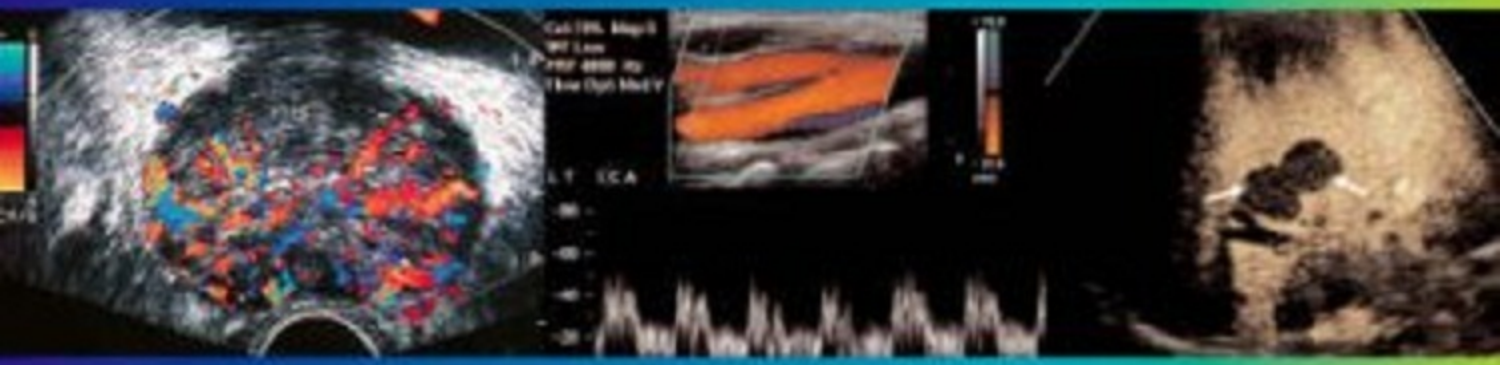

# CLINICAL DOPPLER ULTRASOUND

second edition

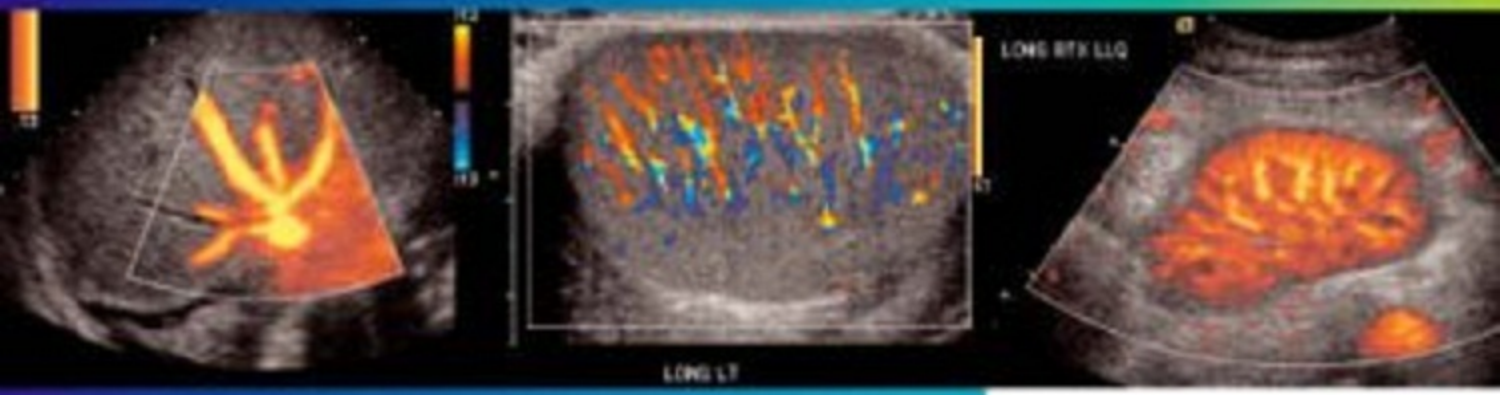


Paul L. Allan  Paul A. Dubbins  Myron A. Pozniak  W Norman McDicken

DVD-ROM included

CHURCHILL LIVINGSTONE
ELSEVIER

**Commissioning Editor:** Meghan McAteer
**Development Editors:** Hilary Hewitt and Louise Cook
**Editorial Assistant:** Nani Clansey
**Project Manager:** Gemma Lawson
**Design Manager:** Jayne Jones
**Illustration Manager:** Bruce Hogarth
**Illustrator:** Hardlines
**Marketing Manager(s) (UK/USA):** Deb Watkins and Emily Christie

# Clinical Doppler Ultrasound SECOND EDITION


Paul Allan BSc, DMRD, FRCR, FRCPE
Consultant Radiologist and Clinical Director of Radiology
Department of Medical Radiology
Royal Infirmary of Edinburgh
Edinburgh, UK

Paul A. Dubbins BSc, MBBS, FRCR
Consultant Radiologist
Department of Radiology
Derriford Hospital
Plymouth, UK

W. Norman McDicken PhD, FIPEM
Professor of Medical Physics and Medical Engineering
Medical Physics
The University of Edinburgh
Edinburgh, UK

Myron A. Pozniak, MD
Professor of Medical Imaging
Department of Radiology
University of Wisconsin
Madison, WI, USA



CHURCHILL LIVINGSTONE
ELSEVIER

CHURCHILL
LIVINGSTONE
ELSEVIER

An imprint of Elsevier Limited



First published 2006

First edition 2000



ISBN-13: 978-0-443-10116-8
ISBN-10: 0-443-10116-7

**British Library Cataloguing in Publication Data**
A catalogue record for this book is available from the British Library

**Library of Congress Cataloging in Publication Data**
A catalog record for this book is available from the Library of Congress

**Notice**
Medical knowledge is constantly changing. Standard safety precautions must be followed, but as new research and clinical experience broaden our knowledge, changes in treatment and drug therapy may become necessary or appropriate. Readers are advised to check the most current product information provided by the manufacturer of each drug to be administered to verify the recommended dose, the method and duration of administration, and contraindications. It is the responsibility of the practitioner, relying on experience and knowledge of the patient, to determine dosages and the best treatment for each individual patient. Neither the Publisher nor the author assume any liability for any injury and/or damage to persons or property arising from this publication.
**The Publisher**

Printed in China
Last digit is the print number: 9 8 7 6 5 4 3 2 1

# List of contributors

**Paul Allan BSc, DMRD, FRCR, FRCPE**
Consultant Radiologist and Clinical Director of Radiology
Department of Medical Radiology
Royal Infirmary of Edinburgh
Edinburgh, UK

**Jonathan D. Berry BSc, MBBS, FRCR**
Specialist Registrar
Department of Radiology
King's College Hospital
Denmark Hill
London, UK

**Paul A. Dubbins BSc, MBBS, FRCR**
Consultant Radiologist
Department of Radiology
Derriford Hospital
Plymouth, UK

**Karen Gallagher AVS, BN**
Senior Clinical Vascular Scientist
Vascular Laboratory
Royal Infirmary of Edinburgh
Edinburgh, UK

**Peter R. Hoskins BA, MSc, PhD, FIPEM**
Consultant Medical Physicist
Medical Physics
The University of Edinburgh
Edinburgh, UK

**Fred T. Lee, Jr, MD**
Robert A. Turrell Professor of Medical Imaging
Department of Radiology
University of Wisconsin
Madison, WI
USA

**W. Norman McDicken PhD, FIPEM**
Professor of Medical Physics and Medical Engineering
Medical Physics
The University of Edinburgh
Edinburgh, UK

**Imogen Montague MB ChB, MRCOG**
Consultant Obstetrician and Gynaecologist
Department of Obstetrics and Gynaecology
Derriford Hospital
Plymouth, UK

**Myron A. Pozniak, MD**
Professor of Medical Imaging
Department of Radiology
University of Wisconsin
Madison, WI
USA

**Paul S. Sidhu BSc, MBBS, MRCP, FRCP, DTM&H**
Consultant Radiologist and Senior Lecturer
Department of Radiology
King's College Hospital
Denmark Hill
London, UK

# Preface

The first edition of Clinical Doppler Ultrasound was designed as a practical introduction to the principles and practice of Doppler ultrasound in the clinical setting. Since then there have been a number of advances which have required a revision of the original text. These include significant technical advances in ultrasound equipment; the evolution of echo-enhancing agents and their wider availability; and new applications of Doppler ultrasound have been developed.

In this second edition we have remained true to our initial aim to provide practical information and advice on the practice and role of Doppler ultrasound. The contributors to this book all have significant clinical experience in diagnostic ultrasound and all the chapters have been rewritten in the light of more recent knowledge and developments; a new chapter on echo-enhancing agents has been included. The images have been updated and expanded, the references brought up to date and one or two small errors from the first edition have been corrected.

Although other vascular imaging techniques, such as computed tomography angiography and magnetic resonance angiography have seen dramatic evolution during the last few years, the authors remain convinced of the primary role of Doppler ultrasound in the investigation of vascular disorders and this role has developed and expanded with time, rather than contracted. It is important that those performing Doppler ultrasound examinations have a clear understanding of the underlying principles of this powerful tool and we have tried to encourage such understanding with this book.

Paul L. Allan
Paul A. Dubbins
W. Norman McDicken
Myron Pozniak 2006

# Physics: principles, practice and artefacts

# 1

W. Norman McDicken and Peter R. Hoskins

A number of techniques have been developed which exploit the shift in frequency of ultrasound when it is reflected from moving blood. This frequency shift is known as the 'Doppler effect'.[1] Five types of diagnostic Doppler instrument are usually distinguished:

1. Continuous wave (CW) Doppler
2. Pulsed wave (PW) Doppler
3. Duplex Doppler
4. Colour Doppler imaging (CDI; colour velocity imaging)
5. Power Doppler imaging

The characteristics of an ultrasound beam, the propagation of ultrasound in tissue and the design of transducers as found in B-mode imaging are all relevant for Doppler techniques.[2–6]

## THE DOPPLER EFFECT AND ITS APPLICATION

For all waves such as sound or light the Doppler effect is a change in the observed frequency of the wave because of motion of the source or observer. This is due either to the source stretching or compressing the wave or the observer meeting the wave more quickly or slowly as a result of their motion. In basic medical usage of the Doppler effect, the source and observer (receiver) are a transmitting and a receiving crystal usually positioned next to each other in a hand-held transducer (Fig. 1.1a). A continuous cyclic electrical signal is applied to the transmitting crystal and therefore a corresponding CW ultrasound beam is generated. When the ultrasound is scattered or reflected at a moving structure within the body, it experiences a Doppler shift in its frequency and returns to the receiving (detecting) crystal. Reflected ultrasound is also detected from static surfaces within the body but it has not suffered a Doppler shift in frequency. After the reflected ultrasound is received, the Doppler instrument separates the signals from static and moving structures by exploiting their different frequency.

Motion of the reflector towards the transducer produces an increase in the reflected ultrasonic frequency, whereas motion away gives a reduction. The system electronics note whether the detected ultrasound has a higher or lower frequency than that transmitted, and hence extracts information on the direction of motion relative to the transducer.

When the line of movement of the reflector is at an angle θ to the transducer beam, then the Doppler shift, $f_D$, is given by:

$$f_D = f_t - f_r = f_t \,.2.\frac{u}{c}.\cos\theta$$

where $f_t$ is the transmitted frequency, $f_r$ is the received frequency, $c$ is the speed of ultrasound and $u\cos\theta$ (i.e. $u \times$ cosine $\theta$) is merely the component of the velocity of the reflecting agent along the ultrasonic beam direction (Appendix A1). For a typical case of blood flow in a superficial vessel:

Transmitted frequency, $f_t = 5$ MHz $= 5 \times 10^6$ Hz

Velocity of sound in soft tissue, $c = 1540$ m s$^{-1}$

Velocity of blood movement, $u = 30$ cm s$^{-1}$

Angle between ultrasonic beam and direction of flow, $\theta = 45°$

The Doppler shift is therefore:

$f_D = (5 \times 10^6 \times 2 \times 30 \times \cos 45)/154\,000$
$= 1372$ Hz

The shift in frequency is small and within the audible range. In an ultrasonic Doppler instrument, the electronics are designed to extract the difference in frequency, $f_D = f_t - f_r$ (the Doppler shift frequency). The instrument can therefore feed a signal of frequency $f_D$ to some output device such as a loudspeaker, or frequency analyser as discussed later.

So far we have considered an ultrasound beam being reflected from a structure moving at a fixed speed and hence generating a Doppler shift of one particular frequency. In practice, there are many reflecting blood cells and their speeds are different. The ultrasound signals returned to the detector from the different cells therefore have suffered different Doppler shifts and add together to give a complex signal containing a range of frequencies. The Doppler shift frequencies are extracted from the detected complex signal and can be fed to a loudspeaker where they can be interpreted by listening. High-frequency (high-pitch) components in the audible sound are related to high speeds, whereas low-frequency components correspond to low speeds. Strong signals, that is of loud audible volume, correspond to strong echoes that have received a Doppler shift. Strong signals could be due to the detection of many blood cells, say in a large vessel, or to echoes from tissue. Later it is noted that an output display called a spectral display or spectrogram is often used to portray the frequency content of Doppler signals.

In the PW Doppler technique, the electrical excitation signal is applied to the crystal as pulses, each containing say 10 cycles, at regular intervals and therefore a corresponding train of pulses of ultrasound are transmitted. For example, 10-cycle pulses can be transmitted, separated by non-transmission intervals of duration 20 times that of each pulse. Regularly spaced echoes are then received back from a reflector and they can be regarded as samples of the signal which would be received if a continuous wave had been transmitted as discussed above. If the reflector is moving the system electronics can extract a Doppler shift signal from the samples. The Doppler equation again applies to this Doppler shift and can be used to calculate the speed of the reflector.[7]

A bonus of PW Doppler is that since pulsed ultrasound is employed, the range of the moving target may be measured from the echo-return time, as well as its speed from the Doppler shift. The range can be measured from one echo signal; however, the calculation of the Doppler shift and hence speed typically requires 50–100 echoes. As for the CW case, a group of blood cells moving with different velocities produce a range of Doppler shift frequency components in the output signal.

It was noted above that the frequency of reflected ultrasound is shifted upward or downward depending on whether the motion of the reflector is toward or away from the transducer. A numerical example illustrates this point and emphasises the small changes in frequency that the instrument must distinguish. When 2 MHz ultrasound is reflected from an object travelling at 30 cm $s^{-1}$ toward the transducer, it returns to the receiver with a frequency of 2.00078 MHz, a shift of +0.00078 MHz. If the object moves at 30 cm $s^{-1}$ away from the transducer, the ultrasound returns with a frequency of 1.99922 MHz, a shift of -0.00078 MHz. Virtually all Doppler instruments which measure velocity preserve this direction information.

## CONTINUOUS AND PULSED WAVE DOPPLER INSTRUMENTS

Doppler blood flow instruments are required to be extremely sensitive and to be capable of detecting weak signals from moving blood in the presence of much stronger signals from static or moving tissues; the latter give rise to low-frequency Doppler shift 'clutter' signals. The magnitude of the scattered signal from blood is typically 40 dB below that received from soft tissues, i.e. the blood echo amplitude is typically one-hundredth of the soft tissue echo amplitude. The dB unit is a measure of the size of a signal relative to another signal; the second signal

is often a reference signal or perhaps the input signal to an amplifier to which the output is compared. Blood flow signals may be detected even though the vessel is not clearly depicted, for instance in the fetal brain, or the renal artery of the neonate.

The transducer of a basic CW Doppler unit has two independent piezoelectric crystals. Since the transmitting crystal is continually driven to generate a continuous wave of ultrasound, a second crystal is used to detect the reflected ultrasound. When a CW Doppler mode is implemented as part of an ultrasound system which uses array transducers, separate groups of array crystal elements are used for transmission and reception. On extraction of the Doppler shift frequency a filter, the 'wall-thump' filter, is often used to remove large, low-frequency components from the signal, such as those from slowly moving vessel walls. Typically in a Doppler unit operating at 5 MHz, Doppler shift frequencies below 100 Hz are removed by filtering. Basic CW Doppler instruments are small and inexpensive; CW Doppler mode facilities are incorporated into some array systems to allow them to detect high velocities (see section on aliasing artefact).

The transmitted ultrasound field and the zone of maximum receiving sensitivity overlap for a particular range in front of the transducer (Fig. 1.1a). Any moving structure within this region of overlap will contribute a component frequency to the total Doppler signal. The shape of the region of overlap (the beam shape) can be considered as having a crude focus which depends on the field and zone shapes and on their angle of orientation to each other. In practice, the beam shapes are rarely well known for CW Doppler transducers. A 5 MHz blood flow instrument might be focused at a distance of 2 or 3 cm from the transducer and a 10 MHz device at a distance of 0.5–1 cm. CW Doppler instruments normally have ultrasonic output intensities ($I_{spta}$) of less than 10 mW cm$^{-2}$ although they may be significantly higher when used in conjunction with duplex systems to measure high velocities.

A PW Doppler instrument, operating with 5 MHz ultrasonic pulses, may have a pulse repetition frequency (PRF) of 10 000 s$^{-1}$, i.e. 10 kHz. The highest velocity that the instrument can measure is directly proportional to its PRF (see aliasing artefact), therefore the PRF is made as high as possible while still avoiding overlap between successive echo trains. Echo signals, i.e. trains of echoes, are produced as a transmitted pulse passes through reflecting interfaces and regions of scattering targets. After amplification, successive echo signals from a specific depth are selected by electronic gating and the Doppler shift frequency is extracted as described above.

Pulsed Doppler devices can be used on their own by altering slowly the beam direction or the gated range depth while listening to the output, for example in transcranial blood flow studies. Identification of vessels is made easier by combining the PW Doppler mode with a real-time B-scan mode to form a duplex system; however, this obviously adds to the cost and complexity.

Since the ultrasound is pulsed and the excitation time is short, a stand-alone PW unit uses a single crystal transducer for transmission and reception (Fig. 1.1b). On setting the electronic gate to select a signal from a specific range, reflectors within a volume, known as the sample volume, contribute to the signal. The shape and size of the sample volume are determined by a number of factors: the transmitted pulse length, the beam width, the gated range length, and the characteristics of the electronics and transducer. The sample volume is often described as a tear drop in shape (Fig. 1.1b). Sample volume lengths are usually altered by changing the gated range length. In a blood flow unit for superficial vessels, the sample volume length may be as short as 1 mm, whereas in a transcranial device it can be 1 or 2 cm; however, the precise lengths are rarely known.

The ultrasonic output intensity of pulsed Doppler instruments varies considerably from unit to unit. The intensity ($I_{spta}$ -see safety section, pp. 23–24) may typically be a few hundred mW cm$^{-2}$ but can be as high as 1000 mW cm$^{-2}$, particularly when they are required to penetrate bone, as in transcranial Doppler. At present the most common use of stand-alone PW units is in transcranial examinations of cerebral vessels.

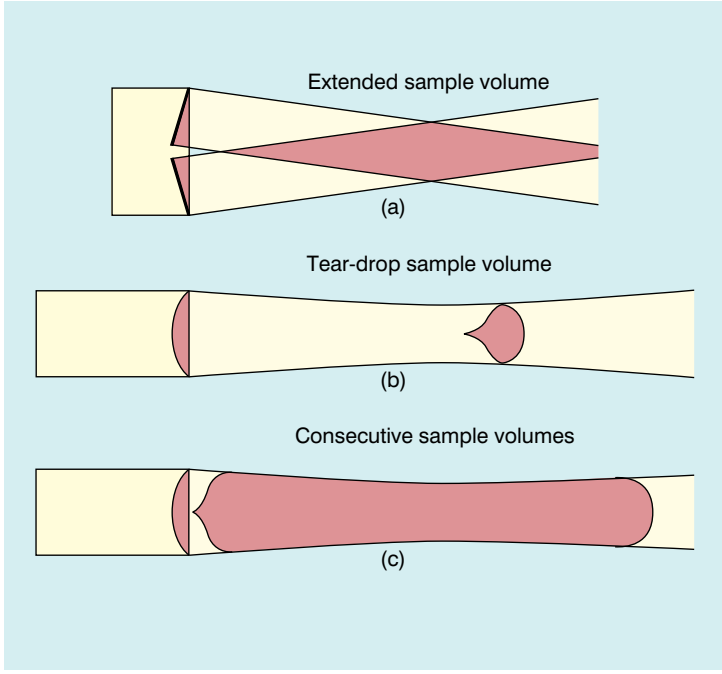


**Fig. 1.1** Sample volumes in Doppler techniques. (a) For dual crystal continuous wave Doppler unit. (b) For pulsed wave Doppler unit. (c) Neighbouring sample volumes along a beam for imaging Doppler units.

### *Technical factors in the use of CW and PW Doppler*

1. Doppler beams are subject to the same physical processes in tissue as B-mode beams, i.e. attenuation, refraction, speed of sound variation, defocusing, etc.
2. Since the stand-alone CW and PW units are used blind, the beam direction and also the sample volume in the PW case must be systematically moved through the region of interest to maximise both the volume and pitch of the audible Doppler signal.
3. PW Doppler is subject to the aliasing artefact in the measurement of high velocities, CW Doppler is not.
4. The sensitivity (gain, transmit power) of the Doppler unit should not be so high that noise detracts from the signal quality.
5. The instrument should be assessed on normal vessels where the blood flow pattern is known and the expected Doppler signal well understood.
6. The wall-thump filter should just be high enough to remove the strong low-frequency signal from vessel walls and any other moving tissue.
7. The final result in many cases should be a distinct display, called a 'spectrogram' or 'sonogram' (see section on the spectrum analyser), with a clearly defined maximum-velocity trace.
8. Since the beam–vessel angle is unlikely to be known, the sonogram cannot be calibrated in velocity and the vertical axis remains as Doppler shift frequency.
9. Care should be taken to ensure good acoustic coupling between the transducer and the patient. Since there is no associated image it is not always apparent that a weak signal may be due to a lack of coupling agent.
10. If possible, information should be obtained on the shape of the sample volume for both CW and PW beams. The sample volume size can then be related to the size of the vessel under study. With CW Doppler there is very little depth discrimination. With PW Doppler the sample volume depth and size are set by the user.

## IMAGING AND DOPPLER

There are three types of imaging used with Doppler techniques. The first, known as 'duplex Doppler', uses a real-time B-scanner to locate the site at which blood flow is to be examined then a Doppler beam interrogates that site. The second type creates an image from Doppler information, i.e. an image of velocities in regions of blood flow.[8] Known as 'colour Doppler', 'colour Doppler imaging' or 'colour velocity imaging' (CVI), it is normally combined with a conventional real-time B-scan so that both tissue structure and areas of flow are displayed. The third type of Doppler imaging is similar to colour Doppler but generates an image of the power of the Doppler signal from pixel locations throughout the field of view and is known as 'power Doppler imaging' (power Doppler).[9] A power Doppler image depicts the amount of blood moving in each region, i.e. an image of the detected blood pool.

### Duplex instruments

Duplex systems link CW or PW Doppler features and real-time B-scanners so that the Doppler beam can interrogate specific locations in the B-scan image (Fig. 1.2). CW duplex is normally only used where very high velocities have to be measured without the aliasing artefact, for example in the estimation of the velocity of a jet through stenosed heart valves. The direction of the CW beam is shown as a line across the B-scan image. In the case of PW Doppler, a marker on the beam line shows the position of the sample volume. The same transducer is usually employed for both imaging and Doppler but two separate ones may be linked together. The Doppler beam is often directed across the field of view so that it does not intersect the blood flow at 90°.

In practice it is difficult to run the B-mode display and the Doppler facility simultaneously, as pulses from one unit are picked up by the other. A time-share solution is employed by many manufacturers, whereby most time is spent in the Doppler mode and the B-mode image is only refreshed at short time intervals. The operator can then check that the ultrasound beam is still intersecting the site of interest. Another option is to switch off the imaging mode once the Doppler beam direction has been fixed and to maximise the PRF for the PW Doppler.

In duplex systems, the transmitted ultrasound frequency in the Doppler mode is often lower than that for the B-mode. The low Doppler beam frequency is to enable higher velocities to be handled before aliasing occurs, while the high

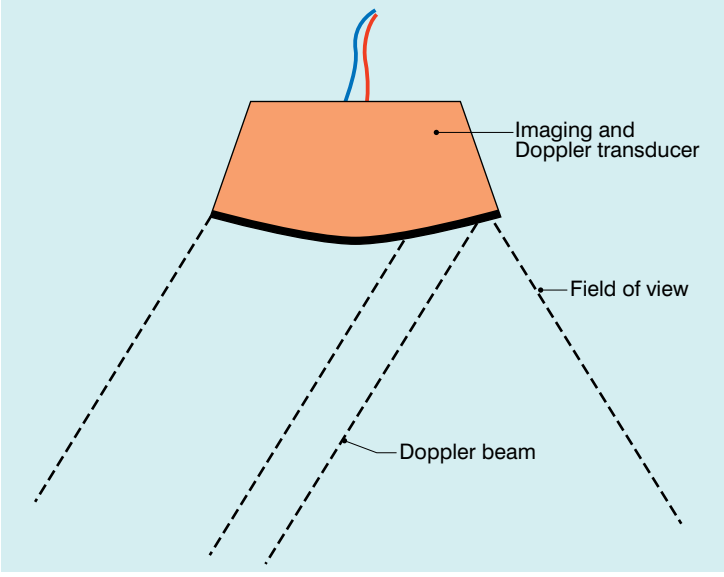


**Fig. 1.2** Duplex system combining real-time B-mode and a Doppler beam of variable position across the B-mode field of view.

B-scan frequency is to optimise resolution in the image. An example could be 5 MHz for Doppler and 7 MHz for B-mode when studies of superficial vessels are undertaken.

### *Technical factors in the use of duplex Doppler*

1. The factors quoted for CW and PW Doppler may also be relevant.
2. A spectrogram can be obtained from a known vessel and a known location within the vessel.
3. The Doppler beam may be refracted and not pass along the line shown in the B-mode image.
4. The beam–vessel angle may be measured manually, allowing blood velocity to be estimated.
5. Simple estimates of blood flow may be obtained from the measured diameter and mean velocity.
6. Spectral broadening due to the use of wide aperture transducers to give good focusing can cause large errors in the measurement of maximum velocity.
7. Since the Doppler beam is held fixed and the PRF is high, particular attention should be paid to the outputs of PW units in relation to safety.

## Colour Doppler imaging

Pulsed Doppler techniques require between 50 and 100 ultrasonic pulses to be transmitted in each beam direction for the determination of velocities of blood in a sample volume. It is therefore not possible to move the beam rapidly through the scan plane to build up real-time Doppler images of velocity of flow. Such imaging became possible when signal processing was developed which could quickly produce a measure of mean blood velocity at each sample volume from a small number of ultrasonic echo pulses. A technique called 'autocorrelation processing' of the signals from blood quickly gives the mean velocity in each small sample volume along the beam (Fig. 1.1c). This real-time colour Doppler imaging processes between 2 and 16 echo signals from each sample volume. In addition, the direction of flow is obtained by examining the signals for the direction of the shift as for CW and PW Doppler devices. Each image pixel is then colour-coded for direction and mean Doppler shift e.g. shades of red for flow towards the transducer and shades of blue for flow away (Fig. 1.3a).

B-scanning and Doppler imaging are carried out with the common types of real-time transducer. Echo signals from the blood and tissues are processed along two signal paths in the system electronics (Fig. 1.4). Going along one path, the signals produce the real-time B-scan image; going along the other path, autocorrelation function processing and direction flow sensing are employed to give a colour flow image. An important exclusion circuit in the autocorrelation path separates large-amplitude signals which arise from tissue and excludes them from the blood velocity processing. The B-mode and mean velocity images are then superimposed in the final display. Strictly speaking, the flow image is of the mean Doppler shift frequency and not the mean velocity, since the beam–vessel angles throughout the field of view are not measured. Colour shades in the image can indicate the magnitude of the velocity, for example light red for high velocity and dark red for low velocity. Turbulence, related to the range of velocities in each sample volume, may be presented as a different colour or as a mosaic of colours.

Doppler images typically contain about 64 genuine lines of information and 128 consecutive sample volumes along each line. The frame rate varies from 5 to 40 frames $s^{-1}$, depending on the depth of penetration and the width of the field of view. As in B-scanning, the appearance of the image is usually improved by inserting additional lines or frames whose data are calculated from the genuine lines, a process known as interpolation. Alteration in flow can occur rapidly over the cardiac cycle, therefore a cine-loop store of say the last 128 frames is of value for review purposes. Doppler spectrograms can be made by selecting the appropriate beam direction and sample volume location in the image and then switching to the PW or CW mode. PW

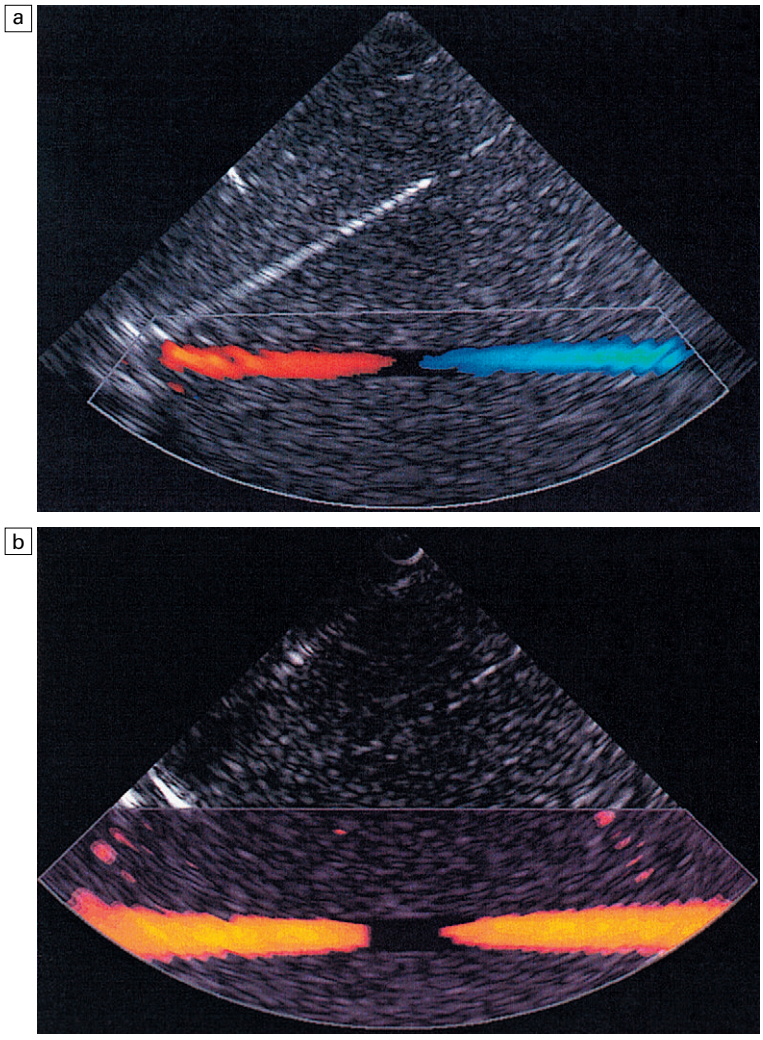


**Fig. 1.3** (a) Colour flow image of flow in a straight tube. When the flow velocity component is along the beam towards the transducer it is colour-coded red, when the component along the beam is away from the transducer it is coded blue. (b) Power Doppler image of flow in a straight tube. Direction of flow is not measured so it is not colour-coded.

and CW Doppler techniques provide more detailed information on blood velocities than colour Doppler, so spectral information is still of value.

### *Technical factors in the use of colour Doppler imaging*

1. The mean Doppler frequency is the quantity which is presented in a colour-coded form in each pixel. When the colour bar is labelled in velocity the beam–vessel angle has been assumed to be zero throughout the image.
2. The velocity component along the Doppler beam is heavily dependent on the angle between the direction of flow and the beam direction (the cosine $\theta$ dependence). The colours depicted in the image are therefore heavily angle dependent.
3. The flow pattern on the colour Doppler display can be related to the structures shown in the B-mode image.
4. CDI is a pulsed technique so aliasing is a problem.
5. A good CDI machine is one which discriminates well between signals from tissue and those from blood.
6. The CDI field of view box should be adjusted to cover only the region of interest and therefore maximise the frame rate.
7. The velocity range covered by the colour scale should be carefully matched to the velocities expected in the study.

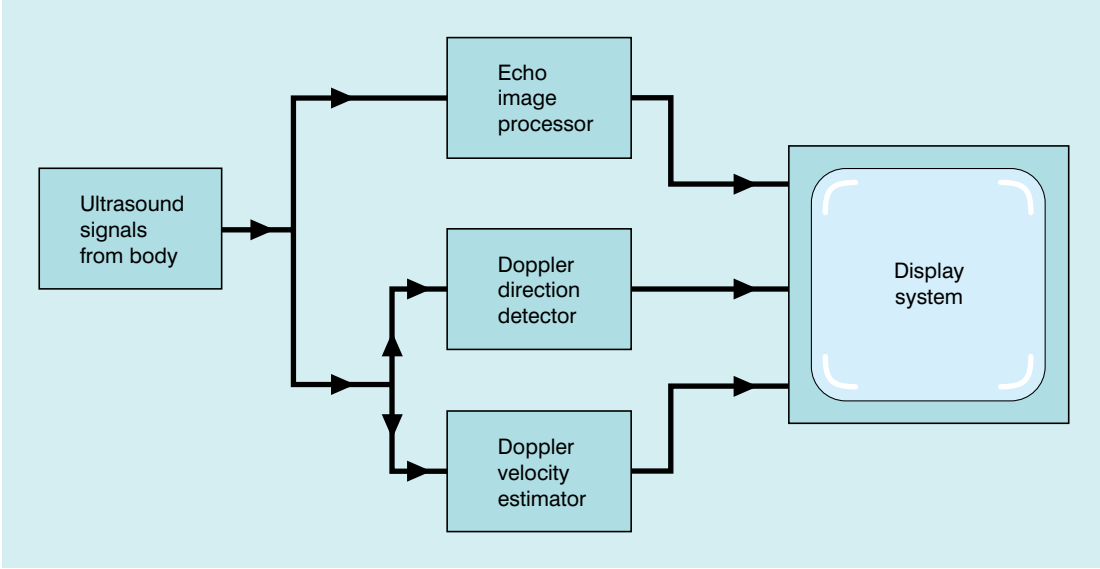


**Fig. 1.4** B-mode and Doppler imaging signal processing paths in a scanning machine.

8. A cine-loop is useful for the review of fast-changing blood flow patterns.
9. A change in the direction of flow, say from toward to away from the transducer, and hence a colour change, need not mean a change in the direction of flow along a vessel. It may merely mean the beam–flow angle has changed from less than 90° to more than 90°.

## Power Doppler imaging

The power of the Doppler signal from each small sample volume in the field of view may be displayed rather than the mean frequency shift (Fig. 1.3b). The power of the signal from each point relates to the number of moving blood cells in that sample volume. The power Doppler image may be considered to be an image of the blood pool. The power mode does not measure velocity or direction and therefore the image shows little angle dependence, neither does it suffer from aliasing; however, it obviously presents less information about blood flow. The attraction of power Doppler images is that they suffer less from noise than velocity images, as the power of the background noise for any sample volume with no blood flow signal is less than the power of the background noise plus Doppler signal when blood flow is present. The background noise may be used to set a threshold above which signals are accepted for Doppler flow. Noise from sample volume regions lacking blood flow is therefore reduced in the power image by a threshold detector. However, when the same signal is used in the velocity imaging mode, the noise will produce a mean velocity value which the machine will treat as a genuine blood velocity and which will therefore appear in the image. The power Doppler mode is therefore less prone to noise and hence more sensitive and can be used to detect small vessels. Further sensitivity can be obtained by averaging power images over several frames to reduce spuriously distributed noise even more. In velocity imaging there is interest in showing quick changes in blood flow and hence less averaging is used.

Power Doppler imaging is fairly easy to use and often provides a more complete image of the vasculature than velocity imaging. This has made it popular in clinical use and it is commonly used initially to locate regions of interest prior to investigation by colour Doppler or duplex methods. It is also possible with some equipment to use the direction information in

the colour Doppler image to colour-code the corresponding power image.

### *Technical factors in the use of power Doppler imaging*

1. In the power Doppler image, the power of the Doppler signal at each pixel is colour-coded.
2. No velocity information is displayed.
3. Most power Doppler systems are direction insensitive; i.e. the display is the same regardless of whether the blood is flowing toward or away from the transducer. However, some machines do display different colours depending on the direction of blood flow by including some directional Doppler information.
4. The power Doppler image is insensitive to angle except near 90° where the Doppler signal may fall below the clutter filter, which cuts out low Doppler shifts, and no signal is displayed.
5. There is no aliasing because the frequency information (i.e. velocity) is not estimated from the Doppler signal.
6. The power Doppler image is very sensitive to movement of the tissue or probe (the flash artefact). Some machines incorporate a flash filter to try to reduce this effect.

## ULTRASONIC MICROBUBBLE CONTRAST AGENTS

A number of agents have been considered which can enhance the scattering of ultrasound from blood and hence could be employed as echo-enhancing or contrast agents. Ophir and Parker[10] have reviewed contrast agents. From this review and more recent experience it has become obvious that agents in the form of encapsulated microbubbles are by far the most likely to be successful echo-enhancing agents in the immediate future. This is due to the large difference in acoustic impedance between the gas in the bubbles and the surrounding blood. In addition, bubbles of a few microns in diameter have a fundamental resonance frequency of a few megahertz. For example, 4 μm diameter bubbles resonate at 4 MHz, which is well within the range of medical ultrasound systems. Bubbles of these dimensions are important since, even with only very thin wall encapsulation, they are able to pass through the capillaries of the lung into the systemic circulation. An investigation by a committee of the American Society of Echocardiography concluded that contrast echocardiography carried a minimal risk for patients and that there were few residual or complicating side-effects.[11] More recent individual studies have confirmed these conclusions; however, more work is required on new agents as they become available.[12]

The development around 1990 of contrast agent microbubbles that can be used by percutaneous venous injection was the breakthrough which gave rise to the current high level of activity in this field. Table 1.1 gives examples of agents which are currently under commercial development. The 'Echogen' agent is different from the others in that it undergoes a phase change from liquid to gas as a result of the increase in temperature following injection into the bloodstream. Large gas molecules are encapsulated in some agents to reduce the rate of diffusion and so increase the lifetime of the bubbles. Typically the lifetime in blood ranges from 2 to 3 min up to 20–30 min. An attraction of contrast agents is the ability to increase the signal obtained from small blood vessels which are difficult to detect by conventional Doppler methods, e.g. cerebral or renal vessels. There is also interest in perfusion studies, for example to observe and measure the wash-in and wash-out of agent in the myocardium in a manner analogous to nuclear medicine studies.

Enhanced scattering is obtained if a bubble is insonated with ultrasound of a frequency equal to that of the fundamental resonance frequency of the bubble. At low power (strictly – low ultrasonic wave pressure amplitude) the oscillations of the bubble are about the centre of the bubble and are directly in proportion to the size of the pressure fluctuations in the ultrasound wave. However, at higher powers the oscillations become distorted and ultrasound at frequencies different from that of the incident wave is

**Table 1.1** Properties of some common intravenous, lung-crossing contrast agents

| Agent | Manufacturer | Type of Agent | Capsule | Gas | Bubble size | Dose (Concentration) |
|---|---|---|---|---|---|---|
| DEFINITY | Bristol-Myers Squibb Medical Imaging | Microsphere | Bi-layer Lipid | Octafluoropropane | Mean diameter 1.1–3.3 μm (98% <10 μm) | $10 \times 10^8$ μbubbles/ml |
| OPTISON | Amersham Health | Microsphere | Albumin | Octafluoropropane | Mean diameter range 3–4.5 μm (95% <10 μm) | $5–8 \times 10^8$ μbubbles/ml |
| SONOVUE™ | Bracco | Stabilised microbubble | Phospholipids | $SF_6$ | Mean diameter 2.5 μm (90% <6 μm) | $2–5 \times 10^8$ μbubbles/ml |
| CARDIOSPHERE | Point Biomedical Corporation | Bi-layer microbubble | Albumin – outer Caprolactone – inner | Nitrogen but gas can be varied | Variable | Variable |

Courtesy of C. Moran.

generated by the bubbles. These frequencies are known as harmonics and are simply related to the fundamental resonance frequency of the bubble, e.g. the second harmonic frequency is twice the fundamental frequency. There is considerable interest in detecting and using the second harmonic, since tissue does not produce this effect to any great extent and the second harmonic signal comes predominantly from the echo-enhancing agent in the blood vessels. Both pulse-echo and Doppler systems have been designed to pick out the second harmonic component in the ultrasound returned to the transducer and use it to enhance the signal from the agent in blood, possibly by as much as 20–30 dB. These systems are being evaluated in clinical practice.[13]

The scattering from contrast agents can also be enhanced if the acoustic pressure fluctuations in the beam are large enough to damage the microbubbles, causing them to leak. An unencapsulated gas bubble then forms next to the original one; however, since it has no outer shell, the scattering from it is undamped and can be around 1000 times higher than that from the encapsulated bubble. This effect has been exploited in a technique known as 'intermittent' or 'transient' imaging, which allows time for the damaged bubbles to be replaced between sweeps of the ultrasound beam.[14]

#### *Technical factors in the use of microbubble contrast agents*

Contrast agents are still very much in the developmental stage. Nevertheless, some technical points of importance are becoming apparent.

1. Check the age and shelf-life of the agent.
2. Microbubble contrast agents are fairly fragile. The handling instructions should be carefully followed and indeed with experience some additional precautions may be identified.
3. The ultrasonic beam may be capable of destroying some microbubbles; higher transmit power will therefore not necessarily produce a stronger echo signal.
4. Several contrast agents require to be insonated at high acoustic pressures to give enhanced backscatter due to bubble destruction. This phenomenon is also known as 'acoustically stimulated emission'. Aspects of its safety still need to be fully evaluated.
5. Determine the physical phenomena which are expected to be present under the operating conditions and which will enhance the echo signal, e.g. harmonic scattering, free bubble creation and bubble destruction.

## INFORMATION FROM DOPPLER SIGNALS

When the Doppler signal which contains information on blood velocities and haemodynamics is being produced it is necessary to interpret it. It is essential to obtain good-quality signals in order to be able to detect disease.

### The spectrum analyser

A Doppler signal may be analysed into its frequency components in order to give a display of the velocities of the blood cells at each instant (Fig. 1.5).[2] Short time intervals of the Doppler signal are analysed, for example a segment of 5 ms duration. This produces an instantaneous spectrum of the frequencies in the sample volume. If an angle correction is then applied, this spectrum will represent the range of velocities in the sample volume. The range of frequencies in each spectrum is then displayed on the vertical axis and the power of each frequency component is presented as a shade of grey. The consecutive velocity spectra are displayed as side-by-side grey-shade lines. In this way a spectral display, or spectrogram, is built up (Fig. 1.6). Note the difference between the instantaneous velocity spectrum which tells us about the pattern of velocities in the sample volume at that instant and the spectral display or spectrogram, which shows how the velocity pattern varies with time. Spectrograms are generated in real time during the clinical examination and it is usually possible to store a few seconds of the trace in an analyser for subsequent review.

The temporal resolution in a spectrogram, that is the smallest discernible time interval,

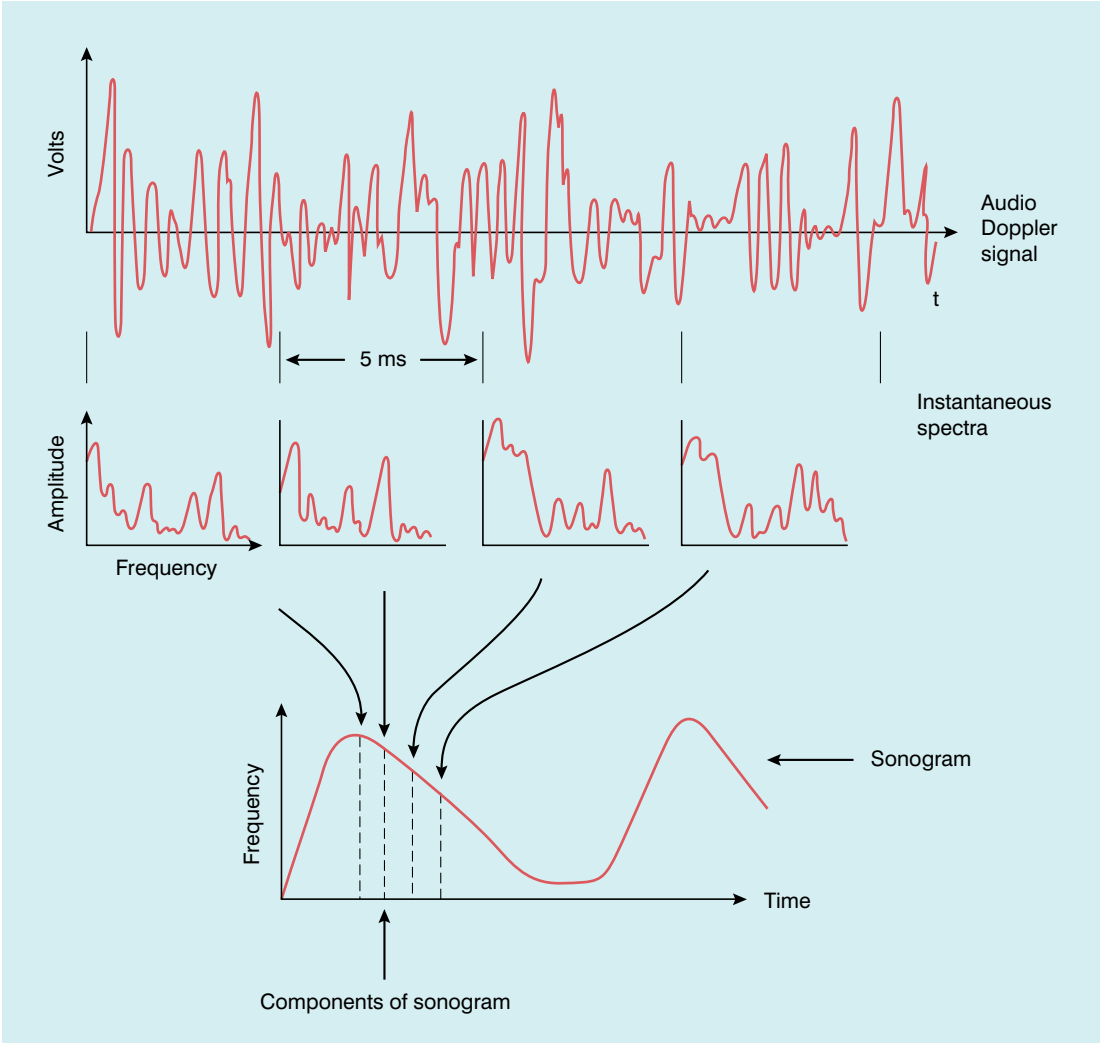


**Fig. 1.5** Schematic representation of the analysis of a Doppler signal to form a sonogram (spectrogram). From McDicken[2] with permission.

equals the length of the portion of Doppler signal used to produce each instantaneous spectrum and is typically 5–10 ms. The frequency (or velocity) axis of the spectrogram usually has about 100 scale intervals each of 100 Hz. The Doppler signal is therefore resolved into frequency components separated by 100 Hz, the frequency resolution of the spectrogram.

It is often desirable to make measurements on a spectrogram, for example an estimate of the time between two events or of the maximum velocity during systole or diastole. Measurement

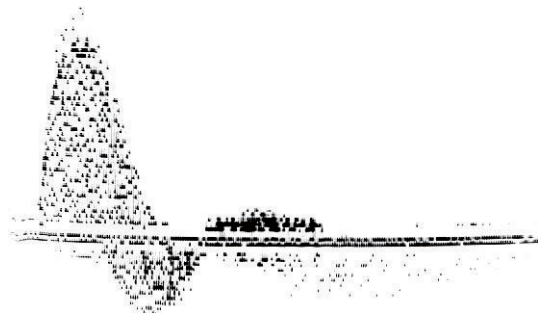

**Fig. 1.6** A sonogram illustrating pixel structure and speckle pattern.

is performed by placing a cursor on the relevant points of interest then a variety of calculations can be performed by the system computer. Indices related to the spectrogram shape and hence to normality or abnormality of flow velocities can be calculated within the analyser and displayed on its screen. These are discussed later in this chapter. The oscillatory shape of a spectrum or a trace derived from it is often referred to as a waveform.

### *Technical factors in relation to spectral analysis*

1. Arrange the frequency and time scales to best display the detailed information in the sonogram by adjusting velocity scale, baseline and sweep speed.
2. Arrange the grey tones, or colours, of the spectral display to give the best 'image' quality by adjusting the Doppler gain.
3. Treat with caution information from weak signals in a noisy background.
4. A clear spectrogram is required before the maximum frequency can be traced.
5. It is usually best to make measurements over at least five heart cycles. However, if this is not possible, perhaps due to respiratory movement, useful information can be obtained from one or two cardiac cycles.
6. Make use of the total storage capacity of the analyser to make a full recording from which the most suitable part of the spectrogram can be selected, using the scroll facility, in order to make measurements.
7. Check thoroughly the reliability of automatic tracing techniques for maximum and minimum velocity.
8. Note whether the vertical axis has been calibrated in velocity by allowing for the beam–vessel angle.
9. To obtain reproducible results, try to use the same beam–vessel angle for all examinations, e.g. 60°.

## SPECTROGRAMS (SONOGRAMS) AND INDICES

A good-quality audible Doppler signal will result in a good quality sonogram. Degradation of a sonogram is due to electronic and acoustic noise which should only be a problem when the gain of the Doppler unit or analyser is very high for the detection of weak signals. Noise in sonograms creates considerable difficulties for the automatic calculation of quantities and they should therefore be used with caution. It is sometimes possible to check traces drawn automatically on a sonogram to see if they have been corrupted by noise. If the automatic mode cannot deal with the noise, then the traces should be drawn manually making use of the eye's ability to distinguish noise from true signal. It should also be remembered that the vertical axis of a sonogram can only be labelled as velocity after the beam–vessel angle has been measured.

### Waveform indices

Waveform indices are derived from a combination of a few dominant features of the waveform.[3] Indices that have the same or similar names in the literature are occasionally defined differently, so a first step is to check the definition of any index to be used. In practice only two classes of index are used to any great extent, those related to the degree of diastolic flow and others related to spectral broadening. The variation in time of the maximum velocity displayed in a spectrogram is commonly used as a source of data for the derivation of an index (Fig. 1.7a). Since the maximum velocity is not always clearly apparent in a spectrogram, some analysers produce a trace which is closely related to the maximum velocity trace. One example is a trace showing the upper velocity boundary below which the velocity components contain seven-eighths of the power of the Doppler signal.

The mean velocity waveform (average velocity waveform) is also employed (Fig. 1.7b). To calculate the mean velocity at each instant, the values

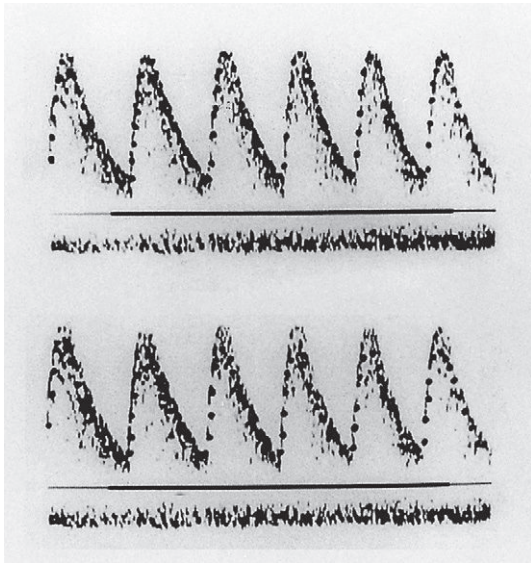


**Fig. 1.7** (a) A maximum-velocity trace on a sonogram. (b) A mean velocity on a sonogram.

of velocity and the intensities of the signal for each velocity component in the instantaneous spectrum are used. The mean velocity is used together with the vessel cross-sectional area to calculate blood flow rate. However, it is difficult to measure mean velocity accurately and there are several other problems associated with calculating flow rates; these are discussed further in Chapter 2.

Since the beam–vessel angle may not always be known, the waveforms or spectrograms will not be corrected for angle. Indices are therefore defined involving ratios of velocities. In such a ratio, the angle factors appear on both the top and bottom and hence cancel each other out, so that the index is independent of beam angle. Errors are also reduced by averaging the calculated indices over several heart cycles.

A number of the most commonly encountered indices are briefly discussed below.

### *A/B ratio*

The A/B ratio is defined as the ratio of two specified velocities, e.g. maximum velocities, at two points in the cardiac cycle (Fig. 1.8). It is usually employed where there is no reverse flow in the waveform.

### *Resistance index (RI)*

In Fig. 1.8:

$$\text{RI} = \frac{\text{S} - \text{D}}{\text{S}}$$

High resistance in the distal vessels produces low diastolic flow in the supplying artery and results in a high value for this index; a low resistance results in a low value as there is higher diastolic flow. It is also known as the Pourcelot index.

### *Pulsatility index (PI)*

The pulsatility index (PI) is defined as:

$$\text{PI} = \frac{\text{maximum velocity excursion}}{\text{mean of the velocity}}$$

It is used in vessels where reverse flow may occur, for example in the lower limbs (Fig. 1.8). The PI may typically have a value of 10 for the normal common femoral artery but be around 2 when proximal disease severely dampens the waveform.

As defined above, the PI index is heart rate dependent. To avoid this, PI can be calculated over a specified time from the start of systole, e.g. for the first 500 ms. The pulsatility index is then labelled 'PI(500)'.

### *Damping factor*

The damping factor is defined as the ratio of pulsatility indices at two sites along an artery. It quantifies the damping of the waveform downstream along a diseased vessel.

$$\text{Damping factor} = \frac{\text{PI (proximal site)}}{\text{PI (distal site)}}$$

The numerical value of this index increases as disease becomes more severe, a value of 2 being typical of a high degree of damping. This index is mentioned for completeness, it is not widely used.

### *Spectral broadening*

Turbulence increases the range of blood cell velocities in a vessel. One index to quantify this broadening of the spectrum of velocities is:

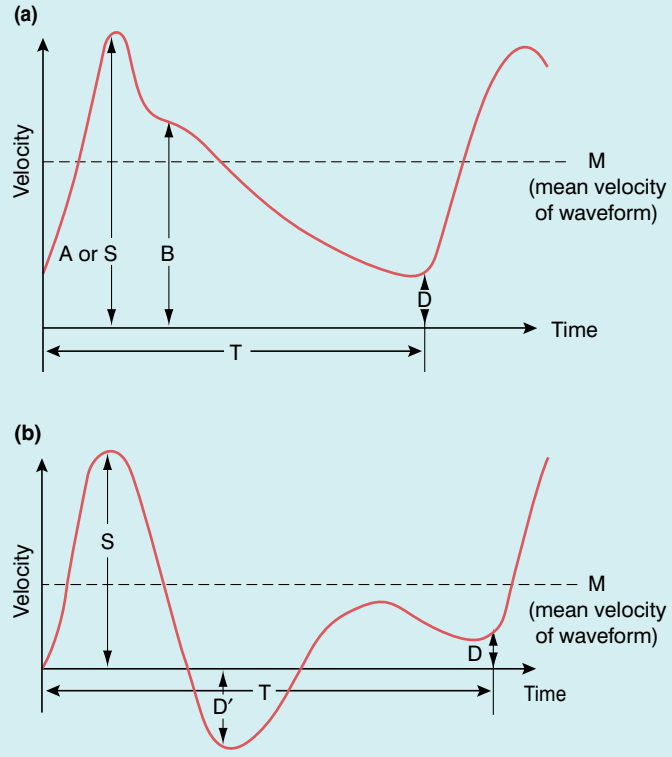


**Fig. 1.8** Waveform indices, normally calculated from a maximum velocity waveform, but the mean velocity waveform can also be used. From McDicken[2] with permission.

$$RI = \frac{S\text{-}D}{S}$$

$S/D$ ratio (umbilical and uterine arteries)

$A/B$ ratio (carotid arteries)

$$PI = \frac{\text{Maximum velocity excursion}}{\text{Mean velocity}}$$

$$= \frac{S\text{-}D}{M} \text{ in } \textbf{(a)}$$

$$= \frac{S+D'}{M} \text{ in } \textbf{(b)}$$

Spectral broadening index (at systole)

$$= \frac{\text{maximum velocity}}{\text{mean velocity}}$$

Conclusions with regard to the presence of turbulence should be made with caution and only after familiarity has been gained with the patterns for laminar and plug flow for the particular instrument being used. Other technical factors can cause spectral broadening; for example 'geometrical spectral broadening', which results from the range of Doppler angles with which ultrasound can insonate a sample volume in the vessel from points on the face of the transducer.

### *Transit time*

The time for the pulse pressure wave to travel along a length of artery can be measured by

placing a Doppler probe at either end of it. From this time and knowing the length, the pulse wave velocity (PWV) is calculated. Alternatively, using the electrocardiogram (ECG) and one Doppler unit the transit time can also be measured, the QRS of the ECG giving the time when the pressure pulse leaves the heart. The time is first measured for the pulse to travel from the heart to the proximal artery site; a second time is then measured for the pulse to go from the heart to the distal site. Subtracting these two times gives the transit time and, if the length of the artery is known, the PWV can be calculated. Any error associated with the assumption that the QRS represents the time at which the pulse leaves the heart is removed by the subtraction.

A normal aorta has a PWV of around 10 m $s^{-1}$. The transit time along 0.5 m is then 50 ms. Pulse wave velocity depends on disease states of the artery wall and blood pressure. This index is also mentioned for completeness, it is not widely used.

### *Technical factors in the application of waveform indices*

1. Use good-quality spectral data to calculate indices.
2. Most indices are calculated using the maximum Doppler frequency as this is relatively insensitive to beam–vessel alignment and sample volume size.
3. Mean Doppler frequency shift is very sensitive to alignment and sample volume size and is not widely used to estimate indices.
4. Indices of waveform shape are insensitive to the beam–vessel angle except near 90° where the end-diastolic component may disappear below the high-pass filter.
5. For obstetrics use, the wall-thump filter must be set low, typically 50–100 Hz, in order that absent end-diastolic flow may be ascertained unambiguously.
6. The most suitable index or measurement for each application can be determined from the literature. Indices are useful in that they allow velocity patterns to be classified and related to disease state. However, they do not extract any more information than can be deduced by direct observation of the whole sonogram.

## ARTEFACTS IN DOPPLER TECHNIQUES

The most important artefacts are mentioned here and methods of dealing with them are suggested. Further details can be found in other texts.[2, 5] Artefacts are usually dealt with by explaining their origin or by recognising that they occur fairly frequently and are not of significance.

### Attenuation

The reduction in echo signal size due to attenuation of the beam in tissue is very familiar from B-mode imaging. The same attenuation processes occur for Doppler techniques, hence stronger signals are detected from superficial vessels than from deep ones. With CW Doppler units this imbalance cannot be compensated. With PW stand-alone and duplex Doppler devices, the signals are from a sample volume at a selected depth and the gain can therefore be adjusted to optimise the signal. In colour Doppler and power Doppler imaging, time gain compensation could help to compensate for attenuation but it is more usual just to process all signals that are above the noise level; obviously those from deep vessels will be closer to the noise level and hence will be more likely to be affected by noise.

### Refraction

Refraction deviates a beam as it crosses at an angle the interface between two tissues in which the speed of sound is different. The direction of the transducer axis may not, therefore, coincide with the actual beam path. With duplex systems a weaker signal than expected from a well-imaged vessel is probably due to refraction of the Doppler beam. This is less of a problem with colour or power Doppler imaging instruments, since the presence of a signal is noted first in the image before any spectral analysis is attempted.

## Shadowing and enhancement

Attenuation of a Doppler beam at a structure may be so large that blood flow behind it cannot be detected, for example at a calcified plaque on a vessel wall. Microbubble contrast agents can also give rise to shadowing problems behind them. Signal enhancement occurs where the beam passes through a medium of low attenuation to reach the vessel, such as a collection of amniotic fluid, or the full bladder.

## Beam width

A wide beam can cause contributions to the Doppler signal from moving structures well off the central axis. This is most likely to be due to a strong reflector such as a heart valve leaflet, but it could also be due to a large blood vessel. A narrow beam may result in only partial insonation of a vessel with the related errors in the Doppler signal; for example, overemphasis of the high-velocity flow at the centre of a vessel occurs when a narrow beam is directed into a vessel but does not encompass the slower-moving blood at the side.

## Spectral broadening

Spectral broadening is another artefact resulting from beam shape. As noted in the discussion on the spectral broadening index, this arises due to ultrasound in the beam insonating a sample volume over a range of angles.

## Speckle and the spectral display

The speckled appearance of a sonogram results from fluctuations in the power levels of the velocity components in neighbouring pixels (Fig. 1.6). These fluctuations are due to fluctuations in the ultrasonic signal received from the random distribution of blood cells. Due to this speckle noise the power level in a pixel cannot be directly related to the number of cells moving with a particular velocity. Averaging the power levels in neighbouring pixels gives a more accurate measure of the number of cells moving with each velocity.

## Inadequate coupling

Weak Doppler signals can be attributed to a lack of coupling liquid between the transducer and the skin. In CW and PW Doppler applications this artefact is not as evident as in imaging techniques, where poor penetration is readily seen.

## Electrical pick-up

Doppler devices are required to be highly sensitive and are therefore prone to electrical pick-up of stray signals. Some such signals can be recognised by their pattern in the sonogram. The spectrum analyser unit may allow the operator to attempt to clean up the sonogram by deleting spurious signals.

## Compression of the spectral display

When a sonogram is compressed, either in its grey shades or in its scale of presentation, information is lost. A sonogram should be treated as a type of image and thus presented with optimum grey-shade contrast and spatial detail. The latter means that the velocity and time axis scales should be selected to show detailed structure in the sonogram. The accuracy of measurements from the sonogram will also be affected by poor presentation.

## Erroneous direction sensing

The direction-sensing circuitry does not always function correctly since its design and implementation are difficult. Flow will then be presented in the wrong direction, either in a sonogram or in a colour Doppler image; if this is suspected then the set-up of the system can be checked by examining a normal artery in which the direction of flow is known.

## Filtering

Filters are used to greatly reduce low frequencies, such as those obtained from arterial walls. Filters also remove information on slow-moving blood but this is not usually a serious problem unless it is desired to measure mean velocity accurately or slow flow specifically (Fig. 1.9).

**Fig. 1.9** Filtering. Raising the high-pass (wall-thump) filter as in the lower sonogram removes low-velocity signals.

## Harmonic generation by large signal distortion

The harmonics of a frequency are higher multiples of that frequency; for example, harmonics of 100 Hz are 200 Hz, 300 Hz, etc. If a signal is too large to be handled by the electronics it becomes distorted and then contains additional harmonic frequency components. When such a distorted signal is analysed, the harmonics appear at regular frequency intervals in the spectral display. Strong blood flow signals exhibit harmonic components as a higher frequency part of the sonogram above that which would probably be obtained if the gain were reduced (Fig. 1.10).

## High or low sensitivity

In colour Doppler and power Doppler imaging, setting up the system with too low a sensitivity causes blood flow signal to be lost. Too high a sensitivity causes spurious echoes to be colour-coded as blood (Fig. 1.11).

## Aliasing

Pulsed Doppler and colour Doppler units have to reconstruct the Doppler shift signal from regularly timed samples of information, rather than the complete signal as used in CW units. The sampling rate is equal to the PRF of the Doppler unit. If the sampling rate is too low, the

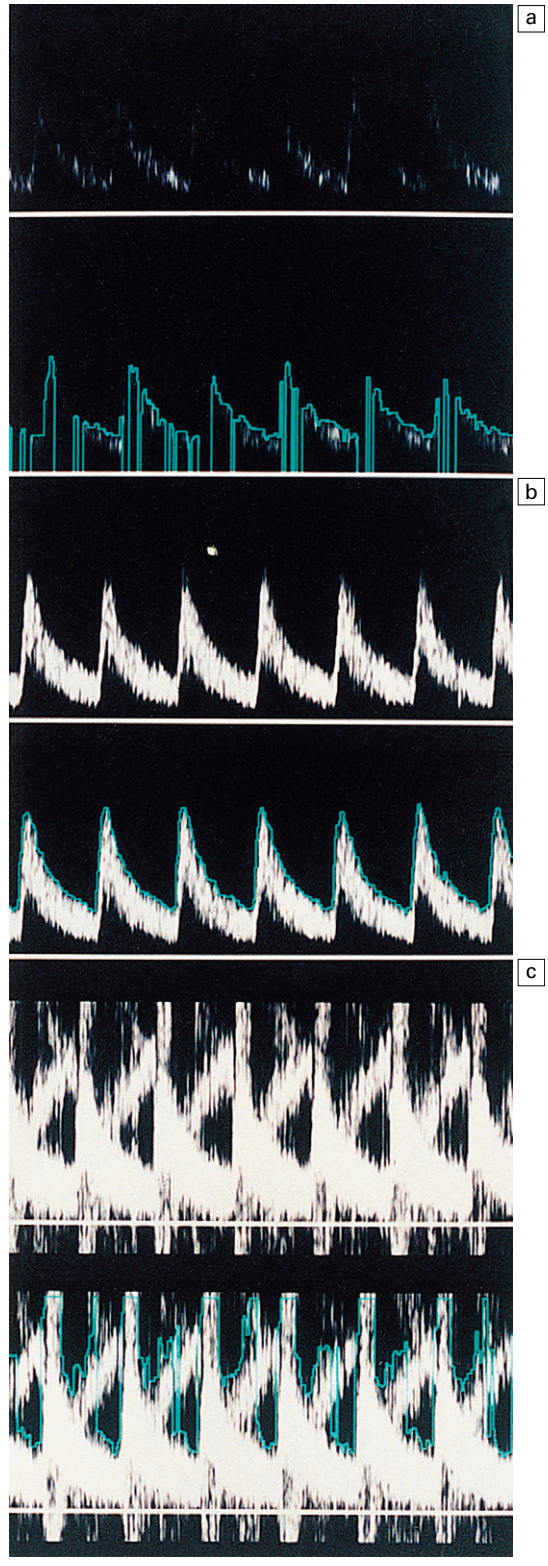


**Fig. 1.10** Increasing gain from (a) to (c). Very high gain distorts the signal and introduces harmonic frequencies.

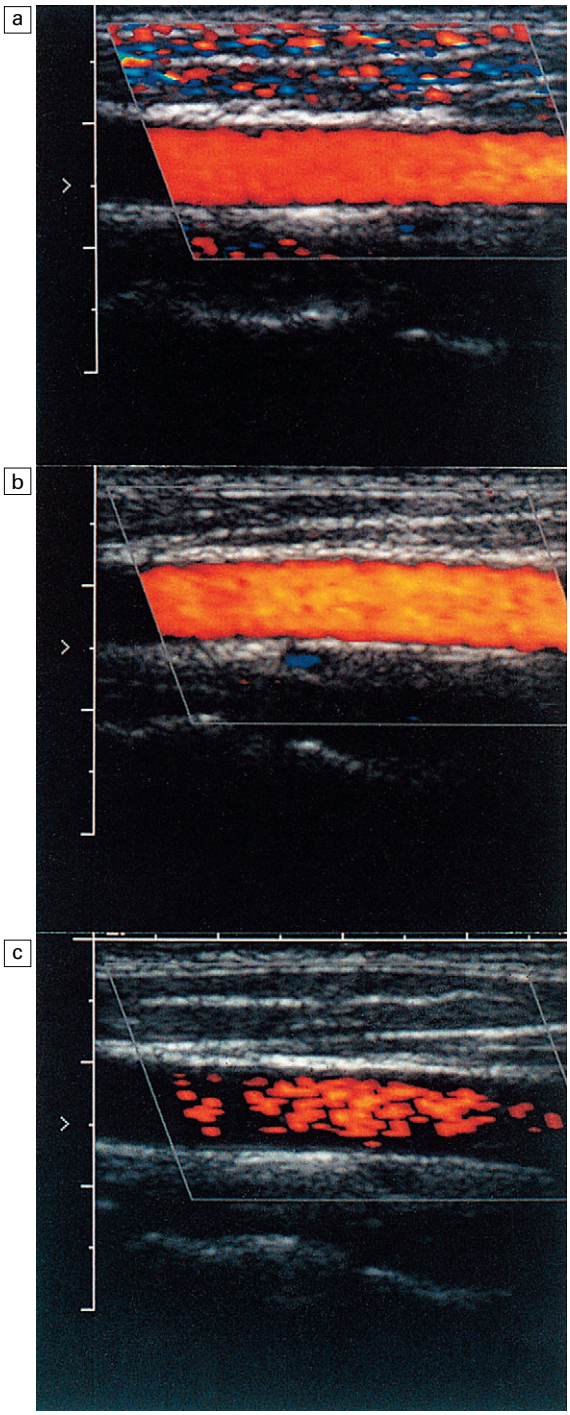


**Fig. 1.11** Variation of gain in a Doppler image. The image content is very sensitive to gain setting: (a) shows too much gain, (b) too little.

frequency of the reconstructed Doppler signal is in error and the direction of flow is presented wrongly. In a spectral display or flow image, this is known as an 'aliasing' artefact (Figs 1.12 and 1.13).

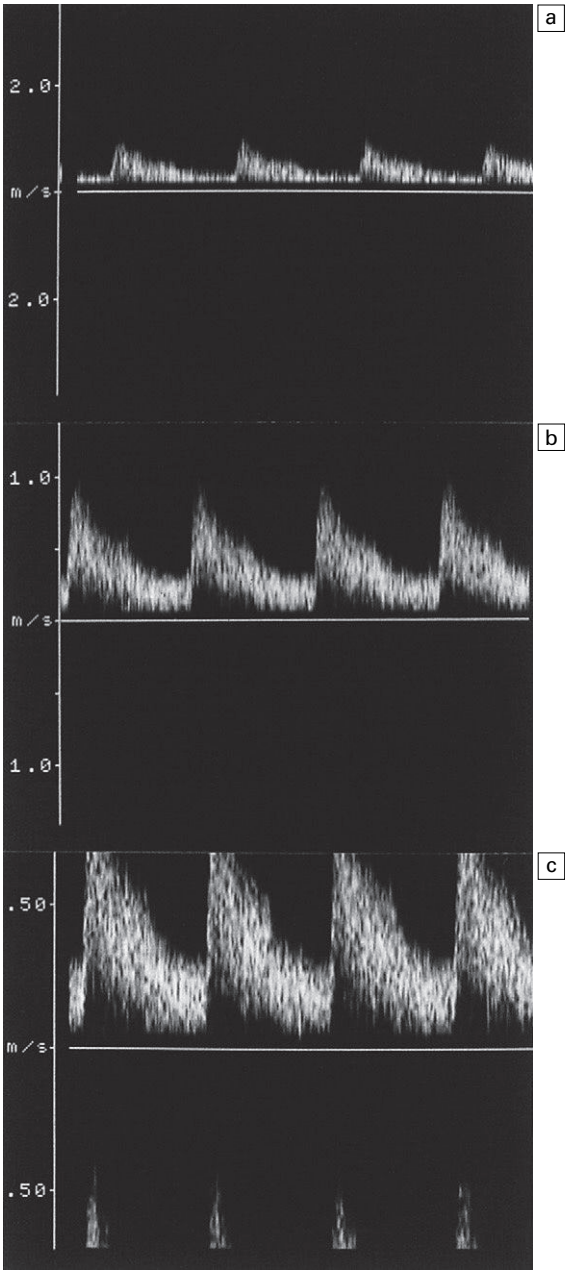


**Fig. 1.12** Aliasing in a sonogram. The highest velocities in (c) appear in the reverse channel.

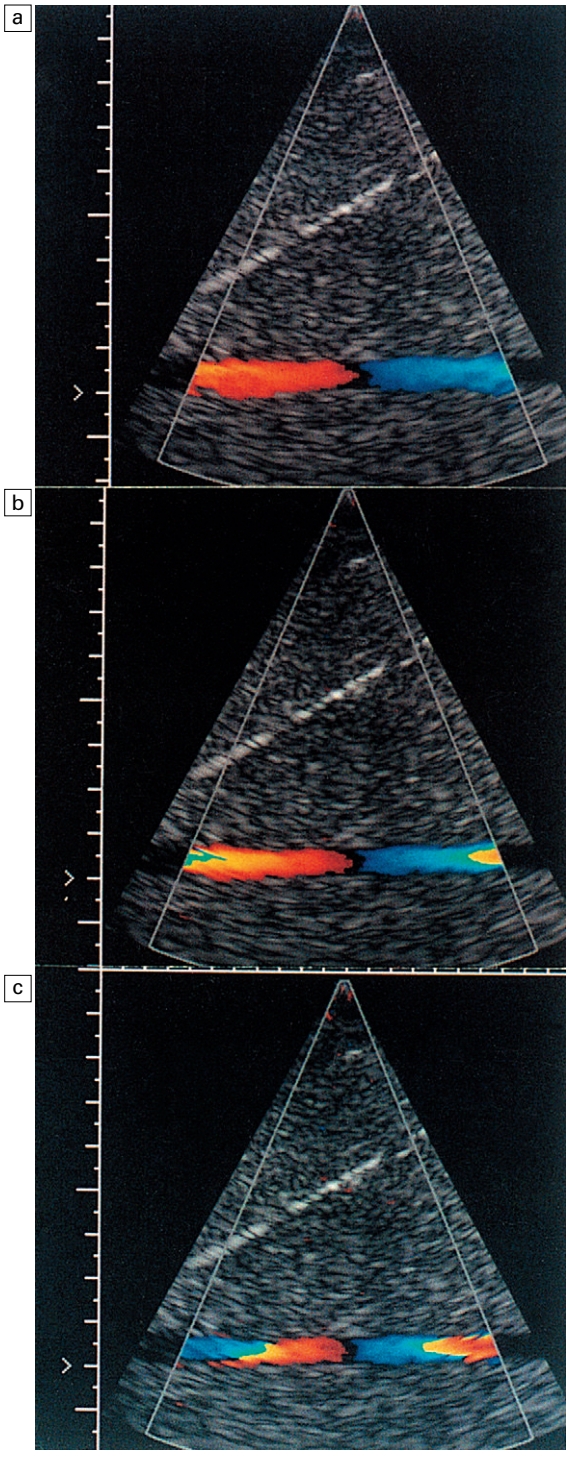


**Fig. 1.13** Aliasing in a colour Doppler velocity image. Note that there is no black space between the red and blue pixels in the lateral colour displays, indicating that the pixel colour-coding has gone off the top of the red colours and wrapped round to the blue colours. However, there is a black space between the colour displays centrally, indicating reversal of flow direction in relation to the transducer.

The aliasing artefact is encountered when high-frequency Doppler shift signals are produced, usually by high-velocity flow. It also occurs when sampling deeper vessels, as the PRF is reduced to allow time for the echoes from a pulse to return before the next pulse is transmitted. If the PRF is too low for the Doppler shift frequencies from the blood in the vessel, aliasing will occur. An approach to raising the velocity level at which aliasing becomes a problem is to use a high PRF (the high-PRF mode), even although the echoes from deep structures have not died out before the next pulse is transmitted. If the deep echoes are strong enough, Doppler signals from deep vessels may then be superimposed on those from a more superficial site. This uncertainty with regard to the source of the signal is referred to as 'range ambiguity'. The high-PRF mode must therefore be used with care. Although this mode can be useful, it increases the intensity of the beam, which is another reason for using it only when necessary.

Figures 1.12 and 1.13 show the aliasing artefact. The high-velocity forward flow components, above the upper limit, appear as high-velocity reverse flow. Aliasing can be of value in colour Doppler imaging since it allows high-velocity jets to be identified. Power Doppler does not suffer from aliasing.

## Effect of beam angle to flow direction

The quality of a Doppler signal depends on beam–vessel angle and, in particular, above 70° it degrades quite rapidly (Fig. 1.14). If the direction of an ultrasound beam is at 90° to the direction of the flowing blood, no Doppler signal is expected since, in the Doppler equation, $\cos 90° = 0$. However, a poor-quality Doppler signal is usually obtained for two reasons. First, the ultrasound beam may converge or diverge slightly from the beam axis, so all of it is never at 90° to the flow. Second, there may be some turbulence in the flow, in which case the blood cells are not all travelling in parallel paths at 90° to the beam.

Colour Doppler images obtained at 90° to the direction of flow appear dark or noisy, corresponding to absent or slow flow (Fig. 1.3).

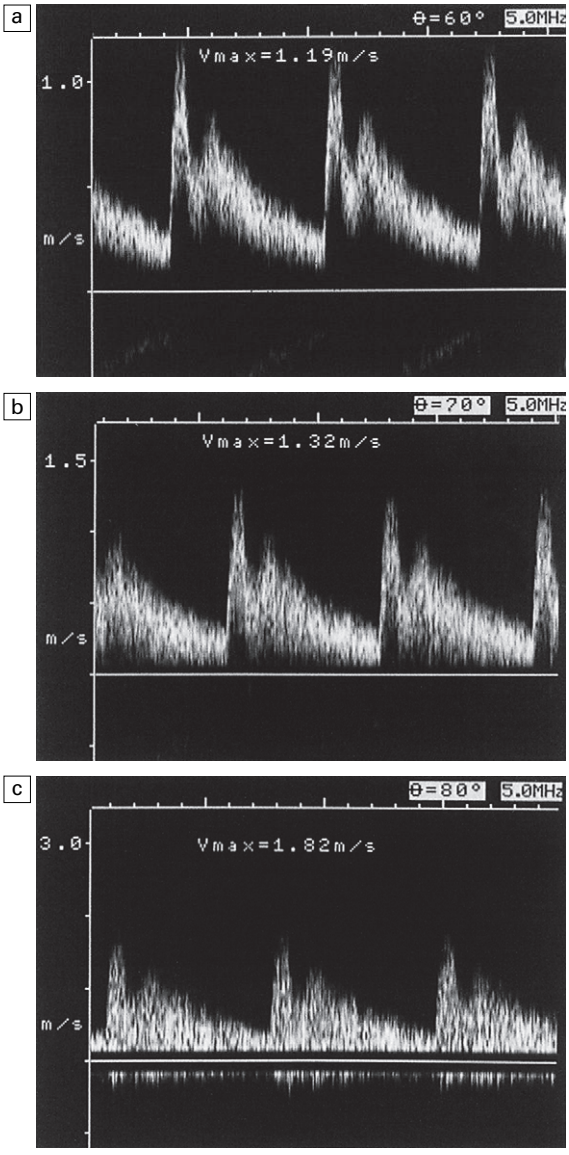


**Fig. 1.14** Variation of quality of signal with beam–vessel angle: (a) at 60°; (b) at 70°; (c) at 80°.

Power Doppler images are relatively insensitive to angle, except near 90°, where the low Doppler frequencies may fall below the clutter filter and no power signal is displayed (Fig. 1.3).

In a vessel in which the direction of flow alters with respect to the ultrasound beam, different regions of the vessel will be colour-coded differently. Note that this may be due to a genuine change in flow direction as seen in the normal carotid bulb, or merely due to the changing beam angle which is particularly common in sector scan imaging.

## Effect of velocity scale

The choice of velocity scale can dramatically change the appearance of a colour flow image (Fig. 1.15). The scale should be chosen to accommodate the range of velocities thought to be present. Too low a scale will cause aliasing and too high a scale results in the flow being depicted as a few dark colours in colour Doppler imaging.

## Unexpected machine artefacts

Doppler technology is developing rapidly and can still have gremlins in it. The operator must therefore check the performance and calibration of the instrument. This is most readily done in a situation where the flow pattern is considered to be well understood, such as in a clearly seen normal blood vessel or a flow test-object. Figure 1.16 shows an unexpected artefact in which the maximum velocity measured varies with the beam position in the field of view. This has arisen because the transducer aperture used is a different size in the different positions, resulting in a different amount of spectral broadening.

## Interference from neighbouring vessels

If part or all of a neighbouring vessel in addition to the vessel of interest is within the sample volume of a CW or PW instrument, the Doppler signal will contain a contribution from the extra vessel. Moving the sample volume or redirecting the ultrasound beam to try to interrogate only the vessel of interest may reduce this artefact.

## Vessel compression

It is easy to compress superficial vessels by transducer pressure. Increased velocity of flow through the restriction in the compressed vessel results in a higher-pitched Doppler sound or a colour change in an image.

## Factors affecting the patient

It is necessary to have as complete a knowledge as possible of the patient's physiological status

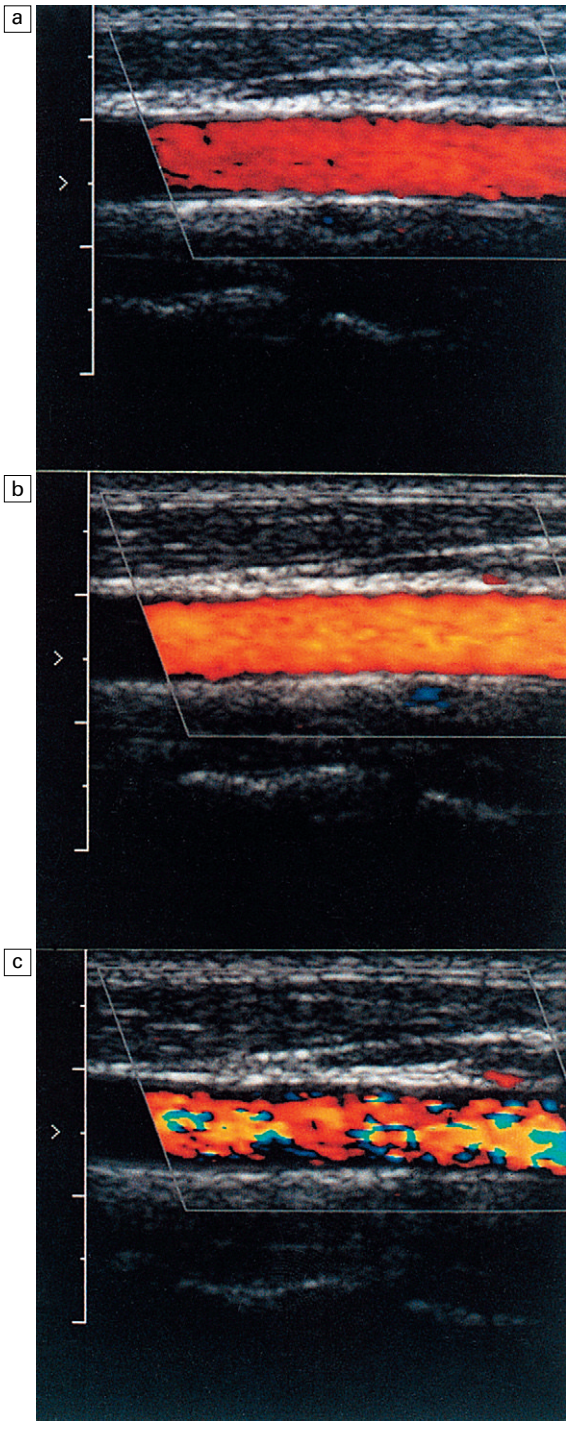


**Fig. 1.15** Effect of changing velocity scale. (a) Maximum velocity 77 cm $s^{-1}$, (b) maximum velocity 32 cm $s^{-1}$, (c) maximum velocity 8 cm $s^{-1}$.

when undertaking blood flow studies, since many factors affect the cardiovascular system. Examples of these factors are exercise, heart rate, temperature, anxiety, posture, food, smoking and other drugs.

## Patient or vessel movement

If movement causes the sample volume of a CW or PW beam to interrogate a different region, the blood flow signal will obviously be altered. It can be difficult to eliminate this factor, especially in abdominal examinations, and it is not always clear whether respiration has actually affected the flow or just moved the vessel.

## Flash artefact

Movement of the patient, an organ, or the transducer during Doppler imaging gives tissues a velocity relative to the transducer and hence scattered ultrasound is Doppler shifted; a large area of the image is therefore colour-coded for the duration of the movement. This artefact is more severe with power Doppler imaging due to its increased sensitivity.

## Beam position within the vessel lumen

The Doppler signal obtained from a vessel depends on how the beam insonates the vessel. The effect is less marked if the beam is wider than the vessel. A narrow beam through the centre of a vessel, however, overemphasises the high velocities while a beam through the side of the vessel detects lower velocities.

## One-dimensional scan

Blood flow often occurs in an unknown direction in space in relation to the transducer, for example in the heart or at a vessel bifurcation. Detecting the flow from one direction only measures the velocity component along that beam direction. Measurement of the actual velocity in these situations requires components to be measured in three directions not in the

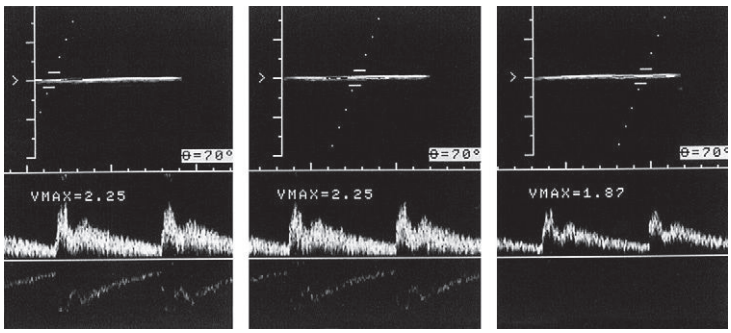


**Fig. 1.16** Variation of sonogram for different beam positions in the field of view. A wider aperture is used near the centre of the array to increase focusing. This increases the range of angles of approach of ultrasound and hence increases spectral broadening.

same plane. However, when laminar flow occurs in a vessel lying in an imaging scan plane, measurement of one velocity component and the beam–vessel angle permits measurement of the actual velocity.

## SAFETY AND PRUDENT USE OF DOPPLER INSTRUMENTS

Ultrasound beams transmit energy into tissue so the possibility of hazard has to be considered. The most likely mechanisms for harmful effects are thought to be tissue heating as the ultrasound energy is absorbed, or cavitation in which microbubbles in the tissue react violently under the influence of the pressure fluctuations of the ultrasound field. The most sensitive structures are considered to be the developing fetus, the brain, the eye, the lung and bone–tissue interfaces.

There is a considerable amount of literature on bioeffects and safety of diagnostic ultrasound. The literature is scrutinised by several national and international bodies who produce statements on safety and the prudent use of ultrasound. Organisations actively monitoring the safety of ultrasound are the World Federation for Ultrasound in Medicine (WFUM), the European Federation of Societies for Ultrasound in Medicine and Biology (EFSUMB),[15] the British Medical Ultrasound Society[16] and the American Institute of Ultrasound in Medicine (AIUM). It is still true to say that there are no confirmed harmful effects of diagnostic ultrasound. Often the possibility of an effect is reported but it is not confirmed by further work. There is a need for well-controlled studies but these are increasingly difficult to conduct since unscanned control populations are almost non-existent in the developed world. Although no harmful effects have been confirmed, there is some concern that the outputs of machines have been increasing by factors of as much as three or five since 1991, as manufacturers seek to produce better B-mode images and more sensitive Doppler units.[17] The situation is summed up in a commentary by ter Haar.[18]

Until the early 1990s, attempts were made to specify the maximum intensities permissible for different clinical applications. This proved to be limiting and impractical, so the approach now is to use the ALARA principle (*a*s *l*ow *a*s *r*easonably *a*chievable) borrowed from the field of ionising radiations. The user is now informed of the output of the machine and has the responsibility to keep the exposure to a low value which will still give a diagnosis. Some systems will display the output on the screen in terms of a thermal index (TI), related to tissue heating and a mechanical index (MI), related to the possibility of producing cavitation. These indices are defined in the Output Display Standard (ODS)[19] developed in the USA.

EFSUMB puts out an annual statement on safety and in its most recent statement it says that the use of B-mode is not contraindicated in routine scanning during pregnancy. However, it is more cautious with regard to pulsed Doppler, saying 'routine examination of the developing embryo during the particularly sensitive period

of organogenesis using pulsed Doppler devices is considered to be inadvisable at present'.

### *Technical factors affecting prudent use and safety*

1. Use the lowest transmit power which will give a diagnostic result. This involves keeping the MI and TI less than one if possible.
2. Use high receiver gain rather than high output power to achieve high sensitivity.
3. Use the minimum scan time possible.
4. Check that the transducer ceases to transmit when the imaging mode is frozen.
5. Take particular care when the fixed beam direction PW Doppler mode is being used near sensitive tissues.
6. Compare the maximum output values (intensity, power, pressure amplitudes) for your machine to those quoted in the published data of equipment surveys.
7. Safety considerations related to contrast agents need to be studied at frequent intervals during their developmental stage.[15]

## FUTURE INSTRUMENTATION

After the basic principle of a new type of Doppler instrument has been established there then usually follows several years of technological and clinical development. During this time the technical performance is improved often by the introduction of new transducers and computer processing of ultrasonic echo signals. The clinical performance is also improved by increased operator experience and the identification of new applications. The introduction of completely new technology typically occurs at the rate of one or two new instruments per decade. Three recent examples are mentioned briefly below.

### Three-dimensional Doppler flow imaging

Just as two-dimensional (2D) colour Doppler flow imaging can be performed by scanning an ultrasound beam through a 2D plane, a 3D colour flow image can be produced by scanning a beam through a 3D volume. At present 3D images are often produced by stacking 2D images next to each other, i.e. a series of parallel scans. These images are proving useful for example in the study of flow through a cardiac valve or complex vascular bed (Fig. 1.17). However true 3D flow imaging would involve measurement of the three velocity components of flow at each sample volume, i.e. at each voxel in the scanned volume. True 3D flow imaging is still at the laboratory development phase and quite far from clinical application.

### Tissue Doppler imaging

All Doppler instruments can be adapted to study tissue motion rather than blood flow. The echo signals from tissue are larger than from blood and the velocities do not reach the high values encountered in blood flow. Nevertheless the signal processing techniques remain valid for Doppler tissue motion.[20, 21] Most commonly it is the myocardium that is studied by both PW Doppler and colour Doppler imaging (Fig. 1.18). The velocity information in 2D tissue Doppler images can be further analysed to give images of strain and strain rate in the myocardium.[22] Doppler tissue techniques have been incorporated in most cardiac imaging instruments.

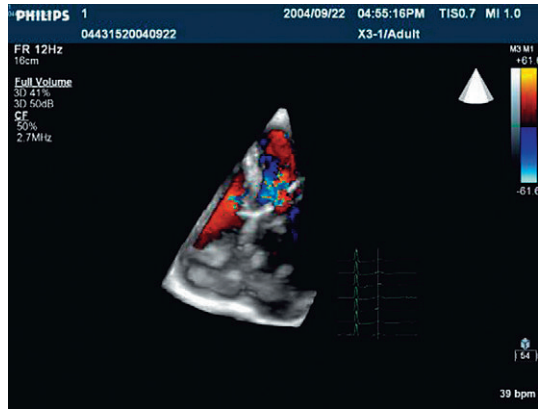


**Fig. 1.17** A 2D projection of a 3D colour Doppler image onto a display screen. The image can be rotated to provide a 3D impression of the flow in the 3D volume scanned. Courtesy of Philips Medical.

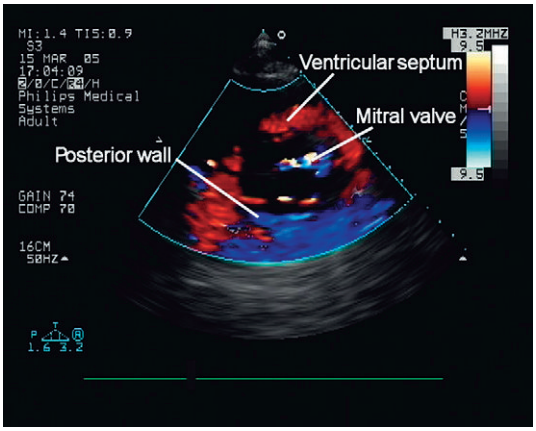


**Fig. 1.18** A longitudinal Doppler tissue image of a section through the left ventricle of the heart.

## Catheter Doppler

High frequency transducers can be miniaturised to dimensions of less than 1 mm making them suitable for insertion into arteries. PW Doppler catheters operating at 20–40 MHz have been commercially available for a number of years. The small transducer crystal is designed to transmit ultrasound along the artery in the direction of the axis of the catheter wire.[23] In practice it can be difficult to know exactly how the ultrasound beam is interrogating the blood flow but high quality low noise signals may be obtained due to the catheter being immersed in the blood. Experimental systems have been made which combine Doppler imaging and grey-shade B-mode imaging.

## APPENDIX A1

The velocity of a structure, say in a plane, can be regarded as the result of combining two other velocities in two other directions in the plane. Each of these two velocities is called the velocity component along its direction. A Doppler ultrasound beam intersecting a moving structure at an angle to its direction of motion will measure the velocity component of the structure velocity along the beam axis (Fig. 1.19a). Figure 1.19b illustrates the point that to fully determine the velocity in 3D space, it is necessary to measure three velocity components in three directions in space. Figure 1.19c shows that if flow is confined to motion parallel to the walls of a straight vessel, velocity along the vessel can be determined with one component i.e. with one ultrasound beam.

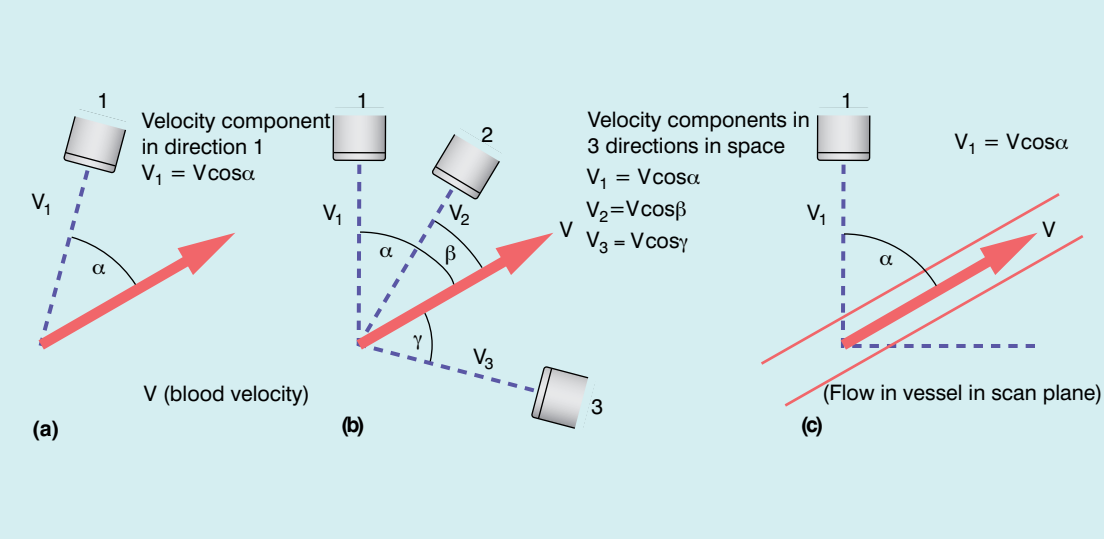


**Fig. 1.19** Velocity components along beam directions.

## REFERENCES

1. White DN. Johann Christian Doppler and his effect – a brief history. Ultrasound Med Biol 1982; 8:583–591.
2. McDicken WN. Diagnostic ultrasonics: principles and use of instruments. London: Churchill Livingstone; 1991.
3. Evans DH, McDicken WN. Doppler ultrasound: physics, instrumentation and clinical applications. Chichester: Wiley; 2000.
4. Hoskins PR. Measurement of arterial blood flow by Doppler ultrasound. Clin Phys Physiol Meas 1990; 1:1–26.
5. Taylor KJW, Burns PN, Wells PNT. Clinical applications of Doppler ultrasound. New York: Raven Press; 1988.
6. Fish P. Physics and instrumentation of diagnostic medical ultrasound. Chichester: Wiley; 1990.
7. Wells PNT. A range-gated ultrasonic Doppler system. Med Biol Eng 1969; 7:641–652.
8. Kasai C, Namekawa K, Koyano A, et al. Real-time two-dimensional blood flow imaging using an autocorrelation technique. Inst Electric Electron Eng Trans Sonogr Ultrasonogr 1985; 32:458–464.
9. Rubin JM, Bude RO, Carson PL, et al. Power Doppler US: a potentially useful alternative to mean-frequency based colour Doppler US. Radiology 1994; 190:853–856.
10. Ophir J, Parker KJ. Contrast agents in diagnostic ultrasound. Ultrasound Med Biol 1989; 15:319–333.
11. Bommer WJ, Shah P, Allen H, et al. The safety of contrast echocardiography – report of the Committee on Contrast Echocardiography for the American Society of Echocardiography. J Am Coll Cardiol 1984; 3:6–13.
12. Williams AR, Kubowicz G, Cramer E, et al. The effects of the microbubble suspension SHU 454 (Echovist) on ultrasound-induced cell lysis in a rotating tube exposure system. Echocardiography 1991; 8:423–433.
13. Burns PN, Powers JE, Fritzsch T. Harmonic imaging; new imaging and Doppler method for contrast-enhanced ultrasound. Radiology 1992; 182:142.
14. Porter TA, Xie F. Transient myocardial contrast after initial exposure to diagnostic ultrasound pressures with minute doses of intravenously injected microbubbles. Circulation 1995; 92:2391–2395.
15. EFSUMB. Guidelines for the use of contrast agents in ultrasound. Ultraschall in der Medizin 2004; 25:249–256.
16. http://www.bmus.org
17. Henderson J, Willson K, Jago JR, et al. A survey of the acoustic outputs of diagnostic ultrasound equipment in current clinical use. Ultrasound Med Biol 1995; 21:669–705.
18. ter Haar G. Commentary: safety of diagnostic ultrasound. Br J Radiol 1996; 69:1083–1085.
19. American Institute of Ultrasound in Medicine/ National Electrical Manufacturers Association. Standard for real-time display of thermal and mechanical acoustic output indices on diagnostic ultrasound equipment. Rockville: American Institute of Ultrasound in Medicine; 1992.
20. Anderson T, McDicken WN. Measurement of tissue motion. Proc Inst Mech Eng 1999; 213 Part H:81–191.
21. McDicken WN, Sutherland GR, Moran CM, et al. (1992) Colour Doppler velocity imaging of the myocardium. Ultrasound Med Biol 1992; 18:651–654.
22. Heimdal A, Stoylen A, Torp H, et al. Real-time strain rate imaging of the left ventricle by ultrasound. J Am Soc Echocardiogr 1998; 11:1013–1019.
23. Doucette JW, Corl PD, Payne HM, et al. Validation of Doppler guide wire for intravascular measurement of coronary artery flow velocity. Circulation 1992; 85:1899–1911.

# Haemodynamics and blood flow

# 2

Peter R. Hoskins, W. Norman McDicken and Paul L. Allan

## PRINCIPLES OF BLOOD FLOW

This section describes the simple principles of blood flow which are of value in understanding the role of Doppler and for performing vascular ultrasound examinations. The underlying principles of fluid mechanics applied to the flow of blood are complex, and discussed in detail in a number of texts including those by McDonald,[1] Caro et al,[2] Strackee & Westerhof,[3] and chapters in the Doppler ultrasound books by Evans et al[4] and Taylor et al.[5]

The blood vessels carry blood from the heart through the pulmonary and systemic arterial circulations and back to the heart through the venous network. Atheroma develops in the arteries and impedes the flow of blood to a greater, or lesser, extent depending on the degree of obstruction that results from its presence.

### Types of flow

The two essential flow states are laminar and turbulent. At low velocity, fluid flow is laminar (Fig. 2.1a). This is characterised by the motion of fluid along well-defined paths called streamlines. At very high velocities, fluid flow is turbulent (Fig. 2.1b); particular elements of the fluid no longer travel along well-defined paths, and there is a random component to the motion of the fluid.

Concepts of laminar and turbulent flow first arose from consideration of flow in long straight tubes. It was found that a dimensionless number called the Reynolds number ($Re$) was useful in characterising the fluid flow. The Reynolds number is defined as:

$$Re = \frac{\rho L V}{\mu}$$

where $\rho$ is the fluid density, $L$ is the vessel diameter, $V$ is the mean velocity and $\mu$ is the fluid viscosity. For a wide variety of fluids the transition to turbulence takes place at a value of $Re$ of about 2000. For flow in which $Re$ is about 2000 the fluid flow will alternate between turbulent and laminar. When velocity is increased so that the $Re$ is above the critical value, turbulence will take a small amount of time to develop. During pulsatile flow it is therefore possible for the flow to be laminar at values of $Re$ higher than the critical value, because turbulence does not have time to develop before the blood velocity has decreased.

There is also a third flow state called disturbed flow, which refers to variations in velocity magnitude and direction which occur at low values of $Re$. The most important phenomenon is that of vortices, which are regions of circulating flow often produced when there is some obvious change in vessel geometry such as a stenosis, or the normal carotid bulb. The pattern of vortex production will change as the degree of stenosis and blood velocity increase. During steady flow at low $Re$ the vortex will be stable and limited to the region immediately behind the stenosis. At low velocity the fluid flow within the vortex is actually laminar. At higher $Re$ there will be vortex shedding at regular time intervals. Again this is not strictly turbulence, as the velocity magnitude and direction at any location is not random, but follows a regular pattern. At even higher $Re$ the vortex shedding will be combined with the random flow patterns

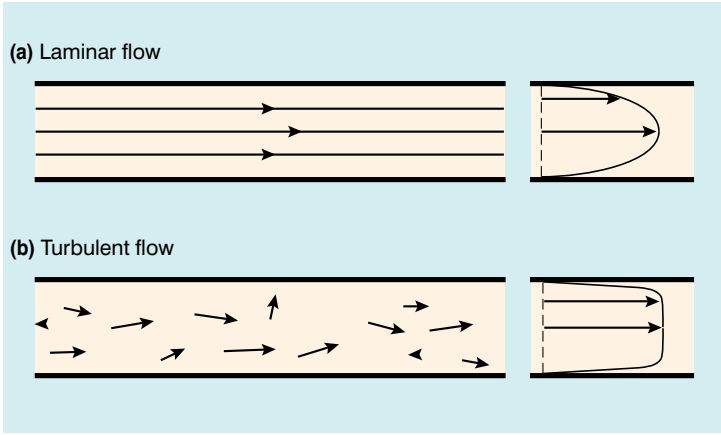


**Fig. 2.1** (a) Laminar flow consists of flow along well-defined streamlines; the velocity profile in a long straight tube under conditions of steady flow is parabolic. (b) The velocity vector magnitude and direction in turbulent flow have random components; the time-averaged profile is blunt.

of true turbulence. Vortices which are shed travel a few diameters downstream and eventually die out as their energy is absorbed through viscous losses. During pulsatile flow, vortex shedding may occur for only a portion of the cardiac cycle.

The effect of the flow state on the Doppler waveform is illustrated in Figure 2.2. Doppler spectra are shown from the normal femoral artery in Figure 2.2a; in this case flow is laminar. Within the sample volume the blood velocity magnitude and direction is similar for all of the red cells, hence the spectral width is low and the waveform outline is smooth. In the poststenotic region of a diseased artery the Doppler waveform is more complex (Fig. 2.2b). The blood which was at rest in the poststenotic region during diastole is accelerated through the sample volume. For this blood, flow is laminar and the initial up-slope of the waveform has a smooth outline with low spectral width, whereas blood which was in the prestenotic region during diastole has to pass through the stenosis, producing disturbed and turbulent flow within the sample volume. The variation in velocity magnitude and direction which this produces results in an increase in the spectral width (Fig. 2.2b), and the waveform outline is no longer smooth.

In the normal circulation, flow is mostly laminar; however, disturbed flow may occur in particular vessels such as the carotid arteries. Flow recirculation is commonly seen in the region of the bulb and there may be disturbed flow in the distal region. For the purposes of clinical Doppler ultrasound, very little practical distinction is made between disturbed and turbulent flow. The presence of spectral broadening is often indicative of pathological change in the vessel. A summary of points concerning flow state is given below:

1. In the normal circulation, flow is mostly laminar.
2. Disturbed flow may occur in particular vessels, e.g. in the region of the carotid bulb.
3. Disturbed and turbulent flow occur in the poststenotic region.
4. Disturbed and turbulent flow both give rise to spectral broadening.

## Pressure and energy

In the circulation the essential principle is that a pressure gradient must be created in order for blood to flow; this is produced by the contraction of the heart and the resultant ejection of blood into the aorta and systemic vessels.

Energy is a useful concept in fluid mechanics. When there is steady flow of an incompressible frictionless fluid, the principles of conservation of energy can be used to give Bernoulli's equation.

| | |
|---|---|
| Energy associated with blood pressure | + |
| Kinetic energy of moving blood | + |
| Potential energy associated with the height of the fluid above ground | = Constant |

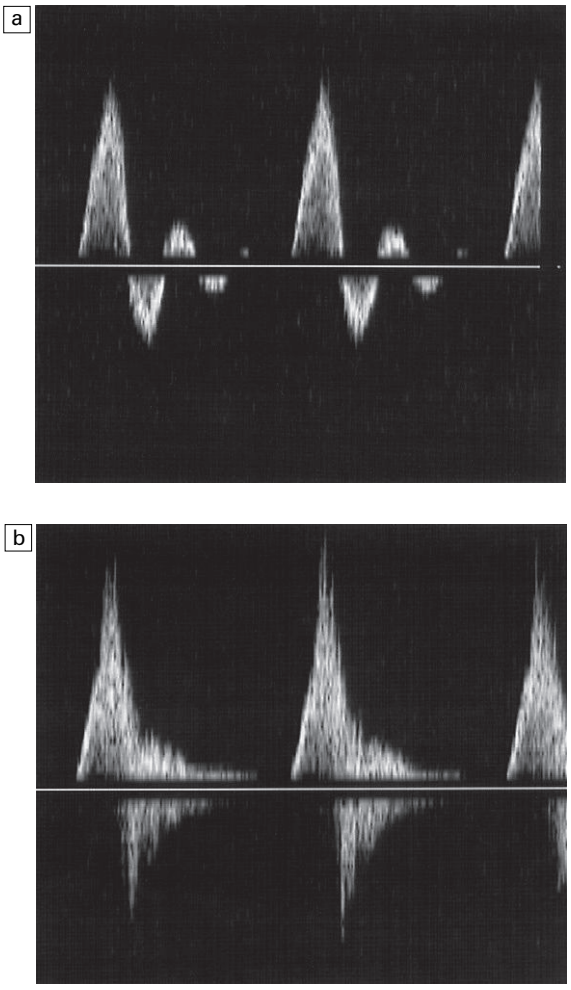


**Fig. 2.2** Femoral artery Doppler waveforms.
(a) From a normal segment; the waveform has a smooth outline and the spectral width is low.
(b) From the poststenotic region; in the early systolic phase the waveform has a clearly defined outline associated with the passage of blood which was at rest in the poststenotic region during diastole through the insonation site. In the later part of the waveform, blood which has passed through the stenosis has developed turbulent, disturbed flow with increased velocity. This appears as a region in which there is spectral broadening and high-frequency spikes.

This is a simple expression which demonstrates that there will be an interchange between the different types of energy within the circulation. In the human body, however, the flow is non-steady and the above equation must be modified slightly to account for the energy required to accelerate the fluid.[4] Energy is conserved in this simple ideal lossless system. In the circulation, energy is lost in the form of heat through viscous effects, manifested through friction of the blood at the vessel wall and between adjacent layers of blood. Energy losses are highest in the region of a stenosis, as there is considerable friction during turbulent flow and vortex motion.

Within a stenosis there will be an increase in blood kinetic energy associated with increase in blood velocity, and according to Bernoulli's equation there is a corresponding fall in blood pressure. If there was no energy loss within the system then the decrease in velocity (and hence kinetic energy) in the poststenotic region would be compensated by a return of the pressure to the prestenotic level. In practice the loss of energy through turbulence and vortex shedding gives rise to a pressure drop across the stenosis whose magnitude is dependent on the degree of stenosis.

The most common application of Bernoulli's equation is in the prediction of pressure drop across a stenosed cardiac valve.[6] The equation may be simplified to:

$$P = 4V^2$$

where $V$ is the measured velocity in m $s^{-1}$, and $P$ is the pressure drop in mmHg. Points concerning pressure and energy are summarised below:

1. The pressure drop across a stenosis is high as a result of energy loss in the poststenotic region.
2. For the estimation of the pressure drop across a cardiac valve stenosis, Bernoulli's equation may be simplified to $P = 4V^2$.

## Velocity profiles

The Doppler ultrasound spectrum is critically related to the detailed variation of velocity within the vessel of interest. The velocity of the blood will vary as a function of its position within the vessel; this is called the velocity profile. The most commonly known velocity profile is called the parabolic velocity profile.

Strictly speaking, a parabolic velocity profile only applies to steady laminar flow in a long

straight tube, when there is maximum velocity in the centre of the vessel and zero velocity at the edge of the vessel (Fig. 2.1a). The profile is radially symmetric, which means that it is the same regardless of which diameter is considered. The shape of the profile is an exact mathematical equation, that of a parabola.

Velocity profiles in vessels in the body are generally more complex; they may not be even approximately radially symmetric and they vary with time during the cardiac cycle. It is worth exploring the various effects that will influence true velocity profiles in the circulation.

### *Entrance effect*

The velocity profile in a vessel is strongly influenced by the distance of the region of interest from the entrance to the vessel. For a long straight vessel, when there is steady flow, the profile is initially flat at the entrance to the vessel. With increasing distance from the entrance the profile will change, becoming parabolic at a distance called the inlet length (Fig. 2.3).

### *Vessel narrowing*

For steady flow, a gradual narrowing taper will tend to sharpen the velocity profile.

### *Vessel expansion*

At regions where the cross-sectional area of the vessel increases, an adverse pressure gradient in the direction of flow is created; that is, there is a pressure decrease in the direction of flow, which tends to retard the flow. For the central high-velocity region, the high momentum opposes this, but at the edge of the vessel the velocities are low and the direction of motion near the wall will reverse if there is a sufficiently rapid increase in vessel cross-sectional area with distance. The phrase 'flow separation' is often used to describe this phenomenon; that is, the high-velocity central jet is located next to a region in which the flow is of low velocity and recirculating. The production of vortices was noted above; both the central jet and vortices die out after a length equivalent to a few diameters and laminar flow is re-established. Figure 2.4 shows the velocity profiles in the region of a small stenosis. When the expansion is less severe, such as a gradually widening taper, the velocity profile simply becomes more blunted.

### *Curved vessels*

Figure 2.5 shows that the velocity profile for steady flow in a curved vessel is skewed towards the outer wall when the entrance profile is parabolic, and skewed towards the inner wall when the entrance profile is flat.

### *Y-shaped junction*

Figure 2.6 shows the velocity profiles from a Y-shaped junction and it can be seen that the profiles are skewed within the two branches, so that the higher velocities occur on the inner aspects of the two branches.

### *Pulsatile flow*

During pulsatile flow the velocity profile will vary throughout the cardiac cycle. Figure 2.7 shows the profiles from a long straight tube with a velocity waveform similar to that found in the femoral artery.

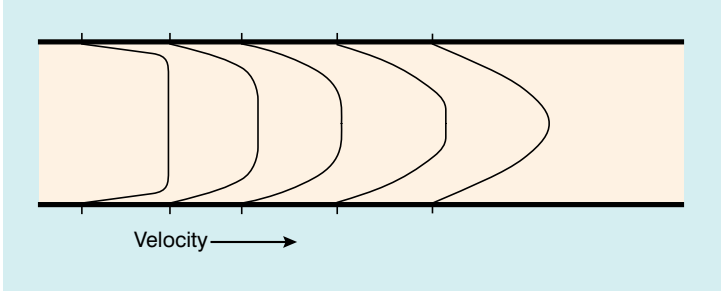


**Fig. 2.3** Velocity profiles during steady flow at different distances from the entrance to a long straight tube from a reservoir. The parabolic velocity profile is restored at a distance from the entrance, the 'inlet length'. After Caro et al,[2] with permission.

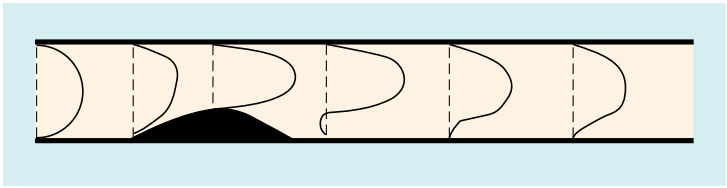

**Fig. 2.4** Velocity profiles from a stenosis model; the region of recirculation in the poststenotic region can be seen on the lower aspect.

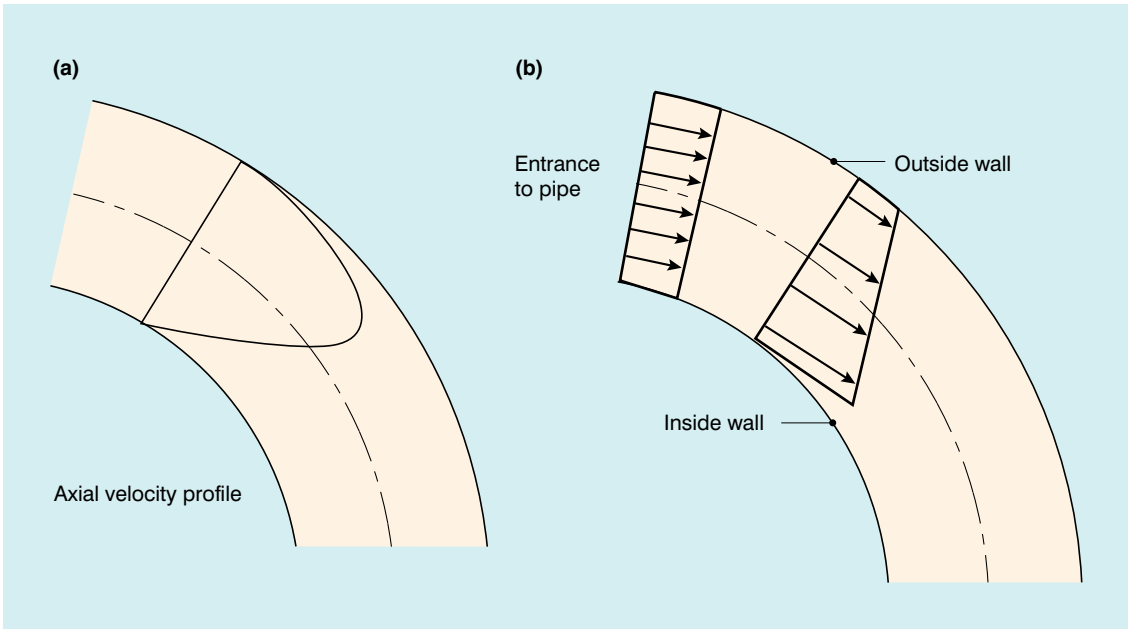


**Fig. 2.5** Velocity profiles within a curved vessel during steady flow. (a) A parabolic velocity profile at the entrance results in higher velocities on the outer aspect of the curve. (b) A blunt velocity profile at the entrance results in the higher velocities occurring on the inner aspect. From Caro et al,[2] with permission.

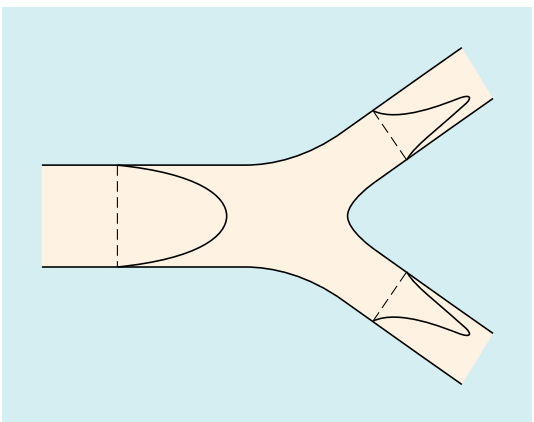

**Fig. 2.6** Velocity profiles in a Y-shaped junction with skewing of the velocity profile and higher velocities on the inner aspects of the two branches.

### *Turbulence*

As discussed above, the velocities during turbulence have a random component, so that it is necessary to take an average value over time. If this is done, then the averaged velocity profile during steady turbulent flow is found to be blunted, with high-velocity gradients near to the vessel wall (Fig. 2.1b).

### *Secondary flow motions*

In many of the geometrical situations described above the components of flow are three-dimensional, which means that there will be some secondary flow motion in the plane perpendicular to the vessel axis. These motions may

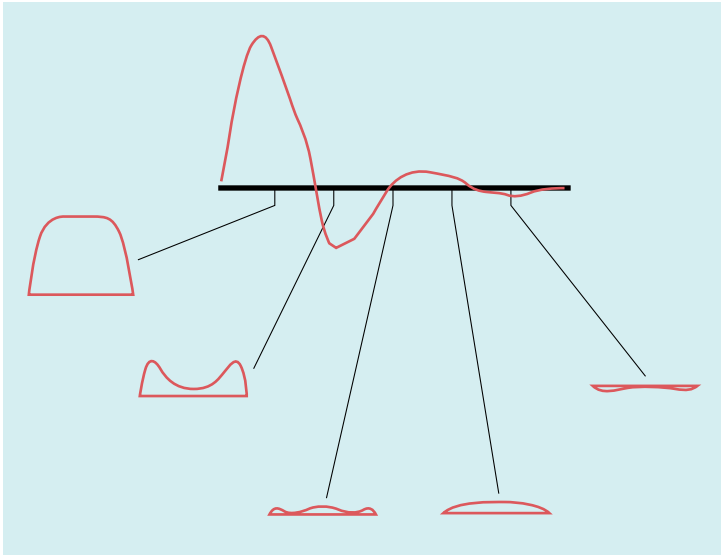

**Fig. 2.7** Changes in the velocity profiles at various moments during pulsatile flow for a velocity waveform similar to that found in the femoral artery. From Evans et al,[4] with permission.

easily be demonstrated using flow models and dye-injection techniques, and there are a few in vivo studies which claim to have demonstrated this.[7,8] A summary of points concerning velocity profiles is given below.

1. Velocity profiles are influenced by a large number of factors, and it generally cannot be assumed that the profile is parabolic.
2. The displayed Doppler spectrum will be critically related to the velocity profile present within the sample volume of the Doppler system.

## A simple flow model

The creation of a pressure gradient within the arterial system is performed by ejection of blood into the arterial tree by the heart. The resistance $R$ to flow of a vessel segment may be defined as:

$$R = \frac{(P_1 - P_2)}{Q}$$

where $Q$ is the flow through the vessel, and $P_1$ and $P_2$ are the pressures at the entrance and exit points of the vessel. One way of expressing this equation is to say that in order to maintain flow at a constant level, the pressure difference must be greater when the resistance to flow increases. Strictly speaking this formula only applies for steady flow conditions; it is therefore useful mainly as an aid in understanding general concepts of flow in arteries, and a more complex version of this equation must be used for pulsatile flow. For a long straight vessel the resistance to flow depends on the fourth power of the diameter. A segment of vessel 2 mm in diameter will therefore have a resistance 16 times that of a similar segment of 4 mm diameter.

A simple model of the flow to an organ is shown in Figure 2.8. The net flow is controlled by a combination of the small vessel (arteriolar) resistance and the large vessel (arterial) resistance. In the non-diseased circulation, the main arteries have relatively large diameters and their resistance to flow is small; the main resistance vessels are the arterioles. The essential clinical manifestations of atherosclerosis may be understood with the aid of this model; an increase in resistance in a large distributing artery because of atheroma must be compensated by a decrease in the resistance of the small arteries and arterioles in order to preserve flow to the capillary bed. As the disease progresses, flow is maintained by arteriolar dilatation until the point is reached where the arteriolar network is fully dilated. Further progression of the proximal disease results in a reduction in flow to the organ and the development of ischaemia

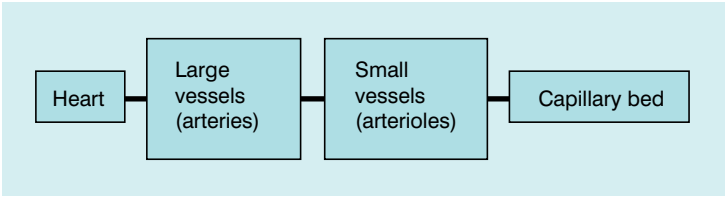


**Fig. 2.8** A simple model of flow from the heart to an organ through a large vessel (arterial) and small vessels (arterioles) to the capillary bed.

because no further compensatory dilatation is achievable. In patients with lower limb claudication, the presence of severe proximal disease results in the distal arteriolar network being fully dilated at rest in order to maintain flow to the lower limb muscles. Whilst this is sufficient in the resting limb, the combination of the proximal stenosis and the maximum arteriolar dilatation means that no further increase in flow can be obtained to cope with the increased metabolic demands of limb exercise.

The concept of a critical stenosis follows from the above model. As the degree of narrowing at a single, isolated stenosis increases, a point is reached at which the distal arteriolar dilatation is at maximum. Consequently, any increase in the degree of stenosis beyond this point leads to a reduction in flow. Experiments performed on animals suggest that this point of critical stenosis is reached with an area reduction of about 75%, which corresponds to a diameter reduction of approximately 50%. Two quantities of interest in Doppler ultrasound are the volume flow rate and the velocity of the blood; the relationship between these two parameters, according to the model developed above, is shown in Figure 2.9.[9] As the calibre of the vessel is reduced, the volume of blood flowing along the vessel is maintained by increasing the velocity. However, above the point of critical stenosis (75% area stenosis), the volume of blood starts to reduce. It should also be noted that the velocity peaks at about 85% diameter stenosis, subsequently tailing off, so that in very tight stenoses the velocity is relatively low.

Two stenoses in series have a larger overall resistance compared with either stenosis considered individually. In practice the combined resistance of stenoses in series is dominated by the one with the smallest luminal diameter.

The concept of a critical stenosis is useful but its application to atherosclerosis should not be taken too far. As atherosclerosis develops, various other compensatory mechanisms come into play in an attempt to preserve perfusion. These include the development of a collateral circulation and a degree of local dilatation of the affected arterial segment. In addition, there is an increase in the extraction efficiency of oxygen from blood. A summary for this section is given below.

1. The degree of constriction of the distal arteriolar bed is one factor used to control the flow rate to the organ.
2. As the resistance to flow of diseased arteries increases, flow rate is maintained within normal levels as a result of distal arteriolar dilatation.
3. Very high degrees of stenosis are accompanied by a low flow rate and low velocities.

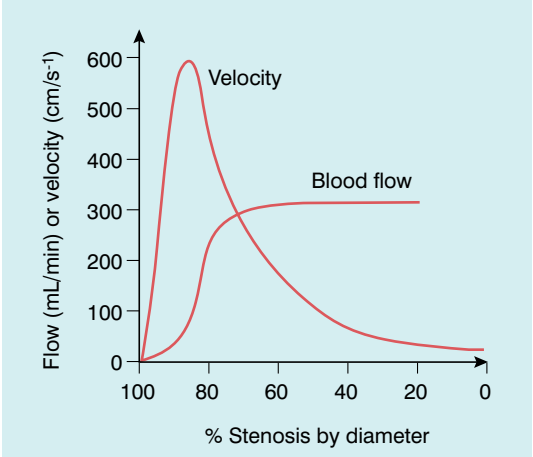


**Fig. 2.9** Flow rate and velocity based upon a single arterial stenosis inserted into an otherwise normal artery. After Spencer & Reid,[9] with permission.

## Pulsatile flow and distal resistance

Doppler ultrasound is commonly used to assess distal resistance to flow. The origin of pulsatile waveforms and their relation to distal resistance are considered here.

For a particular element of blood it is the pressure gradient, not the actual pressure, which accelerates the blood. The pressure gradient is related to the difference between the pressures on either side of the element of blood (Fig. 2.10). When the pressure gradient is positive the blood will be accelerated along the vessel; when the gradient is negative the blood will be decelerated. The corresponding flow waveform is found by detailed calculation of the pressure gradient at the site of interest.

The blood ejected by the heart passes into the aorta. This causes local expansion of the aorta and distal arteries due to the local high pressure. The expanded region passes down the arterial tree in the form of a pressure wave (Fig. 2.11). If the artery were long and straight then, at a particular location along the vessel, the pressure would reach a maximum and then decline to the baseline value (Fig. 2.12a), resulting in a flow waveform with forward flow only (Fig. 2.12b).[10] In practice it is known that flow waveforms in arteries can exhibit periods of reverse flow, and this section is concerned with understanding the origin of this reverse flow.

Periods of reverse flow typically occur in arteries which supply muscle at rest, for example the brachial artery or the femoral arteries. However on exercise, or during periods of reactive hyperaemia, the reverse flow disappears, and there is forward flow throughout the cardiac cycle. This difference in flow waveform is due to differences in the amplitude of reflected pressure and flow waves. As noted above in a long straight pipe there are no reflected waves. However the arterial system is a branching network and the site of the branches will cause a portion of the pressure wave to be reflected and travel back upstream. The major source of reflected waves occurs at the arteriolar junctions, which are the major resistance vessels in the body (Fig. 2.13). When the arterioles are tightly constricted as in the case in resting muscle the amplitude of reflected waves is high leading to reverse flow. On the other hand during exercise or reactive hyperaemia the arterioles are dilated, the amplitude of reflected waves is low and the reverse flow component is lost. This relationship between the degree of diastolic flow and the downstream resistance is used as a diagnostic tool, for example in obstetrics where umbilical artery Doppler waveforms are used to provide an indicator of placental resistance to flow. The normal placenta has a low resistance to flow and umbilical waveforms show flow throughout the cardiac cycle. Absent end-diastolic flow is associated with increased resistance to flow and abnormal placental development; and there is an increased incidence of fetal compromise. Studies in sheep have provided good evidence for the basis for this work.[11]

Before considering the detail of how reflected waves give rise to reverse flow, it is worth considering the simple phenomenon of water waves to illustrate some of the concepts. If a buoy is placed in the ocean it will move up and down with the waves, but the height of the buoy does not provide any information on the direction of travel of the wave. If two waves are travelling towards each other from opposite directions and cross each other at the location of buoy, then the height of the buoy will double as the waves cross

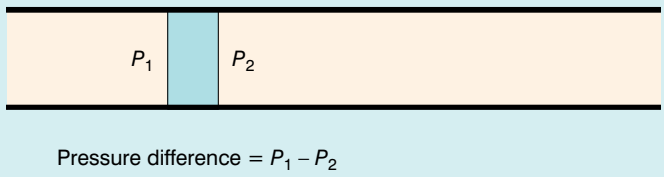


**Fig. 2.10** The force acting on an element of blood is related to the difference in pressures on either side of that element.

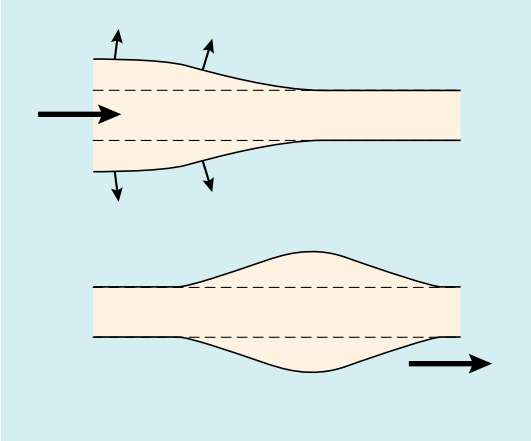

**Fig. 2.11** The blood ejected by the heart causes expansion of the elastic arteries. This expansion passes down the arteries in the form of pressure and flow waves.

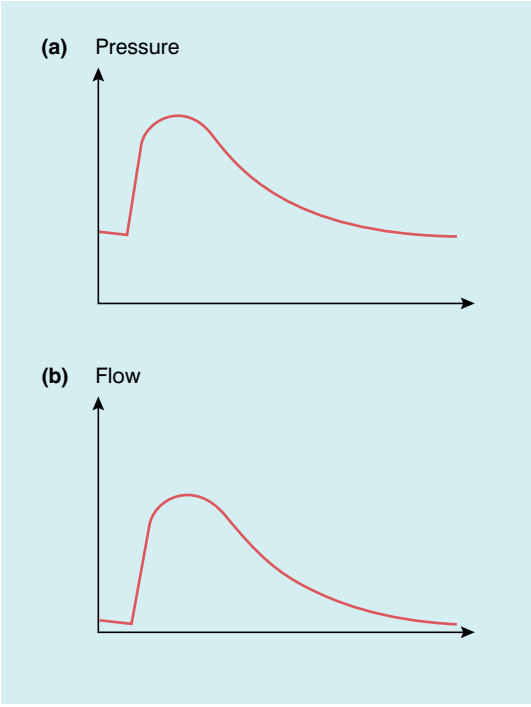


**Fig. 2.12** (a) and (b) Pressure and flow waves in the absence of distal reflection. From Murgo et al,[10] with permission.

due to the additive effect arising from two waves. Returning to the arterial system, there will be a reflected (reverse going) pressure wave which will travel back up the arterial tree and combine

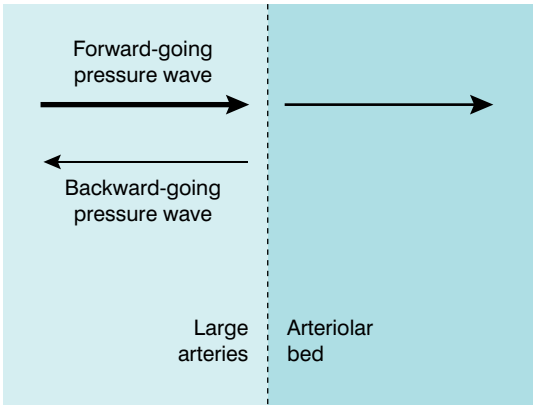


**Fig. 2.13** Reflected pressure and flow waves are produced from the distal arteriolar bed.

with the forward-going pressure wave in an additive manner, hence the combined pressure will be greater (Fig. 2.14). There is also a reflected (reverse-going) flow wave which will also travel back up the arterial tree. However in the case of the flow wave the direction of motion is important. Because the reverse-going flow wave is travelling in the opposite direction to the forward-going flow wave, the result will be a subtraction of the reverse-going from the forward-going wave, which then results in reverse flow (Fig. 2.15).

A summary of this section is given below:

1. Reflected pressure waves from the distal arteriolar bed interact with the forward-going waves to produce the waveform causing increases in pulsatility of the flow waveform.
2. For some arteries the waveform pulsatility as measured using Doppler ultrasound may be a clinically useful indicator of disease.

## QUANTITATIVE FLOW MEASUREMENT

Whilst it is possible to measure blood flow quantitatively, the error is usually rather large, probably between 20 and 100%.[12,13] In some applications such errors may be tolerable, for instance when a large change in flow in the order of 300% from normal to abnormal flow exists. However, one factor which mitigates against blood flow being a sensitive indicator of disease affecting an organ or limb is that circulatory

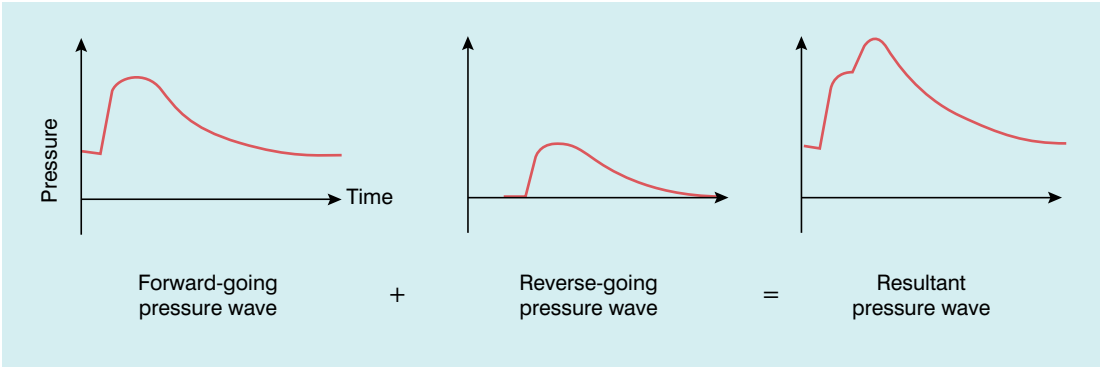


**Fig. 2.14** The resultant pressure wave is a combination of the forward-going wave and the reverse-going wave.

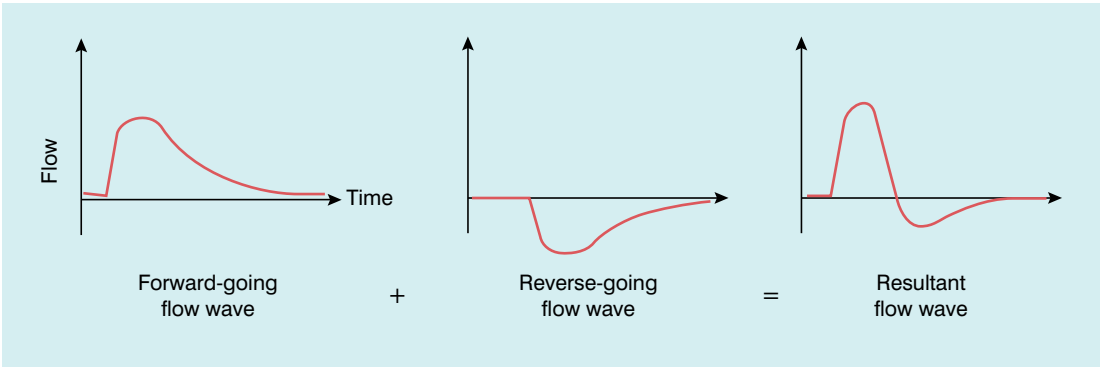


**Fig. 2.15** The resultant flow wave can be considered to be a combination of a forward-going flow wave and a reverse-going flow wave.

regulatory mechanisms can often maintain the level of blood supply until the disease is quite advanced.

A variety of factors must be borne in mind when considering volume flow calculations in relation to the circulation of blood:

1. Flow is pulsatile, therefore the velocity varies over the cardiac cycle. The velocity also varies across the vessel lumen. In addition, turbulence and disturbed flow will result in vectors of flow off the central axis of the vessel, leading to inaccurate angle estimation and correction. Complex flow patterns can occur in curved vessels and near bifurcations, so that the assumption of laminar or plug flow should be carefully examined for each application. Turbulence observed in a sonogram or colour Doppler image makes accurate measurement of volume flow impossible.
2. In practice it is difficult to ensure uniform insonation of a blood vessel, and the resultant error in instantaneous average velocity can be very large, perhaps greater than 50%. Maximum velocity, for use in the calculation of instantaneous average velocity (see below), can be measured to around 5% by ensuring that the ultrasound beam passes through the centre of the vessel. It should always be borne in mind that spectral broadening errors can be large, up to 50%, when maximum velocity is measured by wide-aperture arrays.[14]
3. The calibre of compliant arteries varies with the cardiac cycle. Pulsation of an artery can change its cross-section by up to 20%, hence an instantaneous diameter measurement (see below) should be used if possible.
4. The accuracy of the measurement of the vessel diameter, or cross-sectional area, is inversely

related to the size of the vessel and measurement errors are usually quite large, up to 20% for a 10 mm diameter vessel, rendering the technique of doubtful value for small vessels. The cross-sectional area and the velocity should be measured at the same site; in addition, errors will occur if the scan plane is not exactly at right angles to the axis of the vessel. Special efforts should be made to reduce the error in diameter measurement, since diameter is squared in the formula for cross-section (area = $\pi r^2$) and this increases the error.

5. For laminar flow in a straight vessel the beam–vessel angle can be determined to within 2° or 3°. However, even with this accuracy, if the beam–vessel angle is made greater than 60°, the error in the calculated velocity rapidly rises above 10%, so that the calculated velocities will have significant errors associated with them in this situation.

Knowing the sources of error, steps may be taken to minimise them. A simple approach to measurement is based on the formula:

Instantaneous flow rate = instantaneous cross-section × instantaneous average velocity

'Instantaneous' means the value measured at the point in the cardiac cycle being considered.

The instantaneous average velocity may be calculated by taking the average of the velocities in the spectral display. Both the power level of each velocity in the spectrum and the velocity itself are used in this calculation. The power level for each velocity is a measure of the number of cells moving with that velocity. For this calculation to be accurate, the vessel must be uniformly insonated, which is not easy to achieve due to beam misalignment and distortion.

Another way to obtain the instantaneous average velocity is to measure the maximum velocity and assume a profile for the velocities across the vessel, for example a plug or a parabolic profile. With plug flow all of the blood cells are travelling with the same velocity, so the instantaneous average velocity equals the maximum. For parabolic flow the instantaneous average velocity equals half of the maximum velocity. The maximum velocity is readily measured from a spectral display, provided that part of the beam passes through the centre of the vessel.

The instantaneous cross-section is most easily calculated from the instantaneous diameter measured from an M-scan generated simultaneously with the sonogram; the assumption of a circular cross-section for a given diameter appears to be reasonable for arteries and introduces little error. The diameter can also be obtained from a B-scan provided that it is recorded at the same time and the same location as the spectrum being used from the sonogram.

Averaging the instantaneous flow rate over the cardiac cycle gives the average flow rate.

In practice, these measurements may not be easily achieved on some systems and the following is a more practical formula to use for volume flow rate, in mL $min^{-1}$.

$$\text{Flow rate (mL min}^{-1}) = TAV_{mean}\ (\text{cm s}^{-1}) \times \text{area (cm}^2) \times 60$$

In these cases the time-averaged maximum velocity ($TAV_{max}$) can be calculated over several cardiac cycles and, assuming parabolic flow, divided by two to give a calculated time-averaged mean velocity ($TAV_{mean}$). Some systems will calculate the time-averaged mean velocity directly from the spectral display. Similarly, only a few systems will provide a time-averaged diameter measurement and therefore an instantaneous diameter measurement must be used to calculate area, usually from an image frozen in systole. Alternatively, the area of the vessel can be measured directly from a transverse image of the vessel, providing care is taken to ensure that the section is a true cross-section of the vessel made at systole.

Measurement of volumetric flow is difficult and not generally attempted, as it is easy to produce errors of 100%,[12] but there is little in the literature that gives accurate data on errors in practice. In general terms it should be considered as a research tool and the results treated with suitable caution with regard to the potential errors.

## ARTERIAL MOTION

In the section on pressure and energy above, it was described how the blood ejected from the heart travels down the elastic arteries causing them to distend.

It is possible to examine arterial distension using ultrasound systems. Typically the artery is imaged along the longitudinal plane and the distension at a selected location examined. The artery increases in diameter during systole, and reduces in diameter during diastole. Typically the overall distension is 10% of the diameter, or about 0.5 mm for a 5 mm diameter vessel.

The degree of arterial distension is related to the elasticity of the artery; stiff arteries will not stretch much, whereas elastic arteries will stretch more. It is possible to estimate an index of elasticity, called pressure strain elastic modulus, from distension and blood pressure.[15]

$$\text{Pressure strain elastic modulus} = \frac{\text{change in blood pressure}}{\text{fractional change in diameter}}$$

This provides an easy estimate of arterial stiffness, allowing applications in patients with for example abdominal aortic aneurysm.[16] The pressure strain elastic modulus is a measure of the structural stiffness of the artery and is dependent on the thickness of the arterial wall. It would be very desirable to measure the bulk modulus of the artery, also called the Young's modulus; however this requires knowledge of the wall thickness, which is difficult to measure using ultrasound imaging.

Measurement of wall motion on commercially available systems is slowly being introduced. These are aimed mainly at an assessment of flow mediated dilatation. This is the phenomena whereby the mean arterial diameter will increase slightly following a brief period of absent blood flow. Usually the brachial artery is considered and flow is stopped by an inflated arm cuff. The degree of diameter increase following cuff release is used as a measure of endothelial function. Studies over many years have shown that the overall diameter increase may be measured using ultrasound.[17, 18]

## CONCLUSIONS

The study of haemodynamics involves the application of the principles of fluid mechanics to blood flow in the circulation and provides an insight into the events which occur in both normal and diseased vessels. It is essential to have an understanding of these haemodynamic principles in order to be able to carry out Doppler examinations and to understand the findings which are obtained during the procedures.

## REFERENCES

1. McDonald DA. Blood flow in arteries. London: Edward Arnold; 1974.
2. Caro CG, Pedley TJ, Schroter RC, et al. The mechanics of the circulation. Oxford: Oxford University Press; 1978.
3. Strackee J, Westerhof N. The physics of heart and circulation. Bristol: Institute of Physics; 1993.
4. Evans DH, McDicken WN, Skidmore R, et al. Doppler ultrasound: physics, instrumentation and clinical applications. Chichester: Wiley; 1989.
5. Taylor KJW, Burns PN, Wells PNT. Clinical applications of Doppler ultrasound. New York: Raven Press; 1995.
6. Holen J, Aaslid R, Landmark K, et al. Determination of pressure gradient in mitral stenoses with a non-invasive ultrasound Doppler technique. Acta Med Scand 1976; 199:455–460.
7. Hoskins PR, Fleming A, Stonebridge P, et al. Scan-plane vector maps and secondary flow motions. Eur J Ultrasound 1994; 1:159–169.
8. Stonebridge PA, Hoskins PR, Allan PL, et al. Spiral laminar flow in vivo. Clin Sci 1996; 91:17–21.
9. Spencer MP, Reid JM. Quantitation of carotid stenosis with continuous wave (CW) Doppler ultrasound. Stroke 1979; 10:326–330.
10. Murgo JP, Col MC, Westerhof N, et al. Manipulation of ascending aortic pressure and flow waveform reflections with the Valsalva manoeuvre: relationship to input impedance. Circulation 1981; 63:122–132.
11. Adamson SL, Morrow RJ, Langille BL, et al. Site-dependent effects of increases in placental vascular resistance on the umbilical arterial velocity

waveform in fetal sheep. Ultrasound Med Biol 1990; 16:19–27.
12. Evans DH. Can ultrasonic duplex scanners really measure volumetric flow? In: Evans JA, ed. Physics in medical ultrasound. York: Institute of Physical Sciences in Medicine; 1986.
13. Gill RW. Measurement of blood flow by ultrasound: accuracy and sources of error. Ultrasound Med Biol 1985; 11:625–641.
14. Hoskins PR. Accuracy of maximum velocity estimates made using Doppler ultrasound systems. Br J Radiol 1996; 69:172–177.
15. Peterson LH, Jensen RE, Parnell J. Mechanical properties of aneurysms in vivo. Circ Res 1960; 8:622–639.
16. Wilson KA, Lee AJ, Lee AJ, et al. The relationship between aortic wall distensibility and rupture of infrarenal abdominal aortic aneurysms. J Vasc Surg 2003; 37:112–117.
17. Celermajer DS, Sorensen KE, Gooch VM, et al. Noninvasive detection of endothelial dysfunction in children and adults at risk of atherosclerosis. Lancet 1992; 340:1111–1115.
18. Sidhu JS, Newey VR, Nassiri DK, et al. A rapid and reproducible on line automated technique to determine endothelial function. Heart 2002; 88:289–292.

# The carotid and vertebral arteries; Transcranial colour Doppler

# 3

Paul L. Allan and Karen Gallagher

## THE CAROTID AND VERTEBRAL ARTERIES

### Indications

Ultrasound of the extracranial cerebral circulation is used predominantly in the assessment of patients with symptoms which might arise from disease in the carotid arteries, such as amaurosis fugax and transient ischaemic attacks (TIA), in order to identify those patients with significant changes who will benefit from surgery. Two major trials have shown that endarterectomy for symptomatic patients with significant stenoses [>80% diameter reduction in the European Carotid Surgery Trial (ECST), >70% in the North American Symptomatic Carotid Endarterectomy Trial (NASCET)] confers a significant advantage over medical management in terms of reducing morbidity and mortality.[1,2] The ECST data showed that, during the follow-up period, the percentage of subjects having ischaemic symptoms lasting more than 7 days was 16.8% for those on medical management, compared with 2.8% if surgery was performed. There is no value in having surgery with symptomatic stenoses less than 50% and it is only of marginal benefit for stenoses of 50–70%.[3] A Cochrane Review of the topic[4] concluded that surgery was only beneficial for symptomatic patients with a stenosis of more than 70% on ECST criteria, or 50% on NASCET criteria. The main indications for ultrasound of the carotids are shown in Table 3.1.

**Table 3.1** Indications for carotid ultrasound

- Transient ischaemic attacks
- Reversible ischaemic neurological deficits
- Mild resolving strokes in younger patients
- Atypical, non-focal symptoms which may have a vascular aetiology
- Arteriopaths/high-risk patients prior to surgery
- Postendarterectomy
- Pulsatile neck masses
- Trauma, or dissection
- Screening for disease

#### *Cerebral ischaemic symptoms*

There are many causes of cerebral ischaemic symptoms apart from disease at the carotid bifurcation. These include cardiac arrhythmias, hypotensive episodes, emboli and atheromatous disease elsewhere in the circulation between the heart and the intracerebral arterioles. Many of these can be treated with medical therapy but it is only the extracranial section of the carotid artery which is amenable to surgery, and it is for this reason that so much effort is devoted to the assessment of this area. The main aim is to classify patients into five main groups.

1. Those without significant disease.
2. Those with mild disease (<50% diameter reduction), who will benefit from medical therapy if they are symptomatic.
3. Those with more severe disease (50–70% diameter stenosis), who will be treated medically and may be followed to assess progression of disease, particularly if they are symptomatic.

4. Those patients with severe disease (>70% diameter reduction) who will benefit from surgery if they are symptomatic.
5. Those patients with a complete occlusion, who are therefore not candidates for surgery.

The relationship between the presence of carotid artery disease and the development of cerebral ischaemic symptoms is not straightforward and detailed discussion of this subject is beyond the scope of this book. However, patients who have suffered from temporary ischaemic symptoms, such as TIA, reversible ischaemic neurological deficits, or amaurosis fugax, are significantly more likely to suffer a stroke than asymptomatic subjects: 36% of patients who have a TIA will have an infarct within 5 years of the TIA, compared with an annual stroke rate of 1% for asymptomatic, elderly individuals.[5] Therefore it is reasonable to investigate patients with reversible ischaemic cerebral symptoms in order to identify those with a 70% or greater stenosis who will benefit from endarterectomy. Those with lesser degrees of stenosis can be treated medically and followed up; those who progress to more than 70% diameter stenosis can then be considered for surgery.

The situation regarding the examination of patients with asymptomatic carotid bruits is also complex. The authors, along with many people, would wish to know the status of their arteries if they were found to have an asymptomatic carotid bruit. Although the risk of ipsilateral stroke from an asymptomatic carotid stenosis is low, the Asymptomatic Carotid Atherosclerosis Study (ACAS) reported that surgery is beneficial in reducing the risk of subsequent ipsilateral stroke by some 5% in asymptomatic patients with a stenosis of more than 60% diameter reduction, providing that the centre has a perioperative morbidity/mortality rate of less than 3%.[6] A Cochrane Review of surgery for asymptomatic stenosis concluded that the value of surgery was barely significant and extremely small in terms of absolute risk reduction.[7] Ultrasound will therefore have a role in the identification of those patients who might be considered for endarterectomy, in those centres which offer surgery. However, if there is a policy not to offer surgery to asymptomatic patients, then it might be argued that an ultrasound examination is unnecessary.

The policy for ultrasound in patients with strokes needs some consideration. Patients with a significant, persistent, established neurological deficit will not benefit from carotid surgery whereas individuals with a mild, resolving deficit, who are otherwise candidates for carotid endarterectomy, may be considered for surgery in order to reduce the risk of a subsequent event. It is therefore reasonable to suggest that an ultrasound examination is of benefit in younger patients with milder, resolving neurological deficits but it is of little value in older patients with more permanent neurological signs.

### *Atypical symptoms*

Some patients have unusual symptoms which may or may not be related to carotid disease. Atypical migraine, hyperventilation attacks and temporal lobe epilepsy may sometimes be difficult to diagnose and, in some patients, the possibility of carotid disease might be considered. Ultrasound is of value in excluding carotid disease as a cause of the symptoms in this group of patients, although some care must be given to patient selection to prevent large numbers of unnecessary examinations.

### *Patients at risk of perioperative stroke*

Arterial disease is usually a generalised process, although it affects different arterial territories to varying degrees. Therefore, patients undergoing surgery for conditions such as coronary artery disease, peripheral arterial disease and aortic aneurysms may also have significant carotid disease; there is concern that perioperative morbidity from strokes can be increased in these patients as a result of emboli or inadequate perfusion. Diabetics can also have severe arterial disease and are at risk from perioperative strokes when undergoing major surgery. A review of carotid artery disease and stroke during coronary artery bypass surgery[8] showed that patients with-

out carotid disease had a <2% stroke rate and this only rose to 3% in patients with asymptomatic disease; it also drew attention to the role of aortic arch disease in the aetiology of strokes in coronary artery bypass graft patients. Ivey et al[9] showed that there was no increase in risk associated with asymptomatic bruits in patients undergoing cardiopulmonary bypass procedures, even if there was a haemodynamically significant stenosis; although they felt that patients with a bruit and a history of ischaemic symptoms should be considered for a staged, or simultaneous, endarterectomy if they were shown to have a stenosis of >70% diameter reduction. However, this decision would depend on the relative urgency of the primary condition and many centres, whilst taking note of the carotid disease, will proceed with the main operation and consider subsequent endarterectomy in symptomatic patients.

### *Postendarterectomy patients*

Complications following endarterectomy can be divided into three groups based on the timing of the events.

1. Early occlusion due to thrombosis, occurring within the first 24–48 h after the operation.
2. Stenosis developing over 12–18 months due to neointimal hyperplasia.
3. Recurrence of atheroma over a period of several years resulting in restenosis.

Colour Doppler ultrasound provides a rapid and straightforward method for diagnosis of these complications.

Routine follow-up of asymptomatic patients is not justified by the pick-up rate for developing significant recurrent stenoses,[10] but any patient suffering symptoms related to the operated side should be examined by colour Doppler in the first instance.

### *Pulsatile masses*

Colour Doppler ultrasound provides a rapid technique for the assessment of pulsatile neck lumps. There are a variety of causes for these; the main ones are listed in Table 3.2.

**Table 3.2** Causes of pulsatile neck masses

- Normal but prominent carotid artery and bulb
- Ectatic carotid, brachiocephalic or subclavian artery
- Aneurysm of the carotid artery
- Carotid body tumour
- Enlarged lymph node adjacent to carotid sheath

### *Carotid dissection*

Dissection of the carotid artery may develop from a variety of causes.[11]

1. It may occur spontaneously, usually consequent upon atheromatous change.
2. It may result from the extension of an aortic arch dissection.
3. It may develop following trauma to the neck, such as occurs in whiplash injuries.
4. As a result of iatrogenic causes, such as carotid catheterisation.

Colour Doppler can be used to identify different flow patterns on either side of the flap, or the presence of a thrombosed channel, and monitor subsequent progress.

### *Epidemiological studies and monitoring of therapy*

The carotids provide a convenient window for the assessment of the whole arterial system. Patterns of development of atheroma vary for different arterial areas. Nevertheless it could be expected that changes in the carotids might be related to disease in other vessels, such as the coronary arteries, and that the changes in the carotids might allow some prediction of severity of this disease. In addition their examination could also provide a method for assessing the rate of progression, or regression of disease, if treatment regimens are being investigated, or epidemiological studies are being performed.[12]

By far the largest group of patients will fall into the first group of indications relating to the diagnosis of carotid atheroma and stenosis as a cause of cerebral ischaemic symptoms. In the end the aim of the sonographer is to identify

patients with carotid disease which may be the cause of their symptoms, and to assess the severity of the disease so that appropriate management decisions in relation to surgery or medical management can be taken.

## Anatomy and scanning technique

The main steps in the examination are given in Table 3.3. The patient lies supine, with their neck a little extended by placing a pillow under their shoulders. The patient should be comfortable and excessive extension of the neck should be avoided. In addition, some patients with carotid or veretebral disease may find that neck extension compromises the flow of blood to the cerebral circulation, so if the patient appears to be asleep it is worth checking that they have not lost consciousness. Some patients may not be able to lie supine; if this is the case they can usually be examined adequately in a sitting position.

The examiner can sit beside the patient's thorax and scan the neck from this position, or sit at the patient's head and scan the neck from this location; this latter arrangement was favoured in the early days of carotid ultrasound as it was easier to obtain a standardised probe position, but it is no longer necessary with modern colour Doppler equipment. Furthermore, using this position at the head of the patient for carotid scanning during a general ultrasound list means that the couch and machine have to be moved around in the middle of the list, which is disruptive and time consuming.

A high-frequency transducer (7–12 MHz) is used and the examination starts with a transverse scan of the carotid artery from as low in the neck as possible, to as high in the neck as possible behind the angle of the mandible. This approach will allow the depth and course of the vessels to be ascertained, together with the level of the bifurcation and the orientation of its branches (Fig. 3.1). In addition, areas of major disease will be identified and can be noted for further assessment.

Colour Doppler is then activated and the vessels are examined in the longitudinal plane, again from the lower neck upwards. Areas of abnormal flow are identified with colour Doppler, an initial assessment of their significance is made and the need to undertake a spectral examination can be considered. Just as importantly, areas of normal flow are seen so that the normal segments of the vessel can be identified rapidly and excluded from further investigation. It may be necessary to try a variety of scan planes in order to see the bifurcation in some subjects; the normal approach is from an anterolateral or lateral direction but more posterior planes may

**Table 3.3** Basic steps in the examination

1. Transverse scan from low in the neck up to behind the angle of the mandible to locate bifurcation
2. Longitudinal colour scan to identify areas of abnormal flow and disease
3. Positive identification of the external carotid artery and internal carotid artery
4. Spectral Doppler
   (a) in normal vessels take readings from common carotid artery, internal carotid artery, external carotid artery
   (b) in abnormal vessels take readings from areas of disease in addition to standard readings from common carotid artery, internal carotid artery, external carotid artery
5. Examine the vertebral arteries

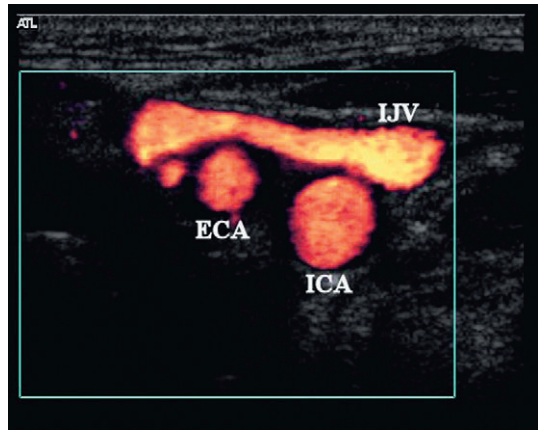


**Fig. 3.1** The left carotid bifurcation on transverse scanning from a lateral approach. The external carotid artery (ECA) and a small branch vessel lie anteriorly with the internal jugular vein (IJV) lying laterally, the internal carotid artery (ICA) lies behind the ECA.

be required and, in a few individuals, the approach may be from under the mastoid process and behind the sternomastoid muscle. In patients who have undergone recent carotid surgery, access can be problematical due to the skin incision and oedema of the soft tissues, so that a variety of approaches may need to be tried, or a lower frequency transducer may be successful; sufficient information can usually be obtained to confirm flow in the vessel, or the absence of flow. Beards are not usually a problem but if they are particularly extensive and luxuriant they may interfere with access; liberal application of gel to exclude air between the hairs usually allows access to the carotids and other cervical structures, although there is some impairment of resolution.

### *Identification of the internal and external carotid arteries*

The common carotid artery on the right arises from the brachiocephalic artery behind the right sternoclavicular joint (Fig. 3.2), where the origin can usually be seen on ultrasound. On the left it usually arises directly from the aorta, so that its origin on the left cannot be seen on scanning from the neck. The level of the carotid bifurcation is usually at about the level of the upper

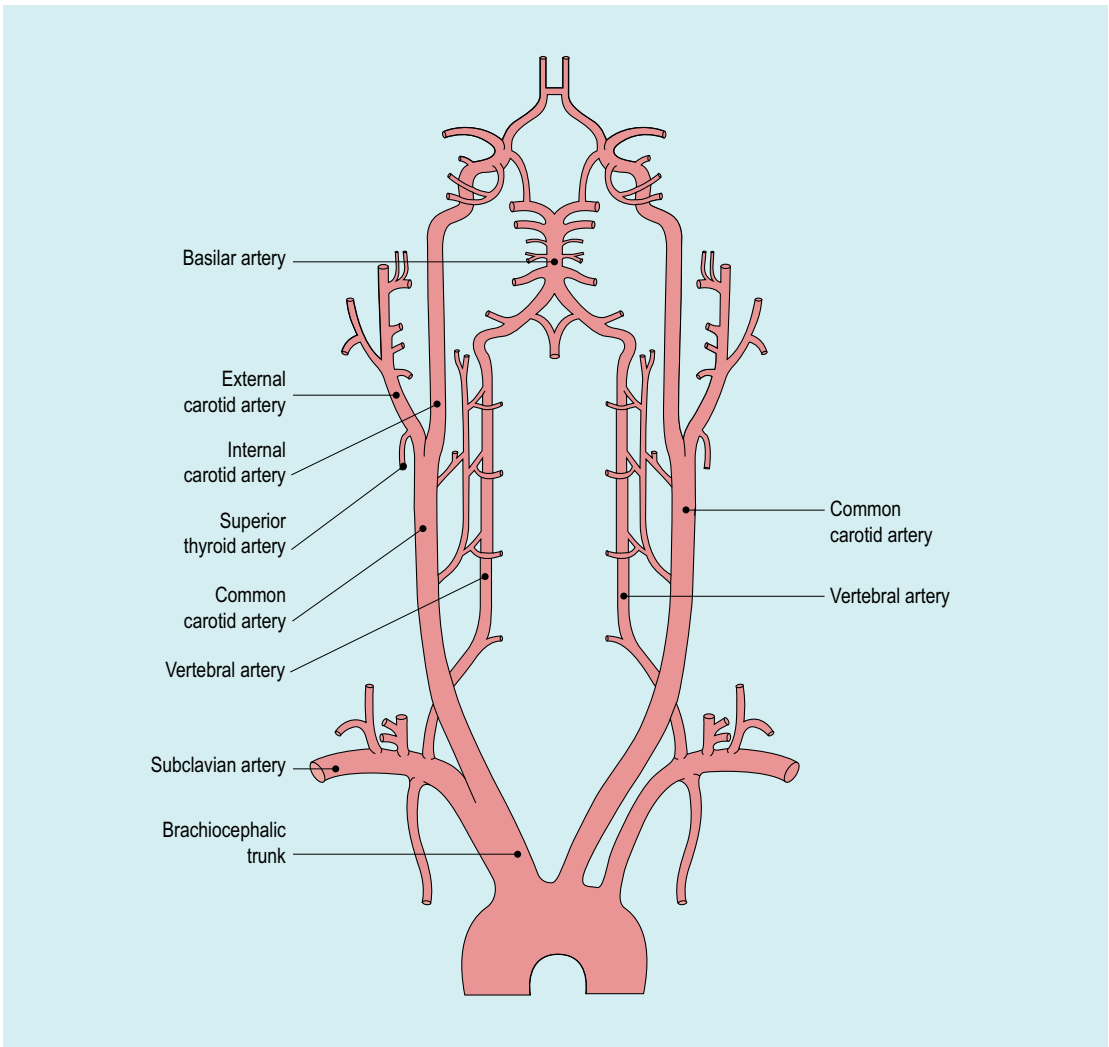


**Fig. 3.2** Carotid and vertebral arteries.

border of the laryngeal cartilage but it may vary considerably. The two branches of the common carotid artery are the internal carotid artery and the external carotid artery. It is essential that they are identified positively, otherwise there is the possibility that disease in one vessel will be mistakenly attributed to the other, which may lead to further inappropriate investigations. The external carotid artery is usually the easier of the two branches at the bifurcation to recognise positively and the criteria to look for are listed in Table 3.4.

The external carotid artery has branches just above the bifurcation (Fig. 3.3); the superior thyroid, ascending pharyngeal and lingual arteries may all arise from the external carotid artery below, or around, the level of the angle of the mandible.

The external carotid artery is nearly always the more anterior of the two branches. In one study it lay anteromedial to the internal carotid artery in 48.5% of bifurcations studied, anterior in 34.5% and anterolateral in 13%; other positions accounted for only 4% of vessels.[13]

The external carotid artery supplies the relatively high-resistance vascular bed of the facial muscles, pharynx, tongue and scalp. Therefore the external carotid artery has relatively less diastolic flow, which makes it appear more pulsatile on colour Doppler and to have a characteristic waveform on spectral Doppler with relatively low diastolic flow (Fig. 3.4a). In addition the dichrotic notch of the pulse wave is usually more prominent in the external carotid artery spectrum than in the internal carotid artery spectrum.

The superficial temporal artery is one of the terminal branches of the external carotid artery, and if this is tapped by a finger as it passes over the zygoma it will produce rapid, clear fluctua-

**Table 3.4** Identification of the external and internal carotid arteries

| |
|---|
| **The external carotid artery** |
| Branches present |
| Anterior position |
| Waveform characteristics: |
| High resistance pattern with relatively little diastolic flow |
| Appears more pulsatile on colour Doppler |
| Dichrotic notch is more prominent |
| Positive 'temporal tap' |
| **The internal carotid artery** |
| The other branch of the bifurcation |
| Bulb at origin |
| Posterior position and course angled posteriorly |
| Less pulsatile waveform on colour Doppler with relatively high diastolic flow |

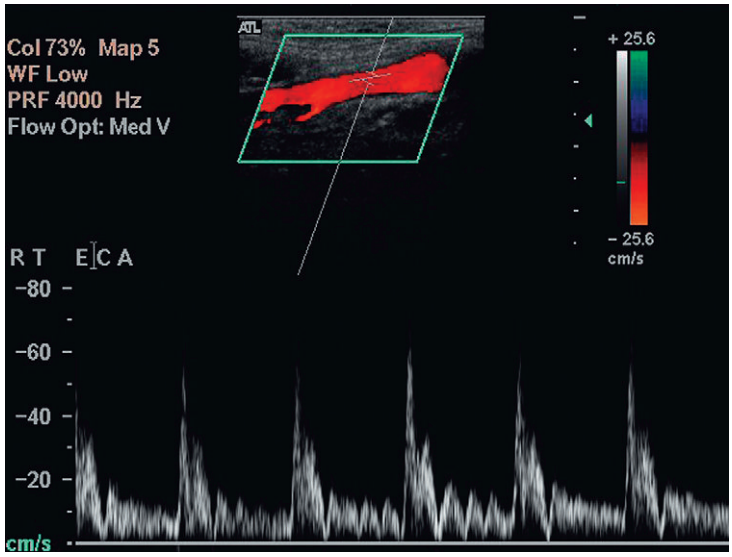


**Fig. 3.3** The external carotid artery showing a branch arising just above the bifurcation and fluctuations induced in the spectrum by tapping the superficial temporal artery at the level of the zygoma.

tions in the waveform in the external carotid artery, whereas there is generally little or no effect in the ipsilateral common carotid artery or internal carotid artery[14] (Fig. 3.4a).

Once the external carotid artery has been identified positively then it can be assumed that the other large vessel arising from the carotid bifurcation is the internal carotid artery. This vessel is nearly always the more posterior of the two branches and tends to run deeply and more posteriorly. It does not have visible branches at this level but the bulge of the carotid bulb is usually apparent in subjects without severe disease. Colour Doppler will show the normal area of reversed flow in the carotid bulb, sometimes referred to as the boundary layer separation zone. The spectrum from the internal carotid artery is less pulsatile and more sustained than that of the external carotid artery, with relatively high diastolic flow (Fig. 3.4b).

Diseased vessels may be more difficult to distinguish as plaques can obscure visual details;

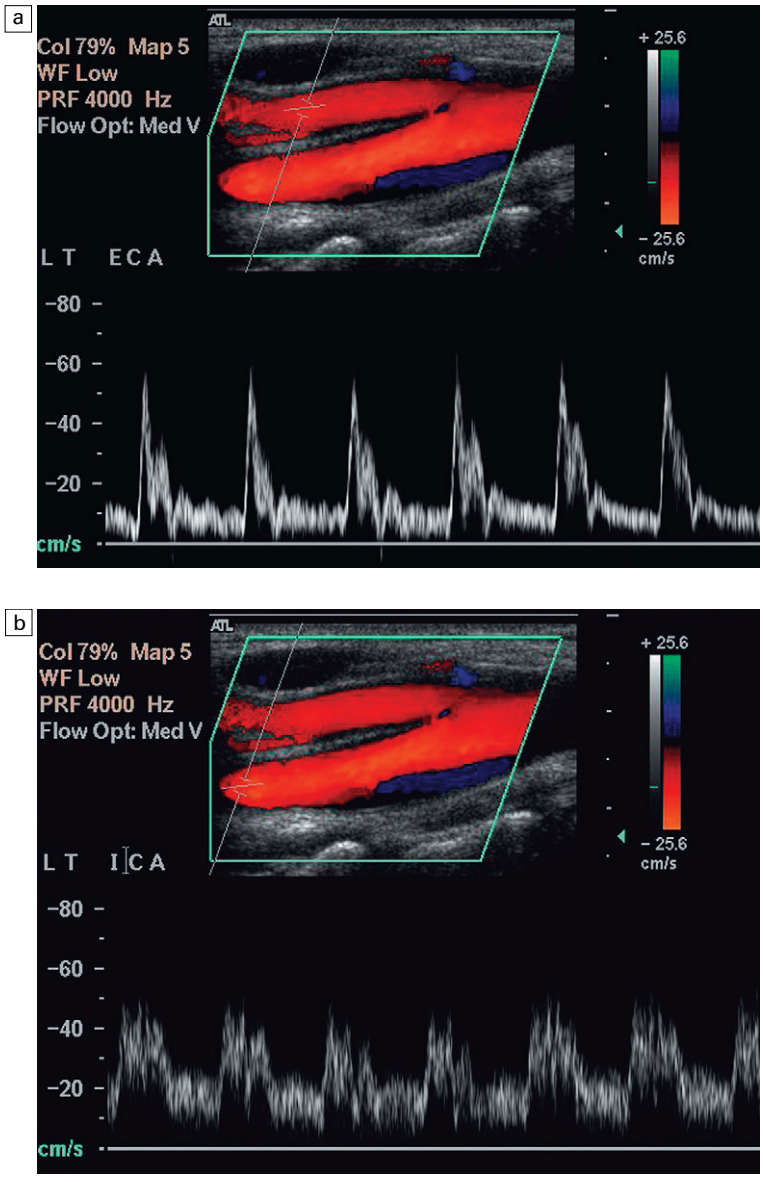


**Fig. 3.4** (a) The external carotid artery and the characteristic spectrum seen in normal vessels. There is relatively low diastolic flow and a prominent dichrotic notch compared with the spectrum from the internal carotid artery. (b) The internal carotid artery and its characteristic spectrum with more flow throughout diastole. The normal area of reversed flow in the carotid bulb is clearly visible.

local and remote disease can lead to alterations in the normal patterns of flow, so that distinction on the basis of the appearance of the waveform may be impossible. In addition some high bifurcations may be very difficult to see well enough to allow reliable assessment; in this situation scanning transversely with colour Doppler switched on may allow localisation of the internal and

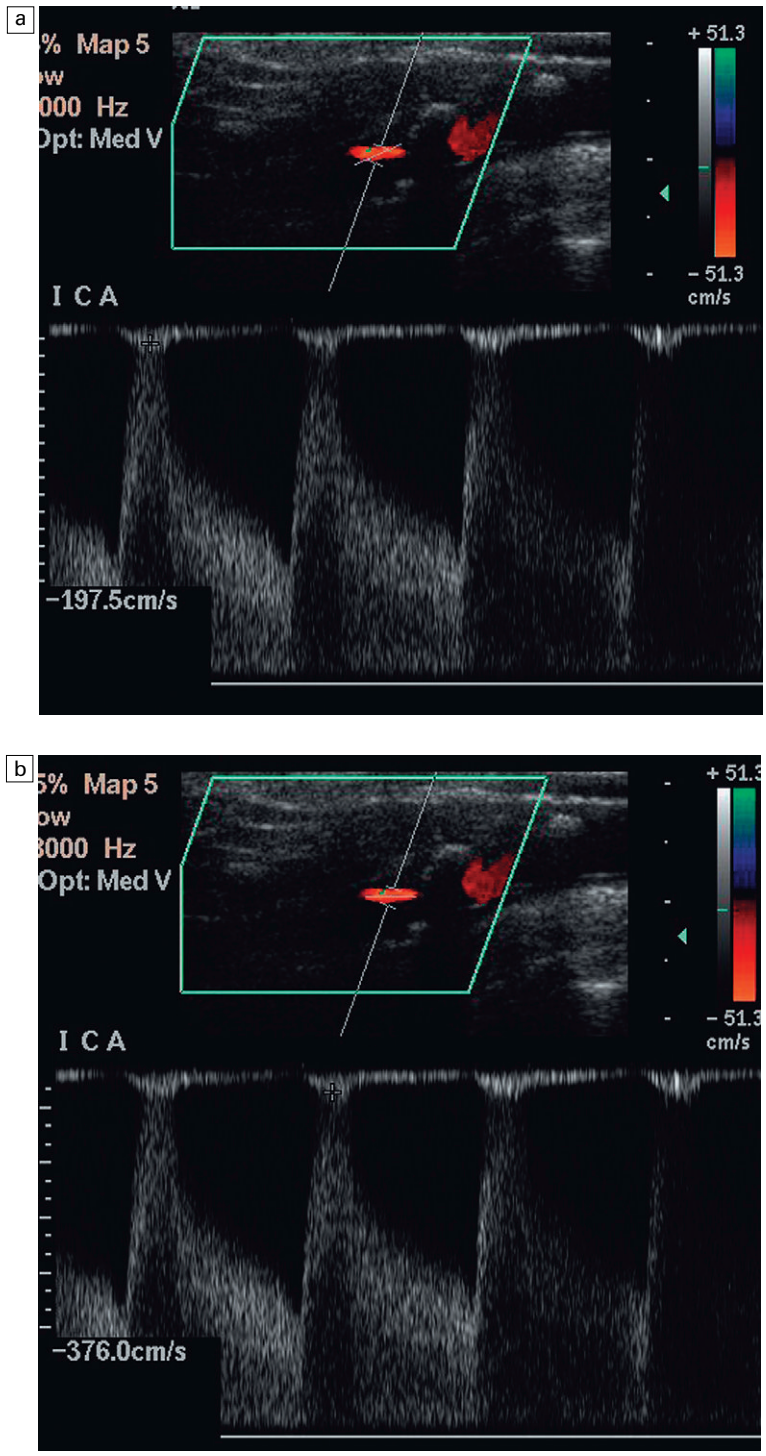


**Fig. 3.5** (a) The angle correction has been made aligning the cursor to the vessel wall resulting in a velocity estimate of approximately 2 m $s^{-1}$. (b) Using colour Doppler, the cursor is positioned along the line of the flow and results in a velocity of approximately 3.5 m $s^{-1}$.

external carotid arteries, so that some spectral information can be acquired.

### Standard velocity measurements

Once the bifurcation and its branches have been identified and assuming that no areas of significant disease are present, it is good practice to take peak systolic velocity measurements from the common carotid artery, the internal carotid artery and the external carotid artery in order to have a record of the examination. These are obtained using spectral Doppler from the upper common carotid artery 2–3 cm below the bifurcation; the internal carotid artery from 1 to 2 cm above the bulb, or as high as possible, in order to allow the normal bulbar turbulence to settle; and from the lower external carotid artery. For routine measurements the sample volume is set at about one-third of the total diameter and placed in the centre of the vessel in order to avoid the natural turbulence at the edge of the lumen and 'wall thump' from inclusion of the vessel wall in the sample volume. The Doppler angle is kept as low as possible, ideally less than 60°; it is good practice to try and keep to a specific angle, such as 55° or 60°, in order to improve the reproducibility of results between examinations. For tight stenoses it is better to reduce the size of the sample volume, as this allows the area of the peak systolic flow signal to be better defined. Colour Doppler allows more accurate assessment of the direction of flow in a stenosis as this may not always be parallel to the walls of the vessel (Fig. 3.5). The precise final location of the sample volume is chosen using a combination of the audible Doppler signal and the spectrum so that the clearest, highest-frequency audible signal and the best spectral trace are obtained; in stenoses, the sample volume should be moved through the length of the stenotic segment in order to locate the peak signal.

### Measuring the intima-medial thickness

This is not always required but should it need to be measured, for instance as part of a population survey, then it can be measured on an image of the distal common carotid wall where the echoes from the intima-media complex are most easily distinguished. The machine settings should be set to give a clear, uncluttered image of the vessel wall and the position of the transducer adjusted to show the characteristic double-line appearance of the vessel wall (Fig. 3.6). The image should be magnified as much as possible to make the measurement easier to perform. The intima-medial thickness (IMT) is best demonstrated in the upper common carotid artery on the posterior wall where the vessel is usually at right angles to the ultrasound beam. The internal carotid artery is more difficult to assess as the vessel slopes obliquely away from the transducer face in many cases. With careful attention to detail it is possible to measure the IMT with satisfactory, reproducible accuracy. The precise upper limit of the normal range is a matter of some discussion. It does increase with age but values of less than 0.8 mm correlate well with lack of coronary artery disease, whereas an increasing thickness above this level (Fig. 3.6) is associated with increasingly severe coronary artery disease,[15, 16] an increased risk of myocardial infarction[17] and also stroke.[18]

### The vertebral arteries

Once both carotids have been examined the vertebral arteries are assessed. The vertebral artery on each side is the first branch of the subclavian artery (Fig. 3.2). It passes posteriorly and upwards to the vertebral foramen in the transverse process of the sixth cervical vertebra (V1 segment), and from there it passes upwards in the vertebral canal to the level of the axis (C2) (V2 segment). It emerges from the vertebral canal at C2, passing behind the lateral mass of the atlas (C1) to enter the skull through the foramen magnum (V3 segment) and runs anterior to the brain stem (V4 segment) to join with the vessel from the other side in front of the brain stem to form the basilar artery.[19]

The vertebral arteries are most easily located by placing the transducer longitudinally over the common carotid artery and angling it medially so that the vertebral bodies are identified; the transducer is then rotated laterally so that the transverse processes of the vertebrae and the

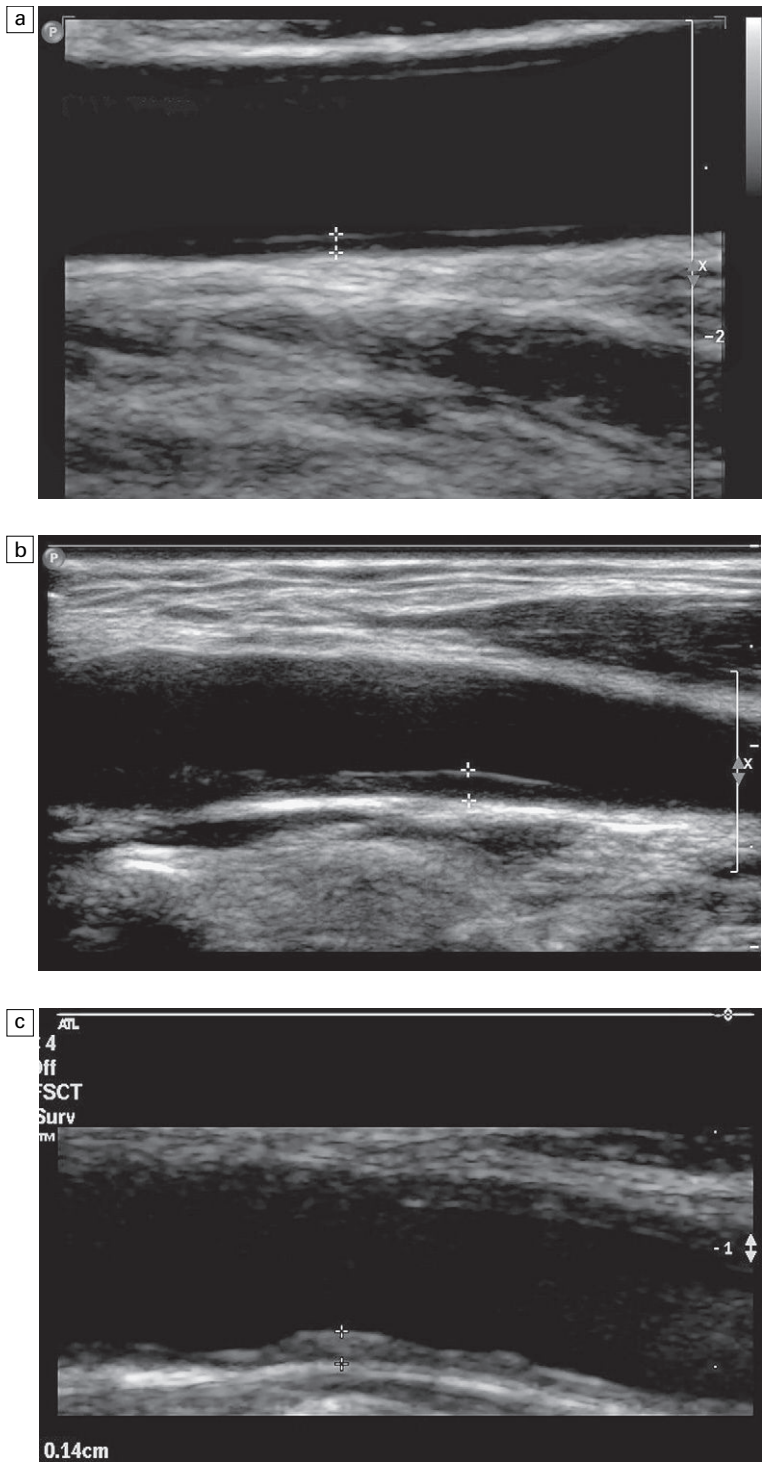


**Fig. 3.6** (a) A normal intima-medial thickness (IMT) of 0.7 mm measured in the upper common carotid artery. (b) Moderate thickening of the IMT at 1.2 mm (c) More marked intimal thickening of 1.4 mm.

spaces between them are visualised, the vertebral artery and vein may then be seen in these gaps (Fig. 3.7). If the vertebral artery cannot be identified in the vertebral canal, it may be looked for in the lower neck as it passes backwards from the subclavian artery towards C6; or in the upper neck behind the mastoid process as it passes around the atlas (C1) and into the foramen magnum.

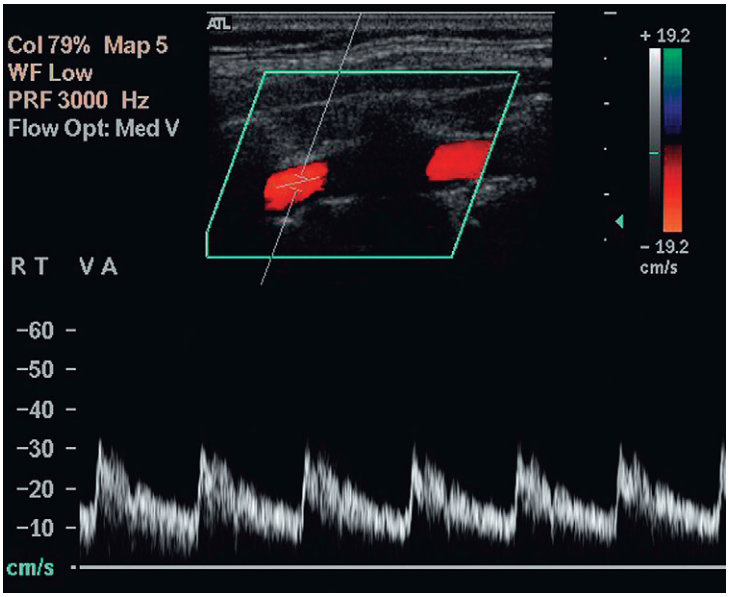


**Fig. 3.7** The vertebral artery seen between the transverse processes of the cervical vertebrae.

There may be marked variation in the size of the vertebral arteries and their relative contribution to basilar artery flow; when there is disparity of size, the left artery is usually the larger of the two and in 7–10% of individuals there are significant segments of hypoplasia, which result in the artery not being visible.[20] Clear visualisation of the vein but not the artery suggests that the artery may be either thrombosed or congenitally absent.

Colour Doppler makes assessment of flow direction in the vertebral arteries straightforward (Fig. 3.8). They should have the same colour as the common carotid artery in front of them. Care needs to be taken in the diagnosis of reversed flow, particularly if the spectral Doppler trace has been inverted during the examination: if subclavian steal is suspected it is worth confirming that the machine is set up appropriately in order to avoid making an error.

## Assessment of disease

### *Measurement of the degree of stenosis*

Two types of information can be used to assess the degree of stenosis: direct measurement using the calipers on the machine; and velocity criteria derived from spectral Doppler.

#### Direct visualisation and measurement

If the stenosis and plaque can be seen clearly then it is possible to measure the calibre of the residual lumen and the original calibre of the vessel. Diameter reduction ratios, or area reduction ratios, are the usual methods for describing the reduction in vessel calibre; percentage residual lumen can also be used. Diameter measurements are generally a little quicker to perform but are slightly less representative of the stenosis, as they do not take account of variations in plaque thickness around the circumference of the vessel and there is the potential to underestimate, or overestimate, the degree of stenosis (Fig. 3.9). Care must be taken to examine a diseased segment of vessel in both transverse and longitudinal views so that the distribution of plaque can be clearly assessed and the most appropriate diameter measurement can be made; this is usually the shortest diameter. Measuring stenoses by area reduction, although more time consuming, overcomes this problem with the eccentricity of the plaque being taken into account as the luminal and vessel areas are measured.

It is important that the type of measurement used is clearly defined as either a diameter reduction or an area reduction, because signifi-

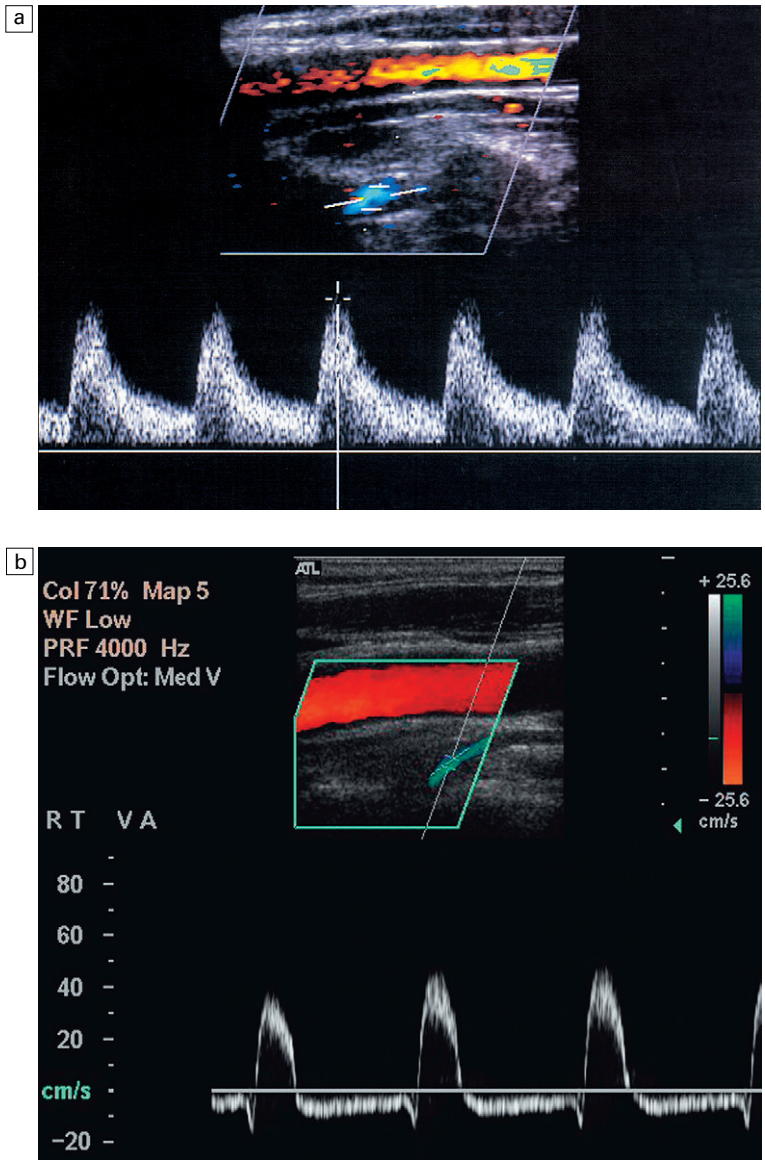


**Fig. 3.8** (a) Reversed flow in the vertebral artery in a patient with a proximal left subclavian artery stenosis. The vertebral artery is the opposite colour (blue) from the common carotid artery. (b) Biphasic flow in the vertebral artery of a patient with a developing subclavian steal syndrome.

cant misunderstandings may occur in the interpretation of the results. For a given stenosis, a 50% diameter reduction corresponds to a 70% area reduction, so that misinterpretation of a 70% area stenosis as a diameter reduction will result in a significant overestimation in the assessment of calibre reduction, possibly leading to unwarranted surgery (Fig. 3.10). It is good practice always to define the value of a stenosis as either an area or a diameter reduction and this is essential if the measurement is in a different form from that normally used.

Most stenoses are relatively short in longitudinal extent, usually no more than a centimetre for the maximum degree of narrowing. Some patients, however, have longer segments of varying calibre reduction and it is important to remember that, although the degree of pressure drop across a stenosis is related primarily to the reduction in radius, it is also related to the

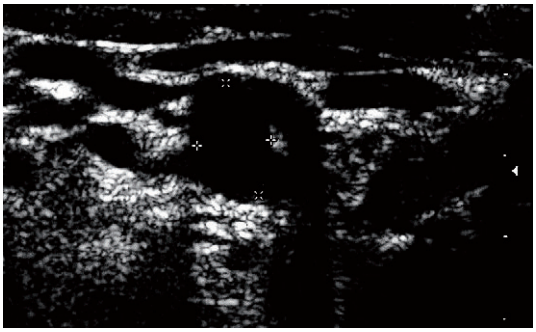

**Fig. 3.9** Transverse view of a plaque in the common carotid artery with the diameter reduction calculated from the diameter measurements. Note that an inappropriate longitudinal scan plane (x–x) could result in a significant underestimation of the degree of stenosis.

length of the stenosis. However, length has a much smaller effect, as the resistance is related to the first power of the length, rather than the fourth power of the radius (Poiseuille's Law):

$$R = \frac{8l\eta}{\pi r^4}$$

If the patient is being considered for endarterectomy, in addition to measuring the degree of stenosis, it is important to assess the level of the bifurcation, the length of the stenosed segment and the diameter of the internal carotid artery above the stenosis. The reason for this is that high bifurcations (<1.5 cm from the angle of the mandible), high distal extent of the stenotic segment (>2 cm above the bifurcation) and a small internal carotid artery (<0.5 cm), or a kinked internal carotid artery, can complicate surgery and prior warning will allow the appropriate surgical technique to be used. Ultrasound can predict these features satisfactorily and supplemental arteriography is not usually necessary.[21]

## Doppler criteria

In many cases the region of the stenosis is not seen clearly due to complex plaque structure and calcification. In these cases direct measurement cannot be used to quantify the degree of stenosis and Doppler criteria must be used. Over the years, much work has been done correlating Doppler findings with degrees of stenosis found on arteriography, or at surgery. It has been shown that carefully obtained Doppler criteria correspond well with the degree of stenosis, and values which allow the severity of internal carotid artery stenoses to be predicted have been developed. However, the literature can be confusing, with apparently widely varying velocities being quoted for specific levels of stenosis. One of the first studies suggested that a peak systolic velocity of >1.3 m $s^{-1}$ was appropriate for diagnosis of a diameter stenosis of 60% or greater.[22] However, other workers have reported velocities of 1.7 m $s^{-1}$ for a 60% stenosis,[23] 2.25 m $s^{-1}$ for a 70% stenosis[24] and 1.3 m $s^{-1}$ for 70% diameter stenosis.[25] This

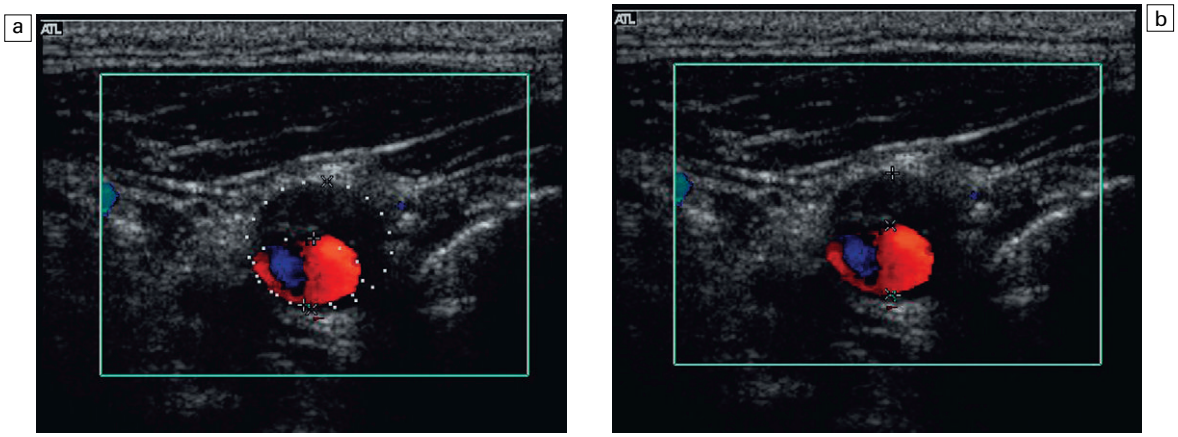


**Fig. 3.10** A stenosis measured with (a) an area-reduction calculation (measured as 62%) and (b) a diameter-reduction calculation (measured as 40%).

apparent lack of consensus emphasises the fact that there is some variation from one department to another depending on the equipment and technique used. Each department must therefore develop and audit criteria which they find work in their environment and complement the clinical criteria and practices used in their institution.

The peak systolic velocity, end-diastolic velocity and the ratio of peak systolic velocities in the internal and common carotid arteries (IC/CC systolic ratio) are the most useful measurements in general practice[24,26] (Fig. 3.11). Spectral broadening and filling in of the window under the spectrum are subjective, difficult to quantify and can be affected significantly by gain control settings; however, they do indicate abnormal flow if they are present. The IC/CC diastolic ratio can also be measured but this does not usually add to the information obtained from the three main criteria. The main levels which need to be distinguished are 50% diameter reduction, where blood flow starts to decline, and 70% diameter reduction, which is the level strongly associated with clinical symptoms and for which surgery will be considered. The values for the criteria which the authors have found to be useful in their practice to predict these levels of stenosis in the internal carotid artery are shown in Table 3.5 and are based on those reported by Robinson et al[24] and Grant et al.[26] It is important to remember that the peak systolic and diastolic values refer only to the internal

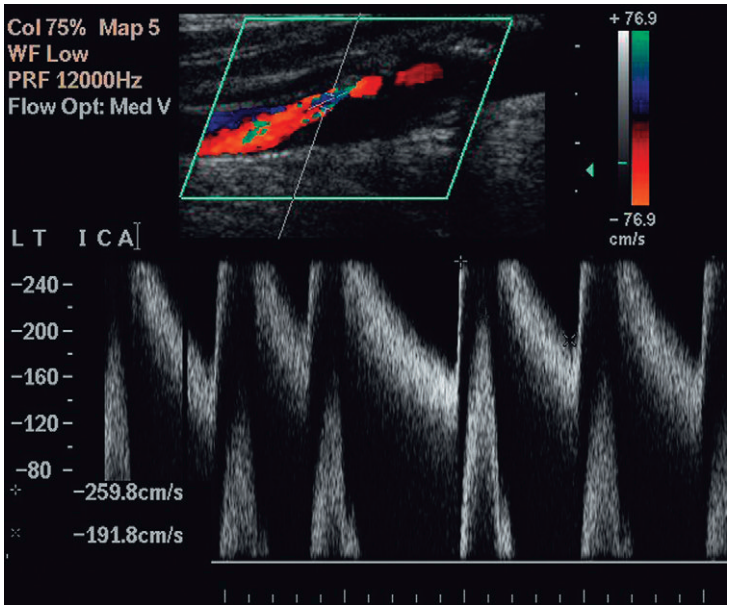


**Fig. 3.11** A stenosis of the internal carotid artery showing a peak systolic velocity in excess of 2.6 m $s^{-1}$ and an end-diastolic velocity of 1.9 m $s^{-1}$. There is aliasing of both the colour and spectral Doppler displays.

**Table 3.5** Diagnostic criteria for Doppler diagnosis of stenoses of 50% and 70%

| Diameter stenosis (%) | Peak systolic velocity ICA[a] (m $s^{-1}$) | End-diastolic velocity ICA (m $s^{-1}$) | IC/CC systolic ratio |
|---|---|---|---|
| 50 | >1.25 | >0.4 | >2 |
| 70 | >2.3 | >1.0 | >4 |

ICA, internal carotid artery; IC/CC, internal carotid/common carotid. From Robinson et al[24] and Grant et al.[25]

carotid artery, not to the common carotid artery or external carotid artery. Furthermore, it should be borne in mind that physiological variations due to heart rate, cardiac output and contralateral occlusion may affect the velocities in a vessel, potentially leading to a false diagnosis of a pathologically high velocity, although these cases should be clarified by the use of the velocity ratios. It should also be remembered that peak velocities decline with very high degrees of stenosis (>90% diameter stenosis)[27] as discussed in Chapter 2.

Attempts have been made to use colour or power Doppler criteria to assess the severity of stenoses.[28, 29] Direct measurement of the residual lumen based on power or colour Doppler can be made but it is essential that care is taken with the gain settings to ensure that there is not any over- or underestimation of the residual lumen; this type of direct measurement will always be less accurate than measurements made on a good B-mode image but, for more severe degrees of stenosis (>50% diameter reduction), they can provide additional confirmatory information. For cases where a diagnosis must be made between 'subtotal', or 'near' occlusion and complete occlusion, then careful setting up of the colour and power Doppler modes is essential for reliable distinction (see below).

In addition to the direct measurement of the residual lumen demonstrated by the colour map, a cursor with angle correction can be placed over the colour map and used to provide an estimate of the mean velocity in the underlying pixel. This allows the mean velocities in a stenotic segment to be estimated. However, these correlate less well with the degree of stenosis than peak systolic or diastolic velocities. Although experienced operators can often get a good idea of the severity of a stenosis from the overall appearances and the colour map changes, it is always better to use the colour map to identify areas of abnormal flow and use this to position the sample volume for spectral Doppler analysis.

### *Effects of disease elsewhere*

The velocities and flow characteristics seen in any given section of a vessel depend not only on local conditions but also on conditions elsewhere along the vessel, in other vessels connected to that vascular territory (Fig. 3.12) and to other factors, such as heart rate, cardiac output and blood pressure (Table 3.6). The best example of this is vertebral or subclavian steal, where a proximal occlusion of the subclavian artery results in reversed flow in the ipsilateral vertebral artery.

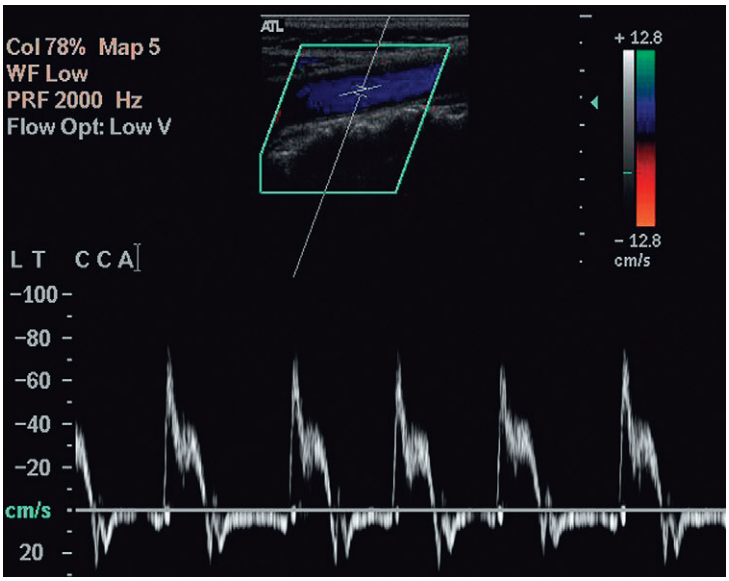


**Fig. 3.12** Common carotid waveform in a patient with aortic valve incompetence showing reversed diastolic flow.

**Table 3.6** Factors affecting the waveform

| | |
|---|---|
| Local | Atheroma and plaques<br>Tortuosity |
| Proximal | Common carotid artery origin disease<br>Aortic valve disease |
| Distal | Carotid siphon disease<br>Intracranial vessel disease |
| Remote | Contralateral carotid occlusion |
| Physiological | High cardiac output states |

Carotid occlusion can lead to an increase in the volume of blood flowing in the contralateral carotid artery. This is achieved primarily by the blood flowing more quickly, therefore there is the potential to mistakenly suggest that an increased velocity measurement is compatible with a degree of stenosis but review of the colour Doppler image should refute this impression in a non-diseased carotid. The use of ratios, mainly the IC/CC peak systolic ratio, helps identify the nature of increased velocities in both normal vessels and those with minor atheroma, as in these circumstances the velocity in both the common carotid artery and the internal carotid artery is increased and the ratio does not alter; whereas if there is significant local disease affecting the internal carotid artery, the velocity in this vessel is increased but the common carotid artery velocity is unchanged, so that the ratio is also increased.

In patients with bilateral severe carotid stenoses, when one side is stented or operated upon, the improvement in flow up the operated vessel will reduce flow up the contralateral carotid and this may result in a decrease in peak velocities on the untreated side that might lead to this stenosis being down-graded in severity. In one series of patients with bilateral significant stenoses on duplex scanning,[30] the stenosis on the non-operated side was reclassified as non-haemodynamically significant in 20% of cases. It is therefore necessary for these patients to be reassessed prior to any management decisions relating to the untreated artery.

### *Carotid occlusion*

Occlusion can affect the internal carotid artery (Fig. 3.13) or common carotid artery separately, or together. Occlusion of the common carotid artery does not always result in occlusion of the internal carotid artery, as sufficient blood flow may be provided by retrograde flow down the ipsilateral external carotid artery to maintain patency of the internal carotid artery. This pattern of abnormal flow may be quite confusing if it is not recognised but it is of clinical importance, as these patients can still suffer ischaemic events in the relevant internal carotid artery territory.[31] The opposite pattern of flow may be seen in a small number of patients with common carotid artery occlusion with reverse flow in the internal carotid artery on the side of the common carotid artery occlusion (a carotid steal phenomenon) and antegrade flow in the ipsilateral external carotid artery. If the lower margin of the occluded segment is above the level of the bifurcation then a characteristic pattern of forward and reverse flow ('stump thump') is seen in the patent residual lumen of the internal carotid artery.

If an occlusion of the internal carotid artery is suspected it is essential that care is taken to ensure that the Doppler settings on the machine are appropriate for locating any low-velocity, small-volume flow that may be present in a

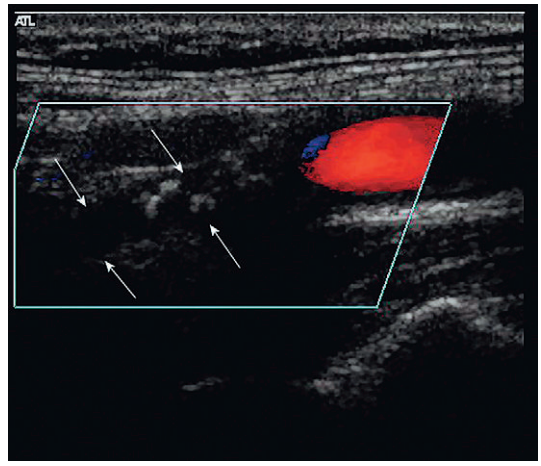


**Fig. 3.13** An occluded internal carotid artery. The occluded lumen is indicated by the arrows.

narrow residual lumen in the segment under investigation. Colour and power Doppler assessments of the vessel should be carried out with the system set for maximum sensitivity in order to identify any small residual lumen ('string sign' or pseudo-occlusion) (Fig. 3.14) or adjacent vessels that might confuse the situation.[32] Spectral Doppler should also be performed carefully at maximum sensitivity, although care must be taken to identify and exclude any waveforms arising from adjacent vessels.[33] Conversely, colour Doppler or power Doppler may show the location of a residual channel in a vessel that was otherwise thought to be occluded; echo-enhancing agents are of value if there is any persisting uncertainty.

Occlusion of the internal carotid artery results in the reduction of diastolic flow in the ipsilateral common carotid artery, so that the common carotid artery waveform becomes more like that seen in the external carotid artery. Reduction of common carotid artery end-diastolic flow may therefore be an initial clue to the presence of an internal carotid artery occlusion, or a very severe stenosis.[34] Care should be taken, however, as the development of collateral channels between the external carotid artery and internal carotid artery circulations in the orbit and meninges can result in 'internalisation' of the external carotid artery flow with relatively high diastolic flow in the external carotid artery; this results in a mistaken impression of a patent internal carotid artery, if it is not recognised. The 'temporal tap' manoeuvre can usually clarify the situation. Occlusion of the carotid on one side may result in increased flow through the contralateral carotid vessels, as discussed earlier.

Recanalisation of an occluded carotid artery is not as rare as might be imagined.[35] One series followed eight patients with internal carotid artery occlusion with serial 6-monthly ultrasounds for a period of up to 8 years, all of the eight patients showed evidence of spontaneous recanalisation occurring between 6 and 96 months.[36]

If there is occlusion of both the internal carotid artery and external carotid artery then the ipsilateral common carotid artery also usually occludes. Before thrombosis occurs, however, a to-and-fro pattern of flow may be seen in the common carotid artery, which signifies that there is no net forward flow of blood up the vessel.

### *Plaque characterisation*

Much effort has been expended in attempting to classify atheroma and plaques on ultrasound, particularly in the carotids, where high-resolution ultrasound gives good images of many plaques. Steffen et al[37] proposed a classification of plaque which takes account of the different types of plaque and its components (Fig. 3.15). Types 1

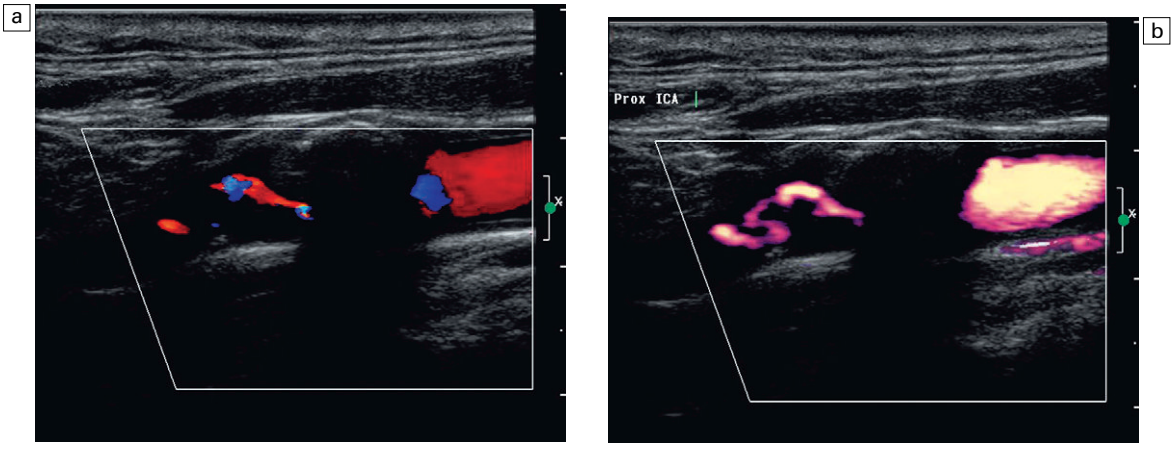


**Fig. 3.14** A thin residual channel on colour Doppler (a) and on power Doppler (b) which is more sensitive for weaker, slower signals and shows the tortuous residual lumen more clearly.

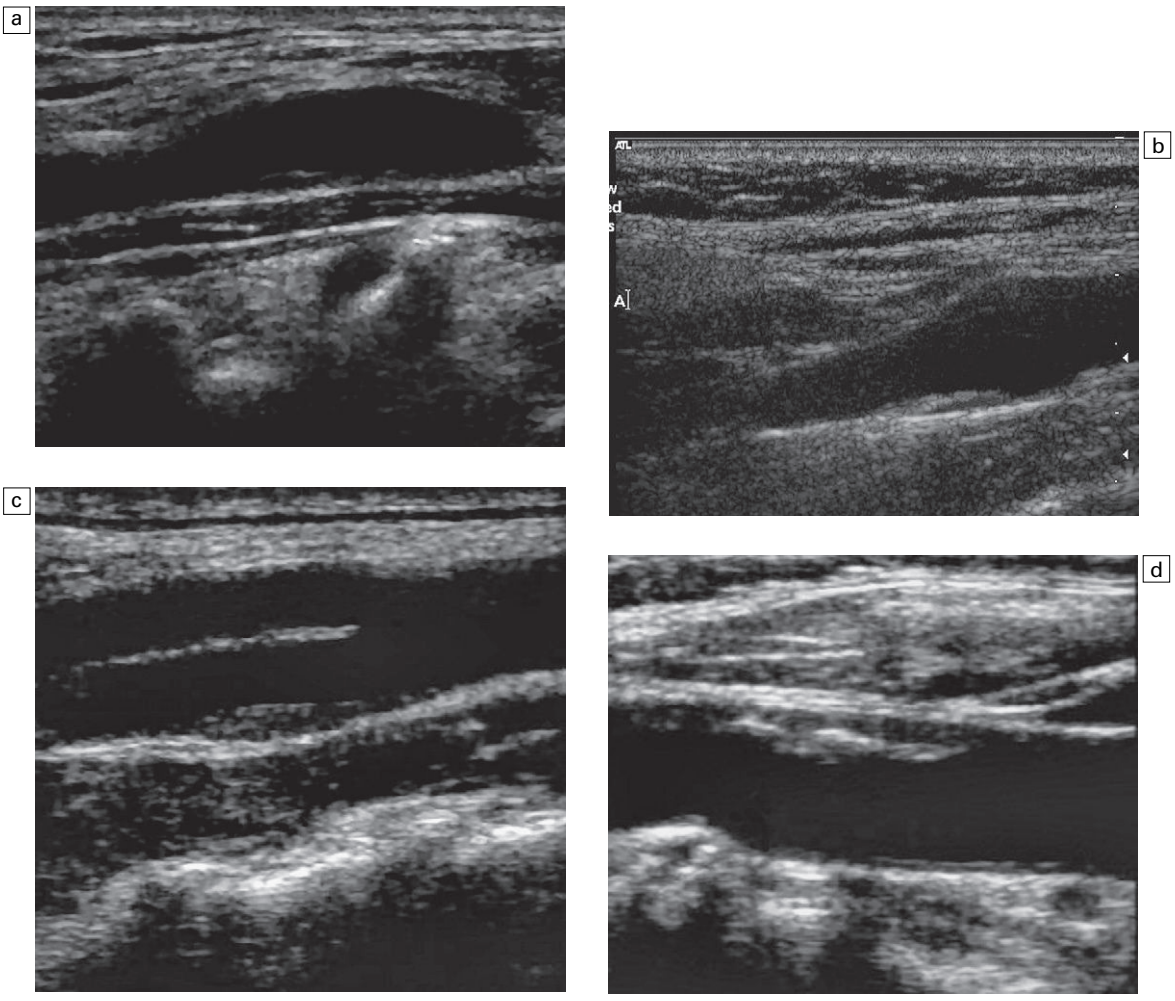


**Fig. 3.15** Different types of plaque seen on ultrasound. (a) Type 1, dominantly echolucent with a thin echogenic cap. (b) Type 2, substantially echolucent lesions with small areas of echogenicity. (c) Type 3, dominantly echogenic lesions with small areas of echolucency of <25%. (d) Type 4, uniformly echogenic lesions.

and 2 were predominant in symptomatic arteries, whereas types 3 and 4 were more common in asymptomatic patients; these findings have been supported by other groups.[38,39] This supports the suggestion that the more friable, lipid-containing, soft plaques are more likely to result in plaque disruption and produce symptoms than firmer, more fibrous and coherent plaques.

The value of ultrasound in predicting the complications associated with plaques is more difficult to define. These complications include intraplaque haemorrhage, surface ulceration and adherent thrombus. The presence of intraplaque haemorrhage has been inferred from the presence of hypoechoic areas within the plaque. However, it is also possible that many of these areas are aggregates of lipid or necrosis, rather than areas of haemorrhage. Sometimes an ulcer in the plaque can be clearly seen, but many plaques are irregular without being ulcerated and, conversely, an ulcerated plaque may not be identified on ultrasound. Thrombus adherent to the surface is suggested by an anechoic or hypoechoic area adjacent to the plaque surface on colour or power Doppler. It is important that the system is set up appropriately, otherwise the lack of colour on the image may be due to technical factors, rather than the presence of thrombus.

Some studies have shown a good correlation between the ultrasound appearances and those found at operation,[40,41] but the results from others have been less satisfactory, with poor prediction of ulceration or haemorrhage.[42,43] Another study from the Seattle group showed that there was no significant difference in plaque constituents between the endarterectomy specimens removed from symptomatic and asymptomatic patients with high grade stenoses.[44] Visualisation of plaque type in high grade (>60% diameter reduction) stenoses is usually inadequate to identify reliably plaque characteristics and the Seattle study would suggest that the degree of stenosis is the more important factor in this group of patients. However, if there is a good view of the diseased segment, the plaque can be described in terms of its type (1–4), extent (focal, diffuse, circumferential) and any obvious associated complications (ulceration, thrombus, haemorrhage) (Fig. 3.16). If visualisation is moderate or poor then discretion is necessary and only those features which are clearly seen should be noted. For example, it may be difficult to distinguish between a plaque ulcer and a gap between two adjacent plaques, or to decide if a colour void associated with the plaque surface is really due to adherent thrombus or to technical factors. Ulceration should only be diagnosed if the plaque and the ulcer are clearly seen, otherwise plaques should be described as smooth or irregular. It should be remembered that many diseased segments are not clearly seen due to the presence of calcification, which makes any attempt at plaque characterisation very difficult, or impossible.

In practical terms, a smooth, homogeneous, predominantly echogenic plaque is less likely to be associated with symptoms, whereas an irregular, heterogeneous or hypoechoic lesion is of greater concern. A stenosis of only 50% (diameter reduction) but with an unstable plaque type in a symp-

**Table 3.7** Classification of carotid plaques

| | | |
|---|---|---|
| **Haemodynamic classification** | | |
| H1 | 0–20% Diameter reduction | Normal to mild |
| H2 | 20–60% Diameter reduction | Moderate |
| H3 | 60–80% Diameter reduction | Severe |
| H4 | 80–99% Diameter reduction | Critical |
| H5 | Occluded | |
| **Morphological components** | | |
| P1 | Homogeneous | |
| P2 | Heterogeneous | |
| **Surface characteristics** | | |
| S1 | Smooth | |
| S2 | Irregular (defect <2 mm) | |
| S3 | Ulcerated (defect >2 mm) | |

From Thiele et al,[45] with permission.

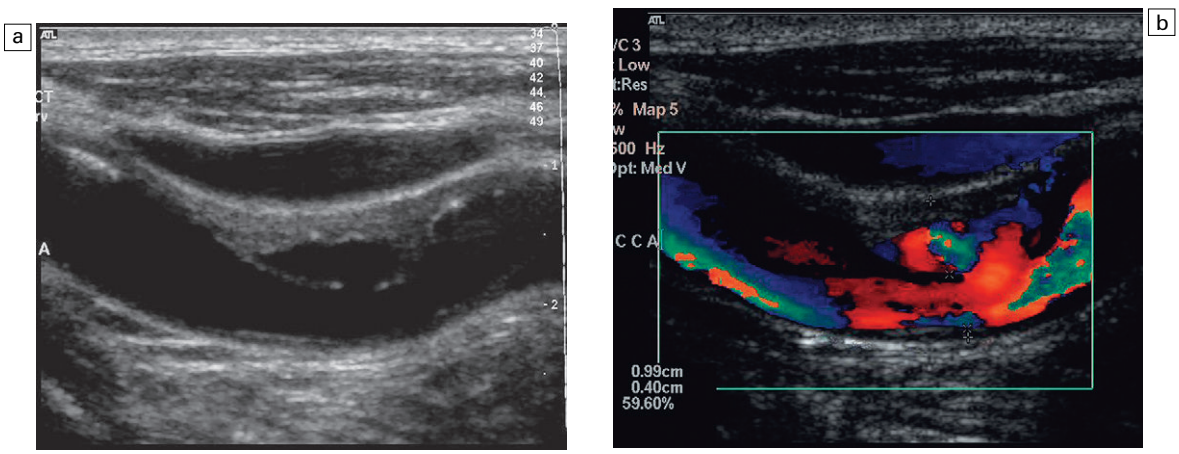


**Fig. 3.16** An ulcerated plaque. A thin rim is seen on the B-scan image (a) but colour Doppler (b) shows flow within the plaque.

tomatic patient might well be a matter of clinical concern and considered for surgery.

An attempt has been made to standardise these descriptions for carotid disease in relation to ultrasound and other non-invasive modalities.[45] This proposes that lesions can be described in terms of the degree of stenosis, the morphological plaque components and the surface characteristics, where these can be clearly visualised. The suggested classification is given in Table 3.7. A lesion listed as H4, S2, P2 therefore represents a lesion which is producing a stenosis of more than 80% diameter reduction (H4), which has an irregular surface (S2) and is heterogeneous (P2). In practice, this type of classification does not add significantly to the information that can be provided by a description of the diseased segment as discussed above. In addition, the original classification for the degree of stenosis does not allow for distinction between <70% and >70% diameter reduction, as H3 covers the range of 60–80%.

### *Pulsatile masses*

The main causes of pulsatile neck masses are given in Table 3.2. Normal but prominent carotids and ectatic carotid or subclavian arteries are easily identified using colour Doppler and do not usually require any further investigation.

Aneurysms of the carotid arteries can also be identified as they are in continuity with the artery. The majority arises following surgery but they may also occur following trauma, including whiplash neck injuries and biopsy of cervical masses. The flow in the aneurysm may be seen with colour Doppler, unless there is thrombosis of the lumen of the dilated segment. In some cases of aneurysm of the common carotid artery, it may be difficult to identify the internal carotid artery above the dilatation and care must be taken to establish whether it is patent or not; flow in the ipsilateral ophthalmic artery is not necessarily evidence of patency, as this may come from collateral filling via the circle of Willis. Aneurysms of the upper internal carotid artery may be difficult to identify with certainty, or the findings may be misinterpreted as a straightforward stenosis or dissection.[46]

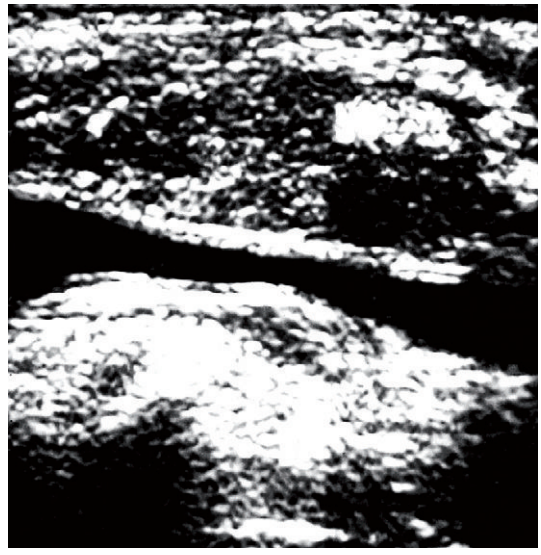

**Fig. 3.17** Tumour recurrence from an oropharyngeal malignancy closely applied to the carotid sheath.

Lymph nodes and other masses adjacent to the carotids will transmit pulsations and require distinction from intrinsic vascular lesions. This is not usually a problem, but occasionally a deposit will surround the carotid artery (Fig. 3.17) and, unless there is a previous history of malignancy, diagnosis can be difficult. Adherence to the carotid sheath can be assessed by gentle palpation and getting the patient to swallow so that relative movement between the mass and the carotid can be assessed.[47] Colour Doppler ultrasound also has an important role in defining the solid nature of a neck lump prior to biopsy and excluding a vascular lesion, such as an aneurysm.

Carotid body tumours are rare but can be diagnosed easily with ultrasound. Characteristically there is a hypoechoic mass between the two branches at the bifurcation, spreading them apart in a 'wine glass' deformity (Fig. 3.18). Colour Doppler shows a highly vascular lesion and the external carotid usually shows a low resistance pattern of flow on spectral Doppler.[48]

### *Dissection of the carotid arteries*

The ultrasound findings in this condition can vary considerably. The vessel may be occluded completely; show a smooth tapering stenosis, with or without a recognisable haematoma/thrombosed

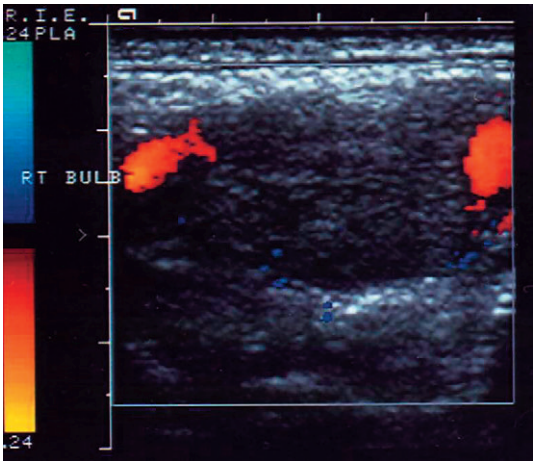


**Fig. 3.18** A carotid body tumour splaying apart the internal carotid artery and external carotid artery. Colour Doppler shows the abnormal tumour circulation.

false lumen being visible (Fig. 3.19); or a membrane with a double lumen may be seen with variable flow patterns in the two channels on either side.[49,50] Recanalisation of the occluded vessel is a recognised occurrence and occurs in up to 60% of cases.[51] Dissection of the vertebral arteries may also occur and is usually manifest as absent flow in the affected artery.[50]

### *Vertebral arteries*

Frequently only cursory attention is paid to the vertebral arteries, unless there are specific signs and symptoms pointing to a posterior fossa problem, when a more detailed examination of the vessels is required.[19] As noted previously, there are several variations of anatomy and size of the vertebral arteries which may affect the ultrasound findings; a further issue to be considered is that disease affecting one artery may be compensated by the other side, or collaterals from the circle of Willis, so that blood flow to the posterior fossa circulation is maintained and local, unilateral vertebral artery disease is of little clinical significance. Nevertheless, some basic patterns of flow can be identified:

1. No flow is detected in the region of the relevant vertebral artery means that the artery is either hypoplastic, absent, or thrombosed. Visualisation of the artery on B-mode without demonstrable flow within it on colour/power and spectral Doppler with the system set to maximum sensitivity suggests that it is thrombosed, or dissected.
2. Demonstration of a focal area of increased velocity at the origin of the vertebral artery (Fig. 3.20), or at some point along its course between the subclavian artery and the foramen magnum, is consistent with a focal stenosis, the significance of which will depend on the clinical situation and the state of the contralateral vertebral artery. Visualisation of the vertebral artery is normally inadequate to make a reliable direct diameter reduction measurement feasible.

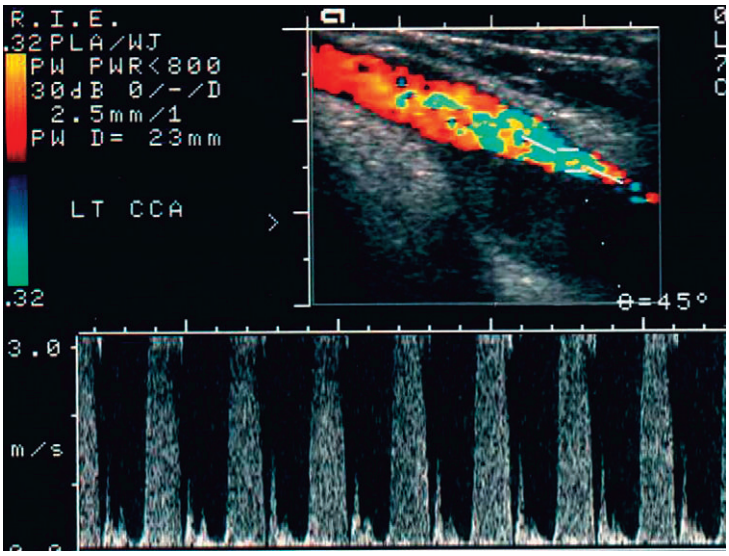


**Fig. 3.19** Dissection of the common carotid artery extending up from a dissection of the aortic arch. One channel has thrombosed, producing a haematoma in the wall of the vessel posteriorly which is narrowing the residual lumen.

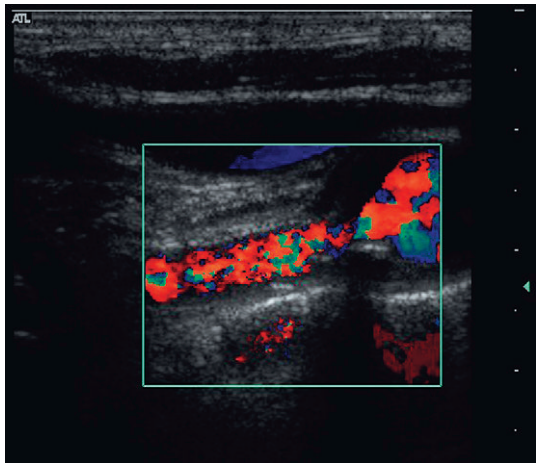

**Fig. 3.20** A stenosis at the origin of the vertebral artery with marked turbulence shown on colour Doppler.

3. A 'tardus parvus' waveform suggests a proximal stenosis; this should be sought by careful examination of the artery from the subclavian artery up to the foramen magnum (Fig. 3.21).
4. The proximal vertebral artery waveform shows reduced or absent diastolic flow, implying a distal stenosis/occlusion (Fig. 3.22).
5. Reversed flow is consistent with subclavian steal syndrome. This occurs when there is an occlusion or tight stenosis of the proximal subclavian artery at its origin and blood supply to the arm is maintained by reversal of blood flow down the ipsilateral vertebral artery.
6. A biphasic vertebral artery waveform may be seen in patients with a developing steal situation from slightly less severe subclavian stenoses and, in some patients, reversed flow may only occur with the arm in certain positions, or after a period of exercise; therefore scanning after a period of arm exercise, such as elbow flexions holding a book, or some other relatively heavy object, should be considered if a steal syndrome is suspected. Alternatively a pressure cuff can be inflated to occlude blood flow to the arm and then released after 2–3 min. The resulting reactive hyperaemia in the arm produces an increased demand for blood and reversal of flow in the relevant vertebral artery.

### *Reporting carotid ultrasound examinations*

Unlike an arteriogram, or magnetic resonance angiography (MRA) examination, there are no easily interpretable images from a Doppler

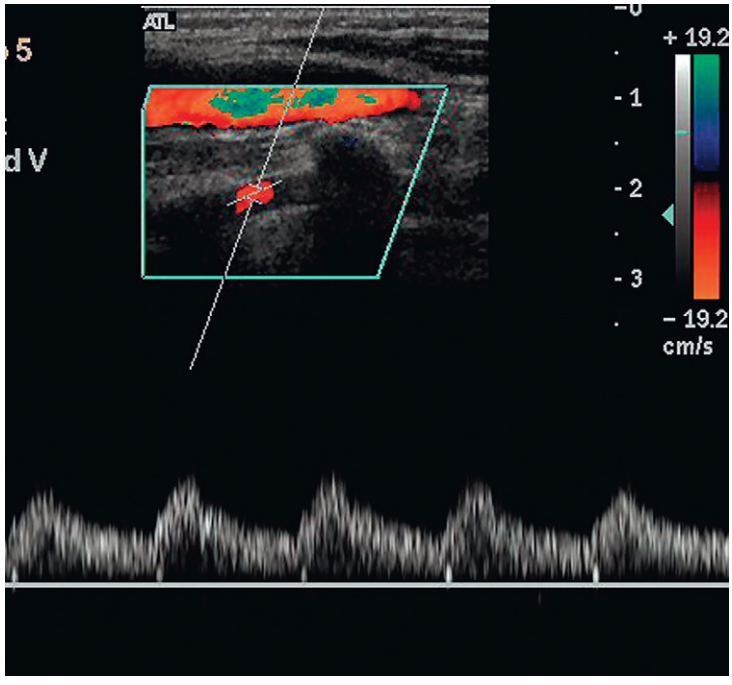


**Fig. 3.21** Vertebral artery with a damped 'tardus parvus' waveform indicating a proximal stenosis.

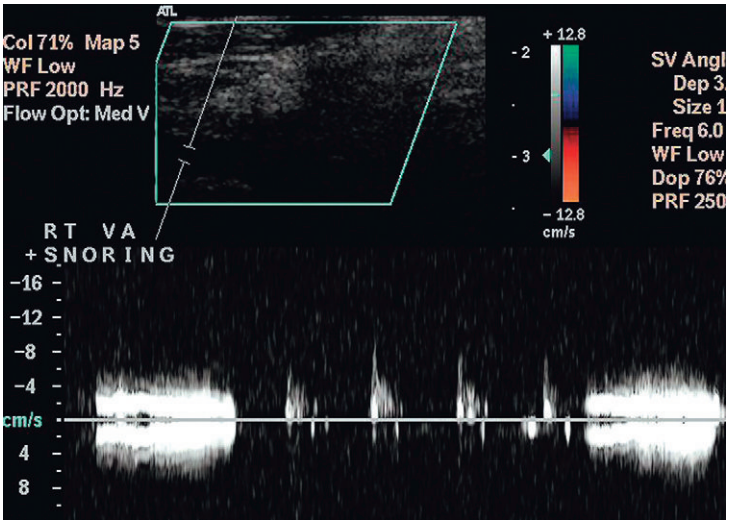


**Fig. 3.22** A difficult vertebral artery to image but spectral Doppler shows absent diastolic flow, this together with the low velocities suggest a distal obstruction. In addition, there is significant interference and noise resulting from the patient going to sleep and snoring during the examination.

examination as the outcome is a mixture of image assessment, Doppler parameters and clinical judgment. It is therefore sensible to standardise the information given in the report of a Doppler examination, to ensure that all necessary data are recorded. The easiest way to do this is to record the data onto a standardised form, which can then be used in reaching management decisions about the patient, or comparing the Doppler examination with any associated MRA, computed tomography angiography (CTA), or arteriogram. The precise details will vary from centre to centre, depending on local preferences. The form used in our institution is shown in Figure 3.23. The main information which should be noted is given in Table 3.8.

## Problems and pitfalls in carotid ultrasound

Problems and pitfalls can arise from a variety of sources. These can be divided into those resulting from poor or faulty technique and those arising from pathological or physiological causes (Table 3.9). Technical aspects of setting up the system are discussed elsewhere (see Appendix) but other aspects which can lead to problems should be considered.

### *Long and eccentric lesions*

The amount of pressure reduction across a stenosis is related primarily to the fourth power of the radius; however, as noted previously, it is also related to the length of the stenosis. This is not relevant for many stenoses, as they are relatively short, but some stenoses, particularly in the common carotid artery, may be longer. There-

**Table 3.8** Carotid examination report information

| |
|---|
| Patient demographic data etc. |
| Patency of CCA, ICA, ECA |
| Any variations of standard anatomy |
| PSV, EDV for each CCA, ICA and ECA |
| IC/CC peak systolic ratio for each side |
| Estimate of degree of stenosis |
| Description of any plaque clearly seen |
| Plaque type: lucent/echogenic/calcified |
| Plaque surface: smooth/irregular/ulcerated/ thrombus |
| Length of any stenosis |
| Diameter of ICA above any stenosis |
| Diagram of any stenosis giving an estimate of plaque disposition |
| Level of the bifurcation in relation to angle of mandible on each side |
| Vertebral arteries |
| Visualised/not visualised |
| Direction of flow |
| Any specific abnormalities identified in relation to the vertebral arteries |

CCA, common carotid artery; ECA, external carotid artery; ICA, internal carotid artery; IC/CC, internal carotid/common carotid.

Please attach patient label

**Vascular Laboratory**

Royal Infirmary of Edinburgh - Little France
51 Little France Crescent
Edinburgh
EH16 4SA

Tel:

**Duplex ultrasound carotid and vertebral assessment**

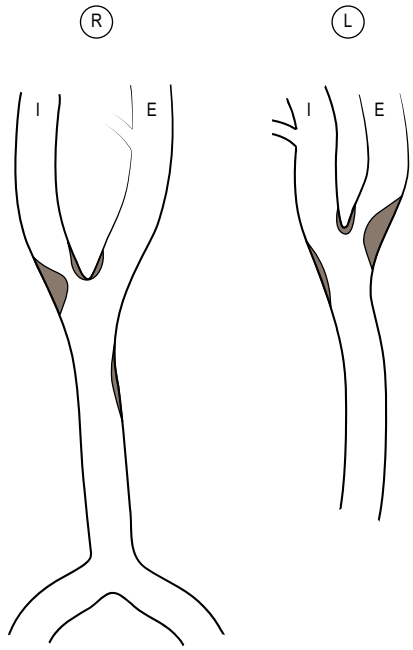


Summary

**Right**

| | CCA | ICA | ECA |
|---|---|---|---|
| PSV (m/s) | 0.7 m/s | 3 m/s | 1.4 m/s |
| EDV (m/s) | | 1 m/s | |
| ICA/CCA | = 4.3 | | |
| % stenosis | <50% | > 70% | < 50% |
| Plaque appearance | mixed smooth | mixed smooth | mixed smooth |

| | Vertebral |
|---|---|
| PSV (m/s) | 0.5 m/s |
| Direction | Antegrade |

**Left**

| | CCA | ICA | ECA |
|---|---|---|---|
| PSV (m/s) | 0.8 m/s | 1.7 m/s | 1.6 m/s |
| EDV (m/s) | | 0.4 m/s | |
| ICA/CCA | = 2.1 | | |
| % stenosis | <50% | 50-69 % | < 50% |
| Plaque appearance | mixed smooth | mixed smooth | mixed smooth |

| | Vertebral |
|---|---|
| PSV (m/s) | 0.6 m/s |
| Direction | Antegrade |

Signature

Please print name and designation

Date

**Fig. 3.23** A specimen carotid examination report form.

fore, whilst a 40% diameter stenosis extending over 5–8 mm length is not haemodynamically significant, a 40% diameter stenosis extending over 5–8 cm may well result in some reduction in pressure and a decrease in flow, resulting in cerebral perfusion problems in some circumstances, and this should be taken into account in the assessment of the patient.

Eccentric lesions may cause problems if the exact disposition of plaque around the circumference of the vessel is not appreciated (Fig. 3.9). Care should be taken to examine areas of disease transversely, as well as longitudinally, as discussed earlier. Another problem with eccentric lesions is that the high-velocity jet may emerge from the stenosis at an unusual angle that is not parallel

**Table 3.9** Problems and pitfalls

| |
|---|
| **Technique related** |
| Incorrect Doppler sample volume position or size |
| Doppler angle too large (>60–65°) |
| Doppler settings too high for low-velocity, low-volume flow |
| Good Doppler angles give poor images and vice versa |
| **Disease related** |
| Long lesions |
| Eccentric lesions |
| Tortuous vessels |
| High-grade stenosis |
| Lesions at the bifurcation |
| Disease elsewhere in the vascular tree |

to the vessel wall, as many people would assume. Colour Doppler is useful in identifying these oblique jets and allows for a more accurate angle correction to be achieved (Fig. 3.5).

### *Tortuous vessels*

Sharp twists in the course of a vessel result in changes to the pattern of blood flow in the lumen: blood on the outer margin flows faster than blood on the inside of the bend (Fig. 2.5); in addition, turbulence is generated, even if plaques are not present. Furthermore, assessing the angle of flow for calculation of velocity can be difficult, so that accurate, representative velocities are hard to define, especially if there is associated disease. Whenever possible, flow characteristics should be assessed as far as possible from the curved segment.

### *High-grade stenoses*

In critical stenoses (>85% diameter reduction, see Ch. 2) velocity decreases; in addition, there is only a small volume of blood flowing through the narrow residual lumen. The signal strength is therefore poor and the Doppler shift is lower than might be expected. It is important to ensure that the machine is set up appropriately to detect these weaker, lower Doppler shifts, if they are not to be missed and a false diagnosis of occlusion reached (Fig. 3.14). The higher sensitivity of power Doppler and the increase in signal strength obtained with echo-enhancing agents are two developments which both individually and together improve the success of ultrasound in discriminating between an occlusion and a small residual lumen.[52]

### *Lesions at the bifurcation*

These can cause problems as a significant amount of plaque may be present in the bulb but, because of the relative dilatation of the lumen which is normally present here, this does not result in any narrowing of the flow channel between the common carotid artery and the internal carotid artery. Although this will not have any effect on the overall flow in the vessel, this disease may provide a source of emboli and may not be recognised if spectral criteria alone are used to identify stenotic segments, as there will not be a significant increase in velocity.

### *Disease elsewhere in the vascular tree*

Vascular ultrasound allows direct assessment of much of the extracranial cerebral circulation from the clavicular region into the upper cervical area and disease in these segments can be measured directly. However, changes in vessels remote from those under examination may affect the findings at any given point. As discussed previously, contralateral occlusion results in increased flow through the patent carotid with higher than normal velocities as a result of this. Aortic valve disease (Figs 3.12 and 3.24) or common carotid artery origin stenosis on the left will not be visualised directly on carotid examination; the presence of disease in these areas can only be inferred from damping of the waveform with, or without, turbulence. Similarly disease more distal in the carotid siphon region will not be detected by cervical carotid examination.

### *Carotid stents*

Insertion of stents into stenotic segments of the common and internal carotid arteries is becoming increasingly recognised as an alternative to endarterectomy for treatment of significant extracranial carotid disease. Insertion of a stent

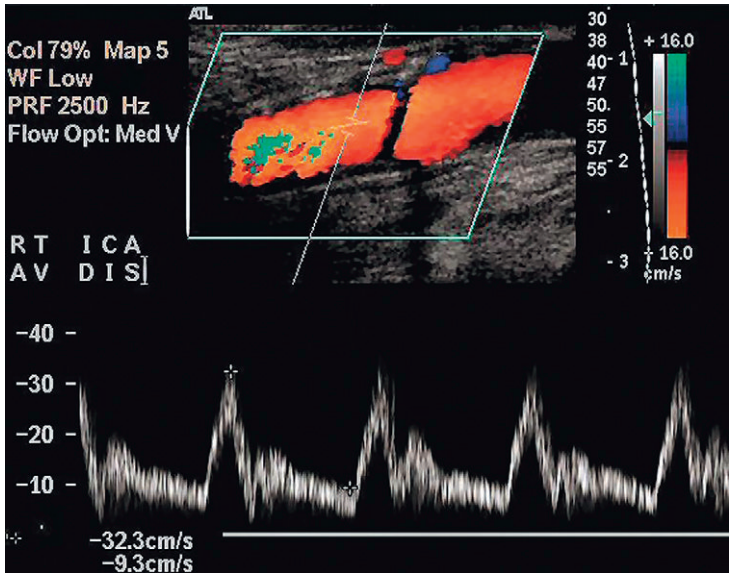


**Fig. 3.24** Carotid waveform in a patient with aortic valve stenosis showing delayed systolic acceleration.

affects the biomechanical properties of the arterial wall resulting primarily in increased stiffness; this means that velocity measurements from a non-stenotic stented segment will be higher than those from an equivalent unstented artery. Lal et al[53] have proposed that a normal velocity through a stented segment can be up to 1.5 m $s^{-1}$. In patients with bilateral severe stenoses, stenting or operating on one side should result in a change in blood flow in the non-operated artery so, as discussed previously, this means that a careful review of the current situation should be made before any decisions are made in relation to the other side.[30]

## Accuracy in relation to other techniques

### *Arteriography*

Many studies have shown that spectral Doppler and colour Doppler have satisfactory accuracy in the diagnosis and assessment of disease when compared with arteriography. Some care must be taken when considering studies comparing the two techniques, as different types of angiography are used as the gold standard: direct carotid injection, arch injection, digital subtraction arteriography (DSA) and venous DSA have all been used. Different methods of measuring the degree of stenosis are also used (Fig. 3.25).[54–56] These will result in different estimations of the degree of stenosis for a bifurcation lesion depending on whether the diameter of the residual lumen is compared with the diameter of the common carotid artery, the diameter of the internal carotid artery, the estimated diameter at the bulb as calculated from calcification in the wall, or from the alignment of the vessels. Indeed, NASCET and ECST[1,2] used different techniques for measuring the degree of angiographic stenosis, so that the results of the two studies are not directly comparable; an 80% ECST diameter stenosis for a given lesion corresponds to a stenosis of 50% in the NASCET study for the same lesion. There is also a degree of variation between different observers in the estimation of stenosis on arteriography, which may be up to 20%.[57] In addition, angiography has some intrinsic procedural risks arising from catheterisation and exposure to contrast and radiation. The risk of minor stroke from carotid arteriography has been reported to range from 1.3 to 4.5% and in the ACAS the combined neurological morbidity/mortality from arteriography in patients with haemodynamically significant stenoses was 1.2%.[58]

The overall performance of Doppler ultrasound compared with arteriography is good. Cardullo et al[59] reviewed 16 spectral Doppler studies with 2146 Doppler–arteriogram comparisons; non-

colour duplex Doppler had an overall sensitivity of 96%, specificity of 86%, positive predictive value of 89%, negative predictive value of 94% and accuracy of 91% for the diagnosis of a diameter stenosis greater than 50%. Subsequently, further studies have confirmed the value of colour Doppler with similar or better levels of accuracy and also its value in improving diagnostic confidence, clarifying difficult situations and reducing examination times.[60, 61] In particular the difficult distinction between a critical stenosis and a complete occlusion can be achieved in nearly all cases with the use of colour Doppler.[33, 62]

### *Magnetic resonance angiography and computed tomography angiography*

Developments in CTA have made the use of CT for the assessment of larger vessels a realistic proposition. MRA is also developing at a rapid pace. These two techniques have an advantage over ultrasound in that they provide information on disease at the origins of the carotids and also in the intracranial circulation. However, they also have significant drawbacks: they both 'image' the blood and infer the wall characteristics from the shape of the blood flowing in the vessel, whereas colour Doppler provides information on the wall of the vessel and any plaque, as well as the flowing blood. MRA is still limited to some extent by signal voids at relatively high velocities, as well as problems from signals arising in plaque haemorrhage and lipid deposits.[63] Another disadvantage of CTA and MRA, apart from exposure of the patient to contrast agents and radiation (CTA), is the significant amount of post-processing and image manipulation required for an accurate assessment of the examination to be achieved. Several authors have suggested that Doppler is satisfactory for initial screening of patients for carotid disease and for identification of patients requiring surgery in most cases but that CTA or MRA are useful additional tests

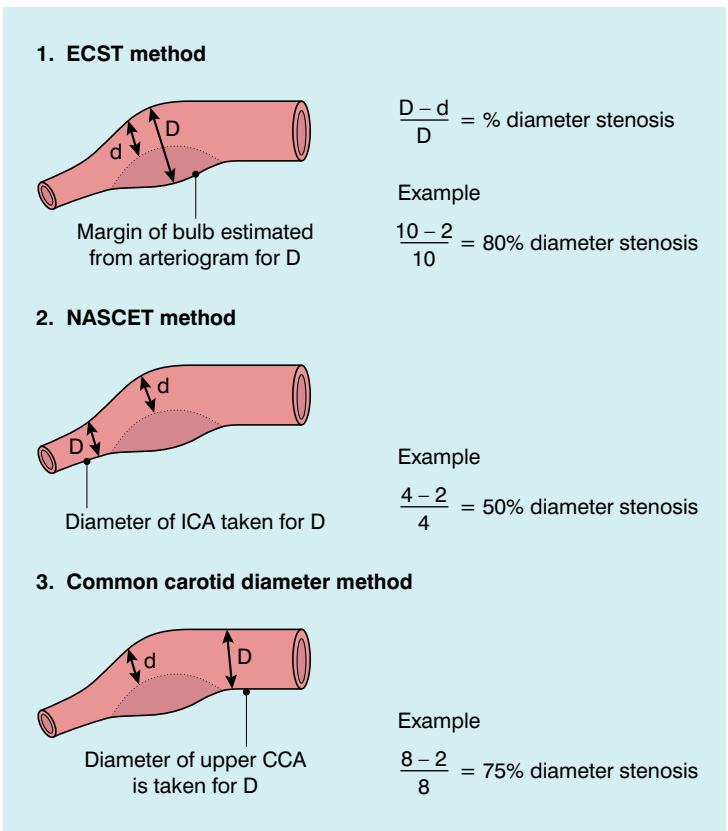


**Fig. 3.25** Methods for estimating percentage diameter stenosis in arteriography.

which can be used instead of angiography if the ultrasound is inadequate or indeterminate, or if clinical uncertainty persists.[64–67] The need for arteriography in the majority of patients being considered for surgery is now very much reduced, although arguments for and against persist.[68–70]

Compared with arteriography, CTA and MRA, Doppler ultrasound is relatively cheap, rapid, non-invasive and accurate for the diagnosis of extracranial carotid disease. Whilst it will not provide information on siphon disease, or aortic arch disease this is not usually a significant problem in most patients in relation to the decision to perform an endarterectomy. If patients are being considered for stenting, then they will need an assessment of the aortic arch and carotid origins, normally by MRA or CTA. If a policy to operate on ultrasound alone is to be implemented then the department/laboratory must ensure that scanning protocols and results are continuously reviewed, audited and validated with care taken to identify patients who will benefit from further imaging.

## TRANSCRANIAL DOPPLER OF THE CEREBRAL CIRCULATION

The use of ultrasound to assess intracranial structures is not a new phenomenon. One of the first clinical applications of ultrasound as a diagnostic technique was in the assessment of midline intracranial structures with A-scan equipment. More recently, high-quality imaging and Doppler studies have been obtained in neonates through the patent fontanelles, or through the relatively thin bone of the neonatal skull. Transcranial Doppler was first described by Aaslid in 1982[71] and the technique of pulsed transcranial Doppler has subsequently been developed in many centres. This technique provides useful information on the direction and velocity of blood flow and the changes which may occur in these with various physiological, pharmacological or pathological conditions; it can also be used to monitor the intracranial circulation during carotid and other vascular surgical procedures.[72,73] However, it is a difficult technique to learn and to perform reliably as the vessels must be located without any imaging information.

Modern ultrasound equipment can now be configured to get some imaging detail and colour Doppler information from within the adult skull in many cases; best results are obtained with dedicated transducers and software. This allows localisation and positive identification of the major arteries and specific segments of these. The main problem is the bone of the skull vault, where it has been estimated that the attenuation can vary from 15–25 dB to 40–60 dB depending on the type and thickness of the bone for a single passage across the skull vault.[74] As the sound pulse has to pass through the skull on both the inward and outward segments of its passage, there is therefore considerable loss of energy. Power Doppler is of value in locating the vessels and the advent of intravascular ultrasound contrast agents has improved the signal-to-noise ratio significantly; it also makes the location of intracranial vessels more straightforward.[75]

### Technique

There are three potential sites of access for transcranial examinations in the adult: the transtemporal window, the suboccipital approach and the transorbital approach. The transtemporal window is used for assessment of the internal carotid arteries, the middle, anterior and posterior cerebral arteries. The window is located by applying liberal amounts of acoustic coupling gel to the hair and skin of the temporal region in front and above the external auditory meatus. Slowly moving the transducer around will allow the point of best transmission to be identified. In some 10% of subjects it may not be possible to get worthwhile images and Doppler signals;[76] there tends to be greater attenuation in older patients, females and Afro-Caribbean patients.[77]

The pituitary fossa and suprasellar cistern are the most recognisable structures in the transverse plane. Once these have been identified, colour Doppler can be used to locate the main arteries and the direction of flow in these vessels (Fig. 3.26). The ipsilateral middle cerebral artery is

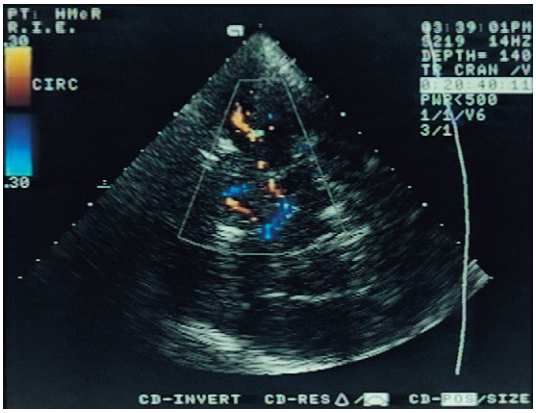


**Fig. 3.26** The anterior and middle cerebral arteries on transcranial colour Doppler ultrasound through the transtemporal window.

seen passing peripherally from the end of the internal carotid artery. It cannot often be seen in its entirety in a single scan plane and the transducer position must be varied to follow it out to the Sylvian fissure, where it turns posteriorly. The origin of the contralateral middle cerebral artery can also usually be identified. The proximal segments of the anterior cerebral arteries are also seen from the transtemporal approach. The direction of flow in the ipsilateral anterior cerebral artery is normally away from the transducer and flow is towards the transducer in the contralateral vessel. This arrangement will be altered if there is occlusion of the ipselateral internal carotid artery and collateral flow through the anterior communicating artery is present. In this situation, flow in the anterior cerebral artery on the side of the occluded carotid will be reversed towards the transducer. The posterior cerebral arteries can be seen arising from the vertebral artery and passing around the cerebral peduncles.

The suboccipital window is located by scanning transversely in the midline under the occipital bone. It is often better to position the transducer slightly to one side or the other of the midline as the nuchal ligament can interfere with the clarity of the image. The vertebral arteries can be seen passing around the atlas and into the foramen magnum. The point where they join to form the basilar artery may be seen if it lies low enough in relation to the foramen magnum.

The transorbital approach is used in pulsed transcranial Doppler to assess the anterior cerebral arteries, but it is not very convenient for colour Doppler examinations as the transducers are relatively larger. Care must be taken, if this approach is used, to ensure that the transmit power is low in order to reduce the risk to the retina.

The major cerebral veins and venous sinuses are more difficult to demonstrate due to their anatomical locations and slow flow within them, but contrast agents have been reported to improve this situation.[75]

## Indications

Transcranial colour Doppler has several advantages when compared with conventional trans-

**Table 3.9** Applications of transcranial Doppler (TCD)

| |
|---|
| **TCD is able to provide useful information and clinical utility is established** |
| Screening children with sickle cell disease to assess stroke risk |
| Monitoring vasospasm after traumatic SAH |
| **TCD is able to provide information but clinical utility compared to other diagnostic tools remains to be determined** |
| Evaluation of occlusive lesions of intracranial arteries in basal cisterns |
| Confirming brain death |
| **TCD is able to provide information but clinical utility remains to be determined** |
| Monitoring thrombolysis of acute MCA occlusions |
| Detection of microembolic signals |
| Monitoring during carotid endarterectomy and CABG |
| Detection of impaired cerebral haemodynamics with severe extracranial ICA disease |
| Detection of vasospasm after traumatic SAH |
| Evaluation and monitoring of MCA territory infarctions |
| **TCD is able to provide information but other diagnostic tests are typically preferable** |
| Detection of L→R cardiac and extracardiac shunts |
| Evaluation of severe extracranial ICA disease |

CABG, coronary artery bypass graft; ICA, internal carotid artery; MCA, middle cerebral artery; SAH, subarachnoid haemorrhage. From 'Assessment: Transcranial Doppler ultrasonography', the American Academy of Neurology.[78]

cranial Doppler. Visualisation of the intracranial anatomy allows rapid localisation and identification of specific vessels and specific segments of particular vessels. The colour Doppler signal allows rapid identification of flow patterns and direction, so compression studies are less necessary in order to assess collateral flow. The ability to perform angle-corrected velocity measurements produces more accurate readings and the ability to measure at specific sites allows better consistency for serial measurements.

Although still largely a research tool, the technique does have several potential applications. These were reviewed in 2004 by the American Academy of Neurology (Table 3.9).[78] In particular the ability to bring the ultrasound machine to the patient allows the technique to be used to monitor cerebral blood flow in a variety of cerebrovascular disorders, such as subarachnoid haemorrhage and stroke.

## CONCLUSIONS

Colour Doppler ultrasound provides a useful technique for the assessment of the carotid and vertebral arteries in the neck. Careful attention must be paid to the standard techniques which are used for the examinations and each centre should use the Doppler criteria for stenosis that provide the most accurate and reproducible results in their experience. The availability of the technique has reduced the necessity for carotid arteriography in most departments. MRA and CTA continue to improve but ultrasound provides information on the nature of the plaque which is not available from these techniques.

## REFERENCES

1. European Carotid Surgery Trialists' (ECST) Collaborative Group. MRC European Carotid Surgery Trial: interim results for symptomatic patients with severe (70–99%) or with mild (0–29%) carotid stenosis. Lancet 1991; 337:1235–1243.
2. North American Symptomatic Carotid Endarterectomy Trial (NASCET) Collaborators. Beneficial effect of carotid endarterectomy in symptomatic patients with high-grade carotid stenosis. New Engl J Med 1991; 325:445–453.
3. Rothwell PM, Eliasziw M, Gutnikov SA, et al. Carotid Endarterectomy Triallists' Collaboration. Lancet 2003; 361:107–116.
4. Cina CS, Clase CM, Haynes RB. Carotid endarterectomy for symptomatic carotid stenosis (Cochrane Review). In: The Cochrane Library, Issue 3. Chichester: John Wiley; 2004.
5. Zwiebel WJ. Duplex sonography of the cerebral arteries: efficacy, limitations and indications. AJR Am J Roentgenol 1992; 158:29–36.
6. National Institute of Neurological Disorders and Stroke. Clinical advisory: carotid endarterectomy for patients with asymptomatic internal carotid artery stenosis. Stroke 1994; 5:2523–2524.
7. Chambers BR, You RX, Donnan GA. Carotid endarterectomy for asymptomatic carotid stenosis (Cochrane Review). In: The Cochrane Library, Issue 3. Chichester: John Wiley; 2004.
8. Naylor AR, Mehta Z, Rothwell PM, et al. Carotid artery disease and stroke during coronary artery bypass: a critical review of the literature. Eur J Vasc Endovasc Surg 2002; 23:283–294.
9. Ivey TD, Strandness DE, Williams DB, et al. Management of patients with carotid bruit undergoing cardiopulmonary bypass. J Thorac Cardiovasc Surg 1984; 87:183–189.
10. Naylor AR, Merrick MV, Sandercock PAG, et al. Serial imaging of the carotid bifurcation and cerebrovascular reserve after carotid endarterectomy. Br J Surg 1993; 80:1278–1282.
11. Bassi P, Lattuada P, Gomitoni A. Cervical cerebral artery dissection: a multicenter prospective study (preliminary report) Neurol Sci 2003; 24(suppl 1): S4–7.
12. Salonen JT, Salonen R. Ultrasound B-mode imaging in observational studies of atherosclerotic progression. Circulation 1993; 87(suppl 3):II56–65.
13. Trigaux JP, Delchambre F, Van Beers B. Anatomical variations of the carotid bifurcation: implications for digital subtraction angiography and ultrasound. Br J Radiol 1990; 63:181–185.
14. Budorick NE, Rojratanakiat W, O'Boyle MK, et al. Digital tapping of the temporal artery: significance in carotid duplex sonography. J Ultrasound Med 1996; 15:459–464.
15. Salonen JT, Salonen R. Ultrasonically assessed carotid morphology and the risk of coronary heart disease. Arterioscler Thromb 1991; 11:1245–1249.
16. Hallerstam S, Larsson PT, Zuber E, et al. Carotid atherosclerosis is correlated with extent and

severity of coronary artery disease evaluated by myocardial perfusion scanning. Angiology 2004; 55:281–288.
17. Geroulakos G, O'Gorman DJ, Kalodiki E, et al. The carotid intima-media thickness as a marker of severe symptomatic coronary artery disease. Eur Heart J 1994; 15:781–785.
18. Kitamura A, Iso H, Ohira T, et al. Carotid intima-media thickness and plaque characteristics as a risk factor for stroke in Japanese elderly men. Stroke 2005; 36:32–37.
19. Buckenham TM, Wright IA. Ultrasound of the extracranial vertebral artery. Br J Radiol 2004; 77:15–20.
20. Berguer R, Kieffer E. The aortic arch and its branches: anatomy and blood flow. In: Kieffer E, Berguer R, eds. Surgery of the arteries to the head. New York: Springer Verlag; 1992:5–31.
21. Wain RA, Lyon RT, Veith FJ, et al. Accuracy of duplex ultrasound in evaluating carotid anatomy before endarterectomy. J Vasc Surg 1998; 27:235–242.
22. Bluth EI, Stavros AT, Marich KW, et al. Carotid duplex sonography: a multicentre recommendation for standardized imaging and Doppler criteria. Radiographics 1988; 8:487–506.
23. Carpenter JP, Lexa FJ, Davies JT. Determination of 60% or greater carotid artery stenosis by duplex Doppler ultrasonography. J Vasc Surg 1995; 22:697–705.
24. Robinson ML, Sacks D, Perlmutter GS, et al. Diagnostic criteria for carotid duplex sonography. AJR Am J Roentgenol 1988; 151:1045–1049.
25. Grant EG, Benson CB, Moneta GL, et al. Carotid artery stenosis: gray-scale and Doppler US diagnosis – Society of Radiologists in Ultrasound Consensus Conference. Radiology 2003; 229:340–346.
26. Hood DB, Mattos MA, Mansour A, et al. Prospective evaluation of new duplex criteria to identify 70% internal carotid artery stenosis. J Vasc Surg 1996; 23:254–262.
27. Spencer MO, Reid JM. Quantitation of carotid stenosis with continuous wave (CW) Doppler ultrasound. Stroke 1979; 10:326–330.
28. Erickson SJ, Mewissen MW, Foley WD, et al. Stenosis of the internal carotid artery: assessment using colour Doppler imaging compared with angiography. AJR Am J Roentgenol 1989; 152:1299–1305.
29. Steinke W, Meairs S, Ries S, et al. Sonographic assessment of carotid artery stenosis. Comparison of power Doppler imaging and color Doppler flow imaging. Stoke 1996; 27:91–94.
30. Sachar R, Yadav JS, Roffi M, et al. Severe bilateral carotid stenosis: the impact of ipsilateral stenting on Doppler-defined contralateral stenosis. J Am Coll Cardiol 2004; 43:1358–1362.
31. Belkin M, Mackey WC, Pessin MS, et al. Common carotid artery occlusion with patent internal and external carotid arteries: diagnosis and surgical management. J Vasc Surg 1993; 17:1019–1027.
32. Krieghauser JS, Patel MD, Nelson KD. Carotid pseudostring sign from vasa vasorum collaterals. J Ultrasound Med 2003; 22:959–963.
33. Mattos MA, Hodgson KJ, Ramsey DE, et al. Identifying total carotid occlusion with colour flow duplex scanning. Eur J Vasc Surg 1992; 6:204–210.
34. Androulakis AE, Labropoulos N, Allan R, et al. The role of common carotid artery end-diastolic velocity in near or total internal carotid artery occlusion. Eur J Vasc Endovasc Surg 1996; 11:140–147.
35. Meves SH, Muhs A, Federlein J, et al. Recanalisation of acute symptomatic occlusions of the internal carotid artery. J Neurol 2002; 249:188–192.
36. Camporese G, Verlato F, Salmistraro G, et al. Spontaneous recanalization of internal carotid artery occlusion evaluated with color flow imaging and contrast arteriography. Int Angiol 2003; 22:64–71.
37. Steffen CM, Gray-Weale AC, Byrne KE, et al. Carotid artery atheroma: ultrasound appearances in symptomatic and asymptomatic vessels. Aust N Z J Surg 1989; 59:529–534.
38. Gronholdt ML, Nordestgaard BG, Schroeder TV, et al. Ultrasonic lucent plaques predict future strokes. Circulation 2001; 104:68–73.
39. Golledge J, Cuming R, Ellis M, et al. Carotid plaque characteristics and presenting symptom. Br J Surg 1997; 84:1697–1701.
40. O'Donnell TF, Erdoes L, Mackey WC, et al. Correlation of B-mode ultrasound imaging and arteriography with pathologic findings at carotid endarterectomy. Arch Surg 1985; 120:443–449.
41. Bluth EI, Kay D, Merritt CRB, et al. Sonographic characterization of carotid plaque: detection of haemorrhage. AJR Am J Roentgenol 1986; 146:1061–1065.
42. Ratliff DA, Gallagher PJ, Hames TK, et al. Characterisation of carotid artery disease: comparison of duplex scanning with histology. Ultrasound Med Biol 1985; 11:835–840.
43. O'Leary DH, Holen J, Ricotta JJ, et al. Carotid bifurcation disease: prediction of ulceration with B-mode US. Radiology 1987; 162:523–525.
44. Hatsukami TS, Ferguson MS, Beach KW, et al. Carotid plaque morphology and clinical events. Stroke 1997; 28:95–100.
45. Thiele BL, Jones AM, Hobson RW, et al. Standards in non-invasive cerebrovascular testing. J Vasc Surg 1992; 15:495–503.
46. Rosset E, Albertini J-N, Magnan PE, et al. Surgical treatment of extracranial internal carotid artery aneurysms. J Vasc Surg 2000; 31:713–723.
47. Mann WJ, Beck A, Schreiber J, et al. Ultrasonography for evaluation of the carotid artery in head and neck cancers. Laryngoscope 1994; 104:885–888.

48. Barry R, Pienaar A, Pienaar C. Duplex Doppler evaluation of suspected lesions at the carotid bifurcation. Ann Vasc Surg 1993; 7:140–144.
49. de Bray JM, Lhoste P, Dubaz F, et al. Ultrasonic features of extracranial carotid dissections: 47 cases studied by angiography. J Ultrasound Med 1994; 13:659–664.
50. Logason K, Hardemark HG, Bärlin T, et al. Duplex scan findings in patients with spontaneous cervical artery dissections. Eur J Vasc Endovasc Surg 2002; 23:295–298.
51. Steinke W, Rautenberg W, Schwartz A, et al. Non-invasive monitoring of internal carotid artery dissection. Stroke 1994; 25:998–1005.
52. Sitzer M, Fürst G, Siebler M, et al. Usefulness of an intravenous contrast medium in the characterization of high-grade internal carotid stenosis with colour Doppler-assisted duplex imaging. Stroke 1994; 25:385–389.
53. Lal BK, Hobson RW 2nd, Goldstein J, et al. Carotid stenting: is there a need to revise ultrasound velocity criteria? J Vasc Surg 2004; 39:58–66.
54. Alexandrov AV, Bladin CF, Magisano, et al. Measuring carotid stenosis. Time for a reappraisal. Stroke 1993; 24:1292–1296.
55. Rothwell PM, Gibson RJ, Slattery J, et al. Prognostic value and reproducibility of measurements of carotid stenosis: a comparison of three methods on 1001 angiograms. Stroke 1994; 25:2440–2444.
56. Phillips DJ. Recent advances in carotid artery evaluation. In: Taylor KJW, Strandness DE, eds. Clinics in diagnostic ultrasound 26: duplex Doppler ultrasound. Edinburgh: Churchill Livingstone; 1990:25–44.
57. Chikos PM, Fisher LD, Hirsch JH, et al. Observer variability in evaluating extracranial carotid stenoses. Stroke 1983; 14:885–892.
58. Executive Committee for the Asymptomatic Carotid Atherosclerosis (ACAS) Study. Endarterectomy for asymptomatic carotid artery stenosis. J Am Med Assoc 1995; 273:1421–1428.
59. Cardullo PA, Cutler BS, Brownell Wheeler H. Detection of carotid disease by duplex ultrasound. J Diagn Med Sonogr 1986; 2:63–73.
60. Carroll BA. Carotid sonography. Radiology 1991; 178:303–313.
61. Sabeti S, Schillinger M, Mlekusch W, et al. Quantification of internal carotid artery stenosis with duplex US: comparative analysis of different flow velocity criteria. Radiology 2004; 232:431–439.
62. Lee DH, Gao FQ, Rankin RN, et al. Duplex and color Doppler flow sonography of occlusion and near occlusion of the carotid artery. Am J Neuroradiol 1996; 17:1267–1274.
63. Sellar RJ. Imaging blood vessels of the head and neck. J Neurol Neurosurg Psychiatry 1995; 59:225–237.
64. Cinat ME, Casalme C, Wilson SE, et al. Computed tomography angiography validates duplex sonographic evaluation of carotid stenosis. Am Surg 2003; 69:842–847.
65. Back MR, Rogers GA, Wilson JS, et al. Magnetic resonance angiography minimizes the need for arteriography after inadequate carotid duplex ultrasound scanning. J Vasc Surg 2003; 38:422–430.
66. Herzig R, Burval S, Krupka B, et al. Comparison of ultrasonography, CT angiography and digital subtraction angiography in severe carotid stenoses. Eur J Neurol 2004; 11:774–781.
67. Buskens E, Nederkoorn PJ, Buijs-Van Der Woude T, et al. Imaging of carotid arteries in symptomatic patients: cost-effectiveness of diagnostic strategies. Radiology 2004; 233:101–112.
68. Moore WS. For severe carotid stenosis found on ultrasound, further arterial evaluation is unnecessary. Stroke 2003; 34:1816–1817.
69. Rothwell PM. For severe carotid stenosis found on ultrasound, further arterial evaluation is unnecessary: the argument against. Stroke 2003; 34:1817–1819.
70. Davis SM, Donnan GA. Is carotid angiography necessary? Editors disagree. Stroke 2003; 34:1819.
71. Aaslid R, Markwalder TM, Nornes H. Non-invasive transcranial Doppler ultrasound recording of flow velocity in basal cerebral arteries. J Neurosurg 1982; 57:769–774.
72. Nedey C, Barjoud H, Chatelard P, et al. The role of intraoperative transcranial Doppler monitoring in carotid artery surgery. Ann Vasc Surg 1995; 9:247–251.
73. Doblar DD. Intraoperative transcranial ultrasonic monitoring for cardiac and vascular surgery. Semin Cardiothorac Vasc Anesth 2004; 8:127–145.
74. White DN, Curry GR, Stevenson RJ. The acoustic characteristics of the skull. Ultrasound Med Biol 1978; 4:225–252.
75. Bauer A, Becker G, Krone A, et al. Transcranial duplex sonography using ultrasound contrast enhancers. Clinl Radiol 1996; 51(suppl 1):19–23.
76. Ringelstein EB, Kahlscheuer E, Niggemeyer E, et al. Transcranial Doppler sonography: anatomical landmarks and normal velocity values. Ultrasound Med Biol 1990; 16:745–761.
77. Halsey JH. Effect of emitted power on waveform intensity in transcranial Doppler. Stroke 1990; 21:1573–1578.
78. Sloan MA, Alexandrov AV, Tegeler CH, et al. Assessment: Transcranial Doppler ultrasonography. Report of the Therapeutics and Technology Assessment Subcommittee of the American Academy of Neurology. Neurology 2004; 62:1468–1481.

# The peripheral arteries

# 4

Paul L. Allan and Karen Gallagher

Atheroma occurs to different degrees in different parts of an individual's cardiovascular system and the lower limb arteries are particularly prone to the development of atherosclerosis. Approximately 2% of adults in late middle age in Western countries have intermittent claudication[1] and each year in England and Wales around 50 000 patients are admitted to hospital with a diagnosis of peripheral arterial disease; 15 000 of these will require amputation.[2] There are many factors which may influence the development of disease and, in general terms, the prevalence of peripheral vascular disease detected by non-invasive procedures is about three times greater than the prevalence of intermittent claudication.[3] This chapter concentrates on the use of ultrasound in the assessment of disease in the lower limb arteries, as this is the area where most work is generated, but the value of ultrasound in the investigation of a variety of upper limb arterial disorders is also discussed.

## INDICATIONS

### Peripheral vascular disease

The main indications for performing Doppler ultrasound of the arteries of the upper and lower limbs are given in Table 4.1. The most common indication is the assessment of patients with ischaemic symptoms of the lower limb in order to determine if they are likely to benefit from angioplasty or a bypass graft. The ultrasound findings provide information on the extent and severity of disease; even in patients with limb-threatening ischaemia ultrasound is a useful first-line investigation that can provide the surgeon with all the information that is required for patient management. In subacute cases ultrasound allows any subsequent arteriogram to be scheduled as either a straightforward mapping examination prior to bypass grafting, or as a more time-consuming angioplasty procedure.[4,5] In many cases ultrasound will provide sufficient information for management decisions to be reached. In other cases, if further information is required, the subsequent magnetic resonance angiography (MRA)/computed tomography angiography (CTA)/arteriogram can be tailored appropriately. Ultrasound provides an accurate assessment of the major arteries which allows distinction between patients with significant peripheral arterial disease and those without. At the other end of the spectrum, patients with atypical symptoms that might be due to ischaemia can be examined to exclude the presence of significant arterial disease.

#### *Bypass grafts and angioplasty*

A variety of problems can occur with surgically inserted bypass grafts, especially in the first year after the operation. A graft surveillance programme using ultrasound allows the identification of grafts at risk of failure and early remedial action to be taken. Similarly, patients in whom angioplasty has been undertaken can be followed with ultrasound to confirm residual patency, identify re-stenosis and assess improvements to flow following the procedure.

#### *False aneurysms and other pulsatile masses*

The assessment of pulsatile masses in relation to the arteries of the upper and lower limbs can be performed rapidly and easily using ultrasound.

**Table 4.1** Indications for Doppler ultrasound of the peripheral arteries

- Assessment of disease in patients with ischaemic symptoms of the upper or lower limb
- Follow-up of bypass graft procedures
- Follow-up of angioplasty procedures
- Diagnosis and follow-up of aneurysms of the peripheral arteries
- Diagnosis and treatment of false aneurysms
- Diagnosis of pulsatile lumps
- Assessment of dialysis shunts

Aneurysms can be distinguished from non-vascular masses which lie adjacent to the artery. The complications of catheterisation procedures, including haematomas, arteriovenous fistulae and false or pseudoaneurysms, can be assessed and differentiated; in many cases, pseudoaneurysms can be treated under ultrasound control, thereby removing the need for a surgical procedure.

### *Haemodialysis fistulae*

Arteriovenous fistulae created for haemodialysis can be examined using ultrasound, allowing identification of complications associated with stenosis or occlusion, as well as estimation of blood flow through the shunt, particularly if this is thought to be inadequate or excessive.

## ANATOMY AND SCANNING TECHNIQUE

### Anatomy – lower limb

The arteries of the lower limb arise at the bifurcation of the abdominal aorta (Fig. 4.1), the *common iliac arteries* run down the posterior wall of the pelvis and divide into the internal and external iliac arteries in front of the sacroiliac joint. The *internal iliac artery* continues down into the pelvis and is difficult to demonstrate with transabdominal ultrasound, although transvaginal or transrectal scanning will show some of its branches. The *external iliac artery* continues around the side of the pelvis to the level of the inguinal ligament, it lies anteromedial to the psoas muscle and is normally superficial to the external iliac vein.

The *common femoral artery* runs from the inguinal ligament to its division into superficial and deep femoral arteries in the upper thigh; this division is usually 3–6 cm distal to the inguinal ligament. The deep femoral artery, or *profunda femoris artery*, passes posterolaterally to supply the major thigh muscles. The importance of the profunda femoris lies in its role as a major collateral pathway in patients with significant superficial femoral artery disease. Several other branches arise from the external iliac, common femoral and profunda femoris arteries and occasionally one of these may be mistaken for the profunda femoris artery, especially if it is enlarged as a collateral supply.

The *superficial femoral artery* passes downwards along the anteromedial aspect of the thigh lying anterior to the vein; in the lower third of the thigh it passes into the adductor canal, deep to sartorius and the medial component of quadriceps femoris. Passing posteriorly behind the lower femur it enters the popliteal fossa and becomes the *popliteal artery*, which lies anterior to the popliteal vein and gives off several branches, the largest of which are the superior and inferior geniculate arteries. Below the knee joint the popliteal artery divides into the anterior tibial artery and the tibioperoneal trunk, although the exact level of the division may vary; after 2–4 cm the latter divides into the posterior tibial artery and the peroneal artery.

The *anterior tibial artery* passes forwards through the interosseous membrane between the fibula and tibia. It then descends on the anterior margin of the membrane, deep to the extensor muscles on the anterolateral aspect of the calf (Fig. 4.2). At the ankle it passes across the front of the joint to become the dorsalis pedis artery of the foot which runs from the front of the ankle joint to the proximal end of the first intertarsal space where it gives off metatarsal branches and passes through the first intertarsal space to unite with the lateral plantar artery and form the plantar arterial arch.

The *posterior tibial artery* passes down the deep medial aspect of the calf to pass behind the medial malleolus, after which it divides into the

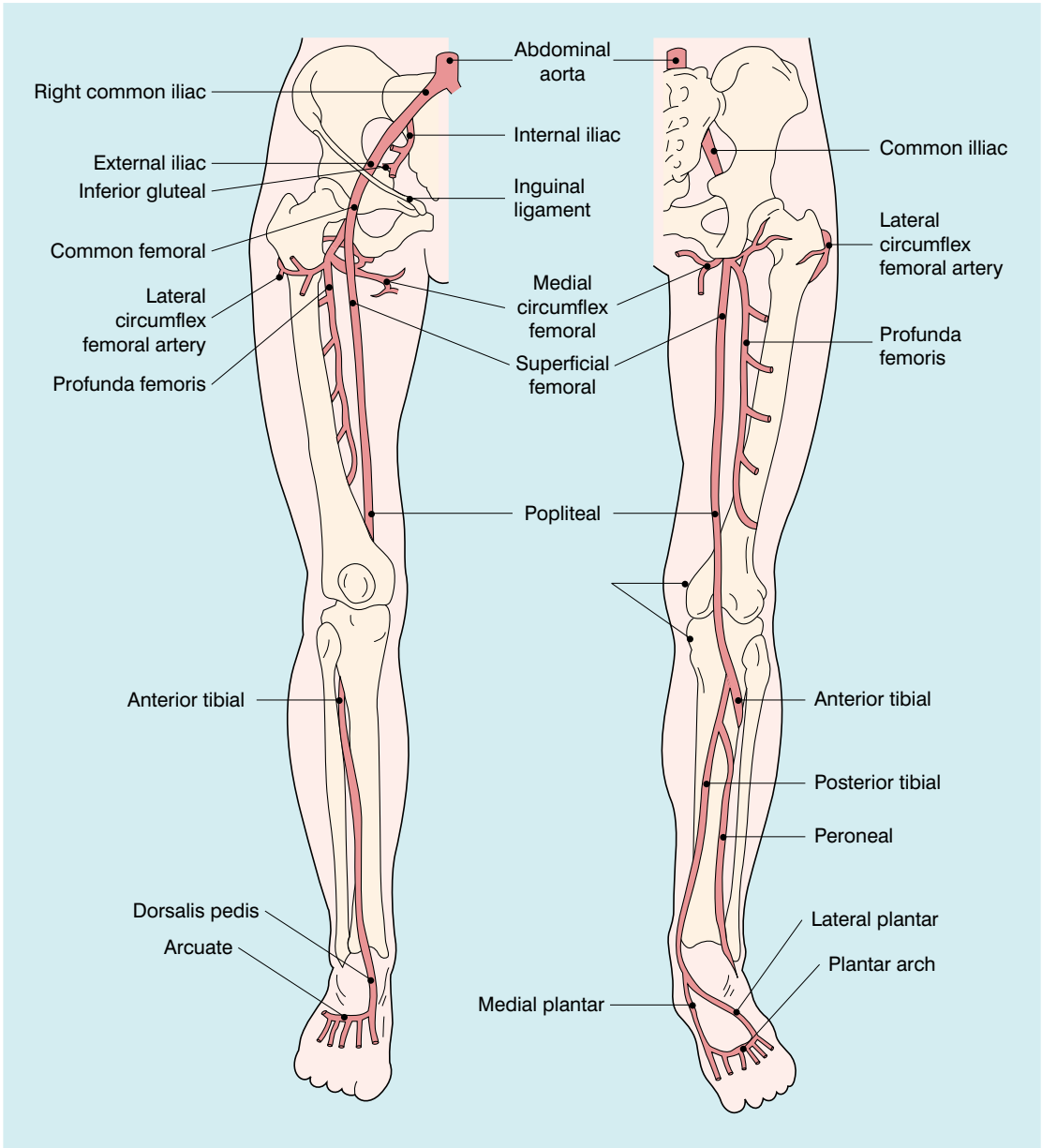


**Fig. 4.1** The lower limb arteries.

medial and lateral plantar arteries of the foot; the lateral plantar artery joins with the dorsalis pedis artery in the plantar arch.

The *peroneal artery* passes down the calf behind the tibia and interosseous membrane and divides into several periarticular branches behind the ankle joint. The size of the calf arteries can be quite variable, the posterior tibial artery is the least variable in calibre but the anterior tibial and peroneal arteries may vary considerably in calibre and overall length in the calf. The arterial supply to the foot is not normally examined but if a bypass procedure to the pedal arteries is being considered then the dorsalis pedis and posterior tibial artery and its plantar branches should be assessed.

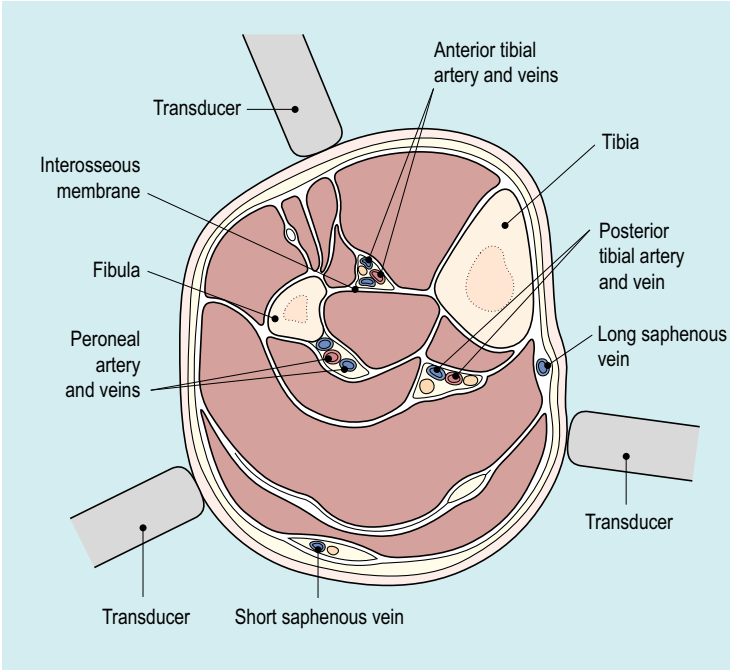


**Fig. 4.2** Cross-section of calf, showing major relations of calf arteries and the three main access points for demonstrating these vessels.

## Scanning technique – lower limb

A full scan of the lower limb arteries can be time consuming. In some cases a full scan from aortic bifurcation to the ankle or foot is required but in other cases the examination can be tailored to specific levels depending on the diagnostic information required. It is therefore useful if the diagnostic question can be clearly defined, so that the most appropriate examination can be performed.

### *Common femoral, profunda femoris and superficial femoral arteries*

The examination begins with the patient lying supine on the couch. The main steps in the examination are given in Table 4.2. A linear array transducer is used; usually 5–12 MHz depending on the performance of the ultrasound system and the build of the patient, lower frequencies may be required to examine the arteries in the adductor canal or in large patients. The distal external iliac/common femoral artery is located using colour Doppler as it leaves the pelvis under the inguinal ligament lateral to the femoral vein. Even if flow appears normal on colour Doppler and there is no evidence of local disease, a spectral Doppler trace should be recorded, as changes in this may indicate the presence of significant disease proximally, necessitating a careful direct examination of the iliac vessels. The bifurcation of the common femoral artery into the profunda femoris and superficial femoral arteries is then examined using colour and spectral Doppler. The profunda femoris artery should be examined over its proximal 5 cm, especially in patients with severe superficial femoral disease, in order to assess the amount of collateral flow, or its potential value as a graft origin or insertion point.

The superficial femoral artery is then followed along the length of the thigh using colour Doppler. It is often better to move the transducer in

**Table 4.2** Basic steps in the examination of the lower limb

1. Patient supine: scan common femoral, proximal profunda and superficial femoral artery down to adductor canal
2. Patient decubitus: scan adductor canal, popliteal artery to bifurcation and tibioperoneal trunk, scan posterior tibial and peroneal arteries
3. Patient supine: scan anterior tibial arteries. Scan iliac arteries and infrarenal aorta

sequential steps, rather than sliding it down the thigh, as most machines require a few frames of sampling at each position to provide a steady image. In addition, the moving transducer generates colour Doppler noise over the image, obscuring vascular details. Doppler spectra are obtained as necessary at points of possible disease. Even in the absence of colour Doppler abnormalities, it is good practice to obtain routine spectral assessments from the superficial femoral artery in the upper, middle and lower thigh, in order to confirm that there is no alteration in the waveform that might suggest disease. Sometimes the artery is difficult to see on colour or power Doppler as the signals are weak or absent. In these cases the artery may be visible by virtue of calcified plaques in the wall of the vessel. Alternatively, the superficial femoral vein, lying behind the artery, can be used as a guide to the position of the artery and spectral Doppler used to demonstrate the presence or absence of arterial flow. Echo-enhancing agents can be used if there is any continuing uncertainty concerning the patency of the artery.

There are three indirect signs of significant disease which might be apparent during the examination and which should prompt a careful review if a cause for these changes has not been identified.

1. Colour Doppler may show the presence of collateral vessels in the muscles of the thigh (Fig. 4.3a).
2. Collateral vessels may be seen leaving the main artery (Fig. 4.3b).
3. The character of the spectral waveform may show a change between two levels, indicating a segment of disease somewhere between the two points of measurement.

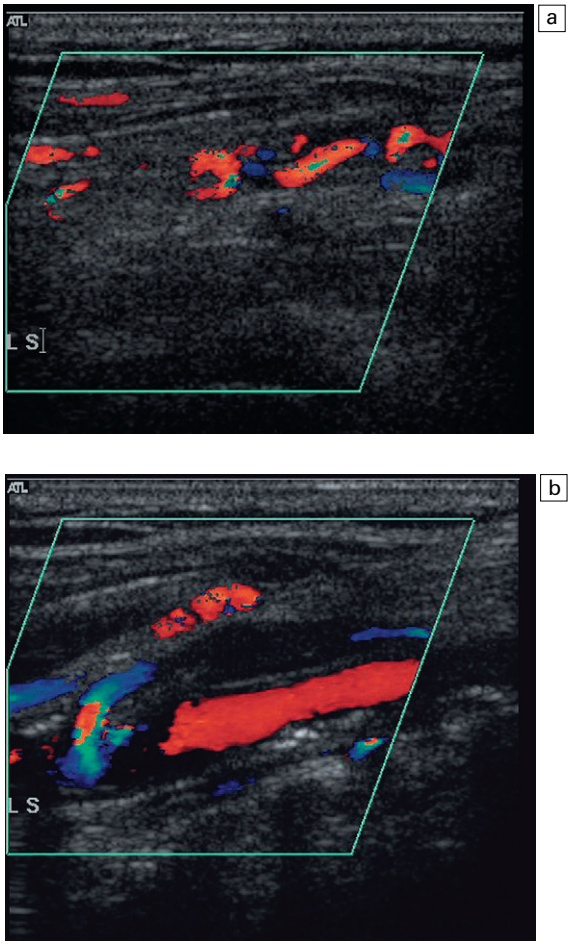


**Fig. 4.3** (a) Collateral vessels in the muscles of the thigh. (b) A larger collateral vessel joining the lower superficial femoral artery.

### *The adductor canal and popliteal fossa*

The patient is then turned into a lateral decubitus position so that the medial aspect of the leg being examined is uppermost (Fig. 4.4). This position is better than the prone position as it allows access in continuity to the lower superficial femoral artery, the adductor canal area, the popliteal region and the medial calf. The region of the adductor canal must be examined with great care as it is a site where a short-segment stenosis or occlusion may be present, and this section of the vessel can be difficult to visualise as it passes deep to the thigh muscles. In some cases the use of a lower scanning frequency may help in visualisation. The superficial femoral artery is examined as far down as it can be followed on the medial aspect of the thigh; the popliteal artery is then located in the popliteal fossa and followed superiorly. In difficult cases a mark can be put on the skin of the medial thigh to show the lowest segment of vessel visualised in the supine position; the popliteal artery is then followed superiorly in the decubitus position until the trans-

**Fig. 4.4** The position of the patient for examination of the adductor canal and popliteal fossa.

ducer reaches the level of the skin mark, ensuring that the vessel has been examined in continuity. The popliteal artery is then examined and followed down to the point of division into the tibioperoneal trunk and anterior tibial artery.

### *Calf arteries*

The complexity of the assessment of the calf arteries depends on the clinical situation. If the examination is to exclude significant proximal disease that would benefit from angioplasty or bypass grafts, then it is usually sufficient to assess the three calf arteries at the upper and mid-calf level, recording whether they are patent or not, in order to provide some assessment of the state of the distal run-off. In other cases a more detailed examination is required to clarify changes seen on MRA/arteriography, or if a distal insertion point for a bypass graft is being sought. The increased sensitivity of power Doppler is useful in detecting weak signals from small or diseased but patent vessels.

The posterior tibial artery is usually the easier of the two branches of the tibioperoneal trunk to locate. Often it can be located by placing the transducer in a longitudinal position on the medial aspect of the mid-calf area behind the tibia, using colour or power Doppler to show the course of the vessel, which can then be followed up and down the calf. In obese or oedematous legs, or if blood flow is impaired by disease, the posterior tibial artery and the other calf arteries may be difficult to locate. Scanning with colour Doppler in the transverse plane using some angulation towards the head or feet may show the relative positions of the posterior tibial and peroneal arteries. Alternatively, the associated veins can be used to identify the region of the relevant artery: squeezing the foot or lower calf will augment flow in the deep veins, allowing these to be identified in either a longitudinal or transverse scan plane. The posterior tibial artery can also be located as it passes behind the medial malleolus, where its position is constant, and then followed back up the leg.

The peroneal artery runs more deeply down the calf than the posterior tibial artery, lying closer to the posterior aspect of the tibia and the interosseous membrane. It can be examined from several approaches: firstly from a posteromedial approach similar to that used for the posterior tibial artery; secondly, it can often also be seen from the anterolateral approach used for the anterior tibial artery as it runs behind the interosseous membrane (Fig. 4.2); thirdly, a posterolateral approach may be of value in some cases.

The anterior tibial artery is examined from an anterolateral approach through the extensor muscles lying between the tibia and fibula. The two bones can be identified on transverse scanning and the interosseous membrane located passing between them. The anterior tibial artery lies on the membrane and can be located using colour Doppler in either the longitudinal or transverse plane. It usually lies nearer the fibula than the tibia (Fig. 4.2).

The foot vessels are not usually examined but the dorsalis pedis artery may be examined in front of the ankle joint before it passes deep to the

metatarsals; this is indicated if the artery is being considered for the insertion of a femorodistal graft.

The advent of power Doppler and echo-enhancing agents has extended the role of ultrasound in the assessment of vascular disease. In the proximal lower limb and iliac vessels, the location of the vessel and confirmation of occluded segments has been made easier and, in the distal part of the leg, they make assessment of the smaller vessels of the calf and foot easier. However, more work is required to evaluate further their role.[6]

### *Iliac arteries*

Examination of the iliac vessels is carried out as part of a general survey of the lower limb arteries, or if the clinical picture suggests a need to confirm or exclude disease affecting these vessels, or if the Doppler findings at the groin suggest the likelihood of significant proximal disease. The ease with which they can be visualised depends on the build of the patient and the amount of bowel gas present. It is usually necessary to use a 3–5 MHz transducer for satisfactory visualisation. Some examiners will prepare patients for iliac Doppler examinations with laxatives and low-residue diets if it is considered likely that these vessels will be examined, although most centres do not do this routinely. However, it is important not to make a false diagnosis of occlusion because the vessel is obscured by bowel gas.

The external iliac artery can be followed up from the groin for a variable distance; the vein, lying behind the artery, can be used to identify the probable location of the artery if this is not apparent. Colour or power Doppler may also help locate the vessel, even if it is not visible on the real-time scan image. Superiorly the common iliac artery can be identified arising from the aortic bifurcation and then followed distally. Firm pressure with the transducer will displace intervening amounts of bowel gas to a large extent, although care must be taken not to compress the artery and produce a false impression of a stenosis. The internal iliac artery may be seen arising from the common iliac artery and passing deeply into the pelvis. This is a useful landmark as visualisation of the internal iliac artery origin, on tracking both the external iliac artery upwards and the common iliac artery downwards, means that the iliac vessels have been examined in their entirety.

The orientation of the iliac vessels as they pass round the pelvis and the use of sector or curved-array transducers can lead to problems with beam–vessel geometry and obtaining satisfactory angles of insonation. However, careful attention to positioning the transducer will usually allow an appropriate angle to be obtained.

## Anatomy – upper limb

The subclavian arteries arise from the brachiocephalic trunk on the right and directly from the arch of the aorta on the left (Fig. 4.5); however, there is considerable normal variation in the patterns of their origination. The origin of the

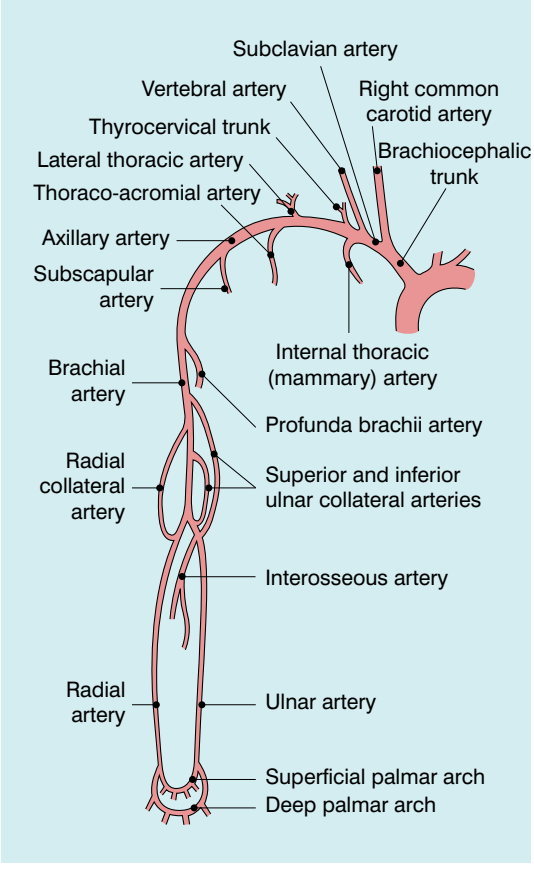


**Fig. 4.5** The upper limb arteries on the right.

right subclavian artery can be examined behind the right sternoclavicular joint, where the brachiocephalic trunk divides into the right common carotid artery and the subclavian artery. The origin of the left subclavian artery from the aortic arch cannot be demonstrated, although the more distal segments can be seen as on the right side. The subclavian artery on each side runs from its point of origin to the outer border of the first rib where it becomes the axillary artery; the subclavian vein lies in front of the artery. The main branches of the subclavian artery are the vertebral arteries, the thyrocervical trunk, the internal thoracic (mammary) artery and the costocervical trunk.

The *axillary artery* runs from the lateral border of the first rib to the outer, inferior margin of the pectoralis major muscle. It gives rise to several branches which supply the muscles around the shoulder; the largest of these are the thoracoacromial trunk, the lateral thoracic artery and the subscapular artery.

The *brachial artery* passes down the medial aspect of the upper arm to the cubital fossa below which it divides into the radial and ulnar arteries; the point of division sometimes lies higher in the upper arm. Apart from muscular branches, the main branches of the brachial artery are the profunda brachii artery, which is given off in the upper arm and passes behind the humerus; the superior and inferior ulnar collateral arteries arise from the lower part of the brachial artery. It divides into the ulnar and radial arteries in the antecubital fossa.

The *radial artery* runs down the radial (lateral) aspect of the forearm to the wrist, where it passes over the radial styloid process, and over the lateral aspect of the carpus. It then passes down through the first interosseous space to form the lateral aspect of the deep palmar arch. It also has a superficial branch which anastomoses with the equivalent branch of the ulnar artery to form the superficial palmar arch. In the upper forearm the radial artery gives off the radial recurrent artery, which anastomoses with the profunda brachii artery, and several muscular branches in the forearm and at the wrist.

The *ulnar artery* passes down the anterior ulnar (medial) aspect of the forearm to the medial aspect of the wrist, where it runs over the flexor retinaculum and then divides into superficial and deep branches which anastomose with the equivalent branches of the radial artery to form the superficial and deep palmar arches. It gives off recurrent ulnar arteries below the elbow and the common interosseous artery, which forms anterior and posterior divisions, running on either side of the interosseous membrane.

## Scanning technique – upper limb

A 7–12 MHz transducer may be used in most cases for examining the arteries in the upper limb, as there is less tissue to penetrate than in the leg. The patient lies in a supine position with their head turned away from the side being examined, the arm is abducted with the elbow flexed and the back of the hand resting on the pillow by the patient's head, so that the axilla and medial aspect of the upper arm can be examined. Alternatively, the arm can be abducted and supported on a suitable shelf, or by asking the patient to hold onto a suitable part of the ultrasound machine. The distal brachiocephalic artery on the right and the mid-subclavian artery on the left can be visualised from a supraclavicular approach by angling the transducer down towards the mediastinum from above the medial clavicle and sternoclavicular joint. The subclavian arteries on both sides are seen behind the subclavian vein as they run up to cross the first rib. In patients with possible arterial compression syndromes, the artery is examined with the arm in various positions so that any narrowing or occlusion may be demonstrated.

The artery beyond the first rib is best examined from below the clavicle and followed distally. It can be followed in continuity as it runs deep to the pectoralis muscles through the axilla and into the medial aspect of the upper arm; from here it can be tracked down to the cubital fossa. The division of the artery into the two main forearm branches usually occurs below the cubital fossa and each branch can be followed to the wrist; if either the radial or the ulnar artery is difficult to trace down from the elbow, then the vessel should be sought at the wrist and followed back up the forearm.

## ASSESSMENT OF DISEASE

The assessment of lower limb atheroma is more complex than for the carotids as the potential for collateral supply around stenoses or occlusions is very much greater. The distinction must be made between haemodynamically significant disease and clinically significant disease. Two individuals may have the same degree of stenosis in their superficial femoral artery, but an 80% diameter reduction which develops acutely will be significantly symptomatic, whereas the same degree of stenosis developing over a period of time, allowing collateral channels to open, may be much less disabling. The findings on Doppler must therefore not be considered in isolation but in the light of the full clinical picture.

Colour Doppler allows the rapid identification of normal and abnormal segments of vessel. In addition, some stenoses may show a colour Doppler tissue 'bruit' due to the tissue vibrations set up by the blood passing through the stenosis. It is valuable to relate the level of any diseased segments demonstrated on ultrasound to bony landmarks which can be seen on angiography; this allows the appearances on the two examinations to be compared and confirm that the abnormality on the arteriogram is at the level of the lesion seen on ultrasound or vice versa. The groin skin crease corresponds to the superior pubic ramus and can be used for lesions in the upper part of the thigh; the upper border of the patella can be used for lesions in the lower part of the thigh; and the tibiofemoral joint space for popliteal lesions.

Some patients will show extensive diffuse disease along much, or all, of the superficial femoral artery but do not show any specific, localised stenoses. It is important to note this appearance, as the overall haemodynamic effect may be severe enough to produce a significant pressure drop along the vessel, thereby reducing limb perfusion, although this pattern of disease is not suitable for angioplasty. Other patients may have several stenoses along the length of the vessel, each of which is not haemodynamically significant but the effects of these are additive, so that there is still a significant drop in perfusion pressure distal to the affected segment.[7]

In addition, the presence of serial stenoses can affect the estimation of the degree of a distal stenosis, if this is not recognised. A significant proximal stenosis or occlusion will result in a drop in perfusion pressure and velocity which makes application of the peak systolic velocity (PSV) and peak velocity ratios, the usual criteria for quantifying a stenosis, problematical.[8] Power Doppler and echo-enhancing agents may allow an estimate of severity but if there is clinical doubt, other imaging should be considered.

The same principles apply to the assessment of disease in the upper limb, but the type and distribution of disease in the arm is different from that seen in the leg. Ischaemic symptoms in the arm may be the result of compression, embolic occlusion, or vasospasm and are less frequently due to localised atheroma.

The main diagnostic criteria which are of value in the assessment of lower limb atheroma are direct measurement of the stenosis, PSV ratios and waveform changes.

### Direct measurement

Direct measurement of a stenosis is often quite difficult in the lower limb arteries as these are relatively small, and it may be difficult to see the lumen clearly in the deeper parts of the thigh, particularly if there is disease present. However, direct measurement of a stenosis may be possible in the lower external iliac, common femoral, profunda femoris and upper superficial femoral arteries. Measurement of the diameter reduction is performed after assessment of plaque distribution in both longitudinal and transverse planes, so that the most appropriate diameter is selected. When a segment of stenosis or occlusion is detected the length of the affected segment should be measured, as this will be relevant to the suitability of the lesion for angioplasty; segments of disease, particularly occlusions, longer than 10 cm will not normally be considered for percutaneous treatment.[9]

## Peak velocity ratios

Direct measurement of a stenosis is often not possible in the lower limb and the severity of the stenosis must then be estimated from the change in peak systolic velocity produced by the stenosis. Normal velocities in the lower limb arteries at rest are approximately 1.2 m $s^{-1}$ in the iliac segments, 0.9 m $s^{-1}$ in the superficial femoral segments and 0.7 m $s^{-1}$ in the popliteal segment.[10] Various criteria have been put forward for the quantification of lower limb arterial stenosis. Those of Cossman et al[11] have produced satisfactory results in the authors' department and have the advantage of being easy to remember (Table 4.3). These criteria are based on the PSV at the stenosis and the ratio of the PSV at the stenosis compared with the velocity 1–2 cm upstream in a non-diseased segment. Colour Doppler allows the position and direction of peak velocity flow in the stenosis to be identified and the sample volume can be placed appropriately, final adjustments of position being performed by listening to the pitch of the frequency shift as the sample volume is moved through the stenosis. A further velocity measurement is then made in a 'normal' segment of artery 1–2 cm upstream from the stenosis and the ratio calculated (Fig. 4.6).

## Waveform changes

The normal waveform in the main arteries of the resting lower limb has three components; four, or occasionally five, may be seen in fit young individuals. These represent the pressure changes which occur in the lower limb arteries during the cardiac cycle. First there is the rise in pressure and acceleration of blood flow at the onset of systole. There is then a short period of reversed flow as the pressure wave is reflected from the constricted distal arterioles. This is followed by a further period of forward flow produced by the elastic compliance of the main arteries in diastole (Fig. 4.7a). These changes are discussed in more detail in Chapter 2.

Exercise modifies this pattern by reducing the peripheral resistance. This results in the reversed component being lost and increased diastolic flow throughout the cardiac cycle (Fig. 4.7b). It is for this reason that ultrasound examination of the lower limb arteries should be performed in patients who have not had significant exercise of the leg muscles for about 15 min. Conversely, examination after exercise, or reactive hyperaemia, may be used in order to 'stress' the lower limb circulation and reveal stenoses which are not significant at rest, when blood flow is relatively low, but which become apparent with the higher volumes flowing when the distal circulation to the muscles opens up.[12]

Disease in the vessel at the point of measurement, above it or below it, can affect the waveform, and if the vessel cannot be visualised in continuity then a change in the waveform between two points is indicative of disease. The two main features which may be altered are the overall shape of the waveform and the degree of spectral broadening as a result of flow disturbance;[10] the major changes are shown in Table 4.4 and illus-

**Table 4.3** Velocity criteria for the assessment of lower limb stenoses

| Percentage stenosis | Peak systolic velocity (m $s^{-1}$) | Velocity ratio |
|---|---|---|
| Normal | <1.5 | <1.5:1 |
| 0–49 | 1.5–2.0 | 1.5–2:1 |
| 50–75 | 2.0–4.0 | 2–4:1 |
| >75 | >4.0 | >4:1 |
| Occlusion | – | – |

From Cossman et al.[11]

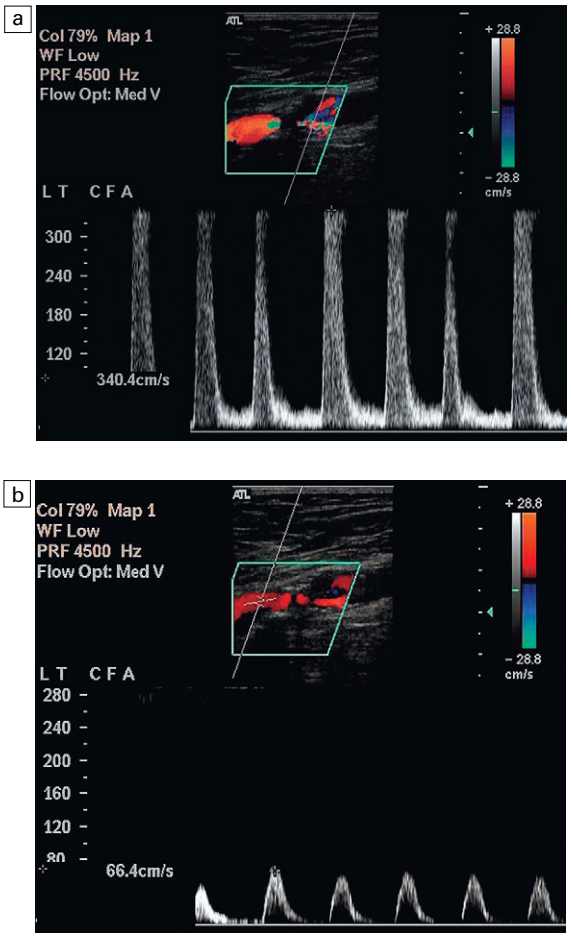


**Fig. 4.6** Measurement of the peak systolic velocity ratio at a stenosis. (a) Velocity at the stenosis is 3.4 m $s^{-1}$. (b) Velocity above the stenosis is 0.66 m $s^{-1}$, giving a ratio of approximately 5.

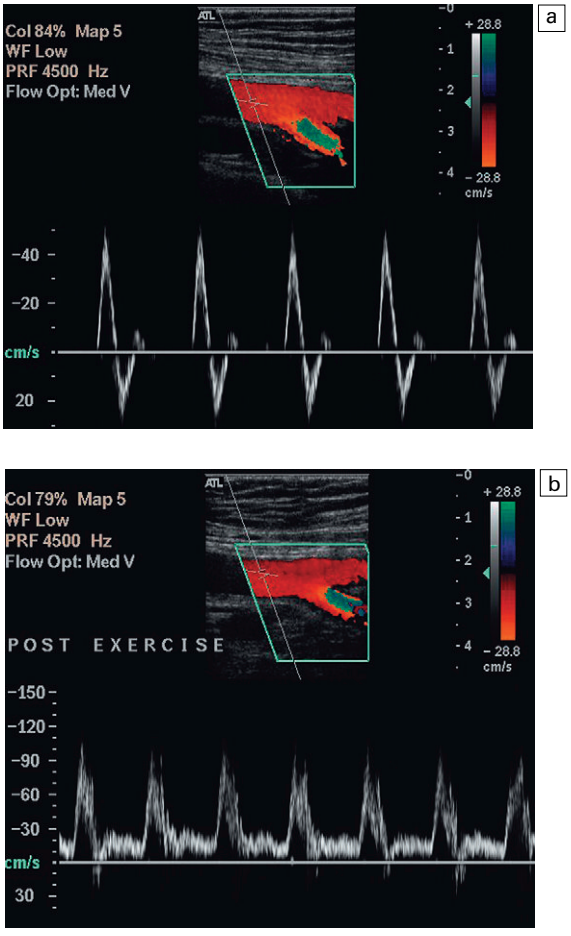


**Fig. 4.7** The normal femoral artery waveform. (a) In a limb at rest three components are visible. Aliasing in the profunda artery is due to the lower insonation angle giving a higher Doppler shift, not a focal stenosis. (b) Following exercise there is increased flow throughout diastole as a result of peripheral dilation.

trated in Fig. 4.8. Proximal disease above the point of measurement results in loss firstly of the third and then of the second components of the waveform, as the normal passage of the pressure wave along the artery is impaired. This interference with the passage of the pulse wave along the vessel is also manifest by the slowing of the systolic acceleration time. The width of the first, systolic complex is increased and the overall height is decreased. These changes result in 'damping' of the waveform, which is most marked when there is a proximal occlusion. The turbulence generated beyond a stenosis shows in the spectrum as spectral broadening and its presence therefore also indi-

**Table 4.4** Waveform changes associated with disease in the lower limb

- Loss of third and then second phase of the waveform
- Increased acceleration time
- Widening of the systolic complex
- Damping of the waveform
- Spectral broadening
- Absent flow in occlusion

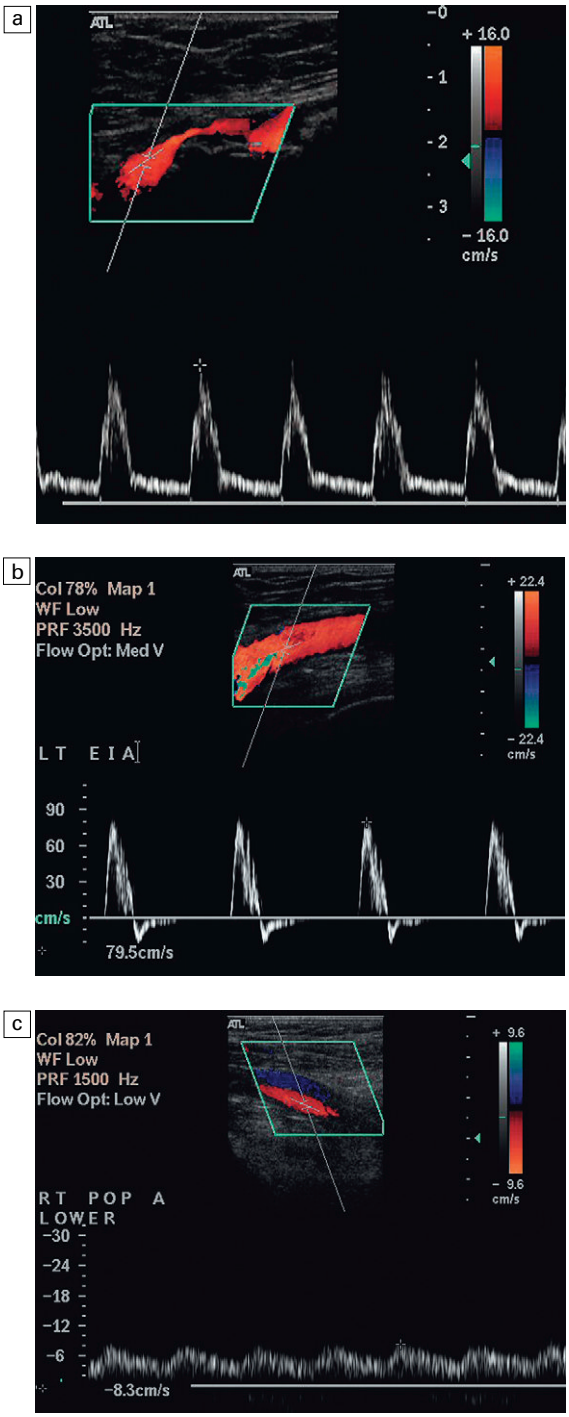


**Fig. 4.8** Abnormal lower limb artery waveforms. (a) Loss of reverse flow and diastolic flow due to distal disease producing peripheral dilatation; a large plaque impinges on the lumen. (b) Broadening of the waveform and turbulence secondary to a proximal stenosis. (c) Damped waveform in the popliteal artery secondary to a proximal occluded segment.

cates proximal disease, although not its severity, as mild turbulence may be due to a minor stenosis close by, or a more severe stenosis further away. The spectral broadening may be seen throughout the spectrum if the stenosis is close to the point of measurement; as the distance from the stenosis increases, the spectral broadening is seen in the postsystolic deceleration phase only. The disturbance of flow created by a stenosis may take several centimetres to resolve. The spectral broadening is lost and the systolic forward flow component is regained, but the reverse component and third component are much less likely to reappear distal to disease. In addition, if the distal limb is ischaemic, this will result in dilatation of the capillaries and increased flow throughout diastole. The presence of some, or all, of these changes requires that the vessel be carefully examined proximally to identify their source.

The presence of distal disease will also affect the waveform, resulting in increased pulsatility, with reduced diastolic flow, evident from the loss of the third component; in addition, the peak systolic velocity is reduced. This situation is most often seen at the origin of a superficial femoral artery with significant distal disease, although the precise changes are variable, depending on the degree of obstruction and the capacity of any collateral channels.[13]

## Assessment of aortoiliac disease

The clinical findings, or the appearances of the waveform at the groin, may suggest the presence of significant disease in the aortoiliac segments.[14] The best method for assessment of these segments is by direct visualisation with colour Doppler and measurement of velocities as for the leg vessels. Satisfactory examinations have been reported in up to 90% of cases with careful scanning and preparation.[15] However, even if adequate direct visualisation is not achieved, the likelihood of significant proximal disease should be noted and, depending on the clinical severity, it can be assessed further using MRA, or by arteriography, if necessary. The main indirect indicators of significant iliac artery disease are spectral broadening, due to the turbulence set up by the stenosis, and

widening of the systolic complex as a result of the stenosis slowing the systolic acceleration. As noted earlier, power Doppler and echo-enhancing agents show promise in improving visualisation and assessment using ultrasound.[6]

### Reporting the examination

The findings from a Doppler examination of the peripheral arteries are best reported on a diagram of the relevant arterial tree. The level and extent of any stenoses can be indicated on this, together with blood flow velocities at areas of stenosis and the standard sites of measurement. Non-visualised areas should also be indicated. For patients with bypass grafts, the location of the graft can be sketched in and relevant velocities indicated.

## ARTERIAL BYPASS GRAFTS

A variety of bypass grafts may be employed to alleviate ischaemic symptoms (Table 4.5). Autologous vein is the preferred material and usually the long saphenous vein is used, although other veins may occasionally be employed. Synthetic materials [polytetrafluoroethylene (PTFE) or Dacron] may be used if the long saphenous veins are unsuitable or unavailable. Infrainguinal femorodistal grafts are the commonest type of procedure; several problems may occur which result in graft failure (Table 4.6) and it has been shown that a programme of graft surveillance in the postoperative period can reduce the number of failed grafts.[16]

**Table 4.5** Types of bypass graft

| |
|---|
| **Types of graft** |
| Femoropopliteal – may arise from external iliac artery rather than common femoral artery |
| Femorodistal – to calf vessels or dorsalis pedis |
| Femorofemoral crossover |
| Iliofemoral |
| Axillofemoral |
| **Materials used for graft** |
| Vein |
| In situ vein |
| Reversed vein |
| Synthetic |
| Polytetrafluoroethylene (PTFE) |
| Gore-Tex |

The timing of graft failure is related to the cause of the problem. Failures occurring within 6–8 weeks of surgery are usually due to technical problems arising from the surgery; 3–5% of grafts fail at this stage, approximately 25% of all graft failures. Failures developing in the period beginning 3 months and extending to 2 years after surgery are usually due to neointimal hyperplasia; 12–37% of grafts fail during this period, approximately 70–80% of all graft failures; most of these will occur in the first 12 months. Beyond 2 years after surgery the usual cause of failure is progression of atherosclerosis, either in the native vessels or in the graft itself.[17] In addition to graft

**Table 4.6** Causes of graft failure

| Intrinsic | Extrinsic |
|---|---|
| Stenosis | Inflow disease progression |
| Proximal or distal anastomosis | Outflow disease progression |
| Mid-graft | Clamp injury |
| Diffuse myointimal hyperplasia | Thromboembolism |
| | Hypercoagulation states |
| Aneurysm | Sepsis |
| Anastomotic | |
| Mid-graft | |

Haemodynamic failure occurs when the graft is patent but the limb remains ischaemic

stenosis or occlusions other problems may occur, including dehiscence at the origin or insertion and false aneurysm formation, arteriovenous fistulae, infected collections and compression or kinking.

The timing of the surveillance scans is based on this time scale for problems. An early scan 4–6 weeks after the operation is performed, subsequently a scan is done at 3 months and then at 3-monthly intervals until the end of the first year. It is not usually necessary to continue beyond this if no cause for concern exists, as the majority of failures will occur in the first year. However, if there are particular reasons for concern, such as mild or moderate stenosis (velocity ratio <2), then surveillance can be extended as appropriate. Surveillance programmes have been shown to be beneficial for in terms of enhanced graft patency and limb survival rates.[16,18] One study followed grafts in 259 legs for up to 10 years and demonstrated 87.4% patency and 88.7% limb salvage rates 5 years after the original operation; 10 years after the operation the equivalent figures were 80.4% patency and 75.4% limb salvage.[19] The situation is less clear cut for synthetic grafts. Whilst some authors suggest that surveillance of synthetic grafts is beneficial,[20] other authors have found that synthetic grafts are more likely to fail without warning signs being demonstrated on Doppler.[21, 22] Symptomatic grafts should always be examined, as a treatable lesion may be demonstrated prior to complete graft thrombosis and failure.

## Technique of examination

It is of value if the request for a graft assessment gives details of the surgery and the type of graft inserted; ideally, a diagram of the course of the graft should be provided. The examination should begin at the groin and the graft located; transverse scanning is helpful with identification of the graft origin. Once located the graft should be followed up to its point of origin from the native artery. The majority of grafts are femoropopliteal and run from the common femoral artery, or lower external iliac artery, to the upper or lower popliteal artery; occasionally the graft may originate from deeper in the pelvis, lower down the superficial femoral artery, or from the profunda femoris artery. The native artery above the graft is assessed and the velocity of blood flow measured with spectral Doppler. The origin of the graft is then examined carefully and any increase in velocity, or disturbance of flow, noted (Fig. 4.9).

The graft is followed down the length of the thigh. Most grafts run along the medial aspect of the thigh; however some grafts, particularly repeat grafts, may follow unusual courses, even crossing the thigh to run down the lateral aspect of the leg. Velocity measurements are obtained at any point of disturbed flow; if no disturbance is present, two to three velocity measurements are taken along the length of the graft to ensure that there is satisfactory flow.

At the graft insertion, the flow above, at and below the anastomosis is examined, any significant changes in the velocities should be assessed as possible signs of stenosis. Some care must be taken in the interpretation of velocity increases at both the origin and insertion of grafts, as moderate changes may be the result of disparity in size between the graft and the native vessel and therefore not pathological in origin, particularly at the distal insertion, if this is into a relatively small calf artery or the dorsalis pedis artery.

Synthetic grafts are relatively straightforward to assess, as any problems usually occur at the origin or insertion, rather than along the length of the graft. Vein grafts, however, can develop problems at any point along their length, particu-

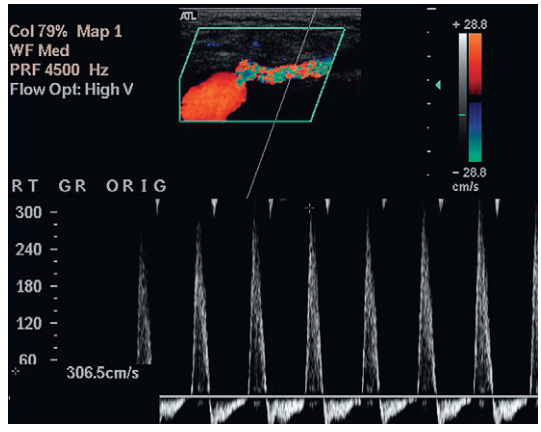


**Fig. 4.9** Origin of a femoropopliteal bypass graft with a high velocity of 3.27 m $s^{-1}$.

larly at sites of avulsed valves or tied perforating veins. Stenoses can occur secondary to surgery, or as a result of intimal hyperplasia, which can be stimulated by the turbulence at an irregularity in the vein wall. In situ vein grafts may also have persistent arteriovenous communications if a perforating or superficial communicating vein has been overlooked during the operation. These may be quite small but their presence should be suspected if there is a rapid, unexplained drop in velocity along the graft, or if pulsatile venous flow is seen in the common or superficial femoral veins. Scanning transversely along the line of the in situ graft makes it easier to identify these communicating vessels and demonstrate their course.

A note should also be made of any collections seen along the track of the graft. In the postoperative period these are usually small collections of serous fluid, haematomas, or small lymphoceles; normally these resorb over a few weeks (Fig. 4.10a). If infection is suspected (Fig. 4.10b) then a fine needle (20–22G) can be used to perform a diagnostic aspiration, although care should be taken not to introduce infection into a sterile collection.

If an occluded graft is demonstrated but the leg is asymptomatic then it is worth checking if the patient has had more than one bypass procedure, as a second, patent graft may be present elsewhere in the leg.

Other bypass procedures that may be performed include aortoexternal iliac/femoral grafts, axillofemoral grafts, femorofemoral (crossover) grafts. These use synthetic grafts and do not usually enter into graft surveillance programmes, although an ultrasound scan may be requested if there are clinical concerns. Distal lower limb grafts to the lower calf arteries, or dorsalis pedis artery are also performed.

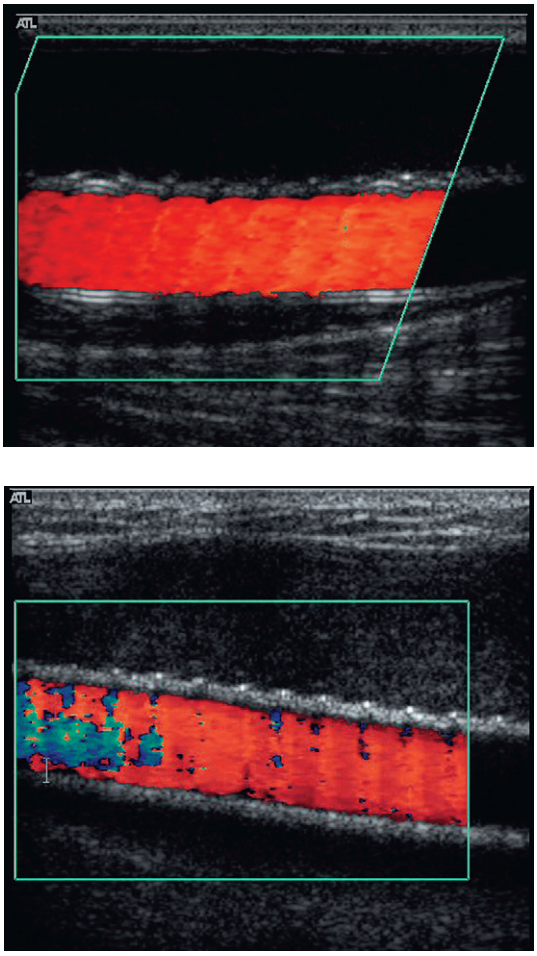


**Fig. 4.10** (a) A small trans-sonic lymphocoele around a femoropopliteal bypass graft; (b) an infected fluid collection around a synthetic graft showing low level echoes within the fluid.

**Table 4.7** Doppler criteria for graft stenosis and grafts at risk

| | |
|---|---|
| Direct measurement of stenosis | Moderate >50% diameter stenosis<br>Severe >70% diameter stenosis |
| Peak systolic velocity changes | >1.5 m $s^{-1}$ = 50–70% diameter stenosis<br>>2.5 m $s^{-1}$ >70% diameter stenosis |
| End diastolic velocity | >1.0 m $s^{-1}$ >70% diameter stenosis |
| Velocity ratio | >2.5 >50% diameter stenosis<br>>3.5 >70% diameter stenosis |
| Peak systolic velocity | <50 cm $s^{-1}$ in narrowest segment |

## Features of a graft at risk

The main features which suggest that a graft is at risk of failing are shown in Table 4.7. There is good correlation between these criteria and the incidence of subsequent graft failure. The finding of a fall in the ankle/brachial pressure index of more than 0.15 in addition to the presence of a stenosis of more than 70%, or low mean graft velocity, is a strong indicator of a graft at risk.[16] Gibson et al[23] found that there was a significantly higher incidence of graft failure if there was a graft related stenosis with a velocity ratio >3.5 and a mean graft PSV of <50 cm $s^{-1}$, calculated from velocities obtained at non-stenotic points along the length of the graft. However, they found that a low mean graft velocity by itself without an associated stenosis was not associated with graft failure.

Other abnormalities which may be seen in relation to a bypass graft are a false aneurysm at the origin or insertion due to dehiscence of the anastomosis (Fig. 4.11), or an arteriovenous fistula.

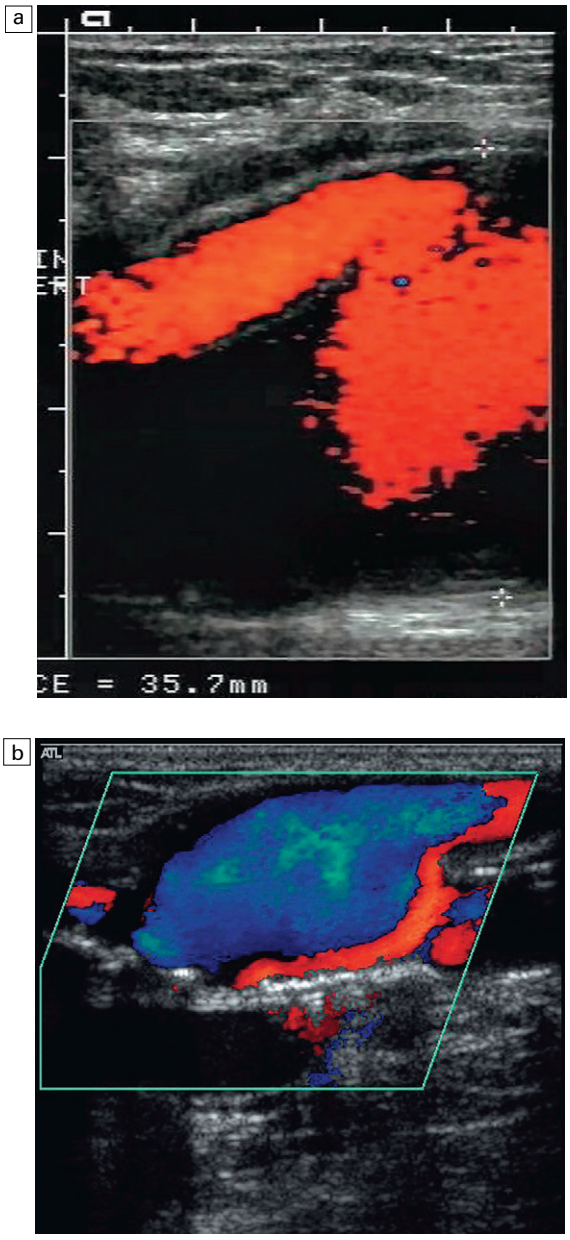


**Fig. 4.11** (a) Dehiscence at the insertion of a graft into the lower popliteal artery; (b) aneurysmal dilatation at the origin of a by pass graft.

## DIALYSIS SHUNTS

Various types of arteriovenous communication may be fashioned to allow for haemodialysis; these are usually in the arm but if no suitable vessels are available the leg may be used (Fig. 4.12). Colour Doppler can be used to examine the supplying artery, the anastomosis, or any interposed venous or synthetic grafts, and the draining veins.[24] Dialysis shunt function is normally monitored by assessing performance during dialysis. The main indications for examining a dialysis fistula are when a shunt which has previously been functioning satisfactorily starts to malfunction, or when a recently created shunt does not seem to be maturing adequately.

In grafts which are not functioning well it should be remembered that problems can occur with the artery anywhere along its length, at the anastomosis, in the vein distal to the anastomosis in the region where dialysis needles are inserted, or in the veins proximally around the groin or clavicle.[25]

### Technique

The examination of upper limb arteriovenous dialysis fistulae begins with the axillary or upper brachial artery, which is then followed with colour Doppler distally until the anastomosis with the vein or graft is identified. The region of the anastomosis is then examined carefully for any evidence

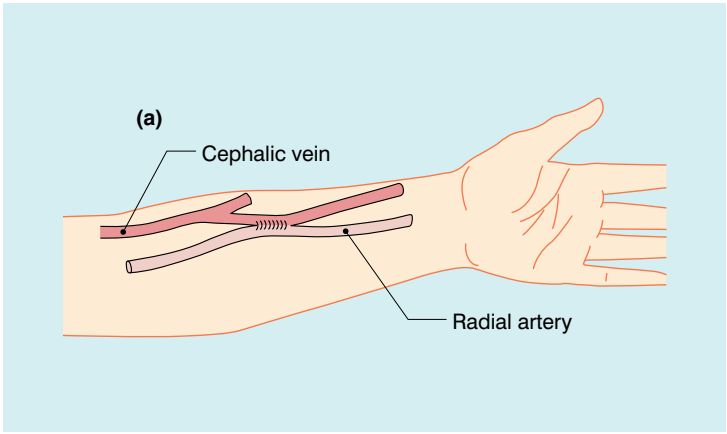


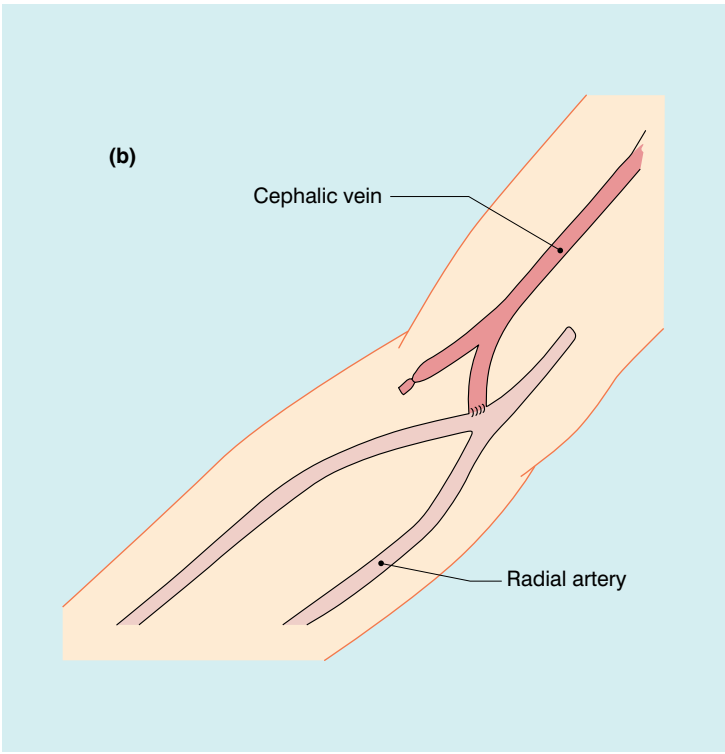


**Fig. 4.12** Diagrams of the different types of arteriovenous fistulae used for dialysis. (a) Radiocephalic anastomosis; (b) brachiocephalic anastomosis;

of stenosis. The amount of flow through such a fistula is normally sufficiently high and turbulent to produce tissue vibrations, which may obscure the lumen but an increase in velocity of two to three times the brachial arterial velocity does not mean that there is a haemodynamically significant stenosis. If the tissue bruit is a problem, making sure that transducer pressure is minimal, and therefore not producing any venous compression, may reduce this visible tissue vibration. Alternatively, gentle compression of the brachial artery with a pressure cuff or manual pressure may reduce flow sufficiently for the tissue vibrations to be reduced and allow visualisation of the vessel and anastomosis.

The venous drainage is then followed back up the arm to the subclavian vein; normally there is a dominant draining vein but several veins may contribute to the drainage of the fistula and each must be followed proximally. If a stenosis is

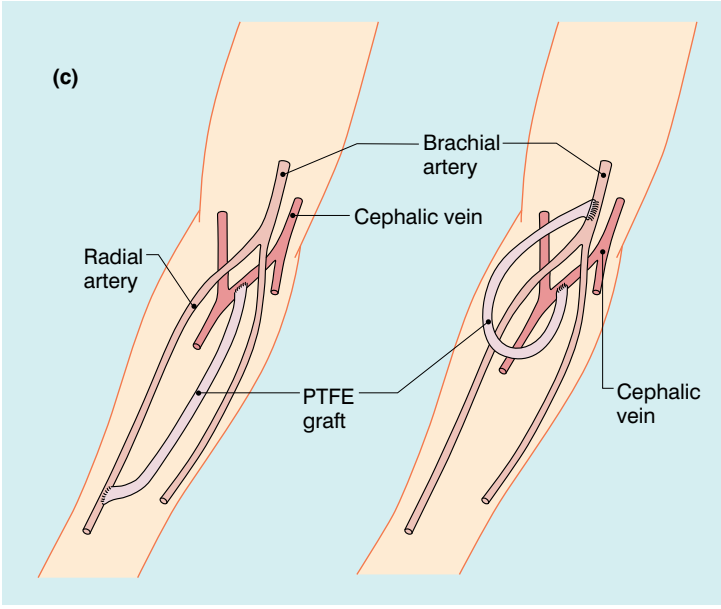


**Fig. 4.12** cont'd (c) two types of fistulae using a synthetic PTFE graft.

suspected on the venous side, then the veins should be examined carefully, making sure that transducer pressure is as light as possible to ensure that inadvertent compression is not responsible for any narrowing which may be demonstrated. There may be a physiological increase in venous velocity as the vein passes through clavipectoral fascia and careful assessment of this region should be carried out if venous problems are suspected.

## Stenosis

A stenotic lesion may affect a dialysis fistula on the arterial side, at the anastomosis, or on the venous side. The criteria used for lower limb arterial lesions do not apply in these circumstances, as flow velocities are generally high with inherent turbulence in the presence of a fistula and visible tissue 'bruits' can occur in the absence of a physiologically significant stenosis. Flow at the arteriovenous anastomosis may be very turbulent and a doubling in velocity at this point does not necessarily mean that there is a haemodynamically significant stenosis present. However, a sudden increase in velocity in the venous limb of the fistula should be assessed carefully, as this may well represent a significant stenosis; Robbin et al[26] showed that a focal increase in PSV ratio of 3 was associated with a 75% stenosis, as demonstrated on arteriography. Ultrasound depicted 92% of significant stenoses, whereas graft volume flow and the resistive index did not correlate with the presence of stenosis. Other workers have suggested a velocity >4 m $s^{-1}$ as a marker of a significant stenosis at an arteriovenous anastomosis.[24] It should also be recognised that a significant stenosis in the artery or at the anastomosis may result in a fall in the velocity and volume of blood flowing along the venous side of the fistula.

Apart from stenosis affecting the inflow, outflow, or anastomosis, other problems which may be identified in relation to dialysis fistulae are true or false aneurysms at the sites of needle insertion, haematomas and abscesses; these result from the repeated trauma of cannulation. Segmental thrombosis may occur on the venous side and complete thrombosis of the fistula may occur, usually affecting the venous rather than the arterial side.

## Fistula steal syndrome

The low resistance of the fistula means that flow to the distal parts of the limb may be impaired if too much blood is diverted through the arteriovenous anastomosis. This is not normally a problem but coexistent arterial disease in the limb arteries above or below the anastomosis can result in significantly impaired perfusion pressure

distally. In one study[27] 10 of 212 patients (8.3%) had signs and symptoms of steal syndrome; this was attributed to stenosis of the inflow arteries in five cases, excessive fistula flow in two cases, arterial disease distal to the anastomosis in two cases, and no attributable cause was found in the remaining patient. Steal syndromes should be assessed by examining the limb arteries above and below the anastomosis to identify any significant stenoses. In patients with excessive flow in a radial artery fistula, antegrade flow may be seen in the ulnar artery but retrograde flow is seen in the distal radial artery as this is reversed with collateral flow through the palmar arches feeding the fistula.[24] Compressing the venous side of the fistula will reduce any excessive fistula flow and if this results in a significant increase in distal flow then it is likely that flow reduction surgery to the fistula will be beneficial. Significant inflow stenoses may benefit from angioplasty.

### Volume flow in the fistula

The assessment of volume blood flow using Doppler ultrasound is beset by various inherent problems which result in a wide standard deviation for most flow measurements, as discussed in Chapter 1. However it is possible to measure dialysis fistula flow sufficiently accurately to divide it into three broad groups: <200 mL $min^{-1}$, which is inadequate for dialysis; 200–800 mL $min^{-1}$, which is satisfactory; and >800 mL $min^{-1}$, which is excessive and may be associated with high cardiac output problems at rates over 1400–1600 mL $min^{-1}$ depending on the cardiac reserve of the patient. A fistula flow rate of at least 200 mL $min^{-1}$ is required for adequate dialysis, ideally rates of 300–400 mL $min^{-1}$ are desirable. Some patients may tolerate flow rates in excess of 1000 mL $min^{-1}$ but others will start to show signs of cardiac decompensation at and above this level of flow.[28] In synthetic PTFE fistulae, flow rates less than 500 mL $min^{-1}$ are associated with a significantly higher risk of failure.[24]

The venous side of the fistula may show branching into two or more venous channels; one of these is usually dominant and used for dialysis needle puncture. However, the multiplicity of venous channels, together with the turbulence of flow, can make assessment of fistula flow volume difficult to estimate on the venous side.[24] On the arterial side it is reasonable to assume that the greatest proportion of blood in the supplying brachial or radial artery will go through the fistula when the arm is in the resting state, and therefore to estimate the blood flow volume in the fistula from the supplying artery. If necessary the distal arterial supply can be occluded with a pressure cuff.

Techniques for measuring volume flow have been discussed in Chapter 1. The most straightforward method for estimating volume flow is by multiplying the time-averaged mean velocity in the vessel by the cross-sectional area at the point of measurement. Three aspects of technique should be remembered: the time-averaged mean velocity must be measured, not the time-averaged maximum velocity; the sample volume for the velocity measurement should encompass the complete cross-section of the vessel; and the cross-sectional area should be measured at right angles to the long axis of the vessel in order to obtain the best estimate of volume flow. If the system calculates the cross-sectional area from the diameter of the artery, then this must also be measured at right angles to the long axis of the artery (Fig. 4.13).

## FALSE ANEURYSMS

These are usually straightforward to diagnose on colour Doppler ultrasound, although occasionally there may be some difficulty if there is also a large haematoma present. The incidence of femoral false aneurysms is increasing as more and more interventional procedures are carried out through femoral puncture sites; rates of 0.2–0.5% after diagnostic arteriography and 2–8% following coronary artery angioplasty and stent placement have been reported.[29] The characteristic appearance is a hypoechoic area which shows swirling blood flow on colour Doppler (Fig. 4.14a). It is important that the relationship of the aneurysm to the femoral artery is identified to ensure that any therapeutic thrombin injection is made into the aneurysm and not the artery. This may be

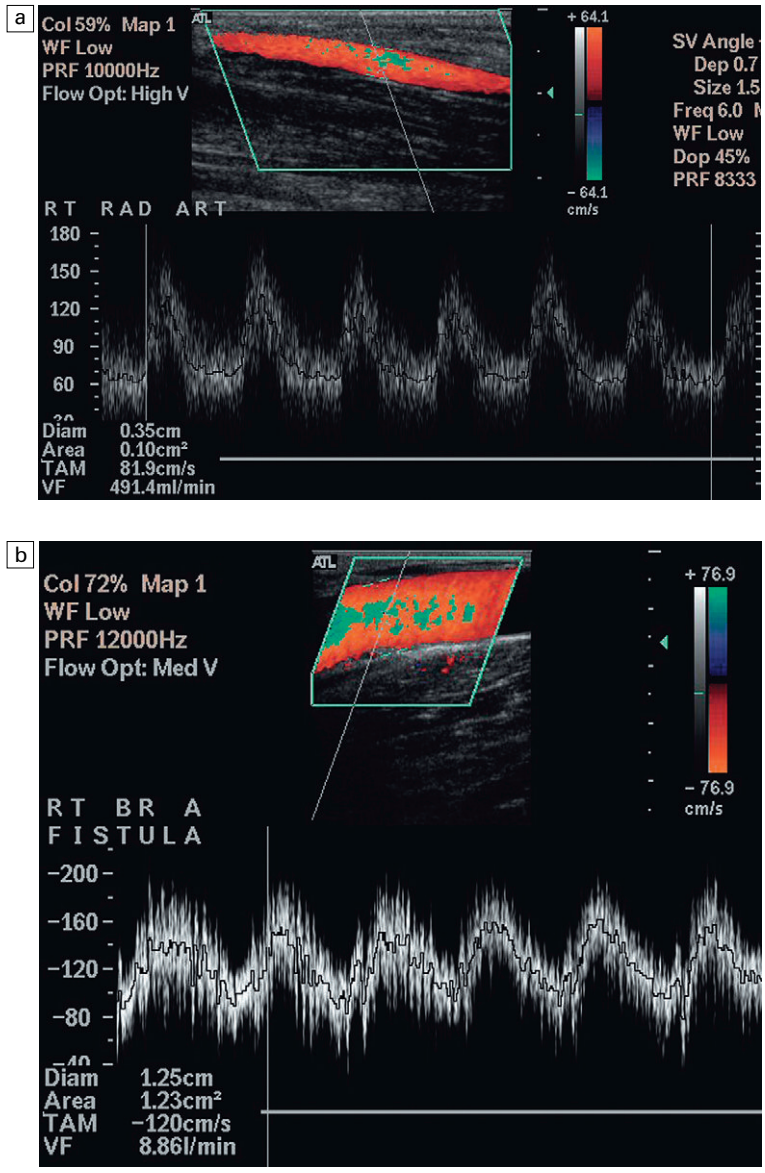


**Fig. 4.13** Estimation of dialysis fistula flow volume. (a) Flow in the radial artery above the fistula is estimated at 491 mL $min^{-1}$. (b) Another patient with a large artery and excessive flow of 8.8 L $min^{-1}$.

difficult to define in the presence of a significant haematoma; in these cases identification of the artery above and below the haematoma and tracking back to the aneurysm area will allow some assessment of the relationships to be reached. Spectral Doppler of the track between the artery and the aneurysm, or at the aneurysm neck, shows a characteristic 'to-and-fro' flow signal as blood flows in during systole and out during diastole (Fig. 4.14b). Rarely, a false aneurysm may be associated with an arteriovenous fistula passing from the cavity to an adjacent vein. The clue to the presence of the fistula is the loss of the 'to-and-fro' flow in the track from the artery, with only forward flow being shown which increases towards end-diastole. The need for intervention to treat a false aneurysm needs careful consideration: thrombin injection, surgery and possibly ultrasound guided compression are all recognised treatments but it should be remembered that a significant proportion of pseudoaneurysms will thrombose spontaneously within 2–3 weeks; in one surgical series, 86% of 147 patients managed conservatively showed spontaneous thrombosis

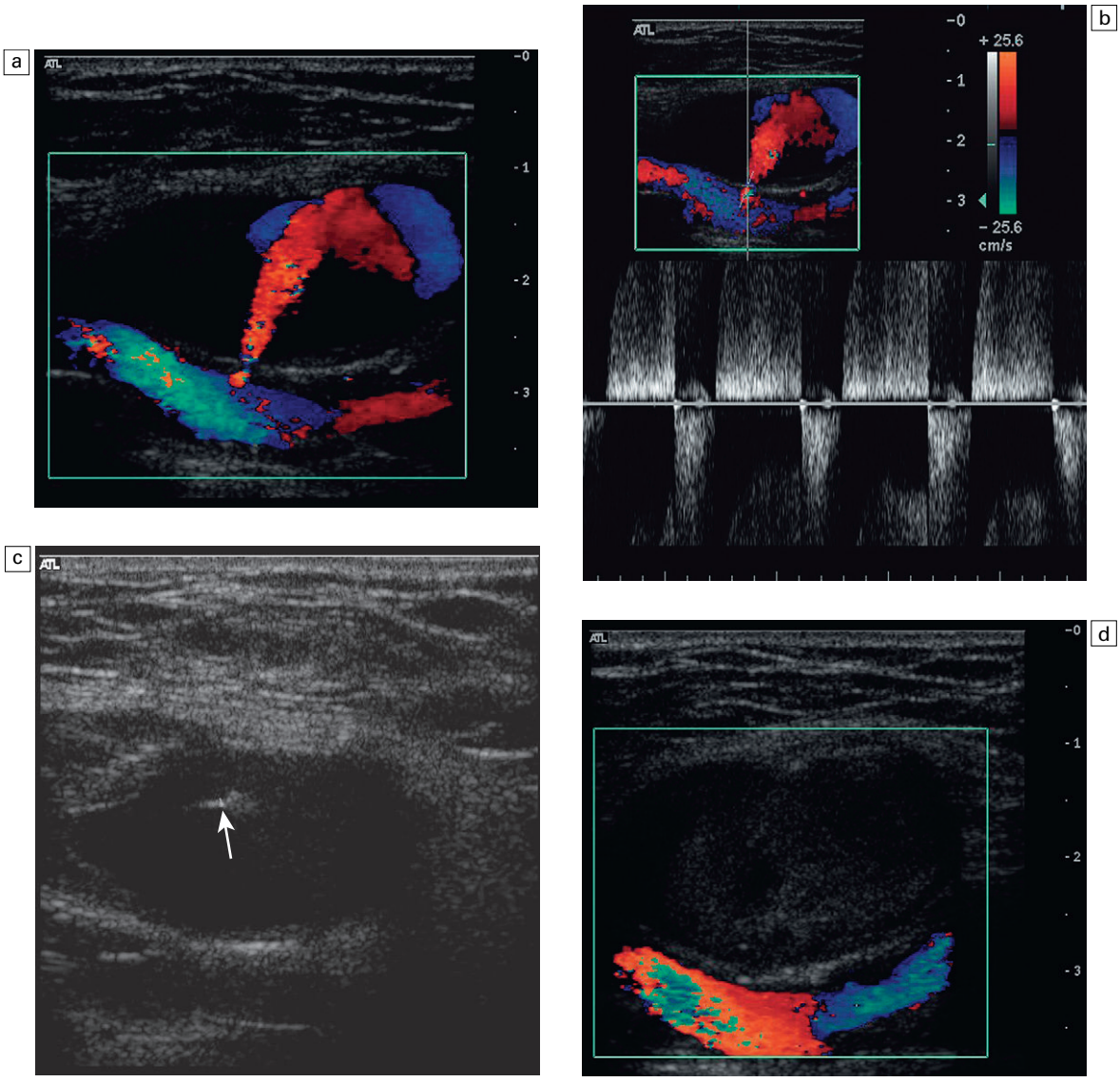


**Fig. 4.14** (a) A false aneurysm showing a patent lumen on colour Doppler; (b) the characteristic 'to-and-fro' flow on spectral Doppler; (c) tip of the needle for thrombin injection seen within the false aneurysm; (d) thrombosed false aneurysm following treatment with thrombin.

of their false aneurysms, or arteriovenous fistulae, within a mean period of 23 days.[30]

## Ultrasound-guided treatment of false aneurysms

### *Thrombin injection*

Bovine thrombin and, more recently, human thrombin are now available in many centres and the treatment of choice for most false aneurysms is injection of human thrombin directly into the aneurysmal sac under ultrasound control. In the great majority of cases, this will produce immediate and complete thrombosis of the false aneurysm within a few seconds. When the needle tip is positively identified within the aneurysm (Fig. 4.14c.), the thrombin solution is injected into the lumen of the aneurysm through a 22–25G needle attached to an insulin type of syringe (1 mL) to allow careful titration of the amount injected; normally 400–1000 IU of thrombin will be

sufficient to produce thrombosis within 20–30 s (Fig. 4.14d). Following the procedure the patient should stay on bed rest for 1–3 h with regular review of the distal circulation in the affected limb and most centres undertake a check ultrasound examination at 24 h. In some cases a small residual region of continuing flow may require a second injection. One study of 101 false aneurysms showed 95% primary success rate after a single injection and 98% after a second injection in three cases; only two patients required surgical repair.[29] Sheiman et al[31] looked at the reasons for failure in a small series of false aneurysms undergoing thrombin injection; they found that arterial laceration of >8 mm was the cause of failure in four out of five cases and local infection the most likely cause in the remaining patient.

Bovine thrombin may produce allergic responses in the patient and induce antibodies to native clotting factors; therefore, it is better to use human-derived thrombin if this is available. Contraindications to thrombin injection include ischaemic skin changes over a large aneurysm, local infection, evidence of nerve compression, or evidence of an arteriovenous fistula. Thrombin injection is reported to have worked satisfactorily after failed compression therapy in patients on full antiplatelet and anticoagulation therapy.[32]

There have been reports of the successful treatment of false aneurysms in other sites by thrombin injection; these include aneurysms in relation to haemodialysis access sites, an anterior tibial artery pseudoaneurysm that developed after a tibial osteotomy and a common carotid artery pseudoaneurysm that developed following an unsuccessful central venous line insertion.[33, 34]

### *Ultrasound guided compression*

If suitable thrombin preparations are not available, then treatment of false aneurysms using ultrasound-guided compression might be considered. The ability of colour Doppler to demonstrate flowing blood in the aneurysm and track allows the operator to apply graded compression using pressure from the transducer, so that flow into the aneurysm is stopped, whilst allowing flow to continue down the native artery. This allows the aneurysm and track to thrombose and therefore remove the need for surgery.[35] There are, however, some circumstances where it is recognised that compression is unlikely to succeed and direct referral for surgery should be considered; these are shown in Table 4.8. The most common contraindications for compression are the age of the aneurysm and warfarin therapy; if it has been present for more than 7–10 days then the track will have started to develop an endothelium and the surrounding tissues are less compliant, so that adequate compression becomes difficult.

The procedure is quite time consuming for the operator and uncomfortable for the patient, so it is better to give some analgesia to the patient prior to the commencement of prolonged compression. The aneurysm and its track are identified and compression is applied by pressing the transducer increasingly firmly down on these until flow in them has ceased but flow is still present in the native artery. This degree of pressure is then maintained for 10–15 min before being released slowly. If flow is then seen in the lumen, compression is reinstated for a further period of 10 min before again gently relaxing the pressure. These cycles of compression and relaxation are repeated until all flow in the aneurysm lumen has stopped. Usually the lumen of the aneurysm thromboses in an irregular fashion from the outside inwards, until complete obliteration is achieved. In one large series,[35] the average time for successful treatment of a simple unilocular aneurysm was 43 min (SD ± 40 min) and 69 min (SD ± 54 min) for complex multiloculated lesions. Another large series showed a 72% primary success rate using compression in 297 false

**Table 4.8** Circumstances when compression of a false aneurysm is less likely to succeed

- Aneurysms more than 7–10 days old
- Associated infection
- Severe pain/discomfort
- Large haematoma
- Aneurysms above the inguinal ligament

aneurysms, 7/12 patients who underwent a second compression episode had successful occlusion giving a secondary success rate of 74%.[36] Following successful obliteration the patient is scanned after 24 h to confirm that the aneurysm remains occluded (Fig. 4.14d). Some operators prefer to dispense with transducer compression and use manual compression with their fingers or a fist pressing over the site of the false aneurysm and its neck; ultrasound is used intermittently to assess the development of thrombosis. A variety of mechanical compression devices have also been proposed but results with these are variable.

## Other pulsatile masses

### *Aneurysms*

Aneurysms of the lower limb arteries may occur in isolation, or as multiple lesions. They are more common in the popliteal arteries but may be found elsewhere in the legs or, more rarely in the upper limb arteries.[37] As with aortic aneurysms they can enlarge over a period of time; their size and rate of enlargement can be followed with ultrasound. Their main clinical significance is that they can act as a source of emboli to the distal lower limb, or may thrombose leading to acute ischaemia.

### *Cystic adventitial disease*

This is a rare condition in which fluid-filled cysts are found in the wall of the artery, usually the popliteal artery, or superficial femoral artery in the adductor canal. The aetiology of these cysts is unclear and various theories, including repeated trauma, ectopic synovial tissue, or a congenital abnormality linking the cyst to the adjacent knee joint space or to adjacent tendons, have been proposed.[38] Signs and symptoms of ischaemia can be variable and confusing.[39] Ultrasound is useful in diagnosis as it will show the narrowing of the lumen, together with the associated cystic lesion producing the stenosis (Fig. 4.15).[40]

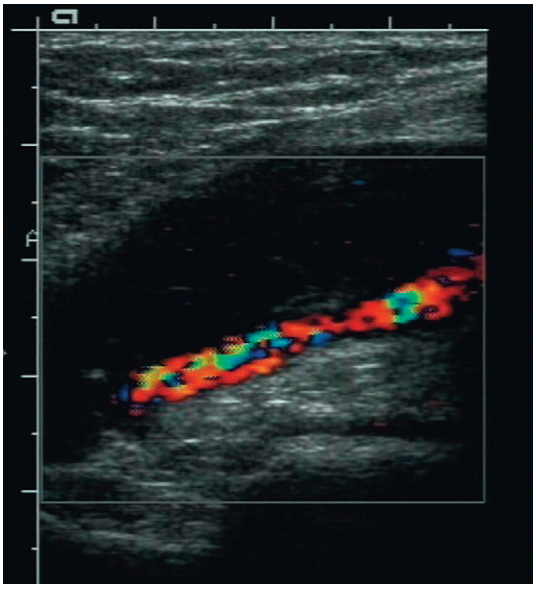

**Fig. 4.15** Cystic adventitial disease of the popliteal artery. The cystic component is seen above the patent lumen.

# BRACHIAL COMPRESSION SYNDROMES

Thoracic outlet syndrome, or compression of the subclavian artery as it crosses the first rib, may be due to congenital fibrotic bands at the insertions of the anterior and middle scalene muscles, or to compression associated with a cervical rib. The accompanying vein is also usually affected. Some degree of compression may be seen in up to 20% of normal subjects.[41] The compression is often positional, typically occurring when the arm is elevated above the head, so various positions of the arm and shoulder may need to be assessed. Sometimes the symptoms only occur with the patient in a particular position such as standing or lying down. Usually the diagnosis is straightforward on clinical grounds, with the pulse in the affected arm disappearing when the arm is in the appropriate position. However, in some cases the diagnosis, or the cause, is less clear cut and colour Doppler can be used to image the subclavian artery as the arm is moved into various positions with the patient supine or erect. The transducer is usually placed in the supraclavicular position but scanning under the clavicle may be useful, particularly when the arm is fully elevated. Careful examination of the artery as it passes over the first rib may show changes in the waveform as the vessel is compressed (Fig. 4.16).

Sometimes access to the subclavian artery in the region of the first rib can be difficult. In these cases, scanning the axillary artery whilst the arm is put in different positions will show any changes in velocity or waveform resulting from arterial compression. A rebound increase in velocity may be noted in the distal arteries on release of compression.[42]

### Popliteal artery compression

In cases of suspected entrapment of an artery or graft in the adductor canal or popliteal fossa, direct examination of the vessel is often restricted by the limited access to the popliteal fossa with the knee flexed. However, careful examination of the lower popliteal artery or posterior tibial artery with the knee in different positions of flexion will demonstrate changes in the arterial waveform resulting from compression. Athletes may get compression of the popliteal artery between the lateral femoral condyle or upper tibia and the hypertrophied gastrocnemius, or soleus and plantaris muscles. This can be demonstrated on Doppler ultrasound by scanning with the foot in a neutral position and then in a position of active plantar flexion.[43,44]

Rarely, athletic patients may get iliac artery compression from a bulky psoas muscle on strenuous exercise. Scanning following a period of exercise shows turbulence, tissue bruits and very high local velocities in the inguinal area.

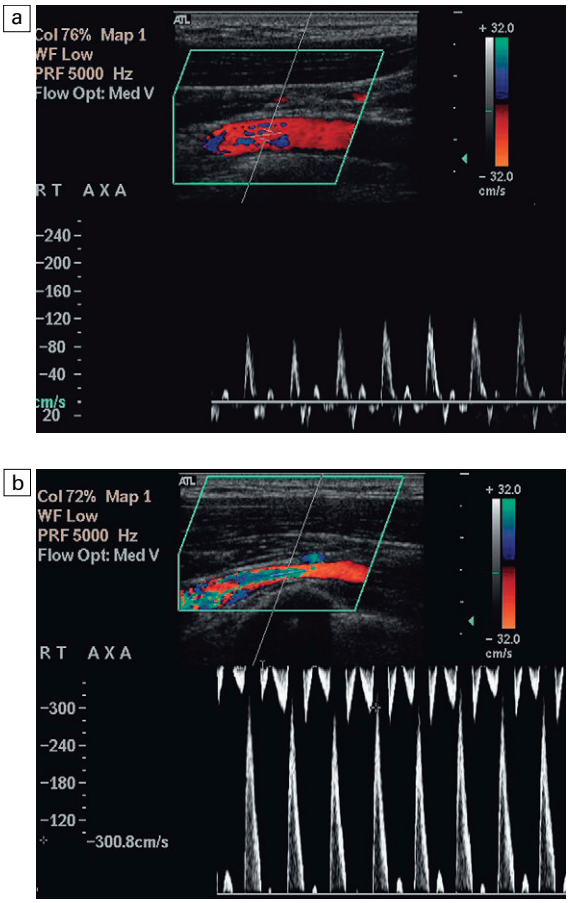


**Fig. 4.16** Compression of the subclavian artery as the arm is elevated/abducted. At rest flow in the axillary artery is approximately 1m $min^{-1}$; (b) showing narrowing of the artery as it crosses the first rib as the position of the arm is changed. The velocity increases to 3 m $min^{-1}$.

## ACCURACY IN RELATION TO OTHER TECHNIQUES

The gold standard for the assessment of the accuracy of Doppler ultrasound is usually arteriography. The reservations on the accuracy of arteriography, which are discussed in Chapter 3 on carotids, are also applicable to peripheral arterial disease. Cossman et al[11] compared colour Doppler with arteriography in 84 limbs, from the iliac to lower popliteal segments, using the criteria discussed earlier. For the detection of stenoses greater than 50%, they found an overall sensitivity of 87% (156/180 segments), specificity of 99% (444/449), accuracy of 95% (600/629), positive predictive value of 96% and negative predictive value of 95%. For the diagnosis of arterial occlusion the overall sensitivity was 81% (76/94), with specificity of 99% (463/466), accuracy of 96% (539/560), positive predictive value of 95% and negative predictive value of 96%.

Polak[45] reviewed five studies performed between 1989 and 1992, including the study by Cossman et al.[11] Colour Doppler was compared to arteriography and the overall sensitivity for the detection of a stenosis greater than 50% was 87.5% (316/361 segments), for an occluded segment the sensitivity was 92.6% (403/435), and the

overall specificity for the identification of normal segments was 97% (1247/1282). These studies have assessed femoropopliteal disease, accurate assessment of infrapopliteal crural vessel disease with duplex is a little more difficult, although a sensitivity of 77% has been reported[46] but if information on these vessels is clinically important then arteriography should be considered if there are any reservations about the duplex examination.

Similar, positive results have been obtained for duplex in upper limb disease with 79% sensitivity, 100% specificity and 99% accuracy for haemodynamically significant (50–70%) stenoses and 98% sensitivity, 99% specificity and 99% accuracy for occlusion being reported by Tola et al[47] who compared duplex ultrasound with intraarterial digital subtraction angiography (DSA) in 578 upper limb arterial segments.

MRA is now being applied to the peripheral arteries with some promising results, particularly with contrast enhancement, but availability and complexity, together with poor resolution in the smaller calf vessels, mean that this is still being developed, rather than a generally available technique. Hingorani et al[48] compared arteriography, duplex ultrasound and MRA in 33 patients undergoing lower limb revascularisation procedures. There was a difference between arteriography and duplex in three cases (10%) and this was considered to be clinically significant in two cases. For MRA, there were differences compared with arteriography in 12 cases (36%) and nine of these were considered to be clinically significant.

CTA can also be used for the assessment of the lower limb arteries[49] but has the disadvantages of radiation and contrast injection. One study[50] looked at 44 patients using a four-slice multidetector CT system. Two vascular radiologists compared the results to DSA images with sensitivities of 79% and 72% for treatable lesions (stenoses >50%) and specificities of 93% each. However, other workers[51] have reported better results with overall sensitivity of 93% and 95% specificity and an overall accuracy of 94%; although results for the infracrural arteries showed only 85% sensitivity. CTA has also been used for the assessment of brachial artery compression and is useful in demonstrating the relation of the artery to adjacent bone and other musculoskeletal structures.

## CONCLUSIONS

Providing that the examination is performed carefully by a skilled operator, Doppler ultrasound provides a relatively cheap and an accurate technique for the assessment of many patients with disease or previous surgery to the peripheral arteries, particularly in the lower limbs. In symptomatic patients it can be used as a first-line test to identify those patients without significant disease, those patients who may benefit from angioplasty and patients who are likely to require surgical bypass. In many centres, ultrasound is now used alone prior to surgery, with CTA or MRA used to clarify the situation in problematic cases. Power Doppler and echo-enhancing agents will increase the diagnostic sensitivity of Doppler ultrasound and the need for arteriography in many cases should be substantially reduced.

## REFERENCES

1. Fowkes FGR. Epidemiology of atherosclerotic disease in the lower limbs. Eur J Vasc Surg 1988; 2:283–291.
2. Department of Health and Social Security, Office of Population Censuses and Surveys. Hospital Inpatient Enquiry. London: HMSO; 1988.
3. Leng GC, Evans CJ, Fowkes FGR. Epidemiology of peripheral vascular diseases. Imaging 1995; 7:85–96.
4. Edwards JM, Coldwell DM, Goldman ML, et al. The role of duplex scanning in the selection of patients for transluminal angioplasty. J Vasc Surg 1991; 13:69–74.
5. Ramaswami G, Al-Kutoubi A, Nicolaides AN, et al. The role of duplex scanning in the diagnosis of lower limb arterial disease. Ann Vasc Surg 1999; 13:494–500.

6. Langholz J, Schlief R, Schürmann R, et al. Contrast enhancement in leg vessels. Clin Radiol 1996; 51(suppl 1):31–34.
7. Flanigan DP, Tullis JP, Streeter VL, et al. Multiple subcritical arterial stenoses: effect on poststenotic pressure and flow. Ann Surg 1977; 186:663–668.
8. Allard L, Cloutier G, Guo Z, et al. Review of the assessment of single level and multilevel arterial occlusive disease in lower limbs by duplex ultrasound. Ultrasound Med Biol 1999; 25:495–502.
9. Whyman MR, Allan PL, Gillespie IN, et al. Screening patients with claudication from femoropopliteal disease before angioplasty using Doppler colour flow imaging. Br J Surg 1992; 79:907–909.
10. Jager KA, Ricketts HJ, Strandness DE Jr. Duplex scanning for evaluation of lower limb arterial disease. In: Bernstein EF, ed. Noninvasive diagnostic techniques in vascular disease. St Louis: CV Mosby; 1985:619–631.
11. Cossman DV, Ellison JE, Wagner WH, et al. Comparison of contrast arteriography to arterial mapping with color-flow duplex imaging in the lower extremities. J Vasc Surg 1989; 10:522–529.
12. van Asten WN, van Lier HJ, Beijnevald WJ, et al. Assessment of aortoiliac obstructive disease by Doppler spectrum analysis of blood flow velocities in the common femoral artery at rest and during reactive hyperaemia. Surgery 1991; 109:633–639.
13. Zierler RE. Duplex and color-flow imaging of the lower extremity arterial circulation. Semin Ultrasound CT MR 1990; 11:168–179.
14. Sensier Y, Bell PR, London NJ. The ability of qualitative assessment of the common femoral Doppler waveform to screen for significant aorto-iliac disease. Eur J Vasc Endovasc Surg 1998; 15:357–364.
15. Rosfors S, Eriksson M, Hoglund N, et al. Duplex ultrasound in patients with suspected aortoiliac occlusive disease. Eur J Vasc Surg 1993; 7:513–517.
16. Bandyk DF. Essentials of graft surveillance. Semin Vasc Surg 1993; 6:92–102.
17. Mills JL. Mechanisms of graft failure: the location, distribution and characteristics of lesions that predispose to graft failure. Semin Vasc Surg 1993; 6:78–91.
18. Fasih T, Rudol G, Ashour H, et al. Surveillance versus nonsurveillance for femoro-popliteal bypass grafts. Angiology 2004; 55:251–256.
19. Landry GJ, Moneta GL, Taylor LM Jr, et al. Long-term outcome of revised lower-extremity grafts. J Vasc Surg 2002; 35:56–62.
20. Sanchez LA, Suggs WD, Veith FJ, et al. Is surveillance to detect failing polytetrafluoroethylene bypasses worthwhile: 12-year experience with 91 grafts. J Vasc Surg 1993; 18:981–990.
21. Dunlop P, Sayers RD, Naylor AR, et al. The effect of a surveillance programme on the patency of synthetic infrainguinal bypass grafts. Eur J Vasc Endovasc Surg 1996; 11:441–445.
22. Hoballah JJ, Nazzal RM, Ryan SM, et al. Is color duplex surveillance of infrainguinal polytetrafluoroethylene grafts worthwhile? Am J Surg 1997; 174:131–135.
23. Gibson KD, Caps MT, Gillen D, et al. Identification of factors predictive of lower extremity vein graft thrombosis. J Vasc Surg 2001; 33:24–31.
24. Wiese P, Nonnast-Daniel B. Colour Doppler ultrasound in dialysis access. Nephrol Dial Transplant 2004; 19:1956–1963.
25. Dumars MC, Thompson WE, Bluth EI, et al. Management of suspected hemodialysis graft dysfunction: usefulness of diagnostic US. Radiology 2002; 222:103–107.
26. Robbin ML, Oser RF, Allon M, et al. Hemodialysis access graft stenosis: US detection. Radiology 1998; 208:655–661.
27. Malik J, Slavikova M, Maskova J. Dialysis access-associated steal syndrome: the role of ultrasonography. J Nephrol 2003; 16:903–907.
28. Landwehr P. Haemodialysis shunts. In: Wolf K-J, Fobbe F, eds. Colour duplex sonography. New York: Thieme; 1995:92–109.
29. Maleux G, Hendrickx S, Vaninbroukx J, et al. Percutaneous injection of human thrombin to treat iatrogenic femoral pseudoaneurysms: short- and midterm ultrasound follow-up. Eur Radiol 2003; 13:209–212.
30. Toursarkissian B, Allen BT, Petrinec D, et al. Spontaneous closure of selected pseudoaneurysms and arteriovenous fistulae. J Vasc Surg 1997; 25:803–808.
31. Sheiman RG, Mastromatteo M. Iatrogenic femoral pseudoaneurysms that are unresponsive to percutaneous thrombin injection: potential causes. Am J Roentgenol 2003; 181:1301–1304.
32. Gorge G, Kunz T. Thrombin injection for treatment of false aneurysms after failed compression therapy in patients on full dose antiplatelet and heparin therapy. Catheter Cardiovasc Interv 2003; 58:505–509.
33. Ghershin E, Karram T, Gaitini D, et al. Percutaneous ultrasonographically guided thrombin injection of iatrogenic pseudoaneurysms in unusual sites. J Ultrasound Med 2003; 22:809–816.
34. Holder R, Hilton D, Martin J, et al. Percutaneous thrombin injection of carotid artery pseudoaneurysm. J Endovasc Ther 2002; 9:25–28.
35. Coley BD, Roberts AC, Fellmeth BD, et al. Postangiographic femoral artery pseudoaneurysms: further experience with US-guided compression repair. Radiology 1995; 194:307–311.
36. Eisenberg L, Paulson EK, Kliewer MA, et al. Sonographically guided compression repair of pseudoaneurysms: further experience from a single institution. Am J Roentgenol 1999; 173:1567–1573.

37. Morrissey NJ. Endovascular treatment of peripheral arterial aneurysms. Mt Sinai J Med 2004; 71:1–3.
38. Flanigan DP, Burnham SJ, Goodreau JJ, et al. Summary of cases of adventitial disease of the popliteal artery. Ann Surg 1979; 189:165–175.
39. Cassar K, Engeset J. Cystic adventitial disease: a trap for the unwary. Eur J Endovasc Surg 2005; 29:93–96.
40. Tsolakis IA, Walvatne CS, Caldwell MD. Cystic adventitial disease of the popliteal artery: diagnosis band treatment. Eur J Vasc Endovasc Surg 1998; 15:188–194.
41. Longley DG, Schwabacher S, Yedlicka JW, et al. Thoracic outlet syndrome: evaluation of the subclavian vessels by colour duplex sonography. Am J Radiol 1992; 158:623–630.
42. Wadhwani R, Chaubal N, Sukthankar R, et al. Color Doppler and duplex sonography in 5 patients with thoracic outlet syndrome. J Ultrasound Med 2001; 20:795–801.
43. Turnipseed WD, Pozniak M. Popliteal entrapment as a result of neurovascular compression by the soleus and plantaris muscles. J Vasc Surg 1992; 15:285–294.
44. Baltopoulos P, Filippou DK, Sigala F. Popliteal artery entrapment syndrome: anatomic or functional syndrome? Clin J Sports Med 2004; 14:8–12.
45. Polak JF. Peripheral arterial disease. Evaluation with color flow and duplex sonography. Radiol Clin North Am 1995; 33:71–90.
46. Karacagil S, Lofberg AM, Granbo A, et al. Value of duplex scanning in evaluation of crural and foot arteries in limbs with severe lower limb ischaemia – a prospective comparison with angiography. Eur J Vasc Endovasc Surg 1996; 12:300–303.
47. Tola M, Yurdakul M, Okten S, et al. Diagnosis of arterial occlusive disease of the upper extremities: comparison of color duplex sonography and angiography. J Clin Ultrasound 2003; 31:407–411.
48. Hingorani A, Ascher E, Markevich N, et al. A comparison of magnetic resonance angiography, contrast arteriography, and duplex arteriography for patients undergoing lower extremity revascularization. Ann Vasc Surg 2004; 18:294–301.
49. Becker CR, Wintersperger B, Jakobs TF. Multidetector-row CT angiography of peripheral arteries. Semin Ultrasound CT MR 2004; 24:268–279.
51. Edwards AJ, Wells IP, Roobottom CA. Multidetector row CT angiography of the lower limb arteries: a prospective comparison of volume-rendered techniques and intra-arterial digital subtraction angiography. Clin Radiol 2005; 60:85–95.
52. Romano M, Mainenti PP, Imbriaco M, et al. Multidetector row CT angiography of the abdominal aorta and lower extremities in patients with peripheral arterial occlusive disease: diagnostic accuracy and interobserver agreement. Eur J Radiol 2004; 50:303–308.

# The peripheral veins

# 5

Paul L. Allan and Karen Gallagher

The peripheral veins may be affected by a variety of disorders, which can be assessed by ultrasound. Deep vein thrombosis (DVT) and thromboembolic disease are the most common indications for investigation of the peripheral veins but venous insufficiency and vein mapping are also reasons for examining the veins. Anderson et al[1] found an average annual incidence of 48 initial cases, 36 recurrent cases of DVT and 23 cases of pulmonary embolus per 100 000 population in the Worcester DVT study.[1] The prevalence of varicose veins and chronic venous insufficiency is more difficult to quantify, but it has been estimated that 10–15% of males and 20–25% of females in an unselected Western population over 15 years of age have visible tortuous varicose veins; 2–5% of adult males and 3–7% of females have evidence of moderate or severe chronic venous insufficiency, with a point prevalence for active ulceration of 0.1–0.2%.[2]

## INDICATIONS

The indications for ultrasound of the venous system are shown in Table 5.1. The most frequent indication for ultrasound of the veins is for the investigation of possible DVT in the lower limb and, occasionally, in the upper limb – especially if there have been central venous catheters inserted for intensive care monitoring, chemotherapy, dialysis or parenteral feeding. Similarly, indwelling femoral catheters are prone to induce thrombosis and patients should be examined early if this is suspected. Ultrasound provides a non-invasive, reliable method for examining the venous system, particularly with respect to the diagnosis, or exclusion, of dangerous proximal thrombus in symptomatic patients.[3] The results for asymptomatic thrombus in the lower limbs are less encouraging and this should be recognised when using ultrasound to screen for DVT in asymptomatic patients.[4]

Recurrence of varicose veins following surgery can pose many problems for the clinician trying to clarify the venous anatomy. Colour Doppler can be used instead of venography and varicography in most cases and may be the only examination required to define the anatomy and function in patients with recurrent varicose veins.[5]

The impact of postphlebitis syndromes and chronic venous insufficiency is a rather larger problem than is apparent from its relatively low clinical profile. In one large epidemiological study of 4376 subjects, 62% had some evidence of varicose veins; signs of chronic insufficiency were present in 22%.[6] Varicography shows perforator veins which are obviously incompetent and some

**Table 5.1** Indications for venous ultrasound

- Diagnosis or exclusion of deep vein thrombosis in the upper or lower limb, spontaneous or related to indwelling catheters
- Assessment of secondary/recurrent varicose veins
- Investigation of chronic venous insufficiency and postphlebitis syndrome
- Vein mapping prior to bypass grafts
- Assessment of primary varicose veins if there is uncertainty following clinical examination
- Localisation of veins for cannulation

incompetent superficial and deep venous segments, but ultrasound has the advantage that the segments of the deep and superficial systems can be examined and the direction of blood flow within each segment can be demonstrated. In addition, it is less unpleasant for the patient and allows multiple assessments to be performed without discomfort. The main disadvantage is that it is fairly time-consuming, particularly in complex cases, and requires a significant degree of expertise in order to perform examinations efficiently.

The superficial veins of the legs and, occasionally, the arms may be used for bypass grafts for the coronary or lower limb arteries. If there is any doubt about their suitability as a conduit following previous varicose vein surgery, or in terms of their calibre, ultrasound can be used to assess the diameter and length of vein available. In addition, the sonographer can map out the course of the vein to allow easier harvesting.

It may be difficult occasionally to locate a suitable vein for central venous cannulation, particularly in patients who have had multiple previous central venous lines, such as intensive care or chemotherapy patients. Ultrasound can be used to clarify the location and patency of potentially suitable veins and, in difficult cases, the puncture may be made under direct ultrasound visualisation.

## ANATOMY AND SCANNING TECHNIQUE

The anatomy of the venous system in the limbs is more complex and variable than that of the arteries. The meanings of the terms 'proximal' and 'distal' may cause confusion as the veins start at the periphery and blood flows centrally towards the heart so that 'upstream' is peripheral and 'downstream' is central, which is the opposite from the situation in the arteries. The convention is that proximal describes locations nearer the heart and distal refers to points further from the heart; these terms are used in this way in this chapter.

### Anatomy – lower limb

The veins of the lower limb are divided into deep and superficial systems. These are linked by a variable number of perforator veins which carry blood from the superficial to the deep systems (Figs 5.1 and 5.2).

#### *The deep veins*

The anatomy of the lower limb veins is rather variable. Generally the veins accompany the arteries but their number may vary and the communications with other veins along the way can show a variety of patterns; however, a general arrangement is usually apparent. In the calf there are veins running with the main arteries: the *posterior tibial*, *peroneal* and *anterior tibial veins*; there are usually two, occasionally three veins with each artery (Fig. 5.3). In addition there are venous channels, or sinuses, which drain the major muscle groups in the posterior calf. These are seen in the upper calf as they pass upwards to join the other deep veins in the lower popliteal region; the *gastrocnemius* and *soleal veins* are the largest of these. The gastrocnemius vein is the more superficial and may be mistaken for the short saphenous vein; clues to its true identity are that it is usually accompanied by the artery to the muscle and it can be followed distally down into the muscle rather than outwards to lie subcutaneously on the fascia around the calf, which is the position of the short saphenous vein.

The calf veins join to form the *popliteal vein*, or veins – there may be two, or sometimes three channels, especially if there is a dual superficial femoral vein. The popliteal vein runs up through the popliteal fossa, lying more posterior and usually medial to the artery. As well as the veins from the calf and calf muscles, it is joined by the *short saphenous vein* at the saphenopopliteal junction.

The popliteal vein becomes the *superficial femoral vein* at the upper border of the popliteal fossa; rarely, the popliteal vein runs more deeply to join with the profunda femoris vein. The superficial femoral vein runs up the medial aspect of the thigh, posterior to the superficial

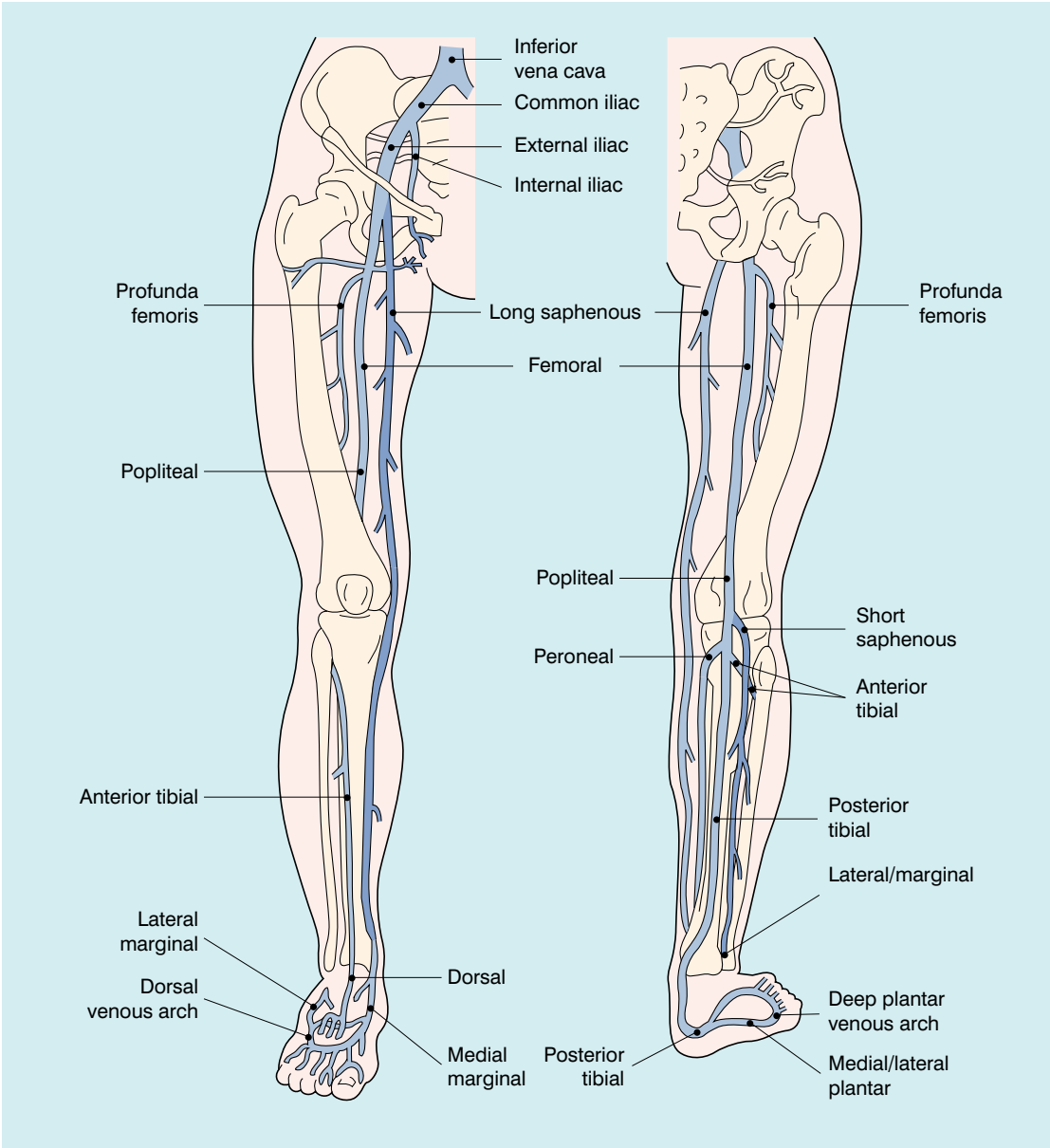


**Fig. 5.1** The veins of the lower limb, showing the superficial and deep systems.

femoral artery to join with the *profunda femoris vein* in the femoral triangle below the groin; the profunda femoris vein drains the thigh muscles. The confluence of the superficial femoral and profunda femoris veins to form the common femoral vein is normally a little more caudal than the bifurcation of the common femoral artery into the superficial femoral and profunda femoris arteries. The superficial femoral vein may have significant segments of duplication (Fig. 5.4) along its length in up to 25–30% of subjects,[7, 8] these dual segments may have a variable relation to the artery, so that they may be overlooked unless care is taken in the examination of the thigh veins with both transverse and longitudinal views being obtained.

In the pelvis and groin, the anatomy is generally consistent. The superficial femoral vein and pro-

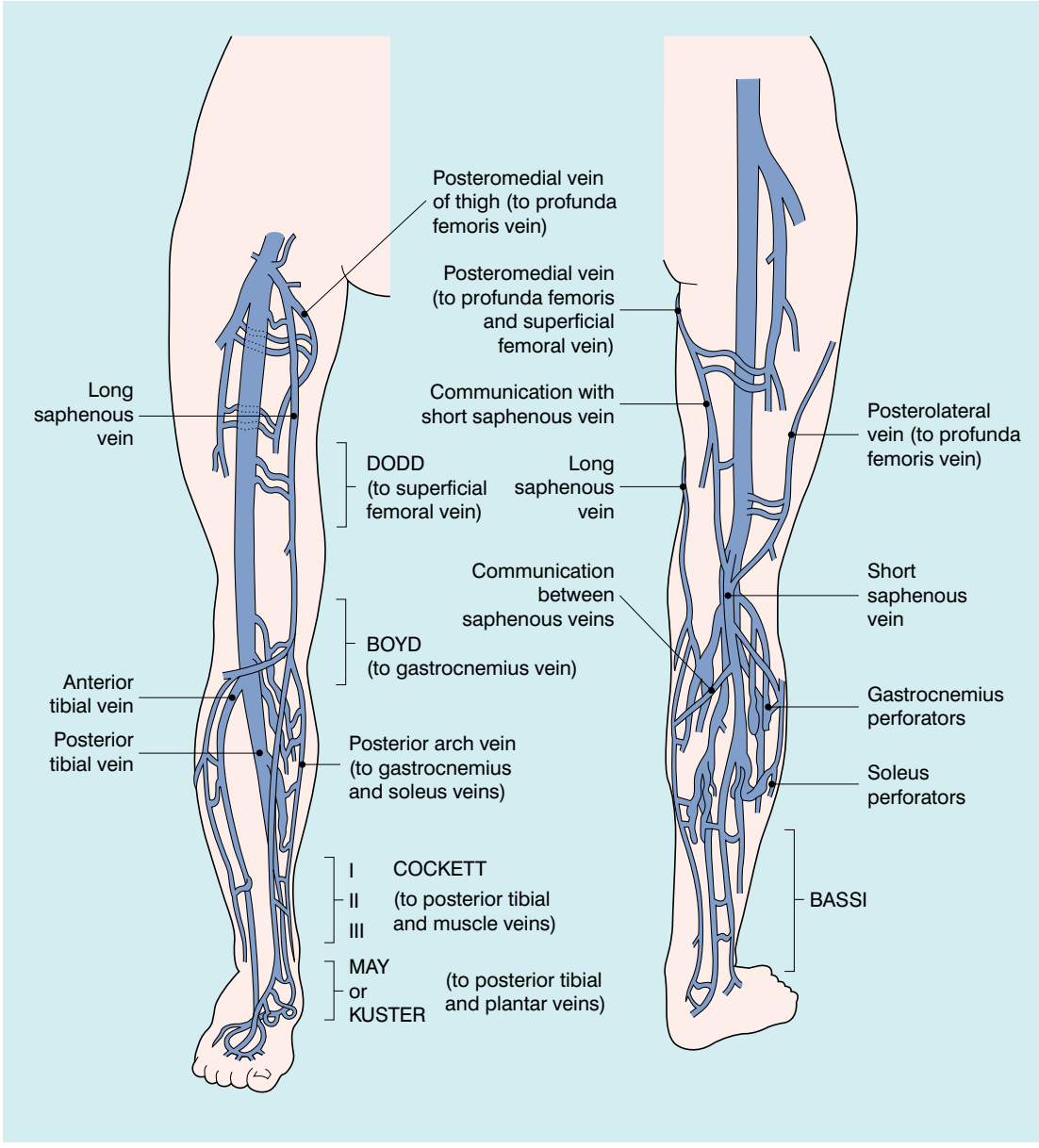


**Fig. 5.2** The major perforating veins in the lower limb.

funda femoris vein join to form the *common femoral vein*, which lies medial to the common femoral artery. The common femoral vein is joined by the *long saphenous vein* at the saphenofemoral junction; the appearance of the common femoral vein, long saphenous vein and artery in transverse section is sometimes referred to as the 'Mickey Mouse' view (Fig. 5.5). The common femoral vein is also joined by veins from the muscles around the hip. These veins are variable in size and number, and occasionally one of these is large enough to be confused with the long saphenous vein or profunda femoris vein but careful attention to the anatomy should clarify the situation. The common femoral vein becomes the *external iliac vein* after it has passed under the inguinal ligament, and then it passes posteriorly along the posterior pelvis, running alongside the

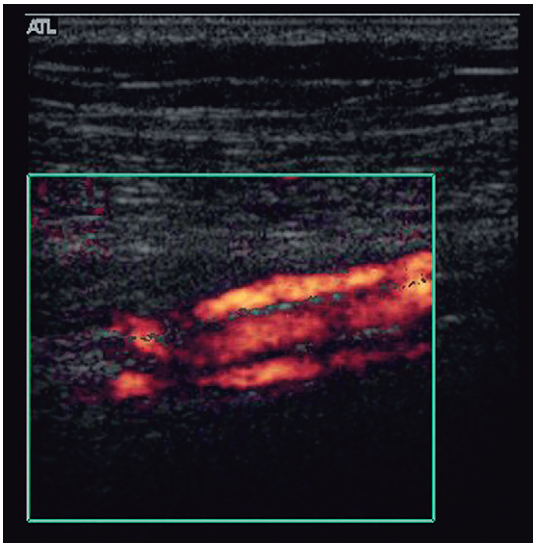

**Fig. 5.3** Power Doppler showing paired deep calf veins running with the artery.

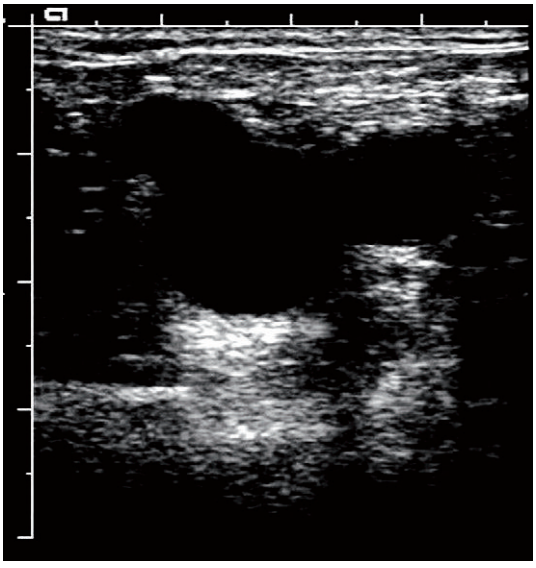

**Fig. 5.5** The saphenofemoral junction showing the 'Mickey Mouse' view.

external iliac artery. The *internal iliac vein*, which drains the pelvic structures, joins with the external iliac vein deep in the pelvis to form the *common iliac vein* (Fig. 5.6). The two common iliac veins then join at the level of the aortic bifurcation to form the *inferior vena cava*, which normally passes cranially on the right side of the aorta. The left common iliac vein passes behind the right com-

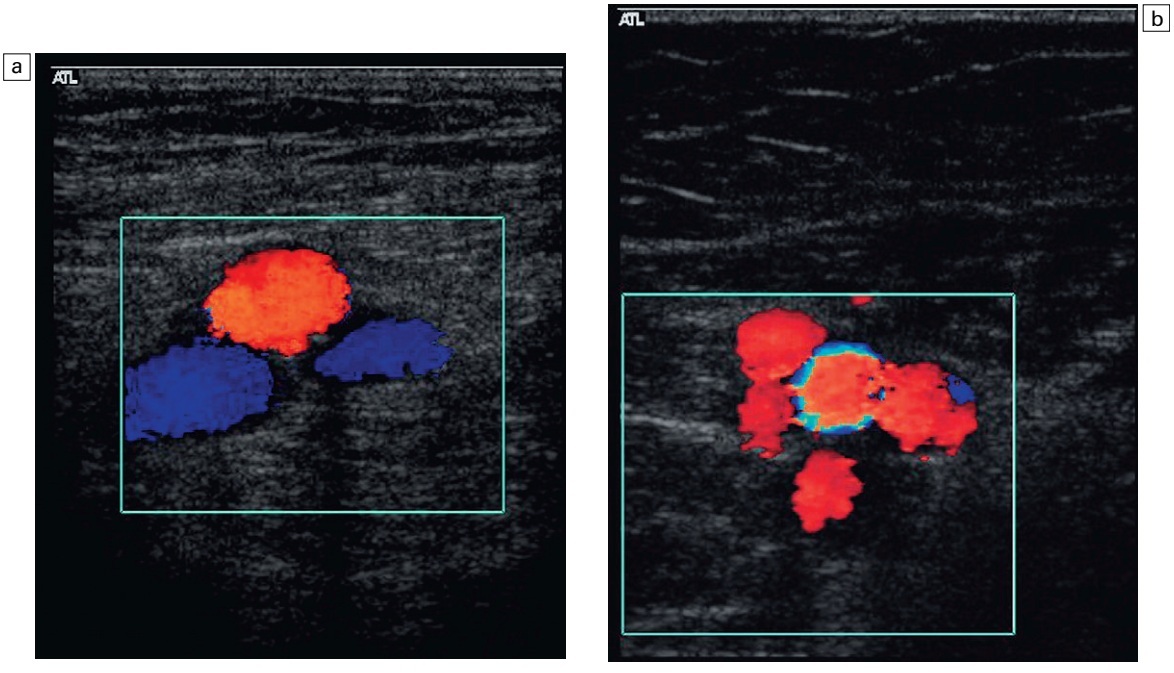


**Fig. 5.4** (a) Transverse view showing dual superficial femoral vein segments; (b) another example of multiple superficial femoral vein segments showing a central artery with four venous channels adjacent to it.

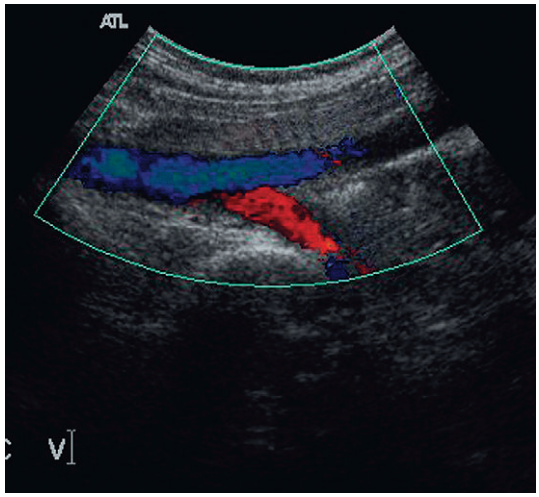


**Fig. 5.6** The confluence of the internal and external iliac veins forming the common iliac vein.

mon iliac artery just distal to this confluence. In a small number of individuals this confluence does not occur and the two common iliac veins continue cranially as dual inferior venae cavae; this reflects the arrangement of paired cardinal veins in the embryo.

The deep veins have a series of valves along their course (Fig. 5.7). These are somewhat variable in their number and location. They are most numerous in the veins below the knee; in the thigh, the superficial femoral vein usually has one just below the confluence with the profunda femoris vein and at several levels below this. The iliac veins, in contrast, have relatively few valves;[9] rarely a valve may be seen in the inferior vena cava.

### *The superficial veins*

The two main superficial venous channels in the lower limb are the long and short saphenous veins. The *long saphenous vein* arises from the medial aspect of the dorsal venous arch of the foot and passes in front of the medial malleolus to run up the medial aspect of the calf and knee into the thigh. In the upper thigh, the long saphenous vein curves laterally and deeply to join the common femoral vein just below the inguinal ligament. The long saphenous vein has two components in the calf: the posterior division passes up from the medial malleolus and communicates with the perforator veins; the anterior division usually joins the posterior division just below the level of the knee joint. Duplication of the long saphenous vein can be seen in the thigh in up to 50% of people,[10] this usually takes the form of parallel channels. The long saphenous vein receives many superficial tributaries and is connected to the deep veins by

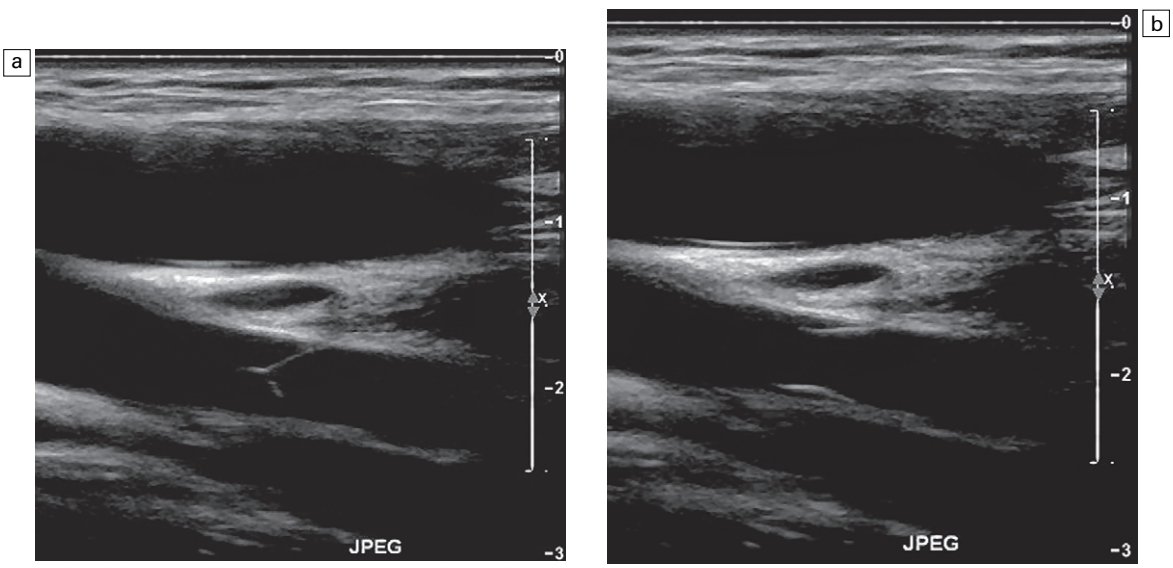


**Fig. 5.7** Normal valves in the profunda femoris vein; (a) valves shut, (b) valves open.

perforating veins; some of these tributaries in the thigh can be quite prominent and may be mistaken for the main vein if their true nature is not recognised. The standard sites for the perforators are at the level of the junction between the middle and lower thirds of the thigh and in the calf, although many other communicating veins have been recorded and described (Fig. 5.2).[11] In the region of the saphenofemoral junction the long saphenous vein receives several tributaries draining the groin, lower abdominal wall and perineum. These veins are of significance in the recurrence of varicose veins following high ligation, as they provide a network of collateral channels which may bypass the resected segment.

The *short saphenous vein* arises from the lateral aspect of the dorsal venous arch of the foot, passing below and behind the lateral malleolus to run up the posterolateral aspect of the calf to the popliteal fossa, where it passes through the deep fascia to join the popliteal vein. Classically, it enters the lateral aspect of the popliteal vein at the level of the popliteal skin crease or within a few centimetres above this but the level of the confluence can be quite variable. Occasionally it passes upwards to join the profunda femoris vein in the lower thigh – a Giacomini vein.[12] Burihan and Baptista-Silva[13] dissected 200 adult cadaver legs and reported 20 different patterns of termination of the short saphenous vein. In 27.5% of legs the short saphenous vein terminated in the principal deep vein of the leg (popliteal or lower superficial femoral vein), in 25% of legs the short saphenous vein, or a branch arising from it, communicated with the long saphenous vein. In the remaining legs, there was a wide variety and combination of communications with other veins, including the deep femoral vein, the mid-thigh perforator vein, muscular veins and even the inferior gluteal vein in three legs.

## Scanning technique – lower limb

The technique varies depending on the clinical indication. The most common indication is the diagnosis or exclusion of DVT in the lower limb. This section therefore concentrates on this aspect and variations in technique for other indications will be dealt with in subsequent sections (Table 5.2). A 4–7 MHz linear transducer is the most suitable frequency as it provides sufficient penetration, particularly in large or oedematous thighs. A higher-frequency transducer may be used for superficial veins, or in thinner legs. It is important to ensure that the system is set up for the slower velocities found in veins, rather than the significantly higher arterial velocities.

It is advantageous if there is a tilting couch available so that the patient can be moved from the horizontal to various degrees of head-up elevation as necessary. In the absence of a tilting couch it is better if the patient can be examined with the thorax higher than the legs, as this produces some distension of the lower limb veins, which makes them easier to identify and the assessment of compression more straightforward.

There are three components to the ultrasound examination of the veins for DVT: imaging, Doppler and compression. Thrombus may be seen in the vein, Doppler may show abnormal, or absent, flow signals and compression refers to the fact that a normal vein is easily compressible – light pressure with the transducer will obliterate the lumen of the vein. Two points should be noted in relation to compression: first, compression should be performed in the transverse plane (Fig. 5.8) for the reason that if it is done in the longitudinal plane a thrombosed vein may disappear as it is no longer in the scan plane, rather

**Table 5.2** Basic steps in the examination for thrombosis

1. Patient sitting on couch/trolley: compression of common femoral vein, superficial femoral vein from groin to adductor canal
2. Colour Doppler with augmentation, examine common and superficial femoral veins
3. Patient decubitus, or with leg elevated: compression and Doppler examination of popliteal vein(s)
4. Patient sitting, if possible, with legs dependent: examine the calf veins with compression and colour Doppler
5. Patient supine: examine iliac veins if thrombus suspected in these

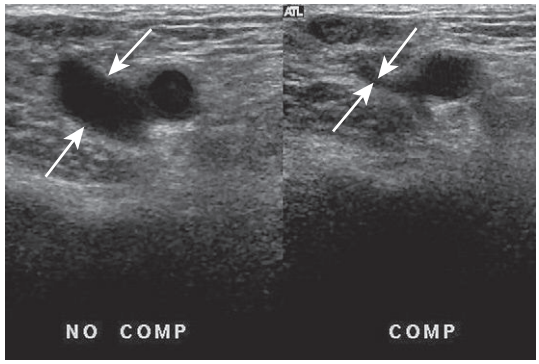


**Fig. 5.8** Normal compression: the lumen of the vein (arrows) is completely obliterated by pressure from the transducer.

than because it has been compressed. Second, fresh thrombus is soft and gelatinous, so that firm pressure can produce a degree of compression, which may give a false impression of patency. The use of colour Doppler should clarify this situation but care must be taken if this is not available. A further reason for scanning in the transverse plane is that dual segments of the superficial femoral vein will be identified more reliably.

The examination begins at the groin, where the common femoral vein is located on a transverse scan and compressed. Compression is then repeated at intervals of 3–5 cm down the length of the thigh to the adductor canal. At this point the superficial femoral vein is difficult to compress from an anterior approach as it is well supported by the bulk of the anterior thigh muscles. Compression is better achieved in this region by placing a hand behind the medial thigh and pushing up with the fingers against the transducer. The scan plane is then changed to longitudinal and the vein examined with colour Doppler, or power Doppler, as the transducer is moved up the thigh. Squeezing the calf gently will augment flow and allow easier detection of areas of flow or thrombosis; alternatively, the patient can be asked to plantar-flex their toes, which results in calf muscle contraction and emptying of the calf veins.

Colour Doppler signals are often sufficient, in conjunction with the findings on compression, to confirm or exclude a diagnosis of DVT (Fig. 5.9). If there is any doubt then a spectral assessment will allow a better appreciation of damped flow, absent respiratory variation and impaired augmentation.

Once the thigh veins have been examined the patient is turned into a lateral position, with the medial aspect of the leg being examined uppermost, so that the popliteal veins can be examined. Again, compression and colour Doppler are used to assess the veins. Some patients, particularly postoperative hip patients, may not be able to move into a decubitus position. In these cases the popliteal veins are examined with the knee partially flexed up off the couch, with external rotation, if possible, so that the transducer can be positioned in the popliteal fossa; a curved array can be of benefit in gaining access in this situation. Alternatively, the leg can be elevated and supported off the couch by an assistant. In addition to the popliteal vein, the main muscular veins draining soleus and gastrocnemius should be assessed, especially if there is pain and tenderness associated with the posterior calf muscles.

The calf veins can be examined after the popliteal vein with the patient in the decubitus position on a tilted couch, or in the supine position with the knee flexed up off the mattress, if the patient is relatively immobile. Alternatively, the patient can sit on the couch with their legs

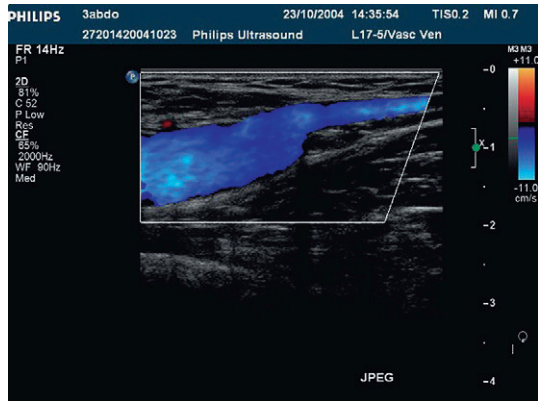


**Fig. 5.9** The normal saphenofemoral junction showing complete colour fill-in across the vein lumen.

over the side so that the dependent calf veins are well distended. The posterior tibial and deeper peroneal vessels are most easily located by scanning in the transverse plane from the medial side of the calf and identifying the arterial signals on colour Doppler (Fig. 4.2). These veins may also be located on a longitudinal scan; again the arterial signal provides a useful guide to the position of the veins. If there are difficulties identifying the posterior tibial veins at the mid-calf level then scanning the lower calf just above the medial malleolus, where the vessels are superficial and constant in location, may be of value; the posterior tibial vessels can then be followed back up the calf with augmentation of flow as necessary in order to assess patency. In the mid- and lower calf, squeezing the calf can produce motion artefacts from movement of the calf muscles which obscure the flow signals from the veins; in these cases, squeezing the foot will produce adequate augmentation of flow. The anterior tibial veins are examined from an anterolateral approach: scanning transversely, the tibia, fibula and interosseous membrane are identified. The anterior tibial vessels are found on the superficial aspect of the interosseous membrane, although it should be noted that these veins are rarely involved in DVT in isolation from the other calf veins. The peroneal veins may also be visualised deep to the interosseous membrane in many patients from this anterolateral aspect, allowing their examination if they have not been identified from a posteromedial approach; a posterolateral approach is also of value in identifying the deeply situated peroneal veins in some patients.

The iliac veins are examined by following the external iliac vein upwards from the common femoral vein into the pelvis. A 3–5 MHz transducer is usually necessary for adequate penetration. Firm pressure may be required to displace bowel gas. This may produce narrowing or effacement of the more superficial segments of vein, resulting in an absence of signal and a possible false diagnosis of occlusion. If the pelvic veins are difficult to trace superiorly then the common iliac vein can usually be identified just distal to the inferior vena cava and aortic bifurcation; this can then be followed peripherally. In some patients it is impossible to identify the deeper pelvic portion of the iliac veins; however, if there is a patent external iliac vein which shows respiratory variation with good augmentation and a patent upper common iliac vein, then it is highly unlikely that there is significant thrombus in the invisible segment. Transvaginal scanning will show the deeper pelvic veins and may be considered if there is a need to visualise these vessels directly. In thinner patients, or patients with good pelvic access, the proximal internal iliac vein may be seen joining the external iliac vein in the pelvis (Fig. 5.5). The inferior vena cava is examined if thrombus is seen extending into this vessel. It is important, whenever thrombus is diagnosed in a leg vein, that the proximal extent of the clot is identified, as this may have a significant impact on management decisions in relation to anticoagulation therapy, or the placing of a filter.

In pregnant women in the later part of pregnancy, the uterus will lie on the iliac veins in the supine position and compress them, thus reducing flow and impairing augmentation in the lower limb veins. This can be alleviated by asking the patient to turn into a semi-decubitus position, with the side being examined uppermost, so that the uterus falls away, allowing better flow in the pelvic veins. An alternative is to examine the patient standing, as the uterus moves forward away from the iliac veins in this position.

## Anatomy – upper limb

The veins of the upper limb are also divided into deep and superficial groups (Fig. 5.10). The *deep veins* are paired and accompany the arteries: the *radial*, *ulnar* and *brachial* veins. There is a variable pattern of communicating veins between the deep venous channels and between the deep venous channels and the superficial veins. The superficial system is more variable than in the leg but there are usually two main channels: the *cephalic vein* on the radial aspect of the arm and the *basilic vein* on the ulnar side. These communicate at the cubital fossa by way of the *median*

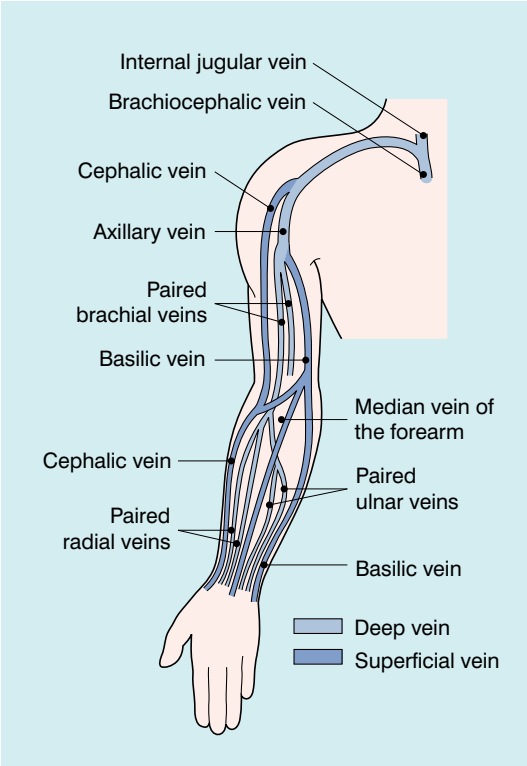


**Fig. 5.10** The veins of the upper limb, showing the main superficial and deep veins.

*cubital vein* and they also communicate with the deep brachial veins at this level. The basilic vein pierces the deep fascia on the medial aspect of the mid-upper arm to join the brachial veins and this combined venous channel becomes the *axillary vein* when it enters the axilla. The cephalic vein passes more cranially along the lateral aspect of the biceps. At the level of pectoralis major it turns medially and deeply to pierce the clavipectoral fascia below the clavicle and joins the upper axillary vein. The axillary vein also receives other tributaries from the region of the shoulder joint and the lateral chest wall.

The axillary vein becomes the *subclavian vein* as it crosses the first rib, where it lies in front of the artery; the main tributary of the subclavian vein is the external jugular vein. The subclavian vein on both sides joins with the internal jugular vein behind the medial end of the clavicle to form the brachiocephalic vein, which is also known as the *innominate vein*.

## Scanning technique – upper limb and neck

Examination of the upper limb veins is normally performed with the patient supine and the arm abducted to about 90°; the patient may require some support for the arm, or they can be asked to hold onto some suitable part of the ultrasound machine beside them. A transducer frequency of 5–12 MHz can be used. The examination begins at the sternoclavicular joint, where the distal brachiocephalic vein can be assessed and the confluence with the internal jugular vein examined, particularly if central lines have been inserted. The subclavian vein is examined from above and then below the clavicle; it is seen lying in front of the subclavian artery as it runs over the first rib. The axillary vein is then followed across the axilla into the upper arm, from where the brachial veins can be examined down to the elbow. The veins below this are not usually examined unless there is some specific reason, such as the presence of a dialysis shunt. Augmentation of flow is obtained by manual compression of the forearm, or upper arm; alternatively, asking the patient to clench their fist will increase venous flow. If there is a suspicion of a possible venous compression syndrome, the arm veins can be examined with the limb in different positions of abduction; comparison of flow on the two sides can be of value.

The internal jugular vein runs in the carotid sheath from the jugular foramen in the base of the skull down to join with the subclavian vein; it lies superficial to the carotid artery. There may be significant variation in size between the two sides. It is normally compressed easily by pressure from the transducer, so a light touch is required. Flow in the vein is influenced significantly by right heart activity, so colour Doppler will show variable forward and reverse flow, with spectral Doppler showing the 'a', 'c' and 'v' waves of the jugular pulse. Respiratory variation will also be seen, with increased forward flow during inspiration when intrathoracic pressure is negative and slowing during expiration when the intrathoracic pressure is positive. Flow can therefore be modified by respiratory

manoeuvres such as deep inspiration, or a Valsalva.

## DIAGNOSIS OF DEEP VEIN THROMBOSIS

Clinical diagnosis of DVT is inaccurate and clinical scoring systems, such as the Wells Score (Table 5.3),[14] have been introduced to stratify risk more accurately. In addition measurements of serum D-dimer can be used to further refine the selection of patients more likely to have a DVT who will benefit from an ultrasound scan.[15] Patients with a low probability for DVT should have a D-dimer estimation. If this is negative, they are highly unlikely to have a DVT and do not require scanning; if the D-dimer is positive, or the patient has an intermediate or high probability score for DVT, then a scan should be performed. D-dimer levels are less useful in patients who have recently undergone surgery as false positives are more common.

The diagnosis of normal or thrombosed veins is based on the compressibility of the veins, the appearance of the veins and the changes which occur to the spectral and colour Doppler findings. The main changes associated with DVT are shown in Table 5.4. The lower limb is examined for possible thrombosis much more frequently than the upper limb, although the features described are also applicable to the arm veins.

**Table 5.3** Pretest probability for deep vein thrombosis (DVT)

| | |
|---|---|
| Active cancer (treatment ongoing, or within previous 6 months) | +1 |
| Paralysis, paresis, or recent immobilisation of the lower extremity | +1 |
| Recently bedridden for more than 3 days, or major surgery within 4 weeks | +1 |
| Localised tenderness along distribution of deep venous system | +1 |
| Entire leg swollen | +1 |
| Calf swelling by more than 3 cm when compared with the asymptomatic leg (measured 10 cm below tibial tuberosity) | +1 |
| Pitting oedema (greater in symptomatic leg) | +1 |
| Collateral superficial veins (non-varicose) | +1 |
| Alternative diagnosis as likely or greater than that of DVT | –2 |

From Wells et al.[14]

In patients with symptoms in both legs, the more symptomatic leg is used.

High: > 3; Intermediate: 1–2; Low: ≤ 0.

### Compressibility

As noted above, a normal vein is easily compressible with only mild to moderate pressure from the transducer, so that the lumen is completely obliterated. A vein filled with thrombus will be held open (Fig. 5.11), although it must be remembered that fresh thrombus has the consistency of jelly, so that it can be compressed to some extent by strong pressure.

### Appearances of the vein and the vein lumen

The lumen of a normal vein is usually anechoic and, on colour Doppler, the whole lumen of the vein should be filled with colour, particularly on augmentation of flow. Although fresh thrombus is anechoic, or hypoechoic, it becomes increasingly echogenic as it matures. In addition fresh thrombus has a tendency to expand the vein and make it look rounder and fuller than a normal vessel.[16] This is accentuated at the upper end of the thrombus where the patent lumen above the clot may be relatively poorly filled with blood due to the distal obstruction by the thrombus (Fig. 5.12).

Fresh thrombus is not particularly adherent to the vein wall, so that some blood may be seen around the periphery of the clot in the vein on

**Table 5.4** Signs of deep vein thrombosis

- Absent or reduced compressibility
- Thrombus in the vein: static echoes, incomplete colour fill-in, expansion of the vein
- Static valve leaflets
- Absent flow on spectral or colour Doppler
- Impaired or absent augmentation of flow
- Loss of spontaneous flow and respiratory variation
- Increased flow in collateral channels

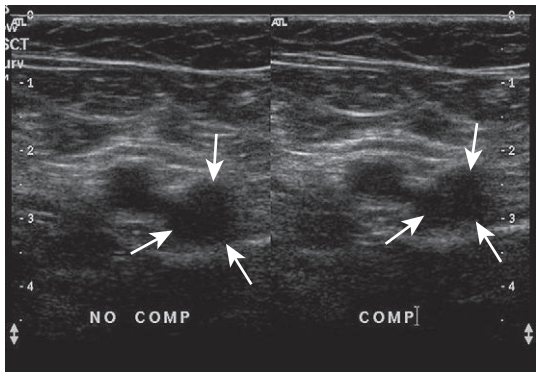


**Fig. 5.11** Positive compression test, the thrombosed vein (arrows) does not change calibre on compression with the transducer.

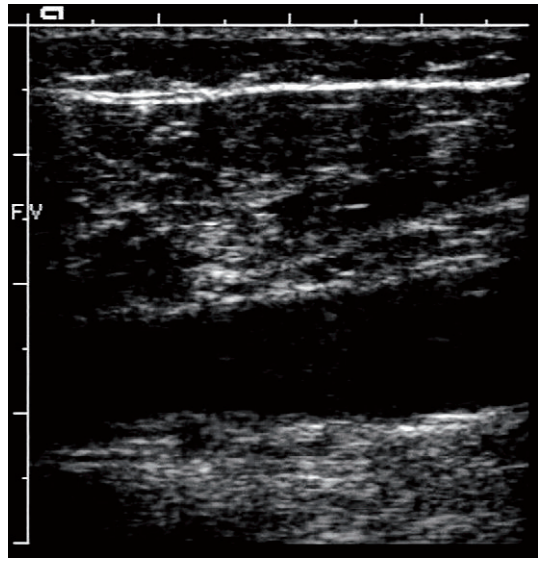


**Fig. 5.12** A vein containing thrombus: low-level echoes are seen in the clot, the patent lumen above the thrombus is narrower than the thrombosed segment.

colour Doppler. Another appearance which may be seen in early thrombosis is that of a thin tail of thrombus extending up the vein from its origin and lying free in the lumen of the vein (Fig. 5.13). Older thrombus becomes increasingly echogenic, adherent to the vein wall and contracts as it becomes more organised and fibrotic. This may result in the vein being reduced to a relatively small echoic structure that may be difficult to locate. Alternatively, the thrombus may retract to one side of the vein, resulting in an asymmetric lumen on colour Doppler.

An exception to the rule that flowing blood is not echogenic is seen in pregnancy, or any other situation where there is slow venous flow and a tendency to hyperviscosity. In these individuals faint, mobile echoes are seen moving up the vein on real-time imaging; these accelerate on augmen-

a

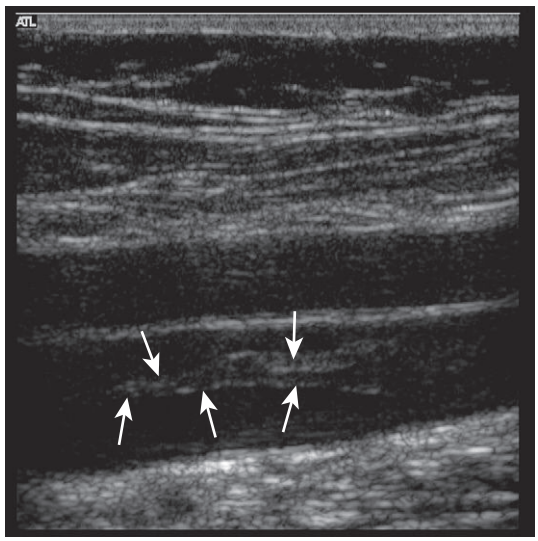

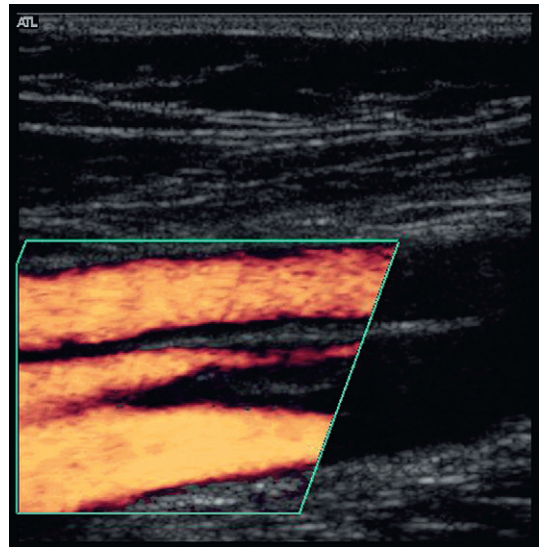

b

**Fig. 5.13** (a) A small tail of thrombus extending up the vein (arrows) which is not sufficiently large to produce any obstruction to flow and could be overlooked if visualisation of this area was poor; (b) power Doppler image of the same thrombus showing flow around it.

tation of flow. These echoes are produced by clumps, or aggregates of red cells, and do not usually cause any significant difficulties in diagnosis with modern, real-time, colour Doppler equipment.

Normal valves may be seen moving gently in the currents from blood passing them, particularly in the larger thigh veins (Fig. 5.7). One of the earliest sites of deep vein thrombus formation is in the sinus above a valve cusp, so that apparent rigidity or fixation of a cusp should raise the suspicion of possible early DVT and a careful examination of the area should be undertaken.

The walls of a normal vein are smooth and unobtrusive. Following recanalisation after a DVT, they become irregular, thickened and echogenic; calcification may also occur in a small number of cases.

## Spectral Doppler findings

### *Spontaneous flow and respiratory variation*

Even at rest and with some head-up tilt there should still be spontaneous flow along the vein which shows some respiratory variation or phasicity, particularly in the proximal leg veins. This variation is produced by the intra-abdominal pressure changes on respiration and is the opposite of the changes found in the jugular vein and arm veins (see above). On inspiration the diaphragm descends and the intra-abdominal pressure rises; this results in decreased flow from the leg veins into the abdomen. On expiration the intra-abdominal pressure decreases and flow from the legs increases. Similarly, if the patient holds their breath, flow in the leg veins slows and may cease until the patient relaxes, when there is relatively high flow from the legs.

If there is thrombus occluding the vein there will not be any flow detected in the vein lumen at the level of the thrombus. Sometimes thrombosis is segmental, with a segment of iliac vein or superficial femoral vein occluded but with patent veins below this level; there is a higher incidence of this in pregnant patients and patients with pelvic tumours. Patent segments below the thrombus may show some slow antegrade flow, particularly if collateral channels are adequate, but this does not show any respiratory variation and the augmentation response is damped.

### *Augmentation*

Normal venous flow is slow and can be improved by compression distal to the point of assessment. There are various techniques for achieving this which are discussed further in the section on chronic venous insufficiency, but for the assessment of possible DVT manual compression of the calf is usually sufficient. The muscles of the calf are squeezed rapidly and firmly in order to propel blood up the veins. In a normal venous system there will be a rapid rise and fall in the frequency shift; whereas if there is a thrombosed segment in the veins, this will increase resistance to flow with damping, or absence, of the augmentation response (Fig. 5.14). It should be remembered that increased resistance to flow anywhere in the vein above the point of compression will result in impaired augmentation the thrombus may be above or below the point of examination. Therefore, the demonstration of impaired augmentation should lead to a careful search for thrombus in that limb; particularly in the calf or iliac segments. The squeeze of the calf muscles should not be violent, or excessive, as patients will often have tender or painful calves; in addition there is a small potential risk of dislodging a fresh friable thrombus, producing a pulmonary embolus. The risk of this is small and reports of this type of event are few.[17]

### *Flow in collateral channels*

When the normal venous channels are occluded, blood may be seen in collateral veins. In the acute stage, intramuscular channels will not have developed significantly but increased velocity and flow may be seen in the two saphenous veins, or the profunda femoris vein, which provide ready-made collateral pathways. Over a period of several weeks the intramuscular venous channels will develop and these may be apparent on colour Doppler; therefore their presence indicates a thrombus of some age, rather than fresh throm-

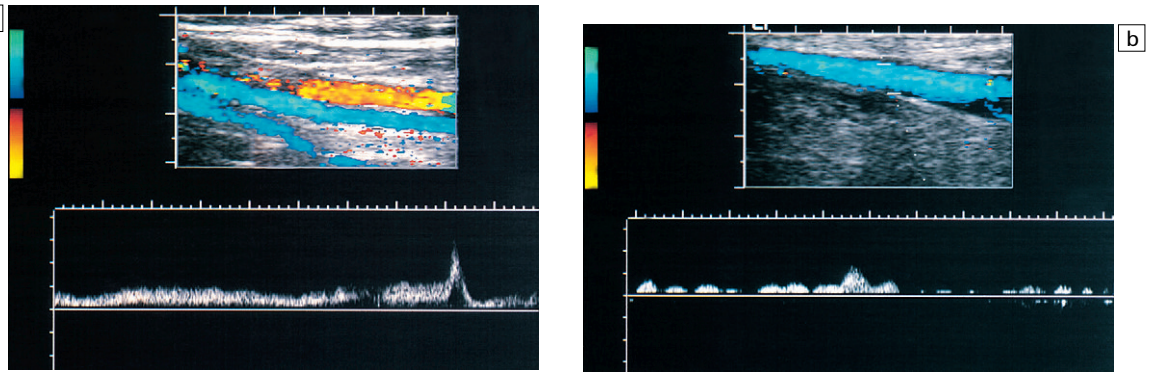


**Fig. 5.14** (a) A normal augmentation response to squeezing the calf; there is a rapid rise and fall in the velocity of blood past the transducer. (b) Abnormal augmentation, with damping of the response as a result of thrombus impeding the flow of blood up the vein.

bus, unless there has been rethrombosis in a segment of clearing clot.

## Distinction of acute from chronic thrombus

The features which suggest older, rather than fresh, thrombus are given in Table 5.5. However, it is not always possible to define the age of a thrombus and, in these cases the management of the patient must be based on the clinical picture.

Fresh thrombus is hypoechoic or anechoic. It is not attached to the wall around the whole circumference of the vein but if it fills the vein, the vein is a little expanded.[14, 18] Increased flow may be detected in the profunda femoris vein, or saphenous veins. As thrombus matures it becomes increasingly echogenic and starts to contract as it becomes organised. Longitudinal studies of thrombosed veins show that some 64–75% of veins will recanalise completely, or in part, by 1 year after thrombosis,[19] although valvular incompetence will be found at some level in the majority of these.[20] The remaining veins will show varying degrees of recanalisation, with a thickened irregular wall around an uneven lumen; or remain as fibrotic, permanently occluded structures. Abnormal collateral venous channels will develop in the soft tissues around any segments which are significantly obstructed for any length of time.

**Table 5.5** Distinction between acute and chronic thrombus

| Acute | Chronic |
|---|---|
| Anechoic or hypoechoic | Increasingly echogenic |
| Expansion of the vein | Contraction of the vein |
| Some compression possible | Incompressible |
| Thrombus 'tail' in lumen | Clot adherent around the wall of the vein |
| Absent or minimal collaterals | Collateral channels in the tissues |

## Upper limb and jugular vein thrombosis

The same principles apply to examination of the upper limb and neck veins. Lack of compressibility of the deep veins of the arm and neck and/or absence of flow on colour or power Doppler are diagnostic of thrombosis. The larger, more proximal veins, such as the axillary and subclavian, cannot be compressed due to their location; diagnosis of thrombosis in these vessels will therefore depend on careful assessment using colour or power Doppler. Indirect signs of thrombosis include loss of respiratory phasicity or cardiac variation, which indicates proximal occlusion and are useful if central vein (innominate or superior vena cava) thrombosis is suspected. Respiratory phasicity can be modified by asking the patient to breathe deeply, hold their breath or perform a Valsalva manoeuvre. Comparison

with the other side may be helpful, assuming that this is normal.

Baarslag et al[21] compared colour Doppler with venography and found 82% sensitivity and 82% specificity for the diagnosis of upper limb DVT; 63% of the patients who had thrombosis had an associated malignant disease and in 14% of those with thrombosis this was associated with an in-dwelling central venous catheter in patients without malignant disease. There is a low risk of clinically significant pulmonary embolus from upper limb DVT; in one series of 65 patients with arm vein thrombosis, none of the patients were found to have symptomatic pulmonary emboli.[22]

## PROBLEMS AND PITFALLS IN THE DIAGNOSIS OF DEEP VEIN THROMBOSIS

Some of these have been discussed already; however, the value of ultrasound as a technique for the diagnosis of DVT depends on the operator performing a careful, complete examination, being aware of potential pitfalls and recognising when a less than adequate examination has been performed. The main problem areas which should be remembered are shown in Table 5.6.

The essential requirement for a satisfactory examination is good ultrasound access to the veins of the limb. Many patients with a possible diagnosis of DVT have swollen or oedematous legs; this situation is aggravated if the patients are also obese. If visualisation is poor then it is possible to miss significant thrombus unless the situation is recognised and appropriate care is taken with the examination and machine settings, as well as with the selection of an appropriate transducer.

Dual superficial femoral veins may be overlooked unless they are actively sought with transverse scanning. If they are not recognised, then one component may be patent and seen on colour Doppler, whereas the other component may contain thrombus and be overlooked (Fig. 5.15).

Similarly, non-occlusive thrombus may be missed if the vein is not seen adequately. If there is only a small amount of thrombus in the vein then good flow signals will be obtained on spectral and colour Doppler and the presence of the thrombus may not be recognised (Fig. 5.13). This is particularly important in obese or oedematous legs.

The calf veins are multitudinous in number and variable in their anatomy. Even with a careful, patient, time-consuming examination it is difficult to exclude completely the presence of a small segmental thrombus in a calf vein or muscular sinus. In a mobile patient with a little calf tenderness or swelling this is not a problem,

**Table 5.6** Problems and pitfalls in the diagnosis of deep vein thrombosis

- Swollen/oedematous/fat legs
- Dual thigh and popliteal veins
- Non-occlusive thrombus
- Segmental calf vein thrombus
- Segmental iliac vein thrombus
- Pregnant patients

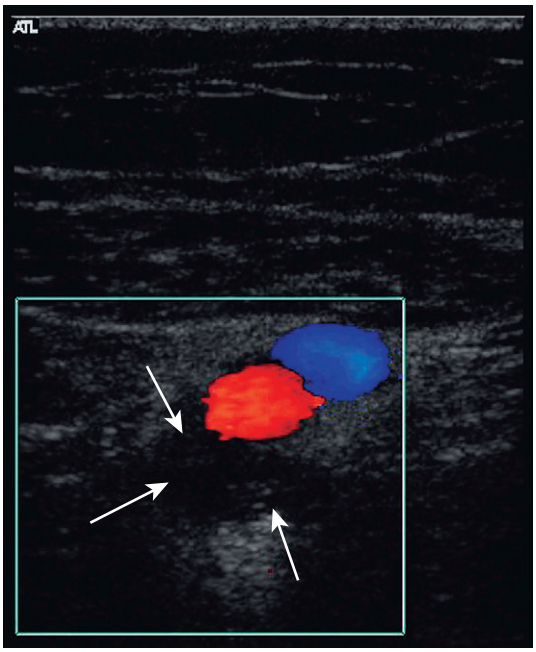


**Fig. 5.15** Dual superficial femoral vein segments; the more posterior segment (arrows) is thrombosed and could be overlooked.

as the body's normal thrombolytic mechanisms will probably clear this. However, in a patient who is immobile following surgery or a stroke, a small segmental calf thrombus indicates that the clotting cascade has been activated and there is a possibility that this small thrombus may increase in size, resulting in a significant, occlusive thrombus. Therefore a follow-up scan should be considered in these patients in order to identify any progression of thrombus from the calf. A study by Labropoulos et al[23] reviewed 5250 patients; isolated calf vein thrombus was found in 4.8% (282 limbs in 251 patients). In these patients, variable patterns of involvement of the calf veins were demonstrated with the soleal veins involved in 20% of cases, gastrocnemius veins in 17%, peroneal veins in 15% and the posterior tibial veins in 12%; in 64% of these positive cases, only a single vein group was involved.

The accuracy of Doppler in the detection of asymptomatic thrombus is less impressive than that for symptomatic thrombus,[4, 24] and the technique is therefore inadequate as a screening tool for the detection of asymptomatic thrombus. This is probably because asymptomatic thrombi are more likely to be small and non-occlusive; in addition, there is a higher incidence of distal thrombi in the calf veins, which may be more difficult to demonstrate with ultrasound.[3]

The external and common iliac veins may not be demonstrated in their entirety due to obesity or overlying bowel gas. Care must be taken to exclude segmental iliac vein thrombosis, especially if this is a possibility following pelvic surgery; however, it is very rare for iliac thrombosis not to include the common femoral vein.[25] The internal iliac veins are difficult to assess but any thrombus arising in these, which extends into the common iliac vein and significantly impedes blood flow, may be suggested by an impaired augmentation response in the femoral veins, or loss of respiratory variation on deep breathing or panting. However, non-occlusive thrombus which is insufficient to produce this effect may be overlooked; transvaginal scanning may be of value in difficult cases. It is important that the proximal extent of any thrombus is defined so that any subsequent extension can be appreciated. In addition, insertion of a caval filter might be considered and it is important to know if access is possible from the groin through the iliac veins. Once a filter has been inserted, the subsequent patency of the cava and iliac veins can be assessed using ultrasound (Fig. 5.16).[26]

During pregnancy several factors are present which increase the risk of thrombosis. These include changes to the coagulation system and physiological changes to venous flow in the leg veins due to a combination of hormonal effects and pressure from the enlarging uterus.[27] Some of the issues relating to the ultrasound diagnosis of thrombosis associated with pregnancy have already been discussed. There is also an increased tendency to develop segmental proximal thromboses in the iliac and upper femoral veins. This is more common on the left side,[28, 29] perhaps reflecting the additional potential compression from the right common iliac artery, which crosses the left common iliac vein just beyond the aortic bifurcation. If isolated iliac thrombosis is suspected and the ultrasound examination is less than adequate, then consideration should be given to

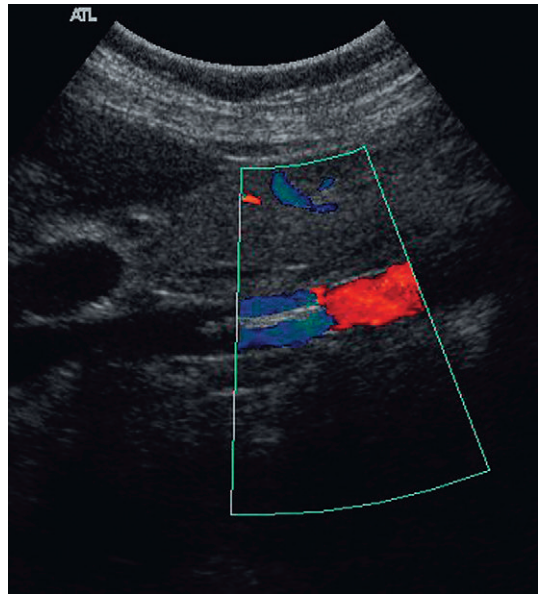


**Fig. 5.16** A caval filter in place. Note the change in colour due to the alteration in direction of flow in relation to the transducer.

further imaging with magnetic resonance (MR), or contrast venography.[27] Patients who have undergone caesarean section will have a higher risk of developing a DVT.

### Other causes of leg swelling, pain or tenderness

Unlike venography, ultrasound allows examination of other structures in the pelvis and leg. Other pathologies may be seen which account for the patient's symptoms of a swollen, or painful, tender leg; these are given in Table 5.7. It is important to remember that, even if a ruptured popliteal cyst is seen (Fig. 5.17), or a superficial thrombophlebitis is demonstrated (Fig. 5.18), the deep veins must still be examined carefully, as a coexistent DVT may otherwise be overlooked. Labropoulos et al[30] demonstrated popliteal cysts in 3% of asymptomatic individuals, rising to 10% of patients with symptoms of possible DVT and 20% of patients with painful knees. Langsfeld et al[31] found popliteal cysts in 3% of patients being examined for possible DVT, 7% of those with cysts had a coexisting DVT.

## ACCURACY IN RELATION TO OTHER TECHNIQUES

Despite these potential problems, ultrasound is a good non-invasive method for the diagnosis of symptomatic DVT, especially between the lower popliteal region and the groin.[3] The key to its value in any given department is that the sonographers must not only be well trained in the technique, but must also be able to recognise an inadequate examination so that appropriate further measures, such as venography or a repeat scan, can be arranged. Should venography be required to clarify areas of doubt, this can be focused on the area of concern identified at the ultrasound examination and only a limited examination may be required.

**Table 5.7** Other causes of leg swelling, pain or tenderness

- Popliteal (Bakers) cysts
- Haematoma/muscle injury
- Superficial thrombophlebitis
- Iliac nodes/pelvic masses
- Arteriovenous fistula
- Lymphoedema

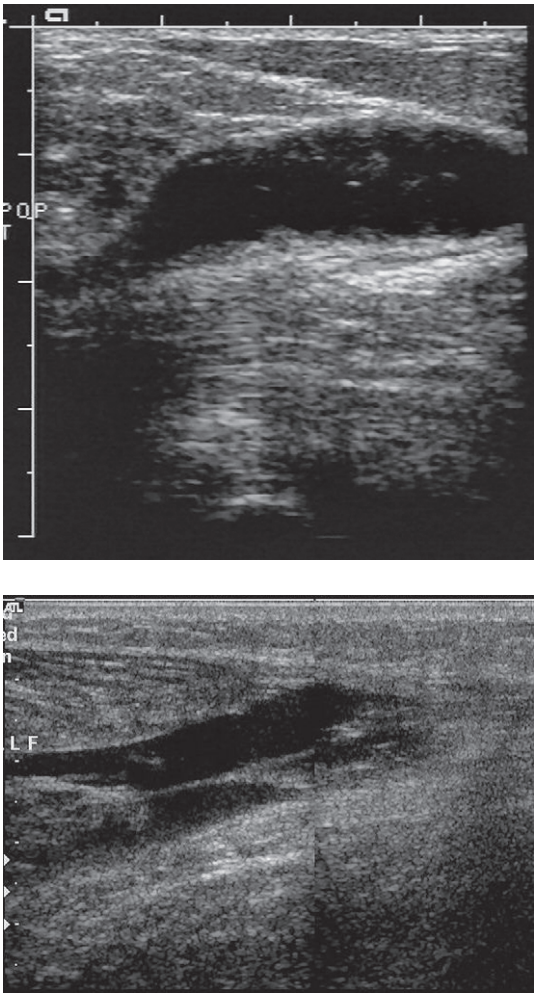


**Fig. 5.17** (a) A popliteal (Baker's) cyst behind the knee joint; (b) another patient with a ruptured popliteal cyst resulting in fluid tracking down through the calf.

Many studies have shown that, in comparison to venography, ultrasound is an accurate technique for the diagnosis of symptomatic DVT in the femoropopliteal segments, even in the absence of colour Doppler.[3] Used alone, compression is an accurate method for detecting DVT, with sensitivities of 89% and specificity of 100%

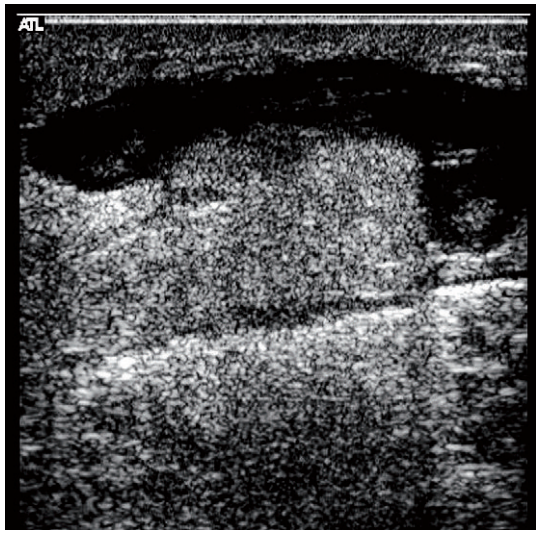

**Fig. 5.18** Thrombosis of the superficial veins is easily recognised but the deep veins should still be examined.

being reported for proximal thrombosis,[32] and sensitivities of 86–92% and specificities of 96–100% for careful examination of the calf veins.[33] The additional use of colour Doppler allows very accurate diagnosis of DVT, particularly in the femoropopliteal segments. With the development of colour Doppler techniques, further studies have shown the value of ultrasound and that the calf veins can be examined satisfactorily in most cases (Table 5.8).[34, 35] The need for an adequate examination must be emphasised. In one study, the initial results in the calf were significantly less accurate than the results for the femoropopliteal segment, but when the examinations were reviewed and only those which were technically adequate were considered, the overall accuracy improved markedly and reached a similar level to that obtained in the upper part of the limb[36] (Table 5.8). In another study,[35] 32% of studies of calf veins were inadequate; if these were excluded then ultrasound showed 93% sensitivity, 98% specificity and 97% accuracy for the diagnosis of lower limb DVT.

In a review of outcomes following negative femoropopliteal ultrasound examinations, Gottlieb and Widjaja[37] showed that only 0.7% of cases developed a subsequent pulmonary embolus, they also reviewed 1797 similar patients reported in the literature and noted that only four (0.2%) of these had developed a pulmonary embolus following a negative ultrasound examination of the thigh area in patients symptomatic for DVT.

It is important to draw a distinction between the accuracy of ultrasound for the diagnosis of symptomatic thrombus and asymptomatic thrombus. The results for the latter are less good as, almost by definition, asymptomatic thrombus will be non-occlusive in many cases and therefore easier to miss. Weinmann et al noted an overall sensitivity in six reported series of only 59% for proximal thrombus, although the specificity was 98%.[3] In addition, asymptomatic thrombus may be small, or involve one or only a few calf vein segments. A further review by Wells of 17 screening studies in orthopaedic patients showed a sensitivity of 62%, specificity of 97% and a positive predictive value of 66% in those studies which had been carried out with an adequate scientific method.[38]

The continuing developments with MR imaging (MRI) and multislice computed tomography (CT) mean that it is now feasible to

**Table 5.8** Results of Doppler ultrasound in the diagnosis of symptomatic deep vein thrombosis

| Author | No. of patients | Sensitivity (%) | Specificity (%) | Regions studied |
|---|---|---|---|---|
| Rose et al [36] | 75 | 96 | 100 | Iliac and femoropopliteal |
| | 75 | 92 | 100 | Femoropopliteal only |
| | 75 | 73 | 86 | Calf only (all studies) |
| | 45 | 95 | 100 | Adequate calf vein studies |
| Baxter et al[34] | 40 | 100 | 100 | Femoropopliteal |
| | 40 | 95 | 100 | Calf only |
| Theodorou et al[35] | 136 | 93 | 98 | Femoropopliteal |

consider using these for the diagnosis of DVT. Several authors have suggested that performing a CT scan of the pelvis and upper legs in patients undergoing CT pulmonary arteriography for pulmonary embolus is a satisfactory way to confirm or exclude the presence of significant proximal thrombus in the leg and pelvic veins.[39,40] However, this technique would not be practical for the assessment of all cases of possible DVT and considerations relating to radiation dose and contrast injection would need to be taken into account. Similarly, MR venography is also of some value[41] as it shows not only the thrombus in the lumen of the vein as a filling defect but can also show thrombus directly due to the methaemoglobin within it; in addition it also shows the perivascular inflammatory reaction to acute thrombosis.[42] As with CT, MR venography is not practical or suitable for initial assessment of all patients with possible DVT, although incidental findings of DVT in abdominal and pelvic examinations can easily be recognised and research into its role is continuing.

## RECURRENT VARICOSE VEINS AND CHRONIC VENOUS INSUFFICIENCY

The venous system of the lower limb is relatively fragile and easily damaged by a variety of insults including thrombosis, trauma and inflammation. Previous thrombosis may not clear completely, resulting in chronic obstruction and damage to the valves. In limbs affected by DVT, 69% had at least one segment of incompetent vein which was more likely to occur in the previously thrombosed segment.[43] This damage results in loss of the protective action of the valves so that a continuous column of blood is present between the heart and the tissues of the calf, ankle and foot. In the erect position this may extend over 1.25 m and the hydrostatic pressure exerted on the tissues interferes with the circulation of blood in the capillaries, the transfer of nutrients and waste matter between blood and the tissues and may also promote local inflammatory responses in the tissues. These changes result in the development of varicose veins, varicose eczema and, ultimately, varicose ulceration. Treatment options include standard varicose vein surgical techniques, pressure stockings, dressings and, more recently, venous reconstruction techniques. The pattern of damaged and incompetent veins can be defined using Doppler ultrasound to examine the deep and superficial veins in order to identify thrombosed or partially recanalised veins. Incompetent venous segments, together with incompetent perforating veins, can be mapped out and appropriate surgical or medical techniques applied. Approximately 1% of the population will have venous leg ulceration at some point in their lives,[2] and up to 22% will have evidence of chronic venous insufficiency.[5]

Diagnosis and assessment of primary varicose veins has traditionally been based on clinical assessment in conjunction with hand-held Doppler devices but it has been shown that a formal colour Doppler assessment prior to surgery will alter the proposed operative procedure in a number of cases. Mercer et al[44] showed that relying on clinical assessment and hand-held Doppler would have resulted in inadequate, or inappropriate operations in 24% of patients undergoing surgery for primary varicose veins. However, applying this principle to all cases of primary varicose veins would result in a heavy workload, so some consideration needs to be given to patient selection and scanning only those in whom there are incomplete, or conflicting clinical findings.[45]

Recurrence of varicose veins after surgery or sclerotherapy may occur. Three main patterns of recurrence have been described.[46] A patent long saphenous vein may be present, suggesting that it has been missed at the time of the operation. Small collateral veins along the line of the long saphenous vein may enlarge to reconstitute the path of the vein (Fig. 5.19). Finally, drainage can occur through venous collaterals which pass along a variety of courses remote from the normal line of the vein. Colour Doppler is useful to assess the pattern of recurrence, so that appropriate surgical intervention may be planned.[47]

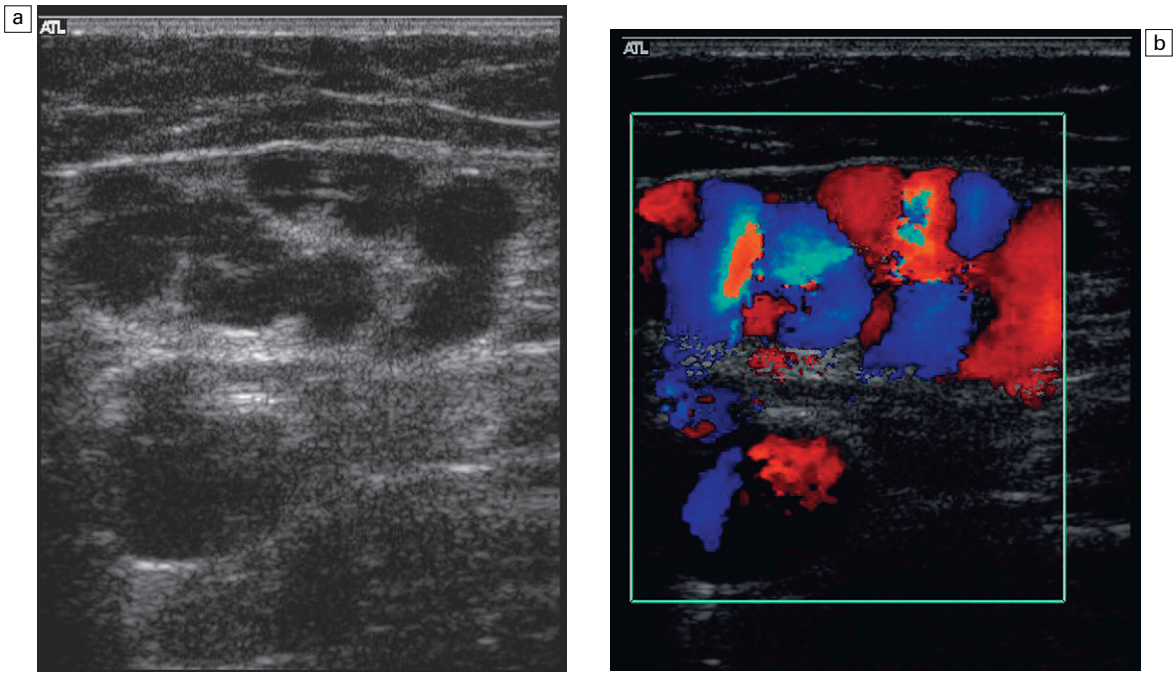


**Fig. 5.19** Collateral channels at the saphenofemoral junction on colour Doppler (a) B-scan image; (b) colour Doppler image.

## Technique of examination

The patient is best examined standing, or with a large degree of head-up tilt if the couch can be elevated, otherwise inadequate pressure will be exerted on the valves to test their competence and misleading measurements will be obtained. As the examination may be time-consuming – particularly if both legs are being examined – it is useful if the patients have some means of supporting themselves, such as a handle or rail on the wall; this enables them to stand in reasonable comfort with their weight on the leg that is not being examined and with slight flexion of the leg under examination. Alternatively, they may support themselves by holding the side of the ultrasound machine. It is useful if they are asked to stand on a low plinth, as this makes examination of the popliteal and calf regions less uncomfortable for the examiner.

Various techniques can be used to assess competence or incompetence of a venous segment.[48] The most convenient method for general assessment is to squeeze firmly the patient's calf, or lower thigh, to promote forward flow. Incompetent valves will allow reverse flow back through them after forward flow has ceased (Fig. 5.20), whereas competent valves will stop any reverse flow. Pressure cuffs that can be inflated and deflated rapidly can be used to produce a similar effect and produce a more standardised stimulus than manual compression.[49] They can also be used to compress a segment of leg in order to squeeze out the venous blood and then released suddenly so that any incompetent segments will show up by reversed filling from above. Alternatively, proximal compression may be applied to induce reverse flow. Getting the patient to perform a Valsalva manoeuvre will also show incompetent segments but there are two disadvantages to this technique. First, the effect will only demonstrate reverse flow as far as the first competent valve, so that any incompetent segments below this will not be demonstrated. Second, it is quite difficult to explain to many patients the exact nature and method for performing a Valsalva. Asking the patient to blow into a high-resistance spirometer circuit can produce the desired sudden increase in intra-

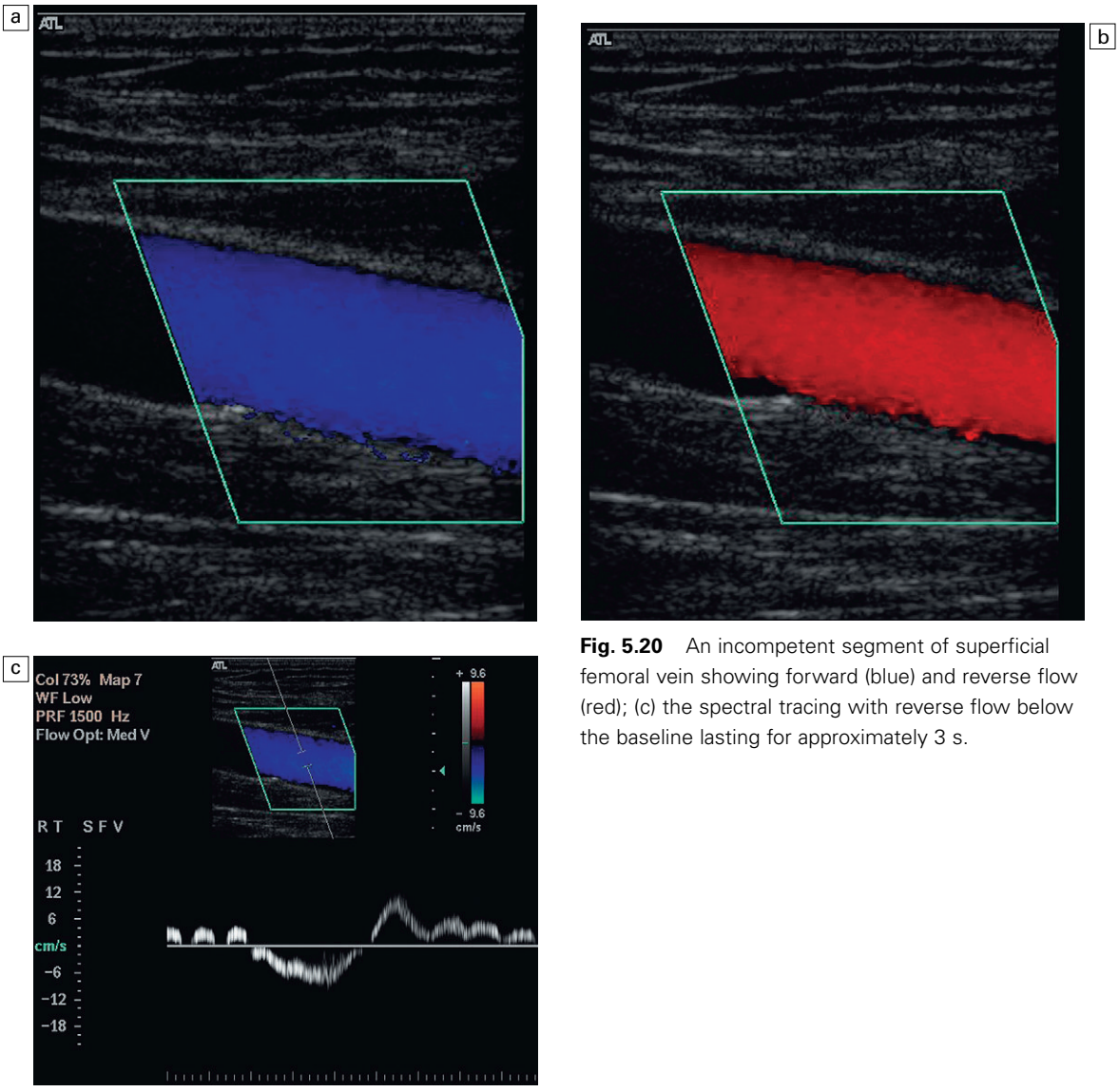


**Fig. 5.20** An incompetent segment of superficial femoral vein showing forward (blue) and reverse flow (red); (c) the spectral tracing with reverse flow below the baseline lasting for approximately 3 s.

abdominal pressure and is easier for many patients to understand. In some patients reflux will be seen simply with inspiration.

Reflux can be defined as reverse flow occurring after the cessation of forward flow. It is generally held to be significant if it lasts for more than 0.5 s,[50,51] although the time taken for reflux to cease does not correlate particularly well with the severity of reflux as measured by air plethysmography.[52] Shorter periods of reversed flow may be seen in normal veins and represent the short period as the valve cusps come together and blood in the venous segment settles under the influence of gravity. Reflux should not be confused with the reversed flow which occurs with turbulence, particularly in the common femoral vein and popliteal veins. The difference is usually apparent on colour Doppler, and turbulence is seen on spectral Doppler as reverse flow occurring at the same time as forward flow (Fig. 5.21).

The examination begins in the groin, where the common femoral vein, profunda femoris vein and saphenofemoral junction are identified

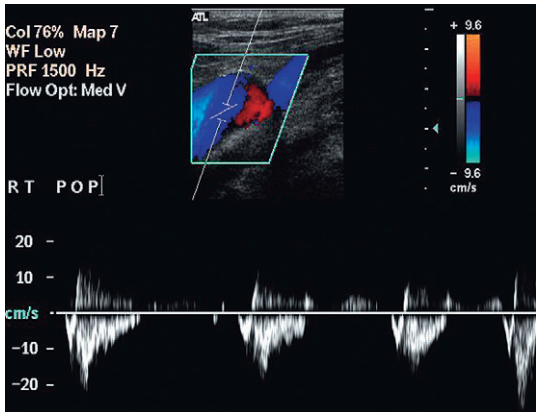


**Fig. 5.21** Turbulence in a vein showing both red and blue signal in the lumen on colour Doppler and simultaneous forward and reversed flow on the spectral display.

and assessed. If there is a history of previous venous surgery the details are sometimes uncertain, or even wrong, and the region of the saphenofemoral junction should be examined carefully to assess the type of surgery, whether it was successful and whether there are any significant collaterals, or recanalised segments which are incompetent. The loss of the normal smooth curve of the long saphenous vein as it passes laterally and deeply towards the common femoral vein is suggestive of previous surgery with subsequent recanalisation or collateral formation.

The patency and competence of the deep and superficial veins of the thigh are then assessed down to the level of the knee. Whilst examining the long saphenous vein the presence of incompetent perforators should be sought (Fig. 5.22), especially if the vein becomes incompetent at a level below the saphenofemoral junction. These can be identified most easily by scanning down the vein transversely whilst applying recurrent compression to the calf or lower thigh and looking for outward flow with colour Doppler. The commonest of these perforating veins is in the lower thigh at the level of the junction of the middle and lower thirds and is called the mid-thigh perforator vein (Fig. 5.2). The use of tourniquets may help clarify difficult cases but this is not usually required with colour Doppler.

The patient is then turned so that the popliteal region can be examined with the knee partially flexed. The veins in the popliteal fossa are assessed and the saphenopopliteal junction is examined. The level of the saphenopopliteal junction should also be noted, especially if this is not in the expected location. As with the saphenofemoral junction, recurrence after surgery can alter the anatomy and pattern of flow so that care is needed in defining the situation.

Examination of the calf veins may also be performed, although the findings tend to be

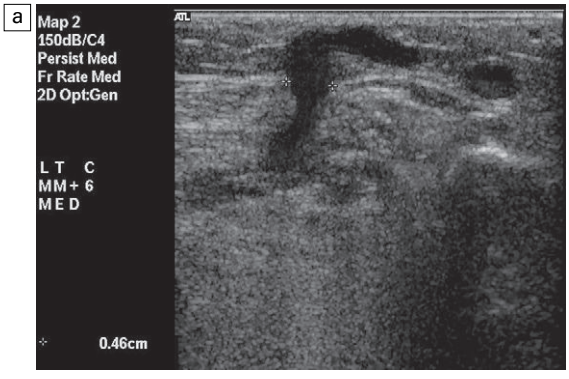


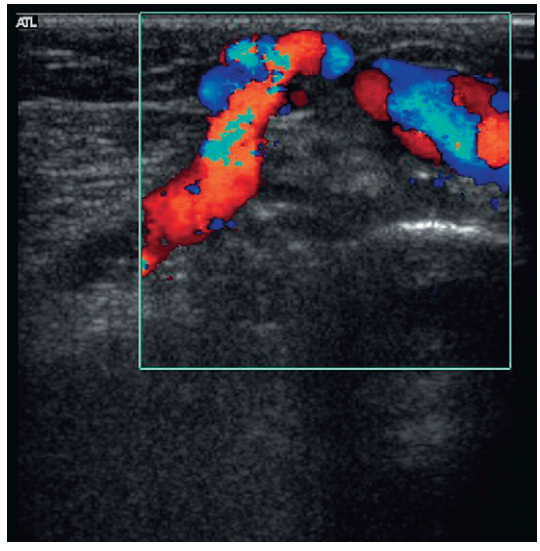


**Fig. 5.22** (a) An incompetent calf perforating vein with a diameter of approximately 5 mm passing through the superficial fascia; (b) colour Doppler shows flow passing from the deep to the superficial veins.

more variable and their significance more difficult to interpret. Incompetence may be seen in a similar fashion to that demonstrated more proximally. Sometimes the veins appear dilated and it is felt that they should be incompetent, but it is very difficult, or impossible, to induce significant forward flow in the vessels, or any subsequent reflux. Any incompetent calf perforator veins should also be sought using colour Doppler, looking for outward flow from the deep to the superficial systems (Fig. 5.2). The anatomy and function of the calf veins and the calf perforator veins may have important implications for the development of varicose changes, and this area is the subject of continuing research.

If necessary, varices can be traced proximally in order to identify the point of communication with the deep or superficial segments. This is usually best done with the transducer at right angles to the line of the vein being followed, judicious compression of lower varices will show the course of the veins on colour Doppler and confirm the presence of reflux, where appropriate. Care must be taken not to compress superficial veins with excessive transducer pressure when following the veins.

## SAPHENOUS VEIN MAPPING

The long saphenous vein is the preferred conduit for arterial bypass grafting in the coronary arteries and lower limb. If there is any doubt concerning the suitability of the vein for the procedure, ultrasound can be used to assess the calibre and available length of the vein. Ideally the vein should be more than 3–4 mm wide for much of its length and more than 2 mm at the ankle if a long, femorodistal graft is being considered.[53] The aim of the examination depends on the surgical procedure being contemplated. If the vein is to be removed for a coronary artery or reversed lower limb arterial graft, then the examination can be limited to confirming the presence of the vein and assessing its calibre over the required length. If an in situ lower limb arterial graft is to be performed then a much more detailed examination is required in order to identify perforating veins and superficial branches communicating with the main vein, as these must be ligated during the operation to stop arteriovenous fistulae developing.

### Technique

The examination is performed with the patient standing, if possible, as this produces distension of the vein, allowing easier location due to dilatation and a better estimation of the calibre of the vessel. If the patient is unable to stand they can be examined sitting with their legs over the side of the couch; if this is not possible then they can be assessed lying supine with a low-pressure tourniquet applied in order to produce distension of the superficial veins.

One of the problems associated with this examination is that ultrasound gel gums up fibre-tipped markers, making it impossible to mark the course of the vein on the skin, or the location of perforators. In order to avoid this problem the skin should not be covered with gel in the normal manner but the gel should be applied to the transducer and this then placed in the region of the saphenofemoral junction. Once the vein has been located the transducer is aligned along its course, the skin is marked over the vein at the lower end of the transducer. The transducer is then moved so that its upper end is on the skin mark, aligned along the vein, and a further mark put at the location of the vein at the new position of the lower end of the transducer. The course of the vein is followed down the limb, with skin markings being made at each transducer length. Care must be taken in the calf, where the long saphenous vein has two main components: the anterior branch usually passes down to the front of the lateral malleolus and is the larger component, with the posterior branch running posteriorly to the posteromedial aspect of the calf. Some operators prefer to mark out the vein with the patient supine as this approximates better to the position during surgery.

Once the main marks have been applied, the location of the saphenofemoral junction, together with any other perforator veins, dual segments

and tributaries, can be identified and marked. This is usually easier to achieve by scanning transversely along the line of the long saphenous vein with regular augmentation of flow from squeezing the calf. The calibre of the vein is measured in the transverse plane, taking care not to compress the vessel with pressure from the transducer.

## CONCLUSIONS

Providing care and attention are paid to examination technique then colour Doppler ultrasound is a reliable method for the diagnosis of DVT in symptomatic patients. The technique has become the first-line investigation for DVT in many centres, allowing any subsequent venography to be restricted to the area of doubt or concern on the ultrasound examination. It is important to recognise that the technique has some limitations and that several pitfalls exist.

Ultrasound also provides a non-invasive technique for the investigation of patients with chronic venous disease, or recurrence of varicose veins following surgery, enabling an accurate assessment of the pattern of incompetence or recurrence to be established and allowing an appropriate surgical approach to be developed. It is also of benefit in the assessment of patients with primary varicose veins, especially if there is uncertainty following clinical examination.

The long saphenous vein can be assessed for its suitability as a bypass conduit for arterial or coronary artery bypass procedures. In addition, ultrasound provides a method for examining the central veins prior to central venous line insertion if problems are anticipated in locating a suitable channel for line insertion.

## REFERENCES

1. Anderson FA Jr, Wheeler HB, Goldberg RJ, et al. A population-based perspective of the hospital incidence and case-fatality rates of deep vein thrombosis and pulmonary embolism: the Worcester DVT study. Arch Intern Med 1991; 151:933–938.
2. Callam MJ, Ruckley CV. The epidemiology of chronic venous disease. A textbook of vascular medicine. London: Arnold; 1996:562–579.
3. Baxter GM. The role of ultrasound in deep vein thrombosis. Editorial. Clin Radiol 1997; 52:1–3.
4. Weinmann EE, Salzman EW. Deep vein thrombosis: a review. New Engl J Med 1994; 331:1630–1641.
5. Phillips GWL, Paige J, Molan MP. A comparison of colour duplex ultrasound with venography and varicography in the assessment of varicose veins. Clin Radiol 1995; 50:20–25.
6. Da Silva A, Widmer LK, Martin H, et al. Varicose veins and chronic insufficiency: prevalence and risk factors in 4376 subjects of the Basle Study II. Vasa 1974; 3(2):118–125.
7. Gordon AC, Wright I, Pugh ND. Duplication of the superficial femoral vein: recognition with duplex ultrasonography. Clin Radiol 1996; 51:622–624.
8. Quinlan DJ, Alikhan R, Gishen P, et al. Variations in lower limb venous anatomy: implications for US diagnosis of deep vein thrombosis. Radiology 2003; 228:443–448.
9. Basmajian JV. Distribution of valves in femoral, external iliac and common iliac veins and their relationship to varicose veins. Surg Gynecol Obstet 1952; 85:537–542.
10. Corrales NE, Irvine A, McGuinness CL, et al. Incidence and pattern of long saphenous vein duplication and its possible implications for recurrence after varicose vein surgery. Br J Surg 2002; 89:323–326.
11. Linton RR. The communicating veins of the lower leg and the operative technique for their ligation. Ann Surg 1938; 107:582–593.
12. Giacomini C. Osservazioni anatomische per service allo studio della circulazioni venosa delle extremitá inferiori. Torino: Tip V Vercillino; 1873.
13. Burihan E, Baptista-Silva JCC. Anatomical study of the small saphenous vein (saphena parva): types of termination. Phlebology 1995; 10(suppl 1); 57–60.
14. Wells PS, Anderson DR, Bormanis J, et al. Value of assessment of pretest probability of deep-vein thrombosis in clinical management. Lancet 1997; 350:1795–1798.
15. Ilkhanipour K, Wolfson AB, Walker H, et al. Combining clinical risk with D-dimer testing to rule out deep vein thrombosis. J Emerg Med 2004; 27:233–239.
16. Hertzberg BS, Kliewer MA, DeLong DM, et al. Sonographic assessment of lower limb vein diameters: implications for the diagnosis and characterization of deep venous thrombosis. Am J Roentgenol 1997; 168:1253–1257.

17. Perlin SJ. Pulmonary embolism during compression US of the lower extremity. Radiology 1992; 184:165–166.
18. Zwiebel WJ, Priest DL. Colour duplex sonography of extremity veins. Semin Ultrasonogr CT MR 1990; 11:136–137.
19. Rosfors S, Eriksson M, Leijd B, et al. A prospective follow-up study of acute deep venous thrombosis using colour duplex ultrasound, phlebography and venous occlusion plethysmography. Internat Angiol 1997; 16:39–44.
20. Franzeck UK, Schalch I, Jager KA, et al. Prospective 12-year follow-up study of clinical and haemodynamic sequelae after deep vein thrombosis in low-risk patients (Zurich study). Circulation 1996; 93:74–79.
21. Baarslag HJ, van Beek EJ, Koopman MM, et al. Prospective study of color duplex ultrasonography compared with contrast venography in patients suspected of having deep venous thrombosis of the upper extremities. Ann Intern Med 2002; 136:865–872.
22. Mustafa S, Stein PD, Patel KC, et al. Upper extremity deep venous thrombosis. Chest 2003; 123:1953–1956.
23. Labropoulos N, Webb KM, Kang SS, et al. Patterns and distribution of isolated calf deep vein thrombosis. J Vasc Surg 1999; 30:787–791.
24. Davidson BL, Elliot CG, Lensing AWA. Low accuracy of colour Doppler ultrasound in the detection of proximal leg vein thrombosis in asymptomatic high-risk patients. Ann Intern Med 1992; 117:735–738.
25. Rose SC, Zwiebel WJ, Miller FJ. Distribution of acute lower extremity deep venous thrombosis in symptomatic and asymptomatic patients. J Ultrasound Med 1994; 13:243–250.
26. Smart LM, Redhead DN, Allan PL, et al. Follow-up study of Gunther and LGM inferior vena cava filters. J Intern Radiol 1992; 7:115–118.
27. Chan WS, Ginsberg JS. Diagnosis of deep vein thrombosis and pulmonary embolism in pregnancy. Thromb Res 2002; 107:85–91.
28. Polak JF, Wilkinson DL. Ultrasonographic diagnosis of symptomatic deep venous thrombosis in pregnancy. Am J Obstet Gynecol 1991; 165:625–629.
29. Macklon NC, Greer IA, Bowman AW. An ultrasound study of gestational and postural changes in the deep venous system of the leg in pregnancy. Br J Obstet Gynaecol 1997; 104:191–197.
30. Labropoulos N, Shifrin DA, et al. New insights into the development of popliteal cysts. Br J Surg 2004; 91:1313–1318.
31. Langsfeld M, Matteson B, Johnson W, et al. Baker's cysts mimicking the symptoms of deep vein thrombosis: diagnosis with venous duplex scanning. J Vasc Surg 1997; 25:658–662.
32. Cronan JJ, Dorfman GS, Scola FH, et al. Deep venous thrombosis: US assessment using vein compression. Radiology 1987; 162:191–194.
33. Atri M, Herba MJ, Reinhold C, et al. Accuracy of sonography in the evaluation of calf deep vein thrombosis in both postoperative surveillance and symptomatic patients. Am J Radiol 1996; 166:1361–1367.
34. Baxter GM, Duffy P, Partridge E. Colour flow imaging of calf vein thrombosis. Clin Radiol 1992; 46:198–201.
35. Theodorou SJ, Theodorou DJ, Kakitsubata Y. Sonography and venography of the lower extremities for diagnosing deep vein thrombosis in symptomatic patients. Clin Imaging 2003; 27:180–183.
36. Rose SC, Zwiebel WJ, Nelson BD, et al. Symptomatic lower extremity deep venous thrombosis: accuracy, limitations and role of colour duplex flow imaging in diagnosis. Radiology 1990; 175:639–644.
37. Gottlieb RH, Widjaja J. Clinical outcomes of untreated symptomatic patients with negative findings on sonography of the thigh for deep vein thrombosis: our experience and a review of the literature. Am J Roentgenol 1999; 172:1601–1604.
38. Wells PS, Lensing AW, Davidson BL, et al. Accuracy of ultrasound for the diagnosis of deep vein thrombosis in asymptomatic patients after orthopaedic surgery. A meta-analysis. Ann Intern Med 1995; 122:47–53.
39. Loud PA, Katz DS, Bruce DA, et al. Deep venous thrombosis with suspected pulmonary embolism: detection with combined CT venography and pulmonary angiography. Radiology 2001; 219:498–502.
40. Lim KE, Hsu WC, Hsu YY, et al. Deep venous thrombosis: comparison of indirect multidetector CT venography and sonography of lower extremities in 26 patients. Clin Imaging 2004; 28:439–444.
41. Fraser DG, Moody AR, Davidson IR, et al. Deep venous thrombosis: diagnosis by using venous enhanced subtracted peak arterial MR venography versus conventional venography. Radiology 2003; 226:812–820.
42. Froehlich JB, Prince MR, Greenfield LJ, et al. 'Bull's-eye' sign on gadolinium-enhanced magnetic resonance venography determines thrombus presence and age: a preliminary study. J Vasc Surg 1997; 26:809–816.
43. Markel A, Manzo RA, Bergelin RO, et al. Valvular reflux after deep vein thrombosis: incidence and time of occurrence. J Vasc Surg 1992; 15:377–384.
44. Mercer KG, Scott DJ, Berridge DC. Preoperative duplex imaging is required before all operations for primary varicose veins. Br J Surg 1998; 85:1495–14977.
45. Kent PJ, Weston MJ. Duplex scanning may be used selectively in patients with primary varicose veins. Ann R Coll Surg Engl 1998; 80:388–393.

46. Stonebridge PA, Chalmers N, Beggs I, et al. Recurrent varicose veins: a varicographic analysis leading to a new, practical classification. Br J Surg 1995; 82:60–62.
47. Bradbury AW, Stonebridge PA, Callam MJ, et al. Recurrent varicose veins: assessment of the saphenofemoral junction. Br J Surg 1994; 81:373–375.
48. Allan PL. The role of ultrasound in the assessment of chronic venous insufficiency. Ultrasound Q 2001; 17:3–10.
49. Markel A, Meissner MH, Manzo RA, et al. A comparison of the cuff deflation method with Valsalva's maneuver and limb compression in detecting venous valvular reflux. Arch Surg 1994; 129:701–705.
50. Iafrati MD, Welch H, O'Donnell TF, et al. Correlation of venous non-invasive tests with the Society for Vascular Surgery/International Society for Cardiovascular Surgery clinical classification of chronic venous insufficiency. J Vasc Surg 1994; 19:1001–1007.
51. Labropoulos N, Tiongson J, Pryor L, et al. Definition of venous reflux in lower-extremity veins. J Vasc Surg 2003; 38:793–798.
52. Rodriguez AA, Whitehead CM, McLaughlin RL, et al. Duplex-derived valve closure times fail to correlate with reflux flow volumes in patients with chronic venous insufficiency. J Vasc Surg 1996; 23:606–610.
53. Leopold PW, Shandall A, Kupinski AM, et al. Role of B-mode venous mapping in infrainguinal in situ vein arterial bypasses. Br J Surg 1989; 76:305–307.

# The aorta and inferior vena cava

# 6

Paul L. Allan

Doppler examination in the abdomen is associated with specific problems which are not encountered in peripheral vascular examinations, and these are particularly relevant to examinations of the aorta, inferior vena cava and their associated vessels.

Respiratory motion and cardiac pulsation impair the examination, but getting the patient to suspend respiration for any length of time results in relative hypoxia and subsequently increased respiratory movement. It is therefore better to scan as much as possible during quiet respiration, asking the patient to hold their breath only for short periods in order to obtain a spectral trace. In most cases only two or three cardiac cycles are needed for assessment.

Many vessels will always seem to be orientated at right angles to the scan plane, especially with sector or curved linear transducers. Different angles of approach and repositioning of both the transducer and the patient may be required in an attempt to improve the Doppler angle.

Bowel gas is also a problem as it can obscure a vessel, or produce distracting motion artefacts as it bubbles past; scanning after an overnight fast may improve the situation, as may an injection of hyoscine. It has been suggested that patients should receive bowel preparation as for an enema, but this author feels that this is not usually justified for the small advantage it may occasionally confer.

Abdominal Doppler examinations are performed on vessels which lie more deeply than the peripheral vessels and this has several consequences. First, lower-frequency transducers are used and this limits the size of Doppler shift which will be obtained for a given velocity. Second, longer-pulse repetition intervals are required to allow the sound to travel the greater distances; this also limits the size of Doppler shift which can be measured as a result of the Nyquist limit (see Ch. 1). Operators should therefore seek to minimise the scan depth and use the highest-frequency transducer compatible with adequate visualisation.

## THE AORTA

### Anatomy

The aorta enters the abdomen at the level of T12 and runs down the posterior abdominal wall to the left of the midline, with the inferior vena cava to its right side. It divides into the common iliac arteries at the level of L4, which is about the level of the iliac crests. Para-aortic nodes are distributed anteriorly and on both sides of the vessel.

The abdominal aorta gives branches to the abdominal organs and to the abdominal wall. The parietal branches to the abdominal wall are not usually large enough to be seen regularly using colour Doppler and will not be considered further. The visceral branches (Fig. 6.1) supply the liver, kidneys, adrenal glands, gonads, spleen, bowel and pancreas. The vessels to the adrenals and gonads are also usually too small to be seen reliably on ultrasound; the renal, hepatic and iliac arteries are covered elsewhere in greater detail.

The splanchnic arteries supply the bowel and associated organs. The *coeliac trunk* (Fig. 6.2) arises from the anterior aspect of the aorta just after it has entered the abdomen. The trunk is only about 1 cm long and divides into three branches: the common hepatic artery, the splenic

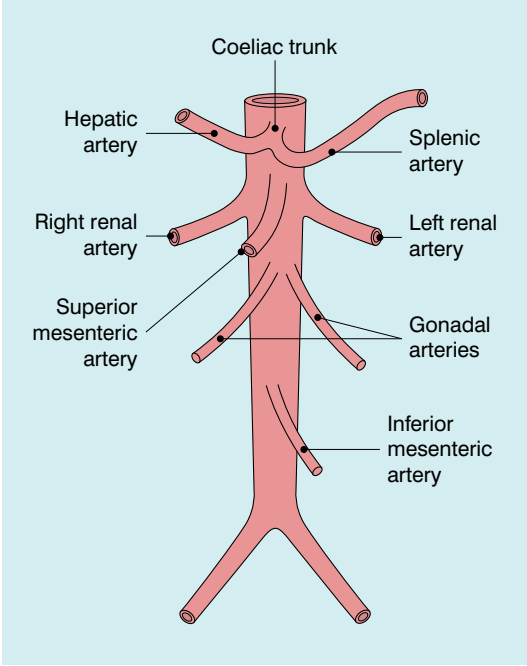


**Fig. 6.1** The abdominal aorta and its major branches.

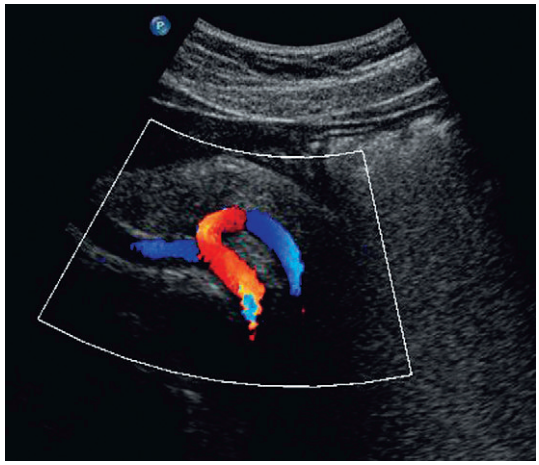

**Fig. 6.2** Transverse view of the coeliac axis showing the splenic artery on the right and the hepatic artery on the left.

artery and the left gastric artery. The *common hepatic artery* passes to the right over the head of the pancreas, where it gives off the gastroduodenal artery which can be seen passing inferiorly between the head of the pancreas and the margin of the duodenum; the other branches from this segment of the hepatic artery are not usually apparent on ultrasound. The artery ascends in the lesser omentum as the proper hepatic artery, in company with the portal vein and common bile duct, to the porta of the liver, where it divides into right and left hepatic arteries. The *splenic artery* passes to the left and runs along the superior margin of the body of the pancreas to the hilum of the spleen. It has a tortuous course and an arterial loop may be mistaken for a small cyst in the pancreas if the situation is not recognised; colour Doppler allows quick identification of the true nature of the 'cyst'. The right gastric artery arises from the splenic artery but is not usually seen on ultrasound.

The *superior mesenteric artery* (Fig. 6.3) arises 1–2 cm below the coeliac trunk and supplies the small bowel and colon to the distal transverse colon. The superior mesenteric vein is seen on the right side of the upper portion of the artery and can be followed to its confluence with the splenic vein, forming the portal vein. The individual branches of the superior mesenteric artery are not usually seen clearly on ultrasound. The *inferior mesenteric artery* (Fig. 6.4) arises from the anterior aorta about 3–4 cm above the bifurcation and runs inferiorly to the left side of the

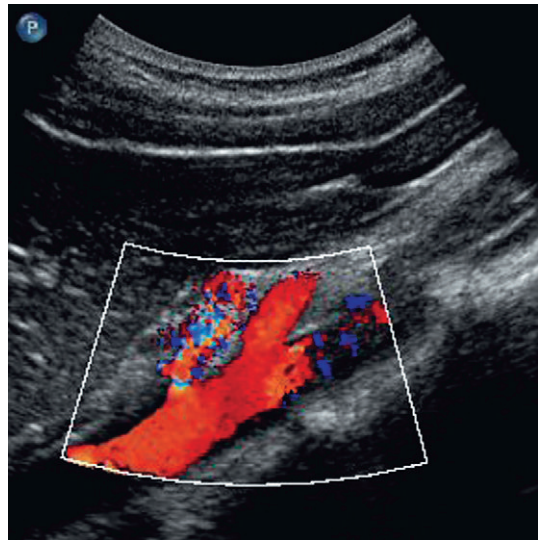

**Fig. 6.3** Longitudinal scan showing the origin of the coeliac axis superiorly and the superior mesenteric artery just below this. Colour Doppler shows aliasing and a tissue bruit around a stenotic coeliac axis origin.

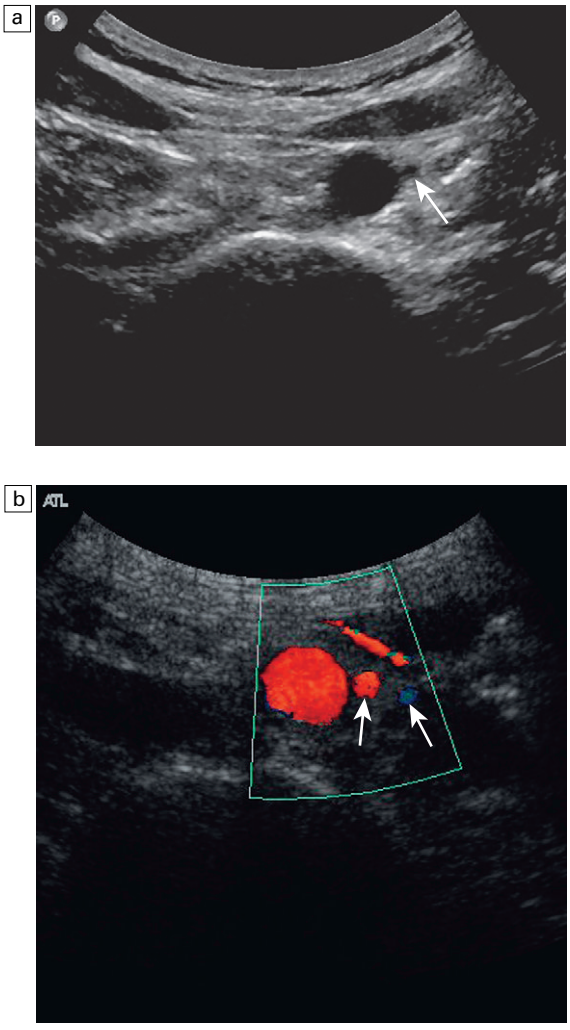


**Fig. 6.4** (a) Transverse scan showing the inferior mesenteric artery lying adjacent to the aorta (arrow); (b) colour Doppler image showing the inferior mesenteric artery and vein (arrows).

aorta. The inferior mesenteric vein may be seen on the left of the artery but diverges as it passes up to join the splenic vein.

Several variations in the anatomy of the splanchnic arteries are well recognised. The most important one in relation to ultrasound is the origin of the right hepatic artery from the superior mesenteric artery. Occasionally the coeliac trunk is absent with its branches arising separately from the aorta; the left hepatic artery may arise from the left gastric artery and accessory hepatic arteries may arise from the superior mesenteric artery or other arteries in the region.

## Scanning technique

### *Aorta*

The upper abdominal aorta can nearly always be examined through the left lobe of the liver; the coeliac trunk and superior mesenteric arteries are also visible from this approach. A 3 or 5 MHz transducer is used depending on the build of the patient. The patient should fast for 8 h prior to the examination, for two reasons: first, fasting will improve visualisation of the aorta and its branches; second, splanchnic blood flow will be in the basal fasting state, rather than the dynamic postprandial state.

If the aorta is the main object of the investigation it is followed distally to its bifurcation. The vessel should be scanned both longitudinally and transversely, taking note of the overall diameter, the presence of any aneurysmal dilatation and any para-aortic masses or pathology. If visualisation from an anterior approach is impaired, then scanning in a coronal plane through the right lobe of the liver will allow the upper aorta to be visualised; scanning in a coronal oblique plane from a left posterolateral approach can provide a view of the mid- and lower aorta, together with the bifurcation. The calibre of the vessel is measured from the outer aspect of the vessel wall, ideally during systolic expansion. The systolic anteroposterior diameter is the easiest and most repeatable measurement to make and this is therefore used for follow-up of aneurysm patients. It is important to ensure that the true anteroposterior diameter is measured, particularly in ectatic, tortuous arteries, as oblique measurements will result in falsely high measurements. Colour Doppler and spectral Doppler are used to assess any potential disturbances of flow which may result from atheroma or dissection.

### *Splanchnic arteries*

The coeliac trunk and its main branches are examined using colour and spectral Doppler. The main trunk is short but it is directed towards the transducer so that an excellent Doppler angle

is achieved. The proximal hepatic and splenic arteries, together with the superior mesenteric artery, are often orientated almost at right angles to the scan plane with an anterior approach (Fig. 6.2), so that some experimentation with points of access is required to get acceptable Doppler angles. The hepatic artery is followed to the right and the gastroduodenal artery can be identified beside the head of the pancreas. The proper hepatic artery is traced towards the porta where it divides into the right and left hepatic arteries. The origin of the superior mesenteric artery is examined (Fig. 6.3) and the vessel traced as far distally as it remains visible. Firm pressure with the transducer may help in displacing bowel gas from in front of the vessel, but care must be taken not to compress the artery and produce a spuriously high Doppler shift. Colour Doppler is used to identify any abnormal areas of flow, including 'visible bruits', or tissue vibrations, which may be seen in cases of severe stenosis. Power Doppler is of less value in the abdomen than in peripheral vessels as arterial pulsation, respiratory movement and bowel gas motion can all cause marked motion artefacts which obscure the signal from the vessel.

The inferior mesenteric artery is sometimes difficult to locate. It can be found by scanning transversely up from the bifurcation and it may be identified just to the left of the aorta, 2–4 cm above the bifurcation (Fig. 6.4).

## Normal and abnormal findings

### *Aorta*

The calibre of the normal aorta varies with the age, sex and build of the patient, being larger in men, older patients and tall patients. The calibre also varies with the level in the abdomen. Goldberg et al found an average diameter of 22 mm above the renal arteries, 18 mm just below the renal arteries and 15 mm above the bifurcation.[1] The normal Doppler waveform in the aorta also varies with location. In the upper aorta there is a narrow, well-defined systolic complex with forward flow during diastole; below the renal arteries the diastolic flow is much reduced and above the bifurcation it is absent, or reversed diastolic flow may occur, with a waveform similar to that seen in the lower limb arteries (Fig. 6.5).[2]

The main abnormalities affecting the aorta are atheroma, aneurysm, dissection and para-aortic masses. *Atheroma* can affect the aorta and produce stenosis (Fig. 6.6), or occlusion; aortic disease, unless severe is usually overshadowed clinically by symptoms arising from the peripheral or the coronary arteries. Sometimes there is uncertainty as to whether aortic disease seen on arteriography is clinically significant. In these cases velocity ratios taken from above and at the

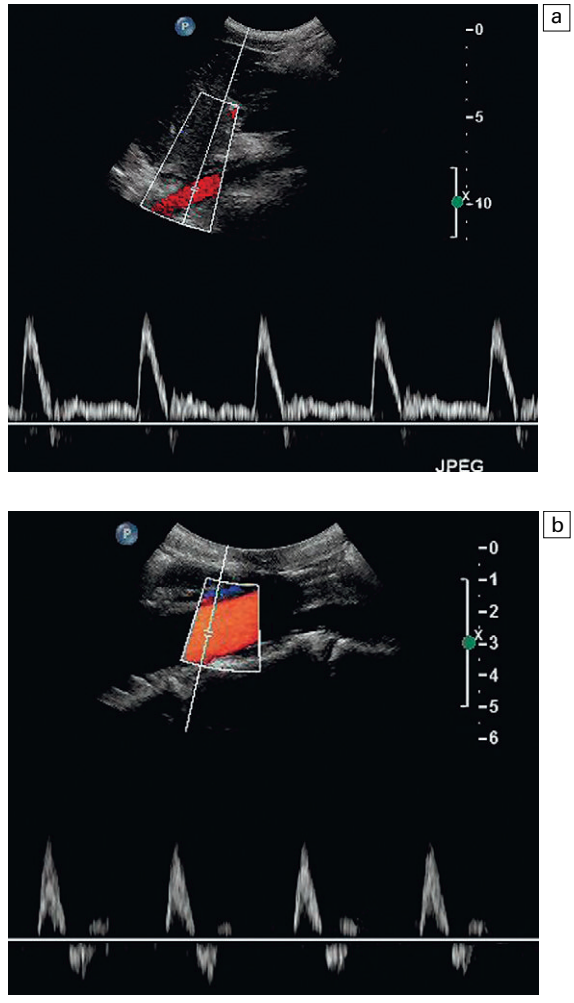


**Fig. 6.5** (a) The aortic waveform in the upper abdomen showing diastolic flow. (b) The aortic waveform above the bifurcation with absent diastolic flow and a waveform similar to that seen in the lower limb arteries.

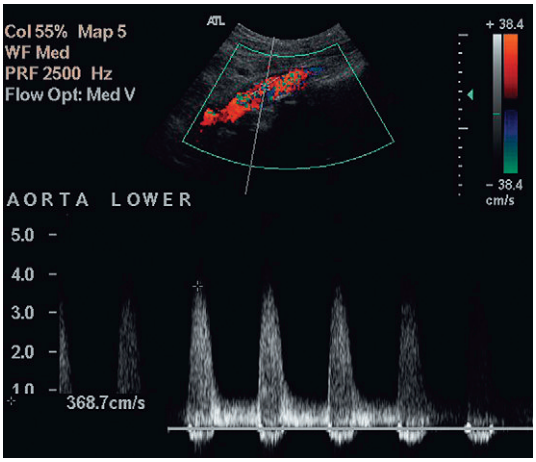


**Fig. 6.6** Colour Doppler image of a stenosis in the middle aortic segment showing significant turbulence and a peak systolic velocity of 3.7 m $s^{-1}$.

stenosis can be used to assess the degree of haemodynamic compromise. However, accurate criteria are not as fully developed for aortic stenosis (Fig. 6.6), as is the case for carotid and peripheral Doppler examinations, but in one study[3] a peak systolic velocity ratio of 2.8 correlated (86% sensitivity, 84% specificity) with aortoiliac stenoses of >50% diameter reduction and a ratio of 5.0 showed some correlation (65% sensitivity, 91% specificity) with stenoses >75%. If the stenotic area is clearly seen, a direct measurement of diameter or area stenosis may be obtained; colour or power Doppler is of value in defining the margins of the residual lumen.

An *aneurysm* of the abdominal aorta can be defined as an increase of the anteroposterior diameter over 3 cm, or a localised increase of 1.5 times the diameter of the adjacent normal aorta. Aneurysms may extend into the abdomen from the thoracic aorta, or may arise within the abdominal aorta, usually affecting the infrarenal segment. Aneurysms are nearly always true aneurysms secondary to degeneration of the connective tissue in the vessel wall. Occasionally mycotic aneurysms secondary to infection, or pseudoaneurysms secondary to trauma, may be seen. Ultrasound diagnosis is normally straightforward; the cardinal measurement is the anteroposterior diameter, which is best obtained by scanning transversely with the ultrasound beam at right angles to the long axis of the vessel, in order to ensure a true anteroposterior measurement. It is also important to locate the upper and lower margins of the aneurysmal segment, particularly in relation to the renal arteries. If these cannot be identified with certainty it should be remembered that the main renal arteries usually arise from the aorta 1–2 cm below the superior mesenteric artery, and this vessel can therefore be used as an approximate marker for the renal vessels.

Colour and spectral Doppler may show turbulent flow within the aneurysm, or indeed very slow flow with very little forward movement of the blood. However, examination of normal-calibre vessels below the aneurysm will show rapid reconstitution of the waveform as the pressure wave is constrained by the narrower calibre. Doppler can also be used to confirm renal blood flow, particularly after surgery, if there is any question that this has been cut off.

Ultrasound is used to monitor the rate of increase in size of the aneurysm over time. However, it should be remembered that the calibre of the aorta increases slowly with age and this should be borne in mind when assessing the significance of any alteration in the size of smaller aneurysms. Measuring any change in the calibre of the adjacent normal aorta may be helpful in assessing the significance of any change in the diameter of an aneurysm. The main complication arising from an aneurysm is leakage (Fig. 6.7) or rupture. Ultrasound can be used to identify any retroperitoneal haematoma which would indicate a leak but computed tomography (CT), if available, provides a more accurate overall assessment of the situation, providing the patient's condition is sufficiently stable to allow investigation. Rarely, an aortocaval or aortoduodenal fistula may develop; high-volume pulsatile flow in the inferior vena cava is seen on Doppler in cases of caval fistula (Fig. 6.8).

Screening for aortic aneurysms in men over 60–65 is beneficial in terms of reducing mortality;[4, 5] approximately 4% of men and 1%

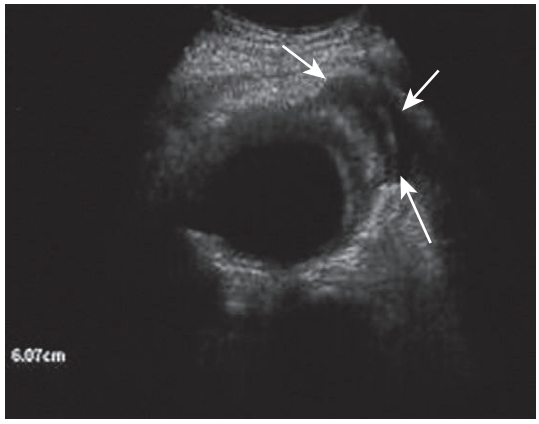


**Fig. 6.7** Transverse image of a leaking aortic aneurysm with a haematoma visible (arrows).

of women over 50 have been shown to have an aorta more than 3 cm in diameter. However, surgery is not normally considered in incidental, asymptomatic aneurysms less than 5.5 cm in diameter.

Ultrasound can also be used in the follow up of patients who have had endovascular repair of aortic aneurysms. Although contrast enhanced CT is considered the gold standard technique,[6] Doppler ultrasound with echo enhancing agents has been shown to be a useful method for assessment and may show leaks that have not been apparent on CT.[7]

*Dissection* of the abdominal aorta nearly always results from the extension of a dissection of the thoracic aorta extending into the abdomen (Fig. 6.9). Rarely, it may originate in the abdominal aorta, or result from trauma. The aorta is usually dilated to some extent but dissection can occur in the presence of a normal-calibre aorta. The flap may be visible depending on its orientation in relation to the ultrasound beam, and if a dissection is suspected the aorta should be examined from several different approaches in an effort to show the flap. Spectral and colour Doppler will show the presence and character of any flow in the true and false lumens and, even if a flap is not visible, the different flows in the two channels may be apparent on Doppler; reversed flow may be seen in the non-dominant channel due to compression in systole; if one of the channels is thrombosed then the appearances can be a little confusing. Doppler can also be used to assess blood flow in the major branches supplying the bowel, liver, kidneys and lower limbs.[8] Clevert et al[9] reported on the role of ultrasound in the assessment of a series of 68 dissections, 25 of which involved the aortic and iliac segments. For the 13 aortic dissections the sensitivity for colour Doppler was 85%, power Doppler 85% and B-flow 98%; for the 12 iliac dissections, the sensitivity for colour Doppler was 67%, power Doppler 75% and 98% for B-flow when compared with the reference techniques (a mix of CT, magnetic resonance angiography and digital subtraction angiography).

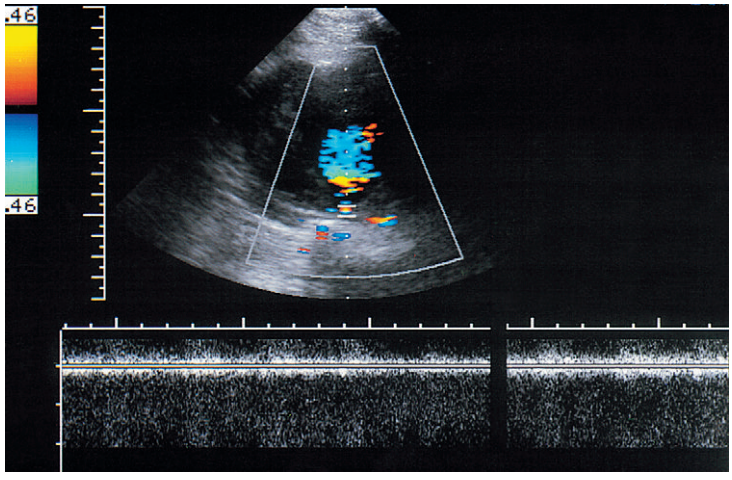


**Fig 6.8** Colour Doppler image of an aortocaval fistula in a patient with an aneurysm. The spectral Doppler gate is on the fistula and the spectral display shows a turbulent signal which is largely off the spectral range at these settings.

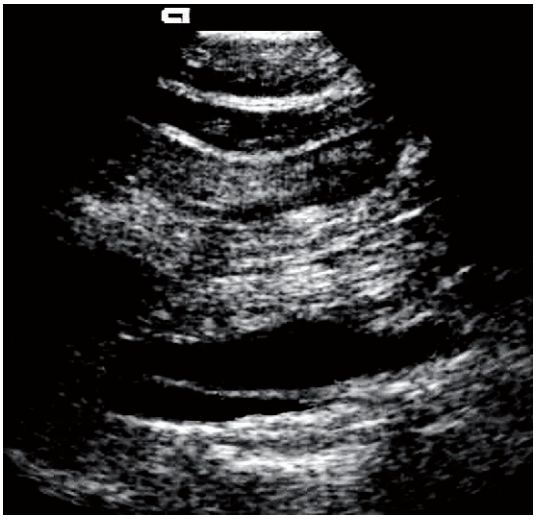

**Fig 6.9** Longitudinal view of the abdominal aorta showing a dissection flap.

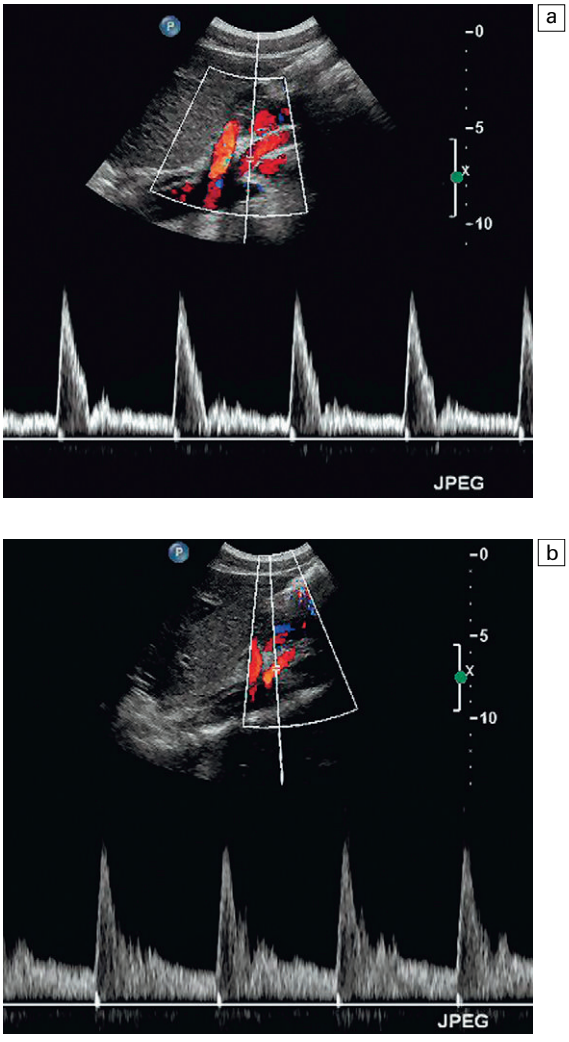


**Fig. 6.10** Flow in the superior mesenteric artery (a) before and (b) after food.

### *Splanchnic arteries*

Blood flow in the superior and inferior mesenteric arteries varies depending on whether the patient is fasting, or has recently eaten. In the fasting state the flow is consistent with a relatively high-resistance vascular bed with low diastolic flow. Following the ingestion of food there is a reduction in the peripheral resistance of the mesenteric vessels, resulting in increased diastolic flow, together with an increase in peak systolic velocity (Fig. 6.10).

The main indication for examination of blood flow in the splanchnic arteries is the investigation of possible *intestinal ischaemia*. One population study[10] showed a prevalence of 17.4% for mesenteric artery stenosis in a population with a mean age of 77 years. Of the patients with mesenteric artery stenosis, 86% had isolated coeliac artery stenosis (Fig. 6.3), 7% had combined coeliac and superior mesenteric artery stenosis, 5% had isolated superior mesenteric artery stenosis and 2% had coeliac axis occlusion; however none of those affected had symptoms of intestinal ischaemia. The usual indication for ultrasound examination is possible subacute or chronic ischaemia, as significant acute ischaemia presents as an acute abdomen and is managed accordingly. The splanchnic circulation is capable of developing multiple collateral channels and this makes the assessment of possible gut ischaemia difficult. The demonstration of stenosis of two of the three splanchnic arteries is strongly suggestive of the diagnosis and, in the appropriate clinical situation, the demonstration of severe stenosis in one vessel with occlusion of another is also supportive of the diagnosis. Colour Doppler is of value in identifying the abnormal segment (Fig. 6.3), although care must be taken not to mistake a high shift resulting from disease with the high shift from normal velocity flow, which is seen due to the low Doppler angle resulting from the orientation of the coeliac trunk and proximal superior mesenteric artery to the ultrasound beam.

In addition, colour Doppler may show a visible tissue bruit if there is a significant stenosis. The proximal 2–3 cm of the vessels is the most common site for disease and a peak velocity of more than 2.8 m $s^{-1}$ in the superior mesenteric artery correlates well with a stenosis of more than 70% diameter reduction with a sensitivity of 92% and a specificity of 96%; whereas the equivalent peak systolic velocity for the coeliac axis is 2 m $s^{-1}$ (87% sensitivity, 80% specificity).[11] Indirect signs of intestinal ischaemia include oedema of the mucosa and bowel wall and also reduced peristalsis. In severe cases gas bubbles may be seen in the portal vein flow; these produce a characteristic popping sound on spectral Doppler (Fig. 6.11).

The problems associated with the diagnosis of mesenteric ischaemia are illustrated by the fact that 18% of patients over 60 years without symptoms of mesenteric ischaemia have been shown to have significant disease on Doppler.[10,12] This emphasises the need to assess the findings in the light of the clinical situation.

Aneurysms of the hepatic and splenic arteries may occur. Splenic artery aneurysms are associated with acute pancreatitis and trauma; hepatic artery aneurysms can be associated with these conditions but may also arise following liver transplantation.

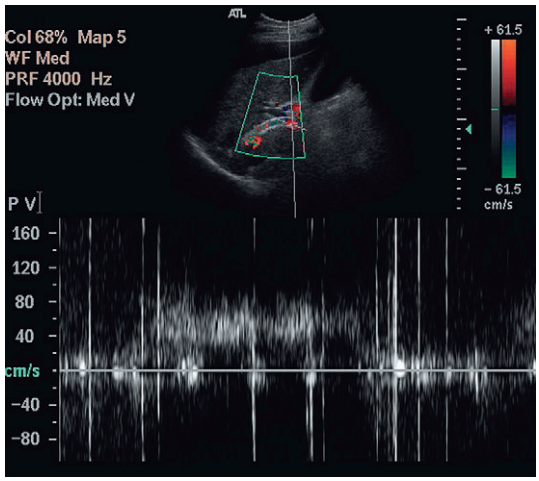


**Fig. 6.11** The spectral display from the portal vein of a patient with severe ischaemia and a transjugular intrahepatic portosystemic shunt (TIPS) showing the characteristic high intensity echoes from bubbles of gas in the blood.

## Other applications

The nature of para-aortic masses can be clarified using colour Doppler and masses can be distinguished from aneurysms.

An aorta which is prominent but of normal calibre in a thin patient, or the aorta in a patient with a marked lumbar lordosis, may be mistaken clinically for a mass or an aneurysm. Ultrasound can confirm the normal calibre of the vessel and the lack of pathology in these patients.

Blood flow in the coeliac and mesenteric arteries is also responsive to a variety of pharmacological agents such as glucagon and somatostatin, or pathological states such as cirrhosis and Crohn's disease.[13] Doppler ultrasound can show flow changes associated with these situations and may hold some promise for the future in the assessment of disease activity, or response to treatment.

Contrast enhanced colour Doppler has been used with some success in the postprocedural assessment of endovascular aneurysm repairs, in some cases detecting leaks not seen on CT angiography.[14,15] However, ultrasound is less good for detecting structural problems with the stent graft, such as stent distortion or fracture.[16] Unenhanced colour Doppler is less reliable when compared with CT angiography and digital subtraction arteriography. One suggested strategy is to alternate CT and ultrasound in the follow-up of stent graft patients[16] as this could result in substantial cost reduction, reduced radiation exposure and reduction in the risk of contrast induced nephrotoxicity.

# THE INFERIOR VENA CAVA

## Anatomy

The inferior vena cava is formed by the confluence of the common iliac veins at the level of the 5th lumbar vertebra and runs cranially to the right of the midline. It passes through the diaphragm at the level of the 8th thoracic vertebra and enters the right atrium. In the embryo there is a complex arrangement of venous sinuses

which form during embryogenesis, and several of these contribute to the inferior vena cava; this means that there are many variations of anatomy which may be seen. The most common variation is that the common iliac veins continue cranially as paired 'venae cavae', with the left component crossing to join the right side at the level of the left renal vein. Many other variations have been recorded; these are more easily assessed using contrast-enhanced CT than ultrasound, but may cause some confusion if they are seen during an ultrasound examination and not recognised.

## Technique

The inferior vena cava can be examined using the techniques described for the abdominal aorta. However, in the supine position the vessel may be narrow in the anteroposterior plane and difficult to define. Scanning transversely with colour Doppler and using the aorta as a guide may allow localisation of the vein in these circumstances; or elevation of the leg(s) by an assistant will increase flow and the calibre of the vein, thus making it more visible. The calibre of the cava will vary with the state of hydration of the patient. In a well-hydrated patient it will be distended, whereas in a dehydrated patient it will be collapsed, narrow and more difficult to visualise. Excessive transducer pressure applied in an effort to disperse bowel gas will also compress the cava, therefore a balance must be sought in order to visualise segments of the vessel in some patients.

## Normal and abnormal findings

Flow in the inferior vena cava is slow and varies with both respiration and cardiac pulsation (Fig. 6.12). On inspiration the diaphragm descends. This results in negative pressure in the chest and increased pressure in the abdomen, and blood therefore flows from the abdomen to the chest; the reverse occurs on expiration. Superimposed on this is the more rapid periodicity resulting from cardiac activity; this is seen particularly in the upper abdomen. The prominence of the caval waveform also depends on the degree of hydration of the patient. A dehydrated patient's cava will be narrow and difficult to see below the renal veins,

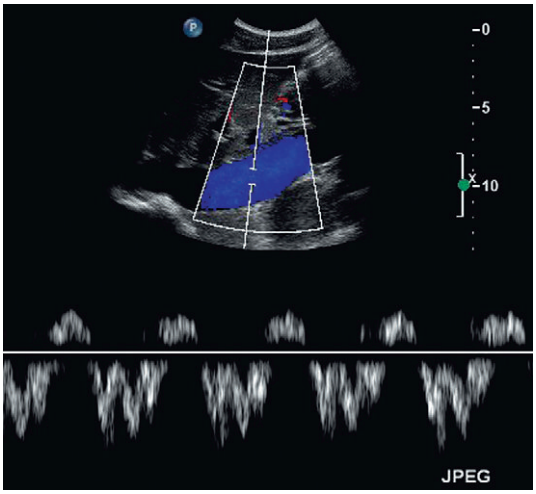


**Fig. 6.12** The inferior vena cava in the upper abdomen showing the variations in flow which occur with respiration and cardiac activity; the various components of the waveform in the inferior vena cava and hepatic veins are described in detail in Chapter 7 and Figure 7.12.

whereas in fluid overload the cava is dilated and there is cardiac periodicity detectable down into the iliac veins.

One of the most common indications for specific examination of the inferior vena cava is to assess whether *thrombus* from a pelvic or lower limb deep vein thrombosis has extended up into the cava. Thrombus may fill the lumen of the cava and even produce some expansion of the vessel; alternatively, a tongue of thrombus may be seen lying free in the lumen, extending up towards the right atrium (Fig. 6.13).

*Caval filters* are inserted in some patients who are at risk of pulmonary embolus from more distal thrombus. There are several types but all are inserted in the mid- or lower cava, below the renal veins. Identifying a metallic, echogenic structure within the inferior vena cava above the level of the renal veins may indicate migration of the filter. There is a small risk that thrombus may extend past the filter, or develop at the site of the filter. Colour Doppler is a quick and easy method for confirming patency of the cava around and above the filter.[17] The metal struts of the filter can be recognised within the lumen of the cava

**Fig. 6.13** A tongue of thrombus extending into the upper inferior vena cava posterior to the left lobe of the liver in a patient with deep vein thrombosis.

and colour Doppler, or power Doppler, will show blood flow past the level of the filter (Fig. 6.14).

Renal tumours and hepatocellular carcinoma are two tumours which have a tendency to invade venous channels and, as a result, *tumour thrombus* may extend into the cava (Fig. 6.15) from the renal or hepatic vein.[18] Compromise of the venous drainage of the liver or kidneys is shown by loss of the normal cardiac and respiratory periodicity of the venous waveform and the tumour thrombus may be clearly seen as it extends into the caval lumen. Some tumours in the retroperitoneum may compress or directly invade the inferior vena cava causing obstruction to the venous return from the lower abdomen and legs. Although the caudal segments of the inferior vena cava and the iliac veins usually remain patent, they will often be dilated, flow will be sluggish or reversed, the flow profile will be flat, and there will be an absence of the normal Valsalva response. Rarely, *intrinsic tumours*, usually mesenchymal in origin, such as fibrosarcomas or leiomyosarcomas may develop in the caval wall, lipomas have also been reported.[19]

Following *liver transplantation* the cava should be assessed to ensure satisfactory flow. The appearances will depend on the type of anastomosis performed. In the past, the segment of donor cava attached to the new liver replaced the equivalent segment of native cava, which had been removed with the diseased liver. Many surgeons now perform a 'piggyback' technique, where the native cava is left in place, the inferior end of the donor caval segment is oversewn and the upper end anastomosed to the native cava. This results in a post-operative appearance which can be confusing if it is not recognised, as there will appear to be two cavae associated with the transplanted liver (Fig. 6.16).

Other postoperative problems which may occur in relation to the cava following transplantation include compression, if the new liver is relatively large; distortion of the cava may also occur if there is relative twisting of the caval channel as a result of fitting the donor liver into the native abdomen. In the longer term stenosis may develop at the sites of anastomosis. Liver transplantation is covered further in Chapter 7.

Retroperitoneal and other abdominal *masses* may compress or occlude the inferior vena cava. The situation is usually apparent, especially with colour Doppler, which shows the cava entering the mass and becoming narrowed or occluded with absent flow. Congenital *webs* can occur, particularly at the upper end of the cava. These may produce a variable degree of caval narrowing and in some cases may predispose to hepatic vein thrombosis and a Budd Chiari syndrome.

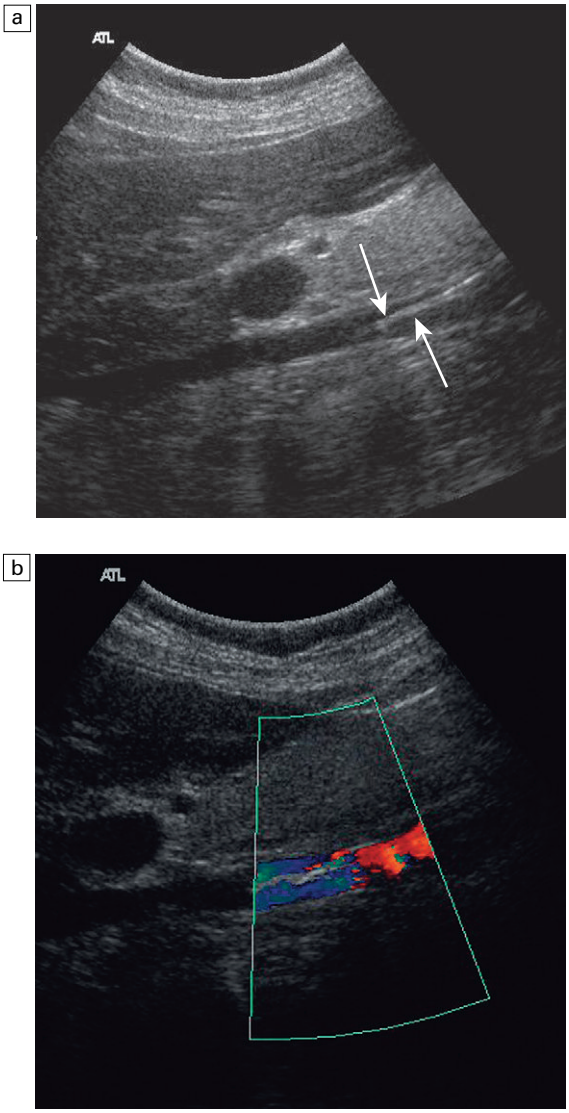


**Fig. 6.14** (a) Real time image of an IVC containing a filter in the lower segment; (b) colour doppler image of the same patient with a caval filter. The change in colour reflects the changing Doppler angle as the blood flows through the sector scan.

*Fistulae* involving the cava may rarely occur spontaneously, often secondary to an aortic aneurysm (Fig. 6.8), or they may be surgically created as is the case with portocaval shunts. In the case of aortocaval fistulae, colour Doppler may show a visible tissue bruit with pulsatile flow in the cava above the level of the fistula; sometimes the fistula itself is difficult to identify. Surgical

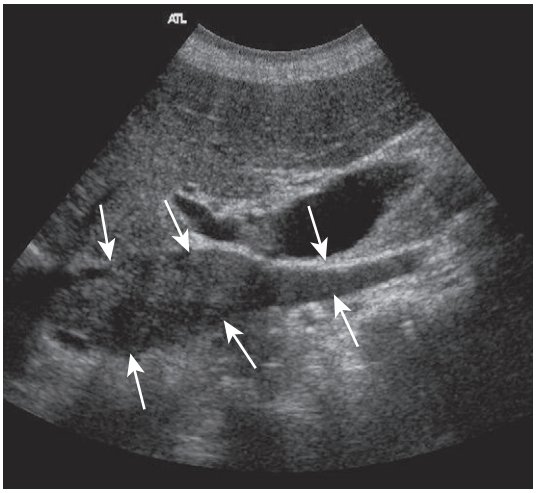


**Fig. 6.15** Tumour thrombus in the inferior vena cava from a renal carcinoma (arrows).

portocaval shunts are usually side-to-side shunts in the upper abdomen at the level where the proximal main portal vein passes close in front of the cava (Fig. 6.17). A tissue bruit may be apparent and the shunt is more easily identified if the liver can be used as a window through to the point of anastomosis; turning the patient up onto the left side may facilitate visualisation. However, these are rarely performed now, having been replaced by transjugular intrahepatic portosystemic shunts (TIPS) (see Ch. 7).

## CONCLUSION

The aorta and inferior vena cava, together with their major branches and tributaries, can be examined in most patients, provided that care and attention is spent in finding the best scan plane and ensuring that the system is set appropriately for the specific examination concerned, both in terms of imaging and Doppler settings. Helical CT and three-dimensional reconstruction is rapidly becoming the technique of choice for imaging the aorta, particularly if percutaneous stent/grafts are contemplated. However, ultrasound continues to have a significant role in relation to both initial diagnosis and follow-up of patients with aortic or caval disease.

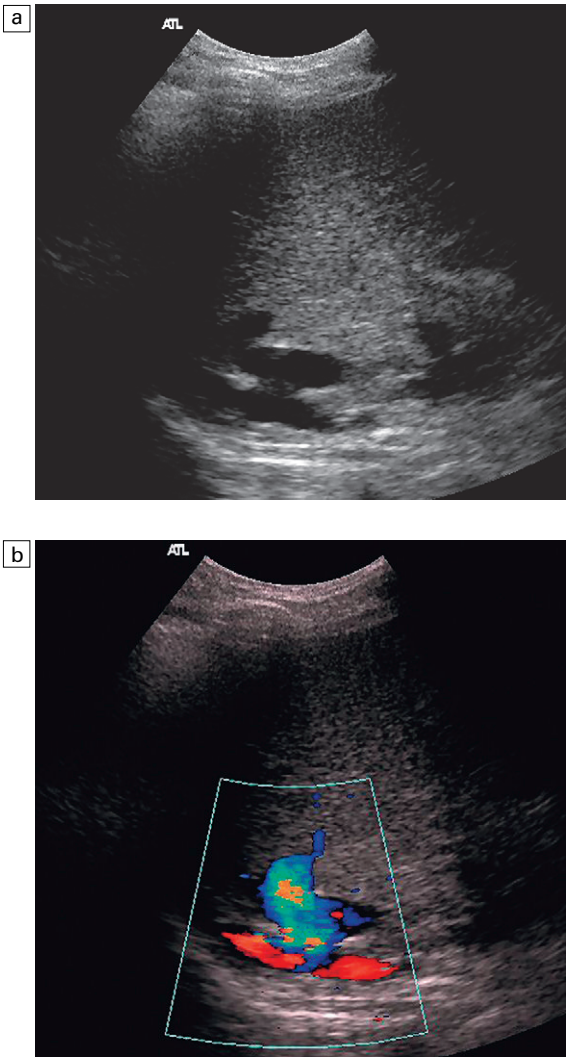


**Fig. 6.16** (a) A real time image of the upper caval region in a liver transplant patient with a 'piggyback' caval anastomosis, showing the native cava posteriorly and the donor cava just anterior to it; (b) colour Doppler image of the same anastomosis.

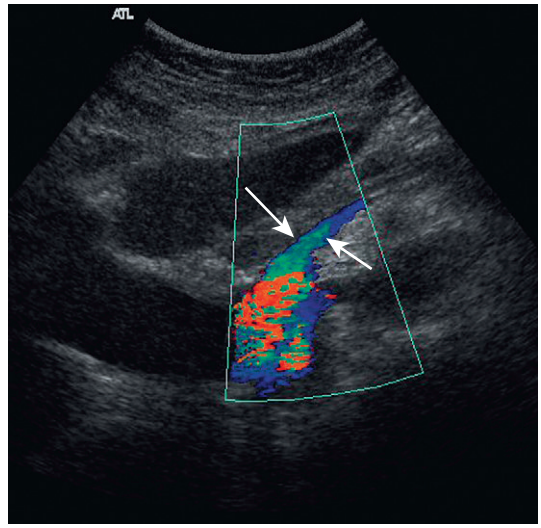


**Fig. 6.17** Colour Doppler image of a portocaval shunt. The portal vein (arrows) has been surgically anastomosed to the inferior vena cava.

## REFERENCES

1. Goldberg BB, Ostrum BJ, Isard HJ. Ultrasonographic aortography. J Am Med Assoc 1996; 198:353–358.
2. Taylor KJW, Burns PN, Woodcock JP, et al. Blood flow in deep abdominal and pelvic vessels: ultrasonic pulsed Doppler analysis. Radiology 1985; 154:487–493.
3. De Smet AA, Kitslaar PJ. A duplex criterion for aortoiliac stenosis. Eur J Vasc Surg 1990; 4:275–278.
4. US Preventive Services Task Force. Screening for abdominal aortic aneurysm: recommendation statement. Ann Intern Med 2005; 142:198–202.
5. Frame PS. Screening for abdominal aortic aneurysm (Editorial). Br Med J 2004; 329:E311–312.
6. Raman KG, Missig-Carroll N, Richardson T, et al. Color-flow duplex ultrasound scan versus computed tomographic scan in the surveillance of endovascular aneurysm repair. J Vasc Surg 2003; 38:645–651.

7. Napoli V, Bargellini I, Sardella SG, et al. Abdominal aortic aneurysm: contrast-enhanced US for missed endoleaks after endoluminal repair. Radiology 2004; 233:217–225.
8. Thomas EA, Dubbins PA. Duplex ultrasound of the abdominal aorta – a neglected tool in aortic dissection. Clin Radiol 1990; 42:330–334.
9. Clevert DA, Rupp N, Reiser M, et al. Improved diagnosis of vascular dissection by ultrasound B-flow: a comparison with color-coded Doppler and power Doppler sonography. Eur Radiol 2005; 15:342–347.
10. Hansen KJ, Wilson DB, Craven TE, et al. Mesenteric artery disease in the elderly. J Vasc Surg 2004; 40:45–52.
11. Moneta GL. Screening for mesenteric vascular insufficiency and follow-up of mesenteric artery bypass procedures. Semin Vasc Surg 2001; 14:186–192.
12. Roobottom CA, Dubbins PA. Significant disease of the coeliac and superior mesenteric arteries in asymptomatic patients: predictive value of Doppler sonography. Am J Radiol 1993; 161:985–988.
13. Perko MJ. Duplex ultrasound for assessment of superior mesenteric artery blood flow. Eur J Vasc Endovasc Surg 2001; 21:106–117.
14. Napoli V, Bargellini I, Sardella SG, et al. Abdominal aortic aneurysm: contrast-enhanced US for missed endoleaks after endoluminal repair. Radiology 2004; 233:217–225.
15. Bendick PJ, Bove PG, Long GW, et al. Efficacy of ultrasound contrast agents in the noninvasive follow-up of aortic stent grafts. J Vasc Surg 2003; 37:381–385.
16. Thurnher S, Cejna M. Imaging of aortic stent-grafts and endoleaks. Radiol Clin North Am 2002; 40:799–833.
17. Smart LM, Redhead DN, Allan PL, et al. Follow-up study of Gunther and LGM inferior vena caval filters. J Intervent Radiol 1992; 7:115–118.
18. Bissada NK, Yakout HH, Babanouri A, et al. Long-term experience with management of renal cell carcinoma involving the inferior vena cava. Urology 2003; 61:89–92.
19. Grassi R, Di Mizio R, Barberi A, et al. Case report. Ultrasound and CT findings in lipoma of the inferior vena cava. Br J Radiol 2002; 75:69–71.

# Doppler ultrasound of the liver

# 7

Myron A. Pozniak

## INTRODUCTION

Recent ultrasound literature has many reports of extensive work and success with ultrasound contrast medium. Practitioners in Great Britain, Italy, Japan, South Korea, Canada, and other countries have reported very impressive results in lesion detection and characterisation with the application of microbubbles.[1] Unfortunately governing agencies across the world have not uniformly endorsed these agents and there is limited ability to apply them in certain countries. This chapter is specifically written for those ultrasound practitioners who do *not* have access to intravenous ultrasound contrast.

The standard abdominal ultrasound (US) examination should include a brief, but precise survey with spectral and colour Doppler.[2–5] This serves a twofold purpose: first, it adds valuable haemodynamic information to the evaluation of the abdominal organs, in most cases reinforcing normality, but occasionally revealing an unexpected finding; second, by consistently integrating Doppler into the routine abdominal examination, sonologists will continually refine their Doppler skills so that significant haemodynamic abnormalities can be identified quickly and evaluated accurately. Although a cursory Doppler survey of the major vessels may add 2–3 min to an abdominal examination, regular practice enables the examiner to become more familiar with the equipment, more adept at perceiving abnormalities, and more expert in analysing the results.

Sometimes altered blood flow may be the only abnormal finding to suggest the presence of pathology. The Doppler survey may reveal a subtle hypervascular lesion of which the examiner was otherwise unaware, or it may display hypervascularity of an observed lesion and awareness of a lesion's vascularity often increases diagnostic certainty. The use of colour Doppler in abdominal examinations also helps to differentiate vascular from non-vascular structures. Care must be taken, however, to ensure that equipment settings are appropriate: if gain, pulse repetition frequency, and filtration are not optimised, slow flow can be missed in vascular structures or artifactual colour can be painted into non-vascular structures.

## GENERAL ASPECTS

Some sonologists place considerable emphasis on the measurement of flow velocity, but too great a dependence on this parameter may generate a false sense of security, or lead to diagnostic errors. Numerous systemic factors affect blood flow in abdominal vessels. These include the patient's state of hydration, cardiac output, blood pressure, vascular compliance, the interval since previous food, and the haemodynamic effects of medications. These factors affect measured velocities in a variety of ways and to varying degrees; so that although the velocity may be above or below the normal levels expected in any individual vessel, it may not necessarily reflect focal disordered haemodynamics. Furthermore, defining flow within a vessel as normal or abnormal by simply comparing the measured velocity to a predetermined normal range is a poor method of establishing a diagnosis, as a few degrees difference in the angle of insonation or improper angle correc-

tion can significantly change the measured velocity. Assigning the proper degree of angle correction may be difficult if the vessel is poorly visualised, curved, or visualised only over a short segment.

Varying the width of the sample volume can be advantageous when examining the abdomen. If the examiner is screening for vascular patency or trying to locate a specific vessel, a large sample volume is appropriate for rapid interrogation of a broad area, for example, when ruling out hepatic artery thrombosis in a liver transplant recipient. If, however, the examiner wants to precisely characterise flow within a vessel and evaluate waveform detail, then the sample volume must be small and placed near the centre of the vessel, thereby interrogating the highest velocity lamina (Fig. 7.1).

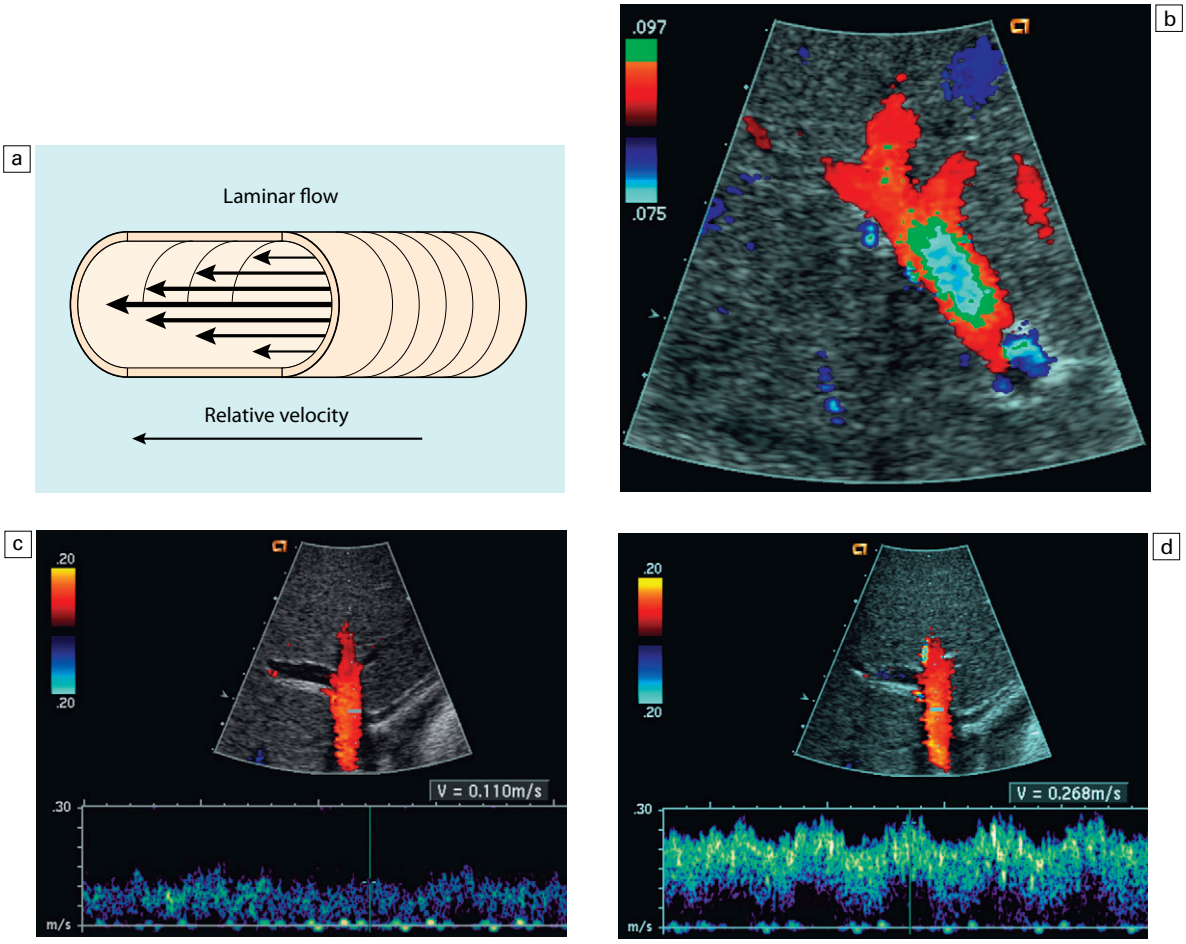


**Fig. 7.1** (a) Schematic representation of normal laminar flow. The velocity along the wall of a vessel is slowed because of drag, therefore the relative velocity is less than that measured at the centre of the vessel. (b) Colour Doppler image of portal vein flow. A green tag was assigned to high-level velocities towards the transducer and the scale was set low to allow aliasing. Colour-encoding thus permits an accurate display of numerous lamina. Note the transition from the slowest velocities, red through orange, green and blue from the periphery to the centre of the vessel. The actual velocity displayed on a spectral tracing will be critically dependent on sample volume placement relative to these various velocity lamina. (c) Normal spectral Doppler tracing of portal vein flow. A small sample volume is placed near the vessel wall. The velocity as interrogated near the wall only measures approximately 0.11 $ms^{-1}$. (d) Spectral Doppler tracing of the same portal vein with the sample volume now placed more centrally interrogating the higher-velocity lamina. The measured velocity is now 0.27 $ms^{-1}$. Simply changing location of the sample volume is sufficient to cause a twofold change in measured velocity.

A wide sample volume, by incorporating the slower lamina along the wall together with the faster central lamina, will broaden the spectral Doppler tracing and mimic turbulence (Fig. 7.2).[6] There is no specific acoustic window that is ideal for all patients and the operator must determine the best approach on an individual basis. This usually requires trying multiple windows at varying degrees of inspiration. During respiration, the upper abdominal organs move back and forth under the US transducer. When patients are able to cooperate, the operator should ask them to intermittently hold their breath during the Doppler examination and to breathe gently at other times. This improves the colour Doppler image and allows acquisition of longer spectral Doppler tracings. Patients who are unable to hold their breath can pose a significant problem and the operator may have to carefully 'ride' the vessel in real time as it moves with respiration. An experienced sonologist may be able to 'rock' the transducer back and forth in synchrony with the patient's respiration, thus maintaining the sample volume over the area of interest and obtaining a longer tracing. If the patient is short of breath or unable to cooperate, short segments of spectral tracings are all that may be possible.

The presence of bowel gas is also an obvious impediment to a successful examination. Making the patient fast for 6–8 h prior to an abdominal examination helps minimise the amount of abdominal gas, thereby increasing the likelihood that an appropriate sonographic window will be available for any particular vessel of interest. In addition, consistently scanning fasting patients decreases the risk of misinterpreting flow dynamics altered by a nutrient load.

Patient obesity is a severe limiting factor for an adequate Doppler examination. Delineation of anatomical detail is impaired when the examination is conducted at lower frequencies. During US imaging, the operator may need to press firmly to displace some of the adipose tissue and position the transducer closer to the area of interest. Such a manoeuvre, however, is not appropriate during a Doppler examination as pressure from the transducer compresses the underlying organ and its vasculature, thereby altering flow profiles and velocities. Compression of an organ or vessel with the transducer causes increased resistance to blood flow (especially diastolic) thereby elevating the perceived resistance to inflow (Fig. 7.3).

## Terminology

In relation to Doppler ultrasound of the liver, it is important to be consistent in the use of terms relating to blood flow: the term *pulsatility* refers to arterial flow, *phasicity* refers to changes in flow

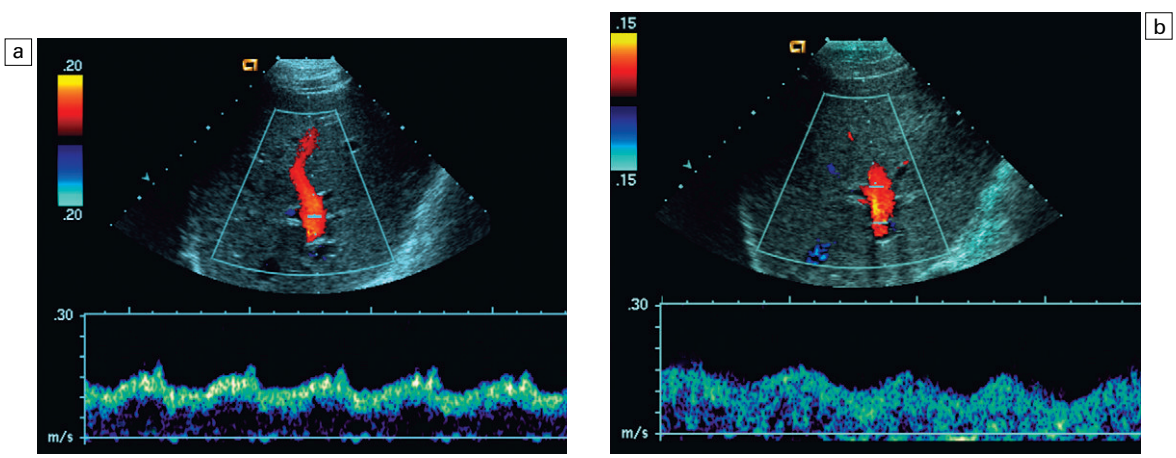


**Fig 7.2** (a) Spectral Doppler tracing of a portal vein with small, centrally placed sample volume. A thin lamina of flow is interrogated and, therefore, the displayed tracing shows a narrow range of velocities with a 'window' below the tracing. (b) The sample volume has been opened wide to incorporate all velocity lamina across this portal vein. Note the 'filling in' of the spectral tracing resulting in a perception of spectral broadening.

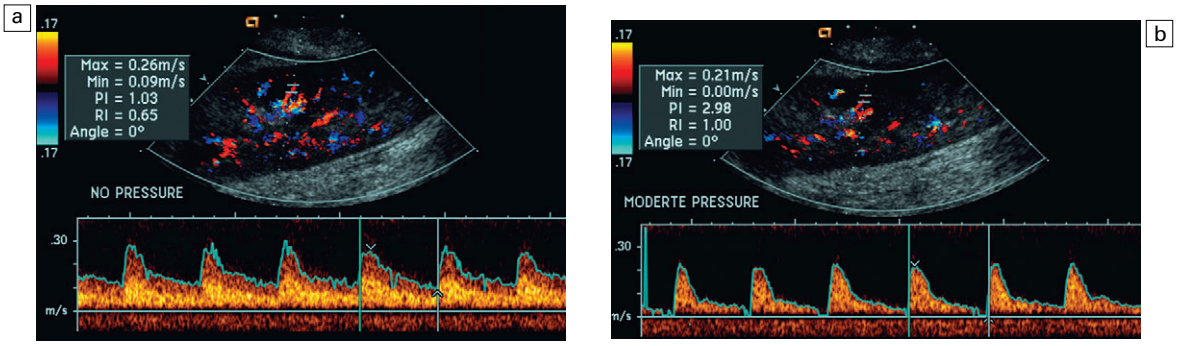


**Fig. 7.3** (a) Spectral Doppler tracing of an interlobar renal transplant artery. This tracing was obtained with the transducer gently contacting the lateral abdominal wall. The resistive measures approximately 65%. (b) The same vessel is now interrogated with moderate pressure applied with the transducer. Note the increase in diastolic velocity with result and elevation in resistive index to 100%. Pressure applied by the sonologist via the transducer can increase the resistance to arterial inflow in any organ or vessel.

secondary to respiration, and the term *periodicity* is recommended when referring to velocity variation in the hepatic and portal veins secondary to cardiac activity. Normal flow in the portal vein towards the liver is properly termed *hepatopetal* (as in centripetal force, not hepatopedal). Reversed portal vein flow is referred to as *hepatofugal* (as in centrifugal force).

## INDICATIONS

A significant percentage of patients referred for right upper quadrant (RUQ) US typically have elevated liver enzymes of unknown aetiology, incidentally detected on screening blood tests. Although sonographic imaging of the liver may reveal diffuse abnormality or focal disease, the majority of studies on these patients are often normal (Table 7.1). Doppler US should be applied to the portal vein, hepatic artery, and the hepatic veins of these patients and indeed in all RUQ examinations.[7] This may reveal flow alterations caused by inflammatory disease, neoplasm, or other disorders which are too subtle or too small to cause imaging irregularities. Alterations in flow profiles and velocities in the hepatic vessels may be the result of either hepatic or cardiac disease, thereby helping to differentiate patients needing cardiac evaluation from those with liver disease who may benefit from liver biopsy, or require further hepatic imaging using computed tomography (CT), magnetic resonance imaging (MRI), or angiography.

**Table 7.1** Indications for Doppler ultrasound of the liver

- Part of the routine examination of the liver and right upper quadrant
- Assessment of portal hypertension
- Pre- and postprocedural assessment of transjugular portosystemic shunt (TIPS) procedures
- Postoperative follow-up of liver transplants
- Assessment of focal liver disease

When portal hypertension is suspected, Doppler US characterises changes in portal haemodynamics and identifies pathways of portosystemic collateralisation.[8, 9] Doppler can confirm the patency of surgical or percutaneous shunts which have been performed in patients with bleeding oesophageal varices.[10]

Identification and differentiation of bland thrombus from tumour thrombus within the hepatic or portal veins by Doppler has significant implications for medical or surgical treatment planning.

Doppler US plays a key role in the postoperative monitoring of liver transplant recipients, confirming patency of the portal vein, hepatic artery, and hepatic veins.

The role of Doppler in the characterisation of parenchymal liver disease and screening for hepatocellular carcinoma (HCC) is controversial. Marked alterations in flow profiles and velocities can be seen and have been described in the literature.[11–20] It is rare, though, to be able to precisely pinpoint a specific diagnosis based on Doppler findings since there is considerable overlap in velocity and waveform alterations among various disease states.[21]

## SCAN TECHNIQUE

The patient is usually scanned while in a supine or left lateral decubitus position (Table 7.2). Depending on vessel orientation and patient body habitus, the portal vein and hepatic artery are best interrogated by either a subcostal approach pointing posterocephalad, or a right intercostal approach pointing medially. Since the portal vein and hepatic artery travel together in the portal triad, along with the common duct, these approaches should satisfactorily interrogate both vessels.

Scanning the left hepatic vein (and occasionally the middle hepatic vein) is best accomplished from a substernal approach. The transducer should be oriented transversely, pointing posterocephalad, and swept up and down across the liver. For the right hepatic vein, a right lateral intercostal approach is used with the transducer pointed cephalad. If the patient's liver extends below the costal margin during inspiration, a subcostal transverse view, angled cephalad, is useful for the confluence of the hepatic veins (Fig. 7.4).

**Table 7.2** Principles of the examination

- General examination of liver parenchyma and abdomen
- Colour and spectral Doppler assessment of the portal vein, superior mesenteric and splenic veins, together with main intrahepatic portal branches
- Colour and spectral Doppler assessment of the hepatic artery from the coeliac axis to the porta, together with main intrahepatic branches
- Colour and spectral Doppler assessment of the main hepatic veins and the upper inferior vena cava

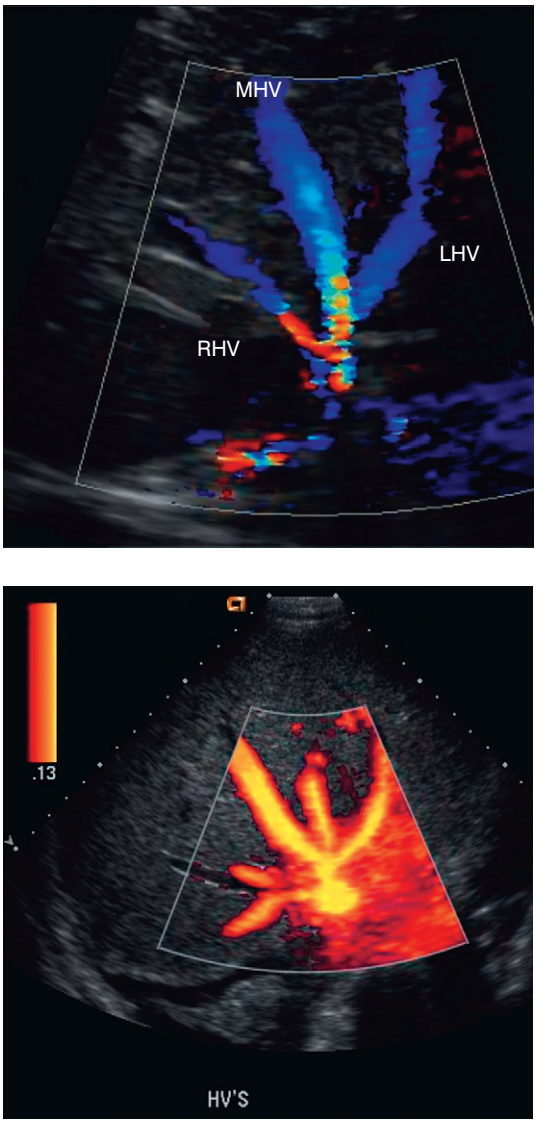


**Fig. 7.4** (a) Colour Doppler transverse view of the liver with a subcostal approach. This colour crow's foot appearance of the three hepatic veins confirms their patency. The direction of flow is away from the transducer and towards the heart. Right, middle and left hepatic vein, RHV, MHV, LHV. (b) Power Doppler image in this patient shows the convergence of five hepatic veins (HVs). The presence of accessory branches is very common.

Some patients, when asked to hold their breath perform a vigorous Valsalva manoeuvre. This results in increased intrathoracic pressure which may impede venous return, affecting flow profiles and velocities, particularly in the hepatic

veins and inferior vena cava (IVC). This effect may alter the hepatic vein profile, creating the perception of hepatic venous outflow obstruction (HVOO). An attempt should be made to scan these patients in neutral breath hold to avoid producing a misleading Doppler tracing.

## VASCULAR ANATOMY AND NORMAL FLOW PROFILES

(Table 7.3)

### Portal vein

The *portal vein* normally supplies approximately 70% of incoming blood volume to the liver. This relatively deoxygenated blood comes to the liver after perfusing the intestine and spleen. It is rich in nutrients after a meal, and arrives at the liver to be processed in the cells of the hepatic sinusoids. The portal vein is formed by the confluence of the splenic and superior mesenteric veins. It is accompanied by the hepatic artery and common bile duct to form the portal triad (Fig. 7.5); this has echogenic margins as it courses into the liver, due to the paraportal extension of Glisson's capsule and the presence of some perivascular fat. In the liver, these vessels progressively branch to supply the liver segments; anatomic variations of the portal vein are rare. The Couinaud system of segmental liver anatomy divides the liver vertically along the planes of the hepatic veins, and horizontally along the planes of the left and right portal veins. The segmental branches of the portal vein enter the centre of the Couinaud segments whose ultrasound appearance has been described by La Fortune et al.[22] The typical portal vein flow profile has a relatively consistent velocity of approximately 20 cm $s^{-1}$ (± 5 cm $s^{-1}$) towards the liver (Fig. 7.6a).[23] The flow velocity is uniform because cardiac pulsation is damped by the capillaries of the intestine at one end of the portal system and by the liver sinusoids at the other end. Slight phasicity may be seen on the portal vein spectral tracing secondary to patient respiration and a mild degree of periodicity may be present, due either to retrograde pulsation transmitted from the right heart via the hepatic vein (A-wave) or to the inflow of blood during hepatic arterial systole.[24] Because these brief pressure surges into the liver transiently increase resistance to portal venous

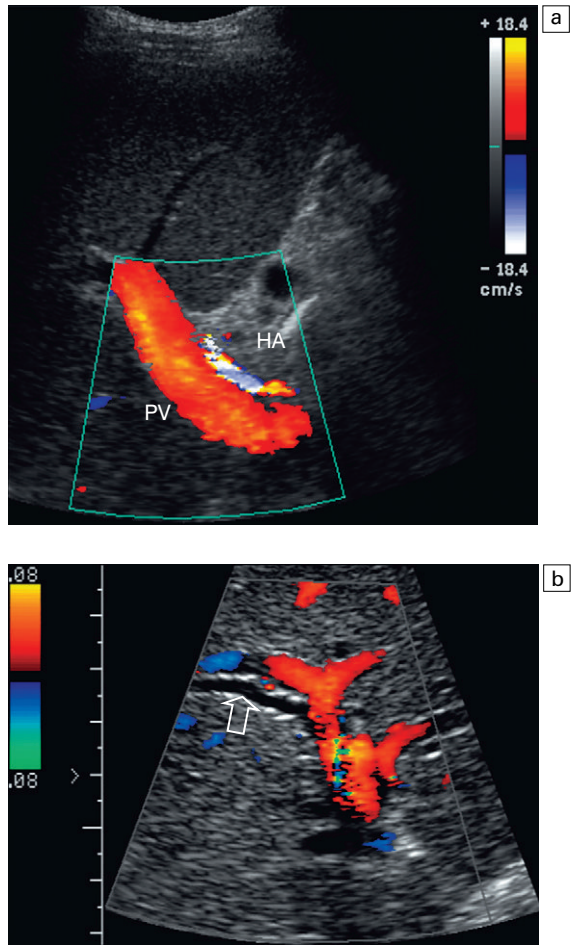


**Fig. 7.5** Oblique colour Doppler images of the porta hepatis. (a) The hepatic artery (HA) accompanies the portal vein (PV) and bile ducts. With the colour scale appropriately set for the slow flow within the portal vein, hepatic arterial flow often reveals colour aliasing during systole. (b) With biliary dilatation colour Doppler provides clear discrimination between vessels and ducts (arrow).

**Table 7.3** Normal hepatic vessel velocities (fasting)

| | |
|---|---|
| Hepatic artery | 30–40 cm $s^{-1}$ systolic, 5–10 cm $s^{-1}$ diastolic |
| Portal vein | 15–20 cm $s^{-1}$ |

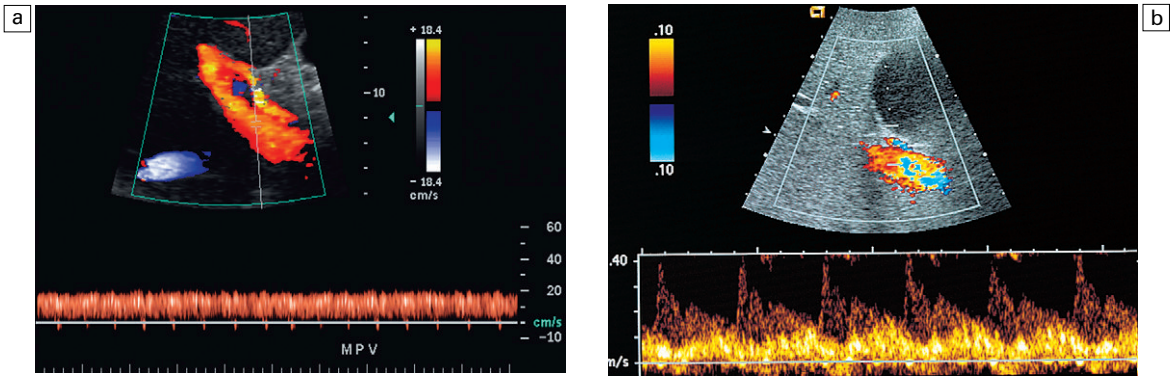


**Fig. 7.6** (a) Spectral Doppler tracing of normal portal vein flow. The flow velocity of 20 cm $s^{-1}$ is relatively uniform and in a hepatopetal direction. (b) Spectral Doppler tracing of a normal portal vein flow. Slight periodicity is present in this patient's portal vein tracing. The dip in antegrade velocity coincides with hepatic arterial systole. Velocity variation may also occur due to pressure change with the hepatic vein A-wave.

inflow, they effect a momentary slowing of antegrade flow in the normal portal vein (Fig. 7.6b).[25] In studies of portal vein flow, Hosoki[26] and Wachsberg[27] reported the presence of some degree of periodicity in 7% and 64% of their respective normal study populations. Although some periodicity may be expected in portal vein flow, reversal of flow, even briefly, should be considered an abnormal finding.

## Hepatic artery

The arterial blood supply of the liver arises solely from the celiac axis in approximately 76% of individuals. The *common hepatic artery* originates from the celiac artery and after the origin of the gastroduodenal artery, it is called the *proper hepatic artery*; this then enters the liver alongside the portal vein (Fig. 7.5a) where it divides into left and right hepatic arteries. There are numerous variants of hepatic artery anatomy. These include accessory vessels which exist in conjunction with normal branches of the hepatic artery and replaced arteries which make up the sole supply of a segment or lobe. For example, a replaced right hepatic artery arising from the superior mesenteric artery may be the sole blood supply to the entire

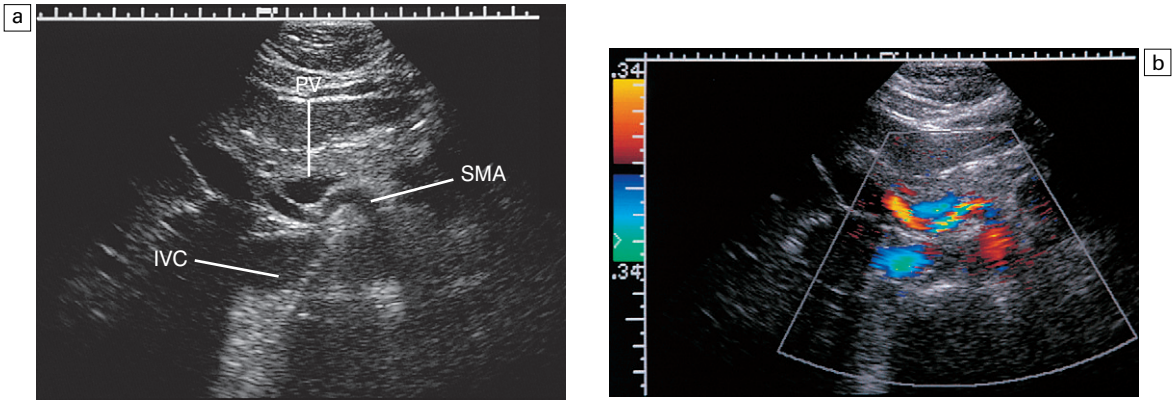


**Fig 7.7** (a) Transverse image of the mid-abdomen at the level of the superior mesenteric artery origin. A tubular structure is seen coursing from the superior mesenteric artery (SMA) to the right lobe of the liver, between portal vein (PV) and the inferior vena cava (IVC). (b) Colour Doppler identifies this tubular structure as a vessel. An arterial signal on spectral Doppler, identification of its SMA origin and a course towards the right lobe of the liver confirm this to be a replaced right hepatic artery.

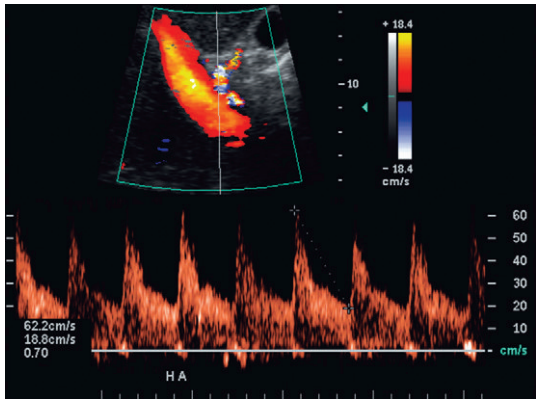


**Fig. 7.8** Spectral Doppler tracing of a normal hepatic artery. Systolic upstroke is brisk with acceleration time <0.07 s. Resistive index measures 70%. Velocity at end diastole approximates 19 cm $s^{-1}$.

right lobe of the liver, a situation occurring in approximately 11–25% of the population.[28] In a slender patient, colour Doppler US may be able to identify the replaced right hepatic artery behind the main portal vein as it courses towards the right lobe from the superior mesenteric artery (Fig. 7.7). The other variants occur less frequently and are more difficult to identify by Doppler US.

The normal hepatic artery in a fasting patient has a low resistance Doppler flow profile, [about 60–70% resistive index (RI)] (Fig. 7.8). During systole, the velocity is approximately 30–60 cm $s^{-1}$; while during diastole, it normally slows to approximately 10–20 cm $s^{-1}$ which is normally less than the velocity of the portal vein flow. The systolic acceleration time is brisk, typically less than 0.07 s. Technically, a good way to evaluate relative flow velocities between the hepatic artery and the portal vein is to increase the sample volume size so that both vessels are incorporated into the same tracing or to swing the sample volume from one vessel to the other in the same tracing (Fig. 7.9).

## Hepatic veins

The hepatic veins are relatively straight, anechoic, tubular structures that converge on the IVC approximately 1 cm below its confluence with the right atrium. The walls of the hepatic veins are relatively hypoechoic which helps to differentiate them from the portal veins in the more echogenic portal triads. There are no valves in the hepatic veins.

In most people, the *right, middle, and left hepatic veins* enter the IVC in a 'crow's foot' configuration when viewed in the transverse plane (Fig. 7.4). The left and middle hepatic veins may enter as a common trunk along the left anterolateral aspect of the IVC. Approximately 30% of individuals have additional hepatic veins that may be identified by colour Doppler; a right superior anterior segmental vein may be seen draining

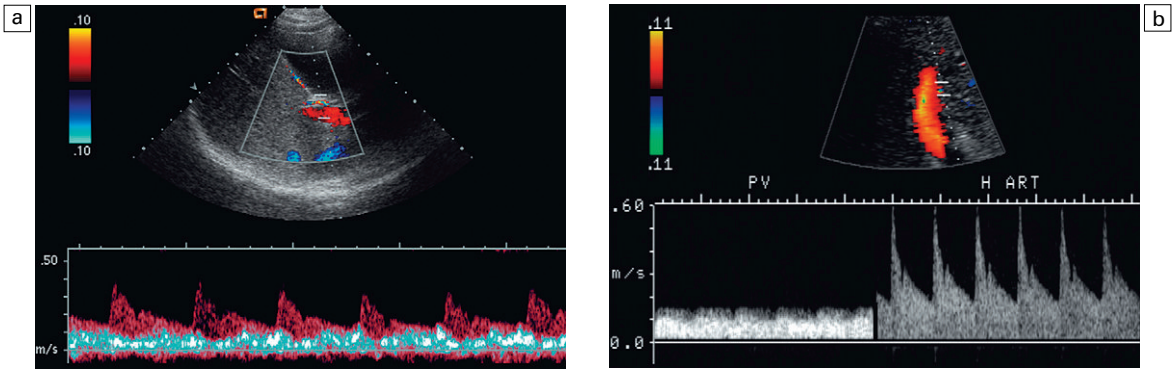


**Fig. 7.9** Combined spectral Doppler tracing of the hepatic artery and portal vein. By opening the sample volume wide (a), or rocking the transducer between the hepatic artery and portal vein in the same tracing (b), the relative velocities between hepatic artery and portal vein can be directly compared. A normal velocity ratio between hepatic artery and portal vein is present in these patients. The hepatic artery diastolic velocity in a fasting patient is normally equal to or slightly less than portal vein velocity.

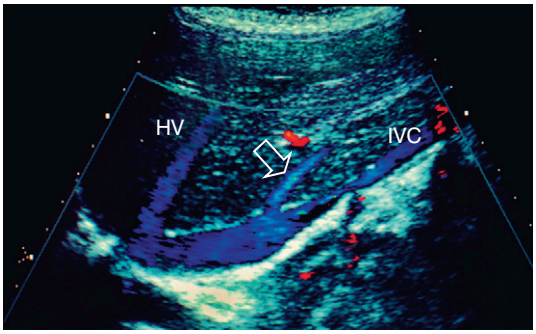


**Fig. 7.10** Longitudinal colour Doppler image of the liver and inferior vena cava (IVC) through the right flank. There is a prominent accessory hepatic vein (open arrow) from the inferior posterior segment of the right lobe of the liver (Couinaud segment 6). This vein joins the inferior vena cava approximately 3 cm inferior to the junction of the right middle and left hepatic veins (HV).

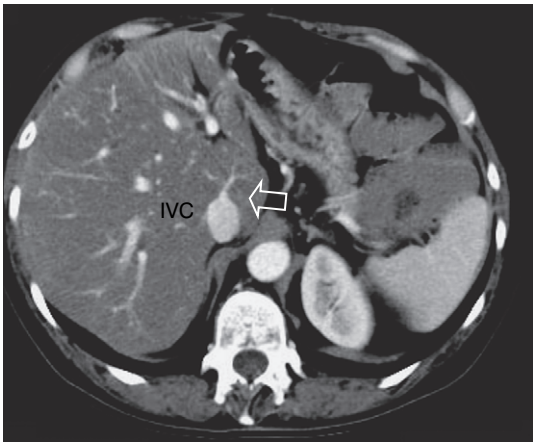


**Fig. 7.11** CT scan at the level of the mid-liver in a patient with marked fatty infiltration. Note several small hepatic veins (arrow) draining directly into the inferior vena cava (IVC). Because of this unique drainage of the central liver, this segment behaves differently in patients with main hepatic vein thrombosis or cirrhosis. The ultrasound appearance may be altered. Hypertrophy may be perceived.

into the middle hepatic vein, marginal hepatic veins may drain into the right and left hepatic veins, and a large accessory right hepatic vein may be seen entering the IVC several centimetres inferior to the junction of the three main hepatic veins in approximately 6–10% of people (Fig. 7.10).

The venous drainage from the central portion of the liver parenchyma, including the caudate lobe, empties directly into the IVC and cannot normally be perceived by colour Doppler since these veins are small and central (Fig. 7.11). This separate drainage pathway is responsible for the unique behaviour of the caudate lobe in liver disease, and for the distinctive enhancement pattern seen on contrast enhanced CT scans of patients with hepatic vein thrombosis.

### *The hepatic venous waveform*

The normal hepatic vein waveform is triphasic as a result of transmitted cardiac activity (Fig. 7.12) and is similar to the jugular vein waveform; indeed, the labels on the hepatic vein components have been transposed from the jugular vein pressure tracing. Most sonographic windows to the liver demonstrate the hepatic veins so that flow towards the heart is away from the transducer, which registers as flow below the baseline but during right atrial systole blood is forced back into the liver and is therefore displayed above the baseline. These directions are best described as being antegrade (towards the heart) and retrograde (away from the heart).

This complicated tracing has been described and normal velocity measurements determined by Abu-Yousef.[24] Figure 7.12b shows the hepatic venous waveform in relationship with an electrocardiogram (ECG) tracing, tricuspid M-mode scan, and atrial and ventricular status. The following stages can be identified:

1. The most distinctive feature is the retrograde A-wave, which is the result of right atrial contraction and coincides with the P-wave on the ECG. Since there is no valve between the right atrium and the IVC, a burst of reversed flow travels down the IVC and into the hepatic veins, which has a mean velocity of approximately 18 cm $s^{-1}$.
2. At the end of right atrial contraction, flow returns to the antegrade direction as the atrium relaxes. However, on right ventricular systole the tricuspid valve is slammed shut and actually bulges back into the right atrium, thus creating its own pressure wave, the C-wave, which may

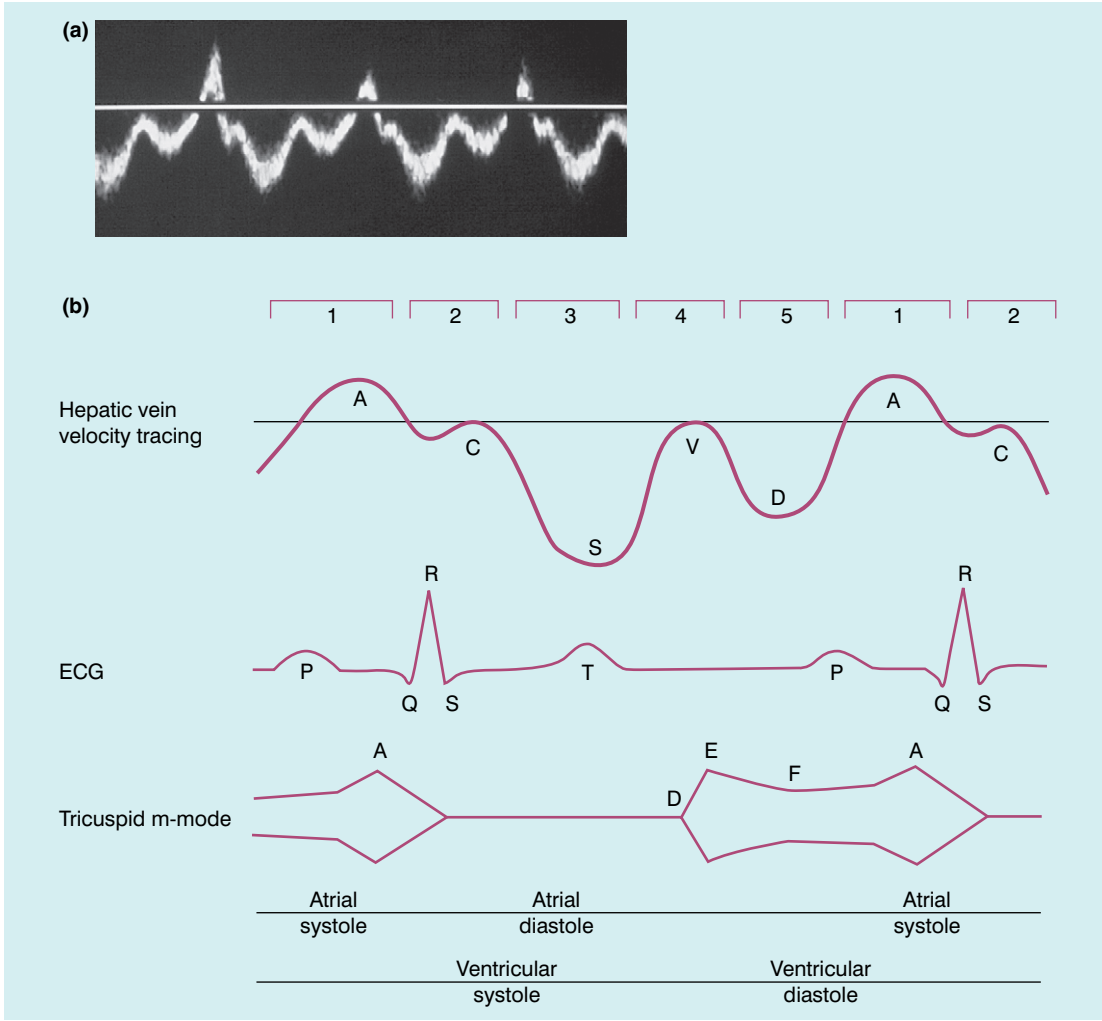


**Fig 7.12** (a) Normal hepatic vein spectral Doppler tracing. (b) Simultaneous tracings of an ECG, hepatic vein spectral Doppler tracing, and mitral valve M-mode tracing with correlation to atrial and ventricular systole and diastole. The divisions at the top of these tracing (1–5) correspond to the discussion in the text.

be perceived as a brief pause in the steadily increasing antegrade flow. This C-wave coincides with the beginning of ventricular systole and occurs immediately after the QRS complex on the ECG.

3. The right atrium continues to dilate and antegrade flow builds to a relatively high velocity of approximately 30 cm $s^{-1}$. Eventually atrial filling approaches completion and antegrade flow starts to slow. This transition, known as the S-wave, occurs during ventricular systole within 0.15 s of the QRS complex.
4. At the end of atrial filling, antegrade velocity decreases, or may even briefly reverse; this is known as the V-wave and has a mean velocity of approximately -1.1 cm $s^{-1}$. In relation to the ECG, this occurs immediately following the T-wave.
5. As the right ventricle enters diastole, the tricuspid valve opens and flow in the hepatic veins increases in the antegrade direction, as both the right atrium and right ventricle fill. Velocity builds to a mean of approximately 22 cm $s^{-1}$ and this phase is referred to as the D-wave. Eventually, the right heart chambers

become filled passively and antegrade flow begins to slow. We then return to the A-wave as the atrium again contracts to begin another cardiac cycle.

This waveform is seen in the hepatic veins and upper IVC in the vast majority of patients. However, not all individuals have a similar degree of periodicity within the hepatic veins. The percentage of patients that manifest an identifiable C-wave is relatively small (Fig. 7.13). The degree of flow reversal of the A-wave and V-wave may vary depending on the patient's cardiac status, state of hydration, heart rate, and the distance of Doppler interrogation from the heart. In a survey of a population of normal volunteers, a 9% incidence of a flattened hepatic vein flow profile has been reported.[29]

Because the heart is located within the thorax, pressure changes caused by respiration affect the hepatic vein flow profile. When the patient forcefully exhales or bears down against a closed glottis, the elevated intrathoracic pressure resists antegrade flow, causing the S- and D-waves to be less prominent. The reversed component of flow increases so the A- and V-waves become more pronounced. Conversely, during forced inspiration with increasing negative intrathoracic pressure, the S- and D-waves become more prominent, while the A- and V-waves are less pronounced and may actually not manifest as reversed flow (Fig. 7.14).

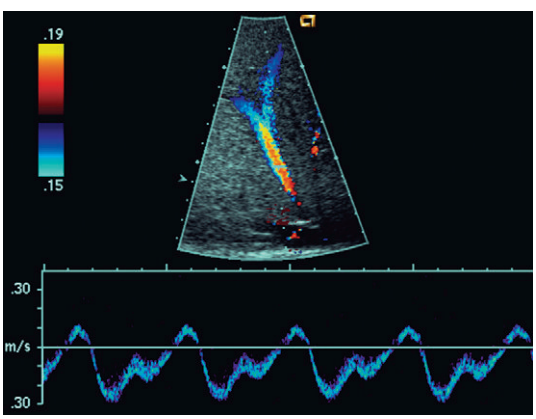


**Fig. 7.13** Normal hepatic vein spectral Doppler tracing. Even though the tracing is acquired within a few centimetres of the heart, the C-wave cannot be identified on this tracing. This is, indeed, the tracing most often visualised in the hepatic vein and inferior vena cava. Only a small component of retrograde flow is present.

## ASSESSMENT OF DISEASE

### Portal vein

#### *Portal hypertension*

In hepatocellular disease, the sinusoids are damaged, destroyed or replaced. As the volume of normally functioning liver parenchyma decreases, the resistance to portal venous flow increases, the portal vein dilates, and portal flow decreases and eventually reverses.[8, 30–33] There is an elevation in portal vein pressure, in excess of normal, by 5–10 mmHg, resulting in portal hypertension.[34] Use of the 'congestive index' has been recommended in helping to diagnose portal hypertension. This index is the ratio of the portal vein cross-sectional area ($cm^2$) divided by the mean portal flow velocity ($cm/s^{-1}$), thereby taking into account portal vein dilatation and decreased flow velocity, the two physiological changes associated with portal hypertension.[35] In normal subjects, this ratio is less than 0.7. Several other indices have been suggested as useful in the prediction of liver disease and its severity. These include hepatic

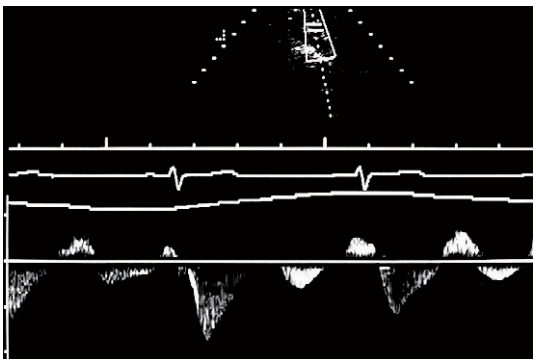

**Fig 7.14** Spectral Doppler tracing in a patient with severe alcohol-induced cirrhosis. Portal vein velocity has decreased although flow does remain hepatopetal through most of the cardiac cycle. Note the marked periodicity, however, which coincided with hepatic arterial systole.

and splenic arteries RIs, modified liver vascular index (portal flow velocity/hepatic artery RI), and portal hypertension index,[36]

$$\frac{(\text{hepatic artery RI} \times 0.69) \times (\text{splenic artery RI} \times 0.87)}{\text{portal vein flow velocity}}$$

As liver disease worsens, the periodicity in the portal vein may become more pronounced, usually coinciding with hepatic arterial systole (Fig. 7.15).[30,37] Finally, with end-stage liver disease, continuous hepatofugal flow is observed, usually with marked periodicity. Blood entering the liver in the hepatic artery normally passes through the hepatic sinusoids to the hepatic veins, but with increasing hepatocellular disease, scarring and fibrosis, the pathway of least resistance for the arterial inflow becomes the portal vein with arterial blood being shunted to the portal vein via vasa vasorum, or via direct arteriovenous shunting at the level of the sinusoids. Thus, the hepatofugal flow leaving the liver in the portal vein is arterial blood shunted from the hepatic artery[38] (Fig. 7.16).

Pronounced periodicity may be seen in the portal vein, which does not coincide with hepatic arterial systole. This is usually due to cardiac disease, such as right ventricular dysfunction or tricuspid regurgitation, and is caused by a prominent reversed component of flow in the hepatic veins, either a 'cannon' A-wave or a reversed S-wave[39,40] (Fig. 7.17).

### *Varices*

As portal hypertension progresses and pressure rises to 15 or 20 mmHg, sufficient pressure exists to cause the development of varices. These collateral pathways shunt blood from the portal to the systemic circulation. The more common

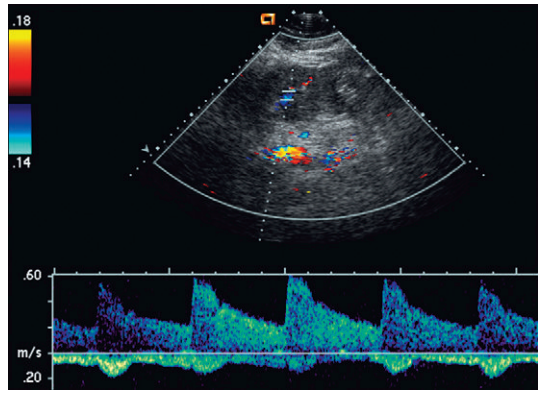


**Fig 7.16** Portal vein spectral Doppler tracing in a patient with severe hepatocellular damage secondary to paracetamol (acetaminophen) overdose. Portal vein flow is hepatofugal throughout the cardiac cycle.

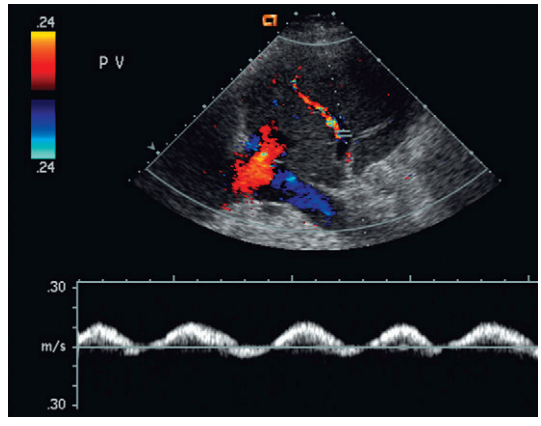


**Fig 7.17** Spectral Doppler tracing of portal vein flow in a patient with severe right ventricular dysfunction and tricuspid regurgitation. There is marked periodicity in the portal vein waveform. Hepatopetal flow decreases, and briefly reverses, coinciding with the large regurgitant component of hepatic vein flow during tricuspid regurgitation.

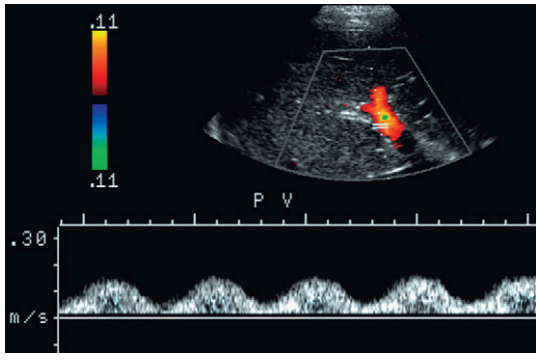


**Fig. 7.15** Spectral Doppler tracing in a patient with severe alcohol induced cirrhosis. The portal vein flow remains continually hepatopetal but the flow profile has developed marked periodicity to the point where antegrade flow almost stops. This coincides with arterial systole.

channels are the short gastric, left gastric and coronary veins; recanalised paraumbilical veins; and splenorenal-mesenteric collaterals (Fig. 7.18). Other, less typical, pathways include pericholecystic, iliolumbar, gonadal, haemorrhoidal, and ascending retrosternal veins. Indeed, almost any vein in the abdomen may serve as a potential collateral to the systemic circulation and may be incorporated in a very convoluted shunt.[41]

*Short gastric varices* coursing between the spleen and the greater curvature of the stomach are best imaged via the left flank, using the enlarged spleen as a window (Fig. 7.19). *Left gastric or coronary vein varices* running from the splenic or portal veins to the lesser curvature of the stomach are best imaged through the left lobe of the liver (Figs 7.19b and 7.20a). Both sets of varices then converge on the gastro-

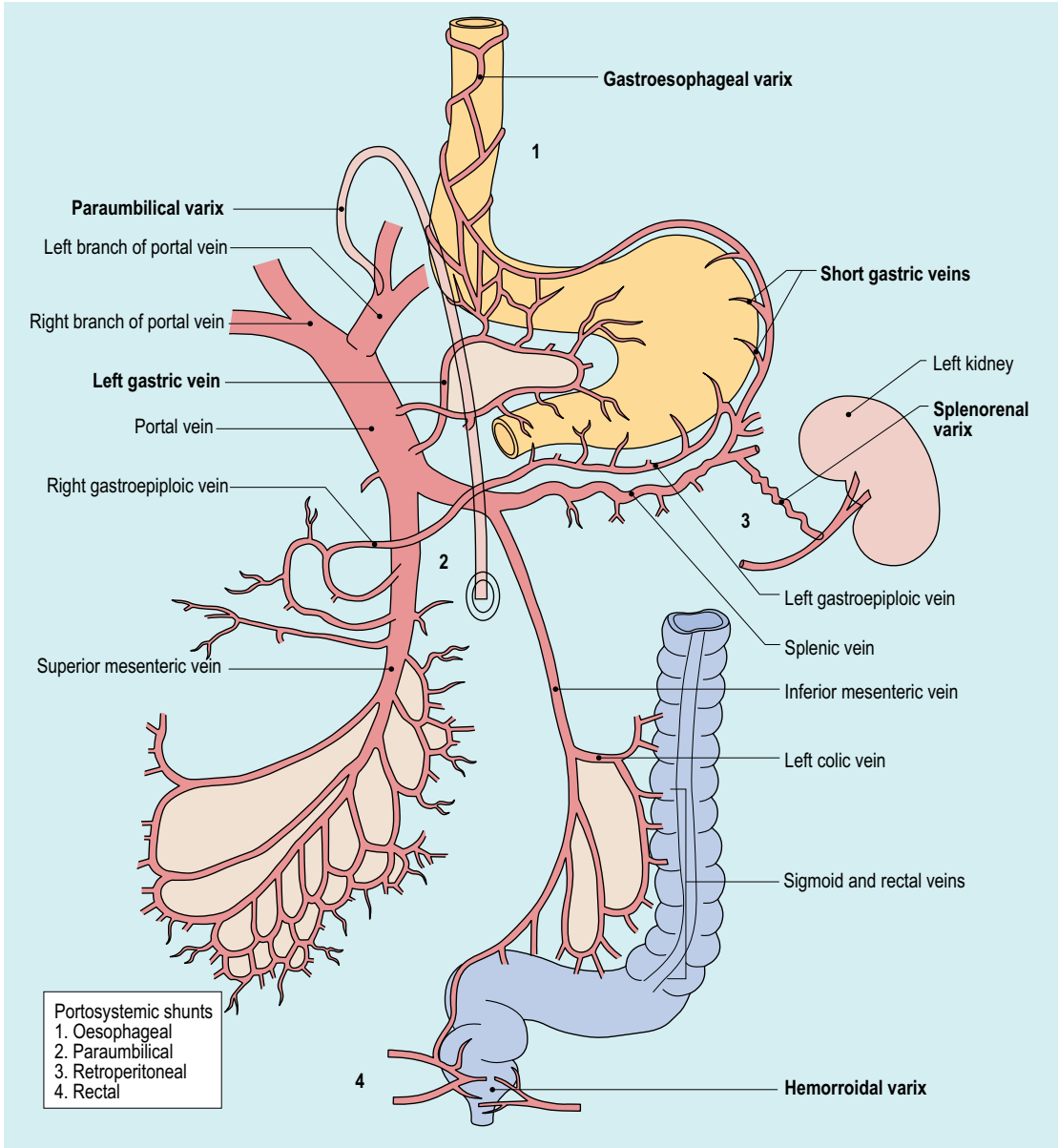


**Fig 7.18** Major portosystemic varices encountered in portal hypertension.

oesophageal junction. From there, blood flow proceeds upwards through oesophageal varices to eventually communicate with the azygous vein and the systemic circulation (Fig. 7.20b). Because of the potential lethal risk from spontaneous, brisk haemorrhage from these varices, a variety of endoscopic, surgical, or percutaneous procedures may be employed to divert blood away from them.[42]

In utero, oxygenated blood flows from the placenta up the umbilical vein to the left portal vein and through the ductus venosus into the IVC and right atrium. After birth, this pathway involutes and the umbilical vein is represented by the ligamentum teres in the falciform ligament. In portal hypertension, *paraumbilical veins* in this ligament can dilate and carry blood from the left portal vein along the anterior abdominal wall to

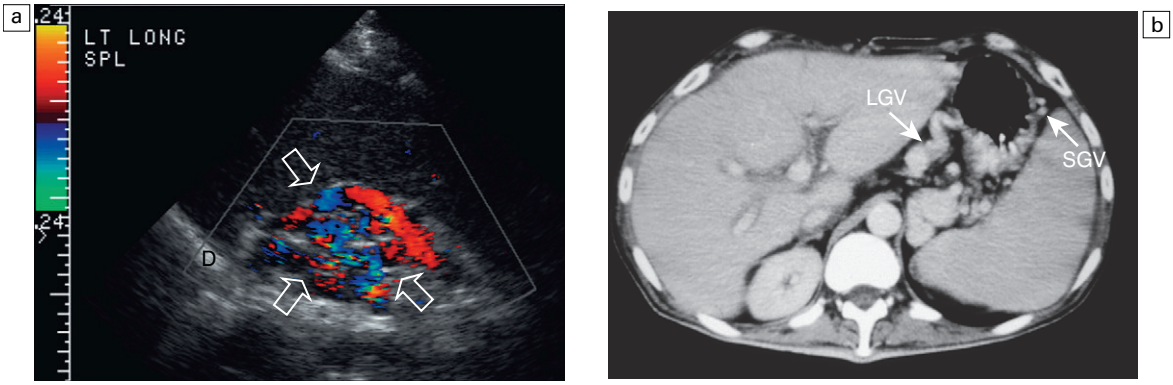


**Fig. 7.19** (a) Longitudinal colour Doppler view of the left flank in a patient with portal hypertension. A tangled web of vessels (arrows) is seen at the splenic hilum and extends cephalad towards the diaphragm (D). These are short gastric varices coursing from splenic veins to the stomach and from there to the systemic circulation via esophageal varices. (b) Contrast-enhanced CT of a patient with portal hypertension. Short gastric varices (SGV) are best imaged from the left flank using the spleen as a sonographic window. The left gastric varix (LGV) is best imaged through the left lobe of the liver.

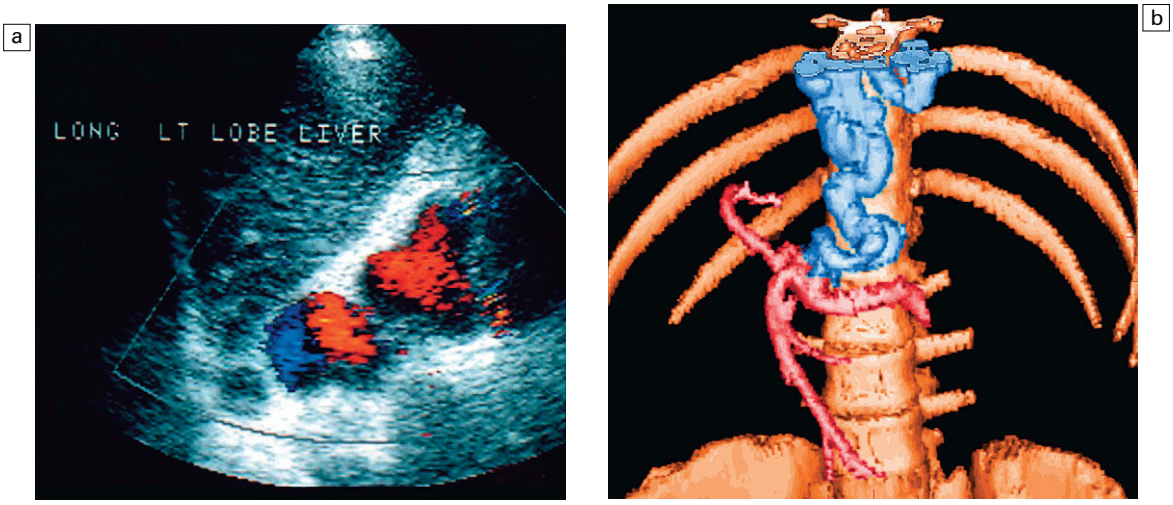


**Fig. 7.20** (a) Longitudinal colour Doppler image in the midline of a patient with portal hypertension. A large tortuous left gastric varix is seen coursing from the region of the coeliac axis towards the gastro-oesophageal junction. Whereas short gastric varices tend to be a plexus of small vessels, the left gastric varix is typically a single large tortuous vessel. (b) Coloured shaded surface displays three-dimensional reconstruction of the portal vasculature. The portal venous system is coloured red. The vessel represents a large left gastric varix. Note the convoluted nature of this vessel as it courses cephalad, eventually branching into multiple oesophageal varices.

the umbilical region (Fig. 7.21).[43] From the umbilicus, the blood may pass to the superior or inferior epigastric veins, or through subcutaneous veins in the anterior abdominal wall, a 'caput medusae', to reach the main systemic venous system. Because inferior epigastric varices run just deep to the rectus muscles, they are not apparent on clinical examination but are easily identified by colour Doppler (Fig. 7.22). Patients with known portal hypertension, who present with an umbilical hernia, should undergo imaging evaluation prior to surgery as the hernia may contain a dilated varix, rather than bowel (Fig. 7.23). One advantage of this collateral pathway is that it shunts blood away from those varices that can cause life-threatening variceal bleeding.[44]

*Splenorenal-mesenteric* collaterals are typically quite large and very tortuous. They are seen in the left flank coursing between the splenic hilum and the left renal vein (Fig. 7.24). Occasionally, this pathway can continue via gonadal veins into the pelvis.

*Pericholecystic varices* can occur in the gallbladder wall and are associated with portal vein thrombosis. US imaging may reveal cystic or tubular structures in the gallbladder wall. These should not be confused with the Rokitansky Aschoff sinuses of hyperplastic cholecystosis. Colour Doppler is useful to show flow within these vessels; the spectral tracing is that of portal venous flow (Fig. 7.25). From the gallbladder, subhepatic collaterals communicate with the abdominal wall and subcostal veins. Haemorrhoidal collaterals are not routinely studied by Doppler.

### *Portal vein thrombosis*

Portal vein thrombosis may be completely asymptomatic in patients with cirrhosis; however, more than half of cases present with life-threatening complications, such as gastrointestinal haemorrhage or intestinal infarction.[45] Portal vein thrombosis must be considered when no Doppler signal is detected within the portal vein. It may be due to blood clot, or to tumour invasion. However, the examiner should first review the system set-up and re-evaluate scale, gain, and filtration settings (Fig. 7.26). If these are found to be set appropriately and there is still no perceptible flow, the patient should be asked to perform a Valsalva manoeuvre. This elevates intrathoracic and right atrial pressure, transmitting higher

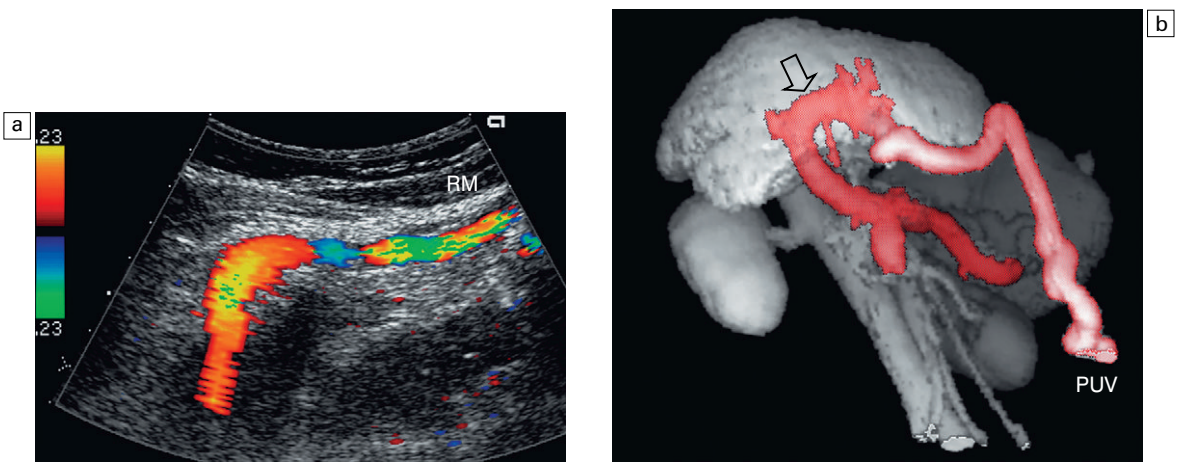


**Fig. 7. 21** (a) Longitudinal colour Doppler image of a patient with portal hypertension. A large vein carries flow from the left portal vein towards the transducer. It courses along the falciform ligament and then turns caudad along the interior abdominal wall coursing towards the umbilicus, deep to the rectus muscles (RM). (b) Shaded surface display three-dimensional reformat of the upper abdominal solid organs and portal venous system. Flow in the main portal vein courses towards the liver but immediately channels into a large left portal vein (open arrow). Flow then continues anteriorly towards the anterior abdominal wall and down towards the umbilicus in a large recanalised paraumbilical vein (pink).

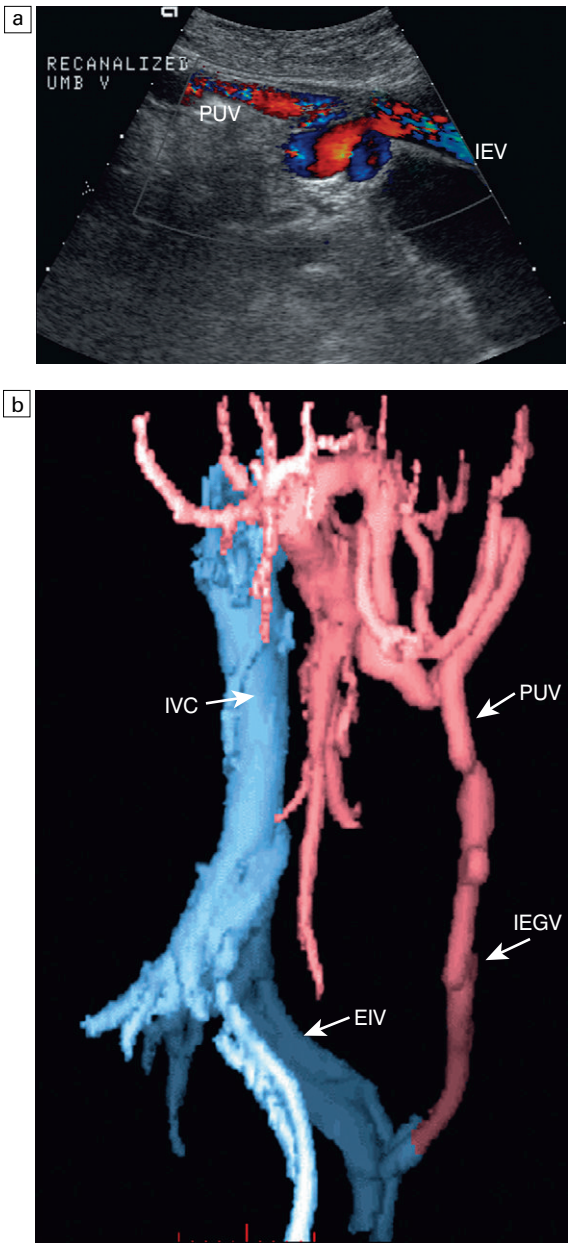


**Fig. 7.22** (a) Longitudinal colour Doppler image directly over the umbilicus. A recanalized paraumbilical vein (PUV) carries blood towards the umbilicus. No caput medussa was present in this patient since flow continues from the umbilical region via the inferior epigastric vein (IEV). (b) 3-D CT angiogram in a patient with portal hypertension. Note the large recanalized paraumbilical vein (PUV) coursing towards the umbilicus. From there flow continues back to the systemic circulation via the left inferior epigastric vein (IEGV) to the left external iliac vein (EIV) and the inferior vana cava (IVC).

pressure to the IVC, hepatic veins and subsequently into the liver parenchyma. This increased pressure causes even greater resistance to portal venous inflow and may convert stagnant portal flow to hepatofugal flow (Fig. 7.27). One may also consider the use of an intravenous US contrast agent to enhance perception of very slow flow.

Early *thrombosis* of the portal vein may be difficult to visualise with US since fresh clot can be markedly hypoechoic (Fig. 7.28).[46] As clot matures, it becomes more echogenic and retracts, allowing partial recanalisation of the portal vein (Fig. 7.29). Patients with long-standing portal vein thrombosis may develop collateral flow into the liver via a lace-like network of veins. This is known as cavernous transformation of the portal vein or a cavernoma.[47, 48] Grey-scale imaging alone can seldom visualise these vessels because of their small size, but colour Doppler reveals a web of numerous serpiginous small veins which typically involve a fairly wide area of the liver hilum (Fig. 7.30). Spectral Doppler shows portal flow in the branches of the cavernoma.

### *Neoplastic invasion*

HCC has the propensity to invade the portal and hepatic veins. Intravascular tumour is classified as stage IV disease and is considered unresectable. Involvement of the portal vein by tumour may cause an increase in its cross-sectional area and a decrease in portal vein flow. Tumour in the portal vein will receive its blood supply from the hepatic artery and spectral Doppler of the 'thrombus' will show an arterial waveform, which usually projects in a hepatofugal direction, supplying the tumour as it grows out of the liver. A bland thrombus will not manifest such a tracing on Doppler, so that invasive tumour can be differentiated from bland thrombus and the diagnosis of stage IV HCC with vascular invasion confirmed (Fig. 7.31).[49]

### *Portal vein aneurysm*

Aneurysm of the portal vein has been reported, but it is extremely rare. The vein may enlarge to a diameter of 3 cm or larger. Spectral Doppler

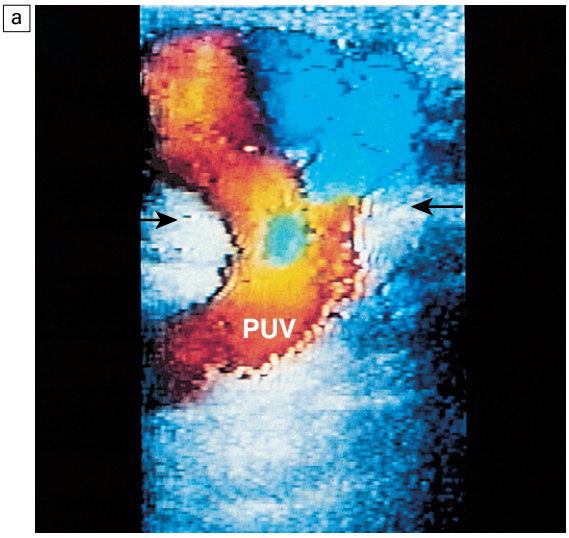


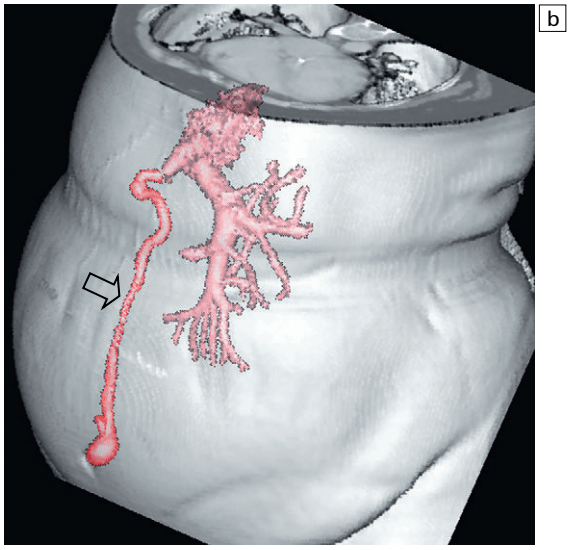



**Fig. 7.23** (a) (b) Three-dimensional rendering shaded surface display. The portal venous phase of the CT angiogram in a patient with portal hypertension. A large recanalised paraumbilical vein (PUV) courses down the anterior abdominal wall (arrow). In the subumbilical region this vessel is seen to dilate into an aneurysmal component of this varix. (c) Photograph of the umbilicus in a patient with alcoholic cirrhosis and end-stage liver disease. This rust coloured mass is a herniated paraumbilical varix that has extended to the rectus sheath and out through the anterior abdominal wall. This varix is simply following the anatomic pathway of the original umbilical vein.

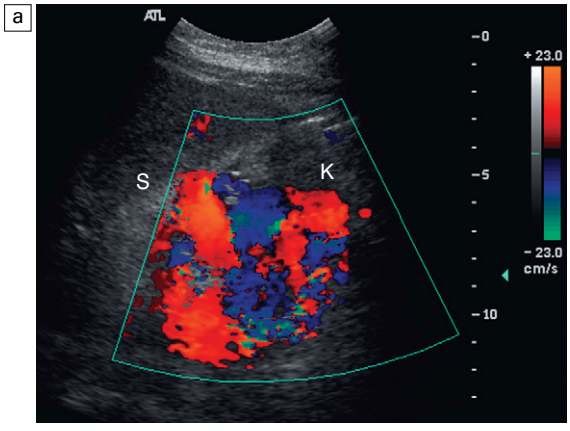


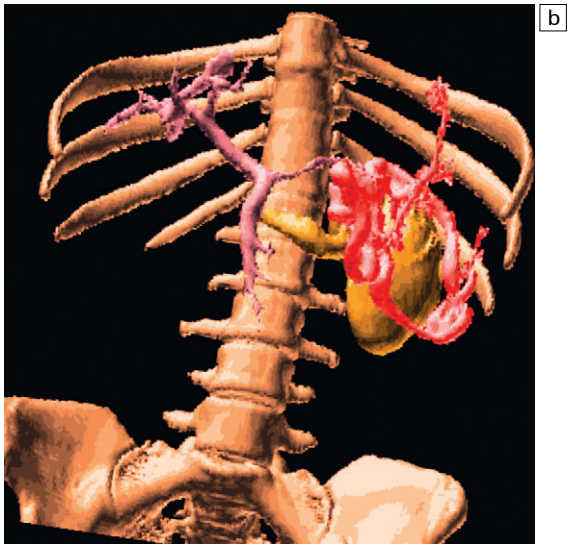


**Fig. 7.24** (a) Longitudinal colour Doppler image of the left flank. A large varix occupies the space between the splenic hilum (S) and the left kidney (K). This represents a convoluted splenorenal varix. (b) Three-dimensional rendering of the portal phase of a CT angiogram. The portal venous system is illustrated in pink. The red vessel represents a large convoluted splenorenal varix. The kidney and its renal vein are illustrated in yellow. (The spleen has been removed for ease of visualisation of this varix.)

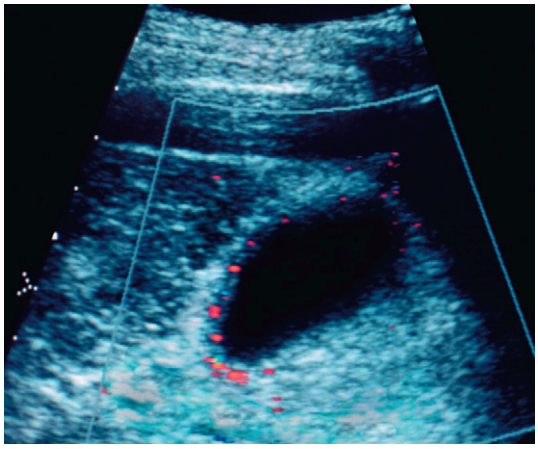

**Fig. 7.25** Colour Doppler image of the gall bladder in a patient with portal hypertension and portal vein thrombosis. Numerous vessels are identified in the gall bladder wall. Spectral Doppler revealed a portal vein waveform as would be expected in varices and not an arterial waveform as would be seen in the cystic artery.

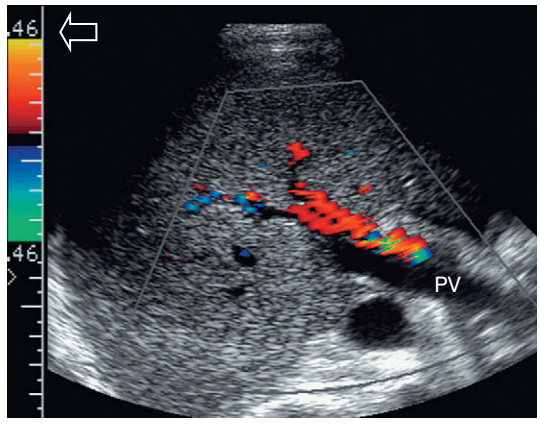


**Fig. 7.26** Colour Doppler image along the axis of the porta hepatis in a patient with portal hypertension. Colour flow is clearly evident in the hepatic artery. The portal vein, however, shows no evident flow suggesting thrombosis. Evaluation of the pulse repetition frequency (arrow) shows that the value was set quite high. This effectively suppresses colour display of slow flow giving the false impression of thrombosis.

should be applied to confirm a portal vein waveform and rule out hepatic artery aneurysm since the latter carries a much higher incidence of complications and rupture.[50,51]

### *Portal vein gas*

Gas may be seen in the portal vein and its branches in a variety of gastrointestinal disorders, such as sepsis, obstruction with distension, necro-

a

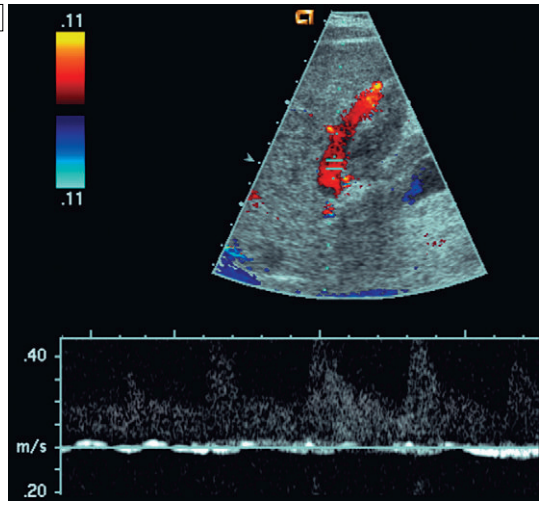


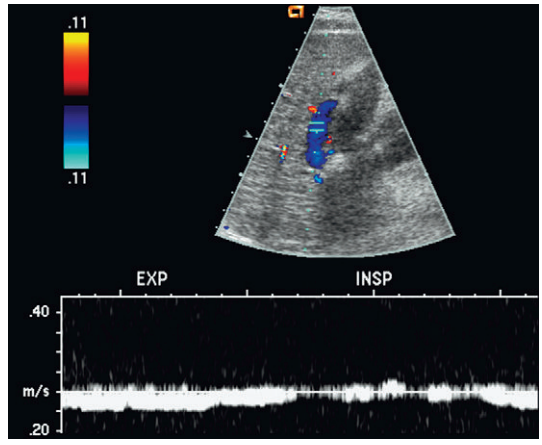


**Fig. 7.27** Spectral Doppler tracings of a patient with end-stage liver disease being considered for liver transplantation. (a) With neutral breath-hold, flow in this portal vein is barely perceived. It oscillates between hepatofugal during arterial systole and hepatopetal during arterial diastole. (b) When instructed to forcefully breathe in and out, this patient's portal flow became more dynamic. During forced expiration with elevated intrathoracic pressure there is increasing resistance to hepatic venous outflow forcing portal vein flow to become hepatofugal. During inspiration with negative intrathoracic pressure, this decreases the resistance to hepatic venous outflow thereby, causing flow to become almost stagnant.

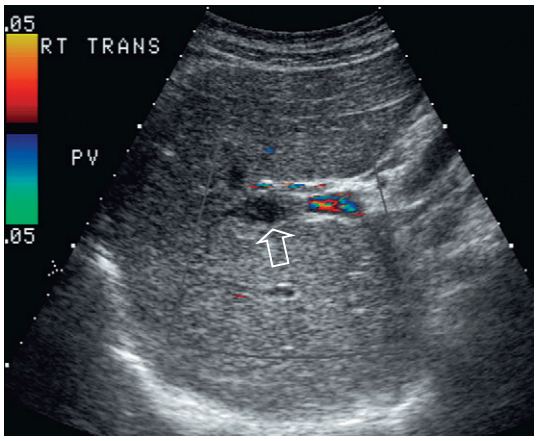


**Fig. 7.28** Oblique colour Doppler image of the porta hepatis. The pulse repetition frequency is appropriately set at a low level. Nevertheless, the trickle of flow is seen in the extrahepatic portal vein but within the liver itself no colour flow is identified. Indeed there are some low level echoes within the portal vein indicating fresh clot (arrow).

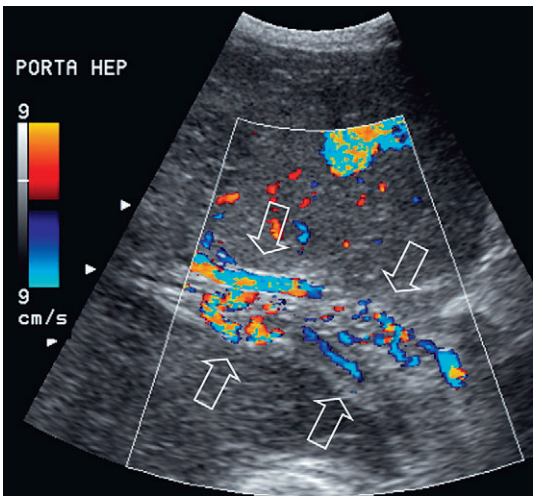


**Fig. 7.30** Oblique colour Doppler image of the porta hepatis. A normal portal vein could not be visualised. Instead there is a plexus of small vessels with hepatopetal flow (arrows). After portal vein thrombosis this web of small vessels reconstitutes portal flow to the liver and is known as cavernous transformation of the portal vein.

tising enterocolitis, infarction or ulceration. Numerous tiny hyperechoic foci can be seen in the portal vein, flowing into the liver. Since these bubbles are moving fairly rapidly, their perception is improved by increasing scanner temporal resolution by limiting the field of view to the area of the portal vein and minimising, or turning off, frame averaging. The spectral Doppler tracing reveals sharp bidirectional spikes superimposed on the Doppler tracing of the portal vein.[52] These spikes do not reflect a higher velocity of the air bubble but represent an artefact resulting from the system being set to display the Doppler shift of red blood cells, so that the much more intense echoes from the air bubbles register as a spikes of noise on the tracing (Fig. 7.32).[53]

a

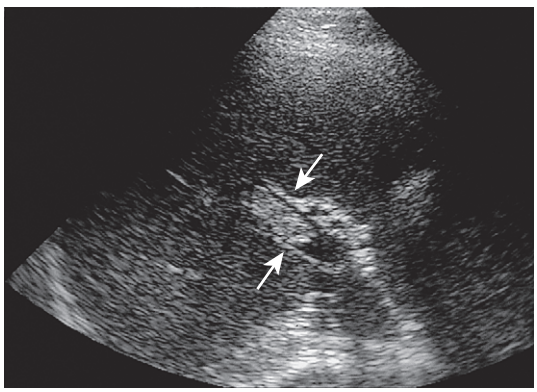

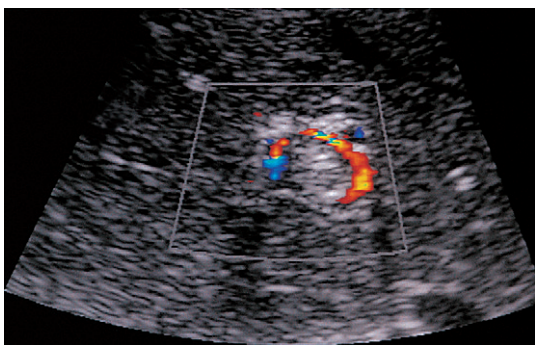

b

**Fig. 7.29** (a) Oblique image of the portal vein in a patient with hypercoagulability. Echogenic thrombus is seen adherent to the portal vein wall (arrows). (b) Colour Doppler image transverse to the portahepatis. Flow is seen coursing past the partially occluding thrombus in a hepatopetal direction.

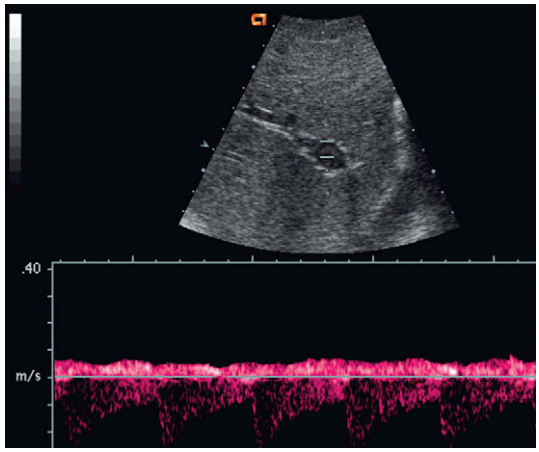


**Fig. 7.31** Spectral Doppler tracing over the portal vein in a patient with hepatocellular carcinoma (HCC). An arterial waveform is present in a plug of tissue identified extending into the portal vein. This represents HCC primarily perfused by arterial flow.

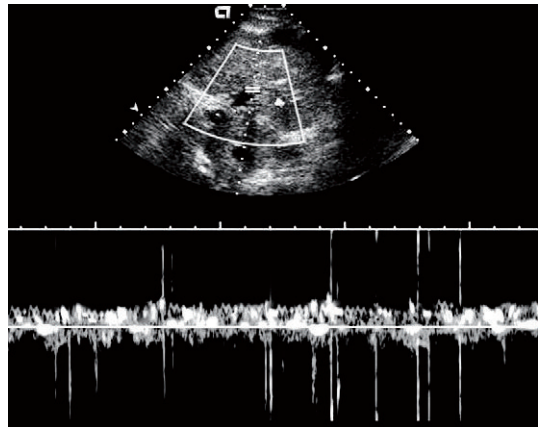

**Fig. 7.32** Spectral Doppler tracing of the portal vein in a patient with pneumatosis intestinalis. The spikes present in this spectral Doppler tracing are caused by air bubbles in the portal vein. These bubbles are traveling at the same velocity as the rest of the blood in the portal vein. With the spectral gain set for blood, the intense sound reflection caused by the passing air bubbles creates spikes of noise.

## Hepatic artery

A comparison of hepatic arterial velocities with those of the portal vein may be used as an indicator of liver disease. The normal portal vein velocity in a fasting patient is about 18 cm $s^{-1}$, the normal systolic velocity in the hepatic artery is 25–40 cm $s^{-1}$ and 10–15 cm $s^{-1}$ in diastole. If the waveforms of the hepatic artery and portal vein can be captured simultaneously on a Doppler tracing, the normal hepatic arterial diastolic velocity will therefore be seen to dip just below that of the portal vein (Fig. 7.9).

Almost all liver disease processes receive their blood supply primarily from the hepatic artery. As the process becomes more severe, or involves a larger area of liver, hepatic artery flow increases. As liver disease worsens, the portal venous inflow encounters progressively increasing resistance, resulting in decreased hepatopetal portal velocity. Therefore, if the Doppler examination shows hepatic arterial diastolic velocities greater than that of the portal vein, the liver parenchyma should be carefully evaluated to rule out focal or diffuse liver disease.[8] This finding, however, is nonspecific and can be seen with neoplasm (both primary and metastatic) and infection (viral, bacterial, parasitic or fungal) (Fig. 7.33). Benign conditions (e.g. haemangioma, fatty infiltration), however, do not perceptibly affect main hepatic artery or portal vein flow (Fig. 7.34).

Hepatic artery resistance has been studied in several disease states. Alterations in resistance may be observed but, to date, have not been shown to be sufficiently specific or sensitive in the diagnosis of any one particular condition.[54,55] Rapid onset of oedema or inflammation of the liver may produce a substantial amount of congestion, leading to higher resistance to hepatic arterial inflow and elevation of the RI. Elevated RI in the hepatic artery has been reported as a predictor of fulminant and severe acute liver failure.[56,57] Hypervascular disorders, especially those with arterial venous shunting, such as neoplasm, can lower the arterial resistance. A tardus parvus waveform and low resistance flow may also be perceived downstream from significant hepatic artery stenosis, or a diaphragmatic crus defect of the celiac axis (Fig. 7.35).

### *Hepatic artery aneurysm*

Aneurysm of the hepatic artery is usually extrahepatic and may be congenital or acquired.

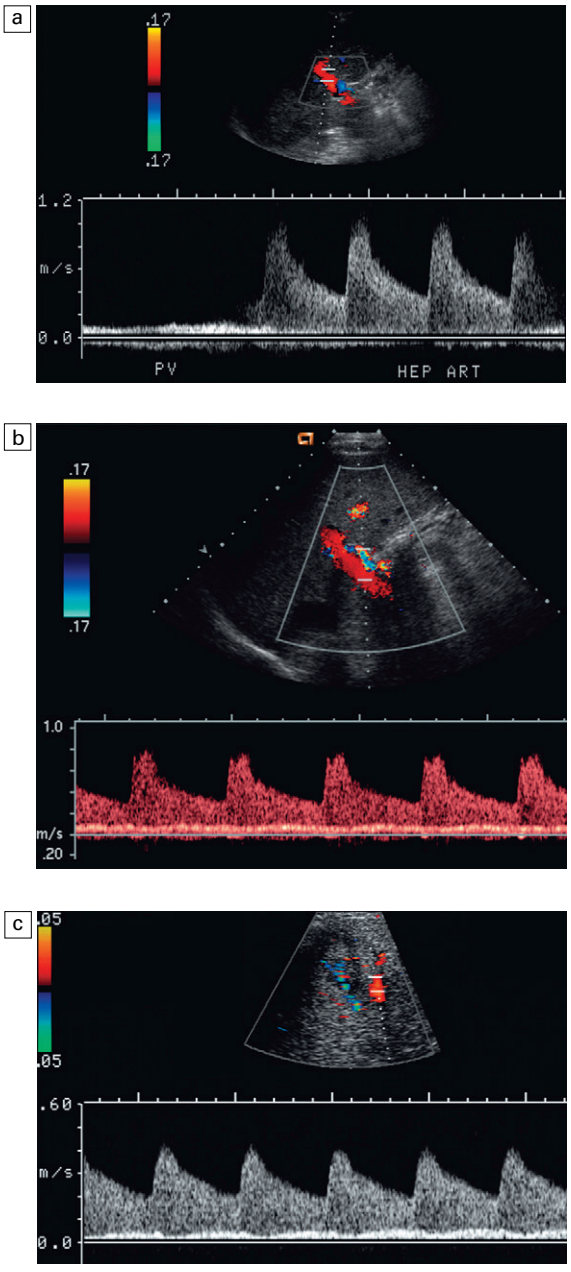


**Fig. 7.33** (a) Spectral Doppler tracing of the porta hepatis in a patient with biopsy proven chemical hepatitis. This tracing was obtained by a slight change in orientation of the transducer during the scan, traversing from portal vein to the hepatic artery. Hepatic arterial velocities are markedly increased with low resistive index and high diastolic flow. Portal vein flow has decreased to the point where it is barely receptable. (b) Combined hepatic artery and portal vein tracing at the porta hepatis in a patient with HIV. In contrast to (a) this tracing was obtained with a sample volume opened wide, including the flow profiles of both the hepatic artery and portal vein in the same tracing. Similar alteration in velocities is again perceived with bounding arterial flow and markedly diminished portal vein inflow. (c) Similar combined tracing in a patient with metastatic lung cancer. The bounding arterial flow is supplying the rapidly growing tumour metastases. Portal venous flow is decreased as the liver sinusoids are being replaced by tumour.

Pancreatitis, trauma, or liver biopsy are the most common aetiologies. Mycotic aneurysms can be seen in immunocompromised patients, those with bacterial endocarditis or those abusing intravenous drugs. Sonography demonstrates a rounded area with swirling flow on colour. An arterial spectral tracing may be perceived but is usually quite distorted due to turbulence.

A clot may eventually develop within the aneurysm or pseudoaneurysm (Fig. 7.36). Communication may develop from the aneurysm to the portal vein or hepatic vein converting the aneurysm to an arteriovenous fistula. Spectral Doppler flow profiles show bounding arterial inflow velocities, swirling turbulent flow within the aneurysm and arterialisation of the venous outflow.[58,59]

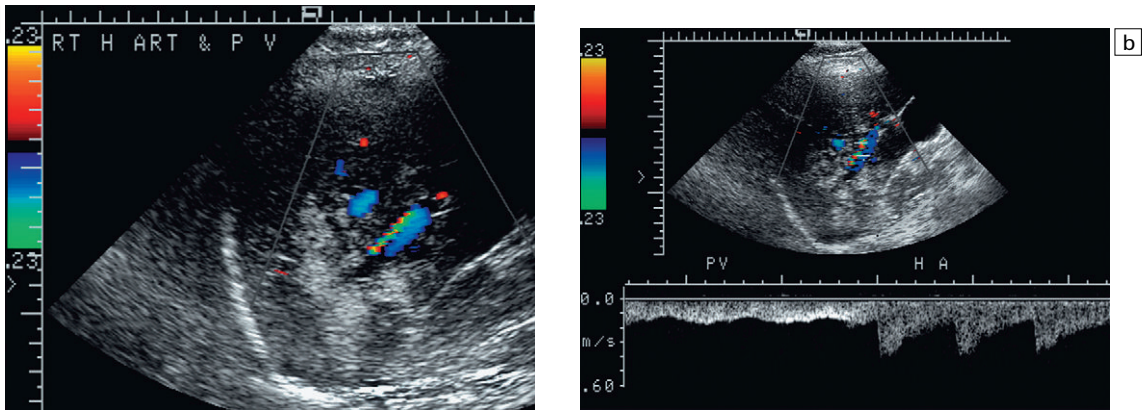


**Fig. 7.34** (a) Transverse image of the right lobe of the liver. A globular but very echogenic mass like infiltrate is perceived in the inferior aspect of the right lobe. The posteroinferior branch of the right hepatic artery and vein are seen coursing into this area on colour Doppler. (b) Spectral Doppler tracing of the hepatic artery and portal vein supplying this mass reveals the velocities are relatively normal. The ratio of flow is not altered between the two vessels. Biopsy proved this mass to be focal fatty infiltration.

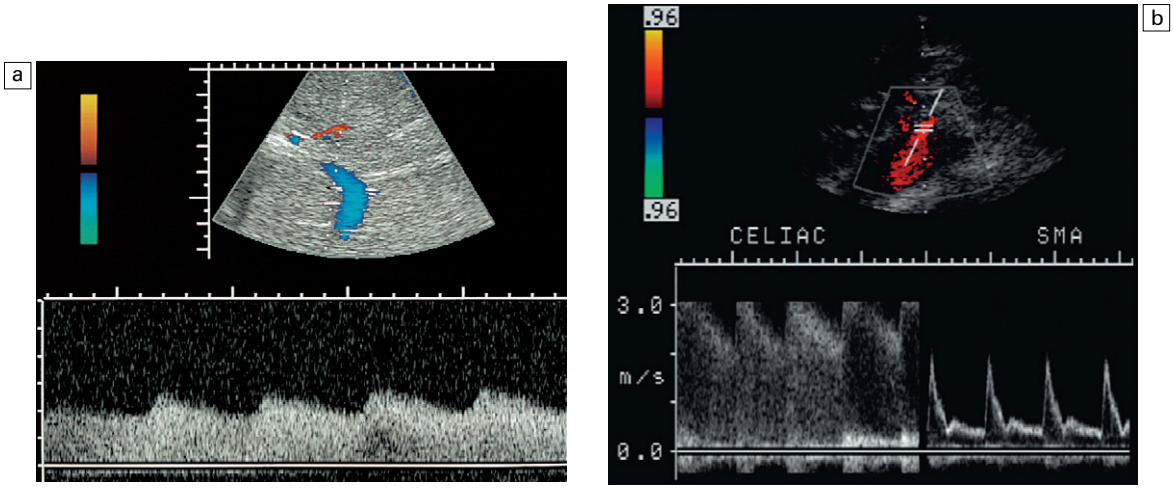


**Fig. 7.35** (a) Spectral Doppler tracing of an hepatic artery in a young patient with upper abdominal pain. The waveform shows a markedly tardus parvus configuration. There is a slow upstroke in systole and very low resistive index. This indicates inflow compromise. (b) Combined spectral Doppler tracing of the celiac artery and superior mesenteric artery (SMA) shows a normal flow velocity in the SMA. The celiac artery, however, shows a very turbulent waveform with a velocity greater than 3 m $s^{-1}$. MR angiography confirms celiac artery compression by the arcuate ligament of the diaphragm.

### *Hereditary haemorrhagic telangiectasia (Osler–Rendu–Weber disease)*

This disease is characterised by multiple small aneurysmal telangiectases distributed over the skin, mucous membranes, alimentary tract, liver, brain and spleen. These patients have a tendency for frequent haemorrhages requiring transfusion. Vascular lesions in the liver can evolve into arterial venous fistulas and aneurysms.[60,61] Ultrasound may reveal large hepatic arteries feeding large, ectatic, serpiginous arteriovenous malformations, which in turn feed large draining veins.[61,62]

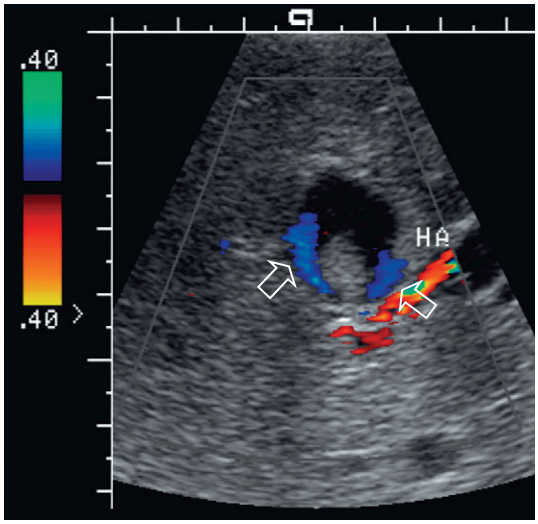


**Fig. 7.36** Transverse colour Doppler image of the mid-liver. A rounded lesion is present with some internal debris layering dependently. Flow is perceived around this debris (arrows). An arterial spectral Doppler waveform was identified in the feeding vessels. Angiography confirmed that this was a partially thrombosed intrahepatic hepatic artery aneurysm.

## Hepatic veins

### *Hepatic venous outflow obstruction*

The term Budd–Chiari syndrome is usually taken to refer to hepatic vein thrombosis. Budd–Chiari, however, refers to liver dysfunction due to any cause of compromised hepatic vein outflow, both thrombotic and non-thrombotic. Ludwig and associates have recommended that the term hepatic venous outflow obstruction (HVOO) should be used instead of Budd–Chiari syndrome.[63] This is appropriate since spectral and colour Doppler are capable of identifying numerous non-thrombotic causes of HVOO and differentiating them from hepatic vein thrombosis.[64] Etiology may be related to pregnancy, tumour, hypercoagulable state or IVC membranes, but the majority of cases are idiopathic.[65] The clinical presentation of HVOO will vary, depending upon how rapidly it develops and the degree of

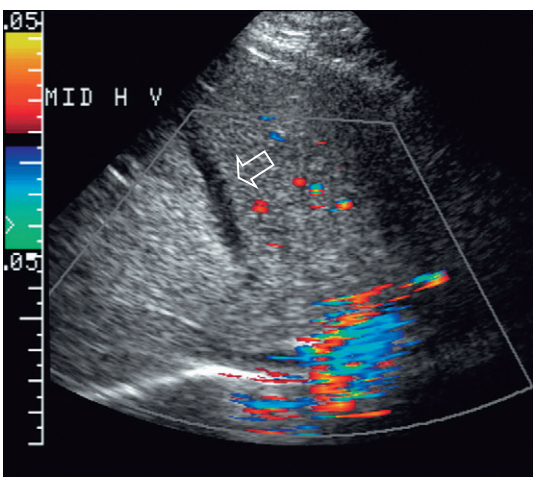


**Fig. 7.37** Transverse colour Doppler image of the upper liver. Even with maximised Doppler sensitivity, no flow was perceived in the middle hepatic vein of this patient (arrow). The hepatic vein had become thrombosed when a central line was inadvertently advanced through the heart into the inferior vena cava and up into the middle hepatic vein. This relatively acute thrombus is hypoechoic compared to the surrounding liver parenchyma. As thrombus matures, however, the echogenicity tends to become isoechoic with the adjacent liver and the thrombus becomes harder to perceive.


**Fig. 7.38** Transverse ultrasound image of the mid-liver. A thrombus is present within the middle hepatic vein (arrows). Fortunately there has been some recanalisation of flow around this clot which is isoechoic to the surrounding liver. In the absence of this flow this clot would have been very difficult to see.

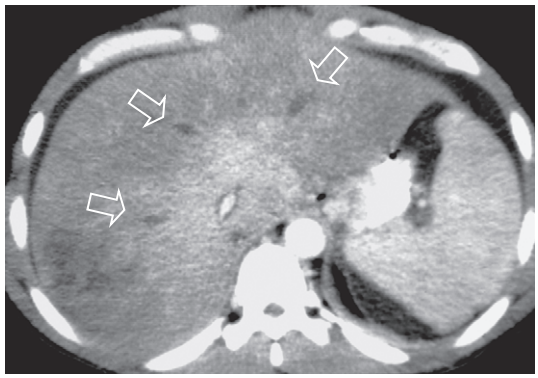

**Fig. 7.39** Contrast enhanced axial CT of the mid-liver. Note the uniform enhancement centrally in the caudate lobe, but peripherally the enhancement is decreased and irregular. The three hepatic veins (arrows) are unenhanced due to the fact that they are thrombosed.

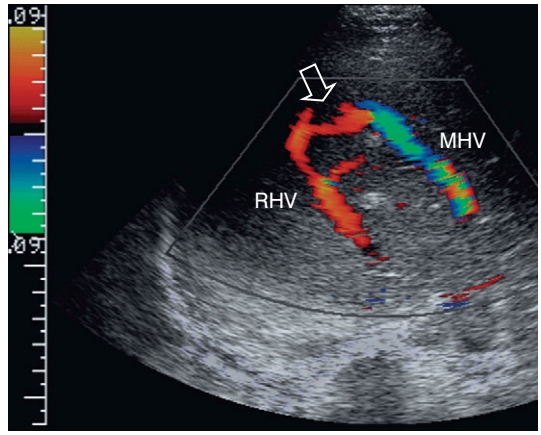


**Fig. 7.40** Transverse colour Doppler view of the mid-liver in a patient with catheter related inferior vena cava thrombus. Flow in the right hepatic vein (RHV) is reversed and coursing towards the transducer. A prominent collateral vein (arrow) then carries flow to the middle hepatic vein (MHV) and back towards the heart. Note the aliasing the more distal hepatic vein due to the higher velocity caused by the increased volume of flow.

obstruction. Approximately 50% of patients first present with RUQ pain and hepatomegaly. Almost all develop ascites, while a few may develop mild jaundice. Patients with chronic, partial obstruction may develop cirrhosis and portal hypertension. If the obstruction progresses to complete occlusion, then shock, hepatic coma and death may ensue.

Sonographic imaging features of HVOO may include echogenic intraluminal material (either thrombus or tumour), diffuse narrowing and compression of the veins from generalised liver swelling, or focal vascular compromise by a mass. Doppler findings include complete absence of hepatic vein flow (Fig. 7.37) or localised flow disturbances due to focal partial obstruction. In addition, the central portions of the hepatic veins (distant from the IVC) that remain patent will display low-velocity continuous flow, rather than the normal flow pattern with periodicity. Finally, liver congestion due to HVOO will also cause flow abnormalities in portal vein flow, such as diminished hepatopetal, bidirectional or hepatofugal (reversed) flow. The diagnosis of complete thrombosis by US imaging is difficult since the echogenicity of the clot is often similar to that of the adjacent liver parenchyma (Fig. 7.38). Because the identification of absent blood flow by Doppler is an exclusionary diagnosis, it is difficult to determine with absolute certainty that the cause is thrombosis.

HVOO may be seen in three disease categories: hepatic vein thrombosis' non-thrombotic focal compromise of hepatic vein drainage (e.g. stricture, web or neoplasm), or reduced compliance of liver parenchyma (e.g. hepatitis, cirrhosis or transplant rejection).

*Hepatic vein thrombosis* most commonly occurs in patients with a hypercoagulation disorder and the use of oral contraceptives increases the risk of hepatic vein thrombosis two and a half times. Hepatic vein injury and phlebitis may also be associated with thrombosis, but in approximately two-thirds of cases, the cause is idiopathic. The caudate lobe has a separate venous drainage to the IVC, which is usually spared from thrombosis, resulting in caudate enlargement and normal enhancement on contrast enhanced CT (Fig. 7.39). Occasionally, thrombosis may be limited to one or two of the hepatic veins, resulting in shunting of blood from the affected lobe to the unaffected side through hepatic venous collaterals (Fig. 7.40). A strategically located mass (either

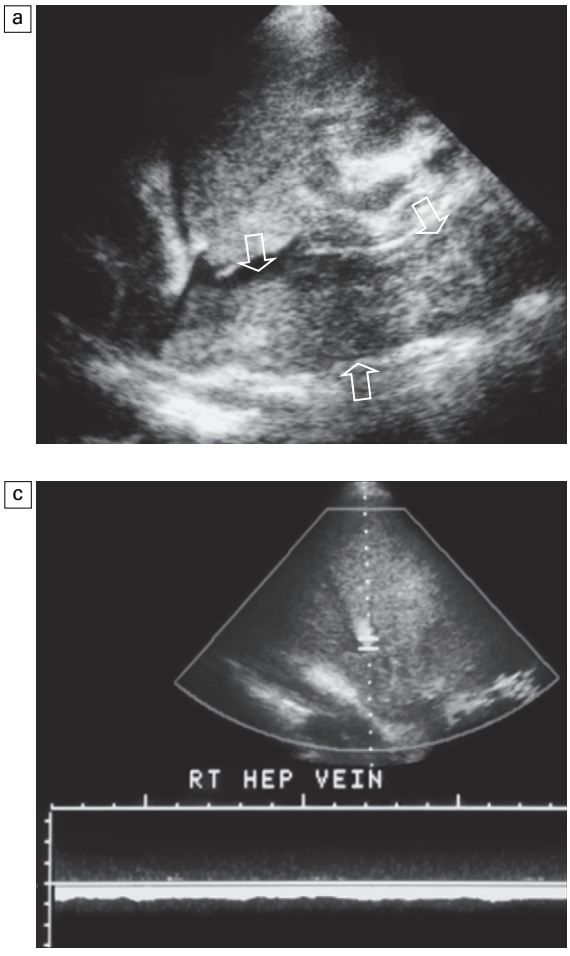


**Fig. 7.41** (a) Longitudinal view of the inferior vena cava in a patient with renal cell carcinoma. A large plug of tumour thrombus is seen extending in the inferior vena cava up to the level of the heart (arrows). (b) Transverse view of the liver. The inferior vena cava tumor thrombus (TT) obstructs the hepatic vein ostia. Note the distention of the hepatic vein (arrows). (c) Spectral Doppler tracing shows flattening of the hepatic vein flow profile and complete absence of periodicity. The triphasic waveform is not present, since cardiac retropulsation cannot get past the tumour thrombus.

benign or malignant) may expand and press upon the ostia of the hepatic veins, resulting in impaired venous drainage. Renal cell carcinoma can extend from the renal vein into the IVC in 5% of cases. Rarely this may extend up to the right atrium and compromise the hepatic vein ostia, which may result in elevation of the liver enzymes (Fig. 7.41). Renal carcinoma metastases to the liver maintain this same propensity for vascular invasion (Fig. 7.42).

*Membranous obstruction (fibrous web)* of the IVC has been reported as one of the major causes of HVOO in South Africa and Asia.[66,67] The aetiology of these is probably acquired since chronic hepatitis B infection is common in these patients, and up to 50% may develop HCC. There is some support, however, for a congenital hypothesis. The obstruction is usually at, or just above, the level of the hepatic vein ostia; this results in damping of cardiac pressure changes into the IVC and the hepatic veins and flattening of the Doppler waveform. The obstruction may eventually lead to hepatic vein thrombosis.

*Diffuse hepatic parenchymal disease* resulting in a reduction of liver compliance can easily compromise hepatic venous drainage as these are a low pressure system (basically the same as the right atrium; i.e. -2/+7 mmHg). Both oedema from acute inflammation and fibrosis from chronic parenchymal disease (Fig. 7.43a) can compromise the hepatic veins, producing a relative HVOO. Some periodicity may be perceived in close proximity to the junction of the hepatic veins with the IVC, but it quickly fades as the sample volume is moved further away from the heart (Fig. 7.43b).[68,69]

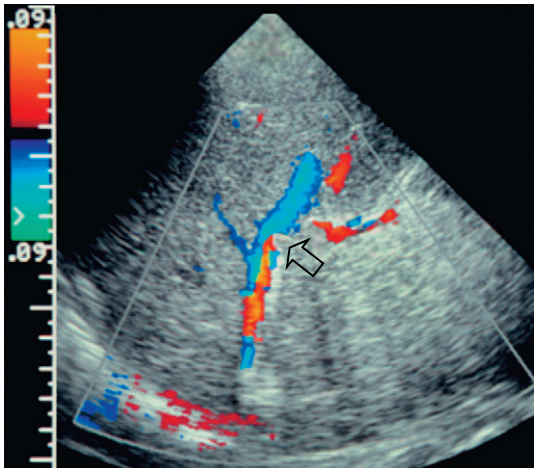

**Fig. 7.42** Oblique view of the right hepatic vein in a patient with renal cell carcinoma metastatic to the liver. A small focus of tumour (arrow) is seen extending from the large echogenic mass in the right lobe into the right hepatic vein. Note distention of the hepatic vein above the tumour thrombus and the turbulent flow with eddy currents beyond the invading tumour.

### *Hepatic veno-occlusive disease*

Non-thrombotic occlusion of small hepatic veins can occur in bone marrow transplant recipients, with alkaloid toxicity or secondary to chemotherapy or radiation therapy. The obstruction of terminal hepatic venules by connective tissue and collagen presents as jaundice, hepatomegaly, pain, ascites and altered liver functions. The associated coagulopathy usually precludes biopsy for diagnosis.[70] Spectral Doppler of the hepatic veins typically shows a normal flow profile. Portal vein flow, however, is typically decreased and may actually reverse.[71] Hepatic artery flow typically shows increased resistance.[72]

### *Altered or increased hepatic vein periodicity*

Near the heart, the normal spectral Doppler tracing of the hepatic vein has a small retrograde component of flow above the baseline, the A-wave. It is relatively small when compared to the antegrade components below the baseline, the S- and D- waves. The ratio of retrograde to antegrade flow decreases during inspiration (which lowers intrathoracic pressure) or when the Doppler sample volume is moved further from the heart (Fig. 7.14). A consistently large component of retrograde flow is an abnormal finding, and if identified, the examiner should consider the presence of cardiac or pulmonary disease (Fig. 7.44). Distortion of the triphasic hepatic vein waveform can occur with many different cardiac disorders including cardiomyopathy, constrictive pericarditis, tamponade, tricuspid or pulmonary valve disease, atrioventricular dissociation, atrial

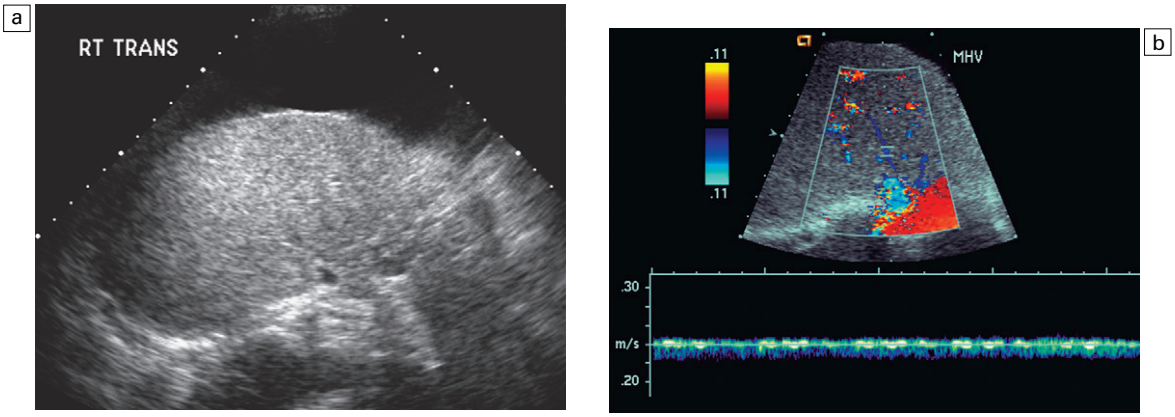


**Fig. 7.43** (a) Transverse image of the liver in a patient with severe cirrhosis. The liver is small, nodular and very echogenic. (b) Spectral Doppler tracing of the middle hepatic within the liver. Patency of the vessel is confirmed by colour Doppler but flow is markedly compromised by compression of this vessel. There is complete absence of periodicity and a relatively slow velocity.

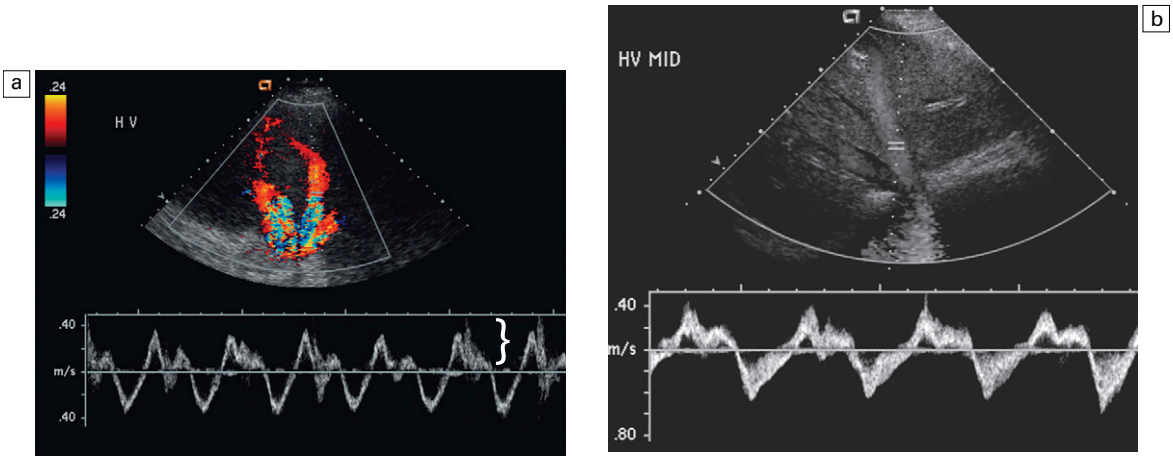


**Fig. 7.44** (a) Transverse spectral and colour Doppler view of the hepatic veins. The hepatic veins are markedly engorged as would be expected with chronic cardiac congestion. Spectral Doppler waveform shows appropriate periodicity within these vessels. The overall amount of retrograde flow, however, is disproportionately large. When summating the area of flow above and below the baseline it becomes apparent that there is relatively little total antegrade flow as would be expected with cardiac congestion. (b) Spectral Doppler tracing in another patient with cardiac congestion. Although periodicity is identified in the tracing it is more disordered than the standard triphasic waveform. Flow away from the heart (above the baseline) is only slightly less than flow towards the heart (below the baseline). This decreased total antegrade flow is a manifestation of cardiac ingestion.

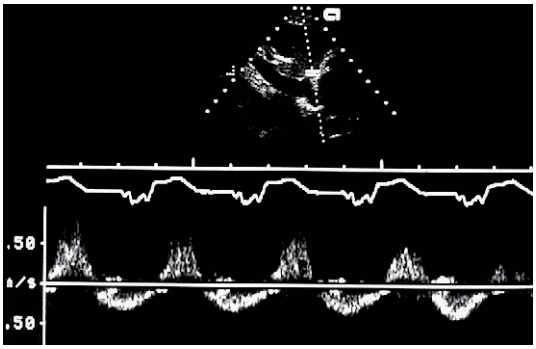


**Fig. 7.45** Spectral Doppler tracing of the hepatic vein obtained concurrently with an ECG tracing in a patient with severe tricuspid regurgitation. Note that the waveform is biphasic. There is a large reversed component of flow but it occurs during the T-wave of the cardiac cycle (during ventricular systole). This is a reversed S-wave, fused with the V-wave. In the absence of an ECG tracing it may be difficult to determine that this is indeed a reversed S-wave. Identifying this large retrograde component of flow and disordered waveform, however, should be enough to channel further workup to a cardiac evaluation.

fibrillation and right ventricular dysfunction. Pulmonary hypertension and massive pulmonary embolism may also distort the hepatic vein waveform.

Specific patterns of hepatic vein velocity profiles have been described in *restrictive cardiomyopathy, pericardial constriction, and tamponade*. A dramatic increase in D-wave amplitude in patients with restrictive cardiomyopathy reflects increased right atrial pressure and rapid early diastolic filling, characteristic of restriction. Reversal of the A-wave is seen in pericardial constriction and tamponade, and represents impaired late diastolic filling of the right ventricle. It is greatest during forced expiration due to the increased intrathoracic pressure transmitted to the pericardium.

*Tricuspid regurgitation* (TR) results in large volumes of blood leaking back through an incompetent or diseased tricuspid valve. In mild TR, the hepatic vein flow profile is characterised by attenuation of the S-wave and a relative increase in V-wave amplitude. In severe TR, systolic

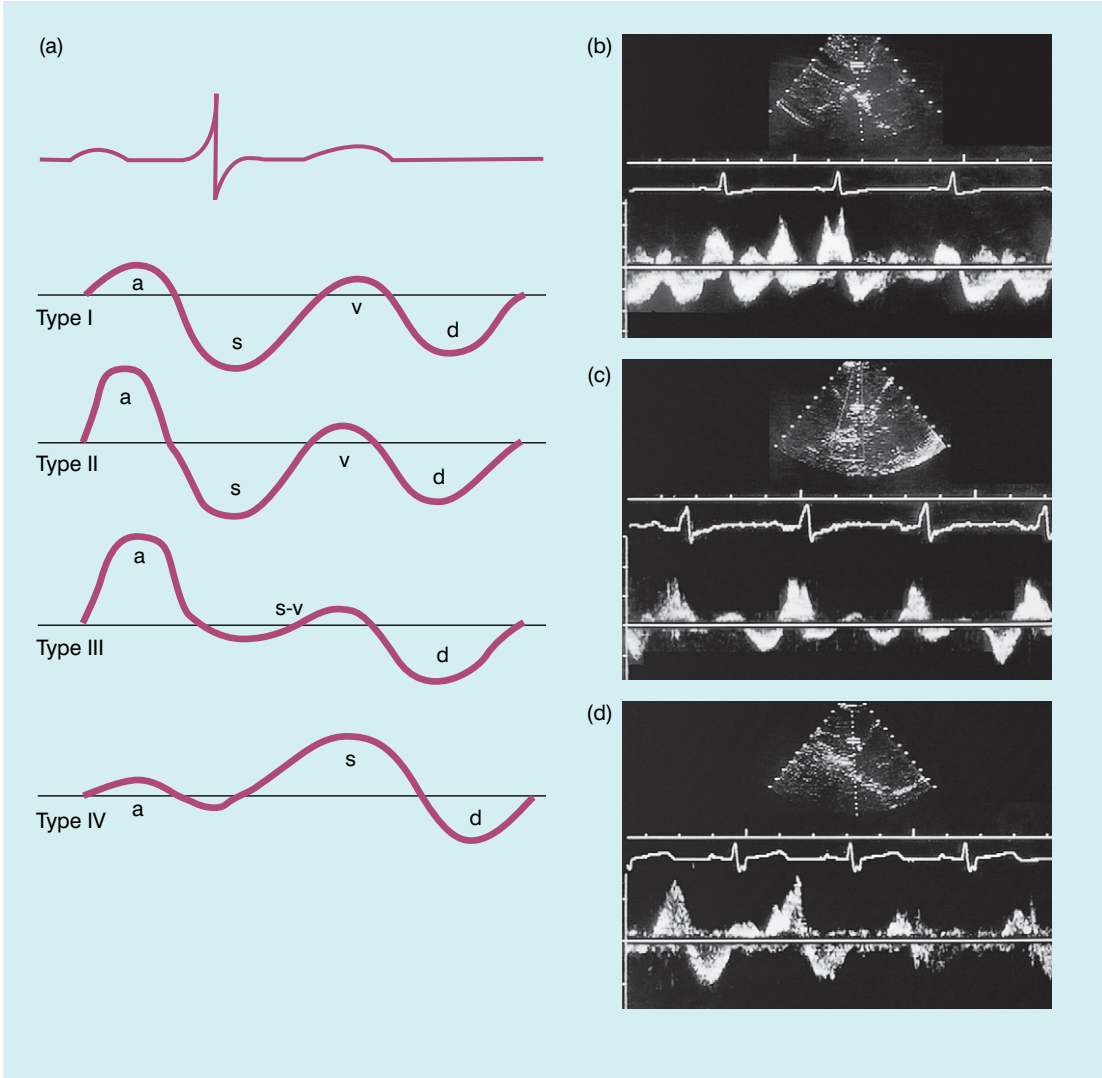


**Fig. 7.46** (a) Hepatic vein flow profiles are characterised into four different types relative to right ventricular dysfunction. With progressively worsening right ventricular dysfunction, the hepatic vein spectral Doppler tracings become more and more distorted. *Type 1*- normal pattern – see Fig. 7.13. The retrograde component of flow (A-wave) follows soon after the P-wave on the ECG tracing. (b) A *type 2* pattern has accentuated A-wave. Greater reversal of flow is secondary to reduced right ventricular compliance and/or increased atrial systolic force. (c) The *type 3* pattern shows an attenuated systolic forward flow (S-wave). This is due to a decrease in the descent of the base of the right ventricle. Also, increased early diastolic flow is seen during the D-wave due to increased early diastolic filling of the right ventricle. Again, note increased A-wave amplitude. (d) *Type 4* pattern is seen with severe right ventricular dysfunction, which is usually accompanied by severe tricuspid insufficiency. Note that the dominant reversed component of flow now occurs well after the QRS. It is not related to the P-wave.

reversal of the S-wave and fusion of the S- and V-waves is seen. Instead of forward flow filling the atrium during atrial diastole, the relatively high ventricular systolic pressure forces blood back through the tricuspid valve into the IVC and the hepatic veins[73] (Fig. 7.45).

In *atrioventricular dissociation*, the atrial and ventricular electromechanical events occur inde-

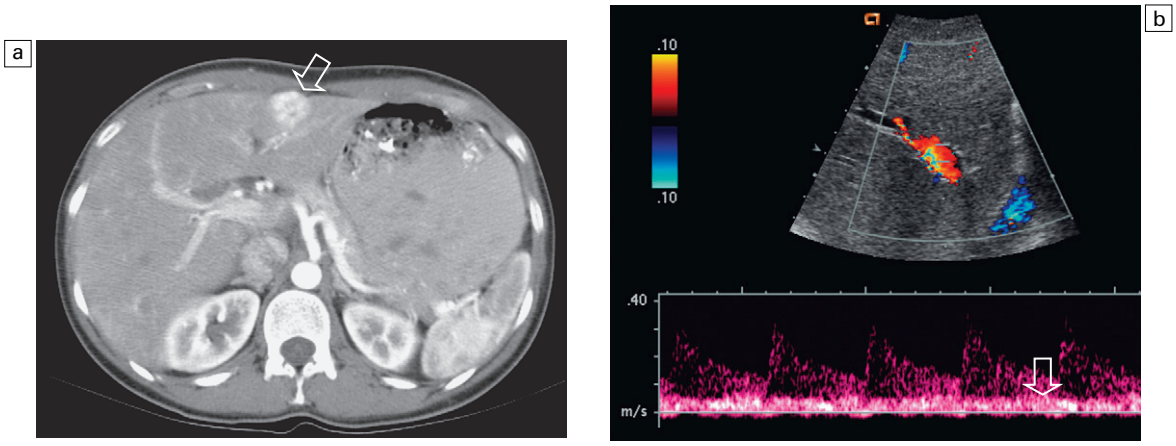


**Fig. 7.47** (a) Contrast enhanced CT scan in a patient with a biopsy proven hepatocellular carcinoma. A brightly enhancing lesion on the early arterial phase is identified in segment 2 (left lobe lateral segment) (arrow). (b) Spectral Doppler tracing of the left hepatic artery and portal vein show changes characteristic of liver disease and neoplasm. Note the relatively high arterial diastolic flow and low resistance. Note, however, the attenuated portal vein inflow (arrow).

pendently of each other. With complete heart block, atrial contraction against the closed tricuspid valve can result in a markedly accentuated A-wave. Clinically, the increased jugular vein pulsations are described as 'cannon' A-waves. The same phenomenon can occur in patients with premature ventricular ectopic beats which follow atrial contraction.

With *atrial arrhythmias*, the A-wave may have a varying relationship to the S-wave due to premature atrial contraction or a variable PR interval as seen in Mobitz I heart block. In atrial flutter, multiple small amplitude A-waves may be present. The lack of organised atrial activity in atrial fibrillation leads to the loss of distinct A-waves in the hepatic vein tracing.

In patients with moderate to severe *right ventricular (RV) dysfunction*, hepatic vein Doppler flow profiles fall into three basic patterns. The first Doppler indication of RV dysfunction is accentuation of the atrial A-wave, due to reduced RV compliance which cannot accommodate all of the right atrial output. Further deterioration of RV function results in attenuated systolic forward flow (S-wave) due to a decrease in the descent of the base of the right ventricle. There is increased early diastolic forward flow (D-wave), because of increased early diastolic filling of the right ventricle and increased A-wave amplitude. Patients with severe RV dysfunction usually have associated tricuspid insufficiency. This results in S-wave reversal. S-wave amplitude changes may also reflect reduced right atrial compliance, reduced RV systolic function or tricuspid insufficiency. A-wave amplitude changes indicate reduced RV compliance or increased right atrial inotropy (Fig. 7.46).

### *Arterialised hepatic vein flow*

An arterial waveform within the hepatic veins is an extremely rare finding. It may be seen with a fistula from the hepatic artery to the hepatic vein following biopsy or surgery. Rarely, erosion of an hepatic artery aneurysm into the hepatic vein will produce arterial pulsations in the veins.

## Focal liver lesions – malignant

### *Hepatocellular carcinoma*

HCC is the most common primary malignant neoplasm of the liver. It most frequently occurs in patients with underlying chronic liver disease, such as hepatitis B infection, and less commonly with alcoholic cirrhosis. US imaging is relatively poor for the detection of HCC with a sensitivity of only 50% for the sonographic identification of malignancy in cirrhotic livers.[74] The

distorted echo-texture of the liver parenchyma, together with the tumour's variable sonographic appearance, makes it difficult to distinguish the neoplasm.

HCC is typically a hypervascular neoplasm and several authors have promoted the use of spectral and colour Doppler in helping to diagnose HCC.[75,76] The tumour typically shows abundant neovascularity, resulting in decreased vascular impedence and resistance. Arterioportal venous shunting also occurs through the tumour.[77] Therefore the Doppler waveform in these tumours typically manifests increased diastolic flow with a low resistance flow profile (Fig. 7.47). A basket pattern of flow within the lesion on colour Doppler has been described as characteristic for HCC;[76] the internal branching vessels within the tumour, combined with the network of surrounding vessels being responsible for this appearance. However, similar findings occur in other conditions. A low RI, high velocity flow with systolic frequency shifts approximating 3 m $s^{-1}$ may be seen in the main hepatic artery but metastases to the liver, especially from hypervascular primaries, can manifest similar changes in the hepatic artery flow profile.

Peripheral portal vein flow alteration has been suggested by some investigators to be valuable in differentiating benign from malignant lesions. Hepatofugal flow can be perceived on spectral and colour Doppler in proximity to HCC or metastatic disease. However, Miller et al[78] showed that this kind of flow profile can also be identified in proximity to large haemangiomas, subcapsular haematomas, and other benign conditions. Therefore, this finding cannot alter the standard differential diagnosis based on grey-scale findings.

Low sensitivity and specificity unfortunately limits the value of US imaging and Doppler in diagnosing HCC. Biphasic CT is now considered the most accurate tool for the early detection of HCC, where a brightly enhancing hepatic lesion during the arterial phase of contrast injection is considered HCC until proven otherwise.

### *Metastases*

Metastatic liver lesions occur with a frequency approximately 20 times greater than primary hepatic neoplasms. Their sonographic appearances are markedly variable, but these do not correlate with cell type. One of the more frequently occurring appearances is that of the target pattern or halo sign. The hypoechoic rim surrounding the lesion is caused by compressed liver parenchyma, or by proliferating tumour at the edge of the lesion.

Colour Doppler may reveal displacement of normal liver vasculature by the expanding metastatic lesion. Little if any flow is usually seen in the metastasis itself. Spectral Doppler can reveal low resistance, high velocity flow in the hepatic artery (Fig. 7.33c). However, this is not consistent enough to be of value in characterising an unknown lesion. If metastasis is suspect, this change in the hepatic artery spectral Doppler waveform can be considered strongly suggestive, but it does not obviate the need for biopsy. Power Doppler imaging can assess vascularity in the majority of small liver nodules, but the pattern distribution of tumoral vascular signals does not provide reliable differential diagnostic criteria.[79]

## Focal liver lesions – benign

### *Hepatic steatosis (fatty liver)*

In response to hepatocellular disease, the liver can accumulate triglycerides within the hepatocytes. This reversible cellular response may be seen with obesity, alcoholic liver disease, diabetes, parenteral nutrition, and numerous other disorders.[80] Ultrasound commonly reveals a bright echogenic liver with poor through transmission. The central vasculature is often poorly visualised due to compression of these vessels by surrounding fat-laden parenchyma. It is well known that fatty infiltration can be patchy and irregular. Occasionally the appearance can be nodular, but most often it is non-spherical in shape with geometric margins or wedge shaped segmental distribution. Doppler ultrasound typically shows no change in the hepatic haemodynamics, or distribution of vessels. Hepatic artery and portal vein velocities maintain a normal ratio. This is in contrast to malignancy which usually shows an increased hepatic arterial velocity. Absence of this velocity alteration may be helpful in further

reinforcing the impression of benign fatty infiltration in cases where the imaging appearance is confusing (Fig. 7.34). If significant doubt exists, CT, MR scintigraphy, or biopsy may be necessary to clinch the diagnosis.[81,82]

### *Haemangiomas*

These are the most common solid benign neoplasms of the liver. They are hyperechoic when small (<3 cm), but the echogenicity of larger haemangiomas can be variable. Colour Doppler adds little to the diagnosis of haemangioma as the flow is typically too slow to register, even at the most sensitive settings. Flow may be demonstrated occasionally with power Doppler (Fig. 7.48). Unfortunately, this may only serve to confuse the diagnosis, as the classic teaching is that flow in haemangiomas is imperceptible. In common with other benign masses, there is rarely any alteration to the hepatic arterial inflow on spectral Doppler. Further evaluation with scintigraphy, or MR, may be necessary to clinch the diagnosis.

### *Focal nodular hyperplasia*

Focal nodular hyperplasia (FNH) is a relatively rare hepatic lesion typically seen in young to middle-aged women. It is believed to be hormone dependent and not premalignant. Ultrasound often reveals a solitary, small lesion (<3 cm), often at the periphery of the liver. The echogenicity is varied with hypo-, hyper-, and isoechoic FNH reported with equal frequency. A central scar has been reported as a dominant feature of FNH, however, it is seldom seen sonographically but, even if seen, it does not help clinch a benign diagnosis since fibrolamellar HCC often also has a central scar. FNH is typically hypervascular with a prominent central artery and radiating branches in a stellate or spoke wheel configuration with centrifugal flow; this is a unique characteristic of this lesion (Fig. 7.49). If doubt still exists in the diagnosis then a technetium 99 sulfur colloid study should be performed as the presence of Kupffer cells within the lesion can successfully differentiate FNH from other pathology.[83–85]

### *Adenoma*

Hepatic adenoma, a rare benign liver tumour, is being seen with increasing frequency. In females it is related to oral contraceptive use, in males to anabolic steroids.[86] Adenomas appear as solid masses with variable echogenicity due to differences

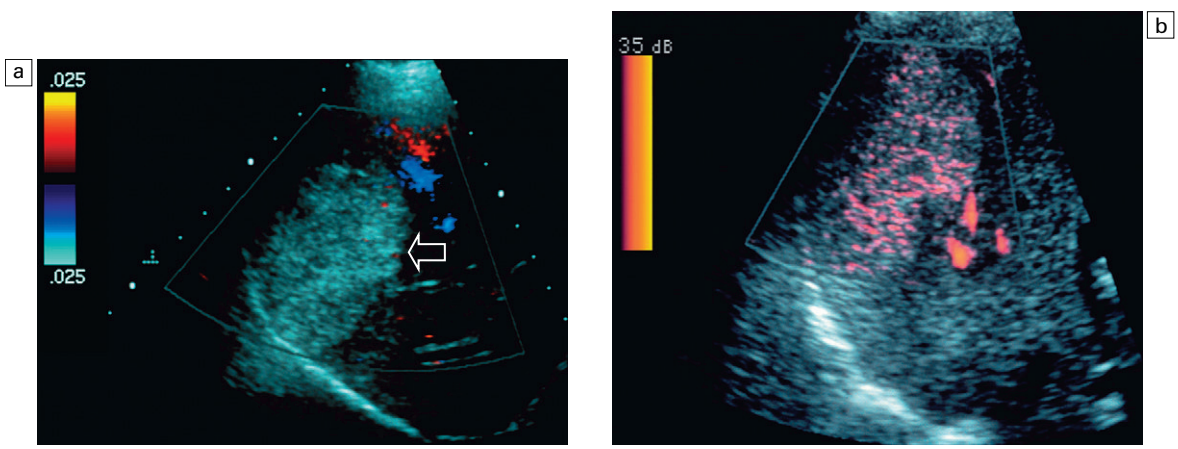


**Fig. 7.48** (a) Transverse colour Doppler image of the right lobe of the liver. A large echogenic mass is easily identified (arrow). No flow is perceived with the mass by colour Doppler despite settings at the most sensitive level. (b) Power Doppler image of this lesion shows a leaf like pattern of signal within the mass. This is most likely an artifact based on motion discrimination. With power Doppler artifact tends to occur within the pixels of high intensity reflection. Biopsy did confirm this lesion to be a haemangioma.

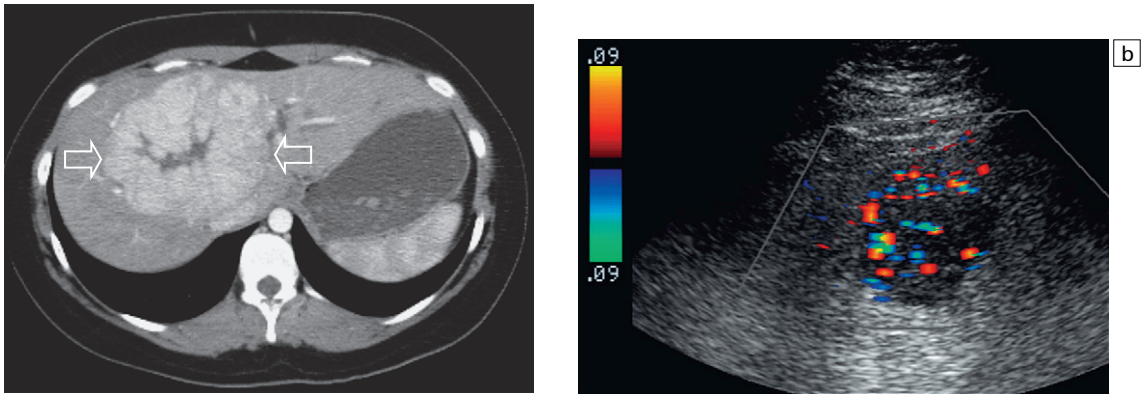


**Fig. 7.49** (a) Arterial phase of a contrast enhanced CT scan through the upper liver. A briskly enhancing round mass with a central scar is clearly evident (arrows). (b) Colour Doppler through the lesion shows it should be hypervascular. Biopsy confirmed this lesion to be focal nodular hyperplasia.

in fat content or haemorrhage. Doppler has not shown utility in their differentiation from other liver masses.

### *Infantile haemangioendothelioma*

Infantile haemangioendothelioma is a rare liver tumour of infancy. It commonly presents as multiple lesions scattered throughout the liver with areas of infarction, haemorrhage and occasionally calcification. The tumour is composed of anastomosing vascular channels lined by one or more layers of endothelial cells. The incidence of congestive heart failure is high because of arterial venous (AV) shunting within the masses. It is considered a benign tumour and most gradually regress after presentation. Some children, however, succumb to the congestive heart failure associated with the high degree of AV shunting. The ultrasound appearance of these lesions usually shows mixed or variable echogenicity. Large feeding arteries and draining veins (Fig. 7.50) can be perceived by colour Doppler with turbulent flow noted on spectral Doppler.[87–89]

## MONITORING TREATMENT OF LIVER DISEASE

### Surgical portosystemic shunts

Numerous variants of surgical shunting have been devised over the years including mesocaval, distal splenorenal (Warren shunt), proximal splenorenal, portocaval, and mesoatrial shunts.[90] As with any surgical anastomosis, stenosis and eventual thrombosis may develop. Imaging of shunt integrity by Doppler ultrasound is sensitive, but because the shunt is usually retroperitoneal in location it can be extremely difficult to visualise. It is mandatory that the sonographer knows the exact type and location of the shunt in order to focus the examination in the correct region. Brisk hepatofugal flow in the main portal vein is a secondary finding that indicates shunt patency, but the definitive diagnosis is made by direct visualisation of the shunt with colour Doppler[91] (Fig. 7.51).

### Transjugular intrahepatic portosystemic shunts

Treatment of portal hypertension and variceal bleeding by interventional diversion of portal flow as an alternative to surgery or sclerotherapy was first proposed in 1969.[92] Transjugular intrahepatic portosystemic shunt (TIPS) placement involves the percutaneous creation of a link between the high-pressure portal system of a cirrhotic patient and the low-pressure hepatic veins. A transparenchymal track is created between the hepatic vein and the portal vein, which is dilated and a stent then inserted to maintain patency. Although the TIPS is most often placed between the right hepatic vein and the right branch of the portal vein, a left hepatic vein to left portal vein

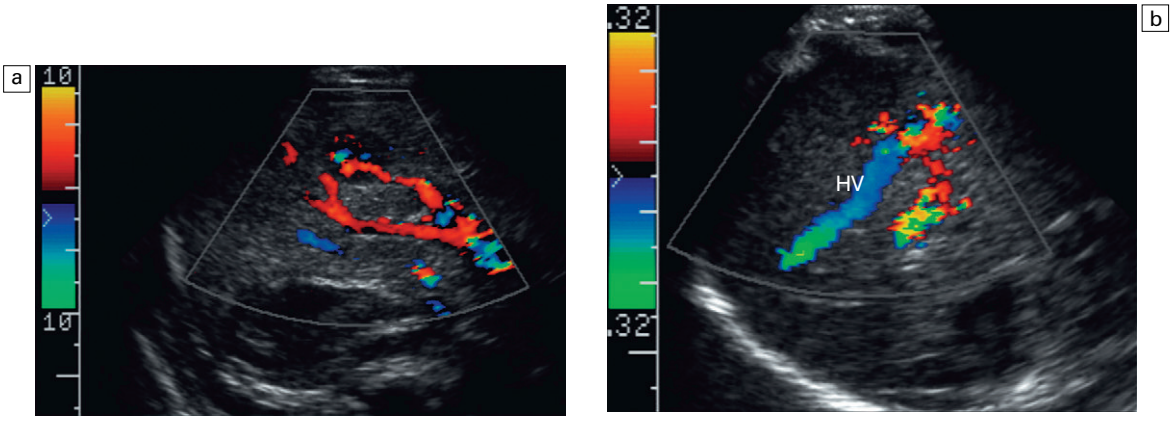


**Fig. 7.50** (a) Oblique colour Doppler image of the right lobe of the liver. A large feeding artery is identified with flow going into a tangled vascular malformation. (b) From this lesion flow is seen draining into a large hepatic vein. Infantile haemangioendothelioma was confirmed at autopsy.

route may be selected for technical or anatomic reasons.

### *Preprocedural assessment*

Imaging evaluation should be performed before TIPS placement to estimate liver size, evaluate for the presence of tumour, confirm patency of the portal vein and hepatic veins, rule out thrombosis, measure vessel size and search for the presence of portosystemic varices. This is best accomplished with CT angiography. Preprocedural Doppler assessment allows a comparative appreciation of the results of the procedure; specifically changes in haemodynamics, spleen size and the amount of ascites. The varices (especially left gastric and recanalised paraumbilical) should be identified prior to the procedure so that they may be occluded by coil placement.

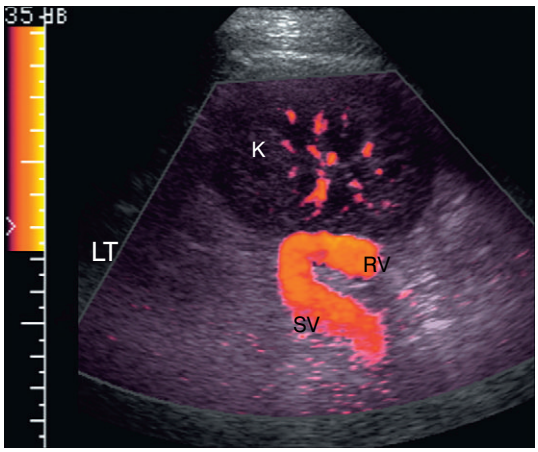


**Fig. 7.51** Oblique longitudinal view of the left flank focused at the upper pole of the left kidney. The candy cane shaped large vessel is identified. The upper portion represents the splenic vein with flow coursing towards the transducer. It has been hooked in surgically to the renal vein. The patient is status postsplenectomy anastomosis of the distal splenic vein to the renal vein. The anastomosis is widely patent with flow confirmed by Doppler.

### *Postprocedural assessment*

Unfortunately, TIPS complications are very common, the most significant being progressive narrowing with eventual thrombosis and occlusion. Clinical monitoring of TIPS function is insensitive. By the time compromise becomes clinically evident, the TIPS is usually occluded. The best way to monitor a TIPS is with Doppler sonography and scanning at regular intervals should be considered mandatory. Prompt identification of a stenosis with timely intervention may prevent progression to thrombosis. A recently thrombosed TIPS may be recanalised successfully, but if the clot is allowed to mature then treatment usually requires placement of a second TIPS.

Routine Doppler monitoring after shunt placement should be considered mandatory as it is an excellent non-invasive modality for sequential monitoring of TIPS patency. An evaluation of

the TIPS should be performed within 24 h after its creation to confirm patency and establish baseline flow directions and velocities. Subsequent evaluation is conducted just prior to discharge of the patient and then periodically thereafter; the frequency varies among centres, but most re-examine the shunt at approximately 3 month intervals.

Optimum scanning parameters and normal US findings following TIPS have been described by a number of investigators.[93–97] Transducers of 2.25–3.5 MHz are usually necessary because of the frequently increased echogenicity and sound attenuating features of the cirrhotic liver, along with the fact that the shunt is usually fairly deep within the body. The Doppler gain should be set as high as possible, without encountering noise. The transducer is focused at the level of the shunt or vessel of interest; the sample volume is placed in the centre with an angle of insonation less than 60° when feasible. This may be difficult to accomplish, especially in the middle segment of the shunt, where the direction of flow frequently runs perpendicular to the insonating beam. The pulse repetition frequency is set as low as possible, but avoiding aliasing. Optimising the scanning parameters will help minimise the chances of making a false positive diagnosis of shunt thrombosis.[93,97]

### *Normal findings*

A complete TIPS evaluation includes a survey of the abdomen to quantify ascites. The radiologist should also look for intrahepatic, perihepatic or subcapsular haematomas; intraperitoneal bleeding (as indicated by increased volume or echogenicity of the ascites); biliary obstruction; and echogenic contents in the common bile duct or gallbladder that suggest haemobilia.[95,98] The shunt is then located between the right portal vein and right hepatic vein. The stent is highly echogenic and appears as two parallel, curvilinear lines, usually uniform in diameter in the parenchyma but slightly flared at the portal and hepatic venous ends (Fig. 7.52). The shunt diameter is easily measured[96] but a curved TIPS that passes obliquely through the plane of insonation may appear artificially narrowed.[95] The stent should extend from within the portal vein, across the parenchyma, and into the hepatic vein. Imaging sometimes reveals malposition of the stent as a result of inappropriate deployment, or subsequent

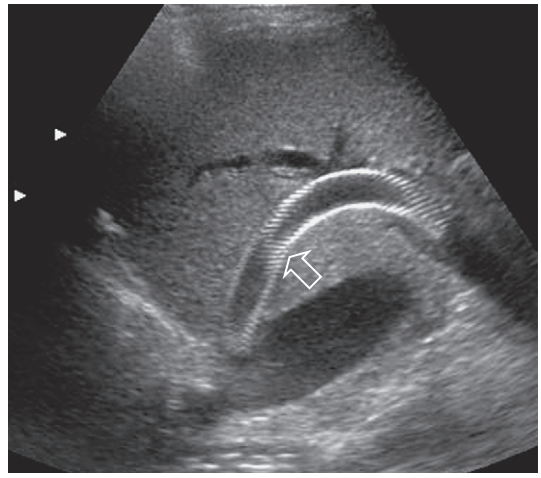

**Fig. 7.52** Grey-scale longitudinal image of the right lobe of the liver. The TIPS catheter is seen coursing from the porta hepatis region to the junction of the right hepatic vein with the inferior vena cava (arrow). This long shunt is composed of two stent elements. Note the subtle narrowing at the mid-shunt where the two stent elements overlap. The mesh like appearance of the shunt is due to the echo reflection off the individual wire elements of the stents.

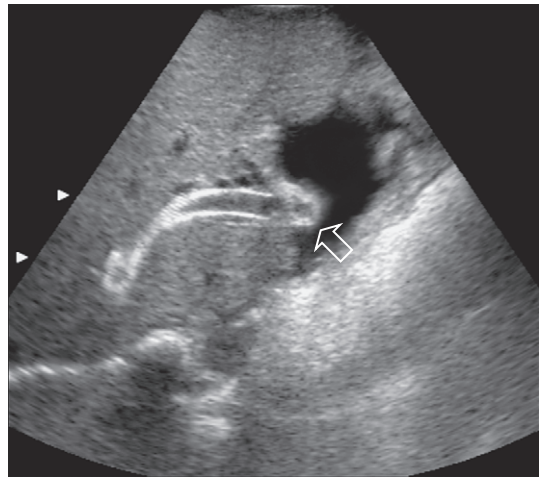

**Fig. 7.53** Transverse view of the TIPS at its junction at the inferior vena cava. The opening of the stent is seen projecting into the right atrium (arrow).

migration down into the portal vein, or up into the hepatic vein and right atrium (Fig. 7.53).

Flow within the stent is then evaluated by Doppler ultrasound. The presence of blood flow is easily confirmed, as the entire shunt lumen fills with colour due to the relatively fast, turbulent flow (Fig. 7.54). Assuming a right portal to right hepatic vein TIPS, the velocity, flow direction and waveform are then checked at the portal vein end, mid-shunt and hepatic vein end. The main portal vein and the left portal vein are assessed and the right hepatic vein is checked both proximal to and just beyond its junction with the stent (Fig. 7.55). Spectral Doppler evaluation should verify that the direction of flow in the shunt is from the portal vein to the hepatic vein. Flow through the normal shunt is non-pulsatile, but flow in a widely patent shunt may show periodicity throughout the shunt due to right atrial pressure changes being transmitted back through the shunt, against the direction of flow (Fig. 7.56). Periodicity is most prominent near the hepatic venous end.[97] In one study, half of the patients with patent TIPS demonstrated some periodicity at the hepatic venous end of the shunt, while the other half had high-velocity turbulent flow.[96] Periodicity may be accentuated within the shunt in patients with tricuspid valve disease or congestive heart failure.[93]

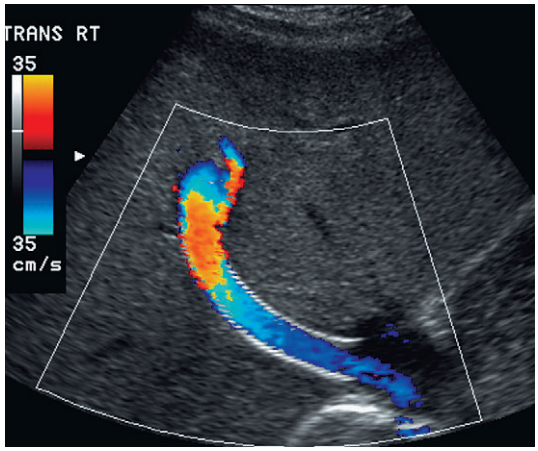


**Fig. 7.54** Oblique colour Doppler image of the TIPS. The entire lumen is saturated with colour indicating patency. Note the non-uniformity of colour encoding – a function of narrowing at the area of stent overlap.

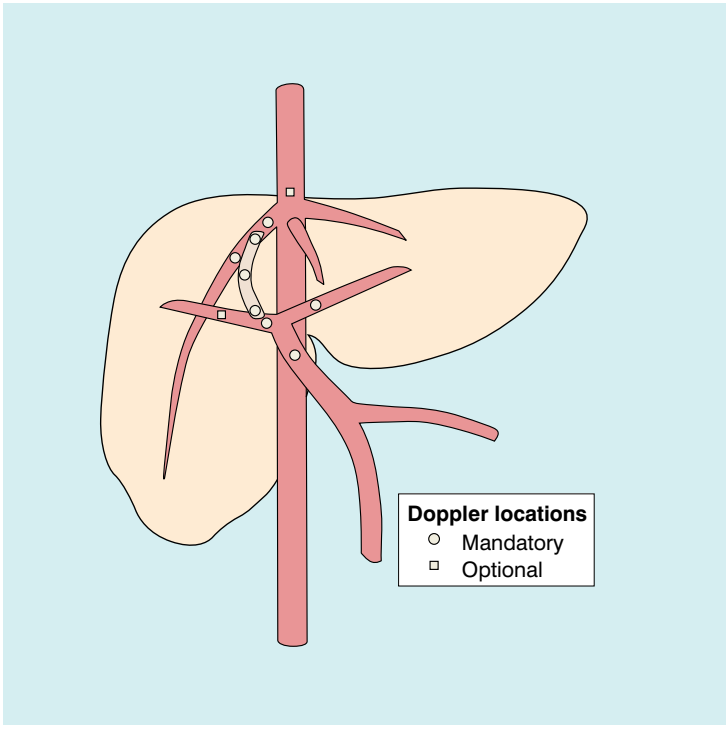


**Fig. 7.55** Illustration of the TIPS and its related vasculature in the standard right hepatic vein to right portal vein configuration. Blue circles indicate those points at which a Doppler tracing should be obtained in a complete TIPS ultrasound evaluation. Figure courtesy of Gerald Mulligan, MD.

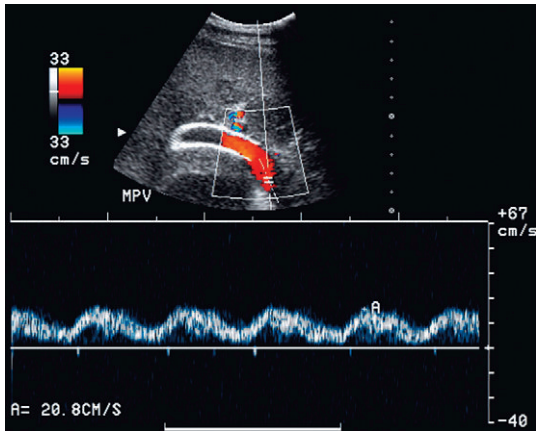


**Fig. 7.56** Doppler tracing obtained at the portal vein end of the TIPS. Note the marked periodicity of flow within the TIPS. The waveform is that commonly seen in hepatic veins and inferior vena cava. Identification of this degree of periodicity at the portal vein and of the stent is a confident indicator of a widely patent shunt.

Flow velocities in the shunt vary widely, ranging from approximately 50 to 270 cm $s^{-1}$.[94,96,97] Velocities can also be quite variable through the shunt itself, usually increasing from the portal venous end to the hepatic venous end of the shunt. The mean velocity of patent shunts has been reported as 95 cm $s^{-1}$ in the shunt near the portal venous end[93] and 120 cm $s^{-1}$ in the middle segment of the shunt.[94] Flow across the shunt is usually quite turbulent, especially when multiple stent components are used, when overriding stents can cause a relative narrowing of the shunt lumen. Normal velocities in the main portal vein are variable. Following TIPS insertion, the mean portal vein velocity has been reported to increase from 7 cm $s^{-1}$ to 24 cm $s^{-1}$ in one study[96] and from 20 cm $s^{-1}$ to 38.4 cm $s^{-1}$ in another.[97] Hepatic arterial flow has also been shown to increase after TIPS, presumably because the shunt diverts the portal venous inflow away from the liver.[95]

In a properly functioning TIPS, flow direction in the portal system is towards the portal vein end of the stent. Therefore, flow in the main portal vein is hepatopetal and its velocity is typically quite brisk (between 20 and 50 cm $s^{-1}$). It must be kept in mind that velocities measured in the stent-bearing portion of the portal vein represent flow in the portal vein, not in the shunt.[95] Flow in the left and right portal veins usually becomes hepatofugal, flowing out of the diseased liver and towards the inflow of the shunt[93] (Fig. 7.57). Depending on the diameter of the shunt and the severity of the liver disease, however, flow may continue to be hepatopetal into the parenchyma. If the patient has patent paraumbilical vein collaterals, these will continue to shunt blood away from the liver. Flow in the left portal vein, therefore, continues in a hepatopetal direction despite normal TIPS function. If portal branch flow changes direction over time from hepatofugal to hepatopetal, a significant flow-limiting lesion is assumed to be present in the TIPS.

The Doppler data are recorded and maintained in a table format for follow-up (Fig. 7.58). Serial documentation provides the best means of identifying any variations in velocity and/or flow direction over time and these changes are the best early indicator of shunt compromise.

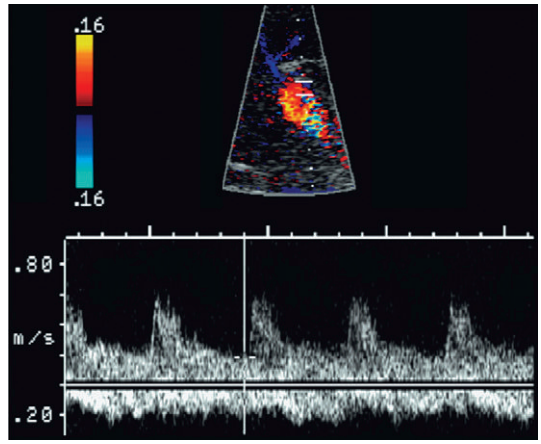


**Fig. 7.57** Combined spectral Doppler tracing of the left branch of the portal vein and hepatic artery in a patient with an appropriately functioning TIPS. The sample volume is opened wide in position so that both vessels are interrogated in the same tracing. Note flow in the hepatic artery is towards the transducer, therefore into the left lobe of the liver. The left portal vein flow, however, is away from the transducer, therefore hepatofugal and towards the inflow of the shunt.

Name: ID:

| | VELOCITIES | | | | DIRECTIONS | | |
|---|---|---|---|---|---|---|---|
| Date | PV End | Mid | HV End | Main PV | Lt PV | HV ↑ TIPS | Comments |
| | | | | | | | |
| | | | | | | | |

**Fig. 7.58** TIPS data sheet. Each patient receiving a TIPS should have a data sheet maintained with velocities and flow directions documented at each visit. Progressive compromise of the TIPS can then be more easily diagnosed as progressive changes in velocities or a change in direction flow become manifest. Velocity measurement in the mid-TIPS tends to be the most erratic. A persistent decrease in main portal vein velocity over the sequence of studies is the most definitive indicator of progressive shunt compromise.

### *Shunt stenosis*

The two most common causes of TIPS compromise are *neointimal hyperplasia* throughout the shunt, or a focal stenosis at the hepatic vein end. Most TIPS will have some degree of neointimal hyperplasia, but this may progress to the point where it limits flow through the TIPS. At the point of maximum stenosis within the TIPS, a high-velocity jet may be perceived by Doppler (Fig. 7.59). Other components of the TIPS and the portal system, however, will show decreased velocities. With sufficient compromise, flow in the branch portal veins becomes hepatopetal and flow in the main portal vein may become hepatofugal.

Focal *hepatic vein stenosis* can occur where the proximal end of the TIPS abuts the hepatic vein. Focal irritation of the vein wall by the stent wires may cause a bar of granulation tissue to build up. This results in decreasing velocities throughout the shunt.[95] A key Doppler finding of this focal stenosis is the presence of poststenotic flow disturbances with a high-velocity jet and turbulence in the hepatic vein or IVC[99] (Fig. 7.60). The sonologist must therefore evaluate flow beyond the end of the stent, sometimes even as far as the right atrium. Flow in all three hepatic veins is normally towards the heart but a stenosis at the junction of the TIPS and the hepatic vein can cause flow compromise peripherally in the vein with damping of periodicity, or segmental flow reversal (Fig. 7.61).

Several investigators have attempted to determine flow velocities which define the presence of TIPS stenosis[93-95,100] but reported findings have varied considerably. In one study, a velocity <50 cm $s^{-1}$ at the portal venous end was 100% sensitive and 93% specific.[93] In another study, a velocity <50 cm $s^{-1}$ in the middle segment of the TIPS was 78% sensitive and 99% specific, with a positive predictive value of 96%, negative predictive value of 91% and accuracy of 92%.[94] [When these investigators used a velocity <60 cm $s^{-1}$ as the criterion, sensitivity increased to 84% but specificity dropped to 89% and accuracy to 87%. At <70 cm $s^{-1}$, sensitivity was 89% but specificity was 83% and accuracy was 85%. In another study, a velocity of 90 cm $s^{-1}$ was applied, but the sensitivity was only 87.5% with specificity of 95%.][101] These varied findings underscore the fact that flow velocities vary widely from patient to patient and that the best method for TIPS evaluation is to use individual patient baseline velocities obtained soon after TIPS placement.[102] A change in velocity of ± 50 cm $s^{-1}$ from baseline has been proposed as the threshold value for predicting haemodynamically significant shunt compromise.[74] It becomes obvious with this spectrum of reports that there is controversy regarding the accuracy of Doppler ultrasound for the detection of TIPS malfunction, nevertheless it is the best non-invasive means for following TIPS.[103]

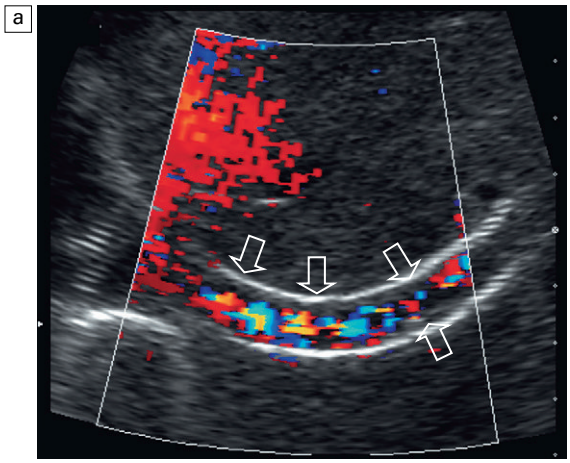


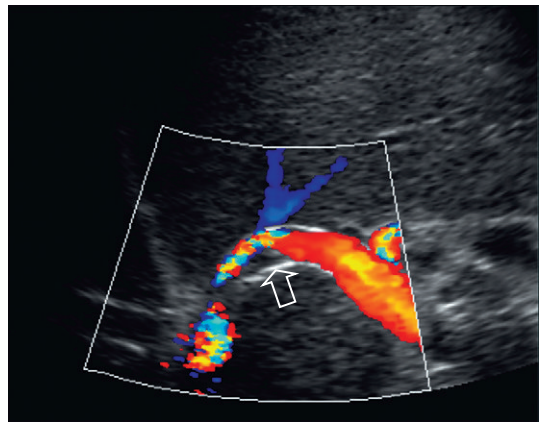


**Fig. 7.59** (a) Oblique colour Doppler image along the length of the TIPS shunt. Turbulent flow is seen across this shunt. Note the absence of flow along the shunt wall (arrows) indicating neointimal hyperplasia along almost the entire length of the TIPS. (b) Flow is seen along the length of the TIPS. At the portal vein it is relatively uniform. At the mid-TIPS there is narrowing and turbulence with the focus of neointimal hyperplasia compromising the lumen. (c) Spectral Doppler tracing at the mid-TIPS shows turbulent flow at the high velocity of greater than 2.5 m $s^{-1}$, well above the accepted normal upper limit of 1.2 m $s^{-1}$ for the mid-TIPS.

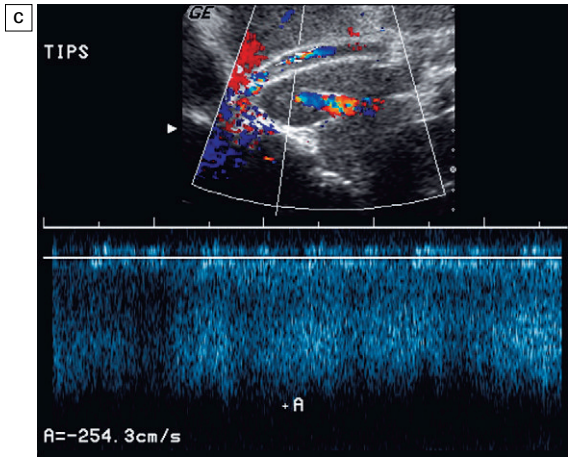


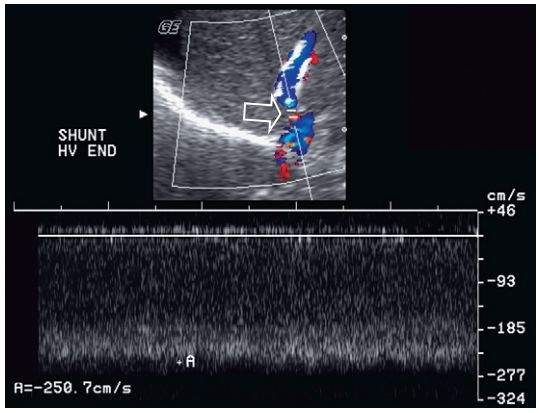


**Fig. 7.60** Spectral and colour Doppler image at the hepatic vein end of the TIPS catheter. Note on the colour image that the catheter ends well short of the inferior vena cava. The diameter of the hepatic vein above the TIPS is relatively narrow (arrow). The spectral Doppler tracing shows a velocity of 2.5 m $s^{-1}$. This high velocity jet is due to the focal stenosis due to the hypertrophy bar of tissue.

If there is significant flow compromise through the TIPS, main portal vein velocity decreases. Flow in the left portal vein may change back to a hepatopetal direction (Fig. 7.62), representing a reversion to pre-TIPS haemodynamics (Table 7.4).[95,97,99]

**Table 7.4** Criteria for compromised TIPS function

- Shunt velocity of <50 cm $s^{-1}$
- Increase or decrease in shunt velocity of >50 cm $s^{-1}$ compared with initial postprocedure value
- Focal region of increased velocity in the shunt or hepatic vein
- Hepatopetal flow in left and right portal vein branches
- Hepatofugal flow in main portal vein

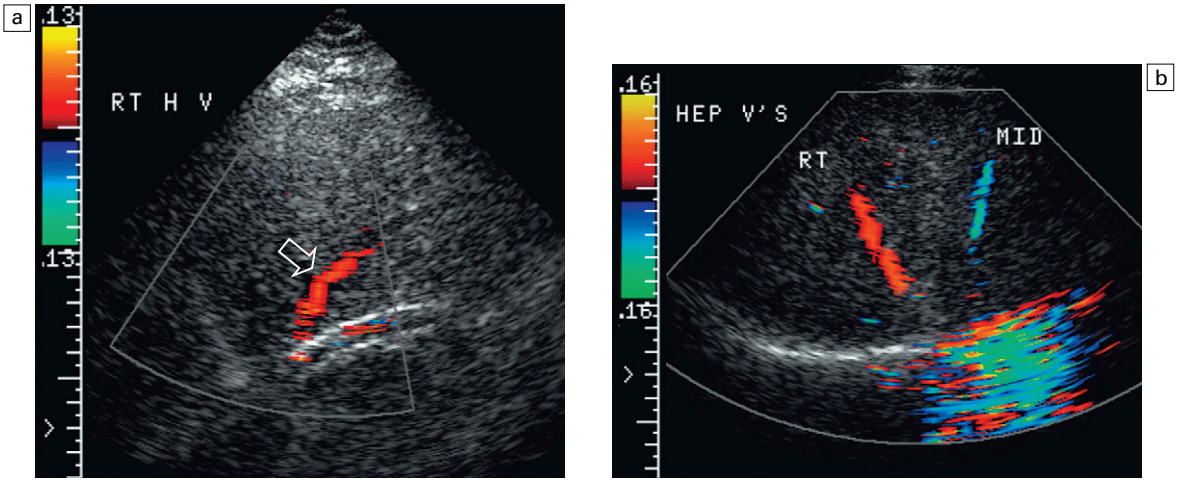


**Fig. 7.61** (a) Longitudinal colour Doppler image including the right hepatic vein and TIPS shunt. Note the poor colour saturation of the TIPS indicating poor flow. Colour signal from the right hepatic vein shows flow coursing through the transducer, which is away from the inferior vena cava. This is a result of focal stenosis at the hepatic vein junction with the TIPS shunt. (b) Transverse image of the same patient as in Figure (a). Flow in the right hepatic vein is indeed coursing away from the heart. It collateralises to the mid-hepatic vein which shows the appropriate flow direction back towards the IVC.

### *Shunt occlusion*

If no flow can be detected in the shunt and flow velocity and direction in the portal vein is the same as it was prior to TIPS placement, shunt occlusion must be considered. The absence of flow by colour or power Doppler within the TIPS is a highly specific indicator of shunt thrombosis (Fig. 7.63).[92,93] However, before concluding that the stent is occluded, meticulous scanning for slow flow should be performed, since flow velocity may be extremely low in a shunt that is

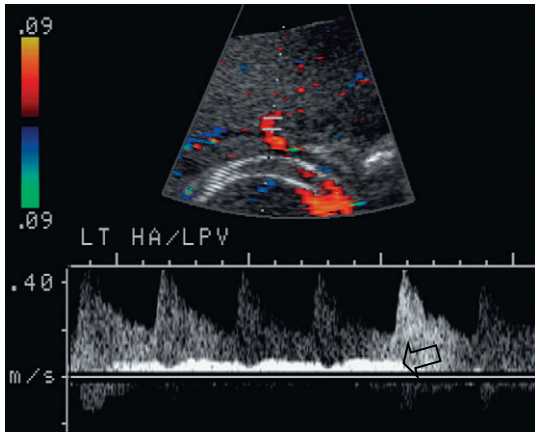


**Fig. 7.62** Spectral Doppler tracing of the left hepatic artery and portal vein including a portion of the TIPS catheter. Absence of colour signal with the shunt indicates TIPS thrombosis. This is further confirmed by the direction of flow in the left portal vein which is hepatopetal. This is in contrast to the normal left portal vein hepatic artery flow direction as illustrated in Figure 7.57.

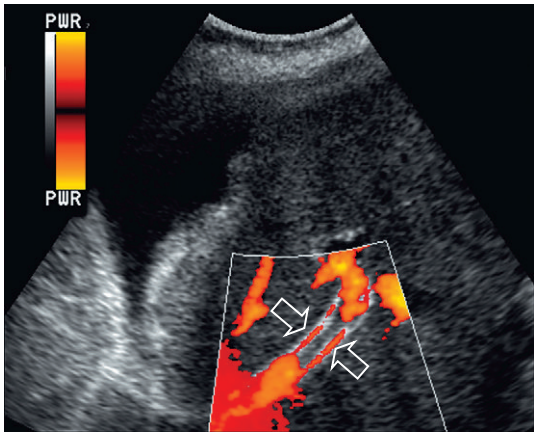


**Fig. 7.63** Power Doppler image of the TIPS catheter. Absence of colour signal within the mid-shunt indicates complete TIPS thrombosis. Note the colour artefact from the stent wires, not to be confused with flow along the wall.

highly stenosed but still patent. Colour Doppler settings (including pulse repetition frequency, gain and filtration) need to be optimised to differentiate true occlusion from very slow flow. A properly functioning TIPS, however, is not a low-flow system, so misinterpretation of thrombosis for technical reasons is rarely a problem. Identifying low flow, however, has the same implication as occlusion, and that is the need for TIPS revision. Indeed, repeat interventions are the key to long-term success of TIPS.[104]

## REFERENCES

1. Beissert M, Delorme S, Mutze S, et al. Comparison of B-mode and conventional colour/power Doppler ultrasound, contrast-enhanced Doppler ultrasound and spiral CT in the diagnosis of focal lesions of the liver: results of a multicentre study. Ultraschall Med 2002; 23(4):245–250.
2. Rao BK. Colour flow Doppler sonography of the abdomen. Curr Opin Radiol 1991; 3:225–229.
3. Czembirek H. Value of abdominal pulsed duplex sonography. Radiologe 1987; 27:98–105.
4. Mostbeck G, Mallek R, Gebauer A, et al. Duplex ultrasound and colour-coded Doppler ultrasound of visceral blood vessels in abdominal diseases. Wien Klin Wochenschr 1992; 4:227–233.
5. Grant EG, Schiller VL, Millener P, et al. Colour Doppler imaging of the hepatic vasculature. AJR Am J Roentgenol 1992; 159:943–950.
6. Kruskal JB, Newman PA, Sammons LG, et al. Optimizing Doppler and colour flow US: application to hepatic sonography. Radiographics 2004; 24(3):657–675.
7. Ralls PW. Colour Doppler sonography of the hepatic artery and portal venous system. AJR Am J Roentgenol 1990; 155:517–525.
8. Iwao T, Toyonaga A, Oho K, et al. Value of Doppler ultrasound parameters of portal vein and hepatic artery in the diagnosis of cirrhosis and portal hypertension. Am J Gastroenterol 1997; 92:1012–1017.
9. Harada A, Nonami T, Kasai Y, et al. Systemic haemodynamics in non-cirrhotic portal hypertension – a clinical study of 19 patients. Jpn J Surg 1988; 18:620–625.
10. Grant EG, Tessler FN, Gomes AS, et al. Colour Doppler imaging of portosystemic shunts. AJR Am J Roentgenol 1990; 154:393–397.
11. Sacerdoti D, Merkel C, Bolognesi M, et al. Hepatic arterial resistance in cirrhosis with and without portal vein thrombosis: relationships with portal haemodynamics. Gastroenterology 1995; 108:1152–1158.
12. Zironi G, Gaiani S, Fenyves D, et al. Value of measurement of mean portal flow velocity by Doppler flowmetry in the diagnosis of portal hypertension. J Hepatol 1992; 16:298–303.
13. Ohta M, Hashizume M, Kawanaka H, et al. Prognostic significance of hepatic vein waveforms by Doppler ultrasonography in cirrhotic patients with portal hypertension. Am J Gastroenterol 1995; 90:1853–1857.
14. Pierce ME, Sewell R. Identification of hepatic cirrhosis by duplex Doppler ultrasound value of the hepatic artery resistive index. Australas Radiol 1990; 34:331–333.
15. Iwao T, Toyonaga A, Shigemori H, et al. Hepatic artery haemodynamics responsiveness to altered portal blood flow in normal and cirrhotic livers. Radiology 1996; 200:793–798.
16. Vilgrain V, Lebrec D, Menu Y, et al. Comparison between ultrasonographic signs and the degree of portal hypertension in patients with cirrhosis. Gastrointest Radiol 1990; 15:218–222.
17. Shikare SV, Bashir K, Abraham P, et al. Hepatic perfusion index in portal hypertension of cirrhotic and non-cirrhotic aetiologies. Nucl Med Commun 1996; 17:520–522.
18. Leen E, Goldberg JA, Anderson JR, et al. Hepatic perfusion changes in patients with liver metastases: comparison with those patients with cirrhosis. Gut 1993; 34:554–557.
19. Moriyasu F. Doppler ultrasound in diagnosis of liver tumour and portal hypertension. Radiol Med (Torino) 1993; 85:44–55.
20. Yasuhara K, Kimura K, Nakamura H, et al. Doppler velocity histogram analysis of hepatocellular carcinoma. J Clin Ultrasound 1995; 23: 225–231.
21. Gorka W, Kagalwalla A, McParland BJ, et al. Diagnostic value of Doppler ultrasound in the assessment liver cirrhosis in children: histopathological correlation. J Clin Ultrasound 1996; 24:287–295.
22. Lafortune M, Madore F, Patriquin H, et al. Segmental anatomy of the liver: a sonographic approach to the Couinaud nomenclature. Radiology 1991; 181:443–448.
23. Zwiebel WJ. Sonographic diagnosis of hepatic vascular disorders. Semin Ultrasound CT MR 1995; 16(1):34–48.

24. Abu-Yousef MM. Normal and respiratory variations of the hepatic and portal venous duplex Doppler waveforms with simultaneous electrocardiographic correlation. J Ultrasound Med 1992; 11:263–268.
25. Gallix BP, Taourel P, Dauzat M, et al. Flow pulsatility in the portal venous system: a study of Doppler sonography in healthy adults. AJR Am J Roentgenol 1997; 169:141–144.
26. Hosoki T, Arisawa J, Marikawa T, et al. Portal blood flow in congestive heart failure: pulsed duplex sonographic findings. Radiology 1990; 174:733–736.
27. Wachsberg RH, Needleman L, Wilson DJ. Portal vein pulsatility in normal and cirrhotic adults without cardiac disease. J Clin Ultrasound 1995; 23:3–15.
28. Lippert H, Pabst R. Arterial variations in man. Munchen: JF Bergmann; 1985:32–33.
29. Shapiro RS, Winsberg F, Maldjian C, et al. Variability of hepatic vein Doppler tracings in normal subjects. J Ultrasound Med 1993; 12:701–703.
30. Westra SJ, Zaninovic AC, Vargas J, et al. The value of portal vein pulsatility on duplex sonograms as a sign of portal hypertension in children with liver disease. AJR Am J Roentgenol 1995; 165:167–172.
31. Gibson PR, Gibson RN, Donlan JD, et al. Duplex Doppler ultrasound of the ligamentum teres and portal vein: a clinically useful adjunct in the evaluation of patients with known or suspected chronic liver disease or portal hypertension. J Gastroenterol Hepatol 1991; 6:61–65.
32. Kuo CH, Changchien CS, Tai DI, et al. Portal vein velocity by duplex Doppler ultrasound as an indication of the clinical severity of portal hypertension. Chan Keng I Hsueh 1995; 18: 217–223.
33. Kozaiwa K, Tajiri H, Yoshimura N, et al. Utility of duplex Doppler ultrasound in evaluating portal hypertension in children. J Pediatr Gastroenterol Nutr 1995; 21:215–219.
34. Gorg C, Schwerk WB, Gorg K, et al. Focal involvement of malignant lymphoma in the liver. Bildegebung 1991; 58:67–70.
35. Moriyasu F, Nishida O, Ban N, et al. Congestion index of the portal vein. AJR Am J Roentgenol 1986; 146:735–739.
36. Piscaglia F, Donati G, Serra C, et al. Value of splanchnic Doppler ultrasound in the diagnosis of portal hypertension. Ultrasound Med Biol 2001; 27(7):893–899.
37. Barakat M. Portal vein pulsatility and spectral width changes in patients with portal hypertension: relation to the severity of liver disease. Br J Radiol 2002; 75(893):417–421.
38. Rector WG, Hoefs JC, Hossack KF, et al. Hepatofugal portal flow in cirrhosis: observations on hepatic haemodynamics and the nature of the arterioportal communications. Hepatology 1988; 8:16–20.
39. Abu-Yousef MM, Milam SG, Farner RM. Pulsatile portal vein flow: a sign of tricuspid regurgitation on duplex Doppler sonography. AJR Am J Roentgenol 1990; 155:785–788.
40. Loperfido F, Lombardo A, Amico CM, et al. Doppler analysis of portal vein flow in tricuspid regurgitation. J Heart Value Dis 1993; 2:174–182.
41. Gorg C, Riera–Knorrenschild J, Dietrich J. Pictorial review: colour Doppler ultrasound flow patterns in the portal venous system. Br J Radiol 2002; 75(899):919–929.
42. Wachsberg RH, Simmons MZ. Coronary vein diameter and flow direction in patients with portal hypertension: evaluation with duplex sonography and correlation with variceal bleeding. AJR Am J Roentgenol 1994; 162:637–641.
43. Saddekni S, Hutchinson DE, Cooperberg PL. The sonographically patent umbilical vein in portal hypertension. Radiology 1982; 145:441–443.
44. Gupta D, Chawla YK, Dhiman RK, et al. Clinical significance of patent paraumbilical vein in patients with liver cirrhosis. Dig Dis Sci 2000; 45(9):1861–1864.
45. Amitrano L, Guardascione MA, Brancaccio V, et al. Risk factors and clinical presentation of portal vein thrombosis in patients with liver cirrhosis. J Hepatol 2004; 40(5):736–741.
46. Parvey HR, Raval B, Sandler CM. Portal vein thrombosis; imaging findings. AJR Am J Roentgenol 1994; 162:77–81.
47. Raby N, Meire HB. Duplex Doppler ultrasound in the diagnosis of cavernous transformation of the portal vein. Br J Radiol 1988; 61:586–588.
48. Weltin G, Taylor KJ, Carter AR, et al. Duplex Doppler: identification of cavernous transformation of the portal vein. AJR Am J Roentgenol 1985; 144:999–1001.
49. Pozniak MA, Baus K. Hepatofugal arterial signal in the main portal vein – an indicator of intravascular tumour spread. Radiology 1991; 180:663–666.
50. Vine HS, Sequeira JC, Widrich WC, et al. Portal vein aneurysm. AJR Am J Roentgenol 1979; 132:557–560.
51. Mhanna T, Bernard P, Pilleul F, et al. Portal vein aneurysm: report of two cases. Hepatogastroenterology 2004; 51(58):1162–1164.
52. Merritt CRB, Goldsmith JP, Sharp MJ. Sonographic detection of portal venous gas in infants with necrotizing enterocolitis. AJR Am J Roentgenol 1984; 143:1059–1062.
53. Maher MM, Tonra BM, Malone DE, et al. Portal venous gas: detection by grey-scale and Doppler sonography in the absence of correlative findings on computed tomography. Abdom Imaging 2001; 26(4):390–394.

54. Joynt LK, Platt JF, Rubin JM, et al. Hepatic artery resistance before and after standard meal in subjects with diseased and healthy livers. Radiology 1995; 96:489–492.
55. Han SH, Rice S, Cohen SM, et al. Duplex Doppler ultrasound of the hepatic artery in patients with acute alcoholic hepatitis. J Clin Gastroenterol 2002; 34(5):573–577.
56. Tanaka K, Numata K, Morimoto M, et al. Elevated resistive index in the hepatic artery as a predictor of fulminant hepatic failure in patients with acute viral hepatitis: a prospective study using Doppler ultrasound. Dig Dis Sci 2004; 49(5):833–842.
57. Deasy NP, Wendon J, Meire HB, et al. The value of serial Doppler ultrasound as a predictor of clinical outcome and the need for transplantation in fulminant and severe acute liver failure. Br J Radiol 1999; 72(854):134–143.
58. Ramchandani P, Goldenberg NJ, Soulen RL, et al. Isobutyl 2-cyanoacrylate embolization of a hepatoportal fistula. AJR Am J Roentgenol 1983; 140:137–140.
59. Falkoff GE, Taylor KJW, Morse S. Hepatic artery pseudoaneurysm: diagnosis with real-time and pulsed Doppler ultrasound. Radiology 1986; 158:55–56.
60. Cloogman HM, DiCapo RD. Hereditary hemorrhagic telangiectasis: sonographic findings in the liver. Radiology 1984; 150:521–522.
61. Ralls PW, Johnson MB, Radin DR, et al. Hereditary hemorrhagic telangiectasis: findings in the liver with colour Doppler sonography. AJR Am J Roentgenol 1992; 159:59–61.
62. Ocran K, Rickes S, Heukamp I, et al. Sonographic findings in hepatic involvement of hereditary haemorrhagic telangiectasia. Ultraschall Med 2004; 25(3):191–194.
63. Ludwig J, Hashimoto E, McGill DB, et al. Classification of hepatic venous outflow obstruction: ambiguous terminology of the Budd-Chiari syndrome. Mayo Clin Proc 1990; 65:51–55.
64. Hosoki T, Kuroda C, Tokunaga K, et al. Hepatic venous outflow obstruction: evaluation with pulsed duplex sonography. Radiology 1989; 170:733–737.
65. Singh V, Sinha SK, Nain CK, et al. Budd-Chiari syndrome: our experience of 71 patients. J Gastroenterol Hepatol 2000; 15(5):550–554.
66. Lee DH, Ko YT, Yoon Y, et al. Sonography and colour Doppler imaging of Budd-Chiari syndrome of membranous obstruction of the inferior vena cava. J Ultrasound Med 1994; 13:159–163.
67. Sakugawa H, Higashionna A, Oyakawa T, et al. Ultrasound study in the diagnosis of primary Budd-Chiari syndrome (obstruction of the inferior vena cava). Gastroenterol Jpn 1992; 27:69.
68. Barakat M. Non-pulsatile hepatic and portal vein waveforms in patients with liver cirrhosis: concordant and discordant relationships. Br J Radiol 2004; 77(919):547–650.
69. Janssen HL, Tan AC, Tilanus HW, et al. Pseudo-Budd-Chiari Syndrome: decompensated alcoholic liver disease mimicking hepatic venous outflow obstruction. Hepatogastroenterology 2002; 49(45):810–812.
70. Boyer TD. Portal hypertension and bleeding esophageal varices: portal hypertension. In: Zakim D, Boyer TD, eds. Hepatology: a textbook of liver disease. Philadelphia: WB Saunders; 1990:592.
71. Brown BP, Abu-Yousef M, Farner R, et al. Doppler sonography: a non-invasive method for evaluation of hepatic veno-occlusive disease. AJR Am J Roentgenol 1990; 154:721–724.
72. Herbetko J, Grigg AP, Buckley AR, et al. Veno-occlusive liver disease after bone marrow transplantation: findings at duplex sonography. AJR Am J Roentgenol 1992; 158:1001–1005.
73. Abu-Yousef MM. Duplex Doppler sonography of the hepatic vein in tricuspid regurgitation. AJR Am J Roentgenol 1991; 156:79–83.
74. Dodd GD 3rd, Miller WJ, Baron RL, et al. Detection of malignant tumours in end-stage cirrhotic livers: efficacy of sonography as a screening technique. AJR Am J Roentgenol 1992; 159:727–733.
75. Taylor KJW, Ramos I, Morse SS, et al. Focal liver masses: differential diagnosis with pulsed Doppler ultrasound. Radiology 1987; 164:643–647.
76. Tanaka S, Kitamura T, Fujita M, et al. Colour Doppler flow imaging of liver tumours. AJR Am J Roentgenol 1990; 154:509–514.
77. Suzuki M, Takahashi T, Sato T. Medial regression and its functional significance in tumour-supplying host arteries: a morphometric study of hepatic arteries in human livers with hepatocellular carcinoma. Cancer 1987; 59:444–450.
78. Miller MA, Balfe DM, Middleton WD. Peripheral portal venous blood flow alterations induced by hepatic masses: Evaluation with colour and pulsed Doppler sonography. J Ultrasound Med 1996; 15:707–713.
79. Gaiani S, Casali A, Serra C, et al. Assessment of vascular patterns of small liver mass lesions: value and limitation of the different Doppler ultrasound modalities. Am J Gastroenterol 2000; 95(12):3537–3546.
80. Marn CS, Bree RL, Silver TM. Ultrasonography of liver: technique and focal and diffuse disease. Radiol Clin North Am 1991; 29:1151–1170.
81. Wang S-S, Chiang J-H, Tsai Y-T, et al. Focal hepatic fatty infiltration as a cause of pseudotumours: ultrasonographic patterns and clinical differentiation. J Clin Ultrasound 1990; 18:401–409.

82. Yates CK, Streight RA. Focal fatty infiltration of the liver simulating metastatic disease. Radiology 1986; 159:83–84.
83. Golli M, Mathieu D, Anglade M, et al. Focal nodular hyperplasia of the liver: value of colour Doppler US in association with MR imaging. Radiology 1993; 187:113–117.
84. Learch TJ, Ralls PW, Johnson MB, et al. Hepatic focal nodular hyperplasia: findings with colour Doppler sonography. J Ultrasound Med 1993; 12:541–544.
85. Kudo M, Tomita S, Minowa K, et al. Colour Doppler flow imaging of hepatic focal nodular hyperplasia. J Ultrasound Med 1992;11:553–557.
86. Okuda K, Kojiro M, Okuda H. Neoplasms of the liver: benign tumours of the liver. In: Schiff L, Schiff E, eds. Diseases of the liver. Philadelphia: JB Lippincott; 1993:1236.
87. Dachman AH, Lichtenstein JE, Friedman AC, et al. Infantile hemangioendothelioma of the liver: a radiologic-pathologic-clinical correlation. AJR Am J Roentgenol 1983; 140:1091–1096.
88. Kew MC. Tumours of the liver: benign hepatic tumours. In: Zakim D, Boyer TD, eds. Hepatology: a textbook of liver disease. Philadelphia; WB Saunders, 1990:1232.
89. Pardes JG, Bryan PJ, Gauderer MWL. Spontaneous regression of infantile hemangioendotheliomatosis of the liver: demonstration by ultrasound. J Ultrasound Med 1982;1:349–353.
90. Boyer TD. Portal hypertension. In: Zakim D, Boyer TD, eds. Hepatology: a textbook of liver disease. Philadelphia: WB Saunders; 1990:602.
91. LaFortune M, Patriquin H, Pomier G, et al. Haemodynamic changes in portal circulation after portosystemic shunts: use of duplex carotid sonography in 43 patients. AJR Am J Roentgenol 1987; 149:701–706.
92. Rosch J, Hanafee WN, Snow H. Transjugular portal venography and radiologic portacaval shunt: an experimental study. Radiology 1969; 92:1112–1114.
93. Chong WK, Malisch TA, Mazer MJ, et al. Transjugular intrahepatic portosystemic shunt: US assessment with maximum flow velocity. Radiology 1993; 189:789–793.
94. Feldstein VA, Patel MD, La Berge JM. Transjugular intrahepatic portosystemic shunts: accuracy of Doppler US in determination of patency and detection of stenoses. Radiology 1996; 201:141–147.
95. Foshager MC, Ferral H, Finlay DE, et al. Colour Doppler sonography of transjugular intrahepatic portosystemic shunts (TIPS). AJR Am J Roentgenol 1994; 163:105–111.
96. Longo JM, Bilbao JI, Rousseau HP, et al. Transjugular intrahepatic portosystemic shunt: evaluation with Doppler sonography. Radiology 1993; 188:529–534.
97. Surratt RS, Middleton WD, Darcy MD, et al. Morphologic and haemodynamic findings at sonography before and after creation of a transjugular intrahepatic portosystemic shunt. AJR Am J Roentgenol 1993;160:627–630.
98. Foshager MC, Finlay DE, Longley DG, et al. Duplex and colour Doppler sonography of complications after percutaneous interventional vascular procedures. Radiographics 1994; 14:239–253.
99. Zemel G, Katzen B, Grubbs G, et al. Sonographic indicators of unsuccessful transjugular intrahepatic portosystemic shunts. Radiology 1994; 193(P)(suppl):167.
100. Dodd GD, Zajko AB, Orons PD, et al. Detection of transjugular intrahepatic portosystemic shunt dysfunction: value of duplex Doppler sonography. AJR Am J Roentgenol 1995; 164:1119–1124.
101. Mituzani P, Saxon R, Alexander P, et al. Duplex US screening after transjugular intrahepatic portosystemic shunt placement. Radiology 1993; 189(P)(suppl):254.
102. Nazarian GK, Ferral H, Castaneda-Zuniga WR, et al. Development of stenoses in transjugular intrahepatic portosystemic shunts. Radiology 1994; 192:231–234.
103. Wachsberg RH. Doppler ultrasound evaluation of transjugular intrahepatic portosystemic shunt function: pitfalls and artifacts. Ultrasound Q 2003; 19(3):139–148.
104. Coldwell DM, Ring EJ, Rees CR, et al. Multicenter investigation of the role of transjugular intrahepatic portosystemic shunt in management of portal hypertension. Radiology 1995; 196:335–340.

# The kidney

# 8

Paul A. Dubbins

The kidney is a highly vascular organ, receiving approximately 20% of the cardiac output. Many of the diseases of the kidney have a major vascular component, and systemic diseases such as hypertension are mediated through the vascular control system of the juxtaglomerular apparatus. The kidney would therefore appear to be a fertile field for examination by Doppler. Renal and renovascular disease might be expected to produce changes in the vascular supply, in the microvascular circulation and in venous return.

## ANATOMY AND TECHNIQUE

Examination of the *renal arteries* requires knowledge of vascular anatomy, anatomical relations, anatomical variations and surface anatomy. It also requires an understanding of the effects of geometry on the ability to record a Doppler signal. The right renal artery is an anterolateral branch of the aorta and courses laterally and posteriorly behind the inferior vena cava and then behind the ipsilateral renal vein to the hilum of the kidney (Fig. 8.1). Its anterior relations are predominantly bowel: the duodenum, small bowel and transverse colon. At the hilum of the kidney it divides into anterior and posterior branches, then into interlobular arteries and subsequently the arcuate arteries, which send out striate branches to the cortex (Fig. 8.2). On the left, the renal artery arises as a posterolateral branch of the aorta and courses posteriorly laterally and inferiorly immediately behind the third and fourth parts of the duodenum, subsequently passing behind the transverse and descending colon (Fig. 8.3). Both arteries therefore trace an arc that runs parallel to the arc of the anterior abdominal wall. Geometrically this favours visualisation but compromises the Doppler examination; however, visualisation is also compromised by bowel which overlies much of the course of both renal vessels.

No single imaging approach can circumvent the difficulties relating to geometry, vessel course and the anterior abdominal relations of gas-filled bowel. Each renal artery must therefore be examined with a flexible technique. Anatomical variations in particular are difficult to image with ultrasound, although supplemental arteries are being identified increasingly with improved equipment resolution and improved sensitivity of colour and power Doppler.

The *renal veins* follow a course parallel to the renal arteries. The right renal vein is the shorter, coursing anteriorly, medially and towards the head in front of the right renal artery (Fig. 8.4). It normally joins the inferior vena cava just cephalad to the right renal artery as it crosses beneath the cava. On the left, the renal vein travels medially and anteriorly, (Figs 8.3 and 8.5) usually superior to the renal artery, passing between the aorta and the superior mesenteric artery, where it may occasionally be compressed by the 'nutcracker effect' between the two vessels. This may cause dilatation of the more proximal portion of the vein but this is not of any clinical significance (Fig. 8.6). The right renal vein usually has no major tributaries but on the left the adrenal, lumbar and gonadal veins usually join the renal vein; of these, only the gonadal vein is regularly imaged on ultrasound as it enters the inferior aspect of the vein near the aorta.

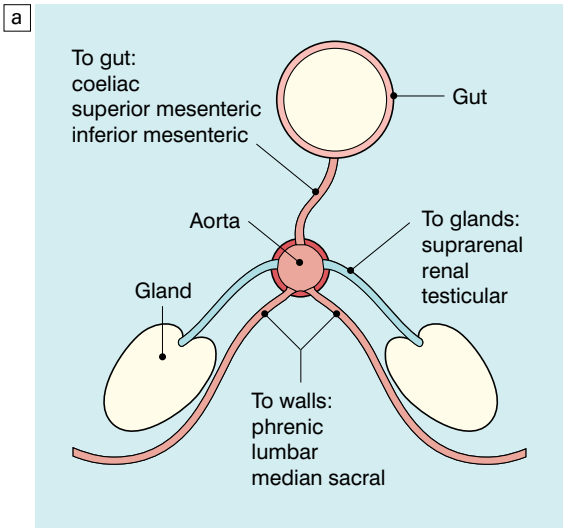


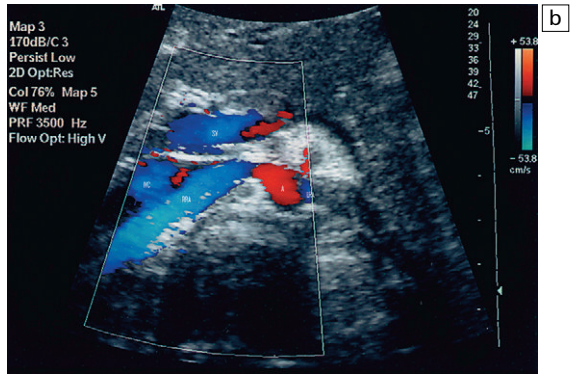


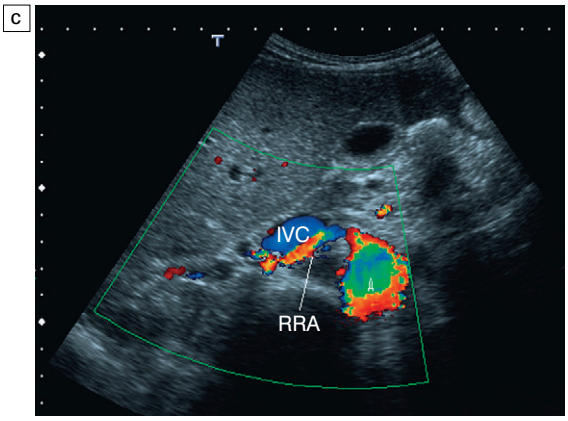


**Fig. 8.1** (a) (b) Axial colour flow image, the level of the origin of the renal arteries. RRA, right renal artery. (c) The origin of the right renal artery is demonstrated as an anterolateral branch of the aorta passing posterior to the inferior vena cava (IVC).

## Technique – patient positioning and scan orientation

With the patient supine, the aorta is localised with a longitudinal scan just to the left of the midline. The probe is rotated through 90° and the superior mesenteric artery identified (Fig. 8.7). Approximately 1 cm below the origin of the superior mesenteric artery, the right renal artery can be identified arising from the anterolateral surface of the aorta. Occasionally the left renal artery can also be demonstrated at its origin from the posterolateral or lateral surface of the aorta. Both renal veins and their junction with the inferior vena cava can usually be demonstrated in this plane (Figs 8.4 and 8.6). On moving the probe slightly to the right of the midline, the right renal artery is seen to turn posteriorly and laterally. In slim patients it is occasionally possible to follow the renal artery and vein into the hilum of the kidney by applying compression with the transducer and slightly oblique angulation. Doppler signal recording is best performed at the origin of the artery, by slight displacement of the probe to the right of the midline and angulation to the left to identify the course of the first short segment of the left renal artery (Figs 8.7 and 8.8). Reversing the angulation to the right approximately 20° from the perpendicular allows signal recording from the posterior and lateral coursing right renal artery[1] (Fig. 8.9).

The patient is then turned into the left posterior oblique position. Scanning just posterior to the right mid-axillary line in the longitudinal plane and angling towards the major vessels, both the aorta

a

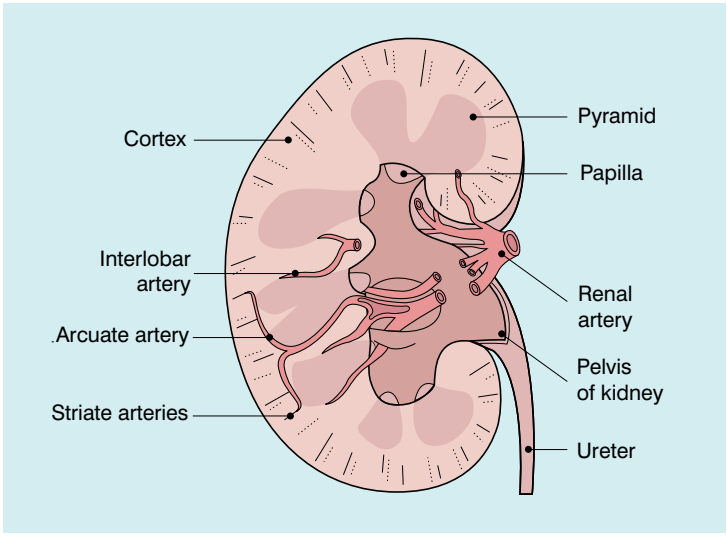


**Fig. 8.2** (a) (b) Colour flow Doppler demonstrating segmental, interlobar, arcuate and interlobular or striate vessels.

b

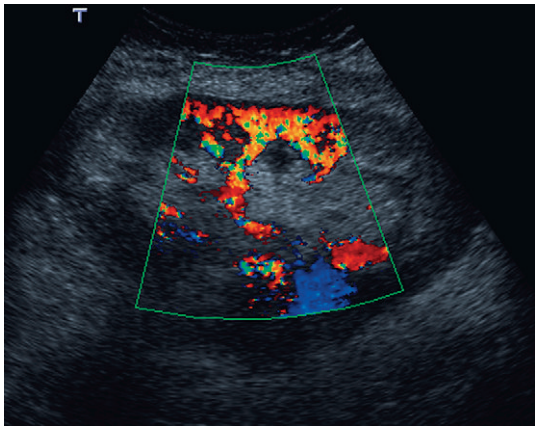

a

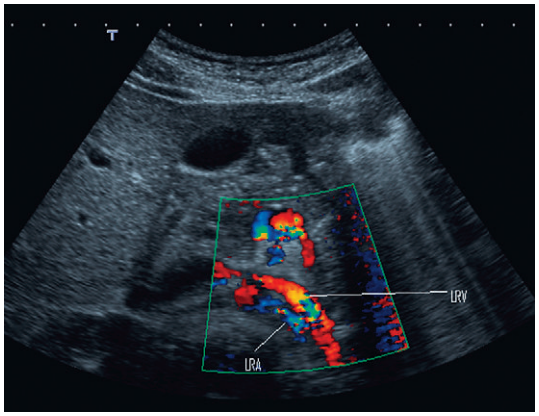


b

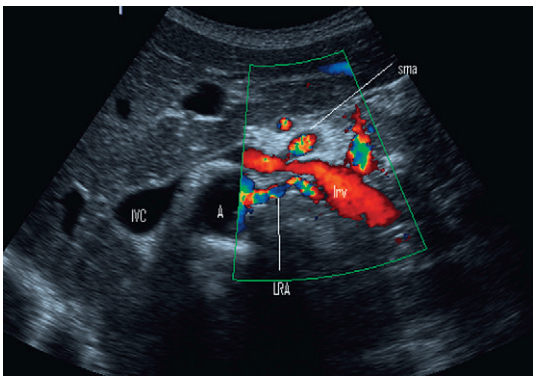


**Fig. 8.3** (a) The origin of the left renal artery from the lateral aspect of the aorta and its course posterior to the left renal vein is demonstrated. (b) The origin of the left renal artery in relation to the aorta, left renal vein and superior mesenteric artery are identified.

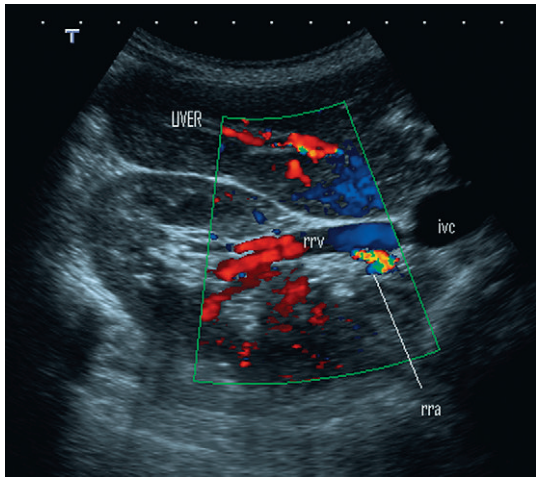


**Fig. 8.4** The course of the right renal vein is demonstrated relative to the right renal artery which lies posteriorly.

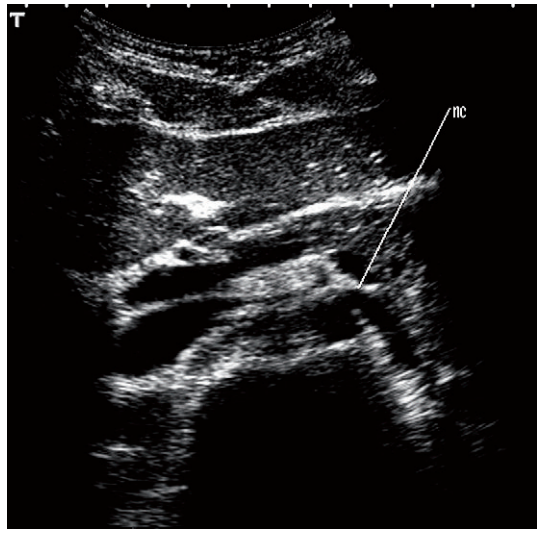


**Fig. 8.6** The nutcracker appearance of the left renal vein as it passes between the aorta and the superior mesenteric artery is identified. There is apparent continuity between the left renal vein and the aorta.

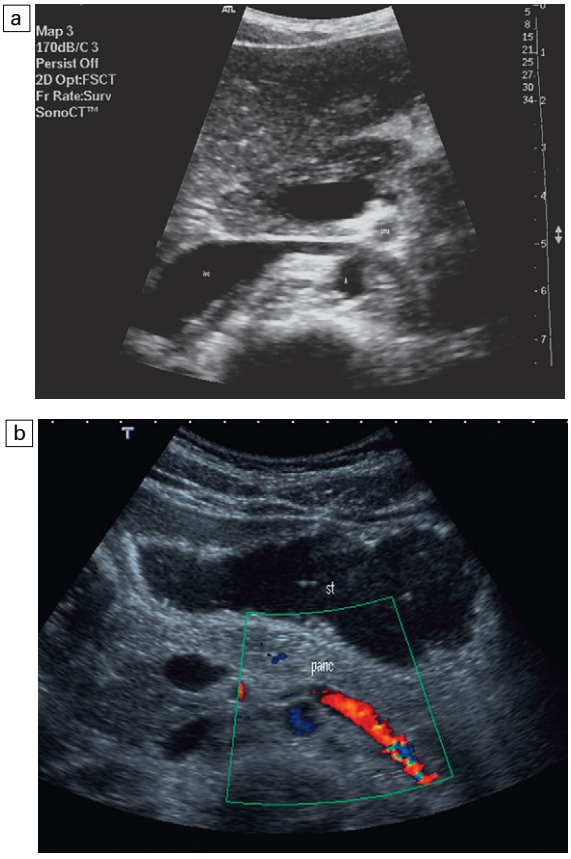


**Fig. 8.5** (a) The course of the left renal vein between the aorta and the superior mesenteric artery is demonstrated. (b) Colour flow Doppler demonstrating the left renal vein. Greater clarity has been achieved by a stomach distended with fluid.

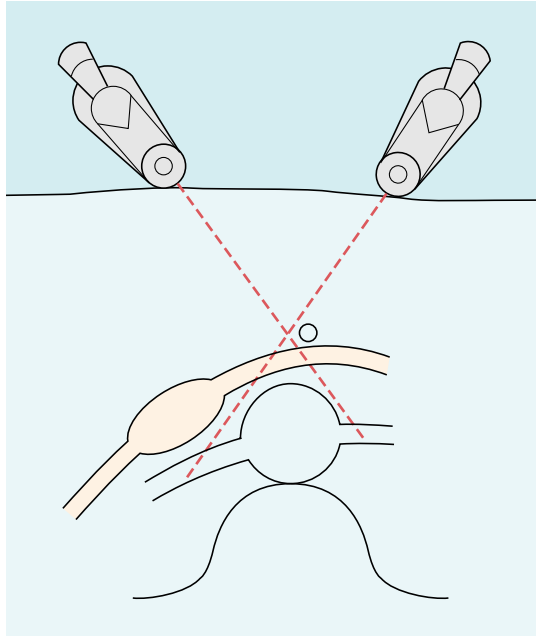

**Fig 8.7** Representation of the approach to Doppler evaluation of the renal arteries from the anterior approach.

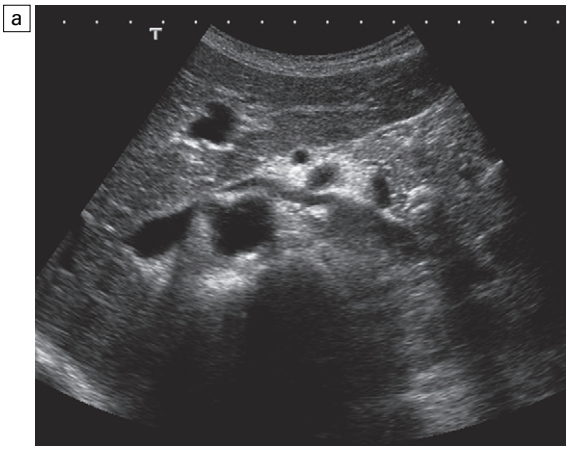


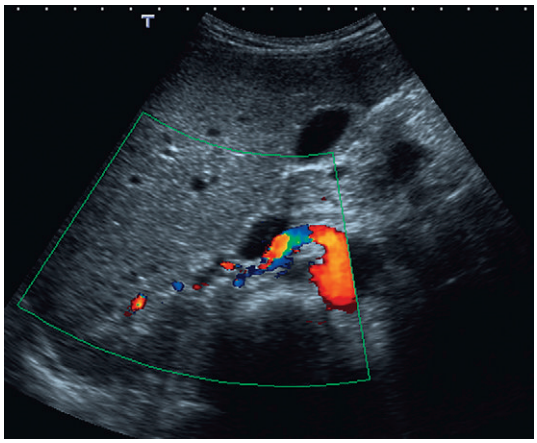


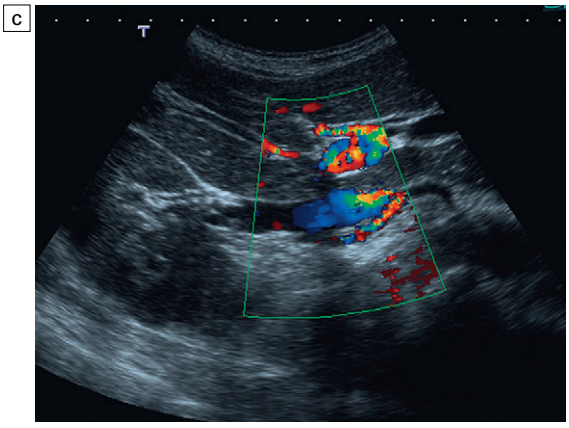


**Fig. 8.8** (a) The anterior origin of the right renal artery is demonstrated. (b) The anterior approach just to the right of midline allows Doppler signal recording within the ostium of the artery. (c) Doppler signal recording within the renal artery as it courses posterior to the inferior vena cava.

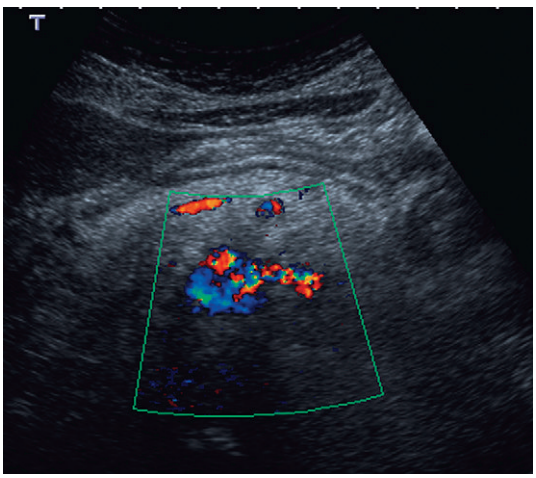

**Fig. 8.9** The probe is angled slightly to the left from a position just to the right of the midline demonstrating the origin of the left renal artery in colour flow Doppler.

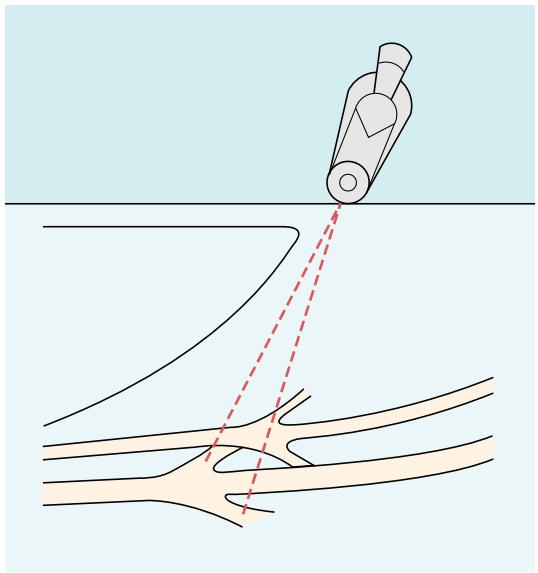

**Fig 8.10** Representation of the approach to the renal arteries scanning from the right flank.

and inferior vena cava can be identified lying parallel to one another (Fig. 8.10). In this plane the section cuts through both the right and left renal arteries and the origins of both can usually be identified (Fig. 8.11). Alteration of the patient position to the right posterior oblique position will identify the junction of the renal veins with the inferior vena cava (Fig. 8.12). Doppler signal recording is possible in this plane from both renal arteries (Fig. 8.13), although occasionally, particularly in heavy or overweight patients, the left renal artery signal is poorly recorded, either because of its depth and difficulties with pulse repetition frequency, or simply because of attenuation of the beam. Scanning from the right flank and angling the probe anteriorly to align the sonographic plane with the coronal plane of the kidney allows the vessels at the renal hilum and within the kidney to be sampled. These can be observed with colour Doppler radiating from the hilum (Fig. 8.14).

The right lobe of the liver acts as an acoustic window to the right renal artery. On the left there is no such acoustic window and visualisation of the left renal artery from origin to hilum is extremely difficult. This may be facilitated by compression, or by using the coronal approach to the kidney and following the course of the renal artery in a retrograde fashion towards its origin, although

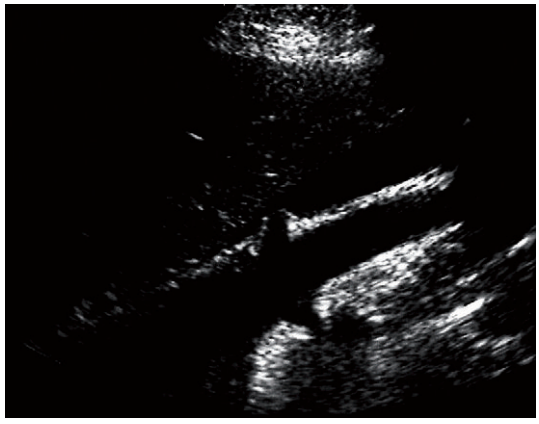

**Fig 8.11** Oblique view through the aorta scanning from the right flank, demonstrating the origin of both renal arteries and the adjacent inferior vena cava. From Dubbins[33], with permission.

**Fig 8.12** Oblique scanning from the right flank, demonstrating the aorta and inferior vena cava, the origin of the right renal artery and the junction of the right renal vein with the inferior vena cava. From Dubbins[33], with permission.

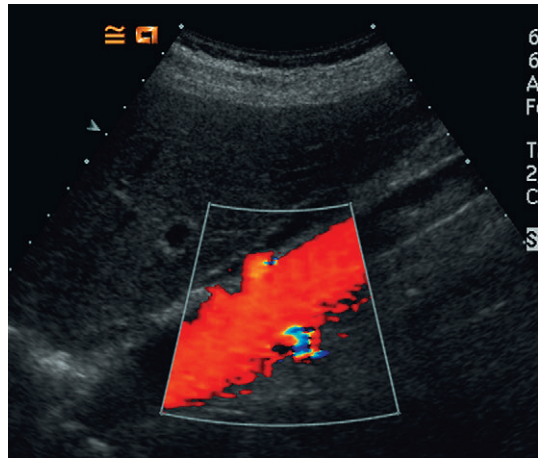

**Fig. 8.13** Colour flow Doppler in the left posterior oblique position demonstrating the origin of both renal arteries.

in this author's experience the left renal artery is rarely seen in its entirety. The origin may be seen in transverse plane, scanning from the anterior approach and angling slightly to the left (Fig. 8.3 and 8.9), or it may be seen with the patient in the left posterior oblique position as described above (Fig. 8.15). The more distal portion of the main renal artery may be demonstrated just proximal to the hilum by the coronal approach, but the mid-portion of the left renal artery is only rarely seen except in slim patients. By contrast

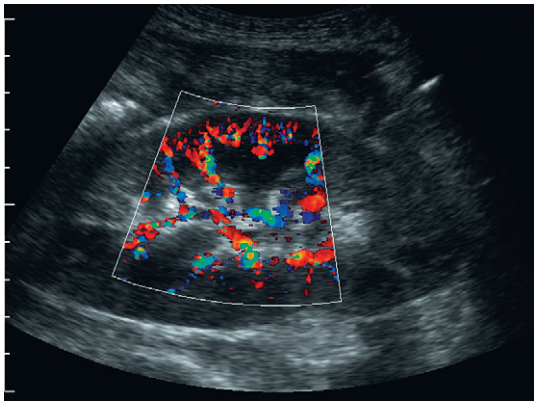


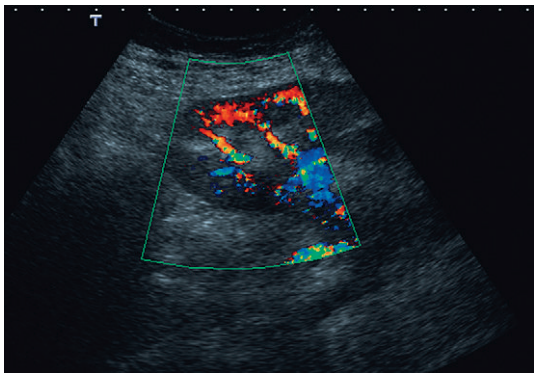


**Fig. 8.14** (a) Colour flow box opened wide to demonstrate global flow within the kidney. (b) Colour flow box identifying focal flow to the upper pole of the left kidney.

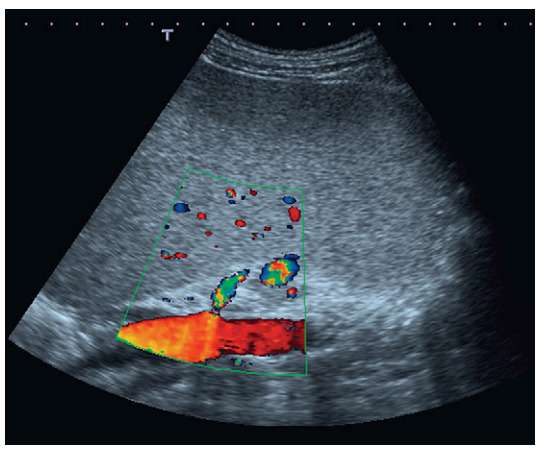

**Fig. 8.15** Origin of the left renal artery and its proximal course identified through an enlarged spleen.

much of the left renal vein is demonstrated with the patient in the supine position; its more anterior and superior location, together with larger diameter, allowing visualisation using the left lobe of the liver as an acoustic window (Fig. 8.16).

### *Anatomical variation*

It has been found that 40% of individuals do not conform to this simple anatomical arrangement, with one or more accessory arteries supplying either or both kidneys. These may arise from the aorta immediately adjacent to the main renal artery, but their origin may be from anywhere along the abdominal aorta down to and including the iliac arteries (Figs 8.17 and 8.18). The polar artery is another common variant, branching early from the main renal artery to pass into either the upper, or more usually the lower, pole without traversing the renal hilum (Fig. 8.19). Multiple renal veins are common, occurring in approximately one-third of the population – the most common of these being an accessory left renal vein traversing to the right behind the aorta – a retroaortic vein (Fig. 8.20).

### *The intrarenal vessels*

Demonstration of the anatomical location and course of the intrarenal vessels is almost exclusively restricted to colour Doppler, although pulsations can be seen on real time at the site of the interlobar vessels, and occasionally at the bright reflectors at the corticomedullary margin which represent the arcuate vessels. The arteries are each accompanied by a vein; they divide into branches to the upper and lower poles and to the anterior and posterior parenchyma (Fig. 8.14). The interlobar vessels course into the renal parenchyma on either side of the renal papillae, giving tiny (invisible) branches to the medulla before arching over the surface of the medulla as the arcuate arteries, giving off multiple small striate branches which extend out towards the cortex. With more modern and sensitive machines, the capsular artery can occasionally be demonstrated at the margin of the kidney, curving around the surface.

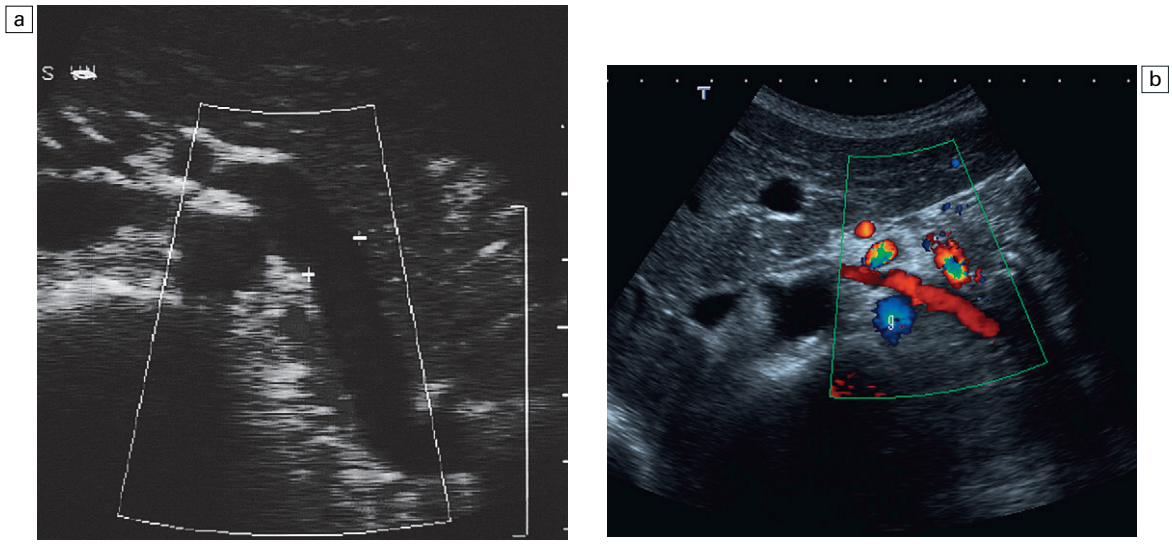


**Fig. 8.16** (a) (b) Colour flow Doppler demonstrating flow towards the transducer in the left renal vein. A large gonadal vessel is demonstrated posteriorly (g).

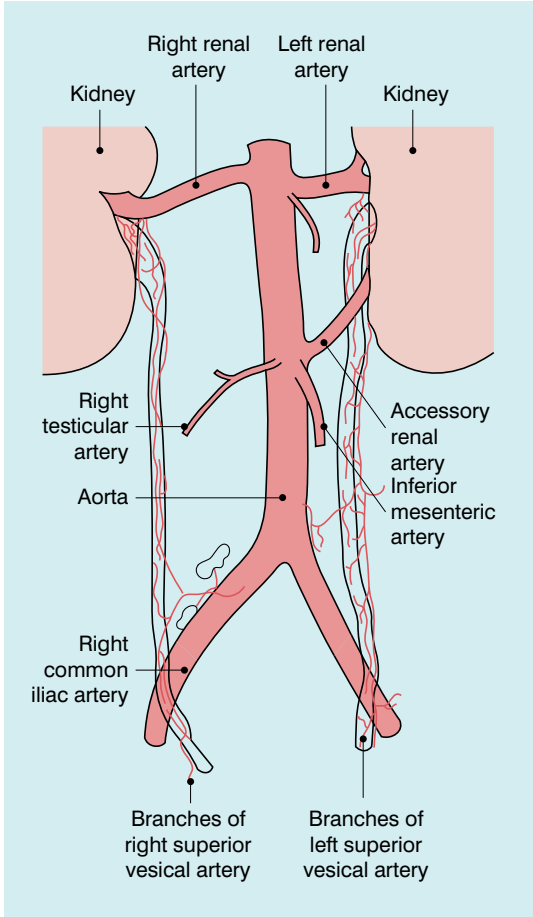


**Fig 8.17** Origin of the renal arteries including an accessory renal artery supplying the lower pole on the left.

It is important to recognise that in the evaluation of the kidneys there are factors other than the Doppler study which contribute to the diagnosis. Both kidneys should be examined carefully with respect to size, echogenicity and smoothness of outline, together with an assessment of the corticomedullary differentiation. The adrenal areas should also be carefully examined to exclude any obvious mass. The time taken to perform a complete vascular examination of the kidney is wasted if the initial examination has missed a renal mass, an adrenal tumour, or a small or absent kidney.

## Technique – Doppler examination

Throughout the course of examination of the renal artery, colour Doppler is frequently switched on to confirm the nature and direction of flow. The optimum pulse repetition frequency is selected to detect moderate flow velocities, although it may need to be modified to detect high velocities if a stenosis with aliasing of the colour signal is present. For spectral Doppler, the sample volume is placed on the selected vessel shown on the colour display. Recording spectral Doppler is better performed in duplex rather than triplex mode, since the processing required for triplex imaging reduces both the frame rate and the pulse repetition frequency, compromising further the discrimination of high-velocity signals at depth.

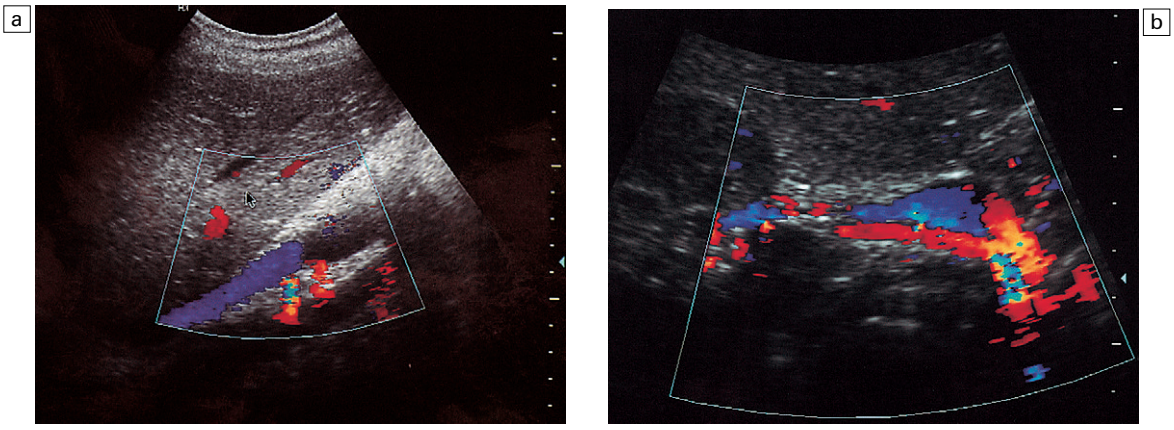


**Fig 8.18** (a) Two right renal arteries. Oblique scan through the aorta and inferior vena cava demonstrating the origin of the two renal arteries from the right lateral wall of the aorta. (b) Transverse scan demonstrating the larger of the two renal arteries (in red) beneath the corresponding renal vein (in blue) coursing towards the hilum of the right kidney. (c) Similar transverse image of the accessory renal artery, which is much smaller than the more superior renal artery, but also beneath the corresponding renal vein coursing towards the hilum of the kidney.

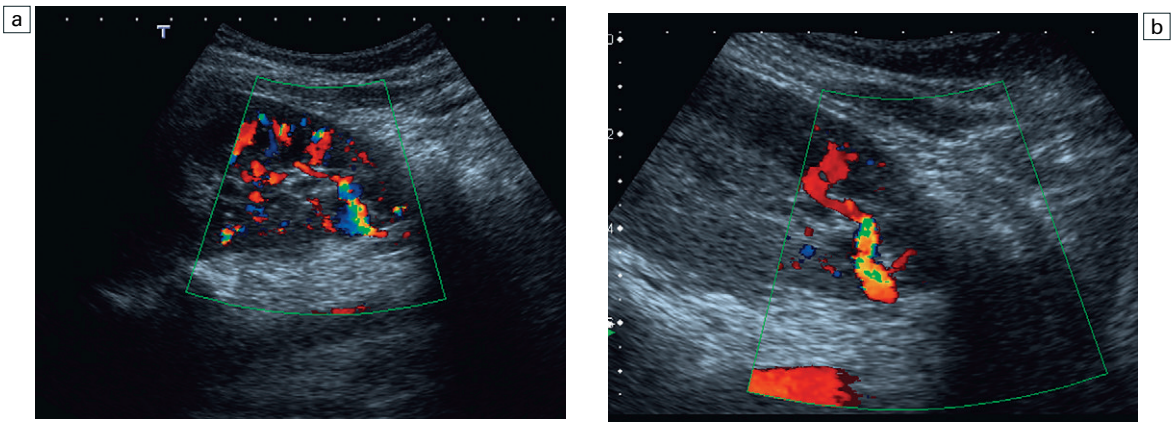


**Fig. 8.19** (a) Coronal colour flow Doppler image of the lower pole of the left kidney. An unusual vessel is demonstrated at the lower pole. (b) Reducing the colour sensitivity the polar vessel is more clearly identified.

Colour Doppler is invaluable in the assessment of intrarenal vessels. With the system set to detect low or moderate velocities, flow can be identified in almost all patients in the vessels at the renal hilum, particularly if the angle of incidence is optimised to achieve angles of less than 60° relative to the course of the vessel. Angling the probe medially from the right or left flank

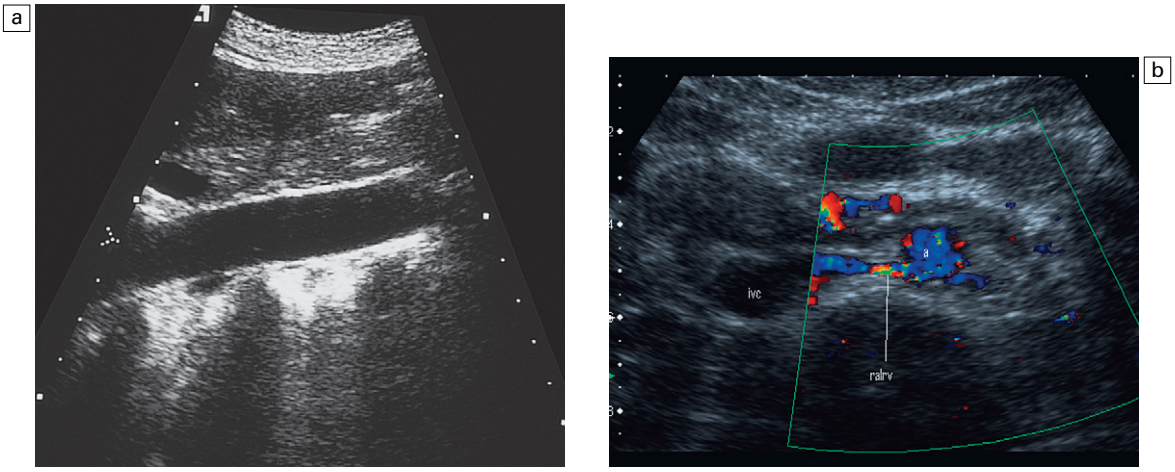


**Fig. 8.20** (a) (b) A retroaortic left renal vein (ralv) is demonstrated in colour passing posteriorly to the aorta (a) before it enters the left side of the inferior vena cava (ivc).

will allow assessment of the intrarenal vessels. Peripheral, smaller vessels may be better demonstrated with power Doppler, although in this situation the directional information is lost. The further development of systems with greater colour Doppler sensitivity has significantly improved vessel identification and discrimination (Fig. 8.21).

Evaluation of global blood flow requires that the colour box be opened to its fullest extent in order to visualise relative blood flow distribution (Fig. 8.22). This is also important in the evaluation of renal tumours so that flow in the lesion can be compared with that in normal adjacent renal tissue. However, this compromises temporal resolution with lower frame rates and pulse repetition frequency; the size of the colour box should therefore be minimised prior to spectral sampling (Fig. 8.23). It is frequently of value to activate the zoom function on the machine prior to interrogation with colour Doppler, as this allows for greater sensitivity of colour signal recording within the intrarenal vessels. Using this technique, the hilar and interlobular vessels are demonstrated in all patients, although arcuate and striate arteries are only seen in slimmer patients. In the case of the arcuate vessels, this is partly due to their course, which is usually at right angles to the incident beam. Advances in


**Fig. 8.21** Colour power Doppler demonstrating perfusion of the renal parenchyma.

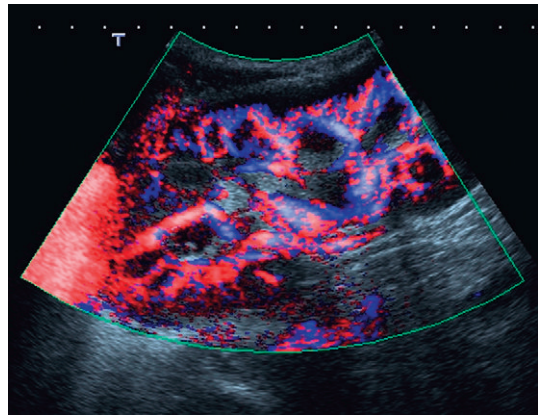

**Fig. 8.22** Greater sensitivity of colour flow Doppler affords directional information as well as identification of the interlobular arteries.

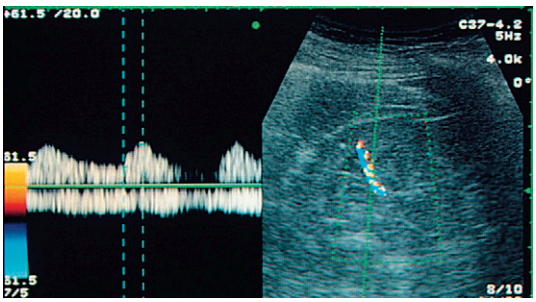


**Fig 8.23** Colour box reduced in size to demonstrate single intrarenal vessel prior to sampling for spectral Doppler.

technology have widened the group in whom the entire renovascular pattern can be identified.[2]

### *Characteristics of the Doppler spectrum*

The typical spectra from the renal arteries are shown in Figure 8.24. There is a rapid systolic upstroke, which is occasionally followed by a secondary slower rise to peak systole (although this is more frequently seen with advancing age, hypertension, etc.). There is subsequently a gradual diastolic decay but with persistent forward flow in diastole.

Renal vein spectra normally reflect the transmitted pulsations from the right atrium. The right renal vein is short and exhibits this feature in all cases except where there is renal vein or caval compromise. The left renal vein, particularly if it is sampled to the left of the superior mesenteric artery, may show only slight variability of flow velocities. This pattern of damped flow may be associated with the nutcracker syndrome and reflect renal venous congestion. However the findings are not constant in this condition and similarly may be found in asymptomatic patients (Fig. 8.25).

### *Indices used in the assessment of renal blood flow*

A multiplicity of indices is used for evaluation of renal blood flow. The wide range indicates that no single index provides all the information that is necessary for adequate evaluation of renal pathophysiology. The indices used, together with normal values, are shown in Table 8.1, and some examples are shown in Figure 8.26. Pulsatility and resistance indices in the renal arteries increase with age and in hypertensive patients. This is presumably consequent upon the effect of the juxtaglomerular apparatus producing vasoconstriction, but also perhaps on the development of hypertensive nephrosclerosis.[3–5] A further cause of variability of Doppler indices relates to differences of opinion as to the optimum site for Doppler sampling. Some authors suggest the renal sinus as the optimum site, while others recommend the interlobar and arcuate artery level.[6] There is significant variety in normal spectral indices but in this author's view this is best minimised by using the same site in order to standardise measurement technique.

*Ureteric jets* are the rhythmic pulses of urine that occur in the bladder approximately four times each minute. These are not necessarily synchro-

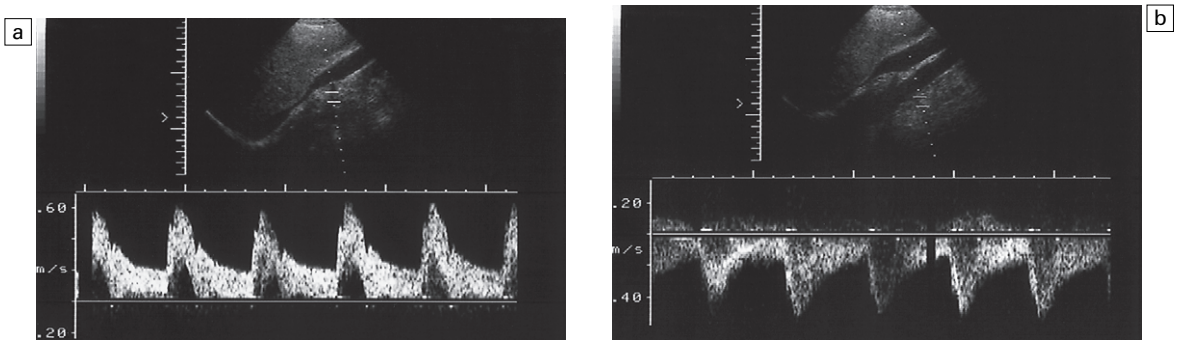


**Fig 8.24** (a) Normal Doppler spectrum from the right renal artery. (b) Corresponding normal Doppler spectrum from the left renal artery using the oblique approach from the right flank.

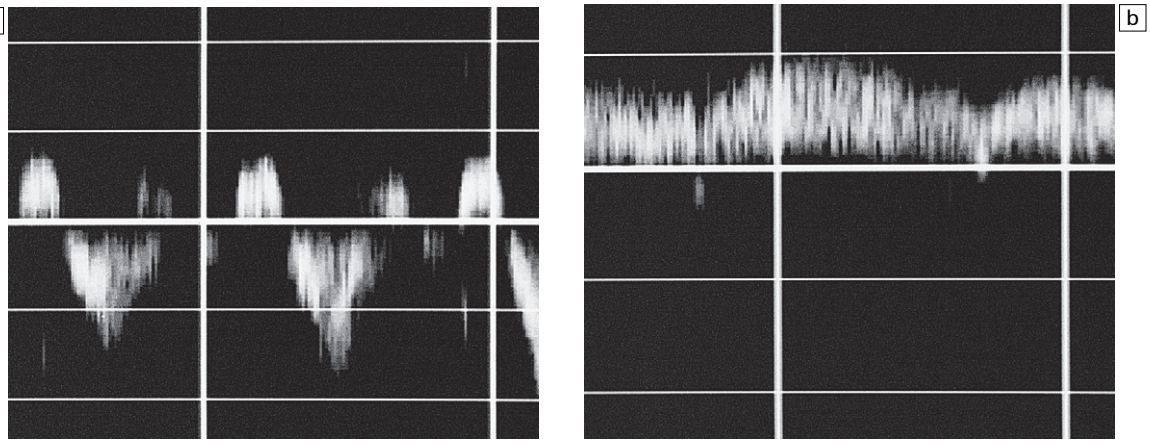

**Fig 8.25** (a) Venous flow within the right renal vein reflecting the pulsatile nature of flow within the inferior vena cava. (b) Damped flow within the left renal vein, presumably modified by the effect of the superior mesenteric artery. From Dubbins[33], with permission.

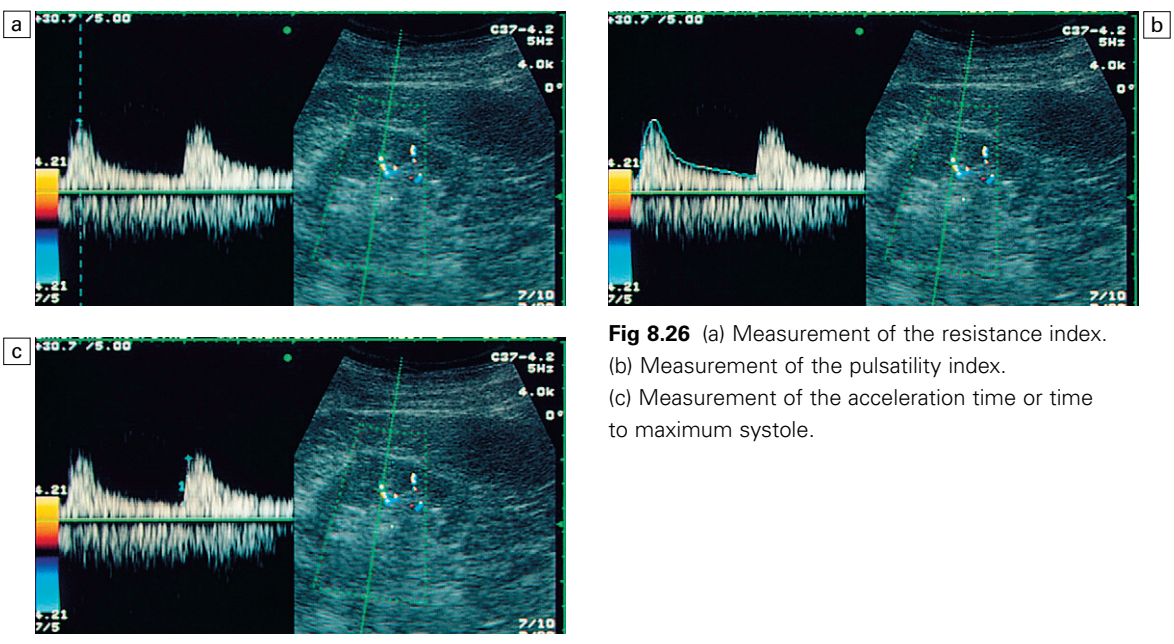

**Fig 8.26** (a) Measurement of the resistance index. (b) Measurement of the pulsatility index. (c) Measurement of the acceleration time or time to maximum systole.

**Table 8.1** Normal renal artery Doppler indices

| Index | Range |
|---|---|
| Pulsatility index (PI) | 0.7–1.4 |
| Resistance index (RI) | 0.56–0.7 |
| Peak systolic velocity (PSV) | 60–140 cm $s^{-1}$ (<180) |
| Diastolic/systolic ratio (D/S) | 0.26–0.4 |
| Renal artery/aorta ratio (RAR) | <3.5 |
| Time to maximum systole (TMS) (systolic rise time) | 42–57 ms |
| Acceleration index | 250–380 cm $s^{-2}$ |

nous but can be identified in approximately 90% of patients of all age groups. Although these jets can be demonstrated on real-time imaging alone, the frequency of their demonstration is much improved by the use of colour Doppler. They are best demonstrated with the patient well hydrated and with a full but not overfull bladder. The probe is placed transversely in the pelvic midline, angling towards the feet. The trigone of the bladder is identified by the two slightly raised ureteric orifices, approximately 3cm apart. Although jets may be seen in real time they are best appreciated on colour when bursts of colour signal, directed medially into the bladder are seen (Fig. 8.27).

### Technique – contrast examination

The role of ultrasound contrast in the evaluation of the kidney has yet to be evaluated. Initially proposed as is a method of Doppler rescue in difficult patients, it is now possible to evaluate renal perfusion and reperfusion.

For the purpose of Doppler rescue, methodology is straightforward. Optimum probe positioning and angulation is selected for the vessel under study and this position is maintained for contrast injection. Colour or power imaging may be used although it is usual to reduce colour sensitivity so as not to cause bloom or flash within the image. Although this technique may destroy the bubbles this is not important in the major vessels since they are immediately reperfused.

Renal parenchymal studies were initially performed in the same way. However, the use of standard imaging and colour settings causes some destruction of the bubbles and compromises the demonstration of certain perfusion characteristics such as perfusion defects, blood pooling and early venous filling.

Most manufacturers now provide specific contrast imaging packages which rely upon the greater sensitivity of harmonics to the bubble oscillation. These may have a low mechanical index (MI), with minimal bubble destruction or a sequenced imaging algorithm of a flash of high MI to destroy the bubbles followed by an imaging sequence of low MI to demonstrate the perfusion/reperfusion sequence.

The probe is placed in a position for optimal visualisation of the kidney (usually coronal to best demonstrate renal vessels) or for best demonstration of focal pathology. Following contrast injection the probe is maintained in the same position and the examination is automatically timed (Fig. 8.28).

There are now available on-line or off-line time/intensity packages which allow the selection of regions of interest within the kidney and the recording of perfusion/reperfusion graphs (Fig. 8.29).

## DISEASES OF THE MAJOR RENAL VESSELS

### General principles

Evaluation of the renal arteries should include an assessment of the aorta, particularly around the origins of the renal arteries, to look for athero-

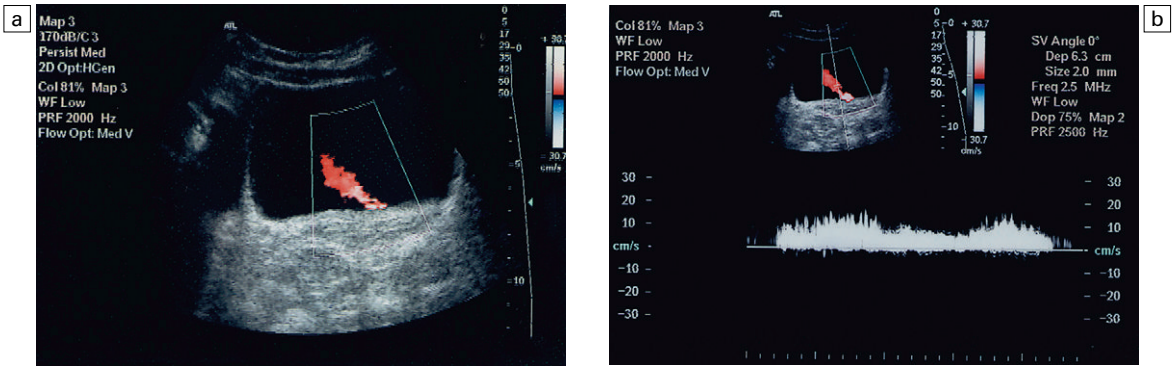


**Fig. 8.27** (a) Colour flow Doppler of left ureteric jet. (b) Spectral Doppler of the burst of urine into the bladder.

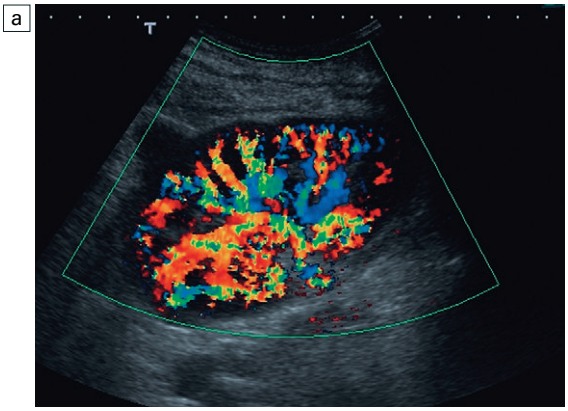


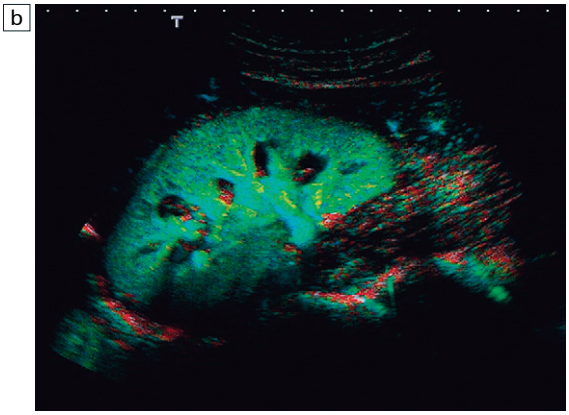


**Fig. 8.28** (a) Colour flow Doppler demonstrating enhancement of the colour signal within the intrarenal vessels after the injection of contrast. (b) Pulse inversion harmonic image in bubble destruction reperfusion mode demonstrating parenchymal perfusion.

matous plaques. The demonstration of atheromatous plaque within the more distal renal artery by direct visualisation is usually rather more difficult, and its presence is inferred from alterations in the Doppler signal. With careful evaluation along the course of the renal artery, it is occasionally possible to demonstrate the irregular beaded appearance associated with fibromuscular hyperplasia. As at other vessel sites, focal dilatation of the artery may represent a poststenotic dilatation associated with a proximal stenotic segment.

## Renal artery stenosis

The pathology of narrowing of the renal artery is largely divided into stenosis produced by atheroma

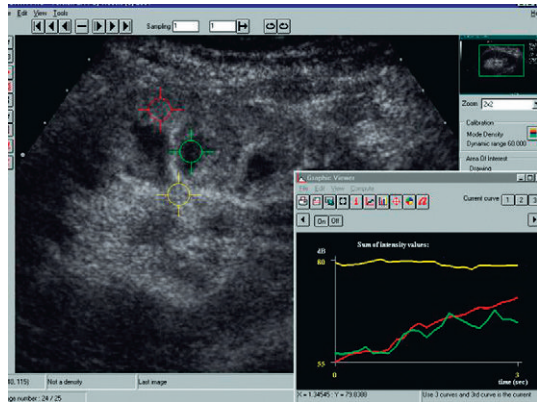

**Fig. 8.29** Time intensity curves for renal sinus, cortex and medullary perfusion.

and that resulting from renal artery fibromuscular hyperplasia. The prevalence of the different types of renal artery disease depends to a very large degree on the age group; fibromuscular dysplasia is predominantly a disease of younger age groups, whereas atheroma becomes more common with increasing age. Atheromatous renal artery stenosis is the cause of the majority of cases of renal artery stenosis. This is particularly the case for those patients presenting with renovascular renal failure, rather than isolated aggressive hypertension. The findings on ultrasound imaging are different in the two conditions.

In cases of atheromatous disease, the stenosis tends to be located near the origin of the artery (Fig. 8.30), although it may occur along the course of the artery. In fibromuscular hyperplasia, the affected segment tends to lie distal to the origin of the vessel. Doppler findings within the main renal artery are variable. For a haemodynamically significant stenosis of more than 50% diameter reduction, there is typically an increase in flow velocity greater than 180 cm $s^{-1}$ associated with spectral broadening (Fig. 8.31); the renal artery/aortic peak systolic ratio (RAR) is increased beyond 3.5. Spectral broadening may be the only sign in stenoses of lesser severity and may predominate in fibromuscular hyperplasia.[7] Colour Doppler findings include narrowing of the luminal diameter and aliasing of the colour signal (Fig. 8.32). The value of using the renal artery/aortic ratio, rather

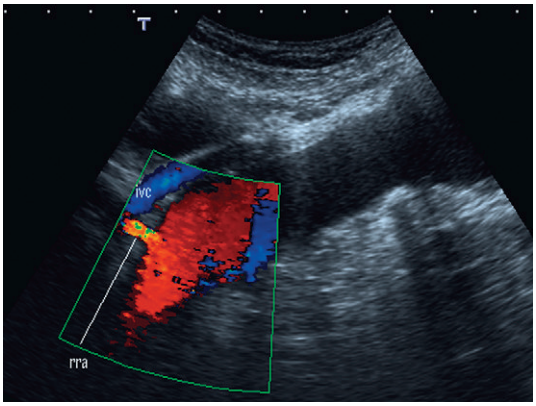


**Fig. 8.30** Colour flow Doppler of the aorta in coronal view. There is marked atheroma of the aortic wall. The origin of the right renal artery is demonstrated beneath the inferior vena cava. The left renal artery was occluded.

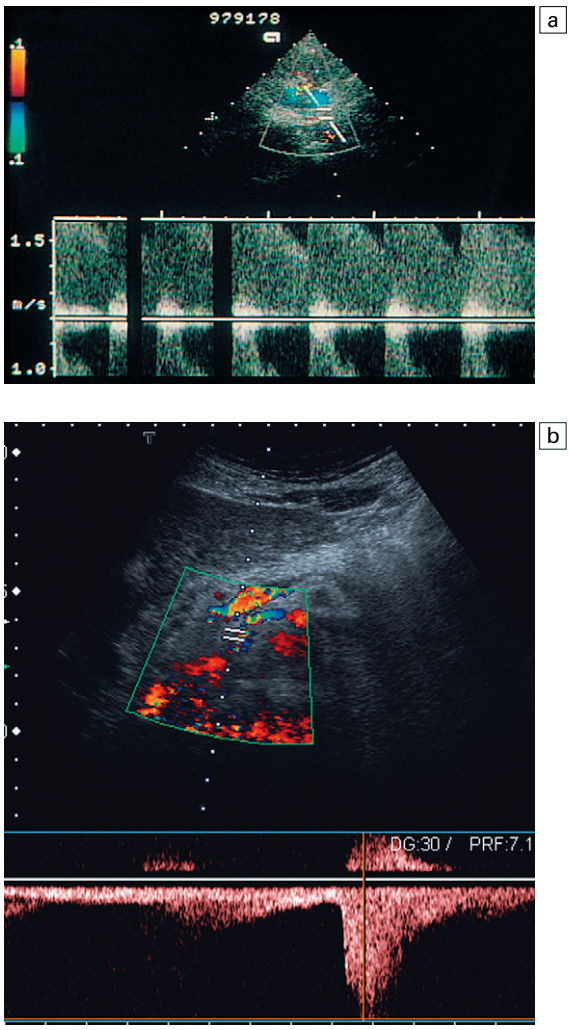


**Fig. 8.31** (a) Right renal artery stenosis. There is increased flow velocity with a liasing of the Doppler spectrum. (b) Right renal artery stenosis. Patient presented with flash pulmonary oedema. Only a single heart cycle is demonstrated because of the dyspnoea. Peak flow velocity within the right renal artery is 240 cm $s^{-1}$.

than absolute measurements of velocity, is that it takes into account poor inflow; it is important to remember that these patients are often arteriopaths and consequently may have poor cardiac output.[8]

However, initial enthusiasm for the technique of direct evaluation of the main renal arteries for signs of renal stenosis has been markedly tempered by the results of more recent studies. Some of these have indicated that the sensitivity of detection may be as low as 20% in comparison to early claims of sensitivities in excess of 80%.[9]

Much of the difficulty relates to the poor imaging of the entire length of the renal artery. Enhanced visualisation of the main renal arteries resulting from the use of effective ultrasound contrast agents has been shown to improve efficacy of the technique allowing Doppler rescue but accuracy of diagnosis of renal artery stenosis remains less than other imaging modalities such as multislice computed tomography (CT).

Similarly the demonstration of accessory renal arteries with ultrasound is unreliable. Where a polar artery is stenosed, and is the cause of renovascular hypertension this will be only rarely demonstrated. Meticulous attention to technique is vital to optimise the opportunity for visualisation of accessory vessels. In addition to the formal structured approach to the renal arteries, a coronal scan through the kidney, whose plane is directed towards the aorta, will allow visualisation of the renal hilum. Moving the colour box towards the aorta, enlarging the box, and/or slightly changing the plane of scan will allow the detection of larger accessory vessels and occasionally renal artery stenosis (Fig. 8.33).

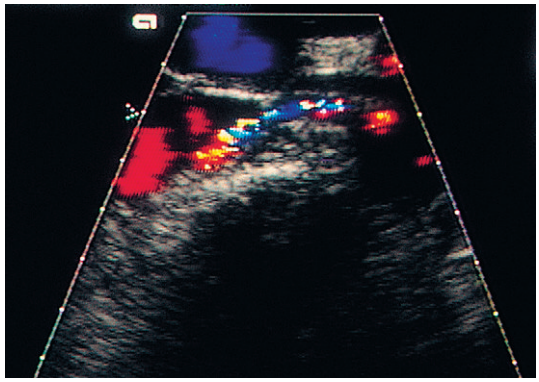

**Fig 8.32** Colour flow Doppler of the origin of the right renal artery in a patient with renal artery stenosis. There is significant disturbance of the flow with a mosaic pattern within the colour signal.

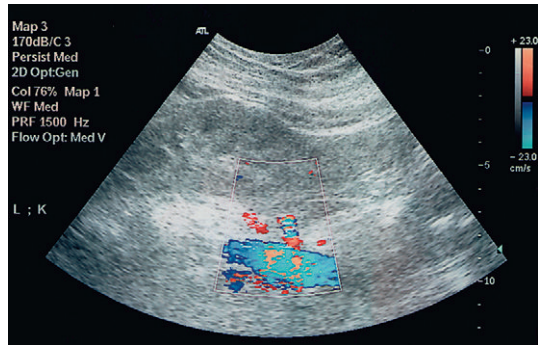


**Fig. 8.33** Coronal view of left kidney. There is significant colour aliasing within a lower polar artery. Diagnosis, polar artery stenosis.

### *Findings in the intrarenal vessels*

The intrarenal vessels can be imaged in most patients. Haemodynamically significant stenoses will produce significant downstream effects within the intrarenal arteries. These have been described as a 'tardus parvus' pattern, with a low-amplitude signal that has a prolonged systolic acceleration time and which appears delayed in relation to the QRS complex of the electrocardiogram (ECG). Duplex indices used to characterise this waveform include a systolic acceleration time above 0.07 s, an increase in the acceleration index in excess of 378 cm $s^{-1}$, a reduced resistance index of less than 0.5 and decreased peak systolic velocities (Fig. 8.34).[10,11] In practice these changes will only reliably identify stenoses greater than 70% diameter reduction. Furthermore, diffusely diseased arteries without a significant focal stenosis may also show these changes, with a significant false-positive rate. Considerable care is therefore necessary in the interpretation of intrarenal waveforms.

### *Screening for renal artery stenosis*

Patients with renovascular hypertension and those with renal failure consequent upon disease of the main renal artery may benefit from a number of possible revascularisation techniques such as angioplasty. Duplex ultrasound is one of a number of techniques which have been proposed as possible screening tools. However, direct signs of renal artery stenosis require visualisation of the main renal artery; most reports would indicate that this is possible in at best only 70% of cases, and that this is only marginally improved by the use of currently available ultrasound contrast, because the problems of obesity and bowel gas remain. Significant interest has therefore centred on the role of the indirect signs from the intrarenal vessels, since these measurements are simpler and quicker to perform and are possible in more than 90% of patients. There are, however, wide variations of 60–90% in the reported sensitivity of this technique, with some authors reporting even lower values.[11,12]

The efficacy of surgical and percutaneous techniques in the treatment of renovascular disease remains controversial. It is therefore important

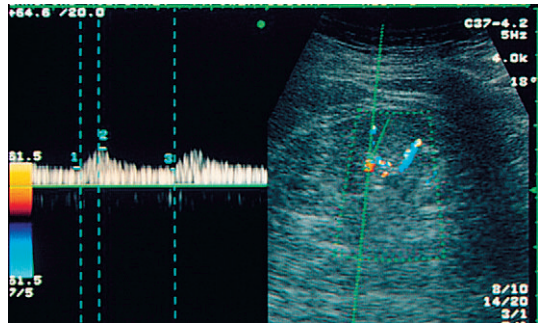


**Fig 8.34** The tardus parvus pattern of renal artery stenosis. Assessment of the intrarenal vessels demonstrates a delay in the time to maximum systole and an increase in the acceleration index.

to ensure that patients are selected who are most likely to benefit from intervention. A renal artery resistance index of 0.8 or greater reliably identifies patients with renal artery stenosis in whom angioplasty or surgery will not improve renal function, blood pressure or kidney survival. Where this is combined with a renal length of less than 9 cm, the outcome is universally poor (Fig. 8.35).

While we would not, therefore advocate the use of renal Doppler as a screening test for renal artery stenosis the technique retains a role in patient selection, in the evaluation of equivocal angiographic findings and follow-up after angioplasty.[13]

## Renal artery aneurysm

Renal artery aneurysms are uncommon. Previously on static B-mode imaging, mistaking the dilated left renal vein, produced by the nutcracker effect on the vein by the superior mesenteric artery, led to false diagnoses of renal artery aneurysm. With modern real-time equipment an aneurysm can almost always be identified in continuity with the renal artery. Colour Doppler will demonstrate the flow direction and characteristic venous pulsatility in the case of a prominent vein, or the disordered arterial flow associated with an aneurysm.

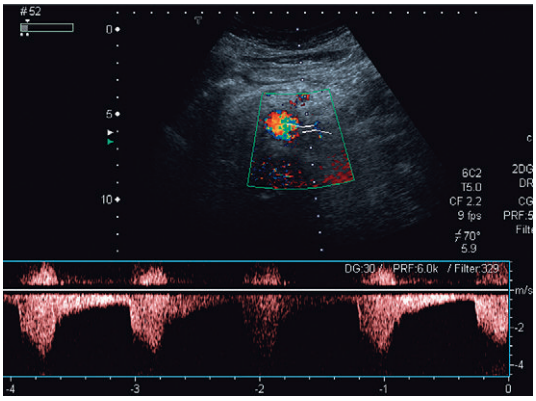


**Fig. 8.35** Left renal artery Doppler demonstrating increased systolic flow velocity in excess of 2 m $s^{-1}$ but reduced diastolic flow and consequent increased resistance index.

## Aortic aneurysm

Ultrasound plays a central role screening for and the diagnosis of abdominal aortic aneurysm. Although it is usually possible to demonstrate the origin of the renal arteries relative to the aneurysm the variability of renal vascular anatomy means that polar vessels may be missed. Where the ostia are involved in the aneurysm this can be demonstrated and flow abnormality detected (Fig. 8.36).

## Aortic dissection

Ultrasound is of value in assessing dissection of the abdominal aorta. Although this is significantly less common than thoracic aortic dissection, it can occur as a consequence of the extension of a thoracic dissection into the abdominal aorta, or subsequent to interventional procedures performed via the transfemoral route. The aortic flap can be identified on real-time ultrasound, while flow within both the true and false lumen can be documented. Flow may be towards the legs in both channels, or may be reversed in the false lumen (Fig. 8.37). The course of the dissection is often spiral; consequently one renal artery may be supplied by the true lumen of a dissection and the other by the false lumen. Documentation of impaired flow within one or other of the renal arteries, or in the intrarenal vessels, is of

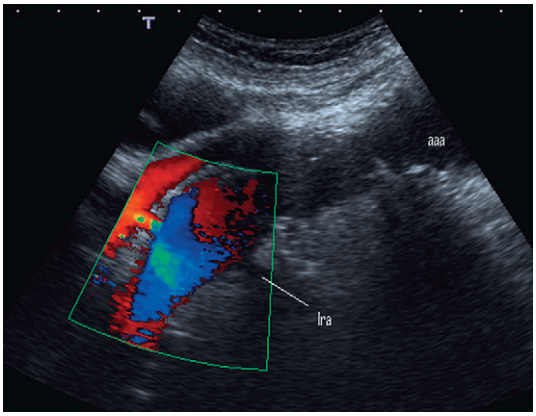


**Fig. 8.36** Distal abdominal aortic aneurysm. Same case as Figure 8.30. The renal arteries are not compromised by the aneurysm, but the origin of the left renal artery is identified. There is no colour flow. Renal vascular compromise caused by atheroma.

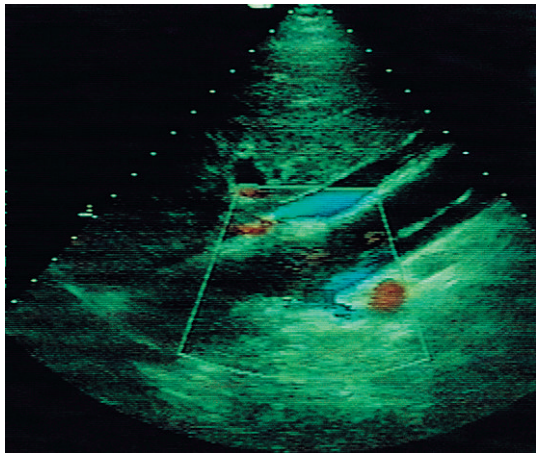

**Fig 8.37** Colour flow Doppler examination of the aorta in a case of aortic dissection. There is reverse flow in the false lumen which modifies flow within the left renal artery. The reverse flow is demonstrated (in blue) underneath the linear echogenic dissection flap. From Dubbins[33], with permission.

significant prognostic value in cases such as this, since it will identify a kidney at risk of ischaemia. In such cases, revascularisation may be considered.[14]

## Arteriovenous malformation/fistula

In the native kidney these are almost invariably post-traumatic following penetrating injury. Small arteriovenous fistulae following renal biopsy are usually short lived, although when large they can compromise renal function and renal survival. These are described in the section on renal transplantation (see Ch. 9). Larger arteriovenous fistulae can be encountered following trauma such as knife injuries. In these cases, both the main renal artery and the main renal vein may enlarge, with increased flow velocities, decreased pulsatility and resistance indices within the renal artery, and high flow velocities within the renal vein.

The site of the arteriovenous communication is identified by reducing the colour sensitivity, so that only high velocity is detected. In this situation no flow is demonstrated within the normal renal parenchyma but there remains a high-intensity colour signal at the site of the fistula. This is frequently accompanied by a tissue 'bruit' visible on colour Doppler as a mosaic of colour extending into the renal parenchyma around the fistula (Fig. 8.38).[15]

## Atheroembolic disease

Embolism of atheroma within the renal vascular tree is a cause of significant renal dysfunction, producing wedge-shaped infarcts and subsequent scarring. Theoretically colour Doppler, and in particular power Doppler with its increased sensitivity to low-flow states, should be able to provide a global view of renal perfusion (Fig. 8.39). While it is possible with both colour and power Doppler to show focal ischaemia and focal infarcts, both techniques suffer from limitations of inadequate penetration to the posterior kidney. Therefore focal colour-free segments in this area cannot reliably be defined as infarcts, as the features may simply be the result of technical difficulties with colour sensitivities. Ultrasound contrast has been advocated as a tool to resolve some of these difficulties. The blood pool contrast agents certainly demonstrate tissue perfusion, even in difficult patients, but gas microbubbles may produce significant sound attenuation, which will degrade the signal from the more deeply

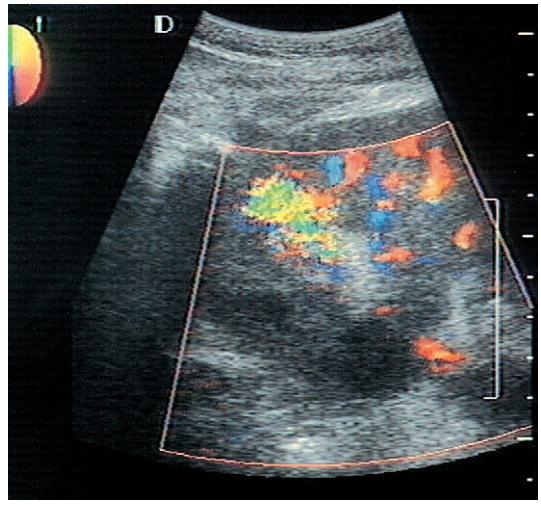


**Fig 8.38** Arteriovenous fistula. Colour flow Doppler demonstrates increased focal flow within the kidney, with a tissue bruit of colour out with the renal vessels caused by vibration of the adjacent renal substance.

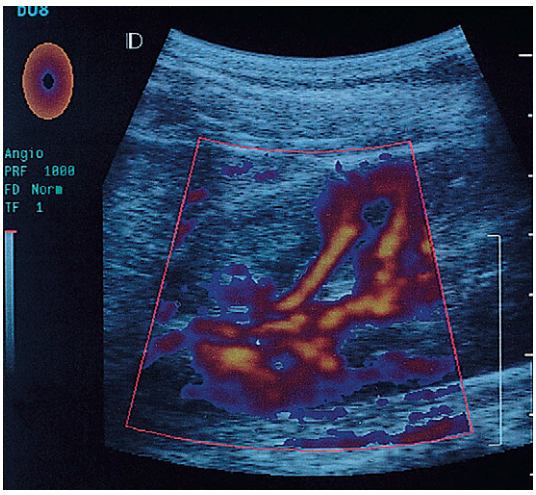


**Fig 8.39** Colour power Doppler evaluation of a patient with focal ischaemia of the kidney. There is normal perfusion in the lower and mid-poles but the anterior surface of the upper pole is avascular.

situated renal parenchyma with the same potential for perfusion defect artefacts. With newer contrast agents it appears possible to maximise Doppler enhancement while minimising the shadowing effect[16] (Fig. 8.40).

## Renal vein thrombosis

This is an uncommon condition in adults; it occurs most commonly in association with the extension of a renal tumour (see below). Rarely, extrinsic compression or haematological conditions which produce an increased tendency for thrombosis may predispose to renal vein thrombosis. In infants, renal vein thrombosis may occur as a complication of dehydration.

Colour Doppler may show no flow in the renal parenchyma, or 'flash flow' where the colour signal is seen only transiently, corresponding to peak systole (Fig. 8.41). Occasionally a 'to-and-fro' pattern may be seen with alternating red and blue colour signals visible within the renal arteries. Spectral Doppler may show absent, or reversed, diastolic flow. A 'W' shape to the arterial diastolic flow component, in association with absent venous flow on colour Doppler, is thought to be characteristic of renal vein thrombosis, although other conditions may produce reversed diastolic flow, including acute tubular necrosis and cardiac abnormalities such as aortic incompetence (Fig. 8.42).[17]

## Renal infection

The findings in renal infection are extremely variable. Infection may be consequent upon the ascending route via the ureter or may be blood borne. Parenchymal infection has been described as global or focal although pathological studies would suggest that these patterns are part of a continuum of disease. Imaging findings include an enlarged kidney, focal masses of varying

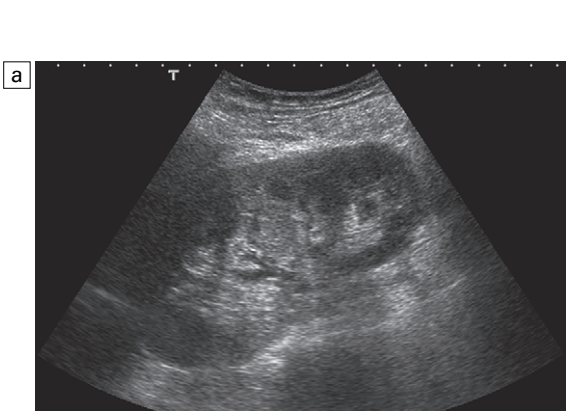


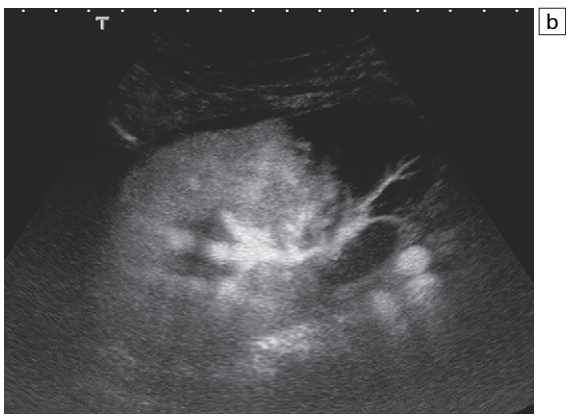


**Fig. 8.40** (a) Focal renal infarct. Kidney appears structurally normal. There is possibly slight decrease in echogenicity of the lower pole. From D.L Cochlin, with permission. (b) Following contrast the lower pole is not perfused.

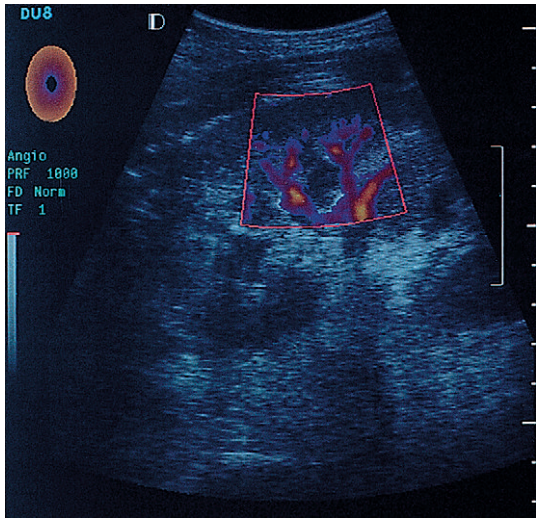


**Fig 8.41** Flash flow of renal vein thrombosis. Poverty of flow to the kidney with only brief demonstration of flow within the central vessels.

echogenicity, capsular thickening (the renal rind) and abscess formation. There may be dilatation of the collecting system with thickening of the urothelium.

Blood flow findings depend upon the influence of the balance between hyperaemia consequent upon infection, and reduced flow consequent upon renal swelling and capsular stretching. Thus there may be a global or focal increase in blood flow, with a reduction in the Doppler indices; or, more commonly, there may be reduction in blood flow and an increase in the Doppler indices. In focal pyelonephritis, this may allow the demonstration of a hypoechoic mass with an associated perfusion defect (Fig. 8.43).[18] Contrast enhanced studies using low MI techniques allow real time demonstration of renal perfusion (Fig. 8.44). When combined with contrast specific imaging packages such as those incorporating tissue harmonics or pulse inversion it is possible to demonstrate focal perfusion defects which may correlate with the subsequent development of renal scars. These techniques remain to be fully evaluated. They are dependent on body habitus. Low MI will afford only modest penetration of the sound beam and although there is significant signal enhancement by microbubbles, sound attenuation by fat and by the bubbles themselves may make it difficult to assess deep structures. This has particular importance for false-positive diagnosis of perfusion defects.

### *Renal abscess*

The development of a renal or perirenal abscess is an uncommon complication of renal infection. The appearances are, however, fairly characteristic, with a renal mass lesion showing central necrosis subsequently developing into an irregular cystic lesion with thick walls. Blood flow is usually increased around the margin of the lesion, producing a 'colour halo', although this is indis-

a

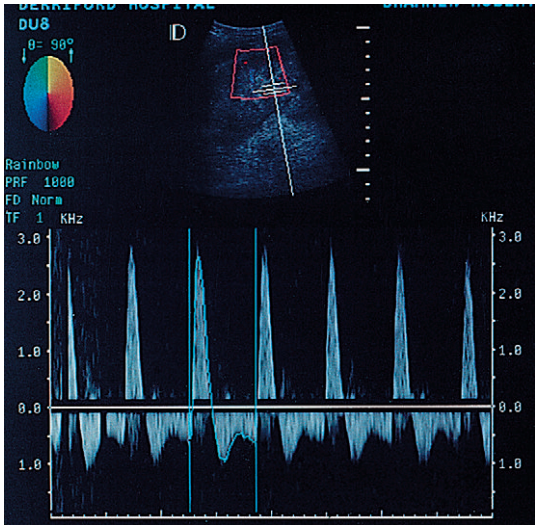


b

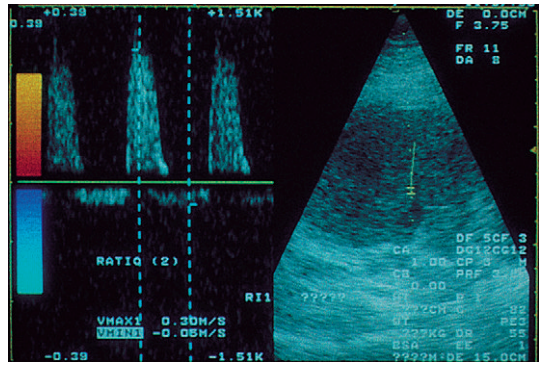


**Fig 8.42** (a) Renal vein thrombosis. Spectral pattern demonstrating the W-shaped flow pattern in diastole characteristic of renal vein thrombosis. (b) Reversed flow in diastole consequent upon aortic incompetence. Image courtesy of Dr D.L. Cochlin.

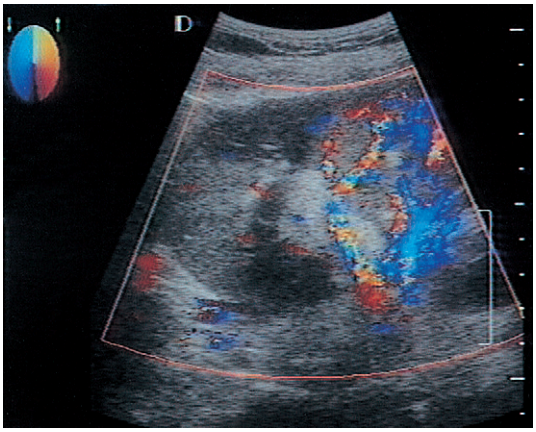

**Fig 8.43** Colour flow Doppler image demonstrating blood flow at the hilum and within the kidney. Note there is absent flow to the upper pole in this patient with focal pyelonephritis.

tinguishable from a necrotic renal tumour. Usually a combination of clinical history and grey-scale features, as well as colour Doppler, will allow the correct diagnosis (Fig. 8.45).

## Renal tumour

Angioneogenesis occurs as part of the disordered growth of renal tumours. As a consequence it was felt that both colour Doppler and spectral Doppler might provide a means of assessment of renal tumours. However, reports are varied in terms of the success of colour Doppler in distinguishing between malignant and benign pathology of the kidney.[19–21] Comparisons with contrast angiography suggest that the accuracy of the technique is likely to be less than has been hoped, as both benign and malignant tumours can be either hypo- or hypervascular. Angiomyolipomas, for example, can be extremely vascular and demonstrate blood pooling while, conversely, transitional cell tumours are characteristically hypovascular.[22] However, in the evaluation of cystic lesions of the kidney the assessment of complexity can be improved by the demonstration of colour flow within septa which is a strong predictor of malignancy (Fig. 8.46).

Examination of renal tumours with colour Doppler requires the colour box to be opened to include the whole of the tumour and a small portion of the adjacent normal renal parenchyma, so as to demonstrate the difference in size, distribution and communication of the abnormal blood vessels. High- and low-velocity blood flow patterns have been described, predominantly in the margin of the tumour but also extending within the tumour mass. Characteristic colour flow patterns are of large irregular marginal vessels extending into the centre of the tumour with an abnormal irregular branching pattern. The pattern of flow is extremely variable. Some tumours are

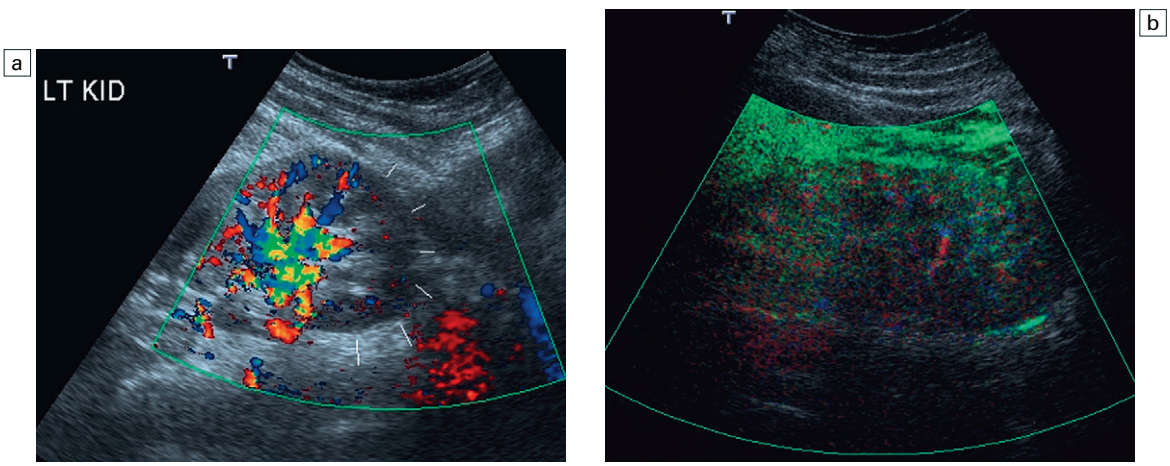


**Fig. 8.44** (a) Focal pyelonephritis. The lower pole of the left kidney is enlarged. There is a possible area of focal ischaemia at the extreme lower pole. From D.L. Cochlin, with permission. (b) The entire kidney appears poorly perfused after contrast injection, but with irregular perfusion defects from the equatorial region to the lower pole. Only the upper pole and parts of the lower pole appear well perfused.

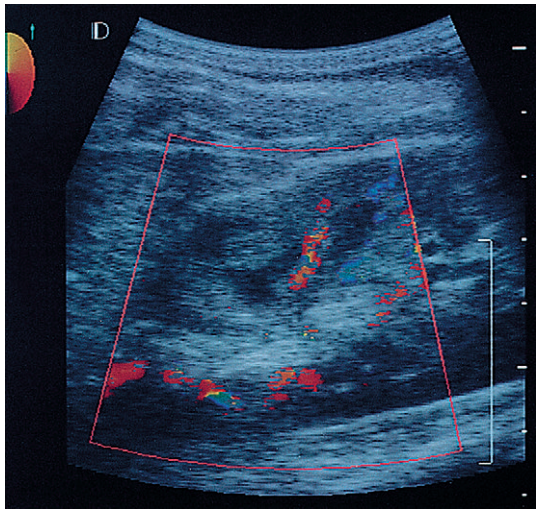

**Fig 8.45** Renal abscess. Colour flow Doppler of the kidney. There is an irregular area within the upper pole of the kidney. There is no flow within the centre of the lesion but circumferential flow.

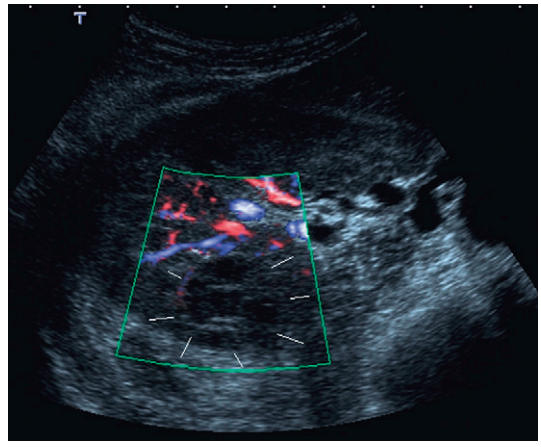

**Fig. 8.46** Benign cystic nephroma of the kidney. There is no evidence of blood flow within the septa of the tumour. From D.L. Cochlin, with permission.

a

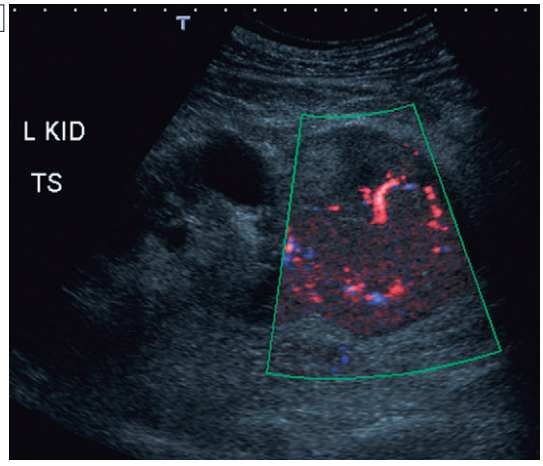


b

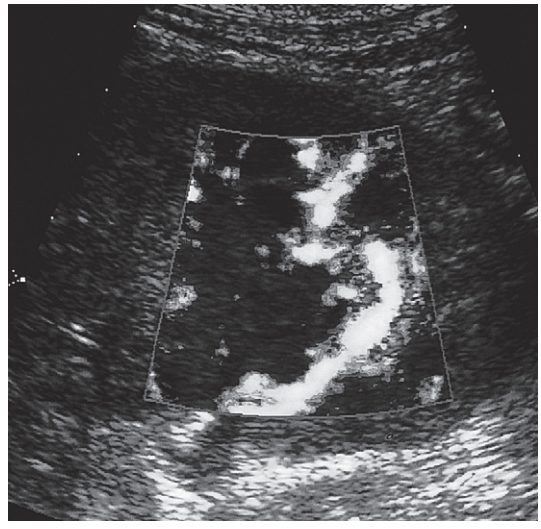

c

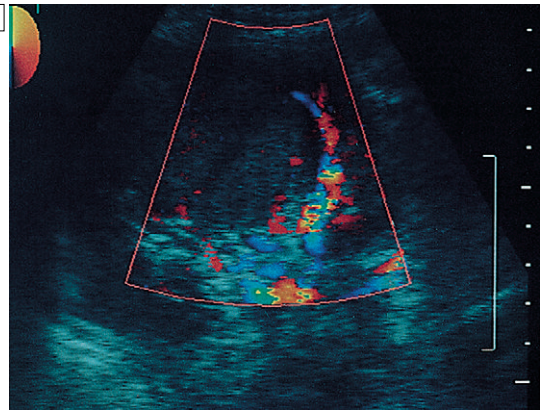

**Fig. 8.47** (a) Colour flow Doppler of a lower pole renal mass demonstrating irregular vessels and colour pooling. (b) Colour power Doppler of renal tumour with irregular peripheral flow and central necrosis. (c) Colour flow Doppler of tumour with relatively avascular appearance and only peripheral flow.

relatively avascular, while others exhibit areas of necrosis producing largely circumferential, irregular flow (Fig. 8.47).

Contrast enhanced ultrasound affords the greater characterisation of intratumoral blood flow. There is improved sensitivity of demonstration of irregular marginal vessels and of neovascularisation of septa with improved confidence of the diagnosis of malignancy. The pattern of contrast enhancement allows the differentiation of tumour from pseudomasses such as the hypertrophied column of Bertin, as well as affording the characterisation of specific renal masses in some cases (Fig. 8.48). The use of three-dimensional

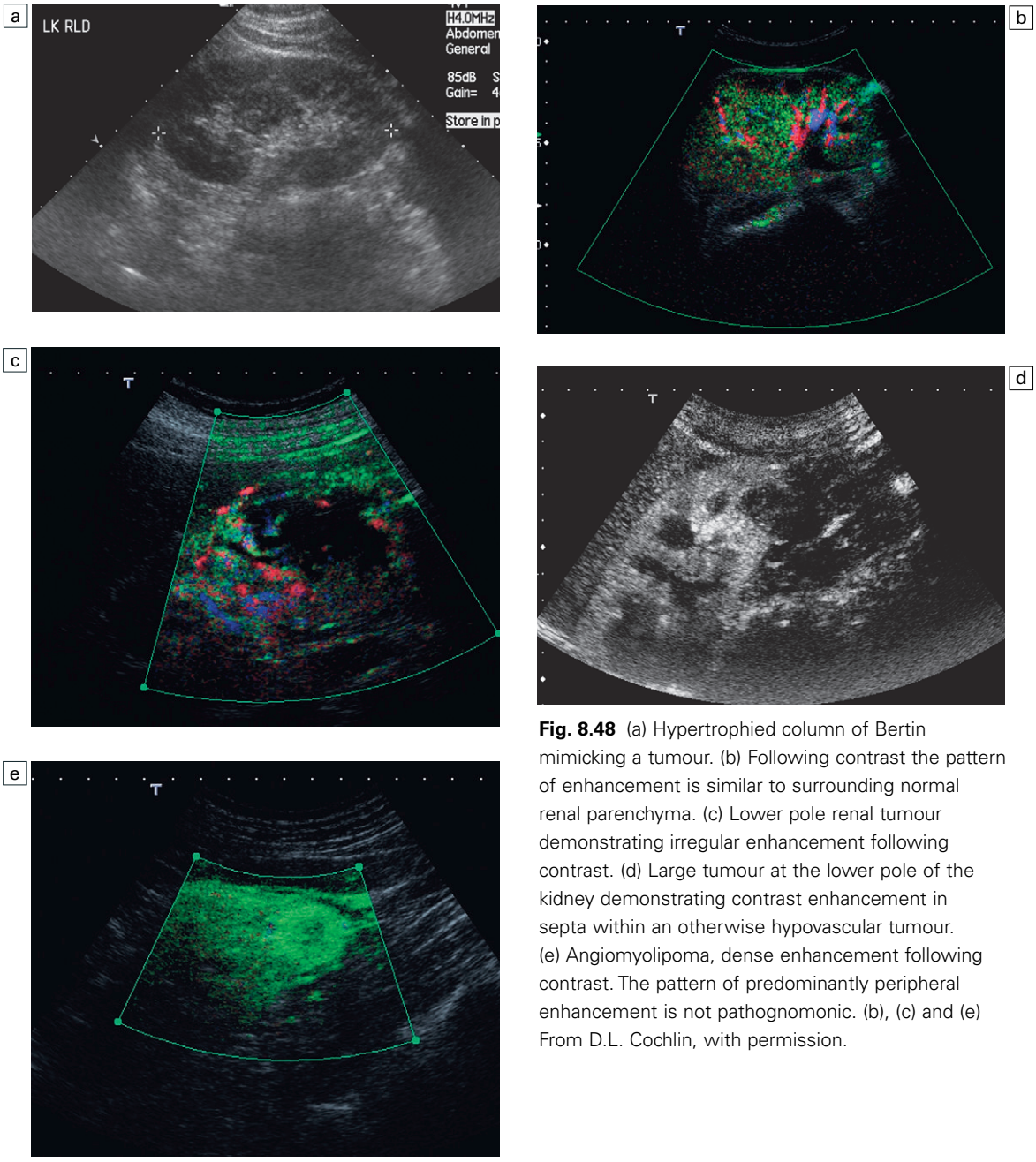


**Fig. 8.48** (a) Hypertrophied column of Bertin mimicking a tumour. (b) Following contrast the pattern of enhancement is similar to surrounding normal renal parenchyma. (c) Lower pole renal tumour demonstrating irregular enhancement following contrast. (d) Large tumour at the lower pole of the kidney demonstrating contrast enhancement in septa within an otherwise hypovascular tumour. (e) Angiomyolipoma, dense enhancement following contrast. The pattern of predominantly peripheral enhancement is not pathognomonic. (b), (c) and (e) From D.L. Cochlin, with permission.

power Doppler, with and without the use of contrast agents, is being explored in an attempt to characterise blood flow patterns specific for benign and malignant tumours, but this work remains in its infancy. Spectral Doppler may show scattered high-frequency signals both at the margin and within the body of the tumour, presumably representing flow through vessels supplying arteriovenous communications.[21] In very large hypervascular tumours with extensive arteriovenous shunting, blood flow within the main renal artery is abnormal with increased systolic flow velocities and spectral broadening.

Colour Doppler may refine the ability of real-time scanning to evaluate invasion/thrombosis of the renal vein. When thrombus is present the renal vein is distended and contains low-level echoes (Fig. 8.49). Colour Doppler demonstrates flow around the thrombus or tumour thrombus. It is only rarely possible to identify blood flow within the tumour thrombus itself and thus distinguish between tumour and non-tumour thrombosis. In total occlusion of the renal vein, no colour flow signal is identified and the spectral flow within the renal artery demonstrates a high-resistance flow pattern with absent or reversed flow in diastole (Fig. 8.50).

## Obstruction

The intravenous urogram once the mainstay of diagnosis of acute obstruction is rapidly being replaced by non-contrast enhanced CT. Ultrasound has long had a role in the demonstration of hydronephrosis, particularly in long-standing

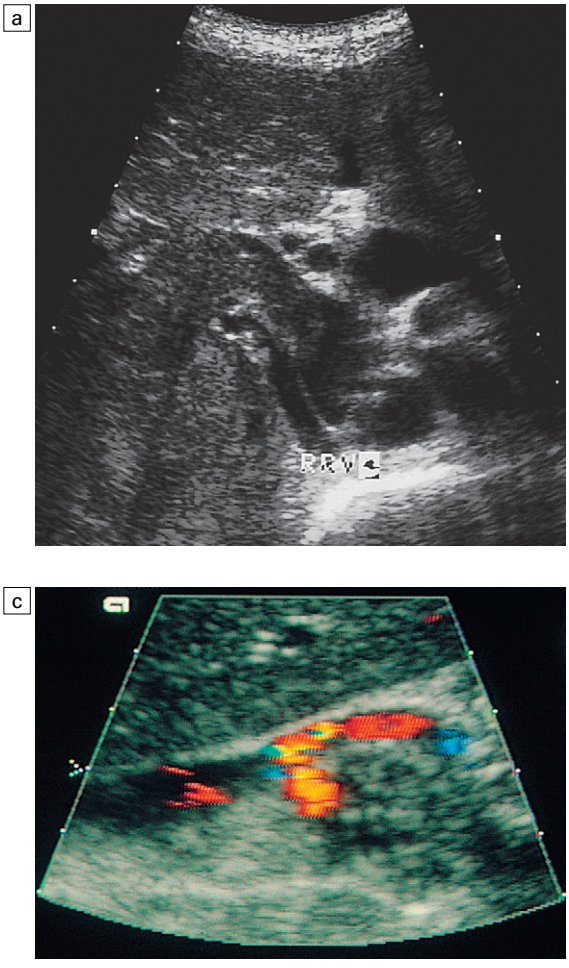


**Fig 8.49** (a) Transverse scan through the left renal vein. The left renal vein is distended and filled with echogenic material, indicating either extension of tumour into the vein or renal vein thrombosis. (b) Same patient – extension of the echogenic thrombus/tumour into the inferior vena cava. (c) Distortion of the inferior vena cava and encasement of the adjacent right renal artery by tumour extending beneath the inferior vena cava from the adjacent right kidney.

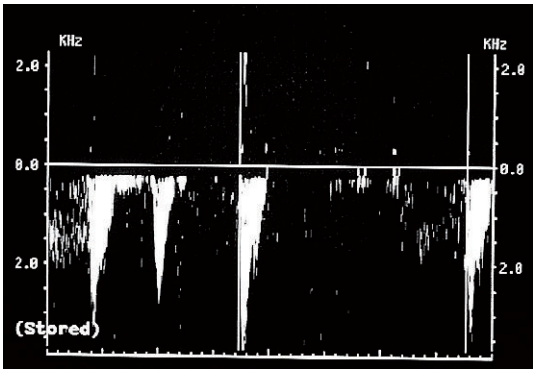


**Fig 8.50** Absent diastolic flow in a patient with renal vein involvement by tumour.

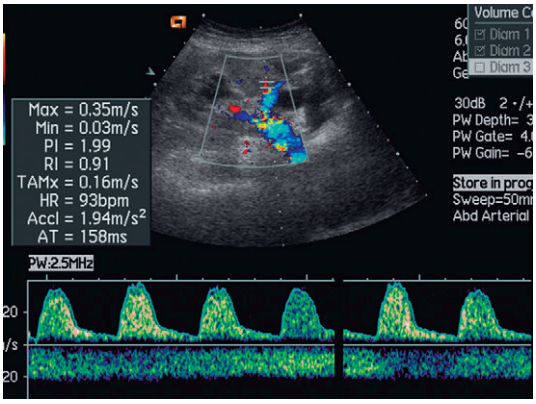


**Fig. 8.51** Renal obstruction. There is significant reduction in the diastolic component flow with a resistance index of 0.91.

obstruction from whatever cause. Features of obstruction on real-time imaging include dilatation of the calyces and of the renal pelvis; dilated ureters can also be identified posterior to the urinary bladder. In acute obstruction, however, there is often no evidence of calyceal or pelvic dilatation and the kidney may appear structurally normal on ultrasound. In this situation, repeat ultrasound after 8–12 h will usually demonstrate the development of pelvicalyceal dilatation.

However, there are alterations in intrarenal pressure consequent upon the obstruction and these may be detected by the use of Doppler techniques. Thus in acute obstruction an increase in the pulsatility index and in the resistance index has been reported. Resistance indices of greater than 0.7, or with the difference between the two sides of greater than 0.05, imply renal obstruction (Fig. 8.51).[23] The findings are time dependant. There is usually no detectable Doppler abnormality in the first 6 h and the change in Doppler spectra gradually returns to normal after 48 h.

However, not all workers have found Doppler ultrasound to be of value in the diagnosis of obstruction; sensitivities vary from 44 to 92%.[24, 25] This author's own experience suggests that in patients in whom an intravenous urogram is contraindicated, such as pregnancy, the combination of Doppler indices with the finding of asymmetric ureteric jets in the bladder is a reliable discriminator of ureteric obstruction, and is a useful screening test to determine which patients should proceed to contrast radiological studies (Fig. 8.52).[26]

a

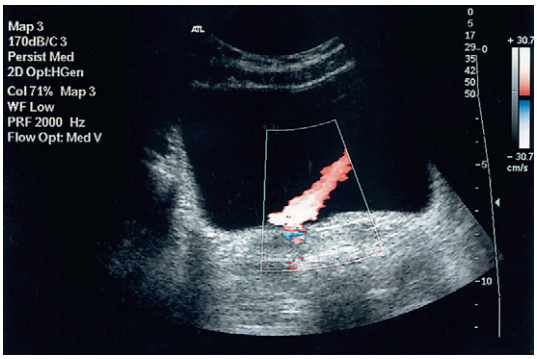


b

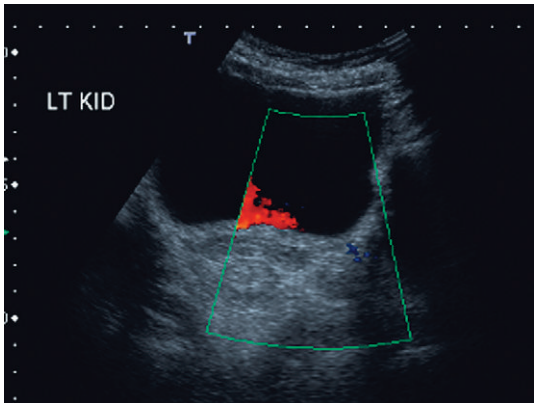


**Fig. 8.52** (a) Normal ureteric jet. (b) Poor flow through the right ureteric orifice on colour flow Doppler in a right ureteric calculus.

Although entry of the urine into the bladder is not usually synchronous, the demonstration of three or more jets on one side without a single jet identified on the other side, or an abnormally directed jet with an abnormal rather diffuse colour signal, implies obstruction of the ipsilateral ureter.

The accuracy of ultrasound findings including Doppler and jet detection is greatest in patients with acute and complete obstruction and is diminished in patients where obstruction is incomplete.

### *Diuretic enhanced sonography*

In cases of renal obstruction, including pelviureteral junction obstruction and calculus obstruction, the use of an intravenous diuretic, such as frusemide, may increase the sensitivity for detection of obstruction. If the ureter is obstructed, the administration of a diuretic will often produce a more marked alteration in the diastolic flow component of the waveform, and therefore a more marked increase in the resistance index.[27] In addition, diuresis will increase the frequency with which normal ureteric jets are identified. This would therefore enhance the detection of abnormalities of ureteric jet production. Similar effects occur in response to a fluid load, and some workers prefer this approach, particularly in children. Diuresis sonography, however, is only indicated when there is a strong contraindication to radiological contrast agents or to ionising radiation.

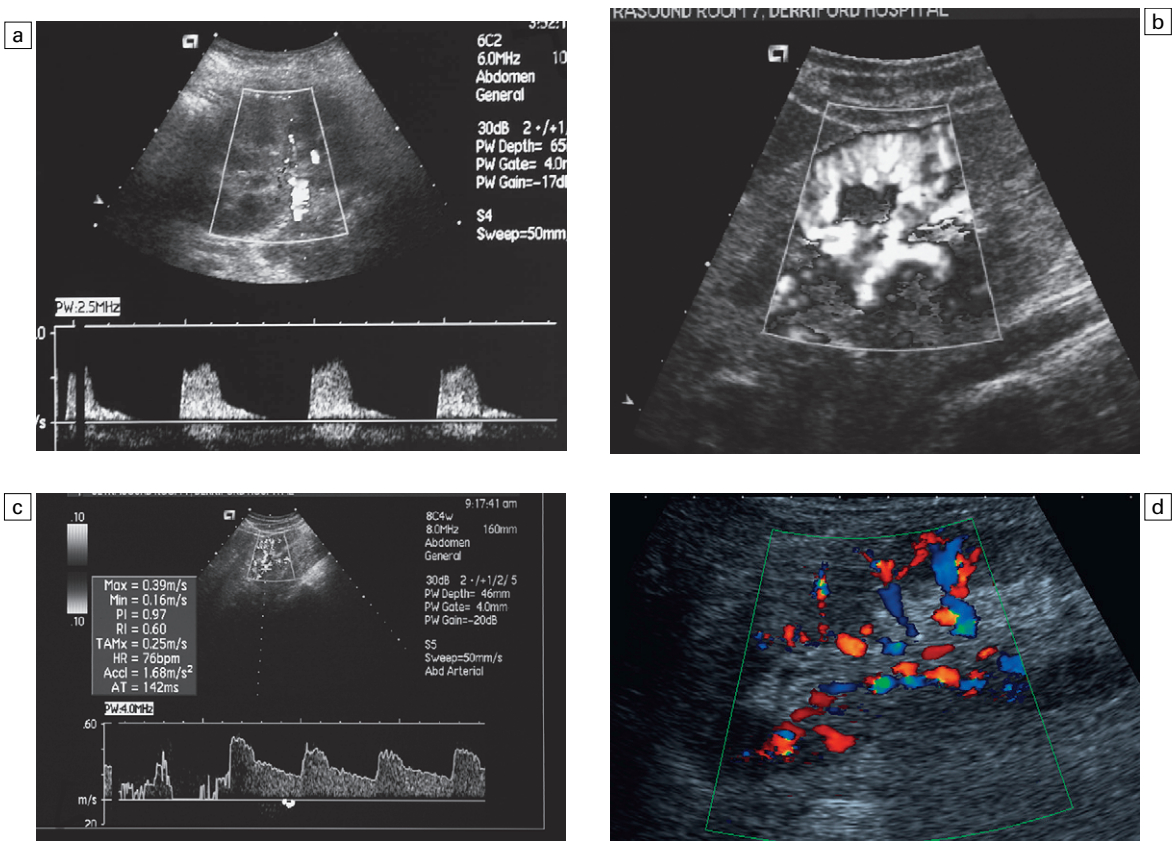


**Fig. 8.53** (a) Diffuse parenchymal renal disease. The patient presented with raised creatinine. There is absent diastolic flow. (b) and (c) Power Doppler and spectral Doppler in a patient with early diabetic nephropathy. The kidney is well perfused. (d) Patchy colour perfusion of a patient with diffuse parenchymal renal disease. Current resolution does not afford the clear demonstration of intrarenal shunting.

## Renal trauma

In cases of renal trauma, CT is normally performed on patients in whom renal injury is likely but ultrasound may be used instead. Colour Doppler can demonstrate reduced or absent flow to the renal parenchyma. While this will not differentiate between vascular transection and severe spasm, it does suggest the need to consider angiography. It is important to optimise colour Doppler settings for the detection of low flow, and therefore institute the lowest high-pass filter together with a low pulse repetition frequency while ensuring that flash artefact is minimised.

## Diffuse renal disease

There are many different causes of diffuse renal disease which may affect glomerular integrity, the tubulointerstitial region of the medulla, or the vessels directly. For the most part, in purely glomerular disease of any aetiology, the grey-scale image and the Doppler spectrum are unaffected until late in the disease process. In renal disease of tubulointerstitial distribution, or that consequent upon a vasculitic process, there is frequently an increase in cortical echogenicity with accompanying enhancement of corticomedullary differentiation. Concomitant with this is an increase in resistance to blood flow with an increase in the resistance and pulsatility indices (Fig. 8.53).[28]

In kidneys with end-stage disease from whatever cause, it is often difficult to detect any blood flow with colour, power Doppler, or with spectral Doppler. When detectable, Doppler spectra are of low systolic amplitude with poor or absent diastolic flow.

Doppler is therefore of limited use in diffuse renal disease. The specificity of the technique in differentiating between the various causes of renal dysfunction is not sufficient to make this of clinical use and allow avoidance of biopsy.[29,30] There is an association between deteriorating serum creatinine and rising Doppler indices but this is not sufficiently reliable to allow the use of Doppler to monitor the disease process.

In a small kidney, the demonstration of absent diastolic flow within the intrarenal vessels is strong evidence that this is consequent upon diffuse renal disease, or small vessel disease. This may be important for differential diagnosis. A small kidney consequent upon renal artery stenosis that may respond to revascularisation will exhibit a tardus parvus pattern within the intrarenal vessels (Fig. 8.34).[31]

## Contrast media

The advent of third-generation ultrasound contrast media now allows the demonstration of blood pool enhancement in the kidney. Currently, the

**Table 8.2** Indications for renal Doppler

| Investigation/purpose | Possible cause/indication |
|---|---|
| 1. To confirm renal perfusion | Renal trauma<br>Reduction in renal size, etc. |
| 2. Diagnosis of renal vein thrombosis | Tumour<br>Dehydration (infant)<br>Hypovolaemia<br>Abnormal clotting |
| 3. Renal obstruction | Contrast hypersensitivity<br>Pregnancy |
| 4. Renal tumour vs pseudotumour | |
| 5. Renal artery stenosis | Equivocal angiogram<br>Follow-up to angioplasty, etc.<br>(Screening) |
| 6. Arteriovenous abnormalities | |
| 7. Aortic aneurysm and aortic dissection | |

duration of enhancement by commercially available ultrasound contrast media is only short lived, being of the order of 2–3 min after bolus injection; this may possibly be extended by the use of infusion techniques. No well defined clinical role has as yet been established for contrast media in the enhancement of Doppler signals from the kidney, although it is possible to demonstrate perfusion defects in focal pyelonephritis and Doppler rescue is possible in a number of cases where the main renal artery is interrogated. Further roles for ultrasound in evaluation of the entire renal vascular supply, the demonstration of abnormal vascular anastomoses in tumours and in the measurement of global and regional volume flow will depend upon extended enhancement intervals, improved algorithms for flow detection and computer packages for flow and perfusion calculation.

## SUMMARY

Doppler techniques now allow the assessment of intrarenal vessels in most patients (Table 8.2). Currently, however, the role of Doppler in the kidney is limited. It may help to resolve problems with mass lesions, including the differentiation of tumours from pseudotumours such as a hypertrophied column of Bertin. It may allow the assessment of renal obstruction when there is a contraindication to X-ray contrast agents. It may clarify the diagnosis of renal artery stenosis in the case of an equivocal angiogram, and it will allow the identification of significant renal venous disease. The greater sensitivity of modern ultrasound systems combined with improved visualisation with echo-enhancing agents may allow visualisation and assessment of the entire renal vascular supply in the future.

## REFERENCES

1. Dubbins P. Renal artery stenosis – duplex Doppler evaluation. Br J Radiol 1986; 59:225–229.
2. Taylor GA, Ecklund K, Dunning PS. Renal cortical perfusion in rabbits: visualization with colour amplitude imaging and an experimental microbubble-based US contrast agent. Radiology 1996; 201(1):125–129.
3. Keogan MT, Kliewer MA, Hertzberg BS, et al. Renal resistive indexes: variability in Doppler US measurement in a healthy population. Radiology 1996; 199(1):165–169.
4. Gill B, Palmer LS, Koenigsberg M, et al. Distribution and variability of resistive index values in undilated kidneys in children. Urology 1994; 44(6):897–901.
5. Boddi M, Sacchi S, Lammel RM, et al. Age-related and vasomotor stimuli-induced changes in renal vascular resistance detected by Doppler ultrasound. Am J Hypertens 1996; 9(5):461–466.
6. Knapp R, Plotzeneder A, Frauscher F, et al. Variability of Doppler parameters in the healthy kidney: an anatomic-physiologic correlation. J Ultrasound Med 1995; 14(6):427–429.
7. Taylor DC, Kezzler MD, Moneta GL, et al. Duplex ultrasound scanning in the diagnosis of renal artery stenosis: a prospective evaluation. J Vasc Surg 1988; 7:363–369.
8. Strandness DE. The renal arteries. In: Strandness DE, ed. Duplex scanning in vascular disorders, 2nd edn. New York: Raven Press; 1993:197–215.
9. Berland LL, Koslin DB, Routh WD, et al. Renal artery stenosis: prospective evaluation of diagnosis with colour duplex US compared with angiography: work in progress. Radiology 1990; 174:421–423.
10. Handa N, Fukunaga R, Etani H, et al. Efficacy of echo Doppler examination for the evaluation of renovascular disease. Ultrasound Med Biol 1988; 14:1–15.
11. Stavros AT, Parker SH, Yakes WF, et al. Segmental stenosis of the renal artery: pattern recognition of parvus and tardus abnormalities with duplex sonography. Radiology 1992; 184:487–492.
12. Strunk H, Jaeger U, Teifke A. Intrarenal colour Doppler ultrasound for the exclusion of renal artery stenosis in cases of multiple renal arteries: analysis of the Doppler spectrum and tardus parvus phenomenon. Ultraschall Med 1995; 16:172–179.
13. Baxter GM, Aitcheson F, Sheppard D, et al. Colour Doppler ultrasound in renal artery stenosis, intrarenal waveform analysis. Br J Radiol 1996; 69:810–815.
14. Thomas E, Dubbins PA. Duplex ultrasound of the abdominal aorta – a neglected tool in aortic dissection. Clin Radiol 1990; 42:330–334.
15. Ozbek SS, Memis A, Killi R, et al. Image-directed and colour Doppler ultrasonography in the diagnosis of postbiopsy arteriovenous fistulas of native kidneys. J Clin Ultrasound 1995; 23(4):239–242.

16. Correas J-M, Kessler D, Worab D, et al. The first phase-shift ultrasound contrast agent: Echogen. In: Goldberg BB, ed. Ultrasound contrast agents. London: Martin Dunitz; 1997:101–120.
17. Tublin ME, Dodd GD. Sonography of renal transplantation. Radiol Clin North Am 1995; 33:447–459.
18. Winters WD. Power Doppler sonographic evaluation of acute pyelonephritis in children. J Ultrasound Med 1996; 15:91–96.
19. Hirai T, Ohishi H, Yamada R, et al. Usefulness of colour Doppler imaging in differential diagnosis of multilocular cystic lesions of the kidney. J Ultrasound Med 1995; 14(10):771–776.
20. Erden I, Beduk Y, Karalezli G, et al. Characterization of renal masses with colour flow Doppler ultrasonography. Br J Urol 1993; 71(6):661–663.
21. Yamashita Y, Takahashi M, Watanabe O, et al. Small renal cell carcinoma: pathologic and radiologic correlation. Radiology 1992; 184(2):493–498.
22. Horstman WG, McFarland RM, Gorman JD. Colour Doppler sonographic findings in patients with transitional cell carcinoma of the bladder and renal pelvis. J Ultrasound Med 1995; 14(2):129–133.
23. Platt JF, Rubin JM, Ellis JH. Distinction between obstructive and non-obstructive pyelocaliectasis with duplex Doppler sonography. Am J Radiol 1989; 153:997–1000.
24. Platt JF. Duplex Doppler evaluation of native kidney dysfunction: obstructive and non-obstructive diseases. Am J Radiol 1992; 158:1035–1042.
25. Tublin ME, Dodd GD, Verdile VP. Acute renal colic: diagnosis with duplex Doppler US. Radiology 1994; 193:697–701.
26. Weston MJ, Dubbins PA. The diagnosis of obstruction: colour Doppler ultrasonography of renal blood flow and ureteric jets. Curr Opin Urol 1994; 4:69–74.
27. Renowden SA, Cochlin DL. The effect of intravenous frusemide on the Doppler waveform in normal kidneys. J Ultrasound Med 1992; 11:65–68.
28. Platt JF, Rubin JM, Ellis JH. Intrarenal arterial Doppler sonography in patients with non-obstructive renal disease: correlation of resistive index with biopsy findings. Am J Radiol 1990; 154:1223–1227.
29. Argalia G, d'Ambrosio F, Mignosi U, et al. Doppler echography and colour Doppler echography in the assessment of the vascular functional aspects of medical nephropathies. Radiol Med 1995; 89(4):464–469.
30. Yoon DY, Kim SH, Kim HD, et al. Doppler sonography in experimentally induced acute renal failure in rabbits. Resistive index versus serum creatinine levels. Invest Radiol 1995; 30(3):168–172.
31. Forsberg F, Goldberg BB. New imaging techniques with ultrasound contrast agents. In: Goldberg BB, ed. Ultrasound contrast agents. London: Martin Dunitz; 1997:177–191.
32. Cosgrove D. Ultrasound contrast enhancement of tumours. Clin Radiol 1996; 51(suppl. 1):44–49.
33. Dubbins P. Urogenital ultrasound: a text atlas. London: Martin Dunitz; 1998.

# Doppler ultrasound evaluation of transplantation

# 9

Myron A. Pozniak

## INTRODUCTION

Graft and patient survival rates following solid organ transplantation are progressively improving due to refinements in surgical technique, advances in human leukocyte antigen (HLA) typing for recipient/donor matching,[1] new and greatly improved immunosuppressive agents,[2] wide acceptance of the national coordinated organ sharing system, and advances in non-invasive transplant monitoring. As the number of transplant recipients grows, there is a corresponding increase in these patients presenting for emergency care to non-transplant centres. The chances for graft survival can be significantly improved with timely identification of the aetiology of transplant dysfunction, allowing prompt medical and/or surgical intervention when necessary.

## RENAL TRANSPLANTATION

In the USA 1-year renal allograft survival rates currently approximate 89% for cadaveric and 95% for living-donor kidney transplants, with 1-year patient survival rates at 94% for cadaveric recipients and 97% for living-related kidney recipients.[3] When screening laboratory test results indicate renal transplant dysfunction, imaging studies are often required to evaluate renal morphology and perfusion. Doppler ultrasound is an ideal tool for this purpose because of its non-invasive nature, ready availability, and ability to detect and distinguish many of the vascular abnormalities that are found with transplant dysfunction. Occasionally, ultrasound can suggest functional problems, such as rejection or acute tubular necrosis.

Examination of the transplanted kidney requires careful attention to scan technique and an awareness of the potential problems. A complete sonographic examination of the renal transplant should cover the points listed in Table 9.1. The most common abnormal findings, which may be demonstrated, are listed in Table 9.2.

### Ultrasound anatomy of the renal transplant

In most cases, the transplant kidney is positioned retroperitoneally in the iliac fossa with an end-to-side anastomosis of the renal vasculature to the common or external iliac artery and vein. The transplanted ureter is implanted directly

**Table 9.1** Renal transplant sonographic examination checklist

- Review any available prior imaging studies. Review the surgical record, especially with regard to the vasculature
- Evaluate the renal collecting system. If dilated, make certain that bladder outflow obstruction is not the underlying cause
- Measure the renal length. Record any change
- Rule out perinephric fluid collections. Record any change in size if previously present
- Rule out lymphocele
- Verify uniform parenchymal perfusion by colour Doppler. Rule out tardus parvus waveform by examining the interlobar or segmental arterial waveforms for resistance and delayed systolic upstroke
- Examine the main renal artery, particularly near its anastomosis (especially if a tardus parvus waveform is observed within the transplanted kidney)
- Verify renal vein patency

**Table 9.2** Renal transplant sonographic findings and possible causes

**Increase in size of transplanted kidney**
- Hypertrophy of the kidney
- Allograft rejection
- Postoperative infection
- Renal vein thrombosis

**Reduction in size of transplanted kidney**
- Ischaemia
- Chronic rejection

**Increased renal arterial flow resistance**
- Compressive effect by transducer, adjacent mass or fluid collection
- Infection
- Advanced stages of rejection
- High-grade obstruction
- Acute tubular necrosis

**Decreased renal arterial flow resistance**
- Renal artery stenosis
- Severe aortoiliac atherosclerosis
- Arteriovenous fistula

**Renal collecting system dilatation**
- Obstructive hydronephrosis
- Ureteral anastomosis stenosis
- Chronic distention of flaccid denervated system
- Sequela of prior obstructive episode
- Bladder outlet obstruction (neurogenic bladder)

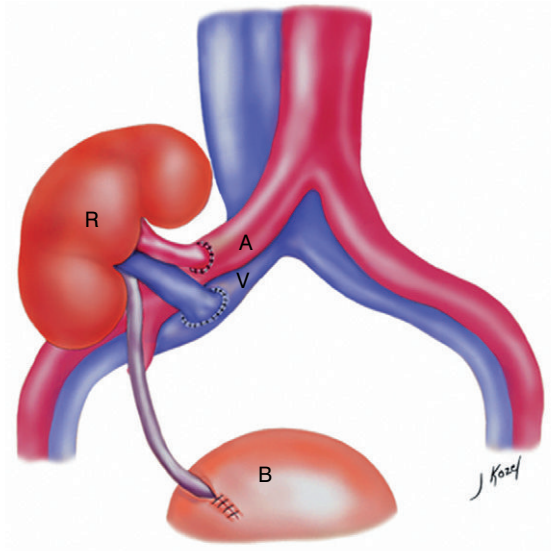


**Fig. 9.1** Artist rendering of a renal transplant (R) located in the right iliac fossa. The transplant renal artery is typically anastomosed to the common iliac artery (A). The transplant renal vein anastomosis is to the common iliac vein (V). The ureter is connected to the urinary bladder (B).

into the superior surface of the bladder or to the native ureter (Fig. 9.1). In approximately 20% of transplants, multiple arterial or venous anastomoses may be required. Because numerous technical variations exist in the way kidneys are transplanted, it is very important that the sonologist and sonographer are familiar with the surgical technique common to their institution and the specific anatomical details of the patient being scanned.[4,5] With the numerous possible variations, proper documentation and communication of the surgical record is very important in ensuring correct understanding and interpretation of imaging findings and Doppler flow profiles in renal transplantation. Ideally, if the transplant has variant vascular anatomy, a drawing is provided which shows the orientation of the kidney and its vasculature, the number and location of anastomoses, and any other atypical anatomical information. If the patient has undergone a simultaneous renal–pancreas transplant, then the kidney is usually found in the left iliac fossa.

## Doppler ultrasound technique

Successful Doppler evaluation of the transplanted kidney can only be accomplished when scan quality is optimal. This requires the use of equipment that provides high Doppler sensitivity. The examiner must optimise the Doppler settings, since improper adjustment can result in slow flow being overlooked and thrombosis being incorrectly diagnosed. Two particularly important scanning factors that must be taken into account to ensure a successful examination of the renal transplant are optimising the angle of insonation relative to vessel orientation of the renal vascular pedicle, and maintaining minimal transducer pressure.

Ultrasound examination of the kidney should first confirm its appropriate location in the absence of any significant fluid collections. Colour Doppler is then used to identify the renal vascular

pedicle. Spectral Doppler is applied to the main renal artery, main renal vein and intrarenal segmetal or intralobar branches at the mid, upper, and lower poles. If any inflow compromise is suspect, then power Doppler can be applied to confirm uniform vascular perfusion throughout the kidney (Fig. 9.2).

### *Scale setting (pulse repetition frequency)*

For the initial scan, the colour and spectral Doppler scales should be set as low as possible. By doing so, the examiner will be able to localise the vessel in question with colour Doppler and then demonstrate adequate excursion on the spectral Doppler tracing. If aliasing occurs, the examiner can always increase the scale setting until the optimal level for that particular vessel is achieved.

### *Doppler gain*

The gain should be set at the highest level possible without creating noise in the image or tracing.

### *Filtration level*

The Doppler filter reduces noise in both colour and spectral modes. If the filtration level is set too high, it can eradicate the display of very slow flow in a vessel. Initially, filtration should be set at the lowest possible level and only increased incrementally when the low setting does not allow for an effective examination.

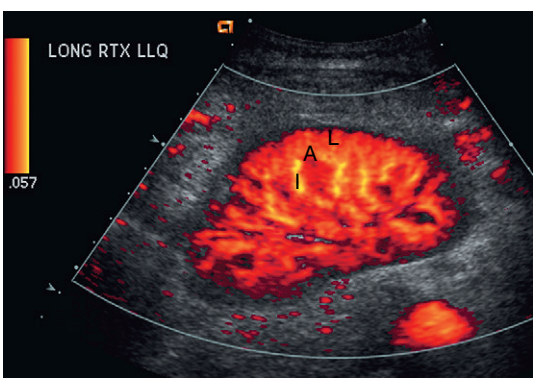


**Fig. 9.2** Longitudinal power Doppler image of a normal renal transplant. With the setting set to a very sensitive level, flow can be perceived in the interlobar (I), arcuate (A), and intralobular (L) arteries all the way out to the capsular surface of the kidney. This is a normal finding and indicates good renal perfusion with normal resistance to inflow.

### *Optimising angle of insonation relative to vessel orientation*

To ensure proper perception of flow by colour Doppler, or an accurate display of the spectral velocity, the angle of insonation should be less than 60°. Finding an appropriate angle can be especially problematic when examining transplanted kidneys because their vessels may be extremely tortuous and a committed search for a suitable Doppler window is required.[6]

### *Minimising transducer pressure*

Often the imaging study is limited because intervening adipose tissue increases the distance from the patient's skin to the transplanted kidney or there is gas in the overlying bowel. By applying sufficient pressure, fat or bowel loops can be displaced. Doing so, however, will compromise the Doppler examination as the renal parenchyma also becomes compressed and inflow during diastole can be impeded (Fig. 9.3). This results in a perceived elevation of the resistive index. Thus, care must be taken not to apply pressure to the kidney or its vessels, so that any diagnosis made on the basis of the resistive index or velocity measurement is more accurate.[7]

## Complications of renal transplantation

### *Functional complications*

These include hyperacute rejection, perioperative ischaemia, acute tubular necrosis, acute rejection, chronic rejection and drug toxicity (most commonly immunosuppressive agents).[8,9] Imaging techniques, including ultrasound with Doppler, are limited in their ability to identify and distinguish these functional complications.[10]

With hyperacute rejection (humeral mediated rejection), graft failure occurs rapidly (within minutes of implantation) secondary to the presence of preformed circulating antibodies. This condition is typically observed in patients

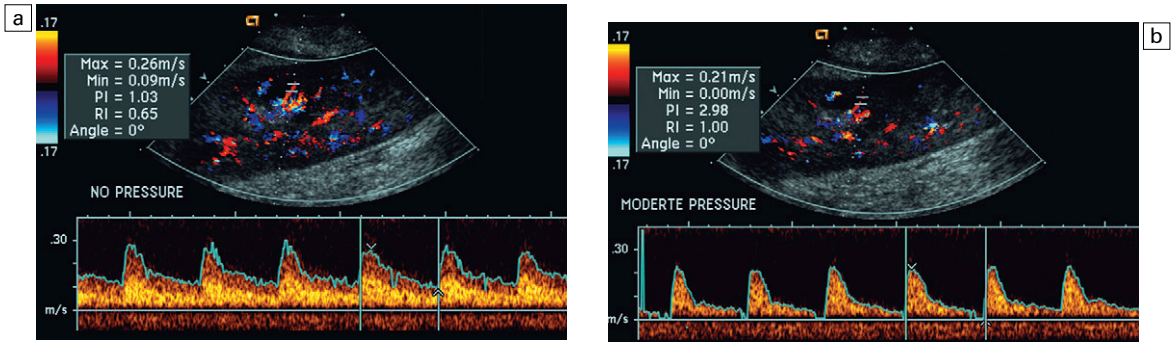


**Fig. 9.3** (a) Renal transplant interlobar artery spectral Doppler tracing acquired with gentle transducer contact. Note the normal waveform and 65% resistive index. (b) When moderate pressure is applied by the transducer, the tracing of the same artery now exhibits an elevated resistive index of 100%. Transducer pressure alone is responsible for this increase in vascular impedance and resultant elevation of resistance.

who have been sensitised by a previous transplant organ or a blood transfusion. This diagnosis is usually made in the operating suite, within minutes of unclamping the vascular pedicle. Since the renal transplant is so short-lived, ultrasound has little role in the evaluation of this condition. Extremely high resistance to inflow can be expected.

Acute rejection is a cellular-mediated process, whereby the immune system attacks the foreign renal allograft. Acute rejection is controlled by the use of steroids, cyclosporine, tacrolimus, sirolimus and other immunosuppressive agents. Occasional elevation in a transplant recipient's immune status (caused by viral illness or non-compliance with immunosuppressive drug therapy) can result in an acceleration of acute rejection to a critical level. The kidney becomes oedematous and swollen, intracapsular pressure rises, and eventually resistance to vascular perfusion increases (Fig. 9. 4). Although early investigators proposed that resistive index elevation was useful in identifying acute rejection as the cause of kidney transplant dysfunction, subsequent laboratory and clinical studies have shown it to be unreliable, and it remains a pathological diagnosis. Indeed, in a canine study it has been found that resistive index actually decreases in the mild to moderate stages of acute rejection. During the early to mid-stages of rejection, the physical effects of increased intrarenal pressure are counteracted by intrarenal hormonal autoregulatory mechanisms. Elevation of resistive index, therefore, does not manifest until the process of acute rejection is quite severe.[11] If a scan being performed in anticipation of transplant biopsy identifies the kidney to be oedematous and swollen with loss of central sinus fat echo and very high resistive indices, thought should be given to deferring the biopsy. Puncturing the capsule of a tense rejecting kidney may cause it to rupture.

Resistive index is rarely affected in the mild to moderate stages of acute rejection and when it is, its specificity is low.[12] It is not until acute rejection progresses to severe levels that the resistive index becomes consistently elevated. Elevation of resistive index, however, can also occur from many other causes such as hydronephrosis, acute tubular necrosis, infection and compression of the kidney by an adjacent mass or fluid collection. Thus, specificity for the diagnosis of acute rejection by Doppler ultrasound is unacceptably low and renal biopsy is still needed to establish the diagnosis.[11–16]

Chronic rejection is primarily a multifactorial process including antibody-mediated rejection, and the pathophysiology is not entirely understood. Doppler indices rarely show any significant alteration in flow profiles with chronic rejection.[15]

Perioperative ischaemia can result in transient compromise of renal function, particularly at the

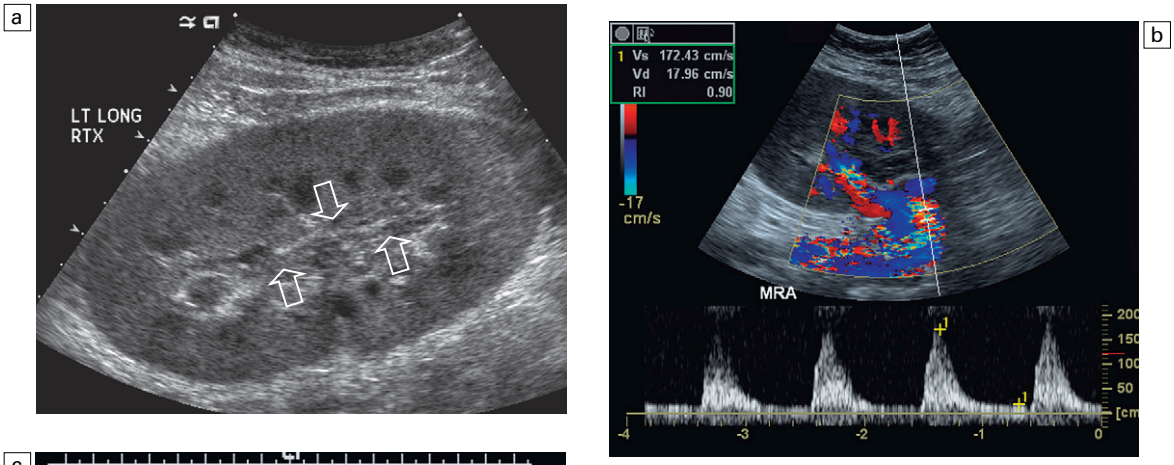


**Fig. 9.4** (a) Longitudinal grey-scale image of a transplanted kidney. Note the rounded globular configuration of the kidney. The central hilar space (arrows) is compressed due to oedema and swelling; therefore central hilar fat has been displaced. (b) Spectral Doppler tracing at the main renal artery level shows a resistive index of 90%. Biopsy confirmed severe acute rejection. (c) Power Doppler image of a severely rejecting renal transplant shows the main central vasculature and a few interlobar vessels but no flow can be seen out to the periphery of this rejecting kidney. The high resistance generated by the rejection process results in this colour Doppler 'pruned tree' appearance. Contrast this to the appearance of normal renal power Doppler flow in Figure 9.2.

level of the distal tubules which are most sensitive to hypoxia. This condition is self-limiting and typically resolves within 1–2 weeks of transplantation. The kidney appears oedematous, especially the medullary pyramids, and Doppler studies will show an increase in the resistive index. Although the imaging and Doppler findings may suggest acute tubular necrosis, they are not specific[11,17] (Fig. 9.5).

### *Anatomical complications*

These include haematomas, seromas, urinomas, abscesses, lymphoceles, obstructive hydronephrosis, focal masses, arterial and venous stenosis or thrombosis, and intrarenal arteriovenous fistula and pseudoaneurysm.[8,9,18] Unlike functional complications, most anatomical complications are readily identified by ultrasound.

Perinephric fluid is a common sequela of renal transplantation and is not considered significant if it is crescentic in shape, or decreases in size over time. Most fluid collections are haematomas or seromas, which result from oozing from the transplant bed; urinomas are relatively uncommon and usually are the result of breakdown at the ureteral anastomosis to the bladder. Doppler examination is of limited value in these cases. High pressure collections, such as haematoma after biopsy or organ rupture may exert mass effect upon the kidney and locally affect haemodynamics. In this case, Doppler may reveal a high resistance spectral tracing in proximity to the fluid pocket (Fig. 9.6).

A patient with a rounded, expansile collection with internal debris and associated signs of infection usually has an abscess. It is usually

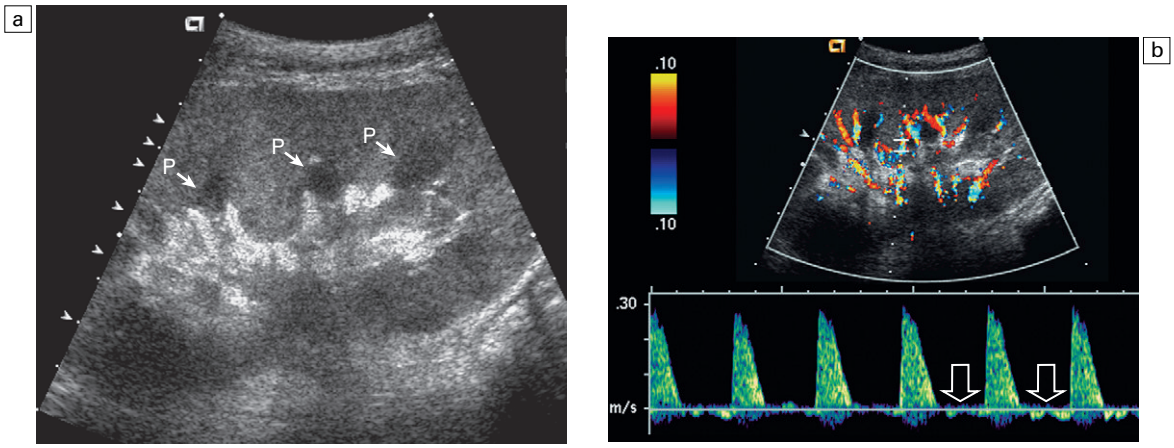


**Fig. 9.5** (a) Longitudinal grey-scale image obtained with 24 h of implantation. This cadaver organ experienced prolonged ischaemic time. Note that the kidney is not particularly rounded and the sinus fat is preserved. The medullary pyramids (P), however, are prominent, hypoechoic and oedematous. (b) Spectral and colour Doppler image of the same kidney. The resistive index is elevated to over 100% since reversed flow can be perceived in diastole (arrows). This combination of findings in the appropriate clinical situation is consistent with acute tubular necrosis. This can be seen in the immediate post-operative state but can also be caused by drug toxicity.

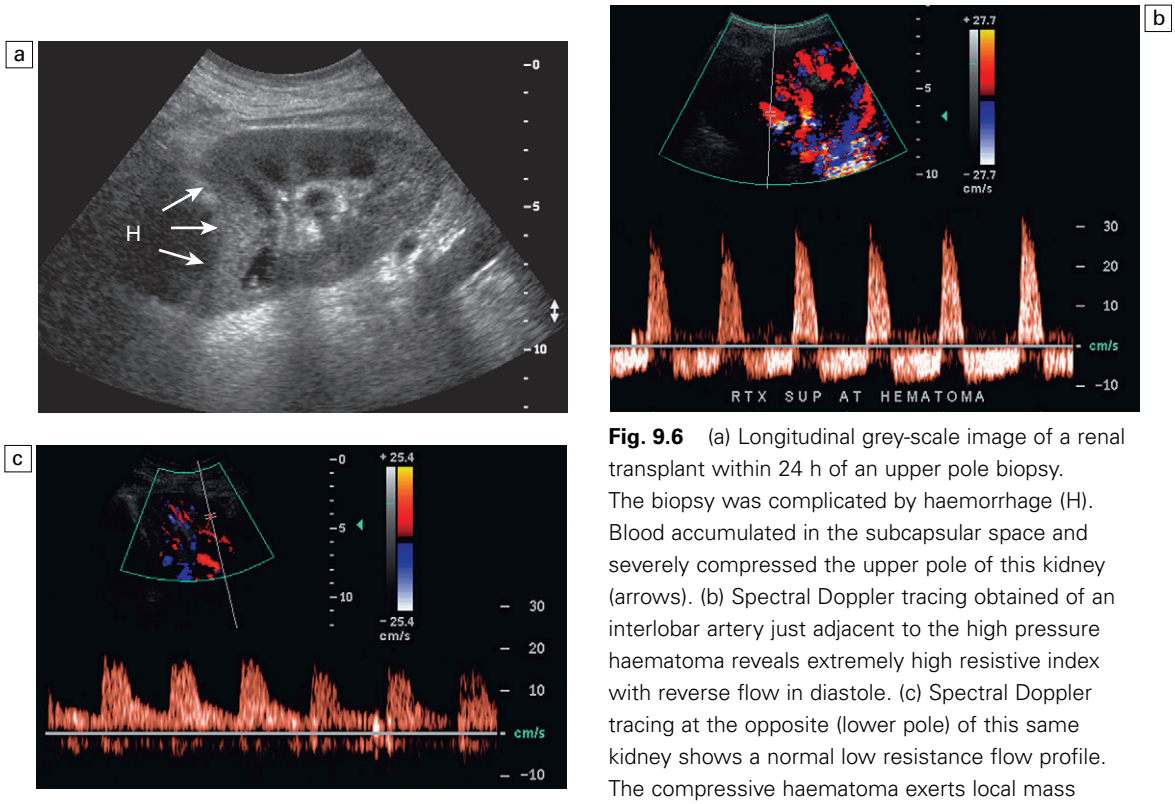


**Fig. 9.6** (a) Longitudinal grey-scale image of a renal transplant within 24 h of an upper pole biopsy. The biopsy was complicated by haemorrhage (H). Blood accumulated in the subcapsular space and severely compressed the upper pole of this kidney (arrows). (b) Spectral Doppler tracing obtained of an interlobar artery just adjacent to the high pressure haematoma reveals extremely high resistive index with reverse flow in diastole. (c) Spectral Doppler tracing at the opposite (lower pole) of this same kidney shows a normal low resistance flow profile. The compressive haematoma exerts local mass effect and elevates resistance to flow.

difficult to diagnose an abscess by sonography alone and computed tomography (CT) is considered a better imaging study for this purpose, especially to determine its extent and percutaneous drainage potential. Occasionally colour Doppler may reveal hyperaemia of the tissues surrounding the abscess.

Lymphoceles usually manifest at about 6–8 weeks postoperatively and are seen as rounded or lobulated collections near the vascular anastomoses. They are the result of surgical disruption of lymphatic channels when the vascular anastomosis to the transplanted kidney is created. An expanding lymphocele may cause ureteric compression and hydronephrosis. If a lymphocele becomes large enough, it may compress or kink the renal vascular pedicle. In this situation, Doppler examination may show findings similar to arterial or venous stenosis (Fig. 9.7).

Intraperitoneal transplantation, as is common with combined pancreas transplantation results in a more mobile kidney. Occasionally ptosis or rotation and torsion may occur in the kidney around its pedicle. This may result in arterial inflow and venous outflow complication (Fig. 9.8).

Transient dilatation of the collecting system as a result of ureteral anastomotic oedema frequently occurs immediately after renal transplantation or removal of the ureteral stent. The presence of a dilated transplant collecting system does not automatically signify an obstructed system under pressure, as the denervated, flaccid collecting system can become markedly dilated, particularly when the urinary bladder is distended.[17,19,20] Platt et al[19] proposed that the identification of an elevated resistive index was useful in distinguishing obstructive hydronephrosis from chronic, low-pressure dilatation of the transplant collecting system. Although this observation may be sensitive, its specificity is very poor because of the many other factors that similarly affect renal haemodynamics. At this time, the Whitaker test remains the 'gold standard' for differentiating high-pressure obstructive hydronephrosis from low-pressure distention of a flaccid renal transplant collecting system.

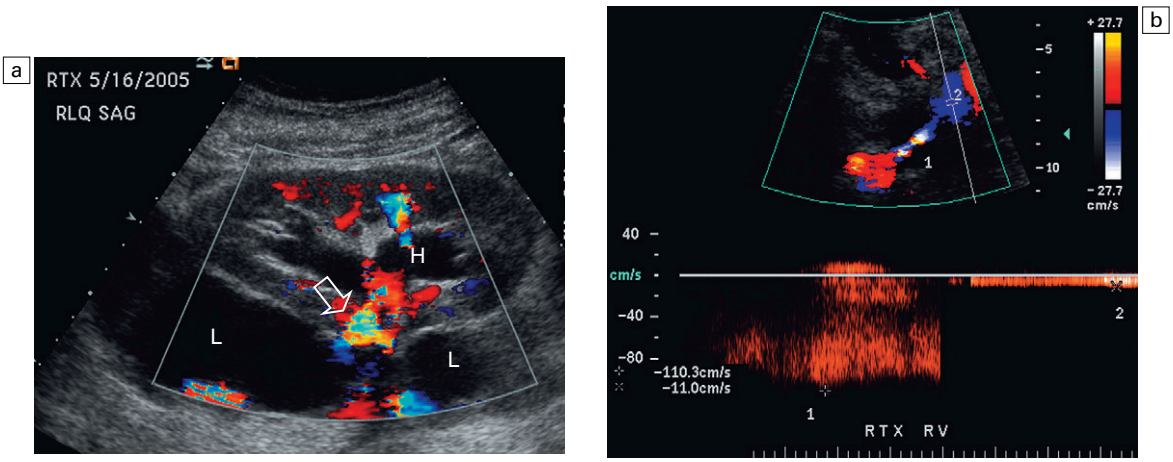


**Fig. 9.7** (a) Longitudinal colour Doppler image of this renal transplant shows a large fluid collection medial to the kidney, surrounding the renal vascular pedicle. This is a lymphocele (L) and it has caused distortion of the pedicle. Colour aliasing can be seen in the renal artery (arrow). There is also obvious hydronephrosis (H) caused by compression of the ureter. (b) Spectral Doppler tracing of the renal vein shows marked compression where it courses past the lymphocele (#1), the measured velocity at this area is 1.1 m $s^{-1}$; whereas within the kidney (proximal to the lymphocele (#2)) the velocity is only 0.1m $s^{-1}$. This 10-fold velocity gradient indicates that this is truly significant renal venous outflow obstruction.

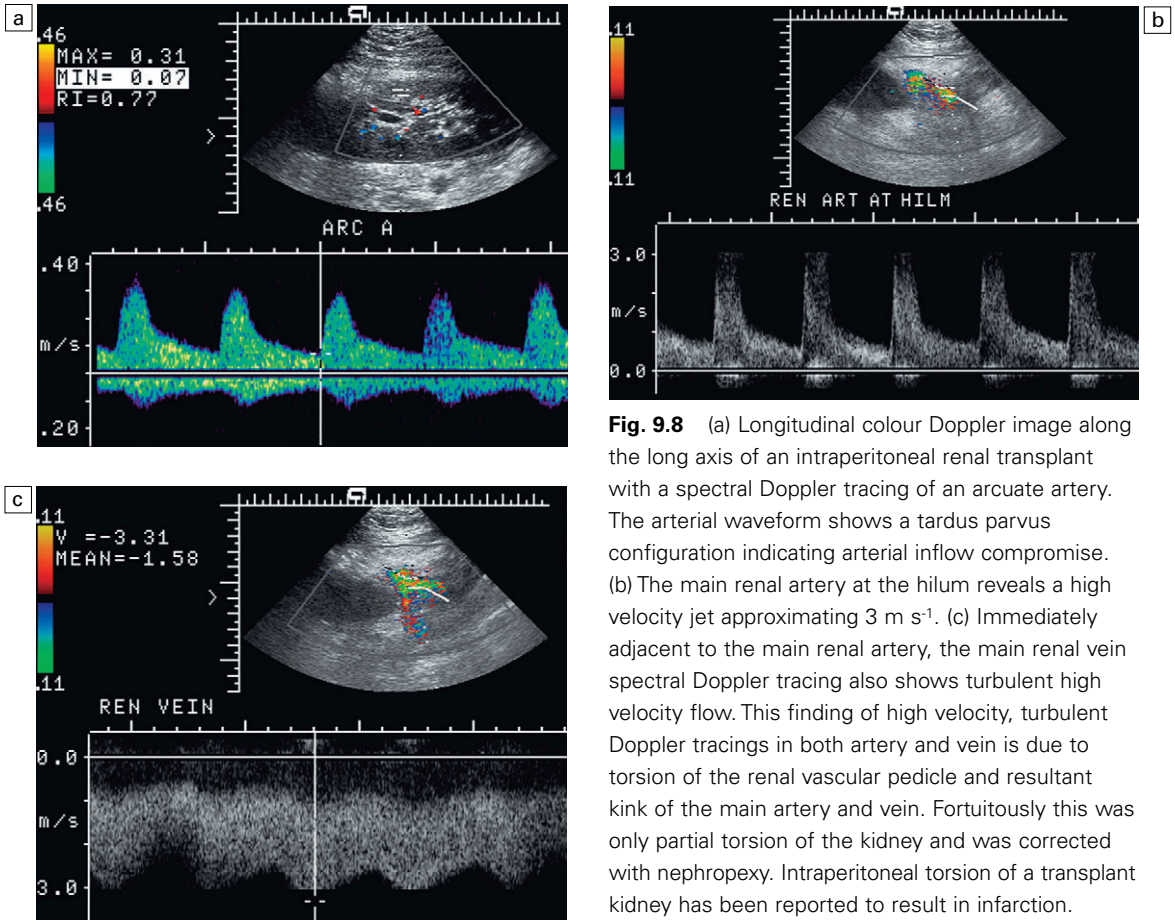


**Fig. 9.8** (a) Longitudinal colour Doppler image along the long axis of an intraperitoneal renal transplant with a spectral Doppler tracing of an arcuate artery. The arterial waveform shows a tardus parvus configuration indicating arterial inflow compromise. (b) The main renal artery at the hilum reveals a high velocity jet approximating 3 m $s^{-1}$. (c) Immediately adjacent to the main renal artery, the main renal vein spectral Doppler tracing also shows turbulent high velocity flow. This finding of high velocity, turbulent Doppler tracings in both artery and vein is due to torsion of the renal vascular pedicle and resultant kink of the main artery and vein. Fortuitously this was only partial torsion of the kidney and was corrected with nephropexy. Intraperitoneal torsion of a transplant kidney has been reported to result in infarction.

### *Vascular complications*

Following renal transplantation, vascular complications are observed in less than 10% of recipients; however, when present, they are associated with a high morbidity and mortality. Complications include renal artery or vein stenosis, compression, kinking, thrombosis, intrarenal arteriovenous fistulae and pseudoaneurysms. If identified promptly, they can often be successfully repaired prior to transplant failure. Doppler sonography is a very effective, non-invasive screening modality for identifying significant vascular complications.[21–23]

#### Renal transplant artery stenosis

This is most often observed within 1–2 cm of the anastomosis, usually as a result of vessel wall ischaemia due to surgical disruption of the vasa vasorum. Stenosis should be suspected if a tardus parvus waveform and relatively low-resistance flow are noted in the intrarenal branches. A tardus parvus waveform is characterised by a delayed upstroke in systole (prolonged acceleration time >0.07 s), rounding of the systolic peak and obliteration of the early systolic notch. A flow velocity greater than 2 m $s^{-1}$ with associated distal turbulence near the renal artery anastomosis is diagnostic of renal artery stenosis (Fig. 9.9). The examiner should conduct a thorough examination from the renal hilum to the iliac artery in search of a focal stenosis, if an intrarenal tardus parvus waveform is observed[24–28] (Fig. 9.10). Occasionally with severe renal artery stenosis the intraarterial waveforms become flattened to the point that it is very difficult to perceive the systolic diastolic

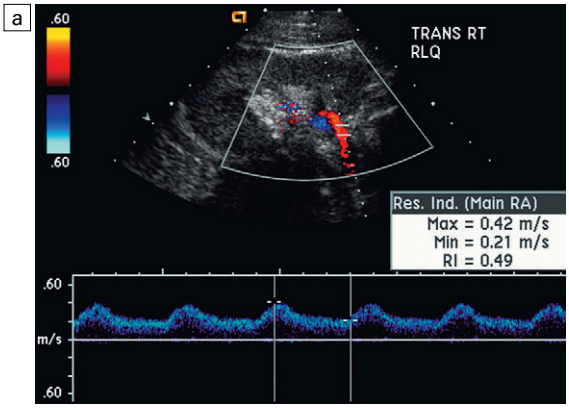


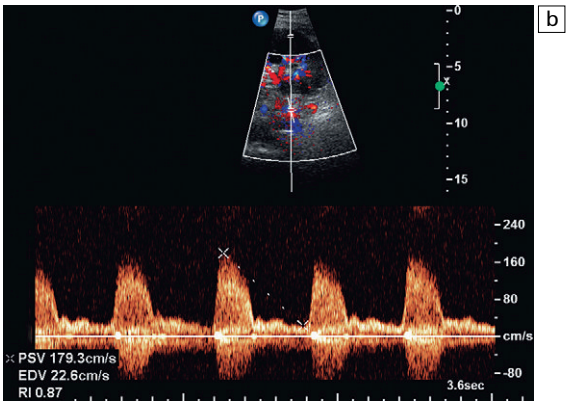


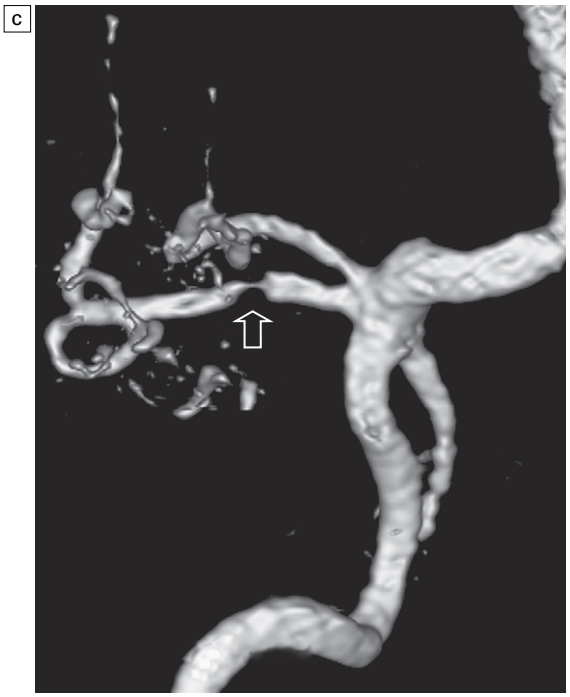


**Fig. 9.9** (a) Renal transplant arcuate artery spectral Doppler tracing in a hypertensive recipient with elevated serum creatinine. The renal arterial waveform manifests tardus parvus waveform with a slow systolic upstroke, and a rounded systolic peak, relatively low resistance. These findings suggest a more proximal stenosis. (b) Spectral Doppler tracing just beyond the anastomosis of the main renal artery to the iliac artery. Note the high velocity (1.79 m $s^{-1}$), turbulent flow characteristic of renal artery stenosis. (c) MR angiogram of this transplanted kidney actually revealed a double arterial anastomosis. The lower pole artery shows a high grade stenosis (arrow) within 1 cm of its anastomosis.

variation. Subtle pulsatile flow is enough to document the patency of the artery and avoid misdiagnosis of thrombosis. This should be further reinforced by the presence of constant outflow in the renal vein (Fig. 9.11).

Approximately 20% of transplanted kidneys require more than one arterial anastomosis due to the presence of accessory arteries. If one of these vessels becomes compromised, then perfusion to the subtended segment of the kidney is decreased. Again, a tardus parvus waveform may be seen, this time limited to the segments perfused by the affected artery. If thrombosis of this artery occurs, then the subtended area shows no flow on colour or power Doppler and an arterial tracing will not be identified by spectral Doppler. The area affected will vary depending on the anatomical vascular distribution (Fig. 9.12).

Renal parenchymal scarring secondary to chronic rejection may result in focal stenosis within branch arteries. This should be suspected if there is irregular distribution of flow on colour Doppler through the kidney. Segmental or interlobar renal artery stenosis can be confirmed by

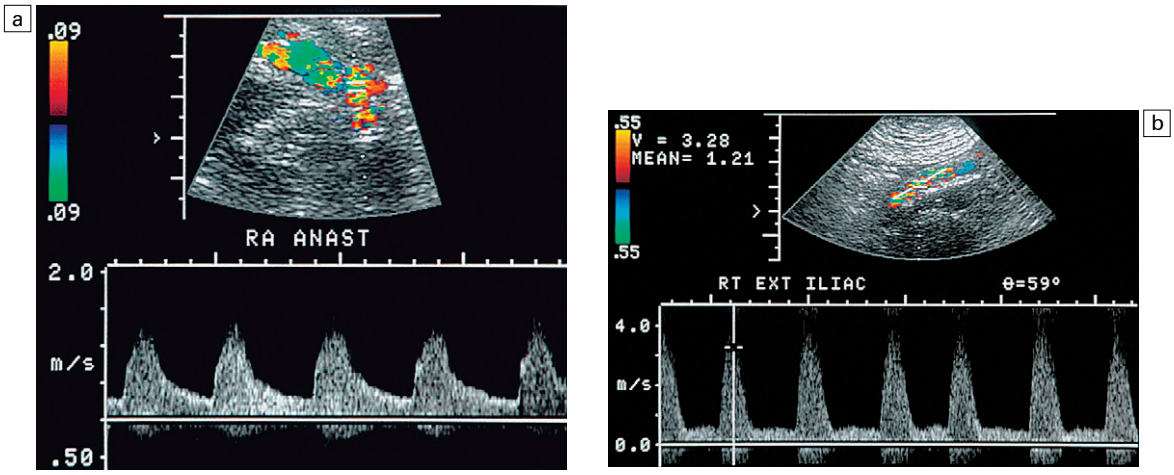


**Fig. 9.10** (a) Spectral Doppler tracing of a transplant main renal artery. Tardus parvus changes were present in this waveform but no anastomotic stenosis was perceived. (b) Spectral Doppler tracing of the external iliac artery. A high-velocity jet is identified with velocities of >3 m $s^{-1}$. This diabetic recipient had an atheromatous lesion in the iliac artery compromising inflow to the renal transplant.

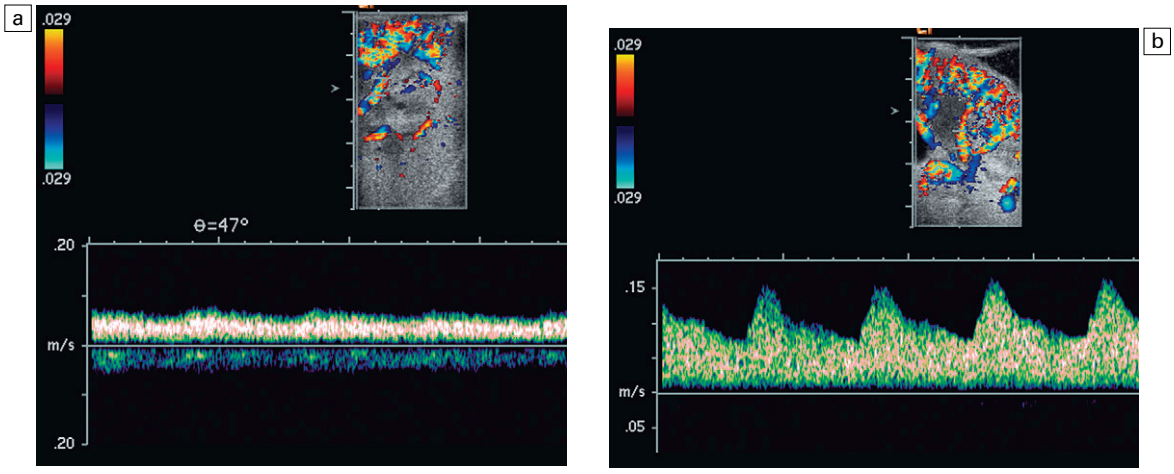


**Fig. 9.11** Intraoperative spectral and colour Doppler ultrasound of a recent renal transplant recipient being reoperated because of non-function and a Doppler suggestion of arterial stenosis. This spectral Doppler tracing of a segmental artery and its adjacent vein shows only a very subtle undulation in the arterial waveform (towards the transducer). The severe proximal stenosis completely wiped out the expected systolic velocity variation. The tracing below the baseline is not mirror imaging of the tracing but venous outflow. (b) As the anastomosis was surgically manipulated a sudden increase in arterial velocity with a more conspicuous arterial tracing became evident on spectral Doppler.

the presence of intrarenal high-velocity flow. Because these lesions are typically multiple and distal, treatment options are limited.[29]

A similar appearance can be seen with scarring after transplant biopsy. If the biopsy needle is guided centrally toward the renal hilum, there is a greater chance of vessel injury. Direct puncture of a major artery usually becomes immediately manifest as an area of turbulence on colour Doppler, a rapidly expanding haematoma, or brisk haematuria due to an arteriourteral fistula. Biopsy in close proximity to a major artery may

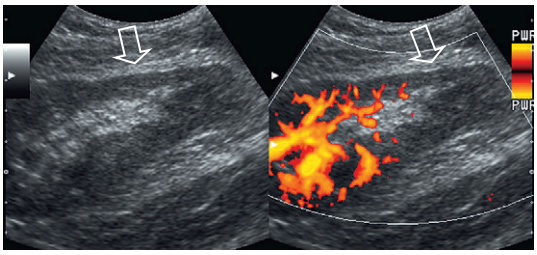

**Fig. 9.12** Side-by-side longitudinal grey-scale and power Doppler image of the low pole of a poorly functioning transplant kidney. Note the thin cortex (arrow) and complete absence of flow on power Doppler at the lower pole. This renal transplant required two arterial anastomoses. Thrombosis of the lower pole artery was suggested and confirmed angiographically. Additionally, ultrasound-guided biopsy of the upper pole identified acute rejection.

present with delayed segmental perfusion as scarring results in progressive compromise of flow to that portion of kidney.

### Renal transplant artery thrombosis

Thrombosis of the main renal transplant artery is a rare event. It is typically due to a technical problem with the surgical anastomosis. Doppler fails to demonstrate any arterial flow.

Rarely severe acute rejection may cause microvascular thrombosis. Colour and Power Doppler show no flow within the kidney. Flow may still be present in the segmental or interlobar branches, but spectral Doppler shows very high resistance because the flow has nowhere to go (Fig. 9.13). It may be difficult to differentiate the two aetiologies, but the non-rejecting kidney with arterial thrombosis is typically not as swollen and oedematous as the acutely rejecting thrombosed kidney.

The spectral Doppler tracing of renal vein flow in microvascular thrombosis may be very confusing. The blood within the vein may be seen to slosh back and forth with cardiac periodicity transmitted down the inferior vena cava (IVC). This to-and-fro flow may mimic high resistance arterial flow, except for the fact that the upstroke is not brisk. In high resistance arterial flow, systole upstroke is brisk with a peak whereas venous to-and-fro flow has a rounded appearance.

### Renal transplant vein stenosis

Renal vein stenosis is an uncommon complication following kidney transplantation, but when present, it is a significant cause of graft dysfunction. Venous stenosis may be seen as a focal narrowing with associated dilatation of the proximal vein. However, to confirm the diagnosis of a significant stenosis, there should be at least a fourfold velocity gradient across the lesion. If the gradient is less than fourfold, it is seldom considered clinically significant, even though it may have a dramatic appearance on Doppler examination (Figs 9.14 and 9.7b).

### Renal transplant vein thrombosis

This is also a relatively rare post-transplantation complication. It is usually seen within the first week following surgery. It is more likely to occur when there is technical difficulty with the venous anastomosis. It may occur with preservation injury, or it may evolve during an episode of severe acute allograft rejection. Extremely high resistance (resistive index typically greater than 100%) will be seen on the renal arterial waveforms with spectral Doppler. In most cases, thrombosis results in partial rather than complete occlusion of the vein and some renal venous outflow can be detected with spectral Doppler. To prevent a false-negative diagnosis, it is important that the examiner conduct a careful imaging and colour Doppler evaluation of the vein when very high arterial resistance is observed[31] (Fig. 9.15).

### Intrarenal arteriovenous fistulae and pseudoaneurysms

These are typically the result of renal transplant biopsy. The true incidence of these complications varies from centre to centre depending on biopsy technique. Arteriovenous fistulae manifest as a flash of colour, or 'visible thrill', in the adjacent parenchyma when the kidney is examined at normal colour Doppler settings. This phenomenon is caused by vibration of the

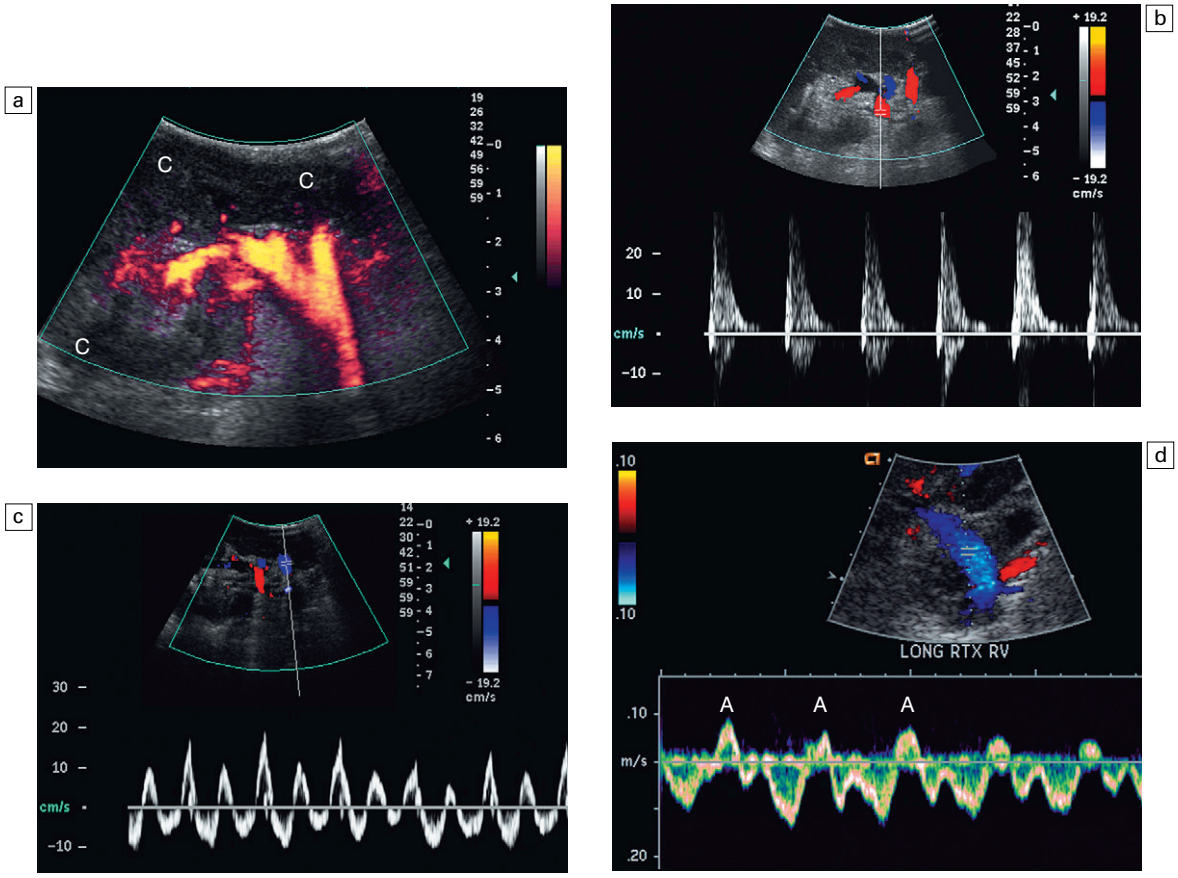


**Fig. 9.13** Longitudinal power, colour and spectral Doppler imaging of this renal transplant recipient with rapidly rising creatinine levels. (a) Power Doppler image shows central flow within the hilum of the kidney, but no flow within the cortex (C) or medulla. Microthrombosis was suspect. (b) Spectral Doppler tracing of the artery shows a brisk spike in systole and essentially no flow during diastole. (c) The renal vein spectral Doppler waveform has an unusual to-and-fro pattern. In summating the area under the tracing above and below the baseline, it becomes evident that there is little total antegrade flow. Due to the microvascular thrombosis, the flow within the vein is simply stagnant moving to-and-fro responding to intrarenal pressure changes between systole and diastole and pressure changes in the inferior vena cava. Contrast this to a tracing of a normal renal vein (d). The retrograde component of flow known as the A-wave (A) occurs during atrial systole. But note how relatively little reversed component of flow there is in comparison to the amount of flow below the baseline that is returning toward the heart.

surrounding tissues secondary to the rapidly flowing blood through the fistula. It is often possible to distinguish the feeding artery and the enlarged draining vein by adjusting the colour Doppler settings to higher velocity. Spectral Doppler tracings will demonstrate a high-velocity, low-resistance flow within the feeding artery. Turbulent, pulsatile (arterialised) flow will be present in the draining segmental vein. If the arteriovenous fistula is large enough, it may be possible to observe pulsatile flow within the main renal vein (Fig. 9.16).

Pseudoaneurysms are typically the result of a biopsy that captured partial thickness of an arterial wall. Therefore, they are extremely rare. They usually appear as a simple cystic structure, or a small collection of paravascular fluid. Colour Doppler, however, immediately reveals that the finding is not a simple cyst (Fig. 9.17). Spectral Doppler tracings show to-and-fro blood flow at

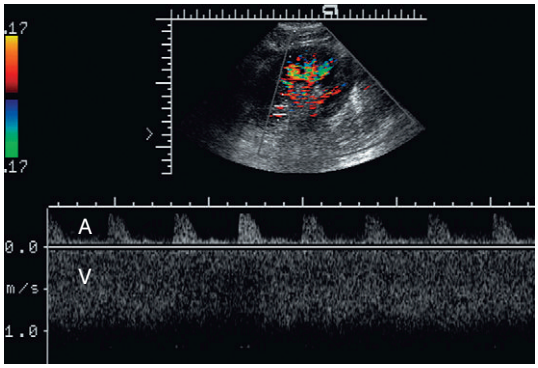


**Fig. 9.14** Spectral Doppler tracing of the renal vascular pedicle incorporating both the arterial (A) and venous (V) waveform. Note the high velocity in the vein approximating 1 m $s^{-1}$. Note the corresponding high resistance arterial waveform. A renal vein stenosis due to scarring was identified at surgery.

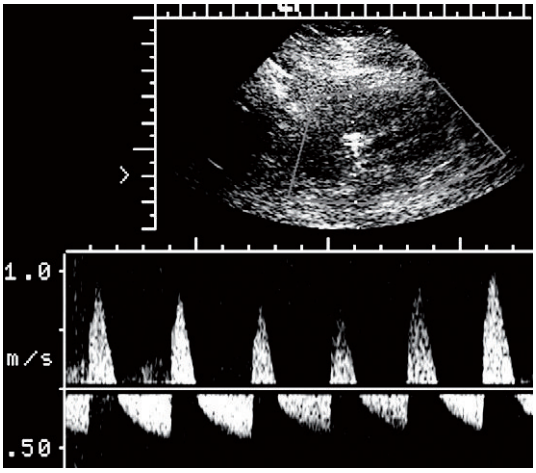


**Fig. 9.15** Spectral Doppler tracing of the main renal transplant artery in a recent recipient with a rapidly rising creatinine. The arterial waveform reveals to-and-fro flow with the retrograde component being essentially equal to antegrade flow. The resistive index measures approximately 140%. No flow could be identified by spectral or colour Doppler in the renal veins. Complete venous thrombosis was confirmed at angiography.

the neck of the pseudoaneurysm and a distorted, turbulent, pulsatile waveform can be observed within the pseudoaneurysm. The vast majority of intrarenal arteriovenous fistulae and pseudoaneurysms resolve spontaneously, but if they

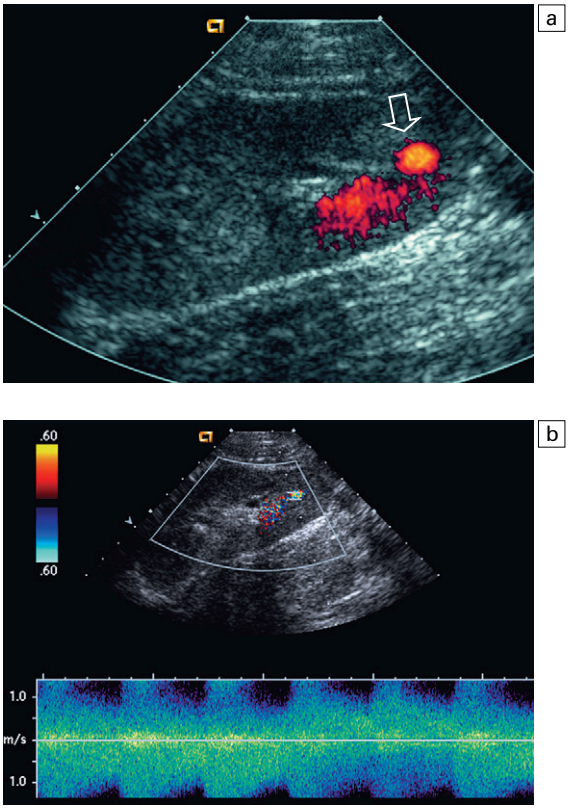


**Fig. 9.16** (a) Power Doppler image of a renal transplant approximately 2 weeks after biopsy. A burst of colour is seen overlying the lower pole (arrow). This flash artefact, due to tissue vibration, suggests an underlying arteriovenous fistula. (b) Spectral Doppler tracing obtained at the fistula site reveals a turbulent, high-velocity arterial waveform; that differentiates it from pseudoaneurysm that has to-and-fro flow.

increase in size over a period of time, angiographic embolisation may be necessary.[32,33]

## LIVER TRANSPLANTATION

More than 22 000 liver transplants have been performed in the world since 1988. The current 1-year graft survival rate in the USA is approximately 82.4% with 1-year patient survival rate of approximately 86%.[34] Improved surgical techniques, development of effective immunosuppressive medications, HLA typing for recipient matching, and establishment of coordinated transplant sharing systems have greatly improved

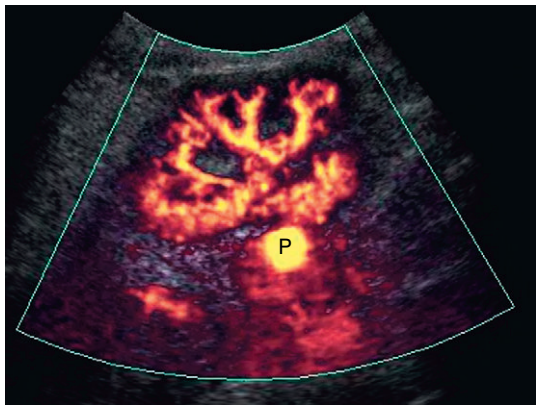


**Fig. 9.17** Power Doppler image of a renal transplant 3 weeks after a biopsy. A rounded area of bright flow represents a pseudoaneurysm (P). There is a higher likelihood of this complication with a more centrally directed biopsy, as was the case with this patient.

the success rate in liver transplantation. Graft survival statistics are further enhanced by prompt identification of liver transplant dysfunction and rapid intervention when appropriate.

## Preoperative assessment

Preoperative assessment consists of confirmation of vascular patency, mapping native vascular anatomy, quantification of diseased liver volume, identification of vascular collaterals secondary to portal hypertension and a search for intra- or extrahepatic malignancy (Fig. 9.18). There are many ways to accomplish this including angiography and ultrasound, but currently CT with CT angiography in the arterial phase and portal phase is the favoured method for the adult. Some centres rely on Doppler and magnetic resonance imaging (MRI), especially for the paediatric candidate.[35] A complete sonographic examination of the liver transplant candidate should cover the points listed in Table 9.3.

## Postoperative assessment

The major complications of liver transplantation are rejection, vascular stenosis or thrombosis, biliary leak or obstruction, and progression of unexpected malignant disease. Acute rejection is clinically monitored by serum liver enzymes, bilirubin, and ammonia levels and diagnosis is established by biopsy. Ultrasound and Doppler have little to offer in the diagnosis of acute hepatic rejection. Doppler ultrasound, however, plays a key role in monitoring for potential vascular complications. A complete sonographic examination of the liver transplant recipient should cover the points listed in Table 9.4. Evaluation of

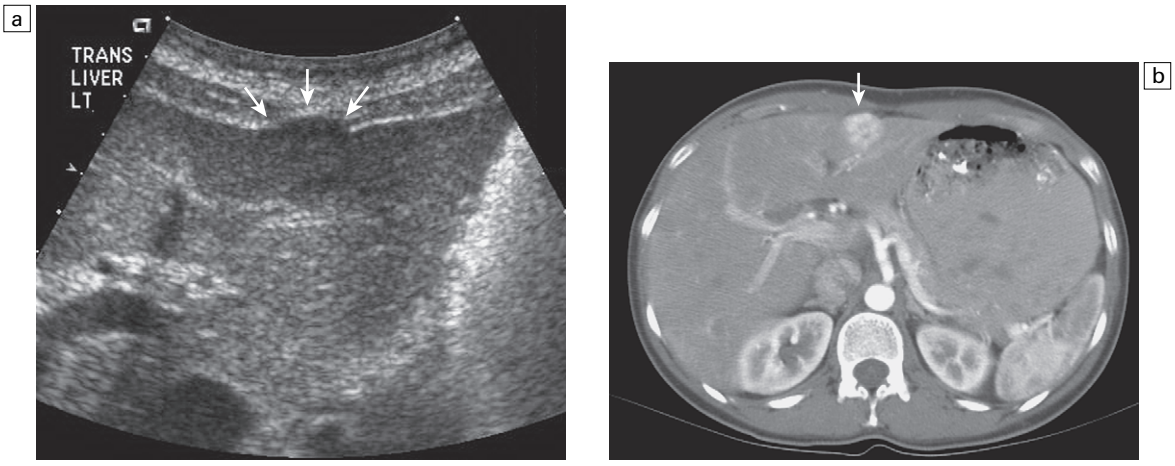


**Fig. 9.18** Transverse ultrasound image of the left lobe of the liver reveals a focal nodule bulging the capsular contour (arrows) (a). Ultrasound imaging alone cannot further characterise this lesion. Arterial phase rapidly enhanced CT (b) shows this lesion to be a hypervascular mass (arrow), most likely a hepatocellular carcinoma. With the addition of ultrasound contrast, some centres are able to use Doppler to identify malignancy during the transplant work-up.

**Table 9.3** Checklist for the pre-liver transplantation ultrasound examination

- Confirm patency of the portal vein. Provide length and diameter measurements of the extrahepatic portal vein
- Identify any anatomical variation of the hepatic artery
- Confirm patency of the inferior vena cava
- Identify and describe collateralisation from the portal to the systemic circulation
- Identify any hepatic mass that may represent hepatocellular carcinoma
- Quantify the amount of ascites
- Estimate the size of the diseased liver
- Provide a measurement of spleen size

the newly transplanted liver requires a precise understanding of the surgical anatomy. Many variations are possible including segmental or reduced-size transplantation, especially in the paediatric population.[36,37] Variations of the arterial anastomoses are necessary when the donor hepatic arterial anatomy is anomalous. Variations of venous anastomoses are necessary when the recipient portal vein is thrombosed. The sonologist must be aware of any variations so that a thrombosed accessory hepatic artery or a stenotic jump graft is not missed (Fig. 9.19).

The liver transplant ultrasound examination should include a general survey of the abdomen and pelvis in order to identify and quantify any haematomas or fluid collections. The liver parenchyma is then examined to rule out any focal abnormality, specifically any fluid collection, area of infarction or possible neoplasm. The biliary system should be evaluated to rule out obstruction or sludge accumulation, especially in a patient with hepatic artery thrombosis. The intra- and extrahepatic hepatic arteries are checked to confirm patency and the waveforms are analysed to rule out stenosis. Patency of the portal vein is confirmed and the Doppler waveform analysed, particularly across the anastomosis (Fig. 9.20). Patency of the three hepatic veins is confirmed and their waveforms are evaluated. Finally, the IVC is checked with special attention to the upper anastomosis (Fig. 9.21).

**Table 9.4** Checklist for the post liver transplantation ultrasound examination

- Survey the liver parenchyma to rule out any focal abnormality, specifically fluid collections, areas of infarction, and possible neoplasm
- Survey and perihepatic recesses, lateral gutters, and pelvis to identify and quantify any haematoma or fluid collection
- Evaluate the biliary system, both intrahepatic and extrahepatic, to rule out obstruction, intraductal sludge and stone formation
- Confirm the presence of both intrahepatic and extrahepatic artery flow, and analyse the waveforms
- Confirm portal vein patency and analyse the Doppler waveform, particularly across the anastomosis
- Confirm patency of the three hepatic veins and evaluate their waveforms
- Evaluate flow in the inferior vena cava with attention to the anastomoses

## Abnormal findings

The most common abnormal findings encountered in liver transplantation are listed in Table 9.5.

The hepatic artery anastomosis is technically the most difficult to create and problems, such as stenosis, thrombosis and fistula formation, have the most significant impact on liver transplant success as they predispose to infarction, intrahepatic abscess, biliary stricture and biloma formation. Doppler findings indicating hepatic artery stenosis include an intrahepatic tardus parvus waveform with low-resistance flow and a high-velocity jet with turbulence at the point of stenosis. A focal high-velocity jet just beyond the hepatic artery anastomosis in excess of 200 cm $s^{-1}$ or greater than three times the velocity in the prestenotic hepatic artery is highly indicative of a clinically significant stenosis.[38] The identification of an intrahepatic tardus parvus waveform with low resistance (<60% resistive index) flow, a prolonged upstroke in systole (>0.08 s)[38] and rounding of the systolic peak, should force a careful survey in the anticipated region of the anastomosis for the high velocity jet (Fig. 9.22).[38,39] It has been shown that searching for the tardus parvus waveform pattern is an excellent screening test for the presence of post-

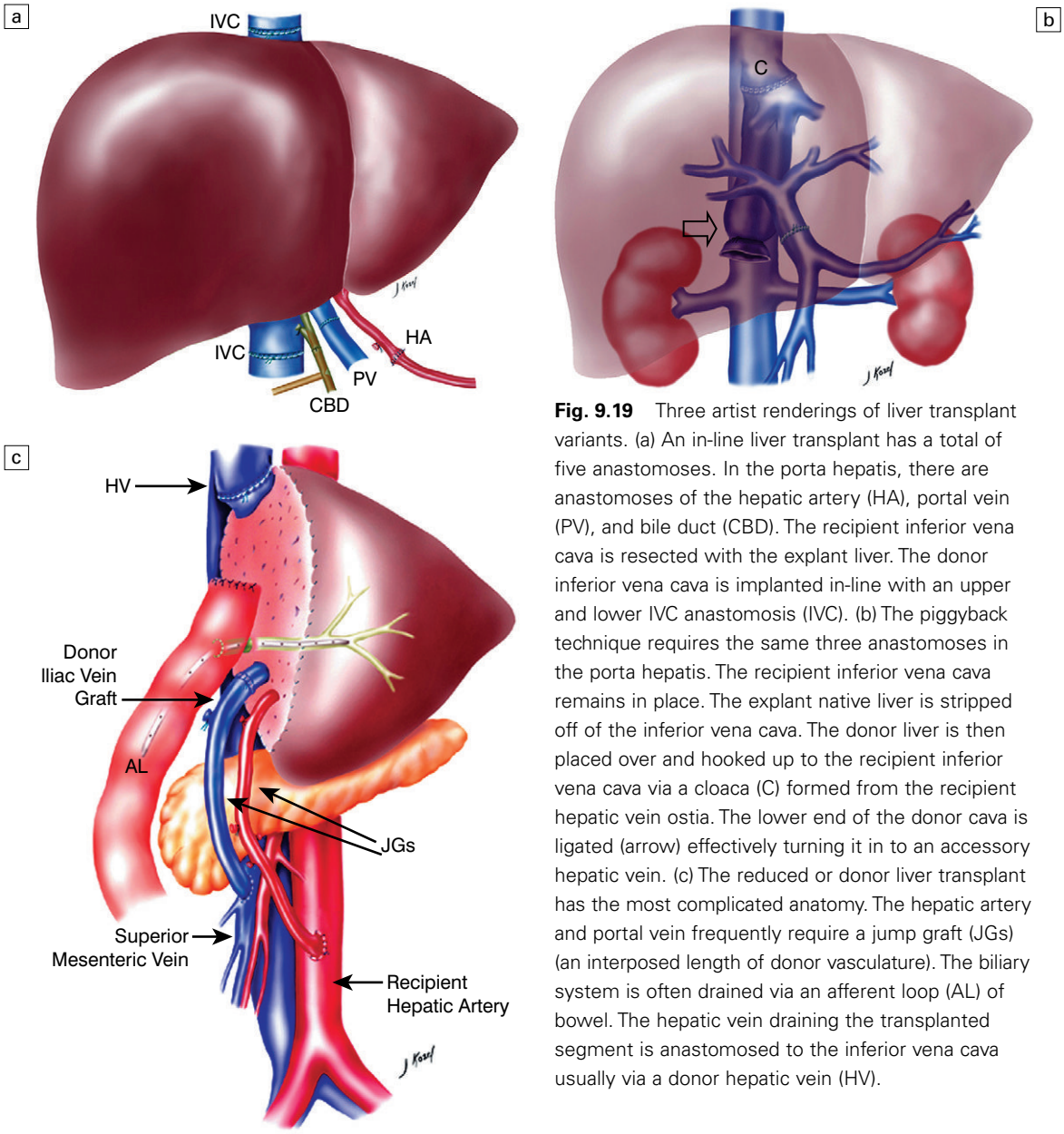


**Fig. 9.19** Three artist renderings of liver transplant variants. (a) An in-line liver transplant has a total of five anastomoses. In the porta hepatis, there are anastomoses of the hepatic artery (HA), portal vein (PV), and bile duct (CBD). The recipient inferior vena cava is resected with the explant liver. The donor inferior vena cava is implanted in-line with an upper and lower IVC anastomosis (IVC). (b) The piggyback technique requires the same three anastomoses in the porta hepatis. The recipient inferior vena cava remains in place. The explant native liver is stripped off of the inferior vena cava. The donor liver is then placed over and hooked up to the recipient inferior vena cava via a cloaca (C) formed from the recipient hepatic vein ostia. The lower end of the donor cava is ligated (arrow) effectively turning it in to an accessory hepatic vein. (c) The reduced or donor liver transplant has the most complicated anatomy. The hepatic artery and portal vein frequently require a jump graft (JGs) (an interposed length of donor vasculature). The biliary system is often drained via an afferent loop (AL) of bowel. The hepatic vein draining the transplanted segment is anastomosed to the inferior vena cava usually via a donor hepatic vein (HV).

liver transplantation hepatic artery stenosis.[40] One article suggests that in the paediatric donor population, the finding of hepatic arterial resistive index <60% is highly predictive of impending hepatic artery thrombosis due to stenosis and thrombectomy and reanastomosis should be considered.[41] Although an intrahepatic arterial tracing may be demonstrated, it should be remembered that a severe stenosis may still lead to biliary ischaemia, or may progress to complete thrombosis.

Absence of an arterial signal along the main portal vein and its branches on spectral and colour Doppler ultrasound indicates hepatic artery thrombosis. Since this is a diagnosis based on the absence of flow, great care must be taken to ensure proper Doppler settings. Scanning by a second experienced sonologist is encouraged,

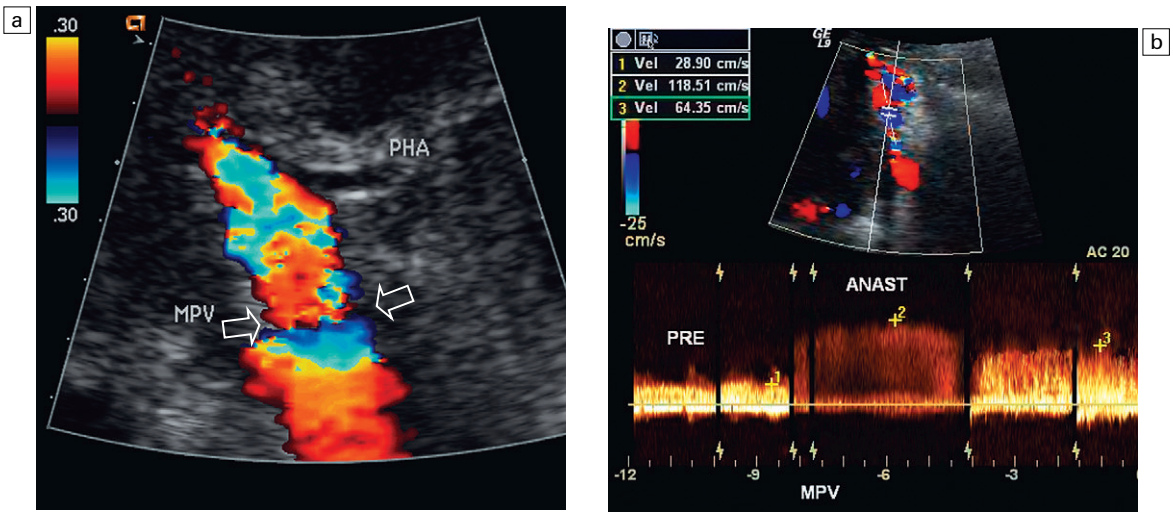


**Fig. 9.20** Colour Doppler image of the porta hepatis (a). The anastomosis between donor and recipient portal vein is evident by the change in calibre which causes the focal aliasing at that level (arrows). Spectral Doppler tracing (b) across the anastomosis and on either side reveals the velocity changes are relatively insignificant in this normal anastomosis.

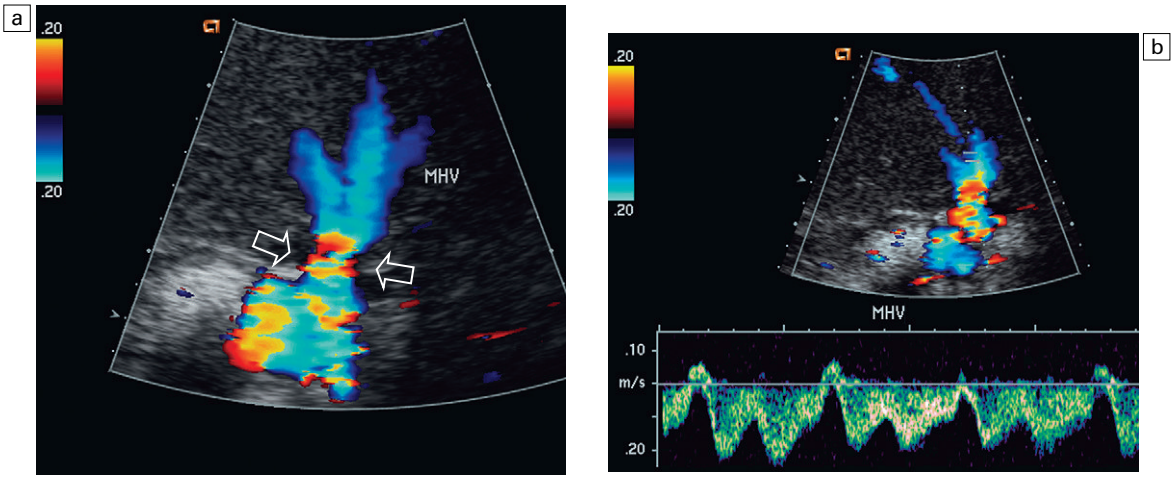


**Fig. 9.21** Transverse colour Doppler image of the hepatic vein/IVC anastomosis (a). Three hepatic veins are indeed patent. Aliasing however is perceived at the caval anastomosis (arrows). Spectral Doppler tracing (b) reveals normal cardiac periodicity transmitting into the liver. Since this waveform must propagate against the direction of flow, its presence within the liver effectively rules out significant hepatic venous outflow obstruction.

since this ultrasound diagnosis routinely leads to arteriography. Use of ultrasound echo-enhancing agents is recommended to improve perception of a weak arterial signal and decrease the rate of false-positive diagnosis of hepatic artery thrombosis and reduce the frequency of hepatic artery arteriography.[42,43]

Studies performed on patients with hepatic artery stenosis and thrombosis have identified certain factors that place patients at a higher risk and warrant more frequent Doppler screening. These factors include bench reconstruction of anatomical variance, the use of an interposition graft, and patients undergoing retransplantation.[44]

**Table 9.5** Differential diagnosis of ultrasound findings in the transplanted liver

**Diffusely irregular parenchymal echotexture**

- Ischaemia or necrosis secondary to hepatic artery stenosis or thrombosis
- Infection or abscess
- Recurrent hepatitis
- Post-transplantation lymphoproliferative disorder or lymphoma
- Geographic or diffuse fatty infiltration
- Hepatocellular carcinoma
- Diffusely metastatic neoplasm

**Focal parenchymal abnormality**

- Abscess
- Infarction
- Recurrent neoplasm
- Intraductal air secondary to choledochojejunostomy or sphincterotomy
- Intraductal sludge or calculi

**High-resistance flow in hepatic artery**

- Preservation injury – common during the first few days after transplantation
- Organ compression by adjacent mass or fluid collection
- Hepatic venous outflow obstruction
- Severe hepatocellular disease

**Low-resistance flow in hepatic artery**

- Hepatic artery stenosis
- Severe aortoceliac atherosclerotic disease
- Diaphragmatic crus sling effect
- Intrahepatic arteriovenous fistula
- Arteriobiliary fistula

**Flattening of hepatic vein waveform**

- Hepatic parenchymal disease, including rejection
- Stenosis or kink of the upper inferior vena cava anastomosis

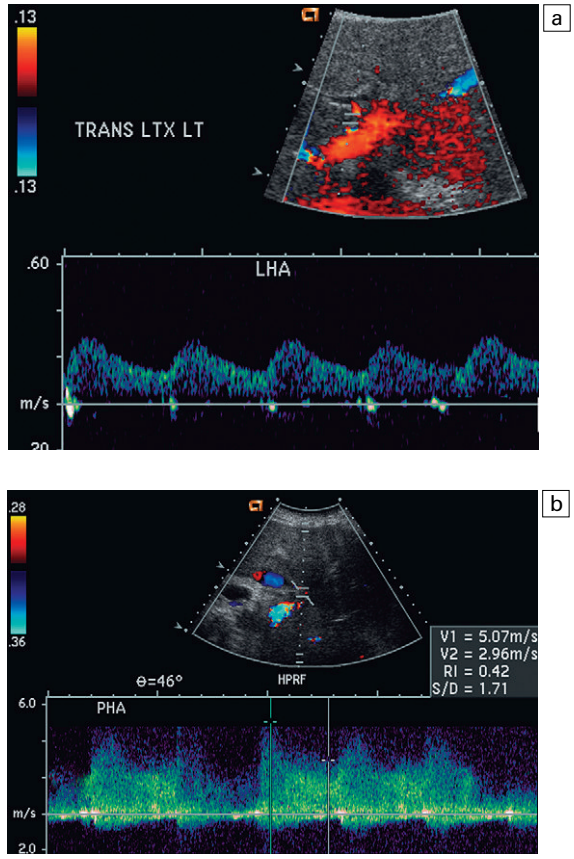


**Fig. 9.22** (a) Colour and spectral Doppler tracing of an intrahepatic arterial flow profile. Tardus parvus pattern with a delayed upstroke in systole rounded systolic curve and relatively low resistance flow is indicative of insufficient hepatic arterial inflow and suggests stenosis. The examiner should carefully walk the sample volume down the hepatic artery and out of the liver looking for the anticipated point of stenosis. In this case, (b) a high velocity jet measuring over 5 m $s^{-1}$ identified the point of stenosis in the subhepatic space.

In cases of hepatic artery thrombosis which are treated conservatively, collaterals will develop and an intrahepatic arterial signal can be detected by Doppler ultrasound as early as 2 weeks after the thrombosis. This typically manifests as a thready tracing with a tardus parvus appearance and can be seen in as many as 40% of patients with documented hepatic artery thrombosis, especially children.[45]

Within the first few days of transplantation, the hepatic artery tracing often shows a relatively high resistance flow. This is a common manifestation of ischaemic reperfusion injury (the anoxia and traumatic insult sustained by the liver during recovery, handling, preservation and surgery). It has been shown to be more common with older donor age and a prolonged period of ischaemia[46] (Fig. 9.23). The high resistance is due to vasospasm and can be reversed with vasodilatory agents such as nifedipine. One must be cautious however to ensure that the transplant recipient is stable enough to be given this drug as a diag-

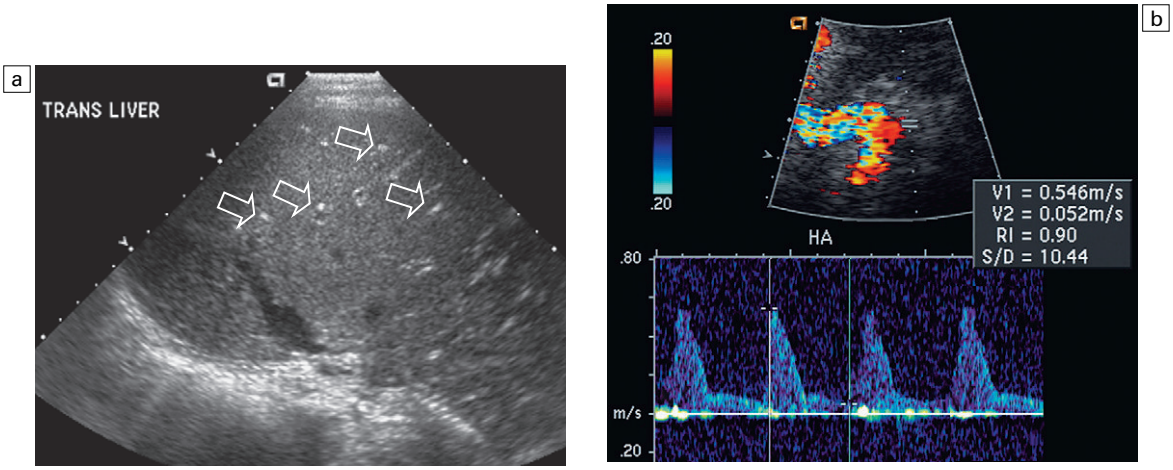


**Fig. 9.23** Transverse ultrasound image of a recently transplanted liver (a). The fat surrounding branches of the portal triad (arrows) stands out prominently against the background of an oedematous, hypoechoic liver; the sequela of ischaemic injury related to the surgical procedure. This is very common within the first few days of transplant. (b) Spectral Doppler tracing of the hepatic artery shows a very high resistance waveform with sharp spikes in systole and very little flow through diastole. Rarely does this progress to thrombosis, but more often evolves into a normal resistance waveform as the oedema and vasospasm resolves.

nostic challenge. Augmenting the Doppler exam with this challenge, however, may obviate the need for an arteriogram if hepatic arterial inflow is compromised to the point where it appears to be occluded (Fig. 9.24). The spasm typically resolves within a few days of transplantation[47] and resistance returns to a normal range.[48] A delayed finding of high resistance, beyond 3–5 days, is a poor prognostic indicator and some of these patients develop arterial thrombosis.[49] The exact cause of thrombosis is not always apparent and in numerous cases is presumed to be secondary to immunological causes and rejection.

At the time of implantation, there must be sufficient length of all of the vasculature to create the anastomoses. A longer pedicle is easier to work with, however, if the vessels are too long a kink may occur as the liver is placed into the fossa and the abdominal wall is closed. Clinically the patient presents with liver dysfunction. A stenosis may be suspect on spectral Doppler. Colour or power Doppler may reveal the tortuosity. Three-dimensional CT angiography may be performed to provide 'the big picture' and determine if a stent of reoperation is the best treatment (Fig. 9.25).

Arteriovenous fistulas are a rare complication of transplantation and are most often the result of a biopsy. Imaging rarely reveals an abnormality, but colour Doppler often shows a localised flash

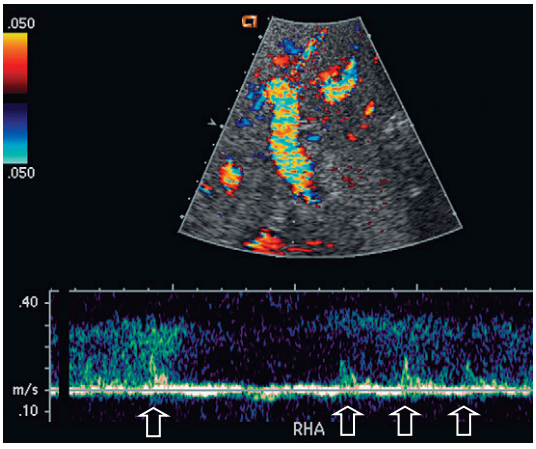


**Fig. 9.24** Spectral Doppler tracing of the porta hepatis on the first postoperative day. The hepatic artery was extremely difficult to identify (arrows) because of the thready, high resistance flow due to severe vasospasm. This patient may be considered a candidate for ultrasound contrast or a provocative test with vasodilating agents to confidently confirm arterial patency.

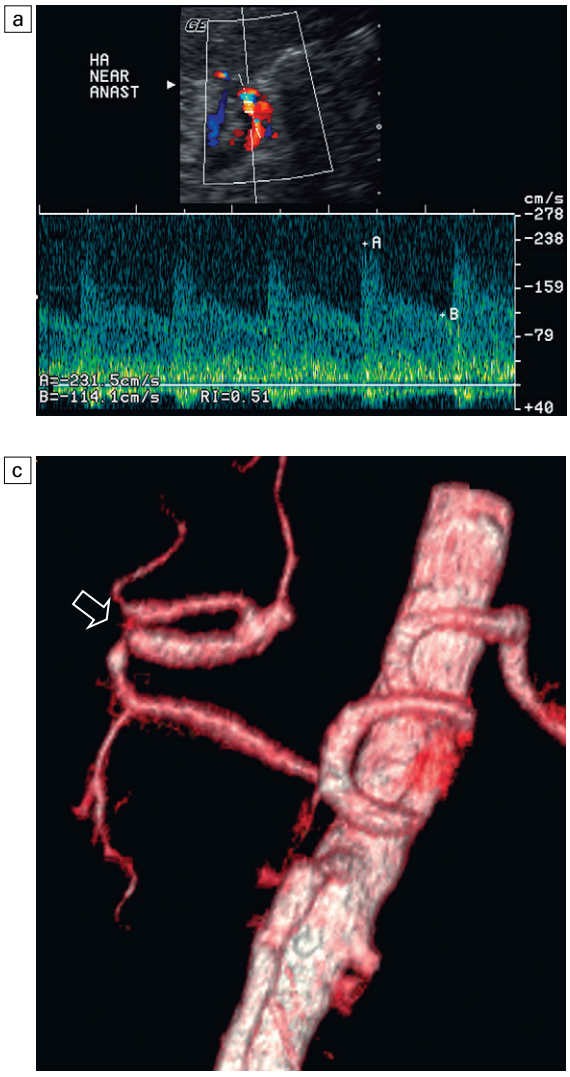


**Fig. 9.25** Spectral Doppler tracing of the hepatic artery in the porta hepatis reveals a high velocity jet suggesting a stenosis (a). Power Doppler image of the subhepatic space (b) reveals a markedly tortuous hepatic artery. The three-dimensional rendering of the CT angiogram during the arterial phase (c) reveals a kink (arrow) due to excessive vessel length in the subhepatic space.

artefact. When Doppler settings are adjusted for high velocities, the feeding artery and draining vein are better visualised. Spectral Doppler reveals a low resistance arterial waveform with high diastolic velocity.[50,51]

The donor portal vein is usually anastomosed end-to-end with the recipient portal vein. Variations may be required if the recipient portal vein is thrombosed, hypoplastic, or of insufficient length. Because the vessel is relatively large, colour Doppler findings can be rather striking (Fig. 9.26). Not all flow disturbances perceived by colour Doppler are haemodynamically significant and compromise of portal vein flow is relatively rare. When it occurs, it may be due to a mismatch between the diameter of the recipient and donor portal veins, to an excessive length of vessel causing a kink, or to a stenosis.[52] If portal vein stenosis is suspected, the velocity gradient across the anastomosis should be measured by spectral Doppler; a velocity gradient of less than fourfold is unlikely to be significant (Fig. 9.26).[53] Nevertheless, recipient donor size mismatch can lead to portal vein thrombosis. This can be treated by surgical thrombectomy, angioplasty or thrombolytic infusion, but in some cases retransplantation may be required.[54]

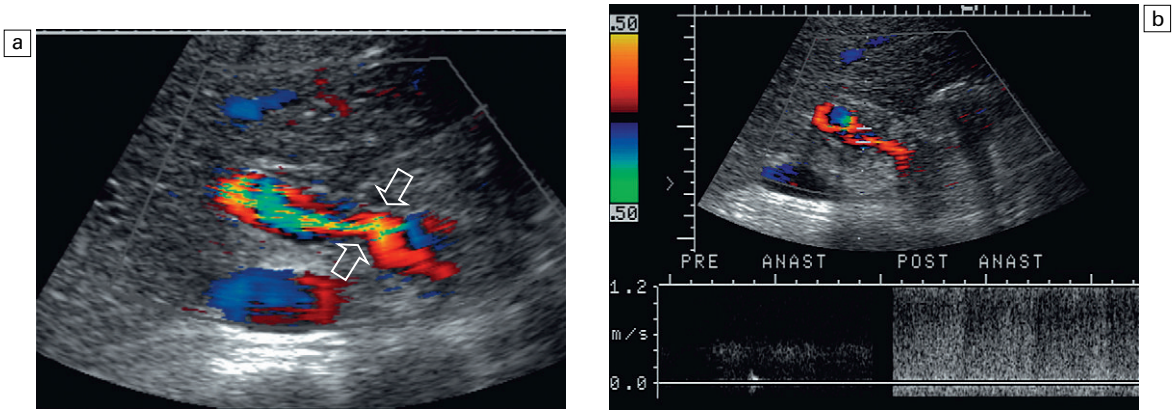


**Fig. 9.26** (a) Colour Doppler image of the portal vein in the region of the anastomosis. Note the area of relative narrowing at the point of anastomosis (arrows). A high velocity jet with aliasing is seen shooting into the donor portal vein. Spectral Doppler tracing on either side of this anastomosis (b) had to be set low to project the relatively slow preanastomotic portal vein flow. As a result, the postanastomotic (poststenotic) tracing shows a high degree of aliasing. This comparative velocity measurement on one tracing can be achieved by moving the sample volume across the anastomosis and allows an accurate comparison of pre- and postanastomotic velocities. Velocity gradients of less than fourfold are not likely to be clinically significant.

Post-transplantation portal vein thrombosis is quite rare and most often attributed to technical factors. It is more likely to occur in the paediatric recipient, especially after split liver transplantation.[55,56] Prompt detection with frequent Doppler evaluation and aggressive surgical treatment in selected cases are required to reduce the mortality and graft loss.

If slow velocity is identified in the portal vein (<1 m $s^{-1}$), it may be due to increased intrahepatic resistance from rejection, or to reduced inflow as can be seen with the collateral steal phenomenon. This occurs when large varices remain unligated, shunting blood from the portal system to the systemic circulation, bypassing the liver.[57–59]

A pulsatile waveform in the portal vein may be observed within the first few weeks after transplantation, especially in patients that received small grafts. This pulsatile flow often disappears without any treatment, although it may sometimes represent vascular complications such as arterioportal shunt.[60]

The donor IVC has a long intrahepatic course and is therefore transplanted along with the liver. The IVC may be inserted in-line with both supra- and infrahepatic anastomoses; the native intrahepatic IVC is excised with the diseased liver. The more common surgical technique retains the native IVC of the recipient in place and the upper end of the donor IVC is anastomosed end-to-side to the native IVC at the confluence of the hepatic veins of the explanted liver. The lower end of the donor IVC is oversewn, which functionally converts it into a hepatic vein. Relative flow volumes through this vessel are much less than when it served as the IVC, therefore clot may be seen partially filling the lumen (Fig. 9.27). This should not cause concern as long as some flow can be perceived. This type of anastomosis is commonly referred to as a 'piggyback'.[61] The incidence of hepatic venous complications in partial liver transplantation is more frequent than that in whole liver transplantation.[62] Any compromise of the upper caval anastomosis, from either stenosis or kinking, may cause hepatic venous outflow obstruction. Ultrasound findings include marked damping, or complete flattening of the hepatic vein velocity profile with complete loss of periodicity, distension of the hepatic veins and a high velocity jet with turbulence just above the caval anastomosis (Fig. 9.28). Hepatic vein or caval anastomotic stricture may be treated with balloon dilatation

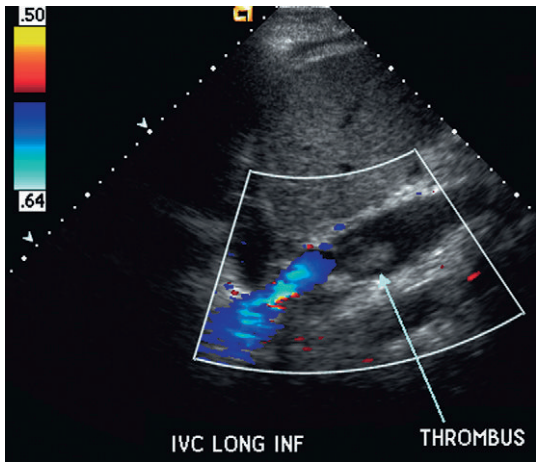


**Fig. 9.27** Longitudinal colour Doppler image of donor inferior vena cava. This liver is anastomosed with a piggyback technique therefore the flow within the cava is only a fraction of what it was previously. As a result clot has formed partially occluding the lumen (arrow).

or endovascular stent placement. If these fail, then surgical intervention with a patch venoplasty of the anastomosis can be performed.[62] Ideally, after a successful procedure hepatic vein calibre should decrease and cardiac periodicity should return to the hepatic vein flow profile.[63,64] Loss of periodicity may also be due to compression of the hepatic veins by the surrounding liver tissue by oedema in the early postoperative period, typically due to preservation injury, or by oedema in the later postoperative period related to rejection.[45,65] Due to the relatively large size of the IVC and the potential for a size mismatch between the donor and recipient cava, a greater than fourfold velocity gradient at the anastomosis is required to confidently diagnose a haemodynamically significant stenosis. A persistent monophasic hepatic vein flow profile is highly

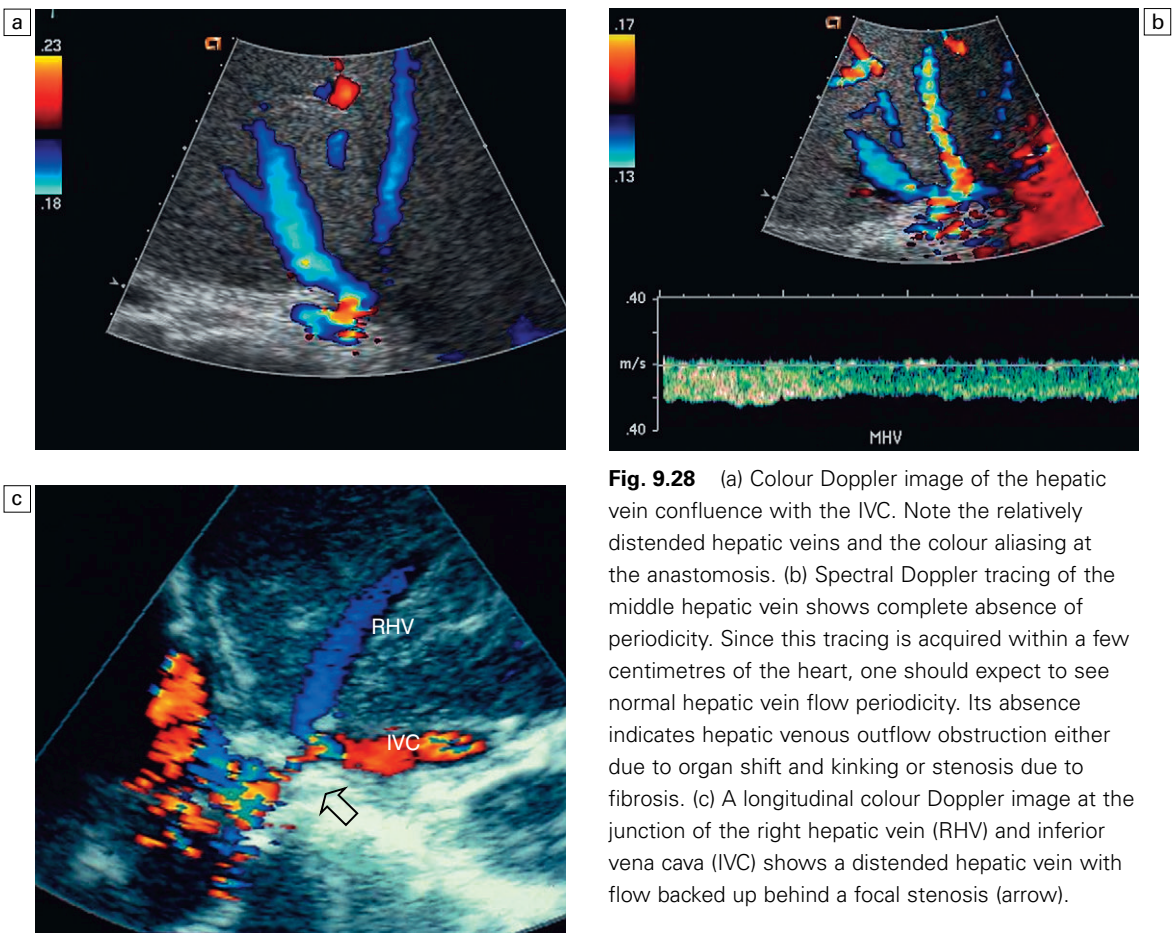


**Fig. 9.28** (a) Colour Doppler image of the hepatic vein confluence with the IVC. Note the relatively distended hepatic veins and the colour aliasing at the anastomosis. (b) Spectral Doppler tracing of the middle hepatic vein shows complete absence of periodicity. Since this tracing is acquired within a few centimetres of the heart, one should expect to see normal hepatic vein flow periodicity. Its absence indicates hepatic venous outflow obstruction either due to organ shift and kinking or stenosis due to fibrosis. (c) A longitudinal colour Doppler image at the junction of the right hepatic vein (RHV) and inferior vena cava (IVC) shows a distended hepatic vein with flow backed up behind a focal stenosis (arrow).

suggestive for hepatic outflow obstruction, but it is not specific. On the other hand, the presence of periodicity within the hepatic vein tracing on Doppler ultrasound can confidently exclude the possibility of significant outflow obstruction.[66]

In those patients with an in-line IVC, compromise of the lower anastomosis may present as lower extremity oedema and renal failure. Ultrasound and colour Doppler imaging of the anastomosis may reveal a kink or focal stenosis with a relatively high velocity jet. As with a piggyback procedure, a size mismatch between the donor and recipient vessels may produce a relatively high velocity jet and a less than threefold velocity increase at the anastomosis is seldom clinically significant. A three- to fourfold gradient is likely to be significant and should be correlated with the clinical findings. A greater than fourfold gradient must be considered haemodynamically significant.

Several authors have studied the possibility of predicting acute liver transplant rejection by identifying changes in the hepatic vein waveform.[67] During rejection, hepatocellular oedema and inflammatory infiltration increase the pressure within the confining capsule of the liver. This reduces the compliance of the liver and results in a dampened hepatic vein waveform. The theory is appropriate but other causes of hepatocellular oedema, such as cholangitis, hepatitis and upper IVC anastomotic stenosis produce similar damping, thereby limiting the specificity of this finding. The diagnosis of rejection is best made by needle biopsy. Ultrasound and Doppler guidance should be used to guide the biopsy needle into the liver, but away from the large central vessels.[68]

Hepatocyte transplantation is now performed at some centres as a temporising bridge until a donor liver can be acquired for the candidate. Patients undergo intraportal infusion of cryopreserved, matched human allogenic hepatocytes. Portal vein thrombosis with liver failure and death has been reported as a complication of this treatment. Portal vein Doppler ultrasound during and after cell infusion is mandatory for these patients.[69]

## THE PANCREAS TRANSPLANT

Whole organ pancreaticoduodenal transplantation is the most reliable means of restoring normal glucose homeostasis, the ultimate goal in the treatment of type I diabetes mellitus. Some studies have suggested that the restoration of normoglycemia for extended periods of time have a beneficial effect on patient quality of life, recurrence of diabetic glomerulopathy, microangiopathy, and progression of peripheral and autonomic neuropathy. There has been steady improvement in results of pancreas transplantation, gains largely due to the evolution of surgical techniques and more potent, selective immunosuppressive medications. In the USA, the current 1-year pancreas graft survival rate (when combined with a renal transplant) is 86%.[70] Despite the remarkable improvements made in the graft survival rates for all types of pancreatic transplantation, the high prevalence of graft loss caused by immunological rejection and surgical complications continues to be a problem. The technical failure rate approximates 8%, with vascular thrombosis being the main cause. Infection, pancreatitis, bleeding, anastomotic leaks and rejection are other causes of transplant failure.[71]

Many sonographic patterns of pancreas transplant dysfunction have been described, including focal or diffuse inhomogeneity of the echo texture, increased or decreased overall echogenicity and graft swelling. Unfortunately, none of these imaging findings is pathognomonic for any one complication of the pancreas transplant. In general, acute inflammatory changes tend to result in an oedematous swollen pancreas and a chronic insult tends to result in a small echogenic gland. These characteristics, however, do not help in solving the immediate clinical dilemma, specifically, differentiation between pancreatitis, rejection and vascular compromise.

A complete sonographic examination of the pancreas transplant recipient should cover the points listed in Table 9.6. When examining a pancreas transplant recipient, it is mandatory that the sonologist know the anatomic details of that patient's transplant (Fig. 9.29). Urological

**Table 9.6** Pancreas transplant – sonographic examination checklist

- Review the surgical record, especially with regard to the vasculature and drainage technique. Review any available prior imaging studies
- Evaluate organ echotexture. Make certain it is uniform throughout
- Rule out pancreatic duct dilatation
- Rule out peripancreatic fluid collections
- Rule out pseudocyst
- Examine the main artery to the transplant, particularly near its anastomosis
- Verify venous patency, particularly with high resistance arterial inflow to the organ
- Verify uniform parenchymal perfusion by colour and power Doppler

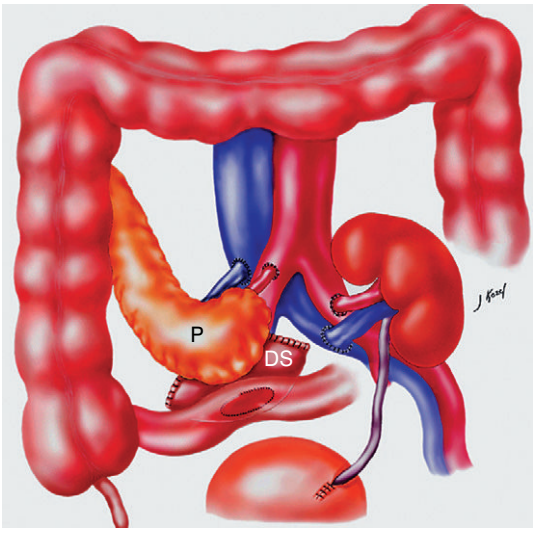


**Fig. 9.29** Artist rendering of a combined renal pancreas transplant. Typically the pancreas (P) is transplanted on the right with an interposed duodenal stump (DS) between pancreas and ileum. The splenic artery and vein, which serve as the vascular pedicle for the pancreas transplant, are anastomosed to the common iliac artery and vein.

and metabolic complications occur frequently in bladder-drained pancreas transplant recipients; and approximately 25% of bladder-drained pancreas allografts ultimately undergo enteric conversion for these complications. Therefore, in the last several years, enteric drainage has become the preferred conduit for managing pancreatic exocrine secretions.

The transplanted pancreas is one of the more difficult organs to monitor by any imaging modality. Ultrasound evaluation of the pancreas transplant can be very difficult. Because the pancreas does not have a discrete investing capsule, it is difficult to define its margins with sonography. Taken out of its normal anatomical location, it becomes more difficult to perceive, especially when camouflaged among bowel loops. Furthermore, in the absence of an adjacent liver, determining its relative echogenicity is difficult. With inflammation of the pancreas and the associated oedema of the adjacent tissues, the already hard to define pancreas becomes even more indistinct.

The one intrinsic anatomical landmark helpful in determining that it is indeed the pancreas being imaged is the pancreatic duct, but this is not always obvious. Identification of the pancreas may be improved by use of colour flow or power Doppler imaging. It identifies flow within the gland and the adjacent transplanted splenic artery and vein. This helps it stand out against the background of bowel loops (Fig. 9.30).

Since the splenic artery and vein end blindly (the donor spleen is removed), there is an increased possibility of them becoming thrombosed. Consequently, Doppler sonography is particularly useful in searching for vascular complications such as thrombosis, or anastomotic stricture.[71,72] Non-visualisation of flow within the organ is a disappointing finding (Fig. 9.31). If identified promptly, however, thrombolytic therapy alone, or in combination with surgical thrombectomy, has been reported to succeed in restoring transplant perfusion. Early diagnosis of pancreas transplant vascular complications is of paramount importance for appropriate treatment and organ salvage.[73]

Although the digestive enzymes are typically drained into the gut via the duodenal stump, some may leak around the pancreas vasculature predisposing to pseudoaneurysm formation, especially in the region of the anastomosis. Arterial flow within a perianastomotic fluid collection, the presence of swirling blood on colour Doppler, and a to-and-fro spectral Doppler waveform

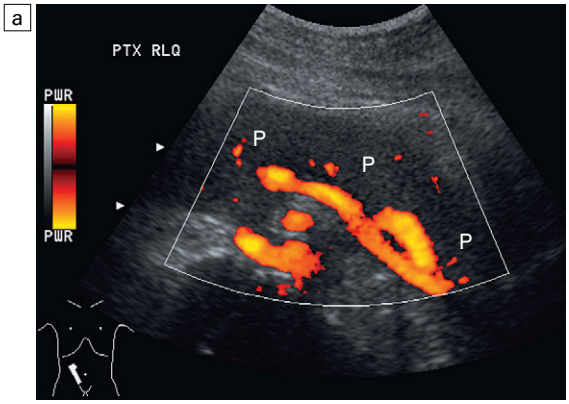


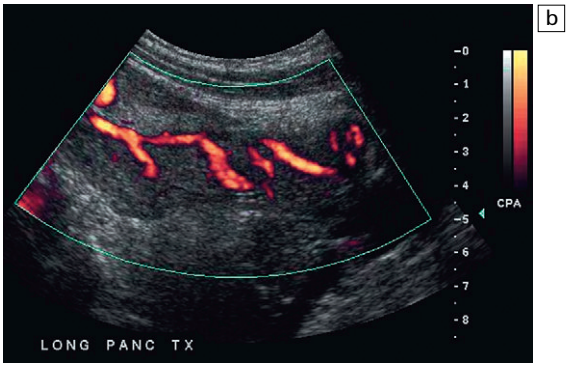


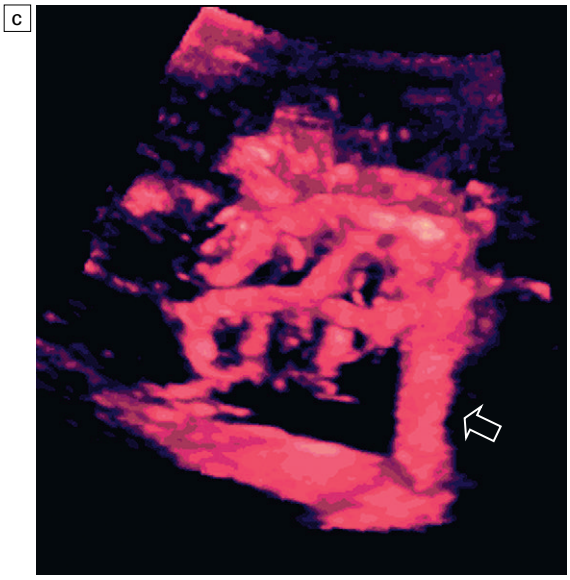


**Fig. 9.30** Power Doppler image of the transplant pancreas (P). (a) The vascular pedicle to the transplant pancreas is a prominent feature that helps to distinguish it from the surrounding bowel loops. (b) Setting scan parameters for slower velocities can depict branch vasculature within the pancreas transplant. This of course may be difficult when there is significant peristalsis in adjacent small bowel loops. (c) If a sufficient sonographic window is available, then a three-dimensional rendering of the vascular pedicle (arrow) can document its integrity.

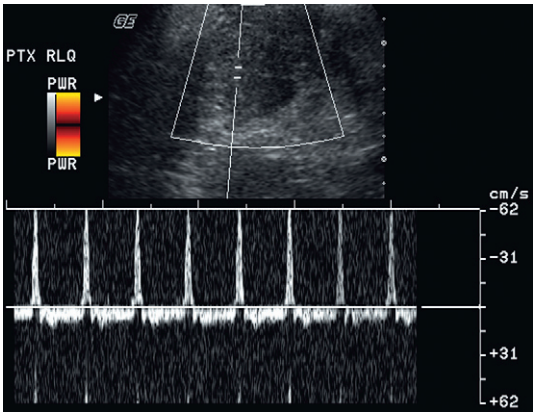


**Fig. 9.31** Power and spectral Doppler image of the pancreas. No colour flow can be identified within the gland. A spectral Doppler of the feeding artery shows extremely high resistance with spike of systolic inflow and reversed outflow throughout diastole.

indicate a transplant associated pseudoaneurysm[74] (Fig. 9.32). Rupture of transplant associated pseudoaneurysm has been described and is a life threatening event.[75] The pancreas transplant, as any other transplanted organ, requires occasional biopsy and this increases the risk of developing an arteriovenous fistula (AVF). Doppler findings are similar to AVFs seen in other locations (Fig. 9.33).

Although ultrasound is excellent in identifying parapancreatic fluid collections, the finding is frequently non-specific. Abscess, haematoma or liquefied phlegmon may all have similar ultrasound appearance of a complicated, debris-filled, irregular collection (Fig. 9.34). The true extent of a fluid collection is better evaluated by CT in which bowel gas does not limit the field of view. Furthermore, follow-up CT examinations

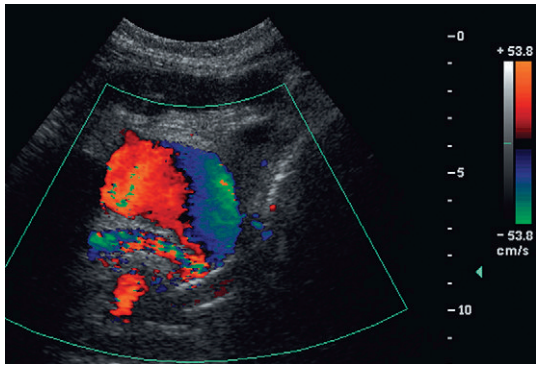


**Fig. 9.32** Colour Doppler image near the anastomosis of the pancreatic vascular pedicle. A rounded collection of colour flow with the classic swirl pattern identifies pseudoaneurysm of the anastomosed splenic artery.

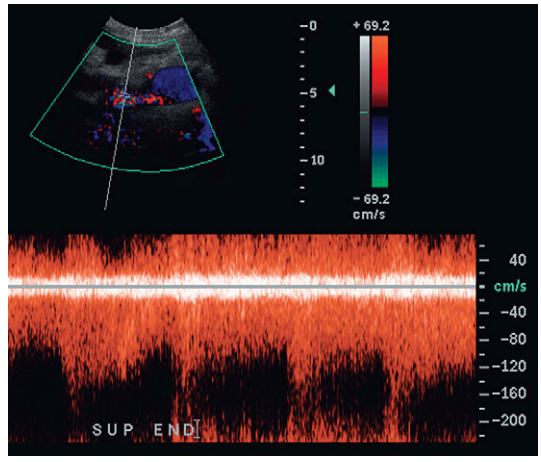


**Fig. 9.33** Colour and spectral Doppler image of a pancreas several days after a biopsy. High velocity, turbulent, low resistance arterial flow is present in an area of flash artifact. This was an arteriovenous fistula; a complication of the biopsy.

can be more reliably compared than ultrasound examinations. The source of a fluid collection is best evaluated by a contrast study or by aspiration.

Preliminary reports suggested that elevation of the resistive index could predict pancreatic transplant rejection. Unfortunately this is not the case, as many rejecting transplants have normal resistive indices. Since the pancreatic graft lacks a capsule, the rejection process will not generate enough intraparenchymal pressure to cause a consistently measurable elevation of vascular resistance.[76] A key role of ultrasound in rejection is to guide the pancreas transplant biopsy. It must identify a safe path to the organ, free of overlying intestine or mesentery. Doppler needs to identify the pancreatic vascular pedicle which must be avoided. The biopsy is monitored in real time, and delayed imaging and Doppler are useful to identify any possible complications.

## POST-TRANSPLANTATION LYMPHOPROLIFERATIVE DISORDER

Post-transplantation lymphoproliferative disorder (PTLD) is a rare but serious complication following solid organ transplantation. The most

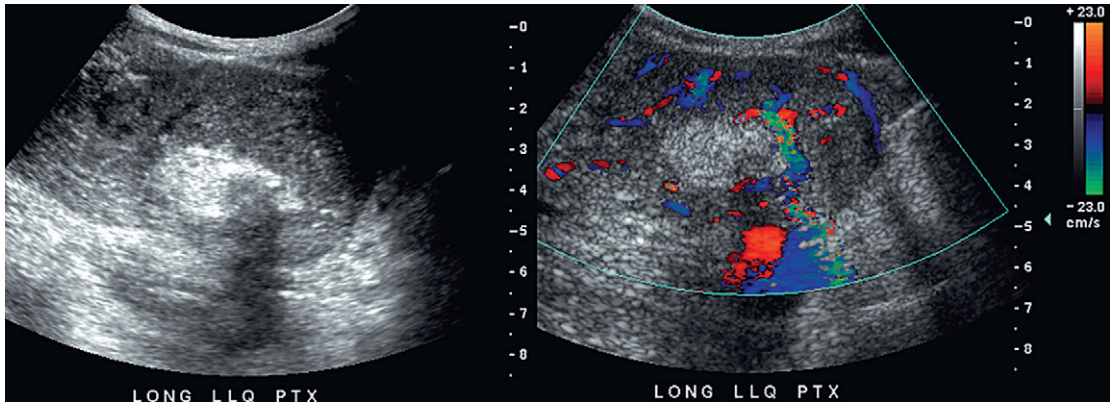


**Fig. 9.34** Grey-scale and colour Doppler images of a pancreas transplant reveal an echogenic rounded area with shadowing from gas. Colour Doppler shows some hyperaemia immediately adjacent to this collection. This was a focal pancreatic abscess.

commonly accepted theory for the pathophysiology of PTLD is that Epstein–Barr virus (EBV)-induced B-cell proliferation, unopposed by the pharmacologically suppressed immune system, causes plasma cell hyperplasia, then premalignant polymorphic B-cell proliferation and eventually malignant monoclonal lymphoma. If untreated, it can be fatal.[77] Reduction or cessation of immunosuppression is the best treatment and usually results in tumour regression. Early diagnosis prior to the development of frank lymphoma is very important and these patients may have a much better response. In a large study of PTLD in renal transplant recipients, it occurred in 2% of 1383 patients and contributed to death in over 50% of these cases.[78]

The liver is the organ most frequently involved by PTLD. It can appear as a focal mass, diffuse infiltration, or a periportal mass.[79] PTLD can affect the transplanted kidney and may manifest as a focal renal mass or diffuse infiltration.[80] The pancreas transplant may be involved, and can present as diffuse enlargement of the allograft or as a focal mass which may be confused with pancreatitis or acute rejection.[81]

Since ultrasound is often the first imaging study performed when laboratory tests suggest transplant dysfunction, it plays an important role in the early diagnosis of PTLD. It may detect urinary or biliary obstruction associated with adenopathy or may perceive a new ill-defined, typically hypoechoic mass. Doppler may show vascular distortion by the adenopathy.[82]

## OTHER IMAGING MODALITIES

MR angiography (MRA) has been found to be sensitive but not specific in the detection of significant vascular stenosis, nevertheless, normal MRA findings reliably exclude the possibility of significant stenosis.[83] CT and CT angiography (CTA) are excellent at identifying transplant and peritransplant fluid collections, abscess formation, vascular complications, etc. However, due to the need for nephrotoxic contrast and the radiation dose, ultrasound is the preferred screening test, with CT and CTA used for confirmation and problem solving.

## SUMMARY

These are very rewarding times in the field of organ transplantation. Advances in organ procurement and preservation; better matching of donors and recipients; refined surgical techniques; availability of new, more effective immunosuppressive agents; and improved post-transplant monitoring of organ recipients have contributed to decreased patient morbidity and improved allograft survival. Although Doppler sonography is only able to make a definitive diagnosis in a small percentage of cases, it is extremely useful as a screening tool in the management of transplant complications. All of this has allowed transplant recipients greater opportunity to return to a more normal lifestyle after surgery.[84,85]

## ACKNOWLEDGEMENTS

I would like to thank Dr Luis Fernandez, Department of Surgery, University of Wisconsin for manuscript review, Carrie Poole and Joan Palmer for manuscript preparation, and Mike Ledwidge, RT, RDMS, for image preparation.

## REFERENCES

1. Takemoto SK. HLA matching in the new millennium. Clin Transpl 2003; 387-403.
2. Gabardi S, Cerio J. Future immunosuppressive agents in solid-organ transplantation. Prog Transplant 2004; 14(2):148–156.
3. US Department of Health and Human Services, Public Health Service. Annual report of the US Scientific Registry of Transplant Recipients and the Organ Procurement and Transplantation Network, 1995-2002. (2004 report, kidney transplant

survivors).Online. Available: http://www.optn.org/AR2004/default.htm July 27 2005.
4. Belzer FO. Transplantation of the right kidney: surgical technique revisited. Surgery 1991; 110:113–115.
5. Solinger HW, Ploeg RJ, Eckhoff DE, et al. Two hundred consecutive simultaneous pancreas-kidney transplants with bladder drainage. Surgery 1993; 114:736–743.
6. Pozniak MA, Zagzebski J, Scanlan KA. Spectral and colour Doppler artifacts. Radiographics 1992; 12:35–44.
7. Pozniak MA, Kelcz F, Stratta R, et al. Extraneous factors affecting resistive index. Invest Radiol 1988; 23:899–904.
8. Benoit G, Blanchet P, Moukarzel M, et al. Surgical complications in kidney transplantation. Transplant Proc 1994; 26:287–288.
9. Hashimoto Y, Nagano S, Ohsima S, et al. Surgical complications in kidney transplantation: experience from 1200 transplants performed over 20 years at six hospitals in central Japan. Transplant Proc 1996; 28:1465–1467.
10. Drudi FM, Cascone F, Pretagostini R, et al. Role of colour Doppler US in the evaluation of renal transplant. Radiol Med (Torino) 2001; 101(4):243–250. [Article in Italian]
11. Pozniak MA, Kelcz F, D'Alessandro A, et al. Sonography of renal transplants: the effect of acute tubular necrosis, cyclosporine nephrotoxicity, and acute rejection on resistive index and renal length. Am J Radiol 1992; 158:791–797.
12. Genkins SM, Sanfilippo FP, Carroll BA. Duplex Doppler sonography of renal transplants: lack of sensitivity and specificity in establishing pathologic diagnosis. Am J Radiol 1989; 152:535–539.
13. Kelcz F, Pozniak MA, Pirsch JD, et al. Pyramidal appearance and resistive index: insensitive and non-specific sonographic indicators of renal transplant rejection. Am J Radiol 1990; 155:531–535.
14. Perrella RR, Duerincky AJ, Tessler FN, et al. Evaluation of renal transplant dysfunction by duplex Doppler sonography: a prospective study and review of the literature. Am J Kidney Dis 1990; 15:544–550.
15. Akiyama T, Ikegami M, Hara Y, et al. Haemodynamic study of renal transplant chronic rejection using power Doppler sonography. Transplant Proc 1996; 28:1458–1460.
16. Saarinen O. Diagnostic value of resistive index of renal transplants in the early postoperative period. Acta Radiol 1991; 32:166–169.
17. Koga S, Tanabe K, Yagisawa TT, et al. Urologic complications in renal transplantation. Transplant Proc 1996; 28:1472–1473.
18. Friedewald SM, Molmenti EP, Friedewald JJ, et al. Vascular and nonvascular complications of renal transplants: sonographic evaluation and correlation with other imaging modalities, surgery, and pathology. J Clin Ultrasound 2005; 33(3):127–139.
19. Platt JF, Rubin JM, Ellis JH. Distinction between obstructive and non-obstructive pyelocaliectasis with duplex Doppler sonography. Am J Radiol 1989; 153:997–1000.
20. Platt JF, Ellis JH, Rubin JM. Renal transplant pyelocaliectasis: role of duplex Doppler US in evaluation. Radiology 1991; 179:425–428.
21. Dodd GD, Tublin ME, Shah A, et al. Imaging of vascular complications associated with renal transplantation. Am J Radiol 1991; 157:449–459.
22. Pozniak MA, Dodd GD, Kelcz F. Ultrasonographic evaluation of renal transplantation. Radiol Clin North Am 1992; 30:1053–1066.
23. Grenier N, Douws C, Morel D, et al. Detection of vascular complications in renal allografts with colour Doppler flow imaging. Radiology 1991; 178:217–223.
24. Baxter GM, Ireland H, Moss JG, et al. Colour Doppler ultrasound in renal transplant artery stenosis: which Doppler index? Clin Radiol 1995; 50:618–622.
25. Roberts JP, Ascher NL, Fryd DS, et al. Transplant renal artery stenosis. Transplantation 1989; 4:580–583.
26. Patriquin HB, Lafortune M, Jequier JC, et al. Stenosis of the renal artery: assessment of slowed systole in the downstream circulation with Doppler sonography. Radiology 1992; 184:479–485.
27. Saarinen O, Salmela K, Edgren J. Doppler ultrasound in the diagnosis of renal transplant artery stenosis-value of resistive index. Acta Radiol 1994; 35:586–589.
28. Handa N, Fukunaga R, Etani H, et al. Efficacy of echo-Doppler examination for the evaluation of renovascular disease. Ultrasound Med Biol 1988; 14:1–5.
29. Stavros AT, Parker SH, Yakes WF, et al. Segmental stenosis of the renal artery: pattern recognition of tardus and parvus abnormalities with duplex sonography. Radiology 1992; 184:487–492.
30. Kribs SW, Rankin RN. Doppler ultrasonography after renal transplantation: value of reversed diastolic flow in diagnosing renal vein obstruction. Can Assoc Radiol J 1993; 44:434–438.
31. Baxter GM, Morley P, Dall B. Acute renal vein thrombosis in renal allografts: new Doppler ultrasonic findings. Clin Radiol 1991; 43(2):125–127.
32. Middleton WD, Kellman GM, Melson GL, et al. Postbiopsy renal transplant arteriovenous fistulas: colour Doppler versus US characteristics. Radiology 1989; 171:253–257.
33. Hubsch PJS, Mostbeck G, Barton PP, et al. Evaluation of arteriovenous fistulas and pseudoaneurysms in renal allografts following percutaneous needle biopsy: colour coded Doppler sonography vs duplex Doppler sonography. J Ultrasound Med 1990; 9:95–100.
34. US Department of Health and Human Services, Public Health Service. Annual report of the US Scientific Registry of Transplant Recipients and the Organ Procurement and Transplantation Network, 1995–2002. (2004 report, liver transplant survivors).

Online. Available: http://www.optn.org/AR2004/default.htm July 27, 2005.
35. Ravindra KV, Guthrie JA, Woodley H, et al. Preoperative vascular imaging in pediatric liver transplantation. J Pediatr Surg 2005; 40(4):643–647.
36. Neuhaus P, Platz KP. Liver transplantation: newer surgical approaches. Baillieres Clin Gastroenterol 1994; 8:481–493.
37. Houssin D, Boillot AO, Soubrane O, et al. Controlled liver splitting for transplantation in two recipients: technique, results and perspectives. Br J Surg 1993; 80:75–80.
38. Dodd GD III, Memel DS, Zajko AB, et al. Hepatic artery stenosis and thrombosis in transplant recipients: Doppler diagnosis with resistive index and systolic acceleration time. Radiology 1994; 192:657–661.
39. Platt JF, Yotzy GG, Bude RO, et al. Use of Doppler sonography for revealing hepatic artery stenosis in liver transplant recipients. AJR Am J Roentgenol 1997; 168:473–476.
40. Sidhu PS, Ellis SM, Karani JB, et al. Hepatic artery stenosis following liver transplantation: significance of the tardus parvus waveform and the role of microbubble contrast media in the detection of a focal stenosis. Clin Radiol 2002; 57(9):789–799.
41. Kaneko J, Sugawara Y, Akamatsu N, et al. Prediction of hepatic artery thrombosis by protocol Doppler ultrasonography in pediatric living donor liver transplantation. Abdom Imaging 2004; 29(5):603–605.
42. Sidhu PS, Shaw AS, Ellis SM, et al. Microbubble ultrasound contrast in the assessment of hepatic artery patency following liver transplantation: role in reducing frequency of hepatic artery arteriography. Eur Radiol 2004; 14(1):21–30.
43. Herold C, Reck T, Ott R, et al. Contrast-enhanced ultrasound improves hepatic vessel visualization after orthotopic liver transplantation. Abdom Imaging 2001; 26(6):597–600.
44. Vivarelli M, Cucchetti A, La Barba G, et al. Ischemic arterial complications after liver transplantation in the adult: multivariate analysis of risk factors. Arch Surg 2004; 139(10):1069–1074.
45. Kok T, Haagsma EB, Klompmaker IJ, et al. Doppler ultrasound of the hepatic artery and vein performed daily in the first two weeks after orthotopic liver transplantation. Invest Radiol 1996; 31:173–179.
46. Garcia-Criado A, Gilabert R, Salmeron JM, et al. Significance of and contributing factors for a high resistive index on Doppler sonography of the hepatic artery immediately after surgery: prognostic implications for liver transplant recipients. AJR Am J Roentgenol 2003; 181(3):831–838.
47. Hall TR, McDiarmid SV, Grant EG, et al. False-negative duplex Doppler studies in children with hepatic artery thrombosis after liver transplantation. AJR Am J Roentgenol 1990; 154:573–575.
48. Stell D, Downey D, Marotta P, et al. Prospective evaluation of the role of quantitative Doppler ultrasound surveillance in liver transplantation. Liver Transpl 2004; 10(9):1183–1188.
49. Propeck PA, Scanlan KA. Reversed or absent hepatic arterial diastolic flow in liver transplants shown by duplex sonography: a poor predictor of subsequent hepatic artery thrombosis. AJR Am J Roentgenol 1992; 159:1199–1201.
50. Otobe Y, Hashimoto T, Shimizu Y, et al. Formation of a fatal arterioportal fistula following needle liver biopsy in a child with a living-related liver transplant: report of a case. Surg Today 1995; 25:916–919.
51. Jabbour N, Reyes J, Zajko A, et al. Arterioportal fistula following liver biopsy: three cases occurring in liver transplant recipients. Dig Dis Sci 1995; 40:1041–1044.
52. Doria C, Marino IR. Acute portal vein thrombosis secondary to donor/recipient portal vein diameter mismatch after orthotopic liver transplantation: a case report. Int Surg 2003; 88(4):184–187.
53. Davidson BR, Gibson M, Dick R, et al. Incidence, risk factors, management, and outcome of portal vein abnormalities of orthotopic liver transplantation. Transplantation 1994; 57(8):1174–1177.
54. Doria C, Marino IR. Acute portal vein thrombosis secondary to donor/recipient portal vein diameter mismatch after orthotopic liver transplantation: a case report. Int Surg 2003; 88(4):184–187.
55. Cheng YF, Chen CL, Huang TL, et al. Risk factors for intraoperative portal vein thrombosis in pediatric living donor liver transplantation. Clin Transplant 2004; 18(4):390–394.
56. Corno V, Torri E, Bertani A, et al. Early portal vein thrombosis after pediatric split liver transplantation with left lateral segment graft. Transplant Proc 2005; 37(2):1141–1142.
57. Durham JD, LaBerge JM, Kam I, et al. Portal vein thrombolysis and closure of competitive shunts following liver transplantation. J Vasc Interv Radiol 1994; 5:611–616.
58. Fujimoto M, Moriyasu F, Someda H, et al. Evaluation of portal haemodynamics with Doppler ultrasound in living related donor liver transplantation in children: implications for ligation of spontaneous portosystemic collateral pathways. Transplant Proc 995; 27:1174–1176.
59. Nishida S, Kadono J, DeFaria W, et al. Gastroduodenal artery steal syndrome during liver transplantation: intraoperative diagnosis with Doppler ultrasound and management. Transpl Int 2005; 18(3):350–353.
60. Tang SS, Shimizu T, Kishimoto R, et al. Analysis of portal venous waveform after living-related liver transplantation with pulsed Doppler ultrasound. Clin Transplant 2001; 15(6):380–387.
61. Salizzoni M, Andorno E, Bossuto E, et al. Piggyback techniques versus classical technique in orthotopic liver transplantation: a review of 75 cases. Transplant Proc 1994; 26:3552.

62. Akamatsu N, Sugawara Y, Kaneko J, et al. Surgical repair for late-onset hepatic venous outflow block after living-donor liver transplantation. Transplantation 2004; 77(11):1768–1770.
63. Carnevale FC, Borges MV, Pinto RA, et al. Endovascular treatment of stenosis between hepatic vein and inferior vena cava following liver transplantation in a child: a case report. Pediatr Transplant 2004; 8(6):576–580.
64. Totsuka E, Hakamada K, Narumi S, et al. Hepatic vein anastomotic stricture after living donor liver transplantation. Transplant Proc 2004; 36(8):2252–2254.
65. Rossi AR, Pozniak MA, Zarvan NP. Upper inferior vena caval anastomotic stenosis in liver transplant recipients: Doppler US diagnosis. Radiology 1993; 187:387.
66. Ko EY, Kim TK, Kim PN, et al. Hepatic vein stenosis after living donor liver transplantation: evaluation with Doppler US. Radiology 2003; 229(3):806–810.
67. Jequier S, Jequier JC, Hanquinet S, et al. Orthotopic liver transplants in children: change in hepatic venous Doppler wave pattern as an indicator of acute rejection. Radiology 2003; 226(1):105–112.
68. Van Thiel DH, Gavaler JS, Wright H, et al. Liver biopsy: its safety and complications as seen at a liver transplant center. Transplantation 1993; 55:1087–1090.
69. Baccarani U, Adani GL, Sanna A, et al. Portal vein thrombosis after intraportal hepatocytes transplantation in a liver transplant recipient. Transpl Int 2005; 18(6):750–754.
70. US Department of Health and Human Services, Public Health Service. Annual report of the US Scientific Registry of Transplant Recipients and the Organ Procurement and Transplantation Network, 1995–2002. (2004 report, pancreas transplant survivors).Online. Available: http://www.optn.org/AR2004/default.htm July 27 2005.
71. Nikolaidis P, Amin RS, Hwang CM, et al. Role of sonography in pancreatic transplantation. Radiographics 2003; 23:939–949.
72. Foshager MC, Hedlund LJ, Troppmann C, et al. Venous thrombosis of pancreatic transplants: diagnosis by duplex sonography. AJR Am J Roentgenol 1997; 169:1269–1273.
73. Spiros D, Christos D, John B, et al. Vascular complications of pancreas transplantation. Pancreas 2004; 28(4):413–420.
74. Tobben PJ, Zajko AB, Sumkin JH, et al. Pseudoaneurysms complicating organ transplantation: roles of CT, duplex sonography, and angiography. Radiology 1988; 169:65–70.
75. Green BT, Tuttle-Newhall J, Suhocki P, et al. Massive gastrointestinal hemorrhage due to rupture of a donor pancreatic artery pseudoaneurysm in a pancreas transplant patient. Clin Transplant 2004; 18(1):108–111.
76. Wong JJ, Krebs TL, Klassen DK, et al. Sonographic evaluation of acute pancreatic transplant rejection: morphology - Doppler analysis versus guided percutaneous biopsy. AJR Am J Roentgenol 1996; 166:803–807.
77. Nalesnik MA. The diverse pathology of post-transplant lymphoproliferative disorders: the importance of a standardized approach. Transpl Infect Dis 2001; 3:88–96.
78. Bates WD, Gray DWR, Dada MA, et al. Lymphoproliferative disorders in Oxford renal transplant recipients. J Clin Pathol 2003; 56:439–446.
79. Pickhardt PJ, Siegel MJ. Posttransplantation lymphoproliferative disorder of the abdomen: CT evaluation in 51 patients. Radiology 1999; 213:73–78.
80. Vrachliotis TG, Vaswani KK, Davies EA, et al. CT findings in posttransplantation lymphoproliferative disorder of renal transplants. AJR Am J Roentgenol 2000; 175:183–188.
81. Meador TL, Krebs TL, Wong You Cheong JJ, et al. Imaging features of posttransplantation lymphoproliferative disorder in pancreas transplant recipients. AJR Am J Roentgenol 2000; 174:121–124.
82. Scarsbrooka AF, Warakaullea DR, Dattania M, et al. Post-transplantation lymphoproliferative disorder: the spectrum of imaging appearances. Clin Radiol 2005; 60:47–55.
83. Kim BS, Kim TK, Jung DJ, et al. Vascular complications after living related liver transplantation: evaluation with gadolinium-enhanced three-dimensional MR angiography. AJR Am J Roentgenol 2003; 181(2):467–474.
84. Lee HM. Quality of life after renal transplantation. Transpl Proc 1996; 28:1171.
85. Park IH, Yoo HJ, Han DJ, et al. Changes in the quality of life before and after renal transplantation and comparison of the quality of life between kidney transplant recipients, dialysis patients, and normal controls. Transpl Proc 1996; 28:1937–1938.

# Doppler imaging of the prostate

# 10

Fred T. Lee, Jr

## INDICATIONS

The most important use of colour Doppler imaging of the prostate remains as an aid in cancer detection. This is particularly relevant in patients in whom cancer is suspected based on prostate specific antigen (PSA) elevation without obvious tumour on grey-scale imaging. Other uses for Doppler imaging are largely confined to detection of prostatitis and inflammatory conditions. Controversy continues surrounding diagnosis and treatment of prostate cancer. This is largely attributable to the wide range of biological behaviour found with this disease. Up to 30% of 80-year-old males will have histological evidence of prostate cancer, yet most will die from other causes. Unfortunately, a more aggressive subset remains an important cause of mortality among men, with 30350 deaths expected in the USA in 2005.[1]

## ANATOMY

The prostate lies immediately anterior to the rectum and inferior to the bladder. Prostatic zonal anatomy has been extensively described by McNeal et al.[2] In summary, the prostate is composed of three major zonal areas; the peripheral zone, the central zone and the transition zone (Fig. 10.1). The peripheral zone is the most posterior, and the central zone is a continuation of the peripheral zone cephalad. The transition zone is the most central area of the prostate, and surrounds the urethra as it courses through the prostate. The anterior fibromuscular stroma lines the prostate anteriorally.

### Prostate vascular anatomy

The prostate is supplied from two arterial sources: the prostatic arteries and the inferior vesical arteries, both arising from the internal iliac system. The prostatic arteries enter the prostate from an anterolateral location on each side, and give off capsular branches as well as urethral branches. Capsular arteries course along the lateral margin of the prostate, and give off numerous perforating branches which penetrate the capsule and supply approximately two-thirds of the total glandular tissue. The areas of penetration into the capsule are commonly referred to as the neurovascular bundles (Fig. 10.2). The inferior vesical arteries run along the inferior surface of the bladder and also provide urethral branches. In addition to supplying the central portion of the prostate, the inferior vesical arteries also give off branches which supply the bladder base, seminal vesicles and distal ureters (Fig. 10.3).[3,4] Both the capsular and urethral branches can be visualised with colour Doppler ultrasound. In the absence of inflammation, neoplasm or hypertrophy the normal prostate is expected to have low level periurethral and pericapsular flow, with only a low level of flow in the prostatic parenchyma.[5]

## EQUIPMENT AND TECHNIQUE

Examination of the prostate by ultrasound requires a high-frequency (5–7.5 MHz) end-fire or biplane transrectal transducer. For the purposes of this chapter, conventional colour Doppler and power Doppler are considered simultaneously. For most general applications,

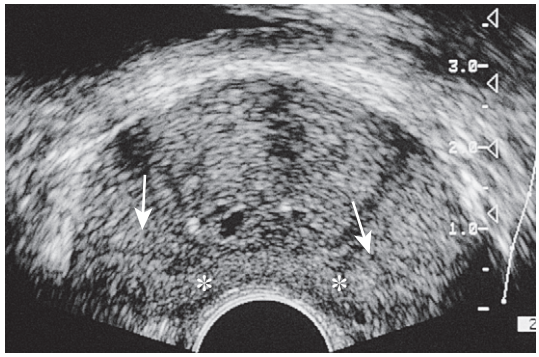


**Fig. 10.1** Axial ultrasound of the prostate in a normal patient. Note peripheral zone (*) separated from the more centrally oriented, periurethral, transition zone by the surgical capsule (arrows).

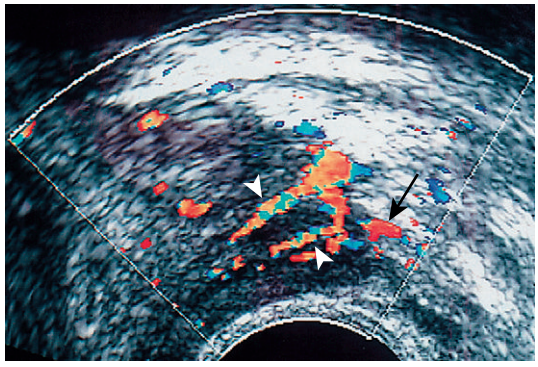

**Fig. 10.2** Axial image of the left neurovascular bundle. Note left neurovascular bundle (arrow) with perforating branches penetrating into the prostate (arrowheads).

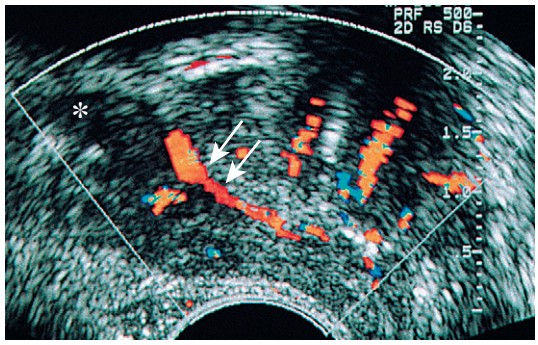


**Fig. 10.3** Sagittal image of the prostate at the level of the seminal vesicle (*) demonstrates periurethral flow (arrows) originating from the inferior vesicle artery.

an end-fire transducer is favoured due to the ease of switching between axial (coronal) and longitudinal imaging planes, as well as the more favourable angle for transrectal prostatic biopsies. For specialised applications such as prostatic volumetry and cryosurgery, a true biplane transducer is necessary.

No specific patient preparation is required although some centres will give the patient a pre-examination enema and have them empty their bladder. The patient is generally placed in the left lateral decubitus position, and the knees brought up to the chest. A digital rectal examination is recommended prior to probe insertion to rule out any obstructing pathology and also to allow the examiner to evaluate the prostate by digital examination. The probe is covered with a condom into which coupling gel has been placed, and the probe lubricated and gently inserted into the rectal canal. Examination of the prostate by grey-scale imaging is first performed, and the length, width and height of the gland measured. The prostatic volume is calculated based on the formula for a prolate ellipsoid (length × width × height × 0.523); this allows correlation of the measured PSA with a predicted PSA based on gland volume. Normal prostatic tissue produces approximately 0.3 ng $cc^{-1}$ of PSA, whereas cancerous tissue produces approximately 3.0 ng $cc^{-1}$ of tumour. Normal levels for polyclonal assays are typically defined as <4.0 ng $mL^{-1}$; unfortunately, up to 20% of prostatic cancers present in patients with 'normal' levels of PSA. A 'predicted' PSA can be generated based on the patient's gland volume × 0.2 for polyclonal assays (or gland volume × 0.1 for monoclonal assays). A level of measured PSA that exceeds predicted PSA increases the suspicion of cancer and increases the positive predictive value of prostatic biopsy.[6]

Most prostate cancers (70%) arise in the peripheral zone, with a minority originating in the central (10–15%) and transition zones (10–15%). Because of this, it is very important that the sonographer carefully examine the peripheral zone for signs of tumour. Virtually all prostate cancers will be hypoechoic in relation to

normal peripheral zone tissues (Fig. 10.4), although a minority of cribriform carcinomas can demonstrate punctate calcifications. Tumours in the peripheral zone have ready access to sites of anatomical weakness, including the neurovascular bundles, ejaculatory ducts and apex of the gland. This results in more aggressive clinical behaviour of peripheral zone tumours when compared to other locations. Transition zone tumours tend to behave in a clinically more benign manner because they are distant from sites of anatomical weakness, and thus need to grow quite large before spreading outside of the gland. The main problem with the diagnosis of transition zone tumours is the heterogeneous echotexture of the normal transition zone. Because normal transition zone tissue can be hypoechoic, hyperechoic or contain calcifications or cysts, it is extremely difficult to diagnose subtle changes in echogenicity that may be associated with neoplasia. Therefore, colour Doppler can play a crucial role in the diagnosis of transition zone tumours by identifying areas of abnormal flow.

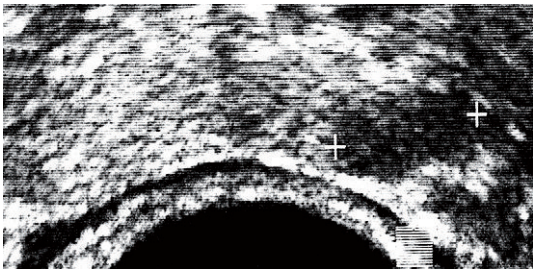

**Fig. 10.4** Prostate cancer. Axial image of the prostate at the mid-gland. Hypoechoic tumour (+) originates in the left neurovascular bundle area.

## COLOUR DOPPLER OF PROSTATE CANCER

Knowledge of the excess PSA for a particular gland is most important from an ultrasound standpoint when an obvious peripheral zone tumour is not found in the face of an elevated measured PSA. As previously mentioned, transition zone tumours are difficult to visualise by grey-scale criteria due to the in homogeneous nature of normal transition zone tissue. Once it is established that the patient is at high risk for prostate cancer by PSA criteria, and no peripheral zone cancer has been found, a careful examination of the transition zone should be undertaken. It is in the search for transition zone tumours that colour Doppler ultrasound has proven to be most useful. Prostate cancer is generally hypervascular when compared to normal prostatic tissue and this is manifested as increased colour encoding at sensitive instrument settings (Fig. 10.5). These can be targeted for biopsy with increased positive biopsy rates compared to blinded sextant biopsies. It is controversial as to whether targeted biopsies using color Doppler alone can replace sextant biopsies.[7] Early work using contrast enhanced color Doppler ultrasound demonstrates an increased sensitivity for the detection of prostate cancer,[8,9] but the exact type of contrast material, imaging algorithm and time after injection has not yet been standardised. Additionally, ultrasound contrast agents have not yet been approved for use in the USA. Spectral Doppler plays a limited role in the specific diagnosis of prostate cancer. Tumours tend to have low resistance (high diastolic) flow, although the exact role and specificity of this finding has yet to be fully elucidated.

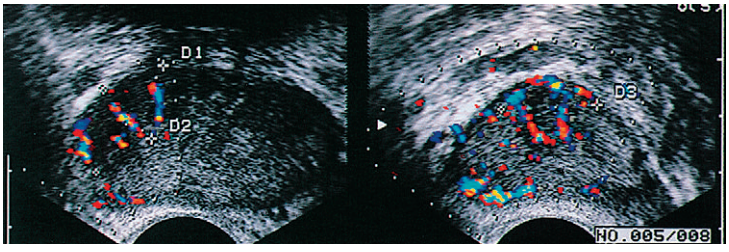


**Fig. 10.5** Transition zone prostate cancer (biopsy proven). Axial (left) and sagittal (right) images demonstrate a hypervascular tumour in the transition zone (arrows).

The use of colour Doppler in the diagnosis of peripheral zone tumours is more controversial. Several authors have found increased colour Doppler flow to have no significant correlation with the presence or absence of tumour at histology. In addition, there has been no colour Doppler method consistently to discriminate tumour from focal prostatitis in areas of increased flow. Others have found biopsy of sites of increased flow useful in the face of an increased measured PSA (greater than predicted) and no other obvious sites of tumour.[10] This has been found to be particularly useful in black males, where the positive predictive value for biopsy of a focal area of increased colour encoding has been found to be twice that of white males (32.2% vs 13.5% respectively).[11] Most authors now feel that colour Doppler is more of a complementary test to grey-scale ultrasound, PSA and gland volume rather than a single factor on which to base biopsy decisions (Fig. 10.6).

## COLOUR DOPPLER OF PROSTATIC INFLAMMATORY DISEASE

Prostatitis is a difficult condition to diagnose and treat. There are several aetiologies of prostatitis, ranging from bacterial to non-bacterial causes. In the case of bacterial prostatitis, the offending organism is usually *Escherichia coli* or other urinary tract pathogens.

Grey-scale findings of acute prostatitis include an hypoechoic rim around the prostate or periurethral areas, and low level echogenic areas within the prostate.[12] Colour Doppler is useful in cases of diffuse bacterial prostatitis. The severity of the inflammatory reaction is mirrored by focal or diffuse increase in the colour signal in the prostatic parenchyma.[13] When focally increased colour signals are seen in cases of prostatitis, there is no reliable non-invasive method to differentiate inflammation from tumour.[13] However, cases of grossly increased flow spread diffusely throughout the gland should be considered prostatitis in the appropriate clinical setting (Fig. 10.7). When the inflammatory process continues to suppuration, a prostatic abscess can develop. On ultrasound, this is seen as a cavity filled with low-level echoes from debris (Fig. 10.8).[14] Colour Doppler may detect increased flow around the rim of the cavity, although this finding is not necessary to make the diagnosis. Cases of bacterial prostatitis are treated by antibiotics, whereas prostatic abscess

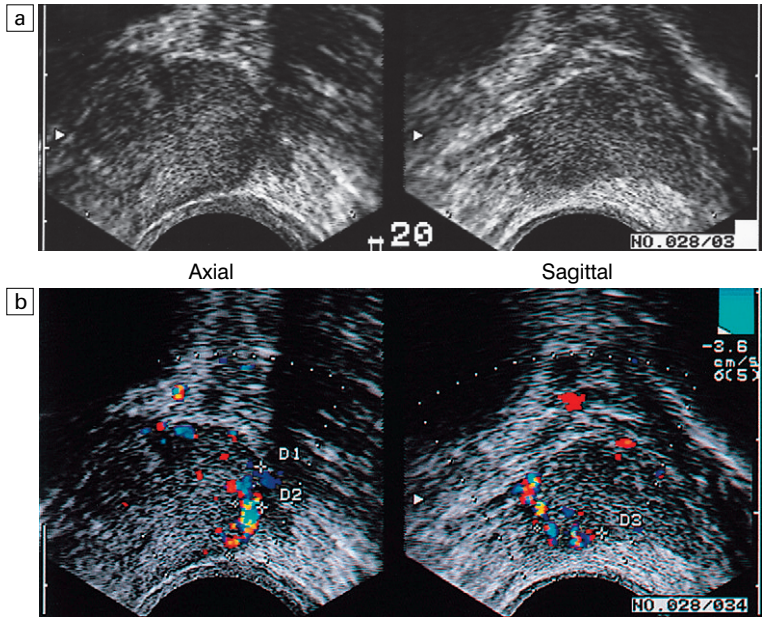


**Fig. 10.6** Peripheral zone prostate cancer. (a) Axial and sagittal grey-scale images demonstrate a subtle hypoechoic area in the left neurovascular bundle (arrows). Biopsy through this area was positive for adenocarcinoma, Gleason score 6. (b) Axial and sagittal colour Doppler images at corresponding locations demonstrate increased colour flow in areas involved by tumour.

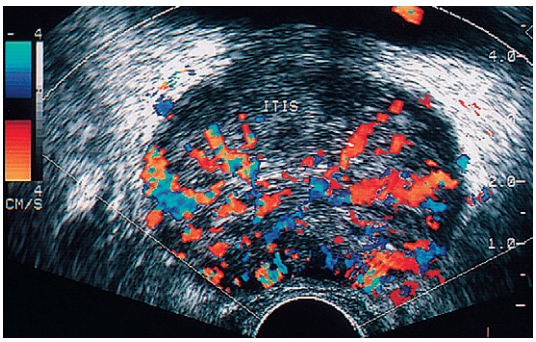


**Fig. 10.7** Prostatitis. Colour Doppler image of diffuse prostatitis demonstrates grossly increased flow throughout the gland.

requires transrectal catheter or transurethral drainage with unroofing of the abscess cavity.

## CONCLUSIONS

Doppler ultrasound of the prostate contributes significantly to the diagnostic value of sonography in the assessment of prostatic disease. Colour and power Doppler identify areas of abnormal blood flow, which can then be examined more closely with grey-scale imaging, or biopsied under ultrasound guidance.

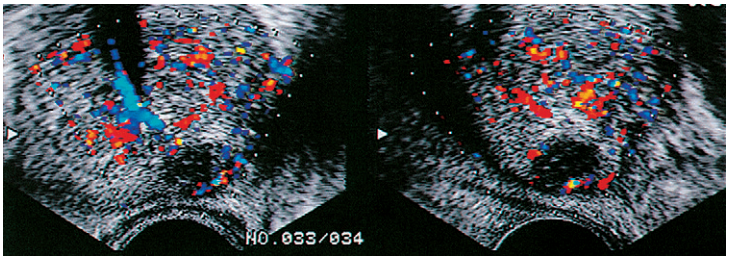


**Fig. 10.8** Prostatic abscess. Markedly hypoechoic lesion with subtle through transmission is present in the peripheral zone of this patient. Note lack of flow in the central portion of this lesion, a finding that would be very unusual for prostate cancer. Drainage confirmed the presence of an abscess.

## REFERENCES

1. Jemal A, Murray T, Ward E, et al. CA cancer. J Clin 2005; 55:10–30.
2. McNeal JE. Regional morphology and pathology of the prostate. Am J Clin Pathol 1968; 49:347–357.
3. Flocks RH. The arterial distribution within the prostate gland: its role in transurethral prostatic resection. J Urol 1937; 37:524–548.
4. Clegg EJ. The arterial supply of the human prostate and seminal vesicles. J Anat 1955; 89:209–217.
5. Neumaier CE, Martinoli C, Derchi LE, et al. Normal prostate gland: examination with colour Doppler US. Radiology 1995; 196:453–457.
6. Lee F, Littrup PJ, Loft-Christensen L, et al. Predicted prostate specific antigen results using transrectal ultrasound gland volume: Differentiation of benign prostatic hyperplasia and prostate cancer. Cancer 1992; 70:211–220.
7. Halpern EJ, Frauscher F, Strup SE, et al. Prostate: high-frequency Doppler US imaging for cancer detection. Radiology 2002; 225:71–77.
8. Frauscher F, Klauser A, Halpern EJ, et al. Detection of prostate cancer with a microbubble ultrasound contrast agent. Lancet 2001; 357:1849–1850.
9. Bogers HA, Sedelaar JP, Beerlage HP, et al. Contrast-enhanced three-dimensional power Doppler angiography of the human prostate: correlation with biopsy outcome. Urology 1999; 54:97–104.
10. DeCarvalho VS, Soto JA, Guidone PL, et al. Role of colour Doppler in improving the detection of cancer in the isoechoic prostate gland (abstr). Radiology 1995; 197(P):365.
11. Littrup PJ, Klein RM, Sparschu RA, et al. Colour Doppler of the prostate: histologic and racial correlations (abstr). Radiology 1995; 197(P):365.
12. Griffiths GJ, Crooks AJR, Roberts EE, et al. Ultrasonic appearances associated with prostatic inflammation: A preliminary study. Clin Radiol 1984; 35:343–345.
13. Patel U, Rickards D. The diagnostic value of colour Doppler flow in the peripheral zone of the prostate, with histological correlation. Br J Urol 1994; 74:590–595.
14. Lee FT Jr, Lee F, Solomon MH, et al. Ultrasonic demonstration of prostatic abscess. J Ultrasound Med 1986; 5:101–102.

# Doppler imaging of the penis

# 11

Myron A. Pozniak and Fred T. Lee, Jr

## INTRODUCTION

Duplex sonography with colour Doppler is the modality of choice for evaluating the penis. The advantages of Doppler over other imaging modalities are ease of performing the study, patient acceptance, versatility, minimally invasive nature, reproducibility, availability and relatively low cost. Colour Doppler allows the examiner to delineate vascular anatomy, display dynamic variations in blood flow, measure arterial velocity and infer adequacy of venous drainage. By combining Doppler with grey-scale imaging and pharmacological induction of erection, both anatomical and physiological abnormalities can be assessed during the flaccid and erect states.[1–5]

## INDICATIONS

The primary application of penile Doppler imaging is to assess the vasculature in patients with erectile dysfunction (ED), the prevalence and the severity of which increase with advancing age.[6] While impotence may be the result of psychogenic, neurogenic, or hormonal factors, vascular disease is one of the leading causes of ED.[4,7] With the introduction of phosphodiesterase inhibitors [specifically sildenafil citrate (Viagra©), Vardenafil HCl (Livetra©), and Tadalafil (Cialis©)], the frequency of Doppler studies for penile impotence has notably decreased.[8] However, diagnostic imaging of ED is still considered useful because ED can be the presenting symptom for a variety of diseases, such as diabetes mellitus, coronary artery disease, atherosclerosis, hypertension and hyperlipidaemia. Most centres will now prescribe a trial of the phosphodiesterase inhibitors as the initial diagnostic/therapeutic test, with only non-responders being sent on for further evaluation.

Doppler and ultrasound imaging can be used to identify arterial or venous injury following acute penile trauma.[3,9,10] Doppler and ultrasound can be used to evaluate patients with Peyronie's disease, an idiopathic process which produces fibrous plaques in the penile tunica albuginea,[3,11,12] specifically to determine if these plaques cause any significant vascular compromise.[13]

## PENILE ANATOMY AND PHYSIOLOGY

The penis contains three longitudinal, cylindrical erectile bodies. Two corpora cavernosa are located in the dorsal two-thirds of the penile shaft, and a single corpora spongiosum is located in the ventral one-third of the shaft. The corpora cavernosa are enclosed by the tunica albuginea, a tough, non-distensible fascial layer. The septum that divides the corpora cavernosa contains fenestrations that create multiple connecting anastomotic channels between the sinusoidal spaces, allowing for free communication across the midline. The dorsal arteries, veins and nerves are situated centrally along the penile dorsum, superficial to the tunica albuginea and deep to Buck's fascia. The urethra is contained within the corpus spongiosum.[14]

On ultrasound, the corpora cavernosa are of uniform hypoechoic echotexture. The tunica can be seen as an echogenic envelope around the corpora. The echogenic walls of the cavernosal

arteries can be seen centrally within the corpora. The corpus spongiosum is of higher echogenicity (Fig. 11.1).

## Arterial anatomy

The *internal pudendal artery* and its branches are the primary source of arterial supply to the penis. The first three branches are the superficial perineal artery, the bulbar artery and a small urethral artery. The *perineal artery* is a large and constant branch that, in 80% of cases, has an internal and external branch. The *bulbar artery*, which supplies the proximal penile shaft, is usually easily identified during angiography because it is associated with a bulbar parenchymal blush in the early arterial phase. The *urethral artery*, which is of small diameter, arises anterior to the bulbar artery. After these branches, the internal pudendal artery continues as the *common penile artery*. It then divides into *left and right penile arteries*, which enter the base of the penis and branch into a dorsal artery and a cavernosal artery. The *dorsal artery* extends along the dorsal aspect of the penile shaft towards the glans and terminates at the level of the arterial corona of the glans; it supplies blood primarily to the skin, subcutaneous tissues and glans. Collateral vessels from the dorsal artery often communicate with the cavernosal artery.

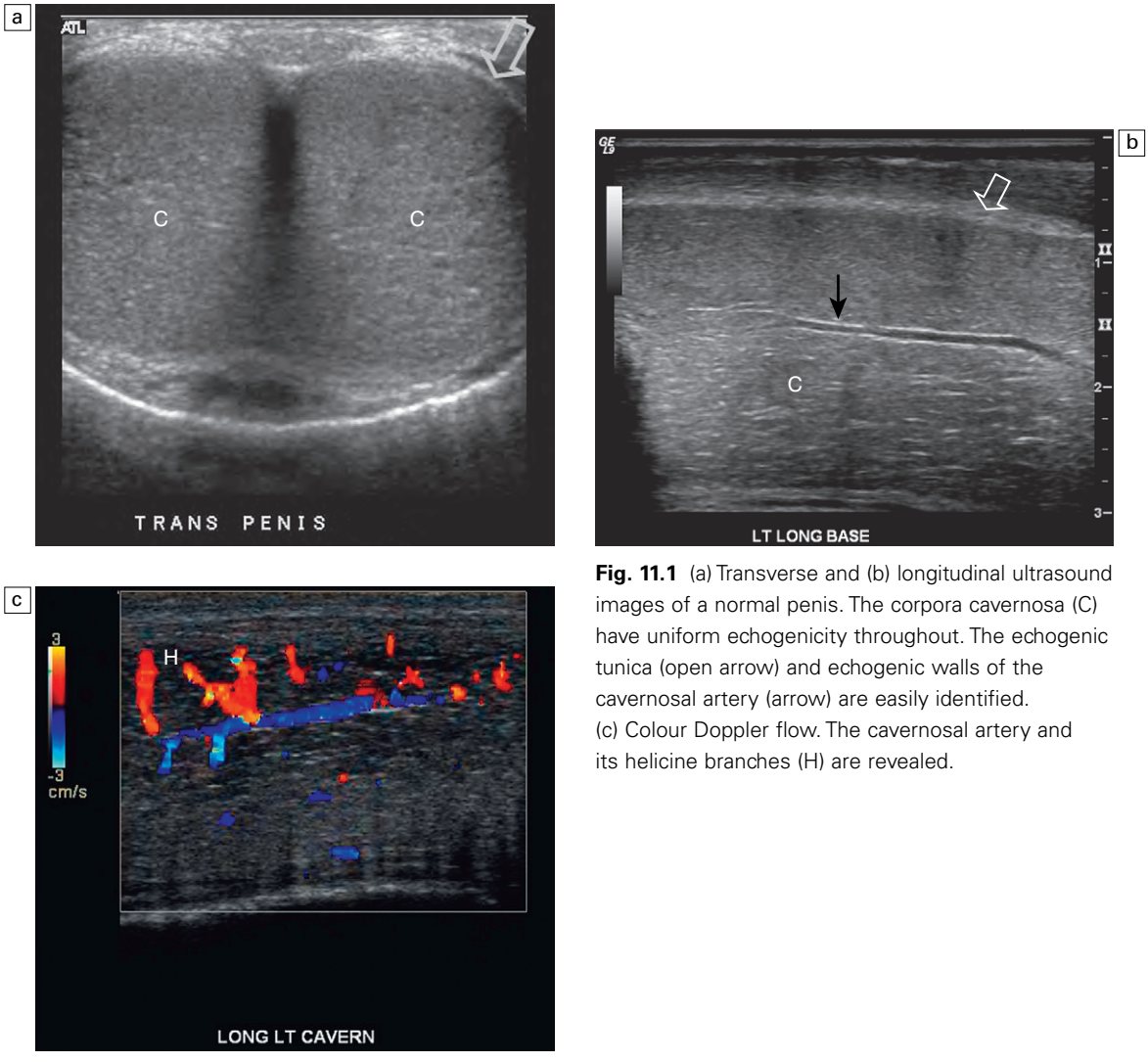


**Fig. 11.1** (a) Transverse and (b) longitudinal ultrasound images of a normal penis. The corpora cavernosa (C) have uniform echogenicity throughout. The echogenic tunica (open arrow) and echogenic walls of the cavernosal artery (arrow) are easily identified. (c) Colour Doppler flow. The cavernosal artery and its helicine branches (H) are revealed.

The *cavernosal*, or *deep penile artery*, enters the tunica albuginea proximally and extends the length of the corpus cavernosum. The cavernosal arteries and their helicine branches are the primary source of blood flow to the erectile tissue of the penis. Just as the cavernosal artery supplies blood to the corpus cavernosum, the *spongiosal artery* supplies the corpus spongiosum (Fig. 11.2).

## Venous anatomy

Venous drainage of the penile erectile tissue (i.e. the sinusoidal spaces) primarily occurs through *emissary (efferent) veins* which drain the corpus cavernosum, penetrate the tunica albuginea and empty into the circumflex veins; these then drain into the deep dorsal venous system of the penis. The emissary veins may also drain directly into the *deep dorsal vein*. The *superficial dorsal vein* drains the distal portion of the corpora cavernosa, as well as the skin and glans. The deep and superficial dorsal veins can be routinely visualised by colour Doppler imaging in the midline of the penile shaft. The most proximal portions of the corpora cavernosa are drained by the cavernosal veins directly into the periprostatic plexus.

## Erectile physiology

When the penis is flaccid, its smooth muscle is in a tonic state, the cavernous sinusoids are collapsed, and the cavernous venules are open.[4] The emissary veins drain the sinusoidal spaces and blood circulates into the dorsal veins. During this state, there is high resistance to blood flow into the penis. Erection starts when an autonomic neurogenic impulse relaxes the cavernosal arterioles and sinusoidal spaces.[2] As erection occurs, there is a marked increase in the volume of arterial inflow into the penis as the cavernous arteries dilate. This is accompanied by relaxation of the smooth muscle of the corpora cavernosa with expansion and elongation of the cavernous sinusoids as they fill with blood. Compression of the cavernous venules between the dilated cavernous sinusoids and the unyielding peripheral tunica albuginea decreases venous outflow. This veno-occlusive mechanism (which depends on neurological stimuli, a sufficient supply of arterial blood, and normal function of the tunica albuginea) maintains sinusoidal distension and rigid erection.[1,2,15]

Five stages of erectile physiology have been defined by Lue: latent, tumescent, full erection, rigid erection and detumescent.[16] During the latent phase, the diameters of the cavernosal arteries are at their greatest and there is maximum inflow of blood with minimal resistance. During tumescence, the sinusoidal cavities of the corpora cavernosa distend with blood. With full erection, blood flow decreases as do the diameters of the

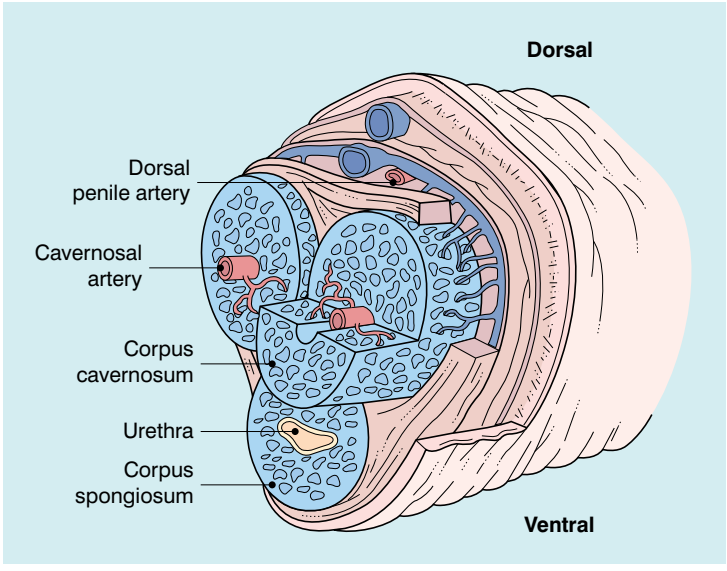


**Fig. 11.2** Normal anatomy. The cavernosal arteries are centrally located in each corpus cavernosus. The urethra courses through the corpus spongiosum. The dorsal penile artery supplies the glands and does not play a direct role in erectile function.

cavernosal arteries. With a rigid erection, blood inflow (and outflow) ceases and the diameters of the cavernosal arteries are at their narrowest. Detumescence occurs when the trabeculae and arteries contract in response to a release of norepinephrine. During the five stages of erection, different arterial diameters and waveform patterns are normally present on Doppler examination.

### *Ultrasound technique*

Various techniques for the sonographic examination of the penis have been described with changes over time primarily due to advances in ultrasound technology.[1-4,17,18] A linear transducer operating at 7 MHz or higher frequency should be employed. Slow flow sensitivity must be optimised. Filters are set at their lowest levels and the Doppler gain is set just below the noise threshold; the pulse repetition frequency is set to the lowest velocity setting possible. All of these settings can then be adjusted if higher than expected velocity distorts the Doppler display.

The evaluation should be performed in a quiet, private setting with the room comfortably warm and darkened, so that the patient is relaxed and not embarrassed. The scan is performed with the patient lying supine and the penis in the anatomical position (lying superiorly against the anterior abdominal wall). During the examination, the patient may be asked to help keep the penis immobilised by gently holding the corona just under the glans penis and then stretching the shaft along the anterior abdominal wall. Scanning is usually performed on the ventral surface of the penis,[1,3] but the probe can be placed on the dorsal or lateral surfaces if necessary.[2,3] Imaging is performed in both the longitudinal and transverse planes from the base of the penis to the glans to visualise anatomical details of the corpora cavernosa, cavernosal arteries and surrounding structures, and also to demonstrate any abnormalities such as fibrosis, scarring, plaques, calcification, haematoma or tumour. The transducer should be applied gently with minimal penile compression. Firm pressure causing vascular compression can resist inflow and affect accuracy of velocity measurement, especially during diastole. The diameter of the arteries and blood flow velocities are measured. Colour Doppler enhances the accuracy of angle correction, which is mandatory for flow velocity determination. In addition, with colour Doppler, blood flow direction can be assessed and the presence of any communications between the cavernosal, dorsal and spongiosal arteries can be detected (Fig. 11.3).

## ERECTILE DYSFUNCTION

The historical evolution of treatment for impotence has gone through several stages. Initially treatment involved the use of penile implants. In the 1980s, implant complication rates were quite high and there was only about a 50% chance of long-term success. These devices failed, migrated or ruptured often necessitating reoperation. This often resulted in stricture and scarring, further complicating the problem. The risk to benefit with the old treatment was high so numerous imaging and testing studies were performed to confirm definitively that the patient had an organic cause of impotence requiring surgery and not some other aetiology that did not require surgical intervention. Treatment of impotence then evolved through the use of vacuum devices and self-injection of prostaglandins such as alprostadil (Caverject) and now is quite successfully accomplished with phosphodiesterase inhibitors.

The initial report of Doppler sonography combined with pharmacological induction of erection to evaluate vasculogenic impotence was by Lue and associates[17] in the mid-1980s. With advances in Doppler technology, the haemodynamic information available greatly enhances the ability to determine if a patient's impotence is due to a vascular aetiology, such as arterial insufficiency, venous incompetence or a combination of the two.[2,4,17–24]

Currently the application of Doppler ultrasound is primarily in young men who present concerned that they have an organic issue. Testing with Doppler is needed to establish the fact that there is indeed no vasculogenic aetiology. The patient is then channelled to psychological counselling. The younger patient is usually reluctant to initially

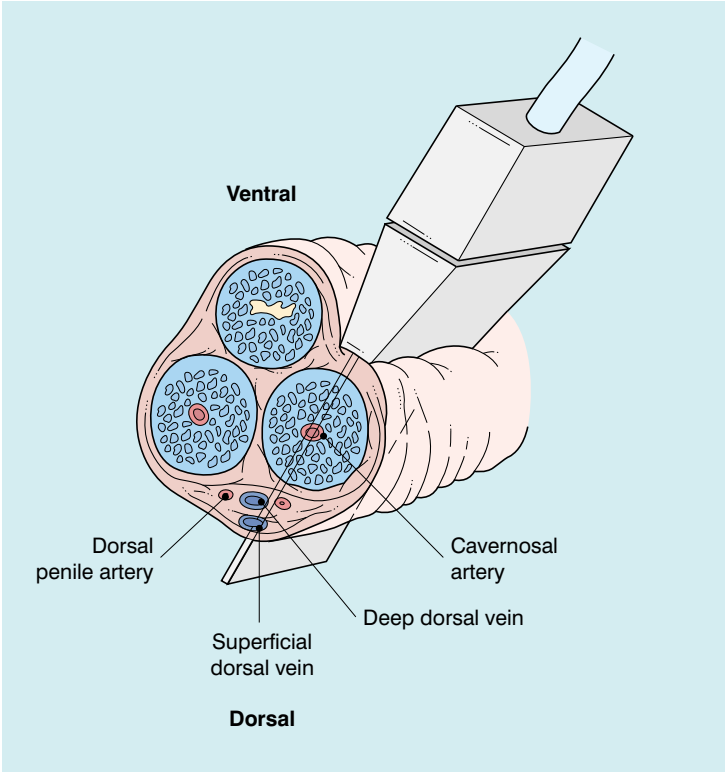


**Fig. 11.3** Ultrasound technique. A linear transducer is placed in a longitudinal plane along the ventral surface of the penis. Since the cavernosal arteries run parallel to the transducer, electronic steering of the Doppler beam is necessary to interrogate at an appropriate angle.

admit the need for psychological counselling until Doppler ultrasound and other tests indeed prove that there is no underlying organic cause for the impotence.

## PHARMACOLOGICAL INDUCTION OF ERECTION

A vasodilating agent is injected into the corpus cavernosum near the base of the penis to induce erection. A number of different agents are available, including papaverine, phentolamine, prostaglandin E1 (PGE-1) and alprostadil. A standard protocol has not been established and a variety of techniques for using these agents has been reported, either singularly or in various combinations. Reported protocols include 15 mg to 60 mg papaverine alone; 30 mg papaverine combined with 1 mg phentolamine; 0.25 mL of a triple mixture of 75 mg papaverine, 2.5 mg phentolamine and 25 g/4.25 mL PGE-1; a 0.2 mL total volume of 6 mg papaverine, 0.2 mg phentolamine and 2 g PGE-1; and 12.5 mg papaverine combined with 10g of alprostadil.[1–4,25–30] PGE-1 is considered to be slightly safer but is considerably more expensive than papaverine. Unfortunately there is a higher incidence of priapism with papaverine and PGE-E1 use is increasing. Gontero et al[31] suggest performing a two-stage assessment with Doppler ultrasound after a starting dose of 20 μg of PGE-1. If erectile response is suboptimal and venous leak is suspect, then an additional 2 mg intracavernosal phentolamine is administered and measurements repeated. They claim high accuracy and a low risk of priapism.[31]

Some patients may have a poor response to the initial injection of the vasodilating agent and may be unable to achieve satisfactory erection. In these cases, manual self-stimulation has been reported to significantly improve erection in many patients.[32] For some patients, a second or third injection may be required before an adequate response is attained.[3,4] However, this may run the risk of priapism, a painful complication of pharmacological induction.

## DOPPLER EVALUATION AFTER VASODILATOR INJECTION

Just as there are differences in the use of vasodilating agents, there is no collective consensus as to how soon, how frequently and how long after injection sonographic measurements should be performed. However, it is now generally recognised that waiting until 5 min after injection, as had previously been the practice, can result in falsely low peak systolic velocity (peak systolic velocity) findings in the cavernosal arteries, since normal maximum peak systolic velocity can occur in less than 5 min following injection.[3] In addition, premature termination of post-injection measurements (i.e. after 5–10 min) can result in false-positive diagnoses of arterial insufficiency, or venous incompetence because of temporal variations in the response to vasodilating agents.[2] Early termination may also result in a false-negative diagnosis of venous incompetence. Suggested protocols are summarised in Table 11.1.

Doppler evaluation following the injection of a vasodilating agent is performed so the penile anatomical vasculature can be visualised and haemodynamic parameters measured. There is considerable debate, however, as to which haemodynamic parameters are significant and what constitutes normal and abnormal values. Connolly et al[4] have suggested that the most important diagnostic indicators are arterial diameter, peak flow velocity and blood flow acceleration.

To obtain accurate readings, it is important that the examiner is familiar with the physiology of arterial inflow to the cavernosal arteries after pharmacological injection. Particular attention must be paid to the Doppler angle, which should be approximately 60°, or less, to the cavernosal artery.[1,3] Measurements are most reliable and most easily reproduced when taken at the base of the penis where the penile vessels angle posteriorly toward the perineum. The arterial diameter and waveform of each cavernosal artery is individually assessed. Peak systolic and end-diastolic velocities are measured and recorded. An asymmetric response of the cavernosal arteries during erection or a lack of arterial dilation may suggest the presence of a significant vascular lesion.[33] The examiner should also carefully search for anatomical penile arterial variants as they may also contribute to vasculogenic impotence.

### Normal Doppler findings

Prior to injection, during the flaccid state, the systolic waveform is damped and a monophasic flow with minimal diastolic component is present

**Table 11.1** Recommended time protocols for sonographic evaluation of pharmacologically-induced erection

| Investigators | Suggested protocols |
|---|---|
| Hattery et al[1] | 5, 10, 15, and 20 min following injection, with delayed measurements occasionally obtained after 20 min if the degree of tumescence or rigidity is still increasing |
| Fitzgerald et al[2] | Immediately after injection and at 5 min intervals for 20–30 min or until waveform progression ceases |
| Herbener et al[3] | Immediately after injection and at 1–2 min intervals until there is a plateau of velocity or until velocities peak and then decrease, with examination normally not exceeding 20 min |
| Herbener et al[3] | 3–5 min intervals until maximum cavernosal artery diameter and peak systolic velocity measurements are obtained |
| Connolly et al[4] | 3–5 min intervals throughout latent, tumescent and full stages of erection for up to 30 min in order to detect patients who show delayed but eventually normal response to injection |

(Fig. 11.4). Following pharmacological inducement of erection, the normal progression of haemodynamic events and the associated Doppler waveform patterns of the cavernosal artery can be classified into different haemodynamic stages.[34] The appearance of the spectral waveform must be correlated with the status of the erection (i.e. flaccid, latent, tumescent, full and rigid).

During the initial latent state, there is a sudden increase in both systolic and diastolic blood flow in the cavernosal artery, and a rounded systolic peak is observed. The flow of blood is unidirectional during systole and diastole, with a pronounced forward diastolic component present (Fig. 11.5). This spectral waveform reflects the low resistance to flow within the sinusoidal spaces. Minimal tumescence normally accompanies this stage. Following that, there is an increase in blood flow to the corpora cavernosa, causing the intracavernosal pressure to increase. As intracavernosal pressure rises, a dichrotic notch appears at end systole and diastolic flow diminishes (Fig. 11.6). When intracavernosal and diastolic pressures are the same, diastolic flow ceases and there is only systolic blood flow. The systolic envelope narrows and systolic velocity may fluctuate. Increasing tumescence normally occurs during this stage.

During full erection, intracavernosal pressure becomes greater than the arterial pressure during diastole because of the veno-occlusive mechanism. Flow reversal may be seen during diastole and the systolic waveform narrows. During this stage, maximal systolic velocity occurs in many patients and strong pulsations are normally seen (Fig. 11.7). In the rigid phase of erection, intracavernosal pressure may equal or exceed arterial systolic pressure, causing additional narrowing of the systolic envelope, and normally a decrease in systolic velocity (Fig. 11.8). Both systolic and diastolic

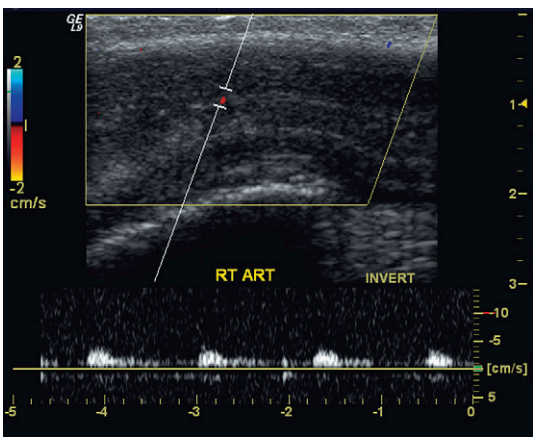


**Fig. 11.4** Spectral Doppler tracing during the flaccid state. Flow velocities are damped and relatively monophasic.

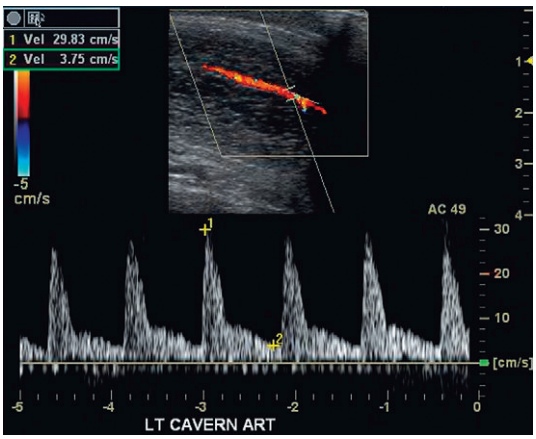


**Fig. 11.5** Spectral Doppler tracing during the initial latent phase of the erectile process. Brisk flow is seen during systole, approaching 30 cm $s^{-1}$. At this state after pharmacological enhancement, diastolic flow is still present in the antegrade direction.

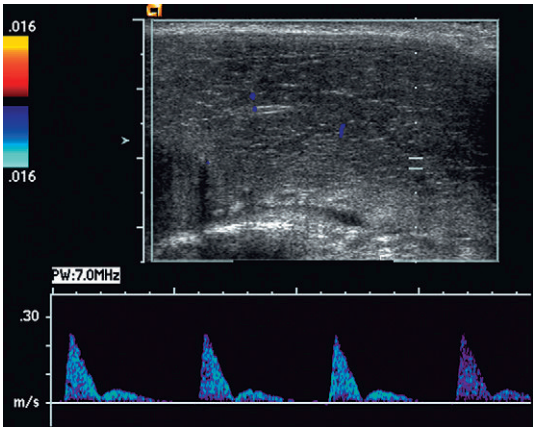


**Fig. 11.6** Spectral Doppler tracing in the early tumescent phase. Systolic waveform is narrowed into a sharp spike. Diastolic velocity decreases and a dicrotic notch are present in early diastole (arrow).

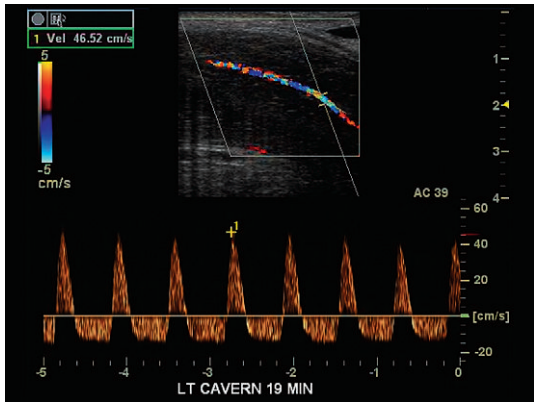


**Fig. 11.7** Spectral Doppler tracing approaching rigid erection. Systolic peak is narrowed, velocity is brisk. Note the reversal of flow throughout diastole.

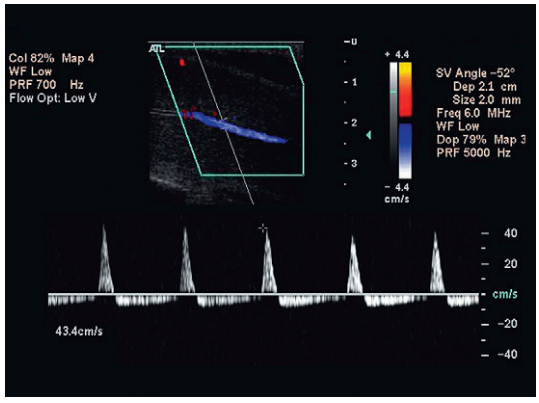


**Fig. 11.8** Spectral Doppler tracing at full rigid erection. Note further narrowing of the systolic inflow peak. Outflow continues through diastole but is at a lesser velocity (compared to Fig.11.7).

flow may cease completely as the pressure in the corporal bodies approaches systolic blood pressure.[4]

## Cavernosal artery diameter

Obtaining cavernosal arterial diameters can be time consuming and the accuracy of the measurement is very dependent on the abilities of the examiner. Considerable controversy exists as to the value of obtaining measurements of the cavernosal artery diameter following pharmacological induction of erection. Some investigators have reported a poor correlation between the degree of increase in cavernosal artery diameter and arteriographic confirmation of arterial integrity. They found that the changes in diameter were not significant enough to be indicative or diagnostic of arterial disease.[5,22,26,33,35,36]

Other authors use cavernosal arterial diameters as a parameter in determining arterial integrity of the penis. Various percentages of increase in vessel diameter after injection have been reported as indicators of normal vessel compliance (Table 11.2). It is argued[1] that as blood flow in the cavernosal artery is a function of velocity and cross-sectional area of the vessels, the ability of the artery to dilate after pharmacological injection is an important reflection of vessel compliance. It is recognised, however, that the degree of change in diameter following injection may not correlate well with other physiological or haemodynamic parameters. Connolly et al[4] contend that because increased blood flow during erection is accompanied by an increase in the diameter of the cavernosal arteries, patients with arterial disease will have minimal or no vessel dilatation following injection because of inadequate vessel compliance or compromised inflow. Thus, they recommend use of the diameter and suggest that the measurement be taken approximately 5 min after injection, since the greatest increase in arterial diameter is observed during the early latent stage of erection when blood inflow is at its maximum.

## Arterial variants

Variant penile arterial anatomy can be seen in a high percentage of patients suspected of having an arteriogenic cause for their impotence.[5,35,41,42] Communications among the cavernosal, dorsal,

**Table 11.2** Criteria indicating normal vessel compliance

| Investigators | Percentage increase in vessel diameter |
|---|---|
| Lee et al[39] | 70 |
| Lue et al[17] | 75 |
| Krysiewicz & Mellinger;[22] James[40] | 60–75 |
| Collins & Lewandowski[24] | 60–00 |

and spongiosal arteries are often found along the shaft of the penis (Fig. 11.9). There may be duplication of the cavernosal artery or cross-communication between left and right cavernosal arteries.[43] Rarely, collaterals from the urethral arteries may also be seen. The incidence of communication between dorsal and cavernosal arteries (dorsal–cavernosal perforators) has been reported in as many as 90% of men.[42] 'Spongiosal–cavernosal communications, or 'shunt' vessels, which course from the corpus spongiosum into the corpus cavernosum are another common variant.[35,43] Any of these collateral pathways may significantly affect arterial Doppler flow profiles during erection.[4,43] Although these anatomical variations do not necessarily result in arterial insufficiency, they may cause inaccurate interpretation if they are not appreciated. For example, systolic peak velocities of the cavernosal artery may be significantly lower in men with a full erectile response if arterial collateral communications are present.[35,43] Careful scanning of the entire penis from the crura to the glans with colour Doppler is essential in identifying these anomalies.

## VASCULOGENIC IMPOTENCE

### Arterial insufficiency

Measurement of peak systolic velocity in the cavernosal arteries after pharmacological injection is considered one of the most important parameters when evaluating patients whose impotence may be due to arterial disease, such as focal stenosis, occlusion, or collateral flow between arteries (Fig. 11.10).[1]

However, what constitutes normal and abnormal values for arterial insufficiency varies, Reported peak systolic velocity values indicative of normal arterial function are summarised in Table 11.3; and reported abnormal values indicative of arterial disease as the cause of vasculogenic impotence are summarised in Table 11.4.

In addition to peak systolic velocity values in each cavernosal artery, a comparison of the values can help in the diagnosis of arterial disease. Asymmetric velocities are considered abnormal if the difference between right and left cavernosal arteries is greater than 10 cm $s^{-1}$,[3, 33] or greater than 10–15 cm $s^{-1}$ by Hattery and associates.[1] Underlying arterial disease should be considered in the artery with the lower peak systolic velocity value.[44]

Other indicators used to increase the sensitivity of detecting potential arterial disease include reversal of blood flow during systole, a penile blood flow index and blood flow (or cavernosal artery) acceleration. During rigid erection, reversal

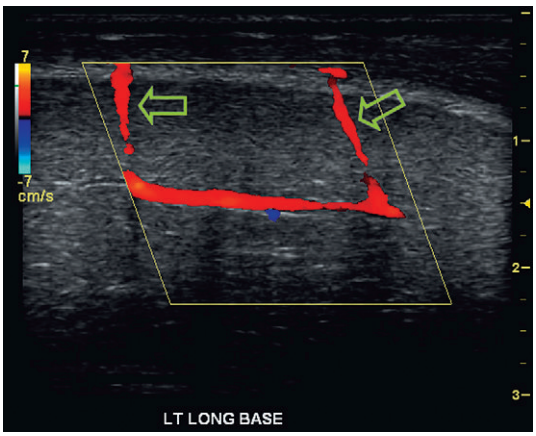


**Fig. 11.9** Longitudinal colour Doppler imaging. Note the presence of two dorsal–cavernosal perforating arteries (arrows).

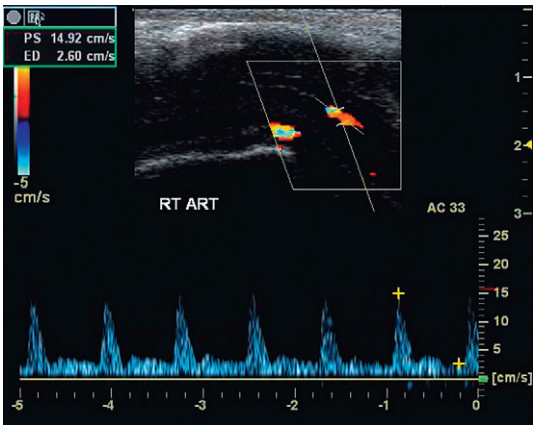


**Fig. 11.10** Spectral Doppler tracing in a patient with arterial insufficiency. Despite appropriate pharmaceutical dose, erectile response was suboptimal. Peak systolic velocity in a cavernosal artery only approximates 15 cm $s^{-1}$. This is well below the accepted range of normal.

**Table 11.3** Criteria for normal peak systolic velocity in cavernosal arteries following pharmacological induction of erection

| Investigators | Peak systolic velocity |
|---|---|
| Lue et al;[17] Paushter[36] | ≥25 cm $s^{-1}$ |
| Porst[45] | 25–30 cm $s^{-1}$ or greater |
| Hattery et al;[1] Connolly et al;[4] Lee et al[39] | ≥30 cm $s^{-1}$ |
| Schwartz et al[34] | Mean peak systolic velocity of 39 cm $s^{-1}$* |
| Herbener et al;[3] Benson & Vickers[33] | ≥40 cm $s^{-1}$ |

*Mean peak systolic velocity values are the combined calculated average of the right and left cavernosal arteries.

**Table 11.4** Criteria for abnormal peak systolic velocity in cavernosal arteries following pharmacological induction of erection

| Investigators | Peak systolic velocity |
|---|---|
| Fitzgerald et al;[2] Quam et al;[5] Lue et al;[17] Paushter;[36] James[40] | Mean peak systolic velocities <25 cm $s^{-1}$* |
| Hattery et al[1] | <25 cm $s^{-1}$ abnormal, 25–30 cm $s^{-1}$ indeterminate with clinical correlation recommended |
| Benson & Vickers[33] | <30 cm $s^{-1}$ considered significant, 30–40 cm $s^{-1}$ regarded borderline to mild |

*Mean peak systolic velocity values are the combined calculated average of the right and left cavernosal arteries.

of diastolic blood flow is considered a normal finding; however, reversal of arterial blood flow direction during systole is always considered abnormal and may indicate an underlying vascular abnormality.[1,3] Systolic flow reversal after pharmacological inducement of erection has been observed in patients with significant proximal penile or cavernosal artery stenosis and occlusion with filling of the distal cavernosal artery secondary to collateral flow.

Lopez et al[46] have described a penile blood flow index, which is calculated by adding the percentage increases in the diameters of the right and left cavernosal arteries to the peak flow velocities of both arteries. If the total value is less than 285 vasculogenic impotence is considered likely to be of an arterial nature; this was 97% sensitive and 77% specific in diagnosing impotence due to arterial disease.

Another Doppler index for identifying arterial disease has been referred to both as cavernosal artery acceleration and blood flow acceleration. This index is calculated by dividing the peak systolic velocity by the systolic rise time (cm $s^{-2}$). The systolic rise time is the time from the start of the systolic curve to its maximum value. Proximal arterial disease would be expected to damp velocity waveforms and prolong the systolic rise time.[4] In a study comprising 30 patients, Valji and Bookstein[23] reported the index more predictive of arterial insufficiency than cavernosal arterial peak systolic velocity by itself. Oates et al[47] found that a systolic rise time of 110 m $s^{-1}$ or greater had a predictive value of 92% for arteriogenic impotence. Mellinger et al[48] reported that blood flow acceleration seemed to correlate well with subjective evaluation of erections.

## Venous incompetence

In some men, venous incompetence, or failure of the veno-occlusive mechanism, may be the

primary cause of vasculogenic impotence.[2] Patients with normal arterial inflow parameters (e.g. peak systolic velocity >25 cm $s^{-1}$) but weak erections will very likely have some degree of venous leakage.[4] Because primary venous leakage is a potentially treatable cause of erectile dysfunction, Doppler examination of the penile venous system may be helpful in identifying these patients who may benefit from additional more invasive studies.[1,49] If surgical or endovascular therapy is considered for the patient, then cavernosography is generally still required.[50,51]

In those patients with arterial inflow issues (peak systolic velocity < 25 cm $s^{-1}$), however, the veno-occlusive mechanism will not be fully engaged, persistent end-diastolic flow can be expected and venous leak cannot be assessed.

A correlation has been shown between end-diastolic blood flow velocity within the cavernosal arteries and the presence of venous leakage. With a normal erectile response, there should be minimal, if any, flow detected with the cavernosal arteries during the diastolic phase 15–20 min after injection. As previously noted, there should be a decrease and eventual absence or reversal of diastolic flow in the normal spectral Doppler waveform during rigid erection. If there is veno-occlusive dysfunction (venous leak), then this decrease or reversal of diastolic flow will not occur.[5,40,49] A persistently elevated diastolic flow in the cavernosal arteries is highly indicative of venous leakage out of the corporal tissue even after maximum peak systolic velocity has been attained (Fig. 11.11). However, just as there are differences of opinion regarding normal and abnormal peak systolic velocity values, various

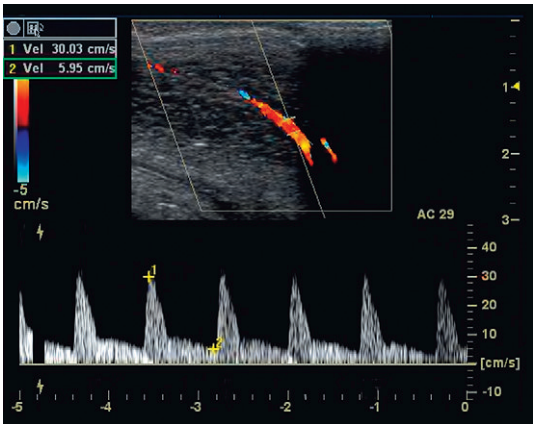


**Fig. 11.11** Spectral Doppler tracing of venous insufficiency. Relatively high velocity persistent forward flow is seen during diastole (approximating 6 cm/sec). This despite appropriate arterial inflow velocities.

criteria exist as to what constitutes abnormal diastolic velocity (Table 11.5). In association with a normal arterial inflow, most authors now consider an end diastolic velocity of >5 cm $s^{-1}$ as the velocity above which a venous leak is present.[5,52]

A potential for a false-positive diagnosis of venous leak does exist, especially in young men. The anxiety during a penile ultrasound examination increases sympathetic drive which results in inadequate relaxation of sinusoidal smooth muscle and consequent failure of veno-occlusion. Additional intracavernosal administration of an alpha-adrenergic antagonist such as phentolamine 2 mg, should be considered. Phentolamine blocks the increased sympathetic drive and helps avoid the false-positive diagnosis of venous leak.[53]

**Table 11.5** Criteria for abnormal mean arterial end-diastolic velocity

| Investigators | End-diastolic velocity |
|---|---|
| Herbener et al;[3] James[40] | >3 cm $s^{-1}$ |
| Quam et al;[5] Benson & Vickers;[33] Paushter;[36] Fitzgerald et al[37] | >5 cm $s^{-1}$ |
| Hattery et al[1] | >5–8 cm $s^{-1}$ |
| Montorsi et al[38] | >10 cm $s^{-1}$ |

## TRAUMA

Injury to the penis may be the result of blunt or penetrating trauma; or from acute bending of the erect shaft. Depending on severity of the insult subcutaneous or intracorporeal haematoma, tunical disruption or urethral tear may occur. The main role of sonography is to exclude albugineal tear because extratunical and cavernous haematoma can be treated conservatively. Surgery is required, however, when rupture of the tunica albuginea cannot be excluded, especially if the patient reports immediate detumescence associated with a popping sound. Surgical repair of an albugineal tear reduces the risk of post-traumatic curvature, and lowers the incidence of erectile dysfunction. Colour Doppler sonography can be used to help localise small albugineal tears. By squeezing the penile shaft, a flush of blood can be forced from the cavernosal bodies through the tear.[54]

Following pelvic trauma, Doppler ultrasound is useful for identifying the presence of injury to the penile vasculature.[3,20] Most non-organic causes of erectile dysfunction in young men are secondary to arterial injury with pelvic fracture. Penile arterial inflow may be compromised by development of a post-traumatic stenosis. Doppler ultrasound can be used to look for a tardus parvus waveform of the affected artery. For patients who experience post-traumatic impotence, Broderick et al[55] found that a systolic velocity less than 25 cm $s^{-1}$ and asymmetric velocities >10 cm $s^{-1}$ were helpful parameters in establishing a compromise of penile arterial inflow. In some centres, vascular microsurgery is being performed on the internal pudendal artery to bypass a focal stenosis.

With severe trauma, the cavernosal artery may rupture. This results in unrestricted blood flow into the cavernosal space, creating an arteriosinusoidal, arteriolacunar, or arteriovenous fistula. Since venous outflow is maintained from the cavernosal space, the patient develops only a partial erection that is not acutely painful. Persistent venous outflow prevents complete erection, stasis and hypoxia. This condition is known as high-flow priapism and colour Doppler sonography is very effective in its identification (Fig. 11.12). It shows a characteristic arterial colour blush consistent with extravasation of blood from the lacerated artery. Spectral Doppler displays turbulent high-velocity flow.[3,10,56,57] In long-standing priapism, this area may appear more circumscribed, mimicking a pseudoaneurysm. Angiographic embolisation of the lacerated artery is currently considered the treatment of choice. Colour Doppler US allows confirmation of successful embolisation by demonstrating disappearance or size reduction of the fistula. If unsuccessful, persistent patency of feeding vessels would be seen.[58]

## PEYRONIE'S DISEASE

Peyronie's disease (induratio penis plastica) is an idiopathic disorder of the connective tissue in which fibrous plaques form in the tunica albuginea with induration of the corpora cavernosa of the penis or a fibrous cavernositis. Its aetiology is unknown and the incidence is stated to be 1%. The disease causes penile deviation and affected patients typically complain of pain during erection.[3,11] Ultrasound imaging can estimate the extent and depth of the plaques, which may be hypo- or hyperechoic and, if long standing, often contain calcification.

Doppler examination of the penile vasculature is of value to determine if any vascular abnormalities exist because of the fibrous plaques.[11,12,59] Doppler ultrasound is helpful in differentiating between veno-occlusive dysfunction (considered the primary vascular cause of impotence associated with Peyronie's disease) and arterial insufficiency.[13] By doing so, Doppler helps establish the correct treatment option for the patient. If Doppler reveals appropriate arterial inflow and an appropriate response to injection, then plaque removal with grafting of bovine pericardium is preferred. However, if the Doppler shows abnormal flow profiles or an inadequate response to injection, in addition to the disfigurement, then implantation of prosthesis should be considered.[60]

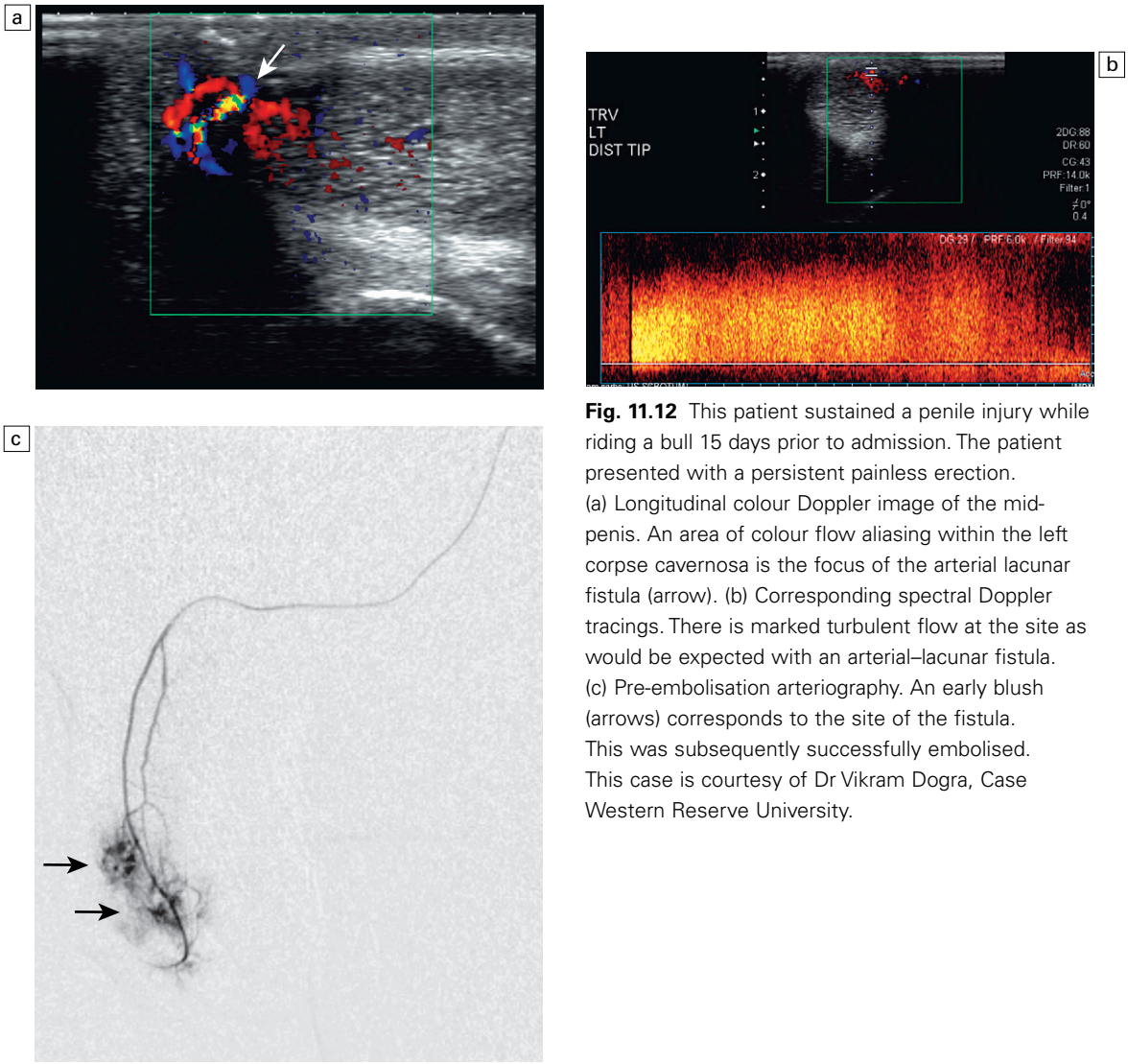


**Fig. 11.12** This patient sustained a penile injury while riding a bull 15 days prior to admission. The patient presented with a persistent painless erection. (a) Longitudinal colour Doppler image of the mid-penis. An area of colour flow aliasing within the left corpse cavernosa is the focus of the arterial lacunar fistula (arrow). (b) Corresponding spectral Doppler tracings. There is marked turbulent flow at the site as would be expected with an arterial–lacunar fistula. (c) Pre-embolisation arteriography. An early blush (arrows) corresponds to the site of the fistula. This was subsequently successfully embolised. This case is courtesy of Dr Vikram Dogra, Case Western Reserve University.

## PENILE TUMOURS

Penile masses are rare. Possibilities include haematoma, cavernosal herniation, Peyronie's plaques, penile carcinoma, metastases, foreign bodies or the penile prosthesis. Doppler may show some interesting flow patterns but rarely adds value to the evaluation.

## OTHER IMAGING TESTS

Doppler ultrasound combined with pharmacological inducement of erection has replaced the use of the penile/brachial pressure index and pudendal arteriography at many institutions for the initial evaluation of patients with suspected vasculogenic impotence.[4] The penile brachial index is now basically a test of historical interest only. Although arteriography is considered the 'gold standard' for assessing the arteries of the penis, unlike Doppler ultrasound, it provides primarily anatomical rather than functional information. If Doppler examination indicates the presence of a surgically correctable lesion, though, many investigators still believe a confirmatory arteriogram (computed tomographic angiography

or magnetic resonance angiography) should be performed before surgery is undertaken.

Colour Doppler ultrasound has also proven helpful in evaluating patients with suspected venous incompetence. However, for patients in whom venous surgery is being considered to correct their condition, dynamic infusion cavernosography is necessary since it provides a more complete preoperative picture of the penile vasculature.[1–3] At many institutions, both cavernosography and cavernosometry are used to determine the presence of veno-occlusive dysfunction and to quantify the degree of venous leakage.

## ACKNOWLEDGEMENTS

Reginald Bruskewitz, MD; Mike Ledwidge, RDMS, RVT; Carrie Poole; Carol Mitchel RDMS and Joan Palmer

## REFERENCES

1. Hattery RR, King BF, Lewis RW, et al. Vasculogenic impotence: duplex and colour Doppler imaging. Radiol Clin North Am 1991; 29:629-645.
2. Fitzgerald SW, Erickson SJ, Foley WD, et al. Colour Doppler sonography in the evaluation of erectile dysfunction. Radiographics 1992; 12:3–17.
3. Herbener TE, Seftel AD, Nehro A, et al. Penile ultrasound. Semin Urol 1994; 12:320–332.
4. Connolly JA, Borirakchanyavat S, Lue TF. Ultrasound evaluation of the penis for assessment of impotence. J Clin Ultrasound 1996; 24:481–486.
5. Quam JP, King BF, James EM, et al. Duplex and colour Doppler sonographic evaluation of vasculogenic impotence. AJR Am J Roentgenol1989; 153:1141–1147.
6. Corona G, Mannucci E, Mansani R, et al. Aging and pathogenesis of erectile dysfunction. Int J Impot Res 2004; 16:395–402.
7. Krane RJ, Goldstein I, Saenz de Tejada I. Medical progress: impotence. N Engl J Med 1989; 321:1648–1659.
8. Weiske WH. Diagnosis of erectile dysfunction – what is still needed today? Urologe A 2003; 42:1317–1321.
9. Armenakas NA, McAninch JW, Lue TF, et al. Posttraumatic impotence: magnetic resonance imaging and duplex ultrasound in diagnosis and management. J Urol 1993; 149:1272–1275.
10. Harding JR, Hollander JB, Bendick PJ. Chronic priapism secondary to a traumatic arteriovenous fistula of the corpus cavernosum. J Urol 1993; 150:1504–1506.
11. Lopez JA, Jarrow JP. Duplex ultrasound findings in men with Peyronie's disease. Urol Radiol 1991; 12:199–202.
12. Amin Z, Patel U, Friedman EF, et al. Colour Doppler and duplex ultrasound assessment of Peyronie's disease in impotent men. Br J Radiol 1993; 66:398–402.
13. Levine LA, Coogan CL. Penile vascular assessment using colour duplex sonography in men with Peyronie's disease. J Urol 1996; 155:1270–1273.
14. Gray's Anatomy, Online. Available: http://education.yahoo.com/reference/gray/subjects/subject?id=262 March 2005.
15. Aboseif SR, Lue TF. Hemodynamics of penile erection. Urol Clin North Am 1988; 15:1–7.
16. Lue TF. Physiology of penile erection and pathophysiology of impotence. In: Walsh PC, Retik AB, Stamey TA, et al, eds. Campbell's urology, 6th edn. Philadelphia: WB Saunders; 1992:707–728.
17. Lue TF, Hricak H, Marich KW, et al. Vasculogenic impotence evaluated by high-resolution ultrasonography and pulsed Doppler spectrum analysis. Radiology 1985; 155:777–781.
18. Mueller SC, Lue TF. Evaluation of vasculogenic impotence. Urol Clin North Am 1988; 15:65–76.
19. Gall H, Bahren W, Scherb W, et al. Diagnostic accuracy of Doppler ultrasound technique of the penile arteries in correlation to selective arteriography. Cardiovasc Intervent Radiol 1988; 11:225–229.
20. Lue T, Tanagho E. Physiology of erection and pharmacological management of impotence. J Urol 1987; 137:829–836.
21. Desai KM, Gingell JC, Skidmore R, et al. Application of computerized penile arterial waveform analysis in the diagnosis of arteriogenic impotence: an initial study in potent and impotent men. Br J Urol 1987; 60:450–466.
22. Krysiewicz S, Mellinger BC. The role of imaging in the diagnostic evaluation of impotence. AJR Am J Roentgenol 1989; 153:1133–1139.
23. Valji K, Bookstein JJ. Diagnosis of arteriogenic impotence: efficacy of duplex ultrasonography as a screening tool. AJR Am J Roentgenol 1993; 160:65–69.

24. Collins JP, Lewandowski BJ. Experience with intracorporal injection of papaverine and duplex ultrasound scanning for assessment of arteriogenic impotence. Br J Urol 1987; 59: 84–88.
25. Bookstein JJ, Valji K, Parsons L, et al. Pharmacoarteriography in the evaluation of impotence. J Urol 1987; 137:333–337.
26. Rajfer J, Canan V, Dorey FJ, et al. Correlation between penile angiography and duplex scanning of cavernous arteries in impotent men. J Urol 1990; 143:1128–1130.
27. Rosen MP, Schwartz AN, Levine FJ, et al. Radiologic assessment of impotence angiography, sonography, cavernosography and cinetrigraphy. AJR Am J Roentgenol 1991; 157:923–931.
28. Shabsigh R, Fishman IJ, Scott FB. Evaluation of erectile impotence. Urology 1988; 32:83–90.
29. King BF, Hattery RR, James EM, et al. Duplex sonography in the evaluation of impotence: current techniques. Semin Intervent Radiol 1990; 7:215–221.
30. Meuelman EJ, Bemelmans BH, Doesburg WH, et al. Penile pharmacological duplex ultrasonography: a dose-effect study comparing papaverine, papaverine/phentolamine, and prostaglandin E1. J Urol 1992; 148:63–66.
31. Gontero P, Sriprasad S, Wilkins CJ, et al. Phentolamine re-dosing during penile dynamic colour Doppler ultrasound: a practical method to abolish a false diagnosis of venous leakage in patients with erectile dysfunction. Br J Radiol 2004; 77:922–926.
32. Donatucci CF, Lue TF. The combined intracavernous injection and stimulation test: diagnostic accuracy. J Urol 1992; 148:61–62.
33. Benson CB, Vickers MA. Sexual impotence caused by vascular disease: diagnosis with duplex sonography. AJR Am J Roentgenol 1989; 153:1149–1153.
34. Schwartz AN, Wang KY, Mack LA, et al. Evaluation of normal erectile function with colour flow Doppler sonography. AJR Am J Roentgenol 1989; 153:1155–1160.
35. Jarrow JP, Pugh VW, Routh WD, et al. Comparison of penile duplex ultrasonography to pudendal arteriography: variant penile arterial anatomy affects interpretation of duplex ultrasonography. Invest Radiol 1993; 28:806–810.
36. Paushter DM. Role of duplex sonography in the evaluation of sexual impotence. AJR Am J Roentgenol 1989; 153:1161–1163.
37. Fitzgerald SW, Erickson SJ, Foley WD, et al. Colour Doppler sonography in the evaluation of erectile dysfunction: patterns of temporal response to papaverine. AJR Am J Roentgenol 1991; 157:331–335.
38. Montorsi F, Bergamaschi F, Guazzoni G, et al. Doppler colour echography in the diagnosis of impotence. Minerva Chir 1993; 48:99–102.
39. Lee B, Suresh CS, Randrup ER, et al. Standardization of penile blood flow parameters in normal men using intracavernous prostaglandin E1 and visual sexual stimulation. J Urol 1993; 149:49–52.
40. James EM. Penile ultrasound. Syllabus special course: Ultrasound 1991. Presented at the 77th Scientific Assembly and Annual Meeting of the Radiologic Society of North America. Chicago: Radiologic Society of North America; 1991:259–266.
41. Breza J, Aboseif SR, Orvis BR, et al. Detailed anatomy of penile neurovascular structures: surgical significance. J Urol 1989; 141:437–443.
42. Bahren W, Gall H, Scherb W, et al. Arterial anatomy and arteriographic diagnosis of arteriogenic impotence. Cardiovasc Intervent Radiol 1988; 11:195–210.
43. Mancini M, Bartolini M, Maggi M, et al. The presence of arterial anatomical variations can affect the results of duplex sonographic evaluation of penile vessels in impotent patients. J Urol 1996; 155:1919–1923.
44. Hattery RR, King BF, James EM, et al. Vasculogenic impotence: duplex and colour Doppler imaging. AJR Am J Roentgenol 1991; 156:189–195.
45. Porst H. Duplex ultrasound of the penis: value of a new diagnostic procedure based on over 1,000 patients [German]. Urologe - Ausgabe A 1993; 32:242–249.
46. Lopez JA, Espeland MA, Jarrow JP. Interpretation and quantification of penile blood flow studies using duplex ultrasonography. J Urol 1991; 146:1271–1275.
47. Oates CP, Pickard RS, Powell PH, et al. The use of duplex ultrasound in the assessment of arterial supply to the penis in vasculogenic impotence. J Urol 1995; 153:354–357.
48. Mellinger BC, Fried JJ, Vaughen ED. Papaverine-induced penile blood flow acceleration in impotent men measured by duplex scanning. J Urol 1990; 144:897–899.
49. Vickers MA, Benson CB, Richie JP. High resolution ultrasonography and pulsed wave Doppler for detection of coporovenous incompetence in erectile dysfunction. J Urol 1990; 143:1125–1127.
50. Frust G, Muller-Mattheis V, Cohnen M, et al. Venous incompetence in erectile dysfunction: evaluation with colour-coded duplex sonography and cavernosometery/-graphy. Eur Radiol 1999; 9:35–41.
51. Fowlis GA, Sidhu PS, Jager HR, et al. Preliminary report: combined surgical and radiological penile vein occlusion for the management of impotence caused by venous-sinusoidal incompetence. Br J Urol 1994; 74:492–496.
52. Bassiouny HS, Levine LA. Penile duplex sonography in the diagnosis of venogenic impotence. J Vasc Surg 1991; 13:75–82.

53. Aversa A, Rocchietti-March M, Caprio D, et al. Anxiety-induced failure in erectile response to intracorporeal prostaglandin-E1 in non-organic male impotence: a new diagnostic approach. Int J Androl 1996; 19:307–313.
54. Bertolotto M, Mucelli RP. Nonpenetrating penile traumas: sonographic and Doppler features. AJR Am J Roentgenol 2004; 183:1085–1089.
55. Broderick GA, McGahan JP, White RD, et al. Colour Doppler US: assessment of post-traumatic impotence. Radiology 1990; 177(suppl):130–134.
56. Hakim LS, Kulaksizoglu H, Mulligan R, et al. Evolved concepts in the diagnosis and treatment of arterial high flow priapism. J Urol 1996; 155:541–548.
57. Sadeghi-Nejad H, Dogra V, Seftel AD, et al. Priapism. Radiol Clin North Am 2004; 42:427–443.
58. Bertolotto M, Quaia E, Mucelli FP, et al. Colour Doppler imaging of posttraumatic priapism before and after selective embolization. Radiographics 2003; 23:495–503.
59. Bertolotto M, de Stefani S, Martinoli C, et al. Colour Doppler appearance of penile cavernosal-spongiosal communications in patients with severe Peyronie's disease. Eur Radiol 2002; 12:2525–2531.
60. Fornara P, Gerbershagen HP. Ultrasound in patients affected with Peyronie's disease. World J Urol 2004; 22(5):365–367.

# Doppler imaging of the scrotum

# 12

Myron A. Pozniak

## INTRODUCTION

Scrotal sonography was first introduced in the mid-1970s. Today, ultrasound is the preferred scrotal imaging technique. Improvements in image resolution with higher frequency transducers, increased Doppler sensitivity and refinements in power Doppler technology have greatly enhanced perception of testicular anatomy and pathology. The haemodynamic information acquired with Doppler adds to the imaging findings and frequently reinforces and occasionally clinches the diagnosis.[1–6] In this era, a thorough ultrasound evaluation of the scrotum must include Doppler imaging of the testes and epididymides.

## INDICATIONS

The two clinical conditions that most commonly warrant an ultrasound examination with Doppler are evaluation of acute scrotal pain and a perceived scrotal mass. Differentiating an acute inflammatory process from testicular torsion is now the domain of colour Doppler. Differentiating a mass as intratesticular versus extratesticular can be accomplished by imaging alone, but colour Doppler adds valuable flow information and helps to further characterise the abnormality. Other common indications for use of scrotal Doppler include evaluation of trauma and infertility.

## TESTICULAR ANATOMY

The normal adult testis is an egg-shaped gland which is approximately 3–5 cm in length and 2–4 cm in width and thickness with a volume of 4 $cm^3$.[7] Testicular size varies with age and stage of sexual development. At birth, the testis measures approximately 1.5 cm in length and 1 cm in width. Before puberty, testicular volume is about 1–2 $cm^3$.[8] The surface of the testicle is covered by the tunica albuginea, a thin, dense, inelastic fibrous capsule. Just within the tunica albuginea is the tunica vasculosa, through which the branches of the testicular artery course before entering into the gland (Fig. 12.1).[8,9] Numerous thin septations (septula) arise from the tunica albuginea and create 250–400 cone-shaped lobules containing the seminiferous tubules (Fig. 12.2).[10–12] These tortuous tubules course towards the mediastinum of the testis and progressively merge to form larger ducts known as tubuli recti (Fig. 12.3). These, in turn, join with each other to form a network of epithelium lined spaces embedded in the fibrostroma of the mediastinum called the rete testis. These continue as 10–15 efferent ductules which pass into the head of the epididymis.

The epididymis is a comma shaped structure that runs along the posterolateral aspect of the testis (Fig. 12.4). Its components are the head (globus major), body and tail, (globus minor). The head is located next to the upper pole of the testis and receives the efferent ductules. The ductules eventually converge through the body and tail and form the vas deferens which continues on in the spermatic cord. Along with the vas, the cord also contains the testicular artery, cremasteric artery, differential artery, the pampiniform plexus of veins, the genitofemoral nerve and lymphatic channels.

The testis and epididymis are enveloped by the tunica vaginalis, a fascial structure composed

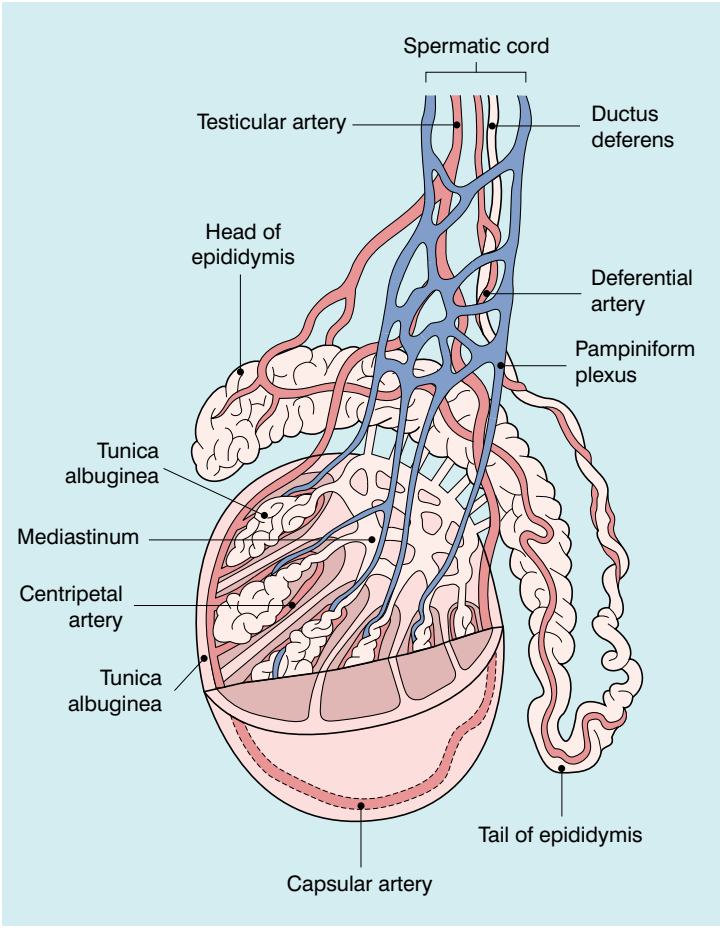


**Fig. 12.1** The testicular artery supplies flow to the epididymis and the testicle. As the testicular artery courses through the spermatic cord, it is surrounded by the pampiniform plexus of veins. The capsular artery, a branch of the testicular artery, courses just beneath the tunica albuginea. The centripetal arteries are branches of the capsular artery and course between the septa supplying the testicular parenchyma.

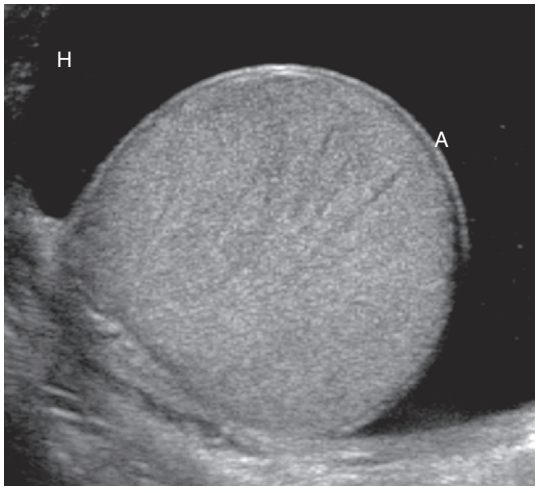


**Fig. 12.2** Transverse view of a normal testicle surrounded by a hydrocele (H). The testicle is of relatively uniform echogenicity. With high resolution equipment, the testicular septa can be perceived as fine lines dividing the parenchyma into the individual lobules. Note the echogenic tunica albuginea surrounding the testicle (A).

of an outer parietal layer and an inner visceral layer which surrounds the entire gland, except along the posterior aspect where the vessels and nerves enter. The extent to which the tunica vaginalis envelopes the testis directly correlates with the risk for developing testicular torsion. The potential space between the parietal and visceral layers normally contains a small amount of lubricating fluid, but a larger fluid collection accumulating here is know as a hydrocele.

## Testicular arterial anatomy

The right and left testicular arteries originate from the aorta just below the renal arteries. They course through the deep inguinal ring to enter the spermatic cord, accompanied by the cremasteric and deferential arteries, which supply the soft tissues of the scrotum, epididymis and vas deferens. The testicular artery penetrates the tunica albuginea along the posterior aspect of

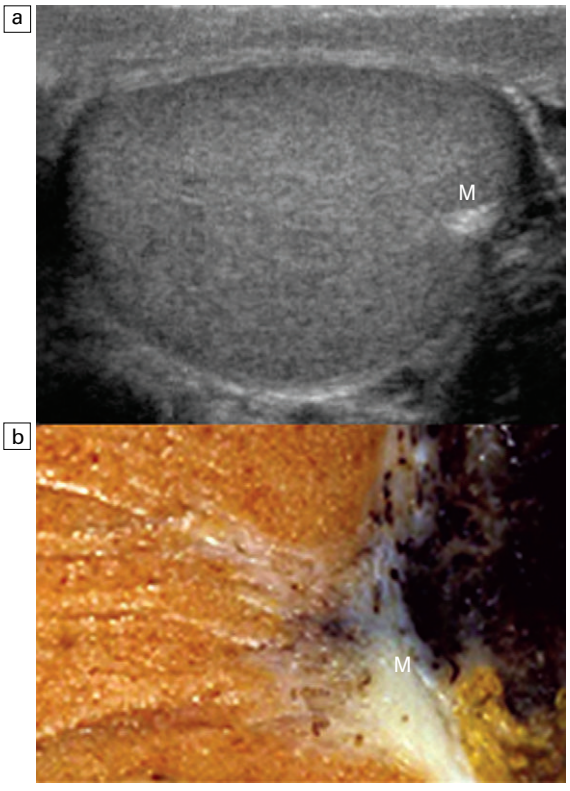


**Fig. 12.3** Transverse view of the left testicle (a). Specimen in the region of the mediastinum testis (b). Mediastinum testis is an echogenic structure. It is the point of confluence of the efferent ductules and the septa. Note the triangular echogenic appearance on the ultrasound (M) and how well it correlates with the dense white fibrous stroma on the specimen.

**Fig. 12.4** Longitudinal view of a normal right scrotum. The slightly hypoechoic epididymis wraps as a comma shape around the testis. The larger more prominent area is known as the globus major or the head of the epididymis.

the testis and gives off capsular branches which course through the tunica vasculosa. These capsular branches then give rise to the centripetal arteries which carry blood from the capsular surface, centrally towards the mediastinum along the septula (Figs 12.5 and 12.6). Some of the branches of the centripetal arteries course backward towards the capsular surface; these are known as recurrent rami. In about 50% of testes, a small branch can be seen passing directly from the testicular artery into the parenchyma, known as the transtesticular artery (Fig. 12.7). Small anastomoses do exist between the testicular artery, cremasteric, and differential arteries. Branches of the pudendal artery may also supply the scrotal wall.

## Testicular venous anatomy

Testicular venous outflow courses mostly through the mediastinum testis, into the spermatic cord, and eventually up through the inguinal canal. As the veins exit the scrotum through the spermatic cord, they form a web-like network that surrounds the testicular artery, known as the pampiniform plexus (Fig. 12.8). This plexus is thought to function as a heat exchange mechanism, pulling warmth away from the testicular arterial inflow, thereby helping to maintain spermatogenesis at a lower, more optimal temperature.

On the left side, the testicular vein usually drains into the left renal vein; on the right side, drainage is directly into the inferior vena cava just below the right renal vein. The testicular veins normally have valves that prevent retro-

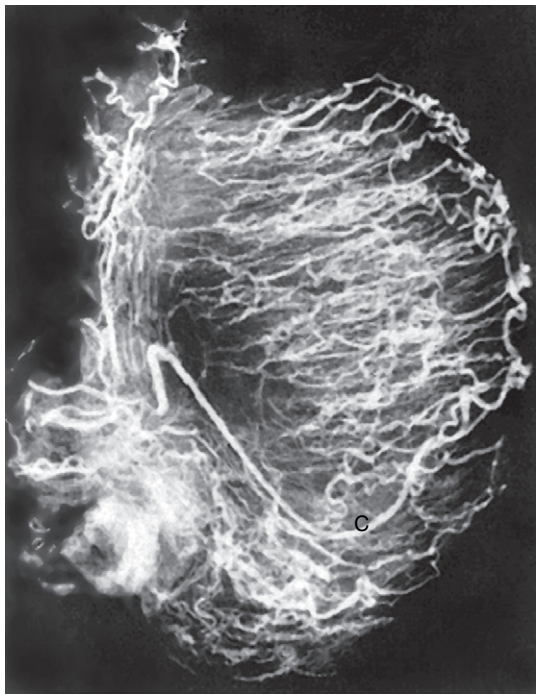


**Fig. 12.5** Microangiogram of the testicle. A prominent capsular branch (C) courses from the testicular artery under the capsular surface. Centripetal arterial branches emanate from it and pass into the lobules of the testicle. With very sensitive Doppler settings, a series of centripetal arteries is seen across this normal testicle. Case courtesy of Dr. Thomas Winter.

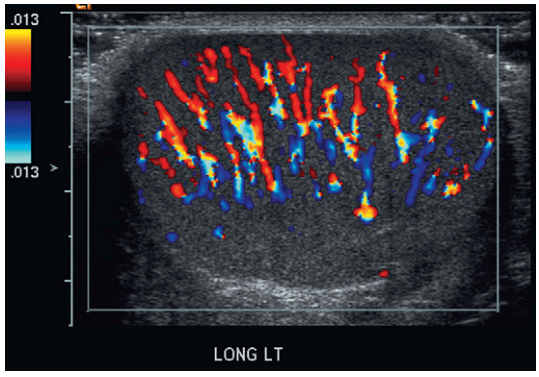


**Fig. 12.6** Longitudinal colour Doppler image of a testicle. With very sensitive Doppler settings, the network of centripetal arteries is seen fanning across this normal testicle.

grade flow of venous blood to the scrotum, but if they are absent or become incompetent; this predisposes to development of a varicocele.[13,14]

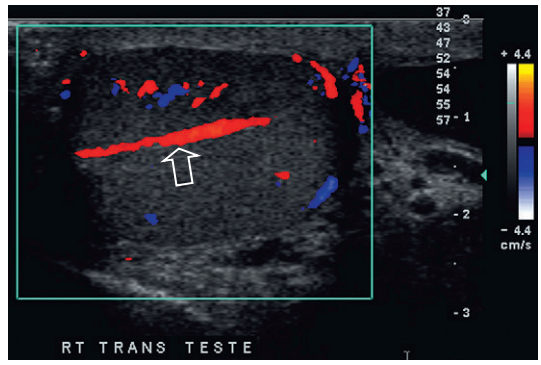


**Fig. 12.7** Longitudinal colour Doppler image of a testicle. A transtesticular artery (arrow) can be seen coursing obliquely through the testicle along the mediastinum. It is a branch of the testicular artery, but is seen in less than half of normal cases.

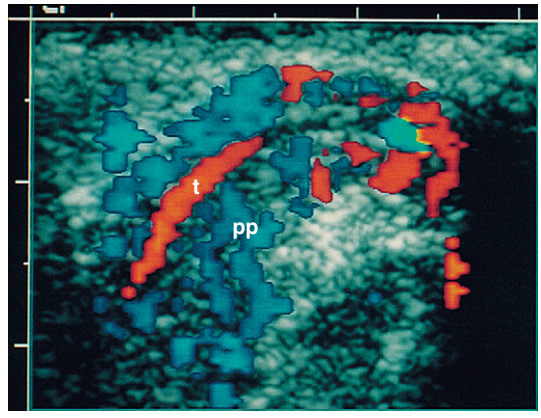


**Fig. 12.8** The pampiniform plexus of veins (PP) is a web-like collection of vessels surround the testicular artery (T) as it passes through the spermatic cord.

## TECHNIQUE

Prior to any ultrasound examination, the testes should be examined with a gloved hand, especially if the sonographic study is being conducted to evaluate a palpable mass. The examination is performed with the patient in the supine position. A towel is placed under the scrotum for support. If the testis is tender, the patient may be asked to hold it in a position which would facilitate the exam. This is particularly useful for the evaluation of a small mass. The patient should be asked to hold it between thumb and forefinger, and the ultrasound transducer is then

gently placed upon it. Some men may have a vigorous cremasteric response during the examination resulting in the testis being drawn upward and puckering the scrotal wall. To avoid shadowing from trapped air, copious amounts of gel need to be worked into the scrotal skin folds (Fig. 12.9). Imaging with the patient standing upright, or while performing a Valsalva manoeuvre, is useful for evaluating the testicular venous system, in particular for determining valvular competence in patients with suspect varicocele, or for improving detection of an inguinal hernia.

A high-frequency (10 MHz or greater) linear-array transducer is used for both grey-scale and Doppler imaging, with direct contact scanning on the scrotal skin. Examination is performed in both the longitudinal and transverse planes for each testis to allow assessment of any differences in size and echogenicity between the two sides. The split screen mode is useful to allow a direct comparison. Oblique imaging of the epididymis and spermatic cord should also be performed. Any extratesticular masses or fluid collections should be noted as well.

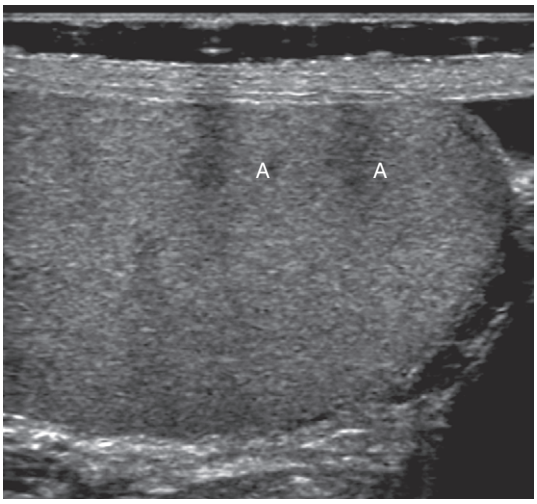


**Fig. 12.9** Longitudinal image of the testicle. Note the layer of gel between transducer and scrotal wall. Two air bubbles are barely perceived, but are enough to cause significant artifact within the testicle (A) which mimics a hypoechoic lesion.

## Doppler technique

Ultrasound examination of the scrotum is not complete without applying colour Doppler. The procedure is a mandatory part of the imaging evaluation to confirm the presence (or absence) of uniform, symmetric vascular perfusion of the testes and epididymides (Fig. 12.10). The settings for colour Doppler scanning must be optimised for low-volume and low-velocity flow.[15] If colour noise is excessive at low-flow settings and interferes with the examination, colour artefact can be decreased by properly adjusting gain and scale settings. Temporal resolution can be improved by minimising the overall image size by using a write zoom or decreasing depth and limiting the size of the colour box. Use of appropriate technical parameters should assure demonstration of intratesticular vessels in all normal cases.[9] The use of power Doppler can be helpful in very low-flow conditions, such as in paediatric patients, and with its evolution scrotal ultrasound has essentially replaced nuclear scintigraphy for the evaluation of torsion.[11,12,16] Spectral Doppler can assess arterial and venous waveforms and

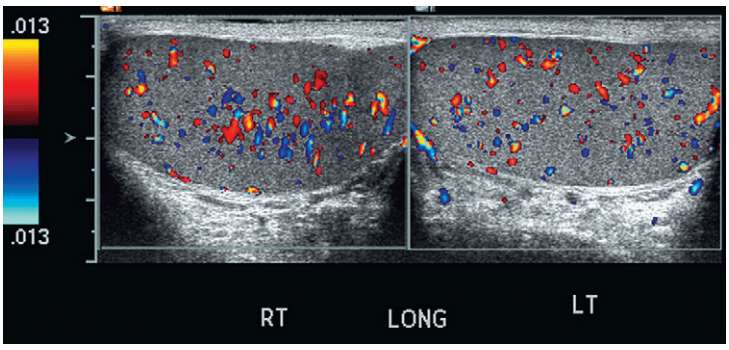


**Fig. 12.10** Longitudinal Doppler ultrasound image of both testicles using a split screen format. Note the symmetry of echotexture and the uniformity and symmetry of colour flow.

quantify velocities[15] (Fig. 12.11), but its application in the scrotum is limited, except for a few conditions such as partial torsion. Then spectral Doppler can best identify the high resistance to arterial inflow caused by venous outflow compromise.

Doppler sensitivity varies greatly between ultrasound systems and software levels. Therefore, the examiner must be familiar with normal flow perception on their equipment. A good 'rule of thumb' is to examine the contralateral side (provided it is normal) to establish a colour flow baseline which can then be used as the standard by which to judge the abnormal testis or epididymis. When comparing flow between sides, be sure to set imaging parameters to the non-affected side; then, without changing any settings, image the affected side. Some advanced ultrasound machines currently adjust imaging parameters automatically as depth and position of colour box changes with scanning. If possible, override this software feature to avoid misperception of asymmetric colour flow.

## Normal ultrasound findings

A normal ultrasound examination of the scrotum reveals uniform, homogeneous echogenicity throughout both testes. The epididymis is usually isoechoic or slightly hyperechoic compared with the testes. The size and echogenicity of testes and epididymides should be bilaterally symmetric.

Colour Doppler should reveal bilaterally symmetric and relatively uniform flow through both testes and epididymides (Fig. 12.10). A fan-like array of the centripetal arteries should be present through the testicles (Fig. 12.6). Venous flow in the epididymides may be seen to fluctuate with respiration.

Spectral Doppler tracings of testicular arterial inflow demonstrate relatively low resistance (Fig. 12.11); this is in contrast to the cremasteric and deferential arteries which have relatively high resistance to flow. The normal testicular artery resistive indices in adults range from 0.46 to 0.78, with a mean of 0.64.[9] Similar findings are reported in the intratesticular arteries of postpubescent boys, with resistive indices ranging from 0.48 to 0.75 (mean, 0.62).[15] In prepubertal boys, however, resistance is higher to the point that diastolic arterial flow may not be detectable.[17] Suprates-ticular arteries to the vas deferens or cremaster muscle, on the other hand, have higher impedance with low-diastolic flow and resistive indices ranging from 0.63 and 1.0, with a mean of 0.84.[1,9,15]

Pulsed Doppler is relatively insensitive in detecting arterial flow in prepubescent patients.[15,17,18] In contrast, power Doppler has been shown to reveal arterial flow in 92% of testes in prepubescent patients, while colour Doppler demonstrates flow in 83% of cases.[4] In postpubescent patients, both Doppler imaging techniques demonstrated flow in 100% of cases.

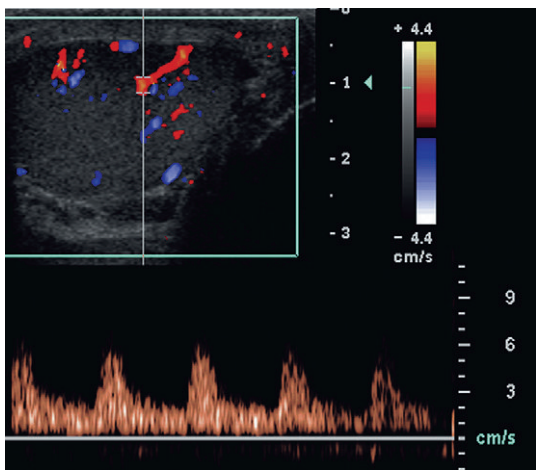


**Fig. 12.11** Spectral Doppler waveform of a normal testicle. The resistive index is a normal (approx. 70%).

# ACUTE SCROTAL PAIN

## Inflammatory disease

Acute epididymo-orchitis is the most common cause of scrotal pain in men over the age of 20 years, accounting for up to 80% of cases of acute scrotal pain, but it is frequently clinically indistinguishable from spermatic cord torsion. Patients usually present with an acutely painful, tender, swollen scrotum, with associated erythema, urinary tract symptoms, fever and leukocytosis. Sometimes, however, the signs and symptoms may be less distinct, making clinical differentiation

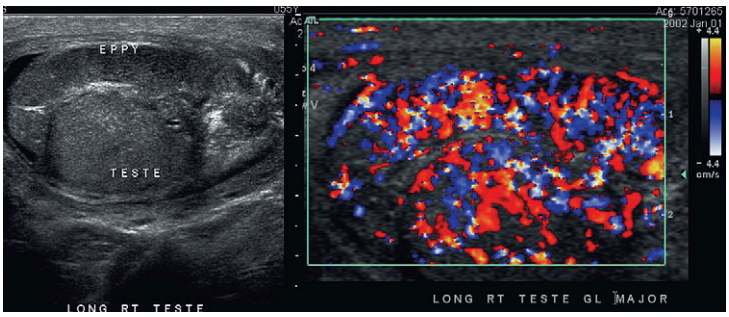


**Fig. 12.12** Longitudinal grey-scale and colour Doppler image of the right testicle. The patient presented with severe pain. Both the testis and epididymis are oedematous, swollen and hypoechoic. Colour Doppler shows exuberant flow through both structures. The diagnosis is epididymo-orchitis.

between infection and torsion extremely difficult. The process typically first manifests in the epididymis and then ascends to affect the testicle, but isolated epididymitis, orchitis, or even focal orchitis can be encountered.

The cause of the infection varies with age.[19] (In adult patients less than 35 years of age, *Chlamydia trachomatis* and *Neisseria gonorrhoeae* (sexually transmitted organisms) are the most common cause. In prepubertal boys and in men over 35 years of age, the disease is most frequently caused by *Escherichia coli* and *Proteus mirabilis*. *Cytomegalovirus* is the most common agent in the immunocompromised patient. In most normal paediatric patients, a bacterial pathogen is not isolated and the inflammation is presumed to be viral in nature, but paediatric patients who have an underlying urogenital congenital anomaly are prone to infection from gram negative bacteria.[20]

The sonographic appearance of epididymo-orchitis varies depending on the stage of the process. The sensitivity of grey-scale sonography for detecting epididymo-orchitis has been reported to be about 80%.[21] In the early, acute stage, the epididymis and/or testicle will be enlarged and hypoechoic. With the onset of tissue breakdown and haemorrhage, the echogenicity begins to increase. [5,12,21] There may be reactive thickening of the scrotal wall. A hydrocele may be present and it may contain debris. If allowed to progress, microabscesses may develop and the appearance becomes more complex and variable. Scarring and necrosis associated with chronic orchitis typically results in a small hyperechoic testis.[22]

The diagnosis of inflammation can be made with greater confidence when hyperaemia is identified by colour Doppler – an asymmetric appearance with more robust flow (an increased number and prominence of discernible vessels) in association with an enlarged, painful, hypoechoic epididymis and/or testis (Fig. 12.12).[1,2,5,21,23] A study by Ralls et al[6] demonstrated 91% sensitivity and 100% specificity for the diagnosis of scrotal inflammatory disease by colour Doppler sonography. Other authors have also reported a sensitivity close to 100%.[9,23] Inflammatory hyperaemia typically shows a low-resistance flow pattern on spectral Doppler;[1] although spectral analysis is occasionally necessary to confirm the diagnosis (Fig. 12.13).[24]

In cases of severe epididymitis, periepididymal swelling may obstruct testicular venous outflow, leading to testicular ischaemia or infarction. An

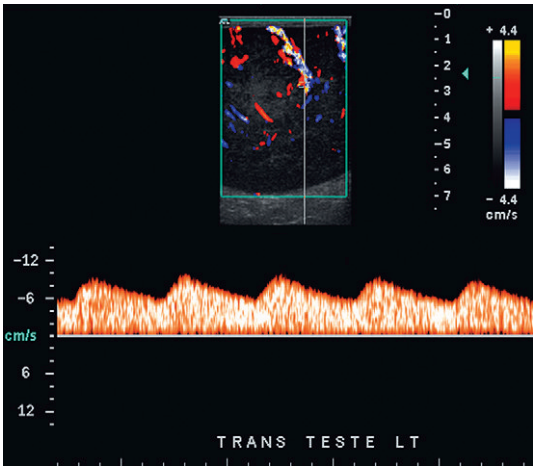


**Fig. 12.13** Spectral Doppler tracing of an area of testicular inflammation. Flow during diastole is relatively brisk resulting in a resistive index of <50%. This appearance is consistent with inflammatory hyperaemia.

enlarged, heterogeneous testicle with reduced or absent colour flow and a contiguous abnormal epididymis will be seen on grey-scale images (Fig. 12.14).[15] Hyperaemia of the epididymis helps to differentiate testicular ischaemia following inflammation from that caused by torsion. A high-resistance waveform, along with decreased or reversed diastolic flow, may be seen on the spectral Doppler tracing and suggests venous infarction.[25]

If left untreated, the process may progress to abscess formation (Fig. 12.15), which usually manifests as an enlarged testicle with a complex, septated collection of fluid debris and tissue of mixed echogenicity. It may be difficult to distinguish from a testicular neoplasm, as both can present as complex cystic/solid masses. Older abscesses may have radiating echogenic septa separating hypoechoic spaces. Increased blood flow around the abscess cavity and no internal flow is present on colour Doppler.[1,21] Surgical exploration may be necessary to rule out the presence of a tumour and débride the abscess.

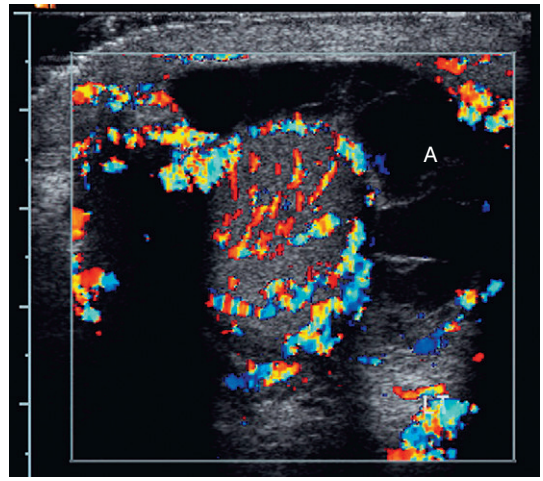


**Fig. 12.15** Transverse view of the scrotum. An inflamed hyperaemic testicle is located centrally within a complex septated fluid collection. The brisk flow in the wall surrounding this collection helps identify it as an abscess (A).

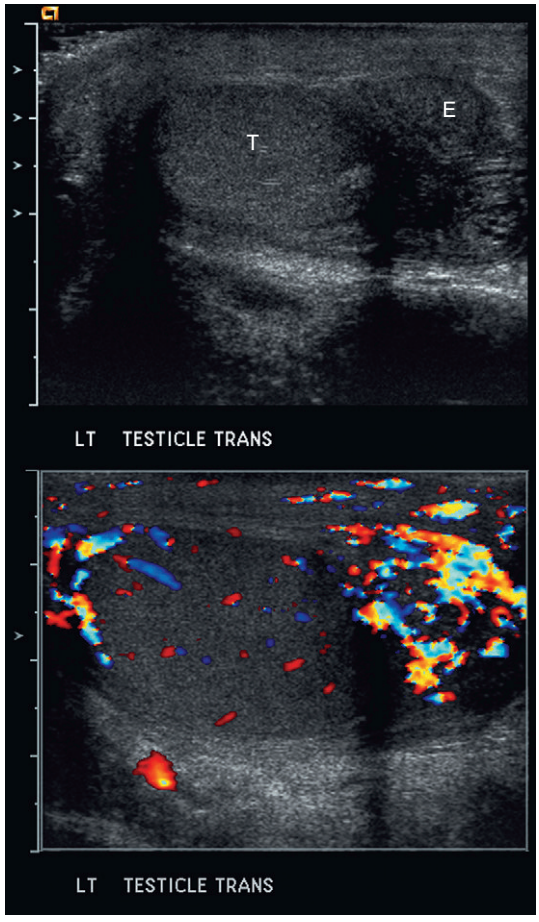


**Fig. 12.14** Longitudinal view of the left testicle with and without colour Doppler. The epididymis (E) is enlarged, but the testicle (T) remains of normal size and echotexture. With colour Doppler, there is brisk flow in the epididymis whereas the testicle shows appropriate if not slightly reduced flow. These findings are consistent with epididymitis.

Occasionally, testicular inflammation may be focal, even rounded, with areas of decreased echogenicity and swelling. Hyperaemia concentrated in the abnormal, tender area may suggest inflammation over neoplasm, but there is overlap in this appearance with neoplasm, especially lymphoma (Fig. 12.16).

## Torsion

Torsion is divided into two types – extravaginal which occurs exclusively in newborns and intravaginal. Extravaginal torsion occurs outside the tunica vaginalis when the testes are not yet fixed and are free to rotate.[26] The testis is typically necrotic at birth. Ultrasound reveals an enlarged heterogeneous testis, a reactive hydrocele, skin

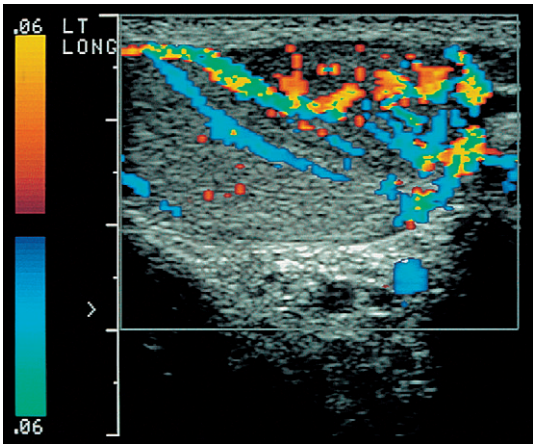


**Fig. 12.16** Longitudinal colour Doppler image of a testicle. This patient complained of severe scrotal tenderness. A focal hypoechoic of the lower pole shows marked hyperaemia in contrast to the upper pole. The diagnosis was focal orchitis.

thickening and no colour Doppler flow in the testis or spermatic cord.[27] Intravaginal torsion occurs most frequent in adolescent boys. A bell-clapper deformity, in which the tunica vaginalis completely encircles the epididymis, distal spermatic cord, and testis, is a key predisposing factor. This deformity is usually bilateral and leaves the testis free to swing and rotate within the tunica vaginalis.

The diagnosis of spermatic cord torsion must be established quickly to allow for prompt surgical intervention, since obstruction of blood flow may result in the loss of testicular viability within a few hours of onset of symptoms. Clinical history and physical findings, however, overlap with that of inflammatory disease to such a degree that even an experienced urologist may have difficulty in differentiating the two conditions. Symptoms and signs include sudden pain in the scrotum, lower abdomen or inguinal area (frequently accompanied by nausea, vomiting and low-grade fever), a tender testicle with a transverse orientation, and a swollen, erythematous hemiscrotum.[15] The false-positive rate of nearly 50% for clinical diagnosis of testicular torsion often results in unnecessary surgical exploration.[28]

Grey-scale sonography by itself has a low sensitivity and specificity when evaluating patients for suspected torsion. Findings will depend on the length of time the torsion has been present.[1,2,5,23,29,30] During the first few hours, testicular appearance is normal, but after about 4–6 h, as the veins are obstructed, there is vascular engorgement and the testis becomes enlarged and oedematous, with a hypoechoic appearance as compared to the contralateral testicle.[6] After 24 h, vascular congestion, haemorrhage and infarction will cause the testis to appear heterogeneous (Fig. 12.17). The epididymis may also be enlarged and hypoechoic because of decreased blood supply.

The addition of colour Doppler increases sensitivity in adults to 90–100% with a high specificity.[1,23,31] Unlike grey-scale imaging, colour and spectral Doppler are almost always abnormal even during the early stages of torsion.[15] Instrument settings should be optimised on the *normal* side to identify low-velocity flow before ascertaining that there is indeed decreased blood flow on the *symptomatic* side (Fig. 12.10). If arterial flow cannot be detected in the symptomatic testicle but can in the contralateral testicle, the diagnosis of torsion can be effectively established.[15] The characteristic finding of ischaemia

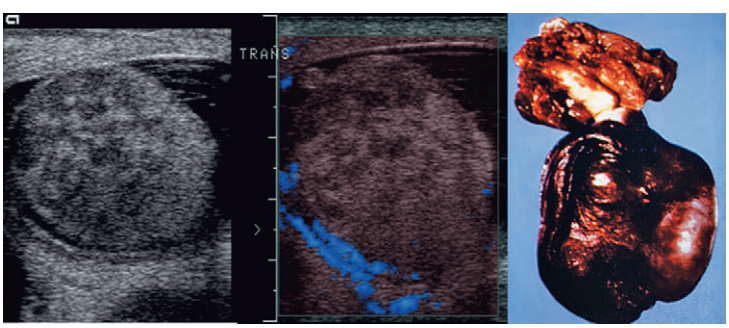


**Fig. 12.17** Transverse imaging view, power Doppler view, and resected specimen of a testicle. Grossly irregular echotexture and absence of flow on power Doppler indicate that this is a severely compromised testicle with torsion. The specimen reveals a frankly necrotic testicle.

is a completely avascular testicle. In the late stages of torsion, colour Doppler may reveal an increase in peritesticular blood flow because of inflammation in the surrounding soft tissues of the scrotum.[1–3,5,32]

Evaluation of the small testicles of prepubescent boys, however, can be very difficult because of inherently low velocity blood flow.[15,31] In addition, if the patient has intermittent torsion and, by the time the patient arrives for the ultrasound examination the torsion spontaneously resolves, flow may appear normal on colour Doppler. Since absence of flow is demonstrated only if torsion is present at the time of sonographic examination, differentiating between normal testicles and testicles with intermittent torsion may be difficult to accomplish.

With full torsion spectral Doppler adds little other than to confirm the obvious fact that there is no flow. With partial torsion, however, the spermatic cord twists only enough to occlude the venous outflow. Because the artery has a thicker wall patency is maintained. The resultant spectral tracing presents a high resistance arterial waveform (Fig. 12.18).[33]

If the spermatic cord spontaneously untwists prior to the ultrasound examination, colour Doppler will likely reveal diffuse, reactive hyperaemia. Although this finding will mimic epididymo-orchitis, resolution of acute scrotal pain concurrent with increased blood flow is highly indicative of spontaneous detorsion.[2,3,12,23] Colour Doppler ultrasound can also be used to monitor non-surgical detorsion of the testicle as the testis is manually rotated; if this manoeuvre is successful,

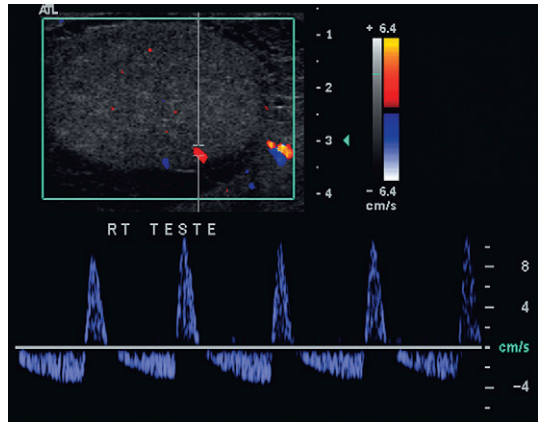


**Fig. 12.18** Longitudinal view of right testicle. This young man complained of intermittent severe pain. The colour Doppler image shows only a few tiny foci of flow, the most prominent at the edge of the testicle. A spectral Doppler tracing shows reversed flow in diastole. These findings support the diagnosis of partial torsion with occluded venous outflow.

blood flow is re-established to the testicle and can be detected on Doppler (Fig. 12.19). This non-surgical approach, however, is only considered a temporising measure. It is *not* a substitute for surgical intervention, which is still necessary to correct the underlying anatomical deformity that predisposes to torsion.

The use of echo-enhancing agents has been studied for improving imaging of small testicles with low-velocity and low-volume flow. In an animal study by Brown et al,[34] the authors examined induced testicular torsion with grey-scale imaging, colour Doppler, power Doppler and spectral Doppler analysis. Injection of contrast media did not enhance grey-scale images, but visualisation

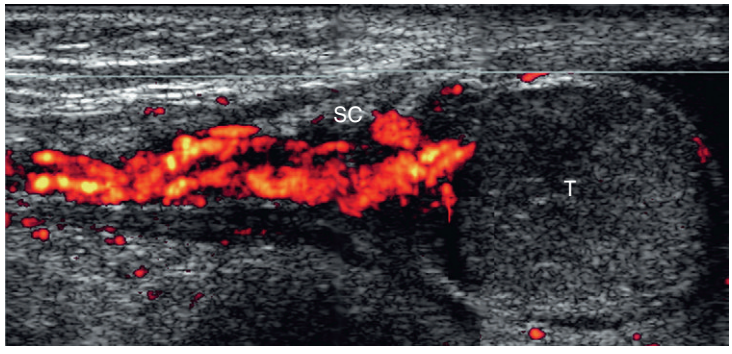


**Fig. 12.19** Longitudinal power Doppler image of the spermatic cord (SC) and testicle (T). This image is a composite of several individual frames. Flow is seen within the cord and suddenly stops with no flow identified in the testicle consistent with torsion.

of all vessels in both normal and rotated testicles was significantly improved with both colour and power Doppler. Asymmetry of blood flow was more obvious. The authors concluded that diagnosis of testicular ischaemia could be made with more confidence using an intravenous ultrasound contrast agent because of improved demonstration of altered perfusion patterns. Similar findings were reported by Coley et al[35] in an animal study comparing unenhanced and contrast-enhanced Doppler analysis of acute testicular torsion. The findings from these studies indicate that use of contrast ultrasonography will likely reduce, and possibly eliminate, the need for scintigraphy in currently difficult-to-visualise testicles.

Hand-held continuous-wave Doppler has no role in the evaluation of testicular torsion because of its inability to provide range-gated information. Normal or increased blood flow within the scrotal wall may lead the examiner to incorrectly conclude that intratesticular flow is preserved.

Although testicular torsion may be accurately diagnosed by sonography, this does not guarantee successful surgical salvage. Success depends on a timely diagnosis and the duration of ischaemia. Indeed, the more obvious the ultrasound diagnosis, the less likely the chance of salvage. The testicle devoid of colour flow but with an appropriate ultrasound appearance is much more likely to be salvaged at surgery. The testicle that appears hypoechoic or worse, showing frank degeneration is likely to be removed.[36]

The appendix testis is a Müllerian duct remnant that is attached to the upper pole of the testis. Patients can develop torsion of the appendix testis and usually present with acute scrotal pain. Physical examination reveals a small firm, palpable, tender nodule. Ultrasound evaluation usually reveals a hyperechoic mass with a reactive hydrocele. Color Doppler may reveal increased flow around the twisted testicular appendage but more importantly it rules out testicular torsion and acute epididymo-orchitis (Fig. 12.20). After torsion and necrosis the appendix testis may slough and become calcified

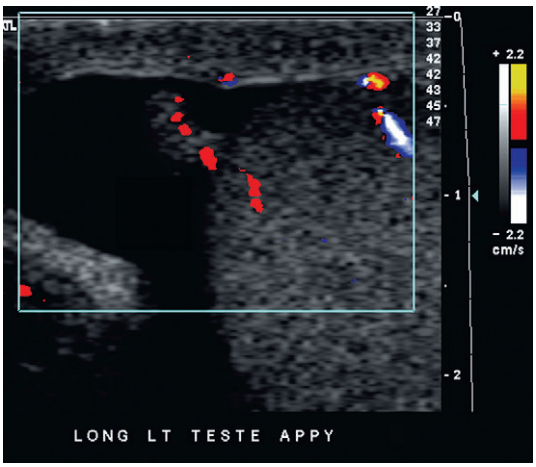


**Fig. 12.20** A longitudinal view of the left testes at the area of maximum tenderness in this patient. The appendix testis was conspicuous as the focus of pain. Note the hyperaemia at the base of this structure. It is quite rare to actually identify colour Doppler flow abnormalities in the appendix testis. Typically patients present well after the structure has necrosed and sloughed.

in which case it becomes known as a scrotal pearl. Twinkle artifact may be present on colour Doppler and should not be confused for true flow (Fig. 12.21).

## Trauma

Testicular trauma typically results from an athletic injury, a direct blow or a straddle injury. Trauma can result in testicular contusion, haematoma, fracture or rupture. Clinical examination of a traumatised, tender testicle can be difficult because of pain and swelling; however, ultrasound evaluation is able to provide information regarding testicular integrity, and the presence of haematoma, haematocele, fracture or rupture. Colour Doppler sonography provides excellent delineation of blood flow throughout the testis, differentiating hyperaemic, contused regions from devascularised or ischaemic areas (Fig. 12.22).

In the case of testicular rupture, sonographic identification is extremely important because prompt diagnosis and quick surgical intervention is required successfully to correct the condition (Fig. 12.23). If surgery is performed within 72 h

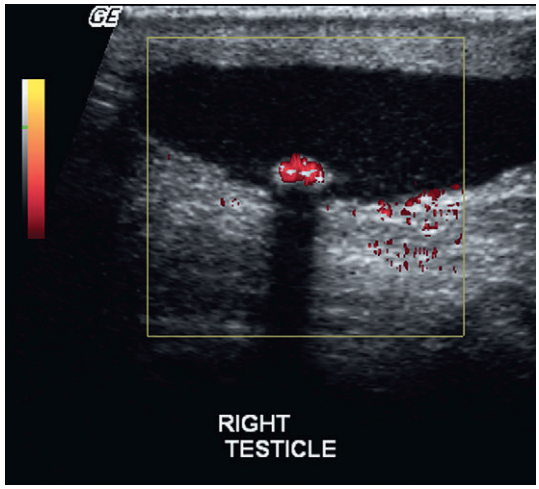


**Fig. 12.21** Image at the base of the right scrotum, distant from the testicle itself. An echogenic structure with acoustic shadowing is layering dependently. Power Doppler reveals colour emanating from this structure indicating frequency shift. This is consistent with twinkle artifact produced when the Doppler beam interacts with crystalline material on this calcified left scrotal pearl.

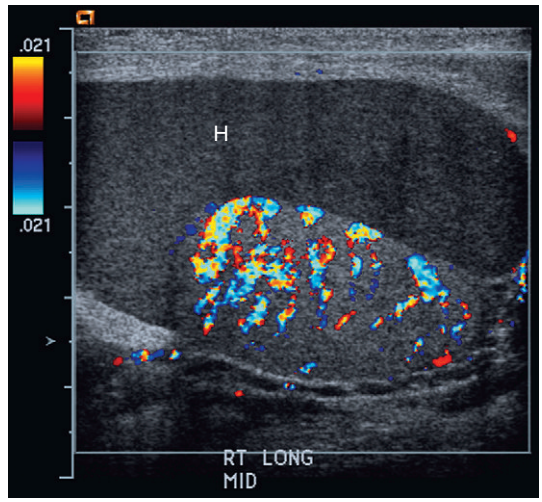


**Fig. 12.22** Longitudinal view of patient with acute trauma. Scrotal swelling and tenderness prevented adequate physical examination. Imaging reveals a large echogenic collection within the tunica vaginalis consistent with an acute haematoma (H). The testicle is hyperaemic, however, integrity is maintained and flow is present throughout.

of the trauma, approximately 80% of ruptured testes can be salvaged.[37] If rupture is present, ultrasound examination may demonstrate a disrupted tunica albuginea; a heterogeneous testicle with asymmetric, poorly defined margins; thickening of the wall of the scrotum; and/or a large haematocele.[16,38] Perception of blood flow will be diminished or absent on colour or spectral Doppler examination.

Unlike rupture, fractures and small haematomas and haematoceles do not require surgery if the tunica albuginea has not been interrupted and Doppler imaging shows normal blood flow to the testicle. Sonographic findings associated with a testicular fracture include a linear hypoechoic band crossing the parenchyma of the testicle, a smooth well-defined testicular outline, an intact tunica albuginea, and often an associated haematocele. Normal Doppler signals indicate unimpaired blood flow and viable testicular tissue. If Doppler signals are absent, ischaemia is very likely and surgical intervention is called for. Acute haematomas are usually hyperechoic relative to adjacent testicular parenchyma.[38] Older

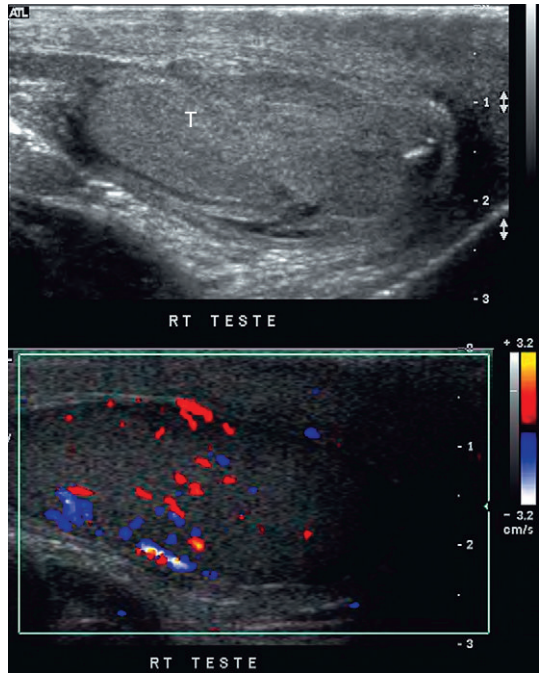


**Fig. 12.23** Longitudinal view of the right testicle (T). Only the upper portion can be clearly identified. The ovoid shape is lost inferiorly where the tunica albuginea has ruptured. Colour confirms flow through the upper part of the testicle, hyperaemia in the mid-testicle, and very little flow in the ruptured segment.

haematomas may have both hyper- and hypoechoic areas, and there may be associated thickening of the scrotal wall. On colour Doppler, haematomas are usually avascular.[1,2,3] Acute haematoceles tend to be echogenic, while low-level echoes or septations may be seen in chronic haematoceles.

## SCROTAL MASS

### Testicular neoplasm

Patients with testicular neoplasms usually present with a palpable scrotal nodule. For palpable scrotal masses, ultrasound is widely considered the imaging modality of choice. The principal role of ultrasound examination in the diagnosis of testicular cancer is to distinguish intra- from extratesticular lesions, because the majority of extratesticular masses are benign, whereas intratesticular masses are considered malignant until proven otherwise.[39,40] Ultrasound can differentiate solid and cystic masses and confirm their extra- or intratesticular location. The main application of ultrasound is to identify those masses which require additional assessment and possible surgical intervention.[41]

On grey-scale images, testicular neoplasms usually appear as a discrete mass whose echo pattern differs from that of the normal testis. Most neoplasms have hypoechoic components although heterogeneity of echotexture is frequently observed (particularly with larger tumours and non-seminomatous germ cell tumours). Sonographic differentiation of seminomas, embryonal cell carcinomas, teratomas and choriocarcinomas can be difficult, especially since 40–60% of testicular neoplasms have mixed histological elements.

*Seminomas* are the most common single-cell type testicular tumour in adult males (40–50%).[42] The 'classic' ultrasound appearance of seminomas has been described as a well-defined, uniformly hypoechoic lesion, with no evidence of calcification, haemorrhage, or cystic areas.[43] Modern high-frequency transducers, however, show fine details of the neoplasm's internal structure and seminomas may appear to be less homogeneous than previously described.

The general ultrasound appearance of germ cell tumours is that of a heterogeneous, small mass with poorly defined margins, anechoic areas due to cystic necrosis, and echogenic foci of haemorrhage.[44] If the tumour invades the tunica, the normal contour of the testicle may be distorted.[11]

*Teratomas* generally appear on ultrasound as extremely heterogeneous masses with well-defined margins and areas of various sizes that may be either hyperechoic or hypoechoic.[11] Dense echogenic foci caused by calcification, cartilage, immature bone, fibrosis, and non-calcified fibrous tissue can cause acoustic shadowing. Old haemorrhage and necrosis may result in hypoechoic areas. Cysts are a common characteristic of teratomas and can cause increased thick-walled anechoic areas with through-transmission.[45]

*Choriocarcinomas* generally appear as small masses on ultrasound, but haemorrhage may also be seen. Areas containing either solid or cystic components associated with viable tissue, necrosis, and haemorrhage may be observed. If calcification is present, a distinct area of increased echogenicity with posterior acoustic shadowing may be present.

Testicular neoplasms have mixed histological components in 40–60% of cases,[46–48] with the most common combination being that of teratoma and embryonal carcinoma (teratocarcinoma). Ultrasound findings of mixed tumours will vary, depending on which cell lines are dominant and if there are no particular ultrasound findings that permit differentiation for possible preoperative planning.

Testicular carcinoid is extremely rare and usually presents as painless testicular enlargement or as a discrete mass. The tumour may be primary, associated with teratoma or metastatic. Primary testicular carcinoid is believed to arise from pluripotential germ cells or from the development of a simplified teratoma without other teratomatous elements.[49] Only 71 cases of testicular carcinoid have been reported in the literature. Very few (<3%) have associated carcinoid syndrome.[50] On ultrasound testicular carcinoid appears as a solid well-defined hypoechoic

intratesticular mass with or without dense calcification. On Doppler it has increased vascularity similar to seminoma[51] (Fig. 12.24).

If a testicular mass is suspected of being a tumour, the rest of the scrotum should be examined carefully to exclude any invasion of the tunica albuginea or epididymis by the neoplasm. Enlargement of the epididymis usually indicates epididymo-orchitis or torsion, rather than neoplasm. An extratesticular fluid collection normally indicates inflammation, torsion or trauma; although testicular neoplasms can be associated with hydrocele. Because a hypoechoic appearance has also been reported with other testicular conditions (e.g. epididymo-orchitis, trauma, spermatic cord torsion, sarcoid), the additional extratesticular findings may help in the differential diagnosis (Fig. 12.25).

Colour Doppler and spectral Doppler sonography are considered to be of minimal benefit in the evaluation and characterisation of adult testicular masses and the diagnosis of testicular neoplasm. This is because vascularity of these lesions is extremely variable (Figs 12.26 and 12.27).[41] Small lesions tend to be hypovascular while larger lesions tend toward hypervascular compared with normal testicular parenchyma. An infiltrative neoplasm of the testicle, such as leukaemia or lymphoma, typically presents as an enlarged hypoechoic area on grey-scale imaging. Colour Doppler may demonstrate hyperaemia in the neoplasm with increased flow in areas of leukaemic or lymphomatous involvement (Fig. 12.28), or flow only along the periphery of the lesion, but the appearance is quite similar to inflammation and clinical or surgical corroboration is required to differentiate these conditions.[52,53]

It has been suggested that colour Doppler imaging may be more useful in evaluating

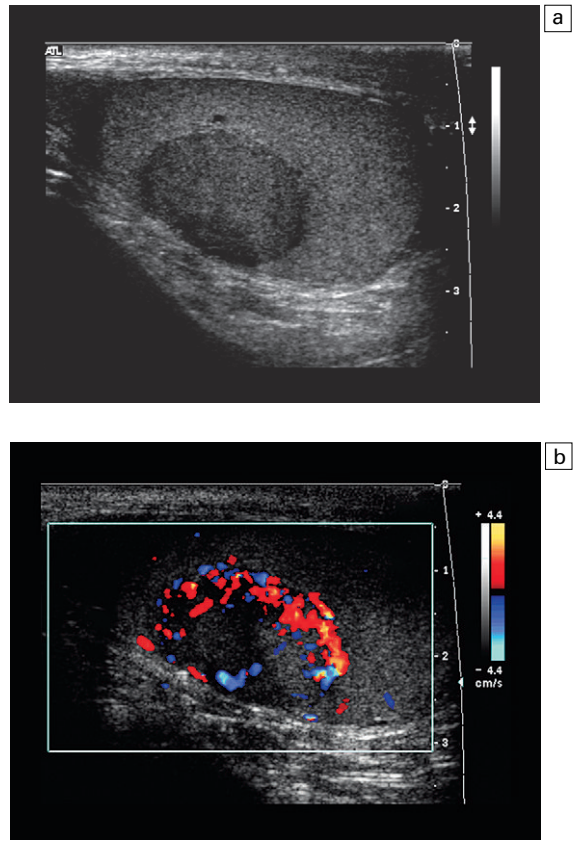


**Fig. 12.24** (a) Right scrotal sonography shows a well-defined solid mass without calcification in the right testis. (b) Colour Doppler shows the hypervascularity of the right testicular mass. Case courtesy of Kyoung-Sik Cho, MD, Asan Medical Center, University of Ulsan, College of Medicine.

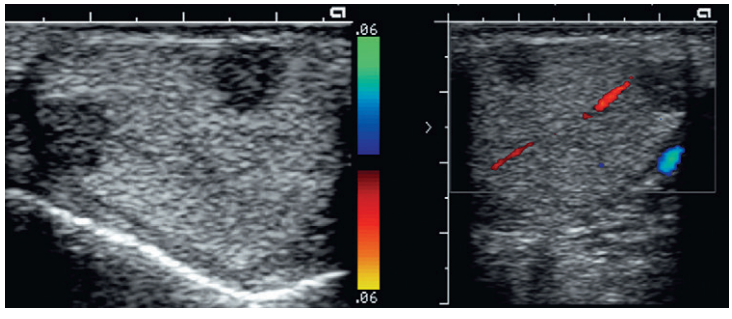

**Fig. 12.25** Longitudinal images of the right and left testicles show two hypoechoic lesions in both. Colour shows essentially no flow within the lesions. These findings are consistent with the patient's known history of sarcoidosis and represent granulomas.

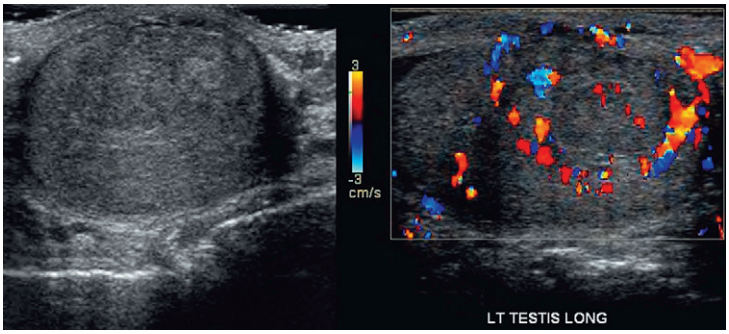


**Fig. 12.26** Grey-scale and colour Doppler longitudinal images of the left testis being evaluated for a palpable mass. The normal testicular echotexture is distorted. There is a slightly hypoechoic mass. Colour Doppler shows a rim of hyperaemia, but the central portion of the mass is relatively avascular.

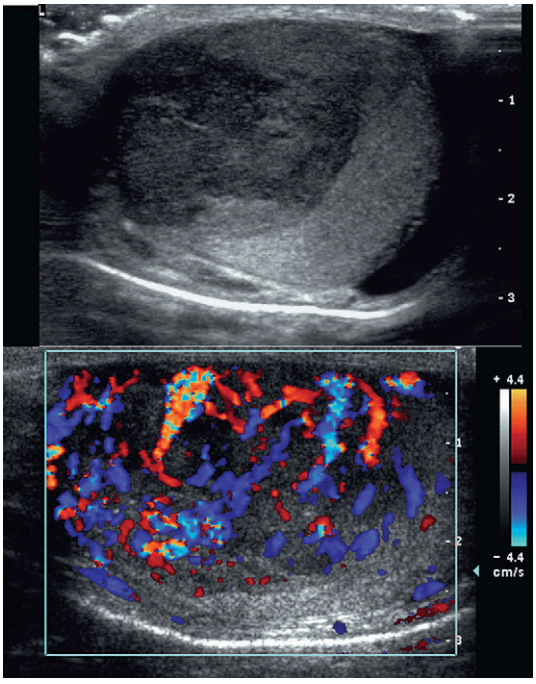


**Fig. 12.27** Longitudinal images of a testis being evaluated for a palpable mass. The large hypoechoic irregular mass replaces the majority of this testis. The colour Doppler image shows marked hyperaemia throughout this large mass. Note the distorted vascular architecture indicates tumour neovascularity.

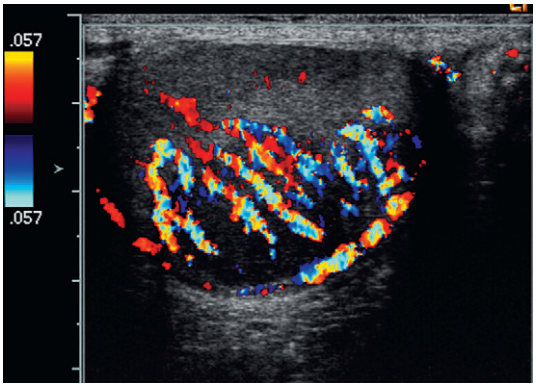


**Fig. 12.28** Longitudinal colour Doppler image of a 59-year-old male with a palpable scrotal mass. Overlying a hypoechoic mass colour Doppler reveals hyperaemia of the capsular artery and centripetal arteries without much anatomical distortion. Colour imaging alone would have suggested an inflammatory process, but the patient is absolutely asymptomatic and therefore lymphoma was entertained and proven at surgery.

paediatric patients in whom testicular neoplasms may be difficult to distinguish with grey-scale imaging but tend to be hypervascular on colour Doppler.[54]

## Benign testicular lesions

Benign intratesticular masses are rare, but recognition is important to avoid unnecessary biopsy, or worse orchiectomy. Almost all intratesticular cystic lesions are benign. The list includes cysts of the tunica albuginea, simple intratesticular cysts, epidermoid cyst, tubular ectasia of the rete testis (Fig. 12.29), and intratesticular spermatocele. Colour Doppler ultrasound helps in confirming their benign nature of these since no blood flow will be seen within these cysts.[55]

Bilateral, eccentrically-located, intratesticular adrenal rest tumours may be seen in patients with congenital adrenal hyperplasia and primary adrenal insufficiency.[56] In most cases, they are hypoechoic oblong lesions peripherally located close to the mediastinum.[57] They are bilateral in 83–100% of cases.[58] They may undergo extensive

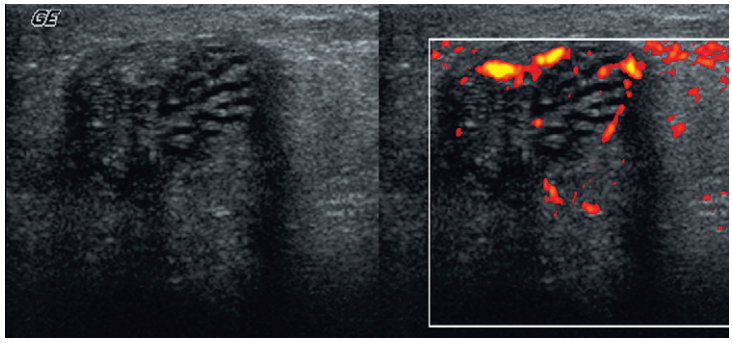

**Fig. 12.29** Grey-scale and power Doppler image focused on the region of the mediastinum testis. A collection of small tubules is present. Power Doppler shows the absence of flow within these tubules, consistent with dilated rete testis.

fibrosis and eventually become hyperechoic with acoustic shadowing. Vascularity on colour Doppler is variable relative to the normal testicle. Vessels may be seen entering from the adjacent testis without change in course or calibre (Fig.12.30). Some lesions may exhibit a spoke-like pattern of converging vessels.[59] There are two theories for the origin of these lesions. One says they originate from hilar pluripotential cells, which proliferate as a result of the elevated level of adrenocorticotropic hormone.[60] The other says they originate from aberrant adrenal cortical tissue that adheres to the testes and descends during prenatal life.[61] Whatever the origin, these should be recognised as benign lesions and first treated with adrenal suppression with dexamethasone.

## Varicocele

Varicoceles are present in approximately 15% of men.[62] Incompetent or absent valves in the internal testicular veins predispose to stasis or retrograde blood flow, resulting in dilatation of the pampiniform plexus. This is responsible for the majority of varicoceles. Varicoceles occur more commonly on the left; this is attributed to the longer course of the gonadal vein and its direct drainage into the left renal vein. Varicoceles are important clinically because of their association with infertility. Diagnosis of varicoceles is important, because treatment improves sperm quality in over half of cases.[63]

On ultrasound a varicocele is seen to consist of dilated (>2 mm diameter), serpiginous channels in the head of the epididymis and spermatic cord. Colour Doppler has been shown to be very accurate in detecting varicocele.[13] At rest and with normal respiration, colour will saturate the tubules at intervals related to respiratory pressure fluctuations (Fig. 12.31). With more vigorous respiration, to-and-fro movement of blood may

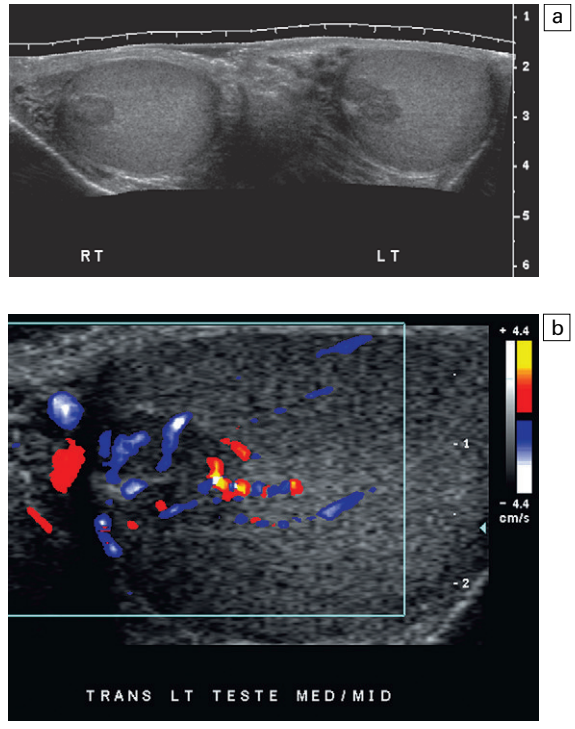


**Fig. 12.30** (a) Transverse panoramic view of both testicles. Hypoechoic masses are identified adjacent to the mediastinum of both testes. (b) Colour Doppler image of the left paramediastinal mass shows hyperaemia. Vessels appear to be passing through this region. The patient had a known history of congenital adrenal hyperplasia and these represent benign rests of adrenal tissue.

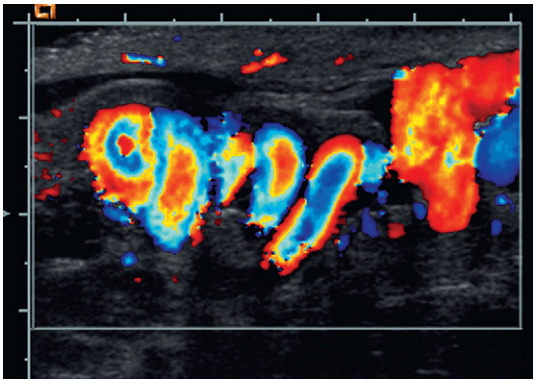

**Fig. 12.31** Longitudinal view of the left spermatic cord in a patient with a palpable thickening and infertility. A serpiginous collection of vessels with a venous flow profile is consistent with that of a varicocele. Note the laminar flow.

manifest as alternating colour in the same vessel, changing between inspiration and expiration. Colour Doppler identification of varicocele is enhanced by having the patient perform a Valsalva manoeuvre or by having the patient stand up. This increases the abdominal pressure and results in the reversal of blood flow into the pampiniform plexus, thereby causing further distention. When the Valsalva manoeuvre is performed, a brief burst of reversed flow is common. This is due to the expulsion of the venous blood in the gonadal vein of the pelvis below the lowest competent valve. As soon as this volume of blood is expressed, then flow usually stops, waiting for the scrotal venous pressure to rise above that created by the Valsalva. When the pressure is released as the patient relaxes, the direction of blood flow reverts to normal (Fig. 12.32).

Whenever a varicocele is identified, obstruction by a retroperitoneal mass, such as a left renal malignancy invading the renal vein should be considered. A brief scan of the upper abdomen should be performed to assess for this possibility.[64]

## OTHER IMAGING PROCEDURES

Computed tomography (CT) is primarily used for staging and follow-up of testicular tumour metastatic to the retroperitoneum or elsewhere. Magnetic resonance imaging (MRI), because of its high cost and limited availability, is reserved for problem solving of difficult cases. MRI has been shown to be diagnostic and cost effective following equivocal scrotal ultrasound, however,

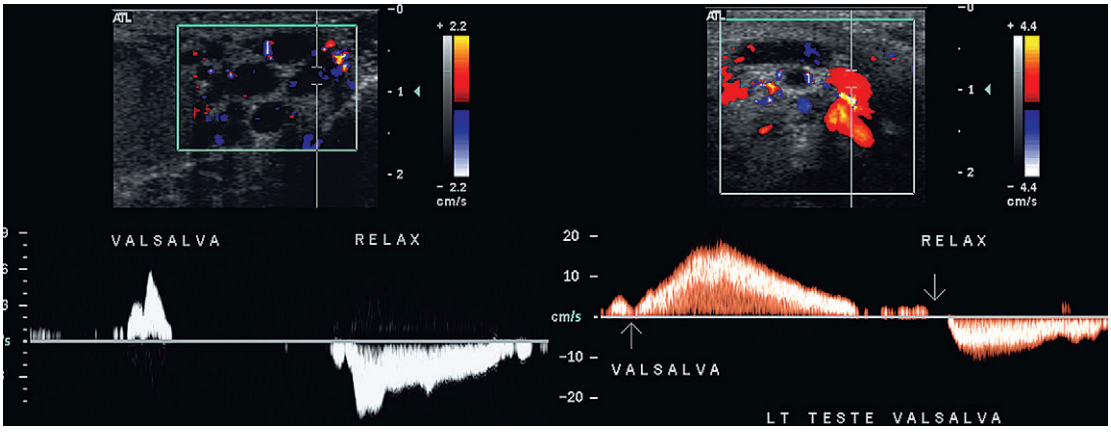


**Fig. 12.32** Spectral Doppler tracings of the left spermatic cord in two patients with a known varicocele. The tracings were obtained as a Valsalva manoeuvre was initiated, maintained, and released. The first patient has a brief reversal of flow at the start of Valsalva; blood below the distal most valve is forced downward, but then because of valve patency, the flow reversal stops. Upon relaxation of the Valsalva, flow surges forward again. The second patient initiates reversal of flow and then maintains persistent flow reversal as renal venous outflow is shunted down the gonadal vein because of the high pressure in the thorax. As pressure builds within the testicle, flow progressively slows until the point of relaxation at which time flow surges forward.

even in an aggressive MRI environment only 1.4% of the scrotal sonograms required the addition of MRI.[65] Currently, other than in select paediatric cases and in the evaluation of cryptorchidism, MRI has not been found to hold significant advantage over ultrasound in the evaluation of the scrotum; but the modality is evolving.[66]

Although scintigraphy continues to be a dependable means of imaging testicular blood flow, it lacks sonography's ability to provide anatomical information, as well as perfusion status, and it exposes the patient to radiation. Therefore, as suggested by Siegel,[15] nuclear scintigraphy should be reserved for those situations when the sensitivity of colour Doppler for low-velocity, low-volume testicular arterial flow is not satisfactory and there are questions regarding the findings (e.g. in the small testicles of prepubescent patients) or when the examiner has limited proficiency with colour Doppler evaluation.

## CONCLUSIONS

The scrotal contents are ideally situated for examination by ultrasound. Their superficial location allows the use of high-frequency transducers and yields very high resolution images of the testes and associated structures. The addition of haemodynamic information by spectral and colour Doppler allows the examiner to make a very specific diagnosis with a high degree of confidence in several very important disease states. Thoughtful fusion of the anatomical and physiological findings will allow many problems to be clarified and managed without the need for further imaging.

## REFERENCES

1. Horstman WG, Middleton WD, Melson GL, et al. Colour Doppler US of the scrotum. Radiographics 1991; 11:941–957.
2. Learner RM, Mevorach RA, Hulbert WC, et al. Colour Doppler US in the evaluation of acute scrotal disease. Radiology 1990; 176:355–358.
3. Luker GD, Siegel MJ. Colour Doppler sonography of the scrotum in children. AJR Am J Roentgenol 1994; 163: 649–655.
4. Luker GD, Siegel MJ. Scrotal US in pediatric patients: comparison of power and standard colour Doppler US. Radiology 1996; 198:381–385.
5. Middleton WD, Siegel BA, Melson GL, et al. Acute scrotal disorders: prospective comparison of colour Doppler US and testicular scintigraphy. Radiology 1990; 177:177–181.
6. Ralls PW, Larsen D, Johnson MB, et al. Colour Doppler sonography of the scrotum. Semin Ultrasound CT MR 1991; 112:109–114.
7. Bannister LH, Dyson M. Reproductive system. In: Williams PL, Bannister LH, Berry MM, et al, eds. Gray's anatomy, 38th edn. New York: Churchill Livingston; 1995:1848–1856.
8. Doherty FJ. Ultrasound of the nonacute scrotum. Semin Ultrasound CT MR 1991; 12:131–156.
9. Middleton WD, Thorne DA, Melson GC. Colour Doppler ultrasound of the normal testis. AJR Am J Roentgenol 1989;152:293–297.
10. Holder LE, Martire JR, Holmes ER, et al. Testicular radionuclide angiography and static imaging: anatomy, scintigraphic interpretation, and clinical indications. Radiology 1977; 125:739–752.
11. Krone KD, Carroll BA. Scrotal ultrasound. Radiol Clin North Am 1985; 23:121–139.
12. Middleton WD. Scrotal sonography in 1991. Ultrasound Q 1991; 9:61–87.
13. Petros JA, Andriole GL, Middleton WD, et al. Correlation of testicular colour Doppler ultrasonography, physical examination and venography in the detection of varicoceles in men with infertility. J Urol 1991; 145:785–788.
14. Giorgio G. Cardiovascular (inferior vena cava). In: Williams PL, Bannister LH, Berry MM, et al, eds. Gray's anatomy, 38th edn. New York: Churchill Livingston; 1995:1600–1601.
15. Siegel MJ. The acute scrotum. Radiol Clin North Am 1997; 35:959–976.
16. Siegel MJ. Male pelvis. In: Siegel MJ,ed. Pediatric sonography, 2nd edn. New York: Raven Press; 1995:479–512.
17. Paltiel HJ, Rupich RC, Babcock DS. Maturational changes in arterial impedance of the normal testis in boys: Doppler sonographic study. AJR Am J Roentgenol 1994; 163:1189–1193.
18. Jequier S, Patriquin H, Filiatrault D, et al. Duplex Doppler sonographic examination of the testis in

prepubertal boys. J Ultrasound Med 1993; 12:317–322.
19. Hermansen MC, Chusid MJ, Sty JR. Bacterial epididymo-orchitis in children and adolescents. Clin Pediatr 1980; 19:812–815.
20. Basekim CC, Kizilkaya E, Pekkafali Z, et al. Mumps epididymo-orchitis: sonography and colour Doppler sonographic findings. Abdom Imaging 2000; 25:322–325.
21. Horstman WG, Middleton WD, Nelson GL. Scrotal inflammatory disease: colour Doppler US findings. Radiology 1991; 179:55–59.
22. Cook JL, Dewbury K. The changes seen on high-resolution ultrasound in orchitis. Clin Radiol 2000; 55:13–18.
23. Burks DD, Markey BJ, Burkhard TK, et al. Suspected testicular torsion and ischaemia: evaluation with colour Doppler sonography. Radiology 1990; 175:815–821.
24. Farriol VG, Comella XP, Agromayor EG, et al. Gray-scale and power Doppler sonographic appearances of acute inflammatory diseases of the scrotum. J Clin Ultrasound 2000; 28:67–72.
25. Sanders LM, Haber S, Dembner A, et al. Significance of reversal of diastolic flow in the acute scrotum. J Ultrasound Med 1994; 13:137–139.
26. Backhouse K. Embryology of testicular descent and maldescent. Urol Clin North Am 1982; 9:315–325.
27. Zerin J, DiPietro M, Grignon A, et al. Testicular infarction in the newborn: ultrasound findings. Pediatr Radiol 1990; 20:329–330.
28. Dubinsky TJ, Chen P, Maklad N. Colour-flow and power Doppler imaging of the testes. World J Urol 1998; 16:35–40.
29. Meza MP, Amundson GM, Aquilina JW, et al. Colour flow imaging in children with clinically suspected testicular torsion. Pediatr Radiol 1992; 22:370–373.
30. Middleton WD, Melson GL. Testicular ischemia: colour Doppler sonographic findings in five patients. AJR Am J Roentgenol 1989; 152:1237–1239.
31. Patriquin HB, Yazbeck S, Trinh B, et al. Testicular torsion in infants and children: diagnosis with Doppler sonography. Radiology 1993; 188:781–785.
32. Leahy PF. Diagnosis of testicular torsion using Doppler ultrasonic examination. Br J Urol 1986; 58:696–697.
33. Dogra VS, Sessions A, Mevorach A, et al. Reversal of diastolic plateau in partial testicular torsion. J Clin Ultrasound 2001; 29:105–108.
34. Brown JM, Taylor KJW, Alderman JL, et al. Contrast-enhanced ultrasonographic visualization of gonadal torsion. J Ultrasound Med 1997; 16:309–316.
35. Coley BD, Frush DP, Babcock DS, et al. Acute testicular torsion: comparison of unenhanced and contrast-enhanced power Doppler US, colour Doppler US, and radionuclide imaging. Radiology 1996; 199:441–446.
36. Middleton WD, Middleton MA, Dierks M, et al. Sonographic prediction of viability in testicular torsion: preliminary observations. J Ultrasound Med 1997; 16:23–27.
37. Cass AS, Luxenberg M. Testicular injuries. Urology 1991; 37:528–530.
38. Jeffrey RB, Laing FC, Hricak H, et al. Sonography of testicular trauma. AJR Am J Roentgenol 1983; 141:993–995.
39. Geraghty MJ, Lee FT, Jr, Bernsten SA, et al. Sonography of testicular tumors and tumor-like conditions: a radiologic-pathologic correlation. Crit Rev Diagn Imaging 1998; 39:1–63.
40. Ulbright TM, Roth LM. Testicular and paratesticular tumors. In: Sternberg SS, eds. Diagnostic surgical pathology, 3rd edn. Philadelphia: Saunders; 1999:1973–2033.
41. Horstman WG, Melson GL, Middleton WD, et al. Testicular tumors: findings with color Doppler US. Radiology 1992; 185:733–737.
42. Mostofi FK. Tumors of the testis. IARC Sci Pub 1994; 111:407–429.
43. Cotran RS, Kumar P, Collins T. The male genital tract. In: Robbins SL, ed. Pathologic basis of disease, 6th edn. Philadelphia: Saunders; 1999:1011–1034.
44. Kurman RJ, Scardino PT, McIntire KR, et al. Cellular localization of alpha-fetoprotein and human chorionic gonadotropin in germ cell tumours of the testis using an indirect immunoperoxidase technique (a new approach to classification utilizing tumor markers). Cancer 1977; 40:2136–2151.
45. Woodward PJ, Sohaey R, O'Donoghue MJ, et al. Tumours and tumour like lesions of the testis: radiologic-pathologic correlation. Radiographics 2002; 22:189–216.
46. Muir CS, Nectoux J. Epidemiology of cancer of the testis and penis. Nat Cancer Inst Monogram 1979; 53:157–164.
47. Carroll BA, Gross DM. High frequency scrotal sonography. AJR Am J Roentgenol 1983; 140:511–515.
48. Mostofi FK. Testicular tumours: epidemiologic, etiologic and pathologic features. Cancer 1973; 32:1186–1201.
49. Terhine DW, Manson AL, Jordon GH, et al. Pure primary testicular carcinoid: a case report and discussion. J Urol 1988; 4: 255–256.
50. Zavala-Pompa A, Ro JY, El-Naggar A, et al. Primary carcinoid tumor of testis. Immunohistochemical, ultrastructural, and DNA flow cytometric study of three cases with a review of the literature. Cancer 1993; 72: 1726–1732.
51. Kim BH Scrotum. In: Kim SH, ed. Radiology illustrated: uroradiology. Philadelphia: WB Saunders; 2003:625–664.

52. Patriquin HB. Leukemic infiltration of the testis. In: Siegel BA, Proto AV, eds. Pediatric disease, 4th series. Test and syllabus. Reston: Am Coll Radiol; 1993:667–688.
53. Mazzu D, Jeffrey RB, Ralls PW. Lymphoma and leukemia involving the testicles: findings on gray-scale and colour Doppler sonography. AJR Am J Roentgenol 1995; 164:645–647.
54. Luker GD, Siegel MJ. Pediatric testicular tumors: evaluation with gray-scale and colour Doppler US. Radiology 1994; 191:561–564.
55. Dogra VS, Gottlieb RH, Rubens DJ, et al. Benign intratesticular cystic lesions: US features. Radiographics 2001; 21(spec no.):S273–S281.
56. Seidenwurm D, Smathers R, Kan P, et al. Intratesticular adrenal rests diagnosed by US. Radiology 1985; 155:479–481.
57. Dogra VS, Gottlieb RH, Oka M, et al. Sonography of the scrotum. Radiology 2003; 227:18–36.
58. Proto G, DiDonna A, Grimaldi F, et al. Bilateral testicular adrenal rest tissue in congenital adrenal hyperplasia: US and MR features. J Endocrinol Invest 2001; 24:529–531.
59. Avila NA, Premkumar A, Shawker TH, et al. Testicular adrenal rest tissue in congenital adrenal hyperplasia: findings at gray-scale and colour Doppler US. Radiology 1996; 198:99–104.
60. Rutgers JL, Young RH, Scully RE. The testicular 'tumor' of the adrenogenital syndrome. A report of six cases and review of the literature on testicular masses in patients with adrenocortical disorders. Am J Surg Pathol 1988; 12(7):503–513.
61. Stikkelbroeck NM, Otten BJ, Pasic A, et al. High prevalence of testicular adrenal rest tumors, impaired spermatogenesis, and Leydig cell failure in adolescent and adult males with congenital adrenal hyperplasia. J Clin Endocrinol Metab 2001; 86:5721–5728.
62. Meacham RB, Townsend RR, Rademacher D, et al. The incidence of varicoceles in the general population when evaluated by physical examination, gray scale sonography and colour Doppler sonography. J Urol 1994; 151:1535–1538.
63. Pierik FH, Dohle GR, van Muiswinkel JM, et al. Is routine scrotal ultrasound advantageous in infertile men? J Urol 1999; 162:1618–1620.
64. Dambro TJ, Stewart RR, Barbara CA. The scrotum. In: Rumack CM, Wilson SR, Charboneau JW, eds. Diagnostic ultrasound, 2nd edn. St Louis: Mosby; 1998:791–821.
65. Serra AD, Hricak H, Coakley FV, et al. Inconclusive clinical and ultrasound evaluation of the scrotum: impact of magnetic resonance imaging on patient management and cost. Urology 1998; 51:1018–1021.
66. Choyke PL. Dynamic contrast-enhanced MR imaging of the scrotum: reality check (editorial). Radiology 2000; 217:14–15.

# Doppler ultrasound of the female pelvis

# 13

Paul A. Dubbins

Ultrasound has assumed a central role in the investigation of gynaecological physiology and pathology. The advent of transvaginal probes has further advanced gynaecological applications to the extent that it is now an indispensable tool in the evaluation of the female pelvis. Ultrasound predominantly assesses structure, although physiological changes can be inferred, for example by sequential ultrasound examinations such as change in the size and the appearance of an ovarian follicle over time, and the pattern of thickening of the endometrium.

The application of Doppler techniques allows the demonstration of changes in perfusion of the uterus and ovaries at different phases of the menstrual cycle. Abnormalities of perfusion indices have been shown also to reflect features of subfertility. Similarly there are marked vascular changes known to take place in pathological conditions. For example, neovascularity is an early and persistent feature of tumour growth with the development of random and chaotic vessels, lack of hierarchical branching, focal calibre variations and blind ending lakes. If documentation of angiogenesis by Doppler techniques was achievable, this might be of value in differentiation of benign from malignant tumours.

More recently it has been suggested that quantification of organ flow may be best achieved using quantitative three-dimensional colour power Doppler. This technique however requires proprietary software which is not yet widely available.

The indications for Doppler ultrasound in the evaluation of pelvic physiology and pathology in the female are therefore potentially large. Many pathologies will produce increased blood flow to the pelvic organs, and hitherto our methods of discriminating between the uncontrolled and irregular angiogenesis of malignant tumour and the angiogenesis associated with benign tumour, or even the hyperaemia of inflammatory conditions, have been insufficiently sophisticated to make a reliable distinction. This chapter presents the current state of knowledge for potential applications of Doppler ultrasound in gynaecological disease, while indicating those areas where the role of Doppler ultrasound is established and considering these in more detail.

## ANATOMY

Knowledge of the course of the pelvic vessels is important for the proper performance and interpretation of the Doppler examination. Although the attention is drawn to the examination of the ovarian and uterine arteries, the anatomical relations of the pelvic organs to the iliac arteries and veins is also important. Pathological conditions affecting the major vessels in the pelvis may complicate uterine or ovarian pathology, such as iliac venous thrombosis, or may mimic gynaecological pathology, such as an iliac artery aneurysm.

The iliac arteries and veins course inferiorly and laterally from the aortic bifurcation and venous confluence respectively on the anteromedial surface of the psoas muscle, to become the femoral artery and vein as they emerge beneath the inguinal ligament in the groin. Surface markings for the common and external iliac artery and vein are approximated by a line drawn from the umbilicus to the site of maximum pulsation in the groin.

The common and external iliac veins lie medial and posterior to the artery. The vessels often form a lateral anatomical relationship to the ovary (Fig. 13.1). The internal iliac artery arises from the medial aspect of the common iliac artery along with the vein approximately 4 cm from the aortic bifurcation. It gives rise to two branches, an anterior and a posterior trunk. At this point, just distal to the bifurcation, the anterior trunk lies posterior to the ureter and to the ovaries. The anterior trunk has several branches, one of which is the uterine artery which runs medially on the surface of the levator ani muscles, crossing above the ureter and ascending in a tortuous fashion lateral to the uterus, giving off uterine branches. It is accompanied through its course by the uterine vein.

The ovary has a dual arterial blood supply. This has assumed greater importance with the advent of minimally invasive procedures for the treatment of gynaecological pathology, for example fibroid embolisation.

The ovarian artery is a branch of the renal artery on the left, although on the right it may arise from the aorta. Throughout its course in the abdomen it lies medial and posterior to the ureter, crossing the external iliac artery and vein to enter the true pelvis, where it turns medially in the ovarian suspensory ligament, passing into the broad ligament where its terminal branches supply the ovary and anastomose with adnexal branches of the uterine artery. The left ovarian vein drains in to the left renal vein and the right into the inferior vena cava. The integrity of venous return is maintained by venous valves within the upper vessel and if these valves become compromised, venous congestion within the pelvis may occur.

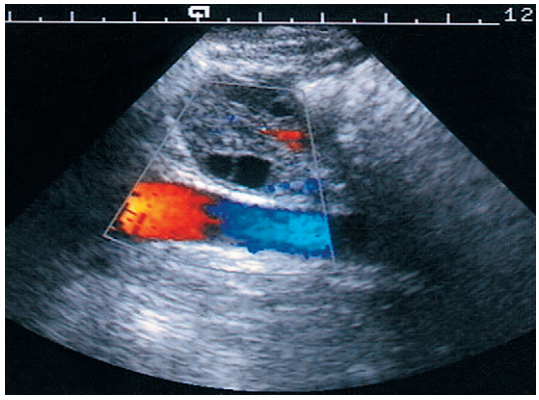


**Fig. 13.1** Colour flow Doppler study of the left iliac fossa using compression. The left ovary is demonstrated anterior to the external iliac artery. There is a small amount of intraparenchymal flow within the ovary. The apparent bidirectional flow within the iliac artery is related to the geometry with the proximal iliac artery, indicating flow towards the transducer while the distal artery shows flow away from the transducer.

## TECHNIQUE

The examination of the pelvic vessels has been significantly altered by the transvaginal technique of evaluation of pelvic anatomy and pathology. The course of the uterine artery is particularly suitable for transvaginal assessment, with ideal geometry for Doppler signal recording (Fig. 13.2). Similarly, however, it is possible to record Doppler signals transabdominally with an empty bladder, when the uterus is normally anteverted, for similar reasons of geometry. When the bladder is full, however, the angle of incidence of the Doppler beam to the uterine arteries is not optimised in spite of good visualisation of the body of the uterus (Figs 13.3 and 13.4). The ovarian arteries, running a somewhat transverse course through the pelvis, are more difficult to assess, although greater sensitivity of signal recording is almost invariably achieved with transvaginal scanning.

Demonstration of the spiral arteries within the uterus and intraovarian vessels requires colour flow or power Doppler for their identification. It is difficult to be prescriptive about colour flow settings but the following generalisations apply.

### Filtration

The lowest possible filtration is needed, particularly when investigating pelvic venous disease and conditions affecting 'perfusion' of tissues.

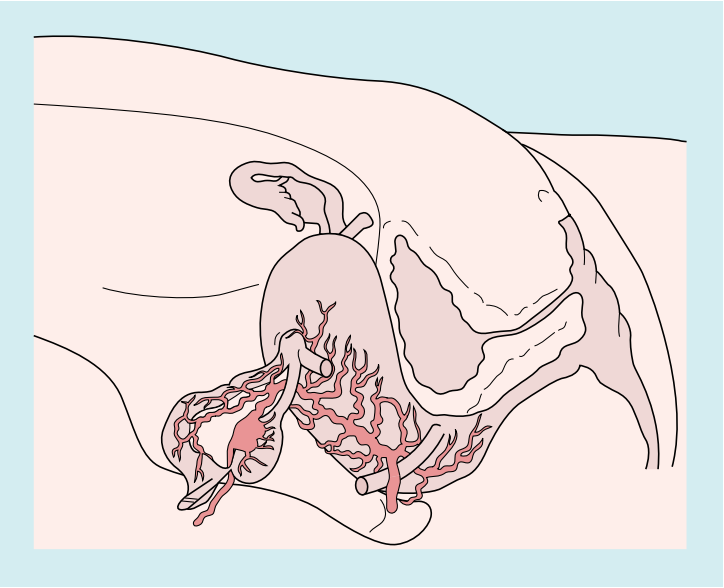

**Fig. 13.2** Uterine and ovarian artery distribution. The uterine artery is a branch of the internal iliac artery and ascends on the lateral border of the uterus. It sends branches to the ovary and to the fallopian tube. The ovary is also supplied by the ovarian artery, a branch usually of the renal artery.

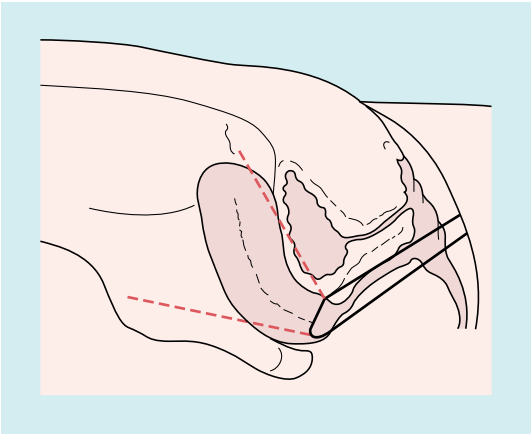

**Fig. 13.3** Sagittal sections through the pelvis demonstrating the optimum geometry achieved by a transvaginal scan with an empty bladder.

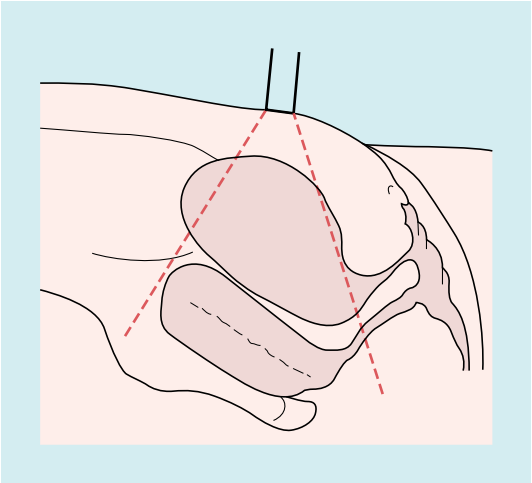

**Fig. 13.4** Sagittal planes through the abdomen demonstrating that with a full urinary bladder the geometry for Doppler assessment of blood flow is suboptimal.

## Colour/B-mode priority

For the most part small vessels are being investigated and it is less critical to exclude 'colour bleed' out with the wall of the vessel; high colour priority should therefore be selected.

## Persistence

A moderate persistence setting should be selected.

## Velocity range

Selection of velocity range depends upon whether arteries or veins are being interrogated. Arterial flow within the uterine and ovarian arteries is usually within the range of 10–50 cm $s^{-1}$ peak systolic velocity, although this may be lower, particularly in postmenopausal ovarian vessels.

Flow velocity in pelvic veins is in the region of 1–10 cm $s^{-1}$. Velocity range settings should be chosen to reflect these predicted velocities.

## Motion artefact

Most machines now have specific algorithms to reduce motion artefact and these should be employed.

## Spectral Doppler settings

These reflect the colour Doppler settings but the need to use low filtration is particularly important in order to detect slow flow in veins and diastolic flow in arteries.

## Angle of insonation

As with all Doppler applications, it is important to optimise the angle of insonation of the Doppler beam on the vessel but this may be compromised by the direction of flow and the limitations that transducer position, both abdominally and intravaginally; provide for variation of this angle. Where possible angles of less than 60° should be employed, although this is less important if velocities are not being measured. Although Doppler indices such as the resistance index and the pulsatility index are widely used in gynaecology and are angle independent, these are often supplemented in clinical applications by measurements of peak systolic velocity, which will require stringent attention to angle optimisation and correction.

## Sample volume

The vessels under study are small and therefore sample volume size should be at a minimum.

## Volume flow quantification

Using proprietary software it is possible to identify a region of interest in colour power mode. On or off line assessment of vessel distribution and power values allow the development of numerical 'perfusion' indices. This may be of value in evaluation of, for example ovarian masses given that malignant lesions contain vessels of larger size and greater density than benign masses.

Three-dimensional (3D) quantification (including 3D power Doppler) is not yet widely available but may allow the semiquantitative assessment of blood flow. Volume acquisition is undertaken after careful selection of the colour power box to enclose only the region of interest (the entire ovary, the follicle, the mass) and the volume mode sweep activated while maintaining the position of the probe entirely stable. Storage of the 3D data is then subsequently analysed. Proprietary software will calculate morphological features such as volume and echogenicity and the number of colour voxels in the region of interest. Derived indices include: the vascularisation index (VI) – the number of colour voxels in the region of interest (ROI); flow index – the mean colour value in the voxels; vascularisation flow index (VFI) – the mean colour value in all the voxels within the sphere. Although there is evidence of different patterns for the dominant follicle and for the right and left ovaries there is currently insufficient work to establish normal features to afford clearly defined clinical applications for this technique.[1]

## Technique for evaluating pathology

It is important when assessing pelvic pathology with Doppler techniques that optimum signal-recording methods are used. Evaluation of vessels is straightforward but in the demonstration of mass lesions, inflammatory processes, etc., careful attention to technique will ensure that the vascular supply is accurately mapped and Doppler spectra precisely recorded.

When a suspected pathological process is identified on real-time ultrasound, it is assessed with colour Doppler. Flexibility of the use of the colour box is important: initially for small- to moderate-sized lesions the whole lesion can be contained within the colour box in order to identify regions of increased vascularity, but this large field of view compromises the frame rate and pulse repetition rate, affecting the detection of high velocities and potentially also pulsatile flow. Therefore a smaller colour box is then selected and individual zones within the lesion are interrogated sequentially. Attention is paid to the size, distribution and communications of the vessels together with the vessels of supply and drainage.

Throughout the procedure the machine settings are varied to optimise the system for very high and very low velocities. Sampling with spectral Doppler is performed at multiple sites, as some vessels may demonstrate apparently normal flow patterns, while others will demonstrate abnormal flow patterns and Doppler indices. Failure to record signals in this obsessive way will result in a lower accuracy of the technique.

Selection of the ROI for quantification requires similar attention to technique with the potential for interobserver variation. Drawing the ROI is currently largely achieved using a freehand technique. Standardisation of the technique, agreement between operators in respect to what is included in the ROI (exclusion for example of cystic areas) will ensure that the pixel intensity is reproducible.

Ultrasound contrast media will enhance the signal in all vessels including those to the pelvic organs. This has the potential to improve the visualisation of a wide variety of pelvic pathology, but it is not yet established whether this will improve the differentiation of different pathologies and no distinct application has been identified.[2]

## NORMAL APPEARANCES

Colour flow Doppler will demonstrate the uterine arteries coursing along the lateral aspects of the body of the uterus (Fig. 13.5). The branches of the uterine artery extending towards the ovary and the ovarian artery can be identified in the broad ligament and on the superior aspect of the ovary, respectively. Because of their tortuosity, only short segments of the arteries are usually identified in any particular scan plane (Fig. 13.6).

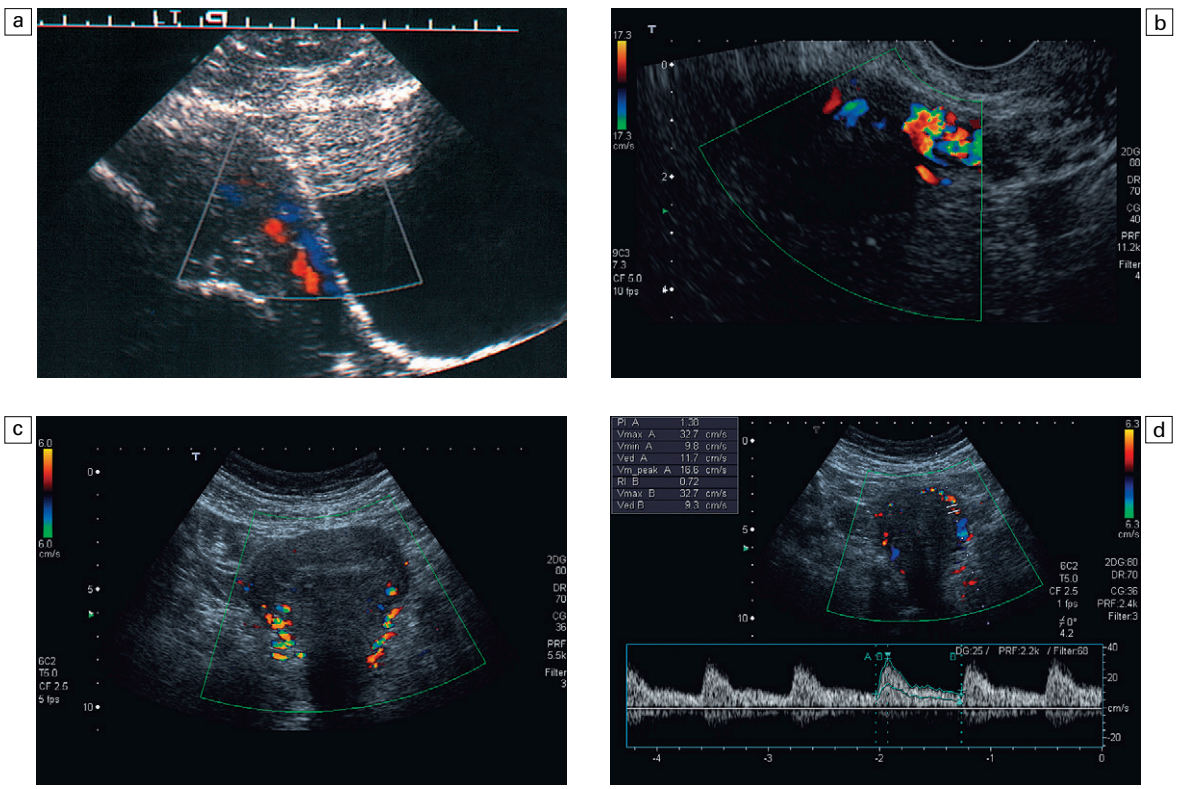


**Fig. 13.5** (a) Sagittal transabdominal scan along the left margin of the uterus demonstrating the uterine artery and vein. (b) Sagittal transvaginal scan along the margin of the uterus demonstrating the uterine vessels. (c) Coronal transabdominal scan demonstrating uterine arteries. (d) Spectral Doppler from uterine artery demonstrating automatic calculation of indices.

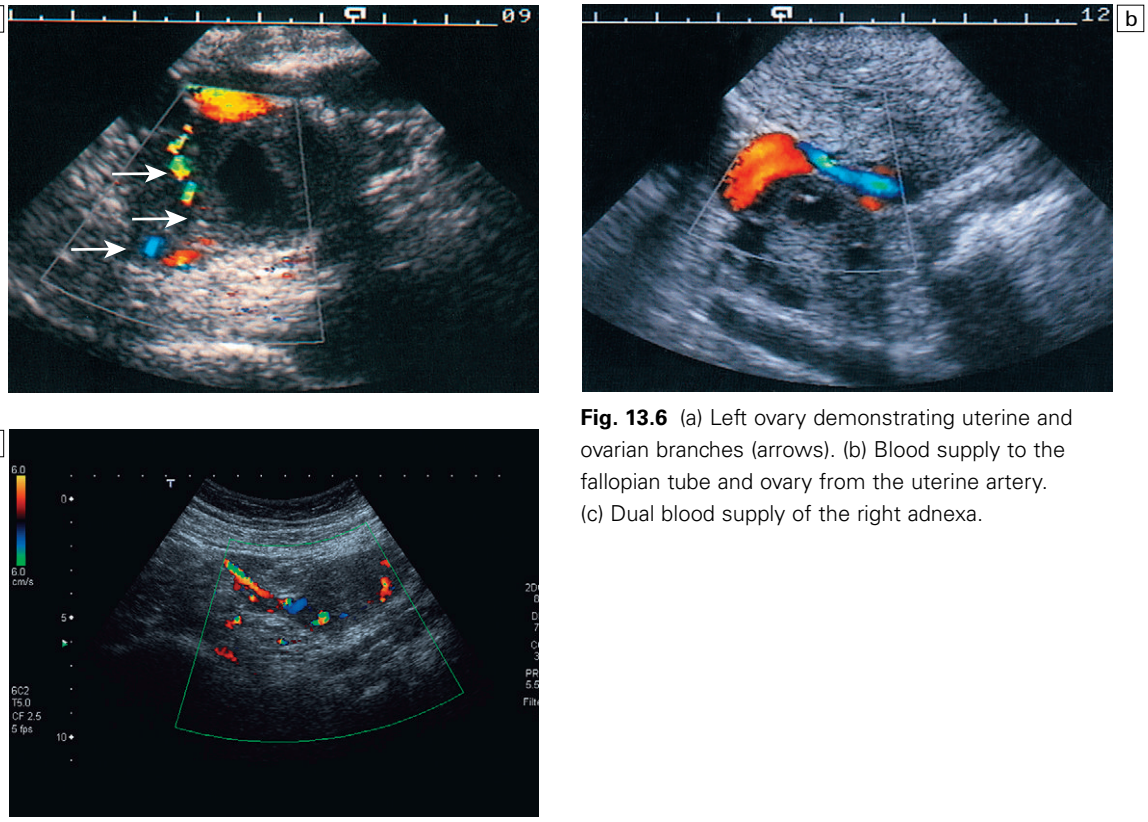


**Fig. 13.6** (a) Left ovary demonstrating uterine and ovarian branches (arrows). (b) Blood supply to the fallopian tube and ovary from the uterine artery. (c) Dual blood supply of the right adnexa.

Colour flow and power Doppler will demonstrate perfusion within the uterus and the ovaries. In the uterus the spiral arteries are arranged perpendicular to the long axis and can be demonstrated extending from the serosal surface of the uterus to the endometrium. No colour flow signal is routinely demonstrated in the normal endometrium or in the subendometrial layer. However recent improvements in colour and particularly colour power sensitivity now allow the documentation of colour power signals within the normal endometrium and subendometrial layer. 3D power Doppler angiography affords the semiquantitative assessment of flow by means of the indices described above. Early reports suggest that the VI and VFI increase in the proliferative phase reaching a peak 3 days prior to ovulation subsequently decreasing to a nadir 5 days following ovulation[3].

The colour flow appearance of the normal ovary depends upon the phase of the cycle and the age of the patient. The normal development of the ovarian follicle is accompanied by a marked change in the vascular pattern which reflects the influence of vascular endothelial growth factor on the corpus luteum. A relatively oligaemic follicle develops may exhibit circumferential flow. However with the development of the corpus luteum a rich vascular wreath is seen supplied by a helical artery. The vascularisation becomes more extensive as vessels invade the central haemorrhagic zone (Fig. 13.7).

## Pelvic veins

Normal venous structures can be seen within the body of the uterus and in both adnexa coursing towards the ovarian vein and the uterine veins.

## Normal Doppler spectra

Normal Doppler spectra vary throughout the menstrual cycle. This variation is particularly

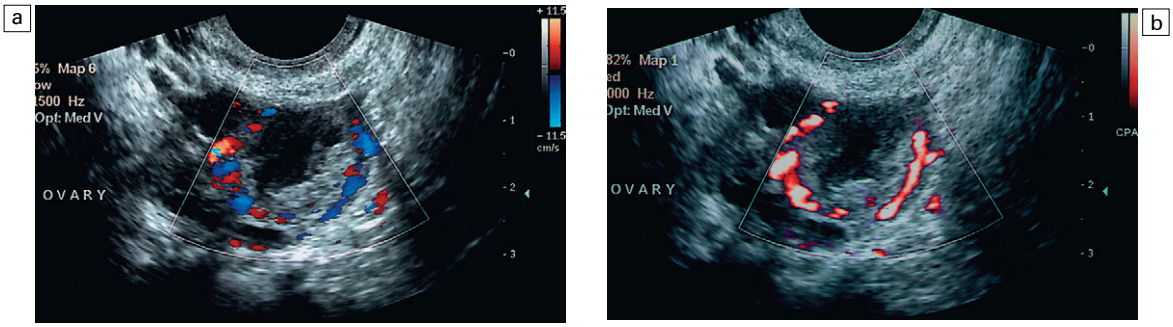


**Fig 13.7** (a) Colour flow Doppler of circumferential flow in corpus luteum. (b) Power Doppler of the corpus luteum.

marked in the ovarian artery which demonstrates a low-resistance pattern at the time of the development of the corpus luteum. However, there is wide variation in reported normal values of stromal ovarian and ovarian artery flow. Typically the resistance index in the early follicular phase is in the region of 0.65–0.7, falling to 0.55–0.6 in the late follicular phase and returning to early follicular phase values in the early luteal phase. However, published normal values range between 0.4 and 0.8 and pulsatility index values vary from 0.6 to 2.5. Similar values for ovarian vascular indices have also been recorded in postmenopausal ovaries but the cyclical variation is lost.[4] Thus an individual measurement of ovarian artery impedance is of limited value in assessment of ovarian function, although the cyclical change of ovarian flow does correlate with development of the corpus luteum.

Cyclical variation in uterine artery flow is well defined and also appears to correlate with fertility; normal values are given in Table 13.1.There is an increase in volume flow and a reduction in resistance index in the luteal phase when compared to the follicular phase. Again, therefore, it appears that cyclical variation is more important in the assessment of normal reproductive physiology, rather than using individual values.[5,6] Normal Doppler spectra are illustrated in Figures 13.8–13.11.

Blood flow to the prepubertal uterus demonstrates a similar pattern to the postmenopausal status with high impedance and absent diastolic flow. Change to the adult pattern of lower indices and forward flow throughout diastole heralds the onset of the menarche.

Pelvic venous diameter is extremely variable but pelvic veins are normally less than 5 mm in diameter and flow velocities between 5 and 10 cm $s^{-1}$. In this author's experience, reverse flow on Valsalva is short lived and of low velocity (<2 cm $s^{-1}$).

**Table 13.1** Variation in Doppler indices in the uterine and ovarian arteries in the menstrual cycle

| | RI OVA[a] | PI OVA[a] | VEL OVA[a] (cm $s^{-1}$) | PI UTA[a] |
|---|---|---|---|---|
| Early follicular | 0.65–0.7 | 1.8–2.2 | 20 | 1.67 ± 0.22 |
| Late follicular/ovulation | 0.55–0.6 | 1.0–1.3 | 40 | 1.89 ± 0.4 |
| Luteal | 0.6–0.65 | 1.3–1.8 | | 2.23 ± 0.67 |
| Non-conception | 0.6–0.7 | 1.8–2.2 | | 3.85 ± 1.1 |
| Postmenopausal | 0.6–1.0 | 1.3–4.0 | | 1.8–3.8 |

[a]RI = resistance index; PI = pulsatility index; OVA = ovarian artery; VEL = velocity; UTA = uterine artery.

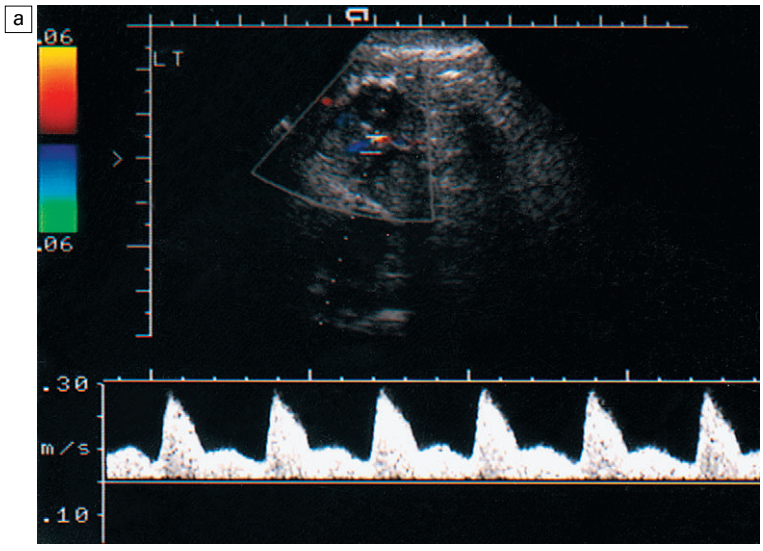


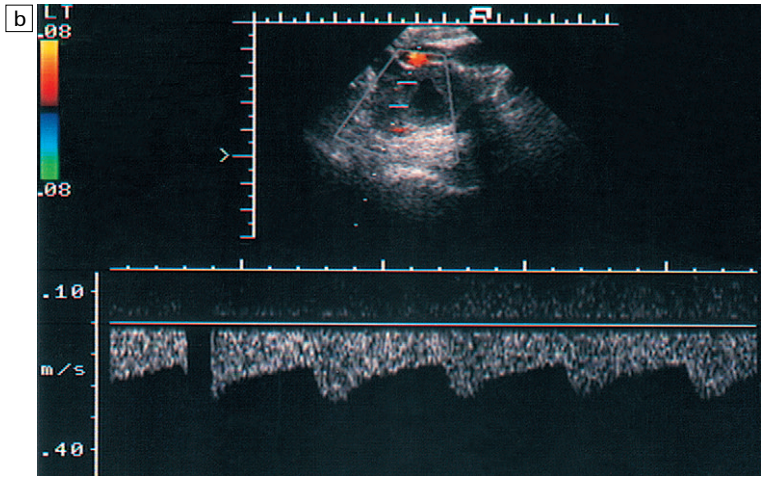


**Fig. 13.8** (a) Doppler spectrum of ovarian blood flow within the follicular phase. (b) Low-resistance blood flow at the time of ovulation.

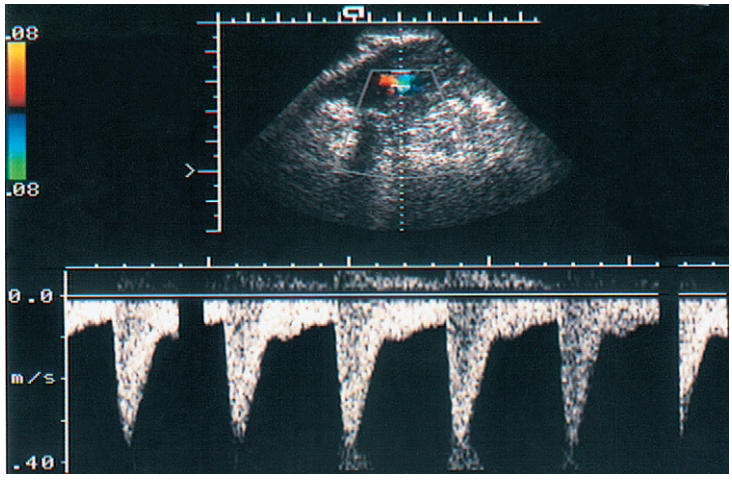


**Fig. 13.9** Doppler spectrum of normal uterine artery blood flow in the late follicular phase.

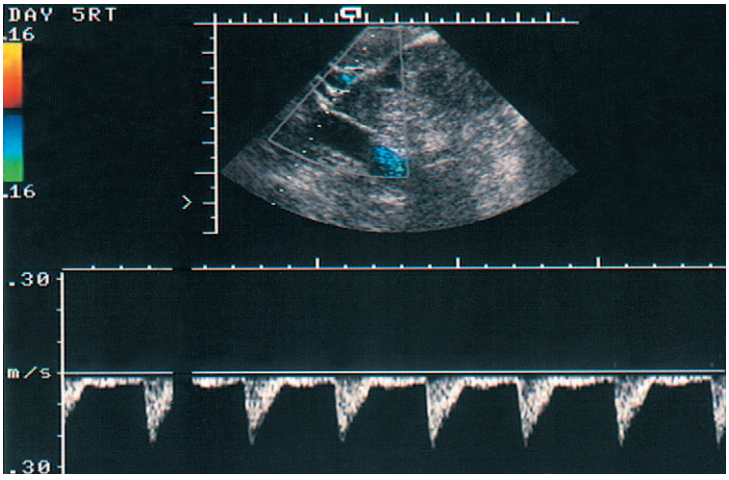


**Fig. 13.10** Doppler spectrum of uterine artery blood flow in the luteal phase.

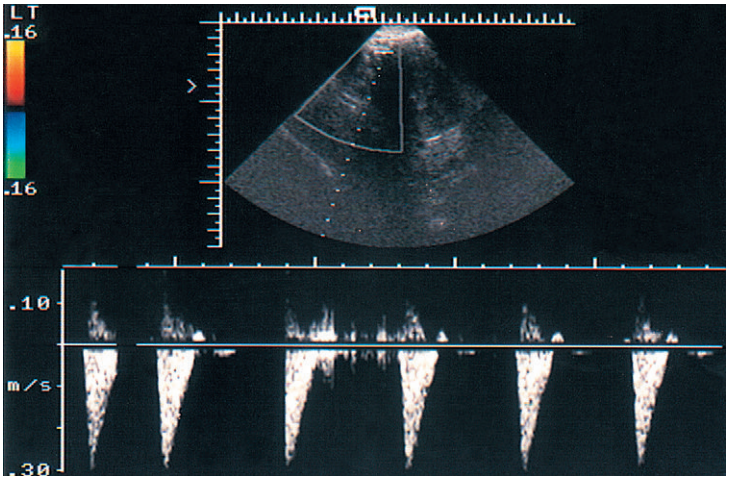


**Fig. 13.11** Doppler spectrum of uterine artery blood flow in the postmenopausal uterus.

## ERRORS AND ARTEFACTS[7]

There are a number of factors which will contribute to alterations in flow and which are not related to pelvic pathology. These are common to all vessels and include the following.

### Hypertension

Indices will be uniformly slightly increased.

### Abnormalities of heart rate and rhythm

Both pulsatility and resistance indices will be decreased in tachycardias and increased in bradycardias. Irregularities such as atrial fibrillation will invalidate the use of any of the Doppler indices.

### Sample volume artefacts

Because of the small size of many of the vessels under study, maintenance of the position of the sample volume within the centre of the vessel is frequently difficult. This has the effect that there may be inaccurate recording of either systolic or diastolic flow velocities, dependent upon vessel movement relative to the sample volume throughout the cardiac cycle. This produces variation in the appearance of the Doppler spectrum and variation in the Doppler indices.

Bowel movement may provide significant imaging artefact, but although this may compromise Doppler signal recording, it is not usually confused for normal or abnormal blood flow patterns.

Bladder distension also has an effect on Doppler spectra, producing a significant increase in the impedance indices compared to the empty bladder.[8]

### Twinkling artefact

The use of colour and power Doppler may produce colour signals even in the absence of flow. This may occur as a consequence of 'over-gain' especially where there is acoustic enhancement such as occurs through a cyst and also may be consequent of motion within adjacent bowel. The twinkling artefact is a feature usually of focal calcification or the reverberation that may be seen in tiny cysts. This is a typical feature of the 'microscopic' echogenicities seen in normal ovaries and those with endometriosis[9] (Fig. 13.12).

## APPLICATIONS

### Menstrual disorders

The use of Doppler techniques to presage puberty has already been described. Similarly in girls with features of precocious puberty the presence of a mature pattern pulsatility index correlates with those patients who exhibit a pubertal response to growth hormone-releasing hormone (GRH).[10]

Women with primary dysmenorrhea have elevated Doppler indices suggesting that this is a more complex condition of the menstrual cycle than had hitherto been suggested.

In menorrhagia there is evidence of reduced pulsatility index values within the uterine arteries. These indices increase with successful treatment for example with danazol.[11,12]

### Fertility

The cyclic changes of blood flow characteristics and Doppler indices within the uterine and ovarian arteries suggest a possible application in the diagnosis and management of subfertility.[13] However there is lack of consensus on the value of flow indices in predicting pregnancy outcome. While some authors have reported differences between groups for example a higher mean pulsatility index in the uterine and ovarian arteries of infertile women in the mid-luteal phase than that in fertile women others have found no uniform relationship. Furthermore there is no confirmed relationship between uterine pulsatility index, subendometrial peak systolic velocity or endometrial thickness and successful pregnancy[14,15] (Fig.13.13). Jarvela et al[16] have suggested that ovarian peak systolic velocity correlates with oocyte recovery development potential of the oocyte and pregnancy rate others have found no such correlation.[17] Ovarian volume appears to be related to ovarian reserve and it may be that 3D depiction of perfusion patterns will be more sensitive than an evaluation of indices and will allow the development of a vascularisation index which correlates with successful pregnancy. Yang et al have suggested that the same may be true for the evaluation of subendometrial vascularity.[18] It is interesting however to note that the changes in flow associated with infertility are seen not only in primary ovarian failure but also in tubal blockage although the cause of this phenomenon is not clear.[5]

An elevated uterine artery pulsatility index is also seen in patients with polycystic ovarian syndrome, although the ovarian artery pulsatility

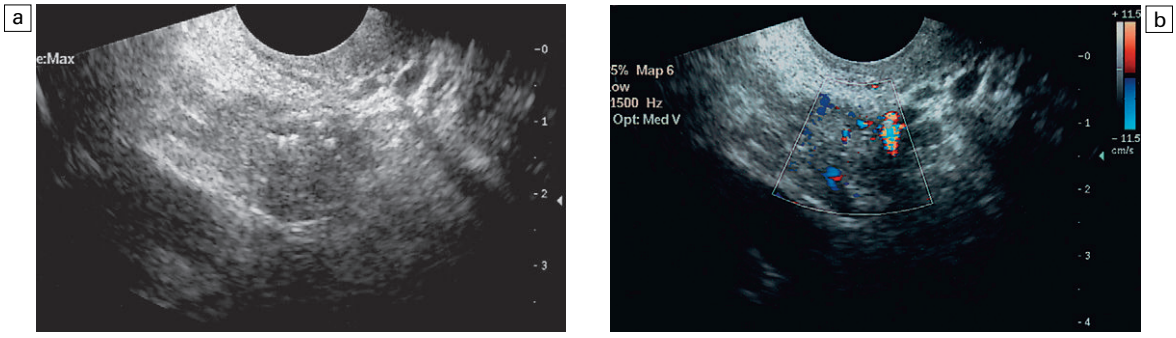


**Fig. 13.12** Twinkling artefact secondary to 'microcalcification' in the ovary: (a) grey-scale; (b) colour flow.

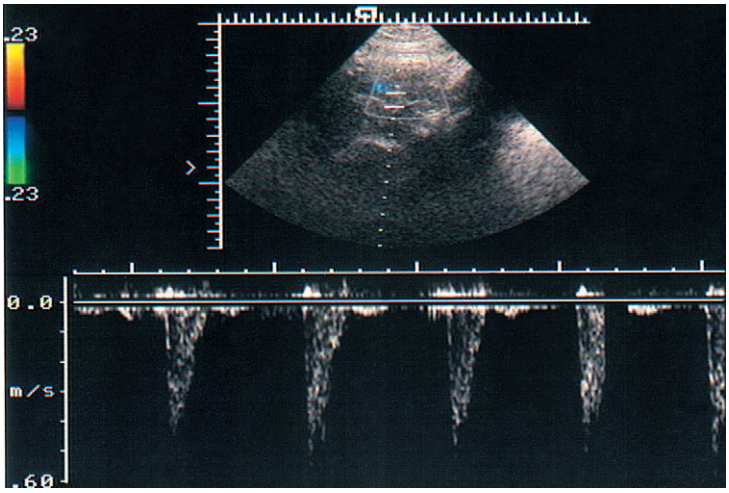


**Fig. 13.13** Doppler spectrum of uterine artery blood flow in infertility.

index is variable although there appears to be an increase in peak systolic velocity in the stroma. In spite of these limitations a high vascular resistance in the uterine artery and ovarian artery in the luteal phase indicates a poor 'baby take-home rate'.

In summary, the role of ultrasound in the investigation and management of infertility is complex. It may be helpful in identifying patients for different treatment regimens but has failed to fulfil the promise of a precise method of assessing uterine receptivity. The role of 3D Doppler in the assessment of vessel density, distribution and flow velocity remains to be established. The best predictor for outcome may be a combination of ovarian morphology and blood flow distribution rather than simple indices although there may be a role for 3D power Doppler.[19]

## Diseases of the uterine body

### *Fibroids*

The vascularity of fibroids is variable. In some patients blood flow to the uterus yields normal resistance and pulsatility indices with uterine vessels simply being displaced around the fibroids. In other cases, the fibroids may demonstrate marked vascularity with increased number and size of uterine vessels (Figs 13.14–13.17) together with a significant reduction in peripheral resistance to blood flow evidenced by reduction in pulsatility and resistance indices below 0.8 and 2.0, respectively. Indeed Wiener et al[20] indicate that the lowest impedance indices of all the uterine pathologies are recorded in uterine fibroids. If the fibroid attenuates sound significantly then it may be impossible to assess blood flow. In cases where it is difficult to

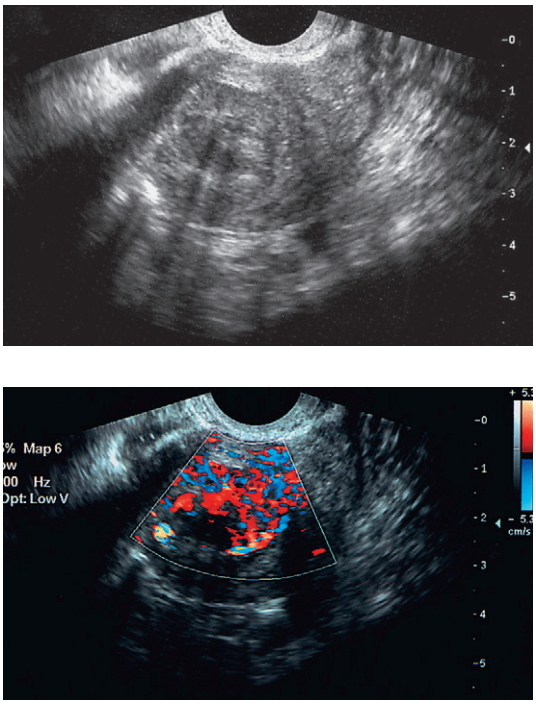


**Fig. 13.14** Submucous fibroid: (a) grey-scale image demonstrates typical fibroid pattern; (b) diffuse colour flow throughout the fibroid.

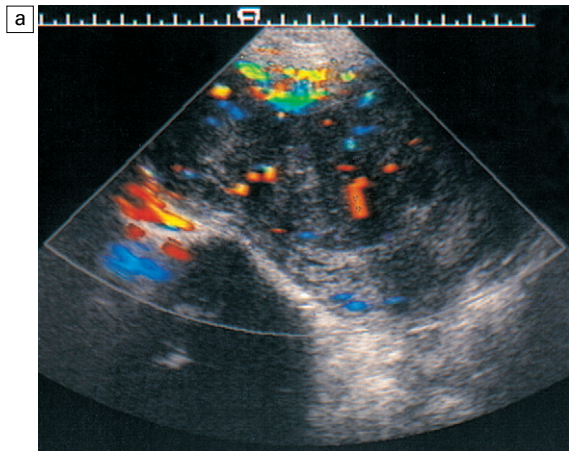


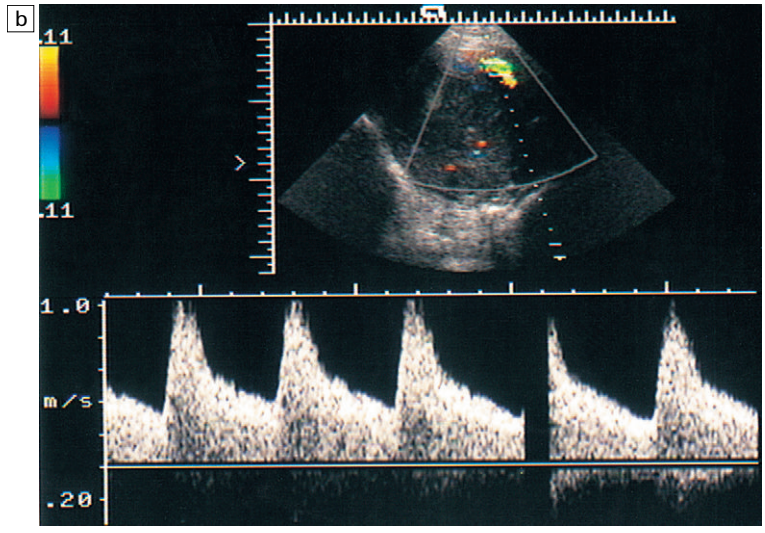


**Fig. 13.15** (a) Irregular blood flow both at the margin and within the uterine fibroids. There was grey-scale evidence of partial necrosis. (b) Doppler spectrum of same patient showing increased systolic and diastolic velocities with reduction in resistance indices indicating uterine hyperaemia with vascular fibroids.

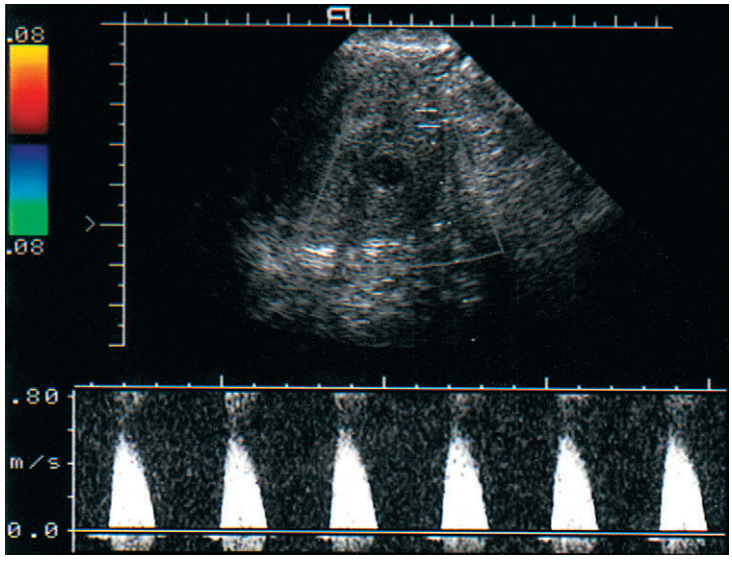


**Fig. 13.16** Doppler spectrum of uterine artery flow in postmenopausal uterus with uterine fibroids. No evidence of increase in blood flow velocities, particularly in diastole.

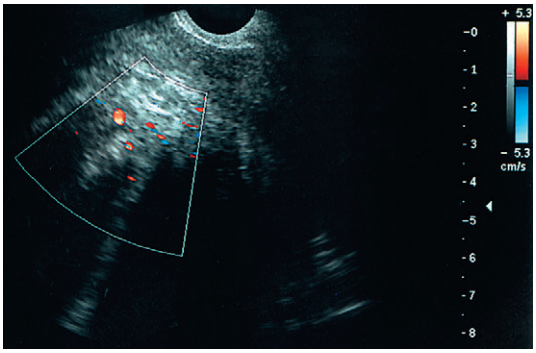


**Fig. 13.17** Attenuation by fibroid prevents any colour signal.

differentiate a subserous fibroid from an extrauterine mass the demonstration of a marginal vessel is said to be a useful discriminating sign (Fig. 13.18).

There is some evidence that vascular fibroids respond better to medical suppressive therapy and this may be useful in their management. There is, however, no evidence that malignant tumours of the myometrium demonstrate any specific Doppler ultrasound features.[21]

### *Endometrial disease*

Endometrial hyperplasia (Fig. 3.19), endometrial polyps and endometrial carcinoma (Fig. 13.20) can produce similar appearances on transvaginal ultrasound. There is broadening and inhomogeneity of the thickness of the endometrium.


**Fig. 13.18** Transabdominal ultrasound demonstrates flow in normal uterine arteries (red) and a junctional vessel between the uterus and the fibroid said to be characteristic of fibroid disease.

Diagnosis of pathology largely depends upon identifying an endometrial thickness greater than 5 mm. While this represents a sensitive method it lacks specificity and does not allow the differentiation of benign from malignant disease.

In the presence of postmenopausal bleeding and in the absence of uterine fibroids it has been suggested that uterine artery and endometrial Doppler are sensitive in the differentiation of significant pathology from endometrial atrophy. When no pathology of the endometrium is present then resistance index values are 0.85 ± 0.08, whereas if there is pathology present these are 0.77 ± 0.03. Furthermore these authors indicate that, in their experience, malignancy has not been found in patients where the resistance index was recorded as greater than 0.83, perhaps allowing a more conservative approach in this group.[21] The greater sensitivity of depiction of vessel distribution with modern colour Doppler and power Doppler affords the demonstration of flow patterns within the endometrium. In carcinoma 81% demonstrate a multiple vessel pattern, 6% a single vessel pattern and 12% a scattered pattern whereas 97% of polyps demonstrate a single vessel pattern and none a multiple pattern (Fig. 13.21). The multiple vessel pattern has been quantified with an endometrial colour score.[22] In practice, the demonstration of a single pedicular vessel is of great value in differentiating endometrial polyp from other pathology. When combined with saline hysterography it demonstrates high sensitivity and specificity for diagnosis of endometrial pathology.

### *Tamoxifen*

Tamoxifen is widely used in the treatment of breast carcinoma and has an oestrogenic effect on the endometrium. This produces significant endometrial thickening and there is an associated increase in the incidence of endometrial carcinoma. There is a concomitant increase in blood flow within the uterine arteries and within the myometrial vessels, which may be demonstrated on colour Doppler and by a decrease in the blood flow indices. However, this is not specific for malignancy and there are no features which will currently allow a specific diagnosis (Fig. 13.22).[23]

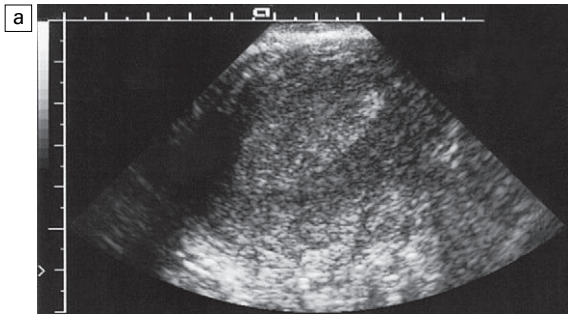


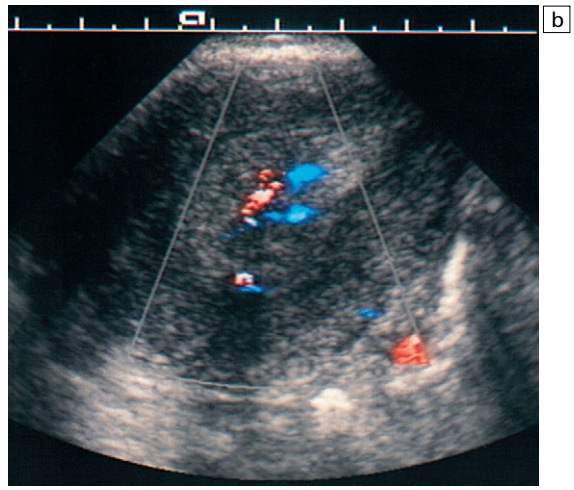


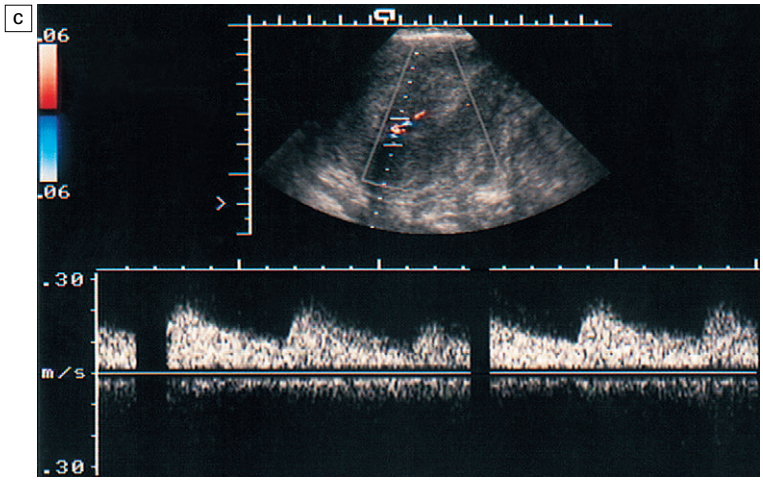


**Fig. 13.19** (a) Transvaginal ultrasound demonstrating endometrial hyperplasia. (b) Same patient. Colour flow Doppler demonstrating endometrial vascularity. (c) Spectral Doppler within the vessels in the endometrium shows resistance indices less than 0.77.

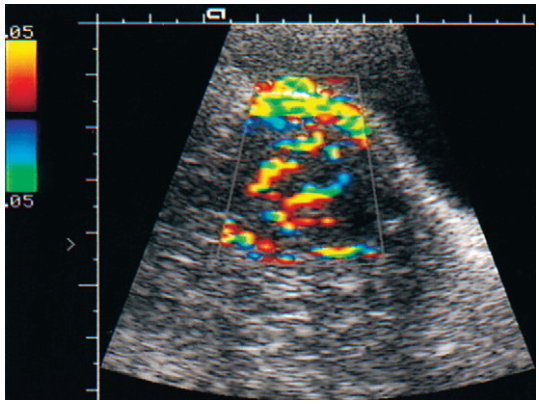


**Fig. 13.20** Transabdominal ultrasound of the uterus with abnormal flow demonstrating gross hyperaemia extending to the surface of the uterus in an endometrial carcinoma with extensive myometrial invasion.

### *Hormone replacement therapy*

Hormone replacement therapy produces no significant change in blood flow characteristics to the normal postmenopausal uterus.[24] However, in the presence of uterine fibroids there may be increased blood flow with particular increase in the diastolic component in patients on replacement therapy.

### *Trophoblastic disease*

The normal appearance of the postpartum uterus is variable, with myometrial heterogeneity and a wide range of appearances of the endometrial cavity. The diagnosis of retained products of conception should not therefore rely on ultrasound appearances although the technique may

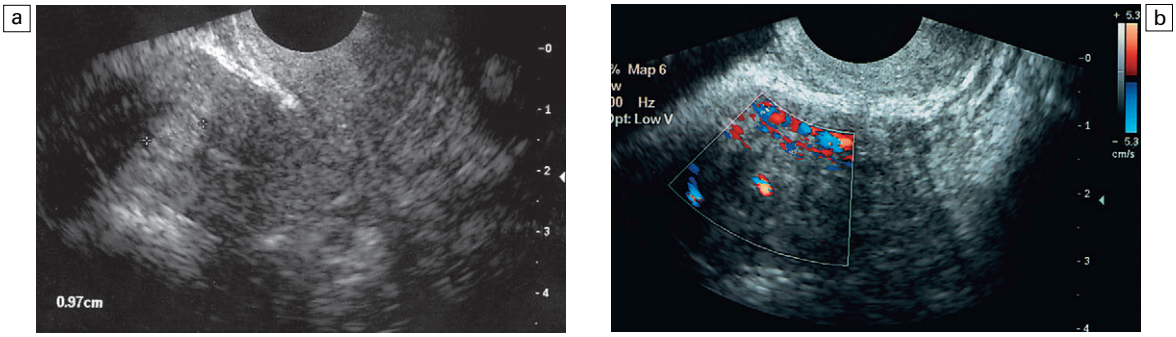


**Fig. 13.21** Endometrial polyp. (a) Transvaginal sonography demonstrates an echogenic lesion within the uterine cavity. (b) On colour flow Doppler there is a single vessel identifying the pedicle.

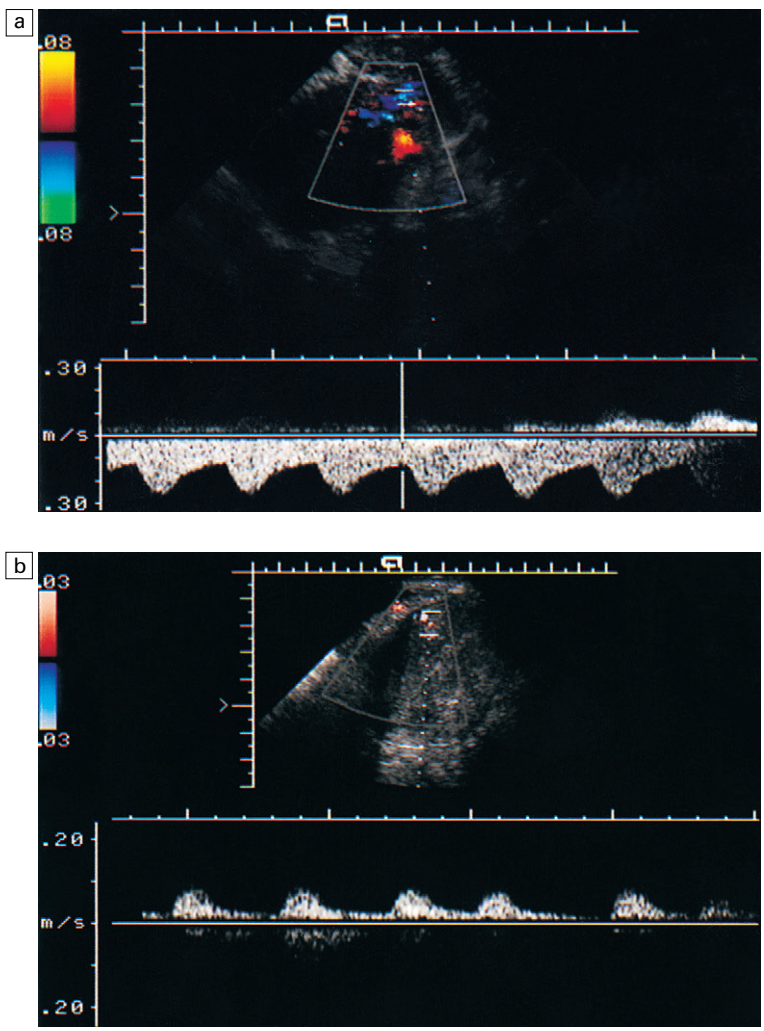


**Fig. 13.22** (a) Spectral Doppler of uterine artery demonstrating increased uterine blood flow in patient on tamoxifen. (b) The return of uterine blood flow to normal values after withdrawal of tamoxifen.

inform the diagnosis. Similarly the vascularity of the postpartum uterus is also variable with areas of enhanced vascularity some even exhibiting a pedicle[25] (Figs 13.23 and 13.24). Ultrasound including colour Doppler however may improve decision making in those patients with postpartum bleeding who have not responded to normal conservative management.

The demonstration of abnormal vessels within the endometrium extending into the endometrium usually following miscarriage or termination of pregnancy was thought to be associated with a diagnosis of arteriovenous malformation. It is now recognised that, although not common, this feature can be associated with a rather prolonged involution of the trophoblast and supplying vessels. In the absence of major symptoms ultrasound may be used to monitor resolution (Fig. 13.25).

Hydatidiform mole, invasive mole and choriocarcinoma are rare neoplasms of the endometrium. Thickening and inhomogeneity of the endometrium are characteristic ultrasound features with a varying degree of formation of vesicles within the uterine cavity. Ultrasound imaging is relatively poor at distinguishing the three levels of severity of the disease and, unless there is evidence of distant metastases, it is unreliable at the assessment of degree of invasion. There is a significant increase in myometrial and endometrial blood flow as evidenced by colour Doppler in all of the trophoblastic tumours; this is usually more marked in the more aggressive tumours. Similarly, Doppler indices are altered in trophoblastic disease: a mean peak systolic velocity of 57.5 ± 20.4 (normal 28.3 ± 3. 41) and a resistance index of 0.56 ± 0.19 (normal 0.86 ± 0.05) have been demonstrated,

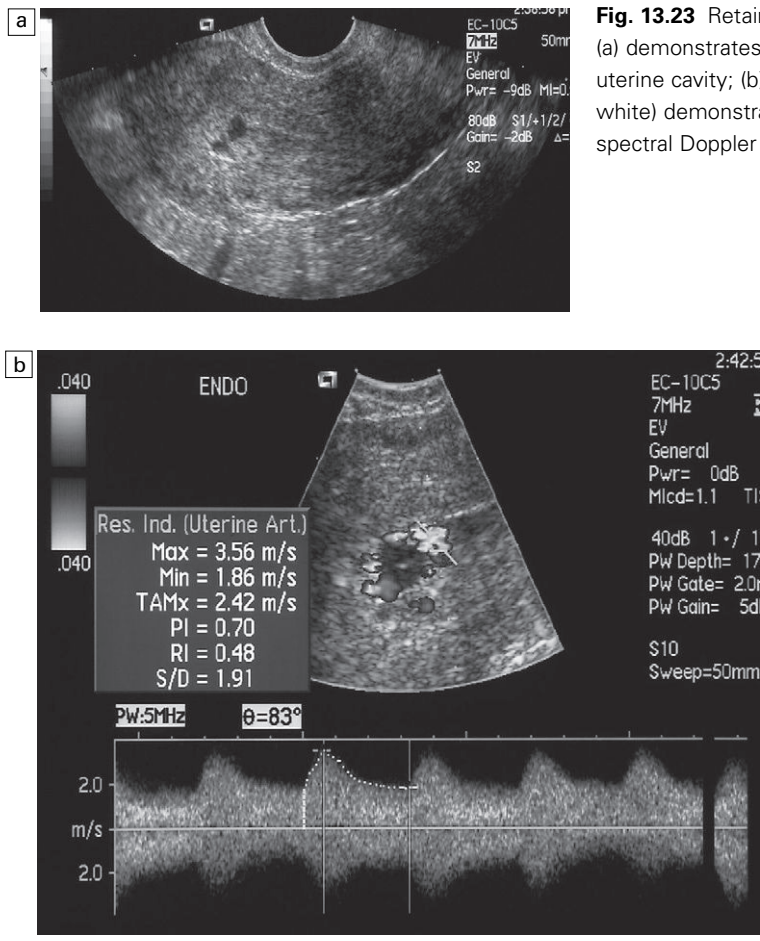


**Fig. 13.23** Retained products of conception: (a) demonstrates residual trophoblast within the uterine cavity; (b) colour flow (depicted in black and white) demonstrates disordered pattern while spectral Doppler yields a low resistance pattern.

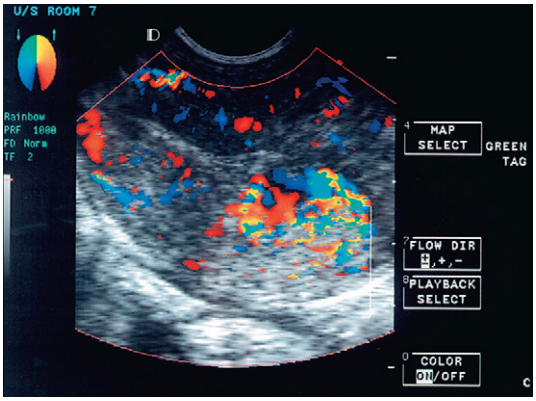


**Fig. 13.24** Colour flow Doppler of flow in trophoblastic tumour.

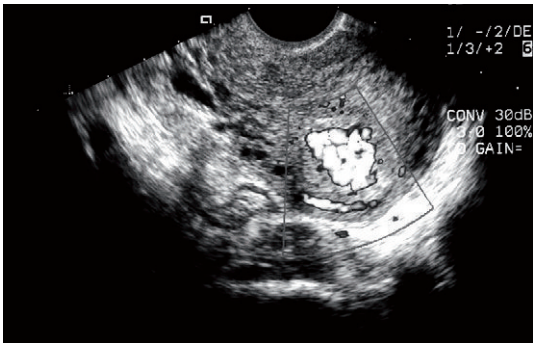

**Fig. 13.25** Colour flow Doppler demonstrating extensive vascular abnormality extending from the endometrium deep within the myometrium. This was an arteriovenous malformation which required embolisation but similar patterns may be seen in some cases of trophoblastic involution, particularly following termination of pregnancy.

although the resistance index may vary from 0.2 to 0.8. Nonetheless, the extent of intratumoral flow correlates with the prognosis: the higher the resistance index, the lesser the need for prolonged treatment cycles.[26] Furthermore, the return of the Doppler indices to normal values is good evidence of successful surgical or medical treatment.

## Ovarian disease

### *Ovarian cancer*

Detection and characterisation of ovarian tumours has depended upon the demonstration of ovarian enlargement and the identification of both cystic and solid masses within the ovary. Criteria for malignancy include the size and complexity of lesions. However, not all malignant lesions demonstrate characteristic ultrasound features. Furthermore, if ultrasound is to have a role in screening for ovarian carcinoma, then features must be sought that would allow the early identification of a potentially malignant lesion prior to the development of frank malignant morphology.

Considerable research work has suggested that malignant tumours demonstrate higher diastolic flow and consequently lower resistance and pulsatility indices than those seen in benign tumours. Similarly, the pattern of colour flow in benign and malignant tumours is reportedly different (Figs 13.26–13.31). However, the reported accuracy of colour flow and spectral Doppler is the subject of wide variability within the literature. Chou et al[27] and Sengoku et al[28] suggest a sensitivity of 100% with a negative predictive value of 100%, while Bromley *et al*[29] and Brown *et al*[30] record sensitivities of only 66% and 50%, respectively. The uncertainty about the value of Doppler is perhaps best reflected in the variation of criteria used by different authors to indicate the presence or absence of malignancy. The cut-off values for the resistance index range between 0.4 and 0.6, while others simply use a visual assessment of the colour Doppler pattern. It is important therefore to compare the results of Doppler findings with the reported sensitivity of ovarian morphology alone in predicting malignancy, which is in the region of 91–98%.[29,31]

More recently there has been renewed interest in the assessment of the pattern of distribution of blood flow[32] and a reassessment of the Doppler spectrum.[33] This work has concentrated on assessment of the diastolic component of the spectrum and the development of a new parameter assessing the pattern of flow decay, the end diastolic velocity distribution slope. In addition there has been early work to assess the value of contrast agents to refine the evaluation of the pattern of flow distribution within the ovary.[34] Although all of these studies are encouraging, to date there has been no validation by larger studies.

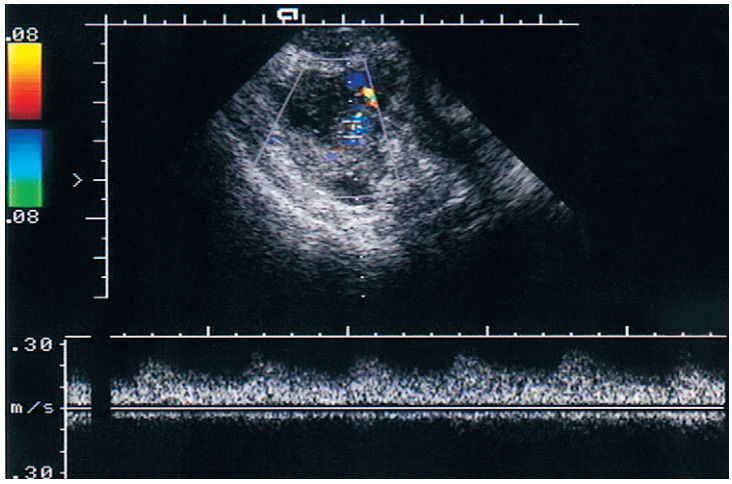


**Fig. 13.26** Solid ovarian tumour with colour flow Doppler at the margin and spectral Doppler demonstrating low resistance.

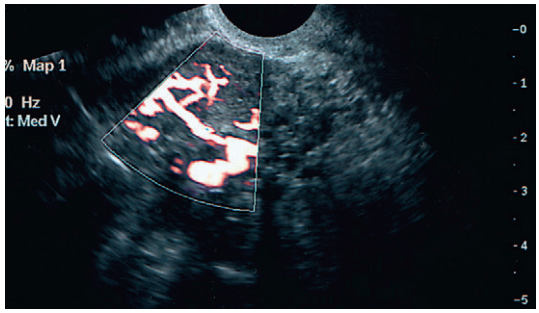


**Fig. 13.27** Solid ovarian cancer. Power Doppler demonstrates disordered pattern of flow with irregular branching vessels, anastomoses and a large draining vein.

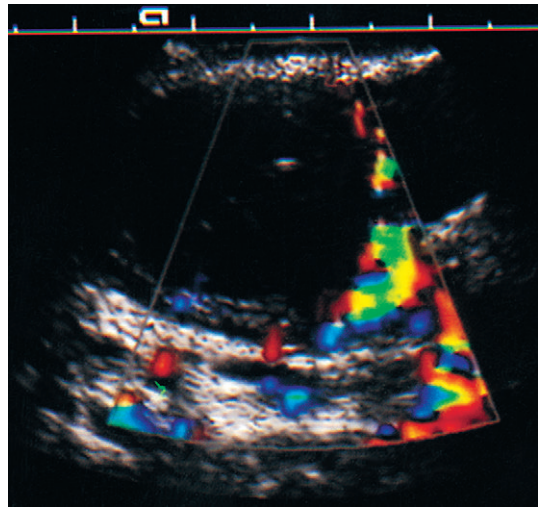

**Fig. 13.28** Colour flow Doppler at the margin of an apparently simple cyst but which subsequently proved to have borderline malignancy detectable in the wall.

Studies attempting to combine a morphological score with Doppler features and indices suggest that although diagnostic sensitivities may be unaltered, there may be significant improvement in positive predictive value from 60% to 94%.[35]

The situation in premenopausal patients is more complex still. The presence of low-resistance flow in a corpus luteum requires that any suspicious lesion be examined in the early proliferative phase of the menstrual cycle to ensure that the neovascularity is not a physiological response (Fig. 13.32).

It is not surprising that the early results have not been borne out by subsequent studies. The process of angioneogenesis is a microscopic one and is at least partly dependent on cell type and morphology.[36]

Carter et al[37] concluded that colour Doppler has neither the sensitivity nor the specificity to distinguish between benign and malignant disease of the ovary. This may no longer be tenable; studies utilising pattern distribution, new indices, 3D colour power and contrast enhancement all promise to improve the assessment of malignant disease. It remains the case, however that the pattern of blood flow within a mass is a single parameter and the

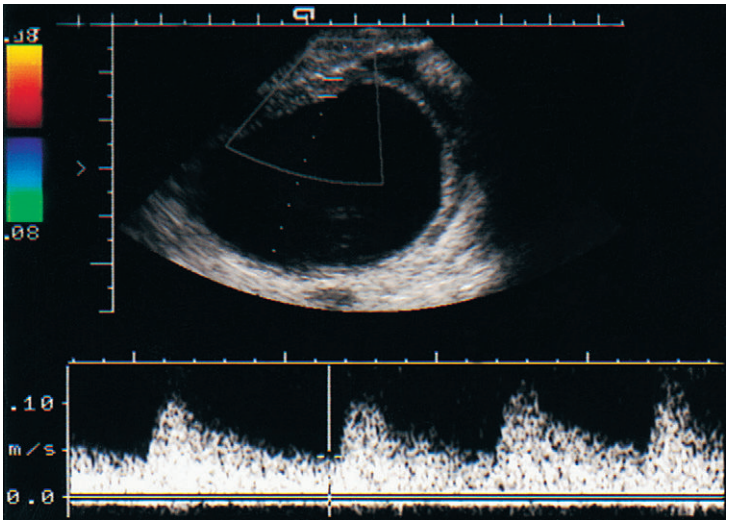


**Fig. 13.29** Simple ovarian cyst with spectral Doppler recorded in the cyst wall with relatively low resistance index of 0.64.

a

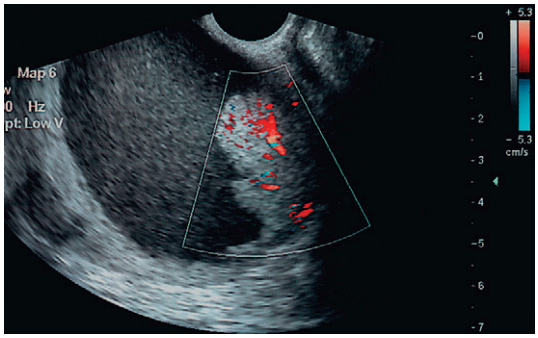


b

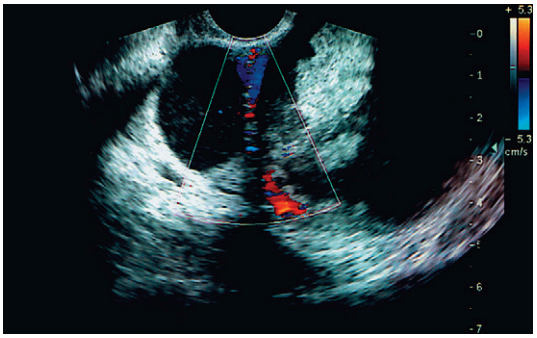

c

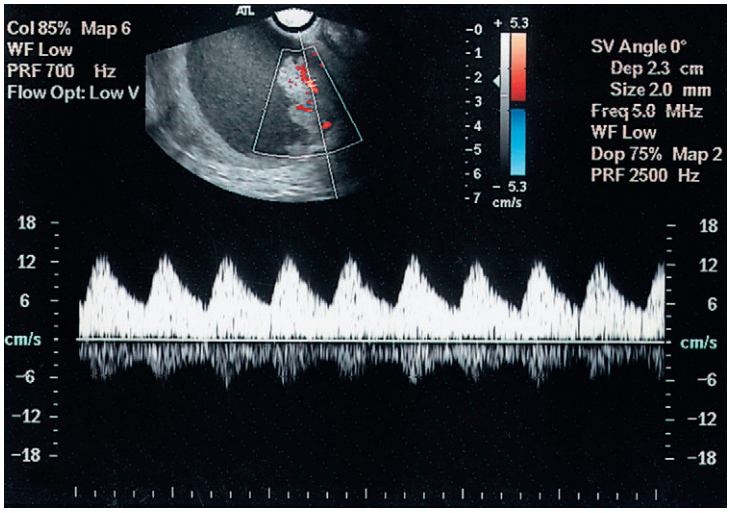


**Fig. 13.30** Heterogeneous ovarian mass with cystic and solid elements. Flow is demonstrated in colour within the solid component (a), and within the septum (b), although spectral Doppler, while showing low resistance, still exhibits a resistance index of greater than 0.5.

evaluation of ovarian tumours with Doppler techniques requires very significant further work if it is to provide a clinically useful tool for wide application.

The diagnosis of ovarian dermoid is usually straightforward on ultrasound. There are a number of cardinal features, the most reliable of which is the echogenic plug. It has been suggested that

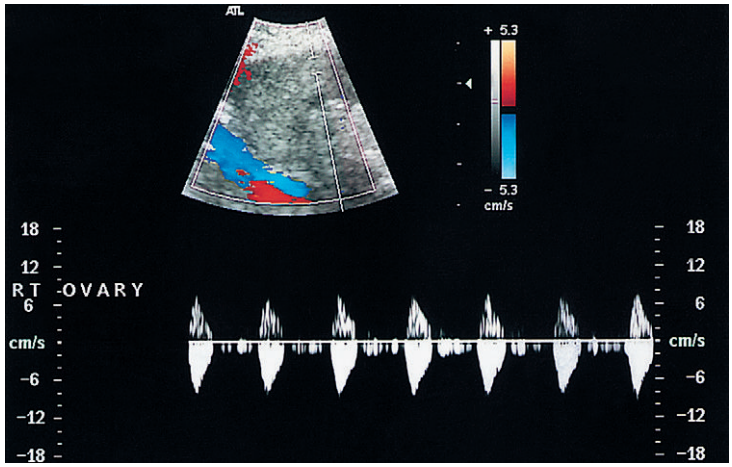


**Fig. 13.31** Spectral Doppler of a postmenopausal ovary showing no diastolic flow. Some artefactual flow is demonstrated in both systole and diastole due to the small size of the vessels sampled.

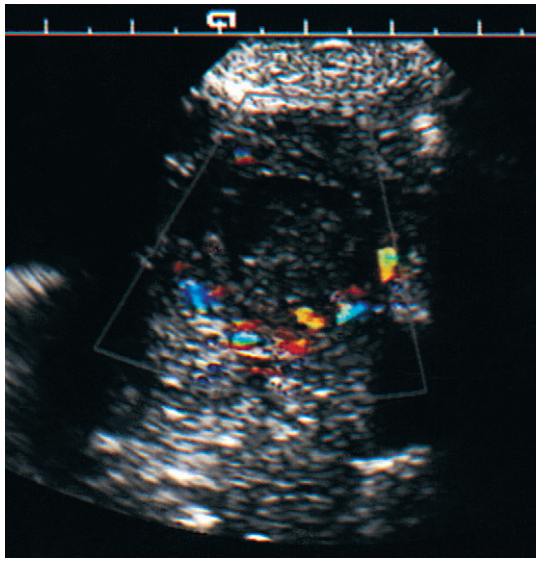

**Fig. 13.32** Colour flow around a complex mass in the ovary of a premenopausal patient. This represented flow in a corpus luteum.

the benign nature of a dermoid can be predicted by the nature of blood flow and similar indices to those described for ovarian cancer (Fig. 13.33). However this lacks further confirmatory evidence and there has been at least one case where a struma ovarii has mimicked a malignant pattern.

### *Screening for ovarian cancer*

Although it is clear that transvaginal ultrasound can identify asymptomatic masses postmenopausally, at present there is an assumption rather than proof that this does more than just affect the 'lead time' to the diagnosis of ovarian cancer. Furthermore, the case for cost effectiveness is far from proven. Screening of first-order relatives of those with ovarian cancer may be justified, and in these patients the addition of colour flow and spectral Doppler may contribute to the security of a negative screening result. Doppler may also be of value in the management of patients who yield masses which appear morphologically benign on transvaginal sonography.[38] There is, however, a diagnostic dilemma when a morphologically normal ovary, or a morphologically benign simple cyst, demonstrates neovascularity. Based on existing studies, about 6% of women screened with ultrasound will have cystic or complex masses. Moreover, in one study an ovarian artery resistance index of <0.4 occurred in 12% of premenopausal patients and 3% of postmenopausal. In this study, only one borderline ovarian tumour and one endometrial malignancy were discovered.[39] The scientific basis for ovarian screening in a low-risk population is therefore unproven and even in patients with a strong family history there is a high false-positive detection rate, particularly in premenopausal patients, using both cancer antigen 125 and ultrasound. It seems unlikely that Doppler, using current methods of data processing, will further improve on the specificity of the screening technique; it could in fact increase the number of false-positive laparotomies if abnormal colour

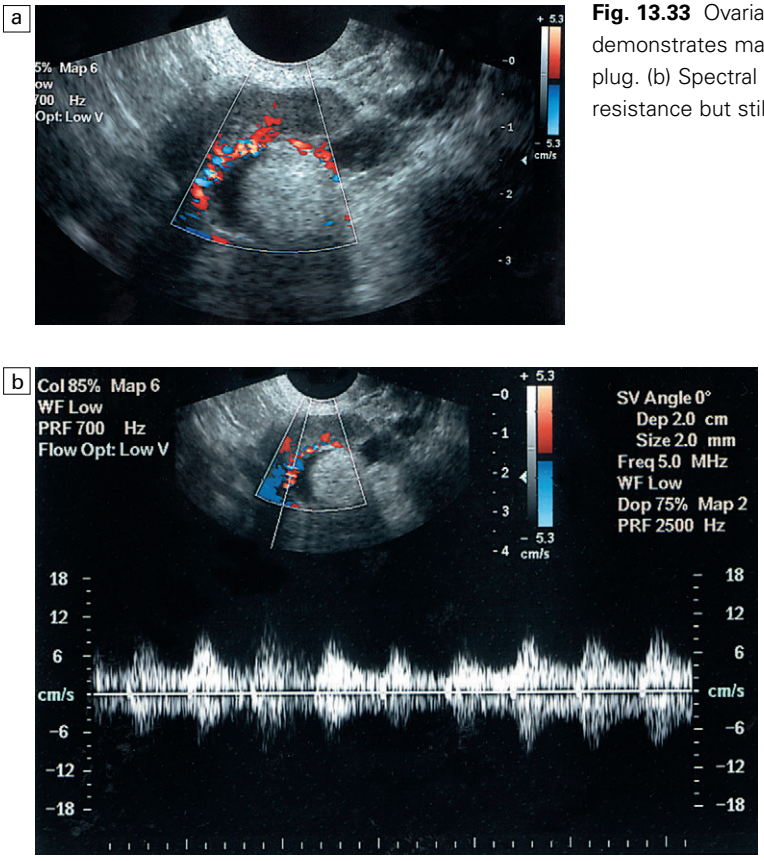


**Fig. 13.33** Ovarian dermoid. (a) Colour flow demonstrates marginal flow around the dermoid plug. (b) Spectral analysis demonstrates low resistance but still out with malignant range.

flow is to be used as another indicator of ovarian abnormality.[40]

## Other adnexal lesions

Inflammatory processes may produce a hyperaemic response, although this is not invariable, and will not allow differentiation of lesions of differing aetiology.[41] Findings in pelvic inflammatory disease are variable. There may be a diffuse increase in the number and size of vessels in the adnexa (Fig. 13.34). *Tubo-ovarian abscess* is the pathology most likely to show evidence of increased Doppler flow with circumferential vessels draped around the cystic component and low resistance indices, often less than 0.5.[42] *Endometriomas* demonstrate a wide variety of appearances on colour Doppler, sometimes with circumferential vessels, occasionally 'spotty' vessels with resistance indices varying from 0.5 to 0.74[43] (Fig. 13.35). Differential diagnostic features remain dependent upon clinical history and other findings. Adenomyosis of the uterus may exhibit focal or diffuse areas of increased echogenicity within the myometrium. The normal vertical alignment of the spiral arteries may be lost (Fig. 13.36).

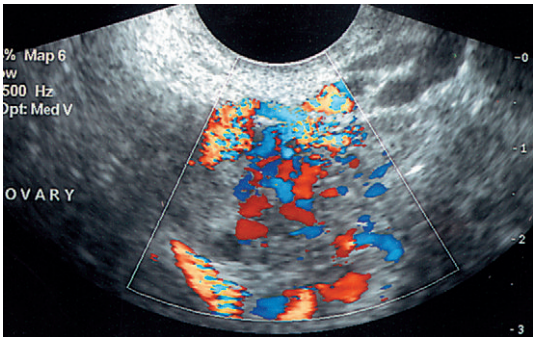


**Fig. 13.34** Colour flow Doppler showing adnexal hyperaemia in pelvic inflammatory disease.

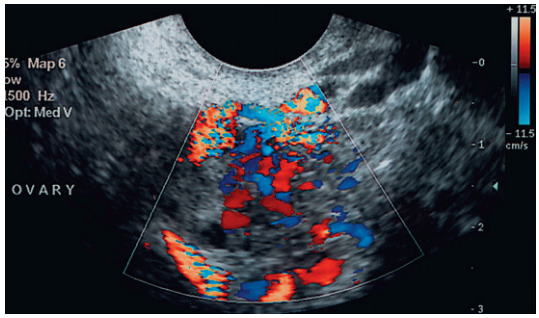


**Fig. 13.35** Irregular, somewhat spotty flow in endometriosis.

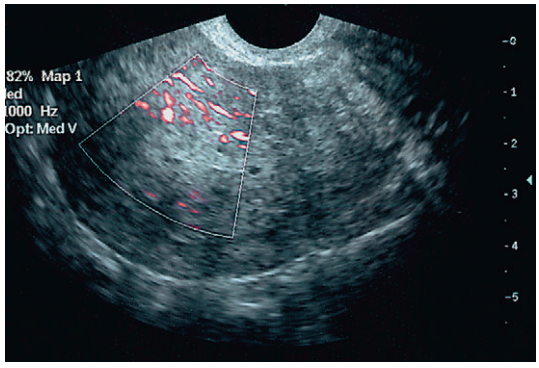

**Fig. 13.36** Adenomyosis of the uterus demonstrating unusual short segment myometrial vessels aligned to the serosal surface.

### *Ovarian torsion*

Ovarian torsion may produce a variety of appearances on ultrasound including a complex cystic mass, a solid mass, and a solid mass with peripherally placed cysts. The absence of colour signal will not distinguish this from other pathologies, since colour Doppler has been demonstrated both centrally and peripherally in torsion.[44] There may be reduction or absence of diastolic flow and a reduced distribution of intraovarian vessels. A particular pattern of torsion described as the whirlpool sign in which the vessels are wrapped around the ovary appears to be specific although it occurs in only a minority of cases.[45] Where there is clinical suspicion of ovarian torsion Doppler studies are reported to be abnormal in all of the cases where torsion is confirmed and in only 2% where torsion was not confirmed.[46] Preoperative assessment with colour Doppler may therefore be used to determine the nature and extent of surgery. Those patients with demonstrable blood flow within the ovary would be submitted for laparoscopic untorsion, while in those with an absence of flow, open surgery and oophorectomy would be the likely procedure, while those with normal flow patterns could be managed conservatively.

## Complications of early pregnancy

The trophoblast is extremely vascular during its development, with two phases of invasion. The vessels contributing to this invasion have thin walls and low peripheral resistance to blood flow. Sampling within the vascular component of the trophoblast will therefore produce characteristic low-impedance signals with resistance indices less than 0.6. Some workers have suggested that this may contribute to the early differentiation of viable from non-viable or complicated pregnancies (Fig. 13.37a). However, the high power output of Doppler, particularly in relation to transvaginal applications, must be considered and, in this author's view, this prohibits its use in most early pregnancy applications. Ectopic pregnancy may be considered an exception to this rule and certain valuable data can be acquired.

### *Ectopic pregnancy*

Ultrasound imaging occupies a central role in the investigation of ectopic pregnancy, with recorded sensitivities of 94% for transvaginal ultrasound.[47] Modern methods of management now suggest that a conservative approach can be adopted in those patients without active trophoblast and that when there is active trophoblast, medical treatment using either systemic or local methotrexate is the preferred first-treatment option. Using colour Doppler as a guide, the vascular trophoblast can be identified within the adnexal region. Sampling the flow within the trophoblast will yield pulsatile flow of low resistance index in the presence of active trophoblast but a resistance index in excess of 0.8 in inactive trophoblast.[48] This may provide a useful guide for conservative, non-operative treatment in these patients (Fig. 13.37b).

Ancillary Doppler findings in ectopic pregnancy are similar to those in a normotopic pregnancy, with flow in uterine vessels and to the corpus

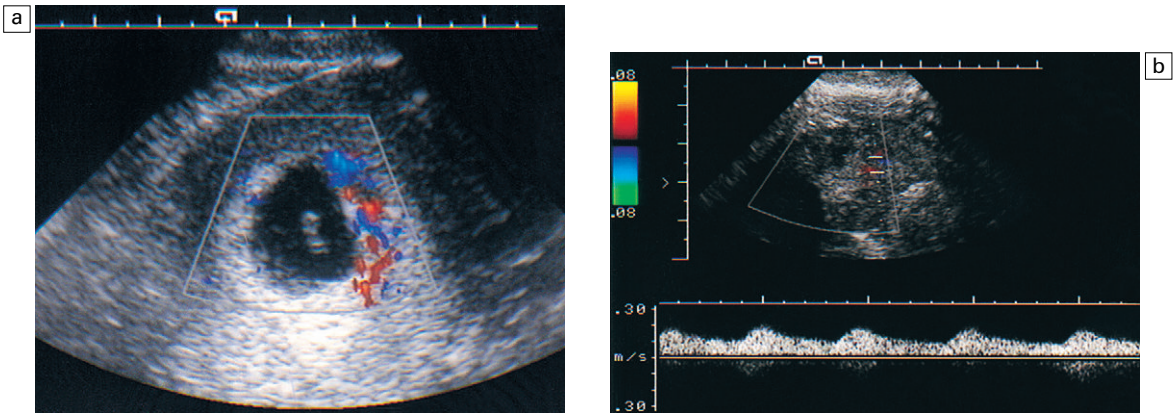


**Fig. 13.37** (a) Normal colour flow pattern in the trophoblast of a normal 7-week intrauterine pregnancy. (This patient subsequently had a termination of the pregnancy.) (b) Vascular trophoblast in the adnexal region. Colour and spectral Doppler demonstrating low-resistance flow, implying active trophoblast and suggesting the need either for administration of methotrexate as medical treatment or operative intervention.

luteum displaying comparable impedance indices, although peak velocities within the uterine arteries are reduced. The reported findings do not, however, appear sufficiently specific to allow differential diagnosis.[49]

### *Cervical ectopic pregnancy*

Although rare, this form of ectopic pregnancy presents particular difficulties with management. Attempts at evacuation of the uterus are usually unsuccessful, accompanied by heavy bleeding and often necessitating hysterectomy. More recently, direct installation of potassium chloride and subsequently methotrexate into the gestational sac can result in regression of the gestation and either complete resolution, or a more safely performed uterine evacuation. Colour and duplex Doppler ultrasound have two roles in this situation: first, to identify the position of the uterine arteries joining the uterus, thus confirming the diagnosis of a cervical pregnancy by its position caudal to the uterine arteries; second, Doppler is used to monitor the regression of the trophoblast by alteration of the pattern of the Doppler signal with time, as this usually mirrors the fall in human chorionic gonadotrophin values.

## Other gynaecological tumours

Duplex Doppler ultrasound has no established role in the assessment either of cervical carcinoma or pelvic metastatic disease, including ovarian carcinoma. Certain metastases may show increased vascularity similar to that of primary ovarian tumours, but there are no data to relate vascularity to susceptibility for certain forms of treatment, nor to the likely response to treatment (Fig. 13.38). Similarly certain cell types in cervical cancer are more likely to demonstrate abundant blood flow but this is of no current clinical value. There is no correlation with stage or degree of local invasion.[50]

## Pelvic congestion syndrome

The association between chronic pelvic pain, dyspareunia and pelvic varices has been termed pelvic congestion syndrome. Its aetiology is not clear but some have ascribed it as being due to dilatation of pelvic veins, congestion of the ovaries with resultant ovarian swelling and cyst formation (Fig. 13.39). In its most marked form there may be vulval and leg varices. Some have suggested a psychological component for the condition but it is difficult to assess a particular psychological profile as cause or effect in women with long-term disabling pelvic pain. There is an association between the symptoms and multiple large serpiginous pelvic veins, usually of diameter greater than 4 mm and, in this author's experience, flow velocities within the pelvic veins of less than 5 cm $s^{-1}$. Reverse flow within the pelvic

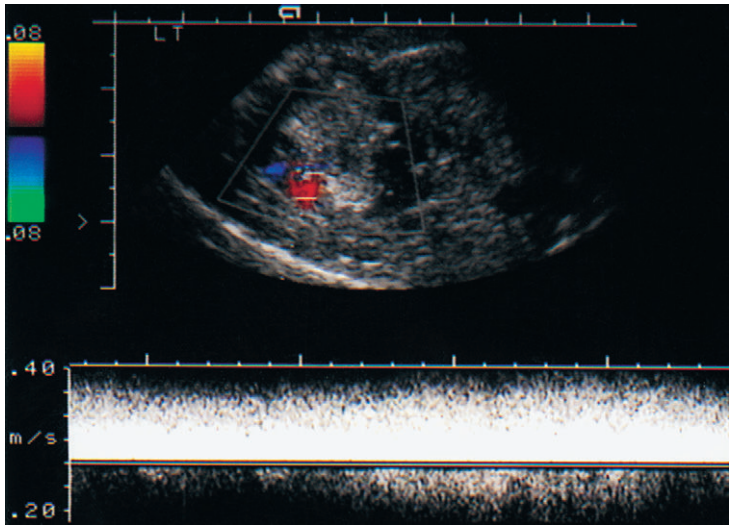


**Fig. 13.38** Echogenic ovarian metastasis in patient with primary breast carcinoma demonstrating high-velocity peripheral flow which is normally indicative of shunting.

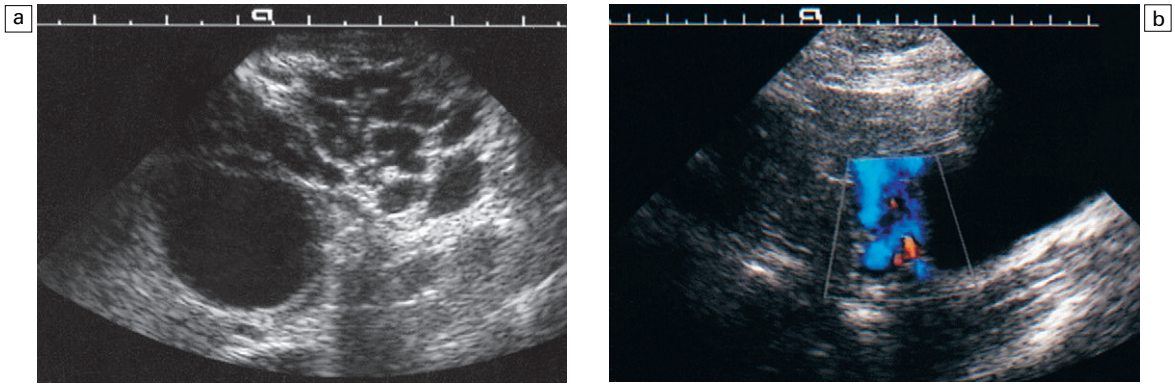


**Fig. 13.39** (a) Large collection of serpiginous vessels in the pelvis adjacent to the right ovary which also contains a cyst. (b) Extension of the distended veins towards the uterine cervix and vaginal vault.

veins during a Valsalva manoeuvre, which exceeds 2 cm $s^{-1}$ peak velocity, appears to be a prominent feature of the syndrome. Further work is necessary, however, to define this association more clearly.

Occasionally it is helpful to use colour Doppler to differentiate distended pelvic veins from hydrosalpinx. The latter will demonstrate no flow even at low velocity settings (Fig. 13.40).

## Other pathologies

Non-gynaecological pathologies can be encountered during pelvic and transvaginal ultrasound examination.

### *Retroperitoneal mass lesions including lymphadenopathy*

The relationship of retroperitoneal masses to the iliac vessels can usually be established without the use of colour flow Doppler.

### *Iliac artery aneurysm*

Common external and internal iliac artery aneurysms can represent a differential diagnostic finding of a pelvic cystic mass. Common and external iliac artery aneurysms are usually easily identified by their relationship to the main arterial trunk, although internal iliac artery aneurysms may require colour flow Doppler for confirmation

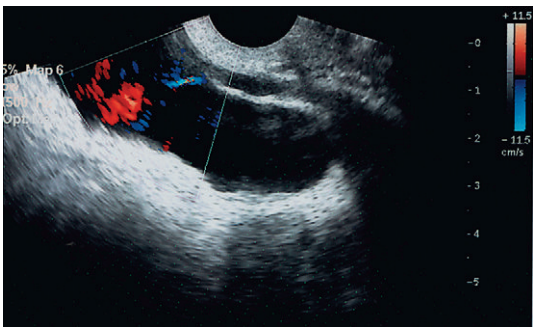


**Fig. 13.40** Hydrosalpinx. Colour flow demonstrates flow in adjacent adnexal structures but not in the tube.

of their nature. Usually a pulsatile but swirling colour signal can be observed within the true lumen with a variable amount of mural clot.

### *Deep venous thrombosis*

Transvaginal ultrasound is not the primary method of diagnosis of deep vein thrombosis but the pelvic extension of clot can be demonstrated by both transabdominal and transvaginal ultrasound, with distension of the iliac veins by intraluminal echogenic clot and either distortion of flow pattern around the clot or complete occlusion.

### *Bowel masses*

Bowel wall thickening is a non-specific feature of bowel pathologies. Similarly, mural hypervascularity is a feature typical of inflammatory bowel pathologies including Crohn's disease, diverticular disease and infective colitides; the degree of vascularity reflects disease activity.

### *Hysterosalpingo-contrast sonography (HyCoSy)*

The use of echo-enhancing agents in the assessment of tubal patency has been shown to be of value in the investigation of infertility. A fine cannula is inserted into the cervical canal under direct vision and between 5 and 10 cc of contrast are injected gently whilst performing a transvaginal scan. This should show the echogenic contrast within the tubes and spill into the peritoneum in similar fashion to that seen with orthodox hysterosalpingography, although the correlation between hysterosalpingography and HyCoSy remains less than 90%. The technique has therefore not fully replaced formal X-ray hysterosalpingograms. The use of colour Doppler in conjunction with ultrasound contrast improves the sensitivity of the technique in the detection of tubal spill.[36]

## SUMMARY

Colour and duplex Doppler have yet to find well-defined applications in gynaecology. The value in ovarian tumour diagnosis is controversial and in tumours of the endometrium unproven. It may improve diagnostic security in patients with morphologically benign ovarian tumours, but hopes that it would enhance the process of ovarian screening have not been fulfilled. In inflammatory pathology there are no reported features that will allow the distinction between different pathological processes, even torsion of the ovary demonstrating intraovarian flow in many cases.

In the assessment and management of subfertility, Doppler techniques appear to have significant value. Ovarian activity and uterine receptivity can be more accurately monitored than by ultrasound morphology alone. Cyclical changes can be documented and the effects of ovulation induction therapy defined.

In ectopic pregnancy it may have a role in the operative planning process, while in malignant trophoblastic disease it appears to be of value in determining prognosis and in treatment planning.

There is a need for considerable research particularly in the areas of neovascularity and signal processing before Doppler techniques are applicable to common gynaecological conditions, and before this author could advocate its widespread adoption in the investigation of gynaecological conditions.

## REFERENCES

1. Jarvela IY, Sladkevicius P, Kelly S, et al. Three dimensional sonographic and power Doppler characterisation of ovaries in late follicular phase. Ultrasound Obstet Gynecol 2002; 20:281–285.
2. Suren A, Osmers R, Kulenkampff D, et al. Visualization of blood flow in small ovarian tumour vessels by transvaginal colour Doppler sonography after echo enhancement with injection of Levovist. Gynaecol Obstet Invest 1994; 38: 210–212.
3. Raine-Fenning NJ, Campbell BK, Kendall NR, et al. Quantifying the changes in endometrial vascularity throughout the normal menstrual cycle with three dimensional power Doppler angiography. Hum Reprod 2004; 19 (2):330–338.
4. Sladkevicius P, Valentin L, Marsal K. Transvaginal gray-scale and Doppler ultrasound examinations of the uterus and ovaries in healthy postmenopausal women. Ultrasound Obstet Gynecol 1995; 6: 81–90.
5. Steer CV, Tan SL, Mason BA, et al. Mid-luteal phase vaginal color Doppler assessment of uterine artery impedance in a subfertile population. Fertil Steril 1994; 61: 53–58.
6. Kurjak A, Zalud I. Doppler and color flow imaging. In: Nyberg DA, Hill LM, Bohm-Velez M, et al, eds. Transvaginal ultrasound. St Louis: Mosby Year Book; 1992:285–294.
7. Meire HB. Doppler – artefacts, errors and pitfalls. Abdom Gen Ultrasound 1993; 5: 83–93.
8. Battaglia C, Artini PG, D'Ambrogio G, et al. Uterine and ovarian blood flow measurement. Does the full bladder modify the flow resistance? Acta Obstet Gynecol Scand 1994; 73: 716–718.
9. Kamaya A, Tuthill T, Rubin JM. Twinkling artifact on colour Doppler sonography: dependence on machine parameters and underlying cause. AJR Am J Roentgenol 2003; 180 (2):215–222.
10. Ziereisen F, Heinrichs C, Dufour D, et al. The role of Doppler evaluation of the uterine artery in girls around puberty. Pediatr Radiol 2001; 31 (10):712–719.
11. Frajndlich R, von Eye Corleta H, Frantz N. Color Doppler sonographic study of the uterine artery in patients using intrauterine contraceptive devices. J Ultrasound Med 2000; 19 (8):577–579.
12. Pepper J, Dewart PJ, Oyesanya OA. Altered uterine artery blood flow impedance after danazol therapy: possible mode of action in dysfunctional uterine bleeding. Fertil Steril 1999; 72(1):66–70.
13. Steer CV, Tan SL, Dillon D, et al. Vaginal color Doppler assessment of uterine artery impedance correlates with immunohistochemical markers of endometrial receptivity required for the implantation of an embryo. Fertil Steril 1995; 63:101–108.
14. Contart P, Baruffi RL, Coelho J, et al. Power Doppler endometrial evaluation as a method for the prognosis of embryo implantation in an ICSI programme. J Assist Reprod Genet 2000; 17 (6):329–334.
15. Schild RL, Knobloch C, Dorn C, et al. Endometrial receptivity in an in vitro fertilisation programme as assessed by spiral artery flow, endometrial thickness, endometrial volume and uterine artery blood flow. Fertil Steril 2001; 25(2):361–366.
16. Jarvela IY, Sladkevicius P, Kelly S, et al. Quantification of ovarian power Doppler signal with three dimensional ultrasonography to predict response during in vitro fertilization. Obstet Gynecol 2003; 102:816–822.
17. Frates MC, Doubilet PM, Durfee SM, et al. Sonographic and Doppler characteristics of the corpus luteum: can they predict pregnancy outcome? J Ultrasound Med 2001; 20 (8) 821–827.
18. Yang JH, Wu MY, Chen CD. Association of endometrial blood flow as determined by a modified colour Doppler technique with subsequent outcome of in vitro fertilization. Hum Reprod 1999; 14(6):1606–1610.
19. Sladkevicius P, Campbell S. Advances in ultrasound assessment in the establishment and development of pregnancy. Br Med Bull 2000; 56(3):691–703.
20. Wiener Z, Beck D, Rottem S, et al. Uterine artery flow velocity waveforms and color flow imaging in women with perimenopausal and postmenopausal bleeding. Correlation to endometrial histopathology. Acta Obstet Gynecol Scand 1993; 72:162–166.
21. Carter JR, Lau M, Saltzman AK, et al. Gray-scale and color flow Doppler characterisation of uterine tumors. J Ultrasound Med 1994; 13:835–840.
22. Alcazar JL, Castillo G, Minguez JA, et al. Endometrial blood flow mapping using transvaginal power Doppler sonography in women with post menopausal bleeding and thickened endometrium Ultrasound Obstet Gynecol 2003; 21(6):583–588.
23. Tepper R, Cohen I, Altaras M, et al. Doppler flow evaluation of pathologic endometrial conditions in postmenopausal breast cancer patients treated with Tamoxifen. J Ultrasound Med 1994; 13:635–640.
24. Van den Bosch T, Van Schoubroeck D, Lu C, et al. Color Doppler and gray scale evaluation of the post partum uterus. Ultrasound Obstet Gynecol 2002; 20 (6):586–591.
25. Zalud I, Conway C, Schulman H, et al. Endometrial and myometrial thickness and uterine blood flow in postmenopausal women: the influence of hormonal replacement therapy and age. J Ultrasound Med 1993; 12:737–741.
26. Zhou Q, Lei XY, Cardoza JD. Sonographic and Doppler imaging in the diagnosis and treatment of gestational trophoblastic disease; a 12 year experience. J Ultrasound Med 2005; 24(1):15–24.

27. Hsieh FJ, Wu CC, Chen CA, et al. Correlation of uterine hemodynamics with chemotherapy response in gestational trophoblastic tumors. Obstet Gynecol 1994; 83:1021–1025.
28. Chou CY, Chang CH, Yao BL, et al. Color Doppler ultrasonography and serum CA125 in the differentiation of benign and malignant ovarian tumors. J Clin Ultrasound 1994; 22:491–496.
29. Sengoku K, Satoh T, Saitoh S, et al. Evaluation of transvaginal colour Doppler sonography, transvaginal sonography and CA125 for prediction of ovarian malignancy. Int J Gynaecol Obstet 1994; 46:39–43.
30. Bromley B, Goodman H, Benacerraf BR. Comparison between sonographic morphology and Doppler waveform for the diagnosis of ovarian malignancy. Obstet Gynecol 1994; 83:434–437.
31. Brown DL, Frates MC, Laing FC, et al. Ovarian masses: can benign and malignant lesions be differentiated with color and pulsed Doppler US? Radiology 1994; 190:333–336.
32. Itakura T, Kikkawa F, Kajiyama H, et al. Doppler flow and arterial location in ovarian tumours. Int J Gynecol Obstet 2003; 83(3):277–283.
33. Shaharabany Y, Akselrod S, Tepper R. A sensitive new indicator for diagnostics of ovarian malignancy, based on the Doppler velocity spectrum. Ultrasound Med Biol 2004; 30(3):295–302.
34. D'Arcy TJ, Jayaram V, Lynch M, et al. Ovarian cancer detected non-invasively by contrast-enhanced power Doppler ultrasound. Br J Obstet Gynaecol 2004; 111(6):619–622.
35. Stein SM, Laifer-Narin S, Johnson MB, et al. Differentiation of benign and malignant adnexal masses: relative value of gray–scale, color Doppler, and spectral Doppler sonography. AJR Am J Roentgenol 1995; 164:381–386.
36. Timor-Tritsch LE, Lerner JP, Monteagudo A, et al. Transvaginal ultrasonographic characterisation of ovarian masses by means of color flow-directed Doppler measurements and a morphologic scoring system. Am J Obstet Gynecol 1993; 168:909–913.
37. Wu CC, Lee CN, Chen TM, et al. Incremental angiogenesis assessed by color Doppler ultrasound in the tumorigenesis of ovarian neoplasms. Cancer 1994; 73:1251–1256.
38. Carter JR, Lau M, Fowler JM, et al. Blood flow characteristics of ovarian tumors: implications for ovarian cancer screening. Am J Obstet Gynecol 1995; 172:901–907.
39. Muto MG, Cramer DW, Brown DL. Screening for ovarian cancer: the preliminary experience of a familial ovarian cancer center. Gynecol Oncol 1993; 51:12–20.
40. Karlan BY, Raffel LJ, Crvenkovic G, et al. A multidisciplinary approach to the early detection of ovarian carcinoma: rationale, protocol design, and early results. Am J Obstet Gynecol 1993; 16:494–501.
41. Quillin SP, Siegel MJ. Transabdominal color Doppler ultrasonography of the painful adolescent ovary. J Ultrasound Med 1994; 13:549–555.
42. Tinkanen H, Kujansuu E. (Doppler ultrasound findings in tubo-ovarian infectious complex). J Clin Ultrasound 1993; 21:175–178.
43. Aleem F, Pennisi J, Zeitoun K, et al. The role of colour Doppler in diagnosis of endometriomas. Ultrasound Obstet Gynecol 1995; 5:51–54.
44. Stark JE, Siegel MJ. Ovarian torsion in prepubertal and pubertal girls: sonographic findings. AJR Am J Roentgenol1994; 163:1479–1482.
45. Vijayaraghavan SB. Sonographic whirlpool sign in ovarian torsion. J Ultrasound Med 2004; 23(12):1653–1659.
46. Ben-Ami M, Perlitz Y, Haddad S. The effectiveness of spectral and colour Doppler in predicting ovarian torsion. A prospective study. Eur J Obstet Gynecol Reprod Biol 2002; 104(1):64–66.
47 de Crespigny LC. Demonstration of ectopic pregnancy by transvaginal ultrasound. Br J Obstet Gynecol 1998; 95:1253–1256.
48. Tekay A, Jouppila P. Color Doppler flow as an indicator of trophoblastic activity in tubal pregnancies detected by transvaginal ultrasound. Obstet Gynecol 1992; 80:995–999.
49. Jurkovic D, Bourne TH, Jauniaux E, et al. Transvaginal color Doppler study of blood flow in ectopic pregnancies. Fertil Steril 1992; 57:68–73.
50. Acazar JL, Castillo G, Jurado M, et al. Intratumoral blood flow in cervical cancer as assessed by transvaginal color Doppler ultrasonography: Correlation with tumor characteristics. Int J Gynecol Cancer 2003; 13(4):510–514.
51. Shlief R, Deichert U. Hysterosalpingo-contrast sonography of the uterus and fallopian tubes: results of a clinical trial of a new contrast medium in 120 patients. Radiology 1991; 178:213–215.

# Clinical applications of Doppler ultrasound in obstetrics

# 14

Imogen Montague and Paul A. Dubbins

The circulatory changes that occur during pregnancy involve modification of vascular structure within the uterus (spiral arteries), the development of a neocirculation (the placenta and the fetus), and a redistribution of blood flow and alteration in circulating blood volume such that the placenta in the third trimester receives 20% of the total maternal circulation and maternal blood volume increases by a similar value. Certain disease processes and certain complications of pregnancy are at least in part mediated by a microvascular abnormality. Thus, for example, impaired trophoblast migration of the spiral arteries is a major component in pre-eclampsia. As a result there has been considerable interest in the application of Doppler techniques to the detection of complications of pregnancy, detection and characterisation of certain fetal abnormalities, as well as an assessment of the value of Doppler in the detection and management of maternal disease.

## THE UTEROPLACENTAL CIRCULATION

The uterine artery is a branch of the anterior division of the internal iliac artery, and divides further into four arcuate arteries, each of which divides into more than 25 spiral arteries. There are therefore between 100 and 200 spiral arteries which enter the intervillus space. During early pregnancy, trophoblast cells invade this space and disrupt the wall of the spiral arteries as part of the process of placental formation. There are two separate waves of invasion. Between implantation and 10 weeks, the trophoblastic invasion is limited to the decidual layer. From about 14 weeks until 22 weeks, the invasion extends as far as the spiral arteries. This invasion of the spiral arteries affects the resistance to blood flow within the spiral arteries and thereby in the arcuate and main uterine arteries.[1]

### Method of examination

The complexity of the uteroplacental circulation makes accurate identification of the vessel under study difficult with either continuous wave or duplex Doppler ultrasound. Flow velocity waveforms are obtained from the lateral lower quadrants of the uterus, angling the transducer on either side of the uterus towards the cervix. Signals achieved in this way are assumed to be originating from the uterine arteries (see Fig. 13.2).[2,3] The uterine arteries are more accurately identified using colour Doppler: the region lateral to the lower uterus is examined and the external iliac artery and the adjacent vein are identified. The uterine artery crosses the external iliac artery on its course from the internal iliac artery to the body of the uterus. In this way more accurate identification of the particular vessel being investigated is achieved. It is important to angle the transducer to improve the angle of insonation whilst maintaining vessel identification on colour Doppler. Spectral waveforms are obtained by placing the pulsed Doppler range gate within the vessel at this point (Fig. 14.1a).[4] The spectral waveform from the normal uteroplacental system is unidirectional, of low pulsatility, and demonstrates frequencies throughout the cardiac cycle (Fig. 14.1b). This is a result of the trophoblastic invasion of the spiral arteries; end-diastolic frequencies increase to a maximum at 24–26 weeks of gestation (see Fig. 14.7).[5]

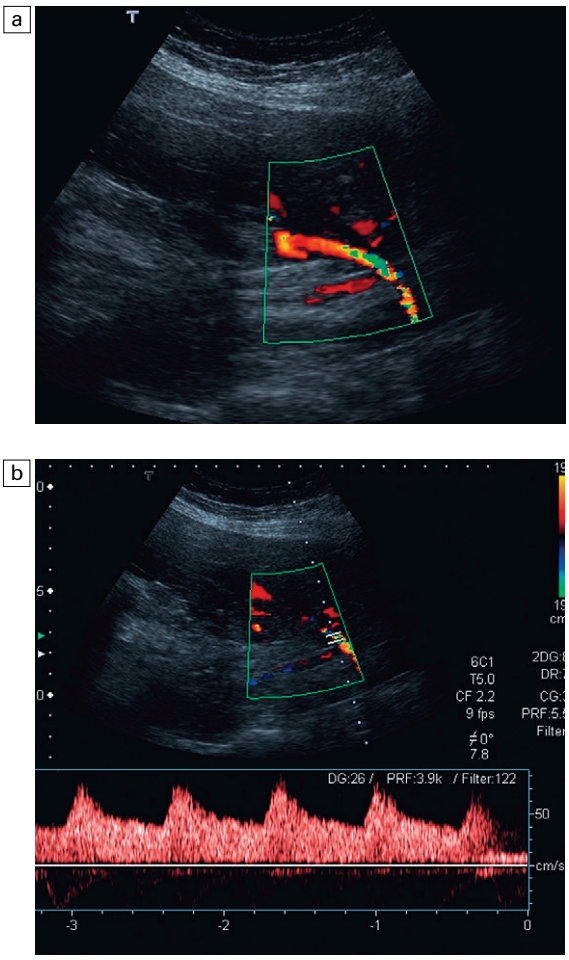


**Fig. 14.1** (a) Course of the left uterine artery as it crosses over the iliac vessels. (b) Normal uterine artery flow in the early third trimester demonstrating high diastolic flow.

It is possible to calculate several indices to quantify waveform analysis; however, the most commonly used in the uterine artery is the resistance index (RI) (Fig. 14.7a). After 26 weeks of gestation the normal range of the resistance index is between 0.45 and 0.58. Decreased end-diastolic flow and consequently raised resistance indices above 0.58 is considered abnormal, as is a notch in early diastole in either uterine artery, suggesting failure of trophoblastic invasion of the spiral arteries (Fig. 14.2).[6,7]

## Problems and pitfalls

A comparative histological study of third-trimester placental biopsy at caesarean section[8] has demonstrated that the uterine artery flow impedance reflects impaired trophoblast migration. Nonetheless, there are a number of reasons for caution. Impedance to flow varies throughout the uteroplacental circulation, with the lowest value seen in the arcuate vessels on the placental side of the uterus and the highest value seen in the uterine arteries on the non-placental side of the uterus.[9] The physiological variations and anatomical complexities of the uteroplacental vascular tree make it difficult to obtain accurate and reproducible measurements using continuous wave Doppler, with interobserver variations ranging from 3.9 to 17%.[10,11] In later pregnancy, between 37 and 40 weeks, maternal position may also alter flow patterns, with the umbilical artery

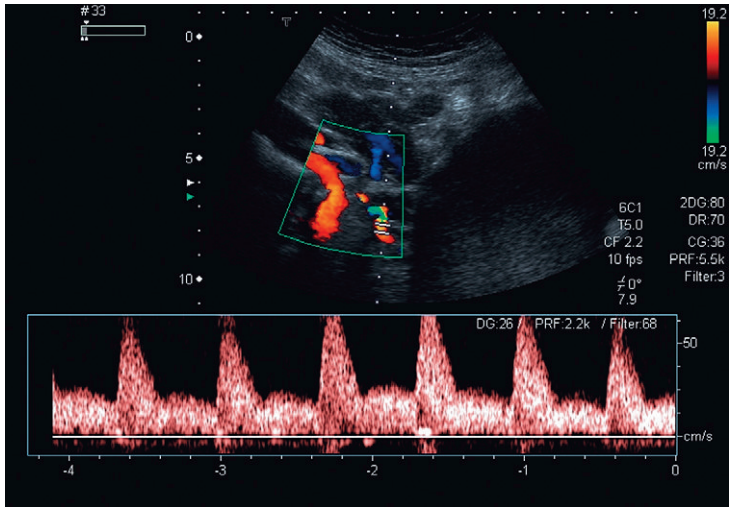


**Fig. 14.2** Uterine artery waveform in intrauterine growth retardation demonstrating low diastolic flow and an early diastolic notch.

resistance being higher in the supine position than in the decubitus.[12] Furthermore, variations in uterine activity (Fig. 14.3), maternal heart rate and exercise also significantly alter the waveform.[13,14] The examination should therefore be performed with the mother resting and only during a period of uterine inactivity. The effect of exercise is more marked in complicated pregnancies, but there are no data evaluating the effect of exercise to improve sensitivity or specificity of Doppler in predicting fetal outcome. The time of day, or recent eating by the mother, do not appear to have an effect on the uterine artery flow.[14,15] Most of the antihypertensive drugs appear to have no effect on fetomaternal blood flow.[16] However, nifedipine appears to produce a reduction in umbilical artery resistance, and this has therefore been suggested as a better drug to use during pregnancy.[17] The effect of smoking on blood flow has been somewhat controversial with researchers reporting either no effect or a significant effect from smoking a cigarette.[18,19] However, because of the dispute and the potential for cigarette smoking to alter flow patterns in chronic smokers, these authors advocate that patients should not smoke for at least 1 h prior to a Doppler study.

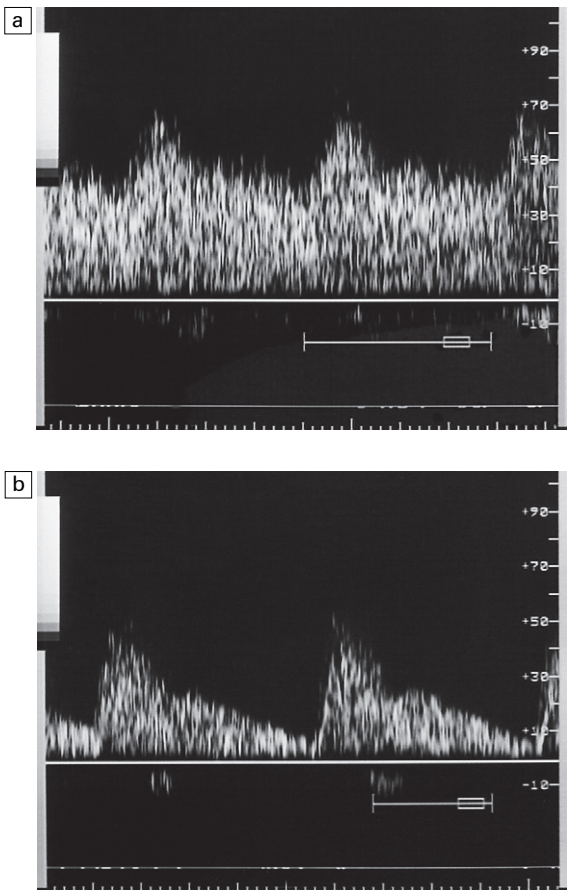


**Fig. 14.3** (a) Uterine artery waveform in labour. Blood flow characteristics in the uterine artery between contractions is normal. (b) During a contraction the overall flow velocity within the uterine artery is reduced. However, the diastolic velocity is reduced further than the peak systolic velocity and there is an early systolic notch.

## Pathology

Although superficially attractive, the use of uterine artery Doppler even in primiparous mothers where the risk of hypertensive complications is greater is neither sensitive nor specific in the detection of pre-eclampsia or small-for-gestational-age infants.[20] This is typical for results seen in low- and moderate-risk pregnancies. The routine use of uterine artery Doppler studies to screen low risk populations for subsequent development of pre-eclampsia and intrauterine growth retardation (IUGR) has a poor positive predictive value. Furthermore, screening can only be useful if there is an intervention available which will improve the outcome, and in obstetrics treatment options for both conditions are limited. Early delivery can only be considered if the pregnancy is sufficiently mature. At present there is no proven intervention to prevent either pre-eclampsia or IUGR. However in a high-risk population the presence of a diastolic notch beyond 24 weeks of gestation may indicate the need for more intensive maternal and fetal surveillance to allow early identification of IUGR or pre-eclamptic toxaemia. This screening technique could potentially be used to rationalise patient care pathways dependant upon their uterine artery Doppler studies.

## Coexistent maternal disease

Uterine artery Doppler appears to be of significantly greater utility when there is pre-existing maternal disease. In chronic renal disease, for

example, an abnormal artery waveform predicts pre-eclampsia and IUGR with a high degree of accuracy. Only 8% of patients with negative Doppler findings in one study developed complications of pregnancy.[21] By contrast, although the resistance index is increased in the uterine arteries of diabetics with a morphological vasculopathy, there is no relationship with short- or long-term diabetic control and it is not a good predictor of diabetes-related fetal morbidity, presumably because these changes are reflecting the risk of acidosis as a result of hypoxia rather than metabolic acidosis.[22,23] In patients with pre-existing, essential hypertension, uterine artery Doppler appears to be useful in defining groups of patients who are at risk of developing complications. If the systolic blood pressure is greater than 140 mmHg, then resistance indices in both uterine arteries is increased. If the systolic blood pressure is less than 140 mmHg, three separate groups may be identified: those with (a) bilateral or (b) unilateral abnormalities of the waveform within the uterine arteries; and (c) those with an entirely normal uterine artery flow. The prognosis appears to be related to the degree of abnormality of uterine artery flow. In systemic lupus erythematosus, one study suggests that an abnormal uterine artery Doppler will identify all those pregnancies with an adverse outcome.[24]

**Table 14.1** Vessels examined by Doppler

| | |
|---|---|
| Maternal | Uterine arteries<br>Arcuate arteries<br>Placental vessels |
| Fetal | Umbilical<br>Aorta<br>Middle cerebral artery<br>Carotid<br>Renal<br>Ductus venosus |

## DOPPLER EXAMINATION OF THE FETOPLACENTAL CIRCULATION

(Table 14.1)

The placenta rather than the lungs is the organ of gaseous exchange in the fetus. Two umbilical arteries convey deoxygenated blood from the fetus to the placenta, and one umbilical vein returns oxygenated blood to the fetal inferior vena cava. The umbilical arteries take origin from the fetal internal iliac arteries coursing alongside the lateral

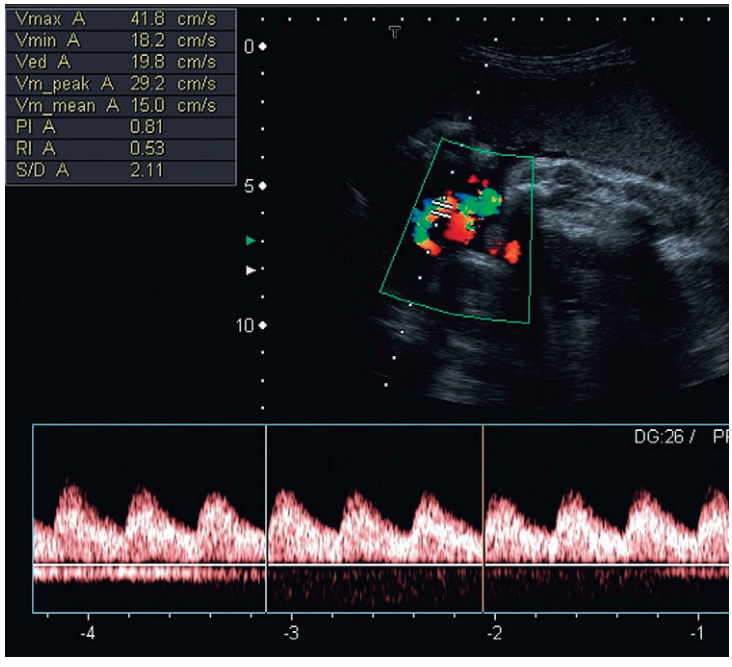


**Fig. 14.4** Normal umbilical artery flow in the third trimester. In the left hand side of the trace coexistent umbilical venous flow is demonstrated. The resistance index is 0.53 and the pulsatility index 0.81.

walls of the bladder in the urachus to the umbilical insertion. The umbilical vein courses posteriorly and cephalad to join the left branch of the portal vein. The oxygenated blood is then shunted through the liver to the inferior vena cava by the ductus venosus. Spectral waveforms from the umbilical artery and vein can usually be easily obtained using continuous wave Doppler ultrasound;[25] a simple Doppler probe is placed on the abdomen and the beam randomly directed into the uterine cavity until the characteristic arterial and venous waveforms are demonstrated (Fig. 14.4). Duplex Doppler allows identification of a loop of cord and the recording of an unambiguous signal from the umbilical vessels. Colour flow Doppler confers *some* advantages on the evaluation of the umbilical artery.

In patients with oligohydramnios it may be the only way to identify a loop of cord. Furthermore, in multiple pregnancies it allows the identification of the individual umbilical arteries.

Ultrasound imaging and colour Doppler allow the optimisation of the angle of insonation to the umbilical vessels and therefore improve clarity of signal reproduction. However, as the Doppler indices relate systolic to diastolic components of flow, optimal angle of incidence is less important. Volume flow assessment within the fetoplacental circulation was much in vogue in the early 1980s but has not found widespread clinical utility and

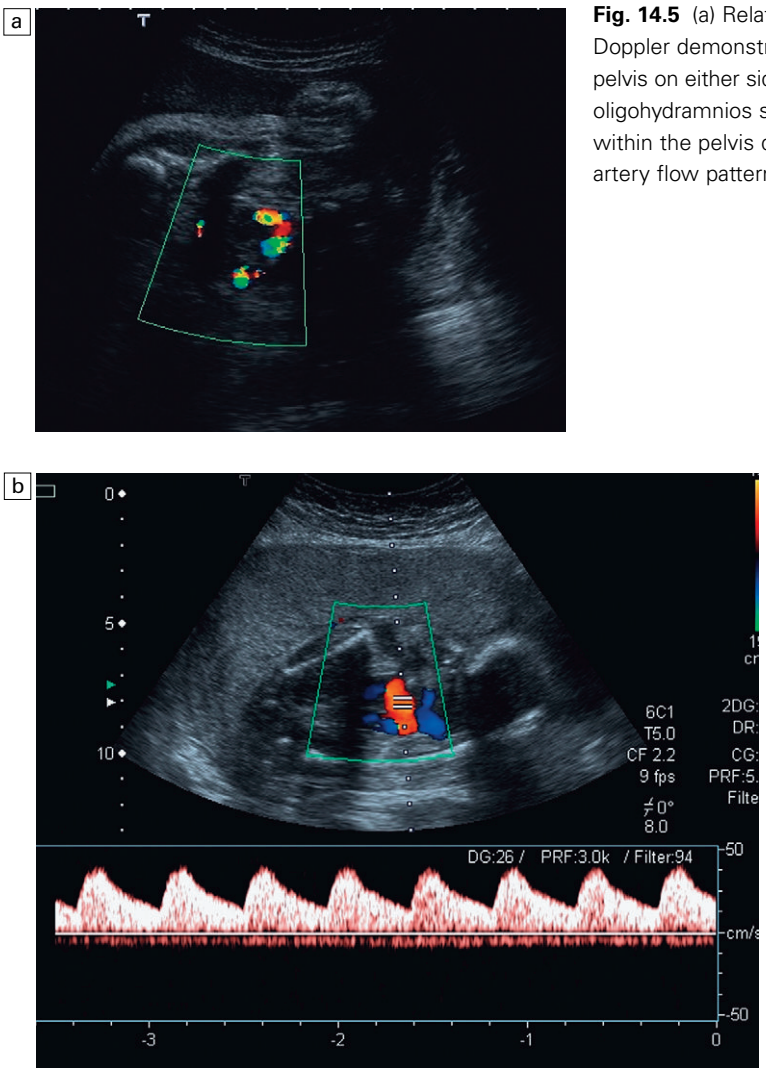


**Fig. 14.5** (a) Relative oligohydramnios. Colour flow Doppler demonstrating umbilical arteries in the pelvis on either side of an empty bladder. (b) Relative oligohydramnios sampling from the umbilical artery within the pelvis demonstrates normal umbilical artery flow patterns.

is not performed in most departments. Early suggestions that different signals were achieved at the placental end of the cord compared to the umbilical end have not been confirmed, and most studies relating abnormal umbilical artery Doppler studies to prenatal outcome relate to sampling of a free loop of umbilical cord. Clinical use of umbilical artery Doppler studies must therefore reflect research results and where possible signals should be recorded from a free loop. However in situations where there is oligohydramnios, and particularly in twin pregnancies with a 'stuck twin', sampling flow from the umbilical arteries within the fetal abdomen as they course alongside the bladder may be the only option to achieve satisfactory Doppler signals (Fig. 14.5).

Doppler waveforms within the umbilical artery change with gestational age in a similar fashion to those of the uterine artery (Fig. 14.6). Resistance and pulsatility indices demonstrate a gradual reduction with increase in gestational age. Normal values of the pulsatility index are shown in Figure 14.7.

## Problems and pitfalls

As end-diastolic values fall, the A/B ratio (peak systole/end diastole) and resistance index tend towards a value of 1. For clinical purposes resistance indices are therefore not sensitive to the quantification of reversed flow, and the pulsatility index is more accurate for situations where there is low, absent or reversed end-diastolic flow. Variations in fetal heart rate[26] and the presence of fetal breathing movement[27] may significantly alter the arterial waveforms, although within the physiological range of 120–160 beats per minute it is not necessary to correct indices for fetal heart rate[28] (Fig. 14.6). Nonetheless, it is important to examine umbilical artery waveforms during a period of fetal inactivity and in the absence of fetal breathing; duplex and colour Doppler ultrasound are of value in enabling the waveform to be sampled rapidly and accurately. Measurement of three consecutive cardiac cycles reduces the coefficient of variation of measurements to less than 5%.[29]

All Doppler devices have inherent filtration which removes low-frequency noise and vessel wall movement artefact. On most current machines the high-pass filter can be varied, but it is important not to set this higher than 100 Hz and preferably lower than 50 Hz, if a false impression of absent diastolic flow is not to be created.

## Pathology and applications

(Tables 14.2–14.4)

### *Intrauterine growth retardation*

Normal waveforms from the umbilical artery are unidirectional and demonstrate forward flow throughout the cardiac cycle. Decreased end-

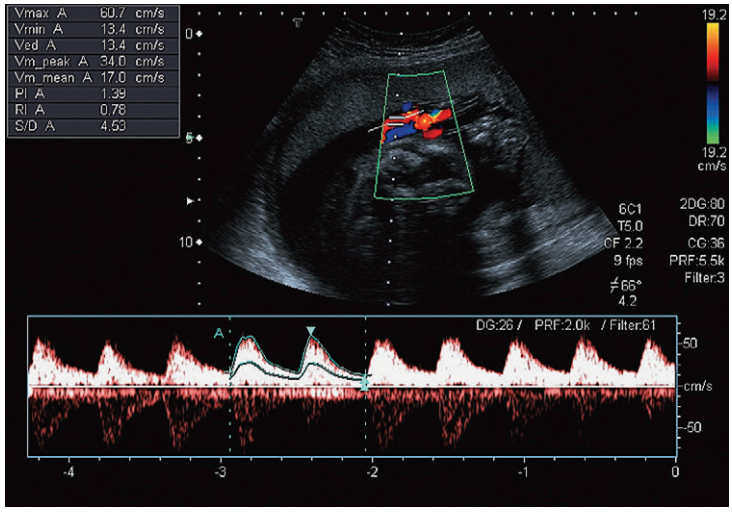


**Fig. 14.6** Umbilical artery waveform at 26 weeks gestation. Note the PI of 1.39 which is just above the mean value for this gestation.

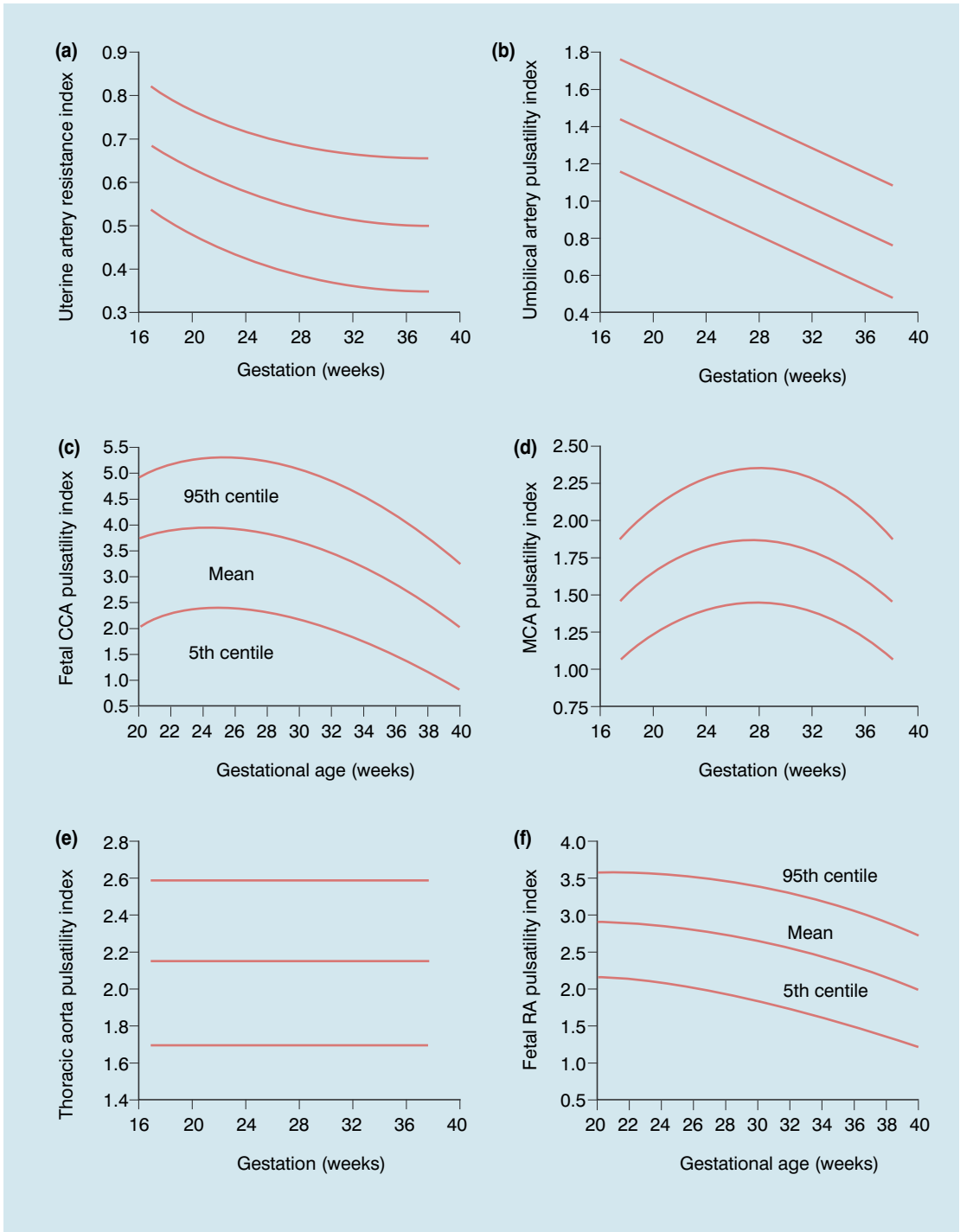


**Fig. 14.7** Normal values during pregnancy for (a) uterine artery resistance index (RI), and (b) umbilical artery pulsatility index (PI). Fetal common carotid artery (CCA) PI (c) falls steeply after 32 weeks gestation, mirrored by the middle cerebral artery (MCA) PI (d). Normal values are also shown for the fetal descending thoracic aorta PI (e) and renal artery (RA) PI (f). Reproduced with permission from Pearce[41].

**Table 14.2** Indications for Doppler examination in pregnancy

| Uterine artery | Umbilical artery | Middle cerebral artery |
|---|---|---|
| ? Screening | Intrauterine growth retardation | Intrauterine growth retardation |
| Pre-existing disease, e.g. renal disease, systemic lupus erythematosus | Post dates | |
| Pre-existing uterine disease | Fetal abnormality | |
| Trophoblastic disease | | |

**Table 14.3** Features of abnormality

| Uterine artery | Umbilical artery | Middle cerebral artery |
|---|---|---|
| Raised indices | Raised indices | Decreased indices |
| Notch | Absent end-diastolic flow | |
| | Reversed end-diastolic flow | Ratio of middle cerebral artery to umbilical artery ≤1 |

**Table 14.4** Factors contributing to abnormal flow

| Uterine artery | Umbilical artery | Middle cerebral artery |
|---|---|---|
| Pre-existing disease | Fetal activity | Direct cerebral compression |
| Exercise | Breathing | |
| Uterine activity | Cord compression | |
| ?Antihypertensives | ?Cigarettes | |
| ?Cigarettes | | |

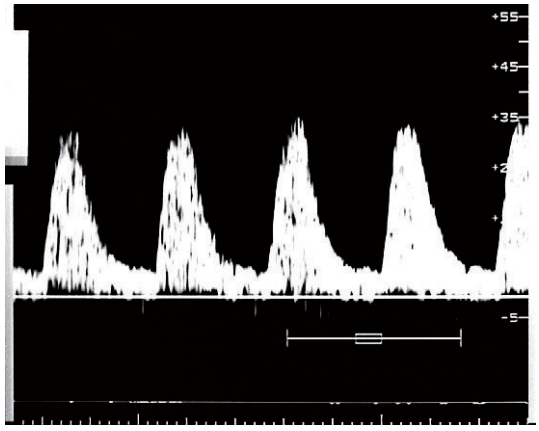


**Fig. 14.8** In intrauterine growth retardation there is reduction of end-diastolic flow.

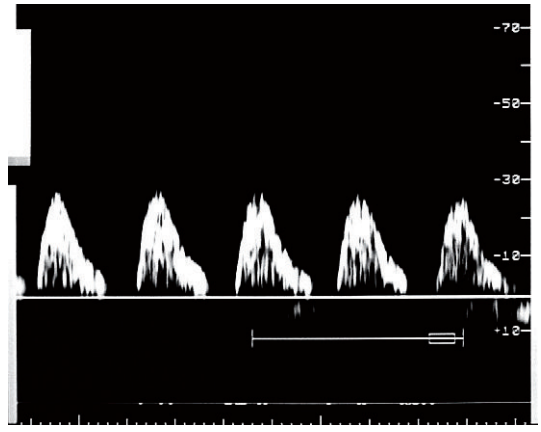


**Fig. 14.9** Severe intrauterine growth retardation with absent end-diastolic flow in the umbilical artery.

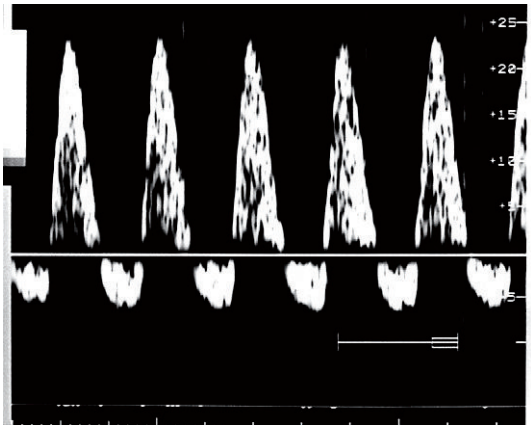


**Fig. 14.10** Reversed diastolic flow in the umbilical artery. This implies a fetus at risk of significant morbidity/mortality.

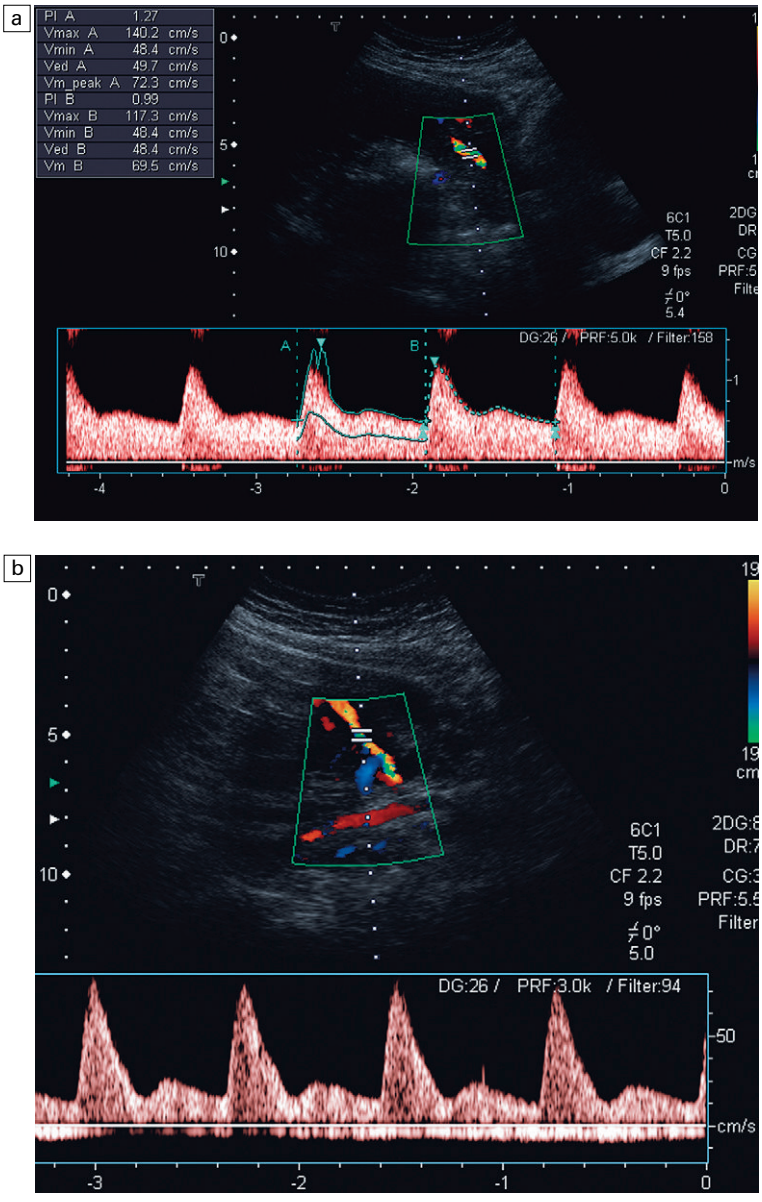


**Fig. 14.11** (a) Normal pattern of flow in the uterine artery on the placental side. (b) Low diastolic flow and persistence of the diastolic notch in the non-placental uterine artery in a patient with previous intrauterine growth retardation.

diastolic flow (Fig. 14.8) and consequently raised Doppler indices are considered abnormal, and are thought to reflect increased placental resistance caused by damage to placental tertiary villi.[30] In more extreme cases, end-diastolic flow may be absent (Fig. 14.9) or even reversed (Fig. 14.10).

Reduction in end-diastolic flow velocities within the umbilical artery waveform is thought to occur as a result of reduced tertiary villi formation and therefore could be an indicator of placental dysfunction, IUGR and fetal distress. In spite of the attraction of the hypothesis that Doppler would provide an early indicator of failure of the tertiary villus, it has not proved of value as a primary screening tool in low risk pregnancies for IUGR. However, in high-risk pregnancies, particularly those in which there is pregnancy-induced hypertension, or which have other clinical or sonographic evidence of fetal growth retardation, the umbilical artery waveform is a good indicator of fetal compromise. Progressive reduction in the diastolic component of umbilical artery flow mirrors the risk and severity of potential fetal compromise.[31,32] Furthermore not only may fetuses at increased risk be identified and managed more intensively, but high-risk pregnancies, such as those with established IUGR or pregnancy-induced hypertension, with normal umbilical artery waveforms appear to carry no greater risk of fetal morbidity or fetal loss than a normal pregnancy. The corrected perinatal mortality rate is reduced when the results of umbilical artery Doppler are made available to clinicians, who are then able to act with more appropriate and timely intervention.[33] The finding of absent or reversed end-diastolic flow in a pregnancy with established IUGR is an indication for the serious consideration of early delivery,[34,35] although there are as yet no precise data indicating the temporal relationship between these end-diastolic flow changes and a subsequent poor outcome. There is some evidence that in pregnancies with previous IUGR, assessment of uterine artery flow will allow the identification of a group of women at high risk of recurrence of third trimester complications. Uterine artery impedance remains high in this group, usually on the non-placental side and there is often an early diastolic notch. Although of potential value in this group there is no established role for uterine Doppler in population screening (Fig. 14.11).

### *Post dates pregnancy*

The management of a post dates pregnancy is extremely difficult. No single parameter has been established that will confidently predict outcome

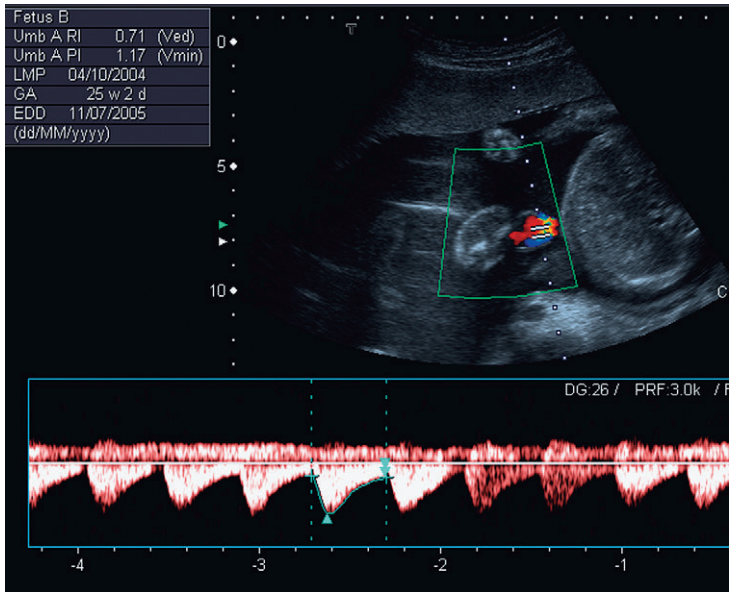


**Fig. 14.12** Umbilical Doppler in twin pregnancy.

a

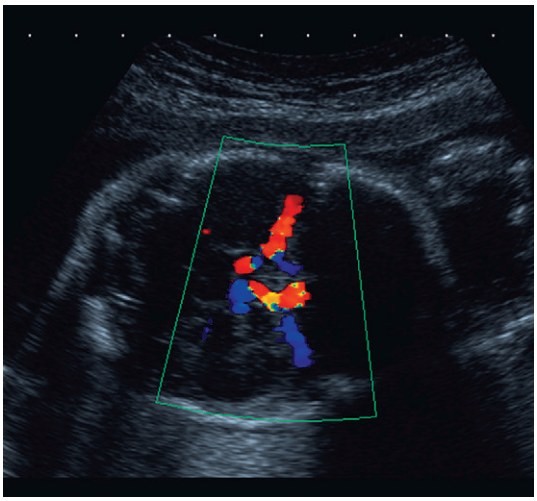

b

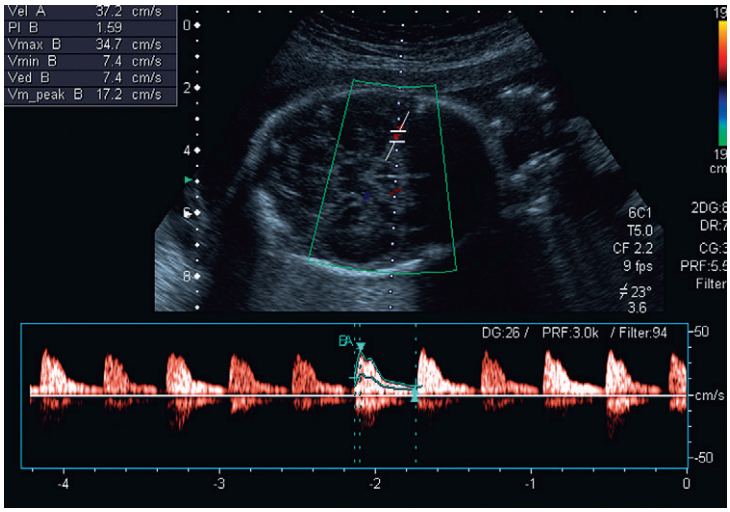


c

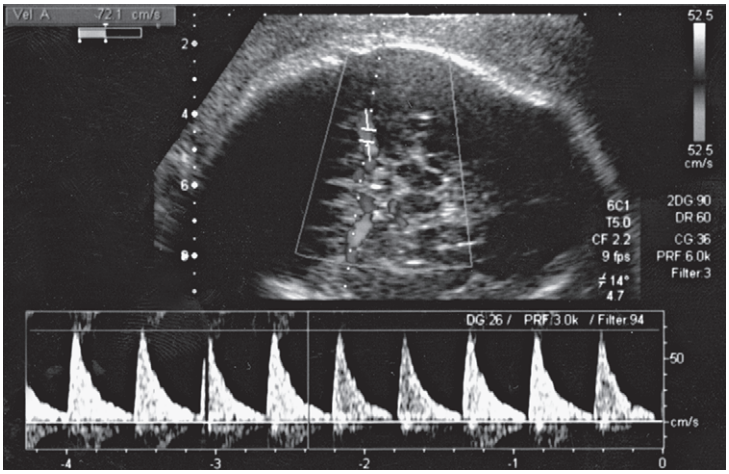


**Fig. 14.13** (a) Colour flow Doppler of the circle of Willis in the fetus. The middle cerebral arteries are demonstrated. (b) Spectral flow within the normal middle cerebral artery. Pulsatility index of 1.6 and a peak velocity of 37 cm $s^{-1}$. (c) Fetal anaemia increase in peak systolic flow velocity to 72 cm $s^{-1}$ is demonstrated.

and, although there has been some enthusiasm for a role for Doppler in the assessment of post dates pregnancy, there is not universal agreement about its value.[36] In these authors' view, therefore, umbilical artery Doppler should be looked upon as one of the factors that may contribute to the monitoring of post dates pregnancies. Absence or reversal of diastolic flow is an indication for immediate delivery, and in this situation an operative delivery may need to be considered. Some authors have advocated the use of the ratio between the Doppler shifts (A/B ratio) in the uterine artery and the fetal middle cerebral artery (UA/MCA ratio) in post-term pregnancy, suggesting that values of <1.05 yield sensitivities of 80% and specificities of 90% in predicting an adverse outcome but this has not been independently confirmed.[37]

### *Twin and higher-order pregnancy*

In uncomplicated multiple pregnancy, there is the same progressive decrease in placental resistance as is seen in singleton pregnancies, with a consequent fall in indices with increasing gestational age. Doppler appears to be of no value in predicting adverse outcomes in unselected pregnancies.[38] However, in pregnancies with discordant growth patterns, Doppler analysis of the umbilical arteries appears to be a useful adjunct to serial growth measurements, allowing recognition of high-risk twin pregnancies which require more intense surveillance[39] (Fig. 14.12).

In twin-to-twin transfusion syndrome, the shared circulation has the result that Doppler waveforms in the umbilical arteries of both twins are similar. Doppler studies of these vessels appear to be of no predictive or management value in this condition, although colour and power Doppler may allow documentation of placental anastomoses and consequent guidance of laser ablation.

In triplet and higher order pregnancies Doppler studies of the umbilical vessels are valuable for the serial surveillance of fetal well-being. Discordant growth with early placental failure becomes more common (in one or more of the fetuses) as the total number of fetuses of a given pregnancy increases. Clinical challenges arise with the management of severe preterm fetal compromise in one or more fetus where preterm delivery of that fetus is indicated, yet can compromise well grown co-fetuses, who can be iatrogenically damaged by preterm delivery. Use of intra-abdominal or abdominal wall insertion umbilical artery Doppler studies is sometimes necessary to be confident of appropriate cord sampling.

### *Diabetes*

Both pre-existing vascular disease and hypertensive disorders of pregnancy are common in mothers with diabetes. In these cases, the value of an abnormal umbilical artery Doppler signal has the same significance in identification of uteroplacental insufficiency as in the non-diabetic population. However, diabetic pregnancies are also at risk of metabolic complications and Doppler flow patterns will not detect these complications, and it is therefore vital that a normal umbilical artery flow does not give either the clinician or the mother false reassurance.[22]

### *Fetal anaemia*

An exciting more recent application of middle cerebral artery Doppler studies is in the field of suspected fetal anaemia due to maternal alloimmunisation. The pregnant woman develops an immune response to paternally derived red-cell antigen that is foreign to the mother and inherited by the fetus. Antibodies may cross the placenta, bind to the fetal red blood cells, causing haemolysis, leading to fetal anaemia. The physiological response to chronic anaemia is the development of a hyperdynamic fetal circulation. Initial studies investigating a potential ultrasound predictor of fetal anaemia looked at many Doppler[40–42] and other parameters such as fetal spleen size.[43] These early studies failed to identify good correlation between ultrasound findings and the presence of fetal anaemia. However, a link between peak velocities of the middle cerebral artery and fetal anaemia was demonstrated[44] (Fig. 14.13). Subsequent studies have shown this technique to be reproducible,[45] and now it has, to a large degree, replaced invasive fetal assessment by amniotic fluid spectroscopy or cordocentesis, both of which carried risks including further sensitisation leading

to exacerbation of the underlying pathology, and pregnancy loss. Use of this technique has accurately predicted anaemic fetuses allowing the timing of any invasive testing (if appropriate) to be at the point when fetal transfusions are clinically required. Middle cerebral artery Doppler peak velocities increase with gestational age.[45]

## Fetal abnormality

Fetuses with autosomal trisomy may also have abnormal placentation with reduced tertiary villi formation.[46] An abnormal umbilical artery waveform should therefore prompt a detailed study of fetal structural anatomy and an assessment of amniotic fluid volume; karyotyping should also be considered.[34] This is particularly important in the presence of early onset growth retardation, (both symmetrical and asymmetrical) which has up to 20% association with abnormal karyotype.

In the presence of a raised alpha-fetoprotein but structurally normal fetus, the appearance of an abnormal uteroplacental Doppler waveform at 20 weeks is associated with a significantly raised perinatal mortality,[47] with the commonest contributor to perinatal mortality being placental abruption. Similarly it has been suggested that fetal and placental morphological features should be combined with Doppler to improve prediction of outcome.[48]

Colour flow Doppler is of value in demonstrating abnormalities of the cord including true knots and a single umbilical artery (Fig.14.14). Similarly the use of colour Doppler will aid in the diagnosis of abdominal wall abnormalities such as omphaloceles and ectopia vesicae (Fig.14.15).

# THE FETAL CIRCULATION

The advent of colour and power Doppler has meant that it is now possible to visualise flow within many of the fetal vessels. These include the aorta, inferior vena cava, carotid, intracerebral and renal arteries. Furthermore, it is possible to study cardiac and cardiopulmonary haemodynamics.

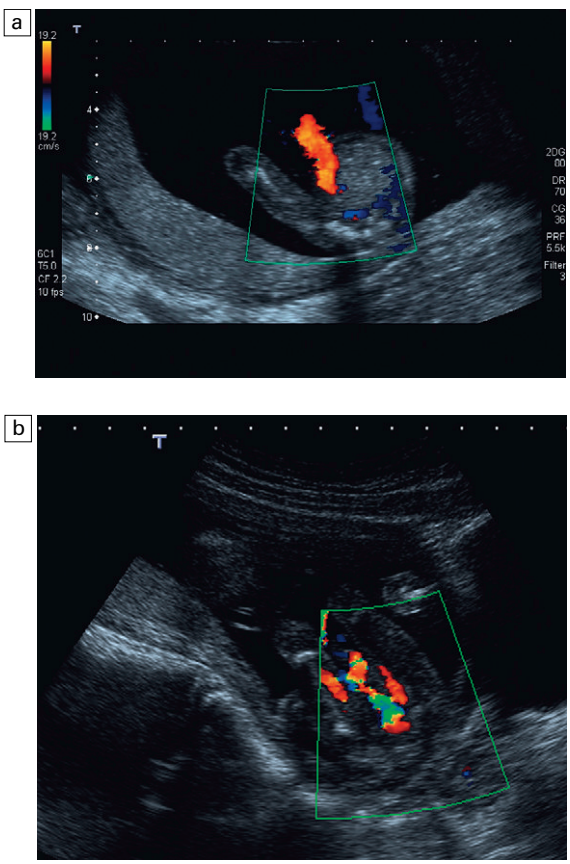


**Fig. 14.14** (a) Colour flow Doppler through the pelvis of a fetus with a single umbilical artery. (b) Single umbilical artery in the pelvis flanked by two femoral arteries.

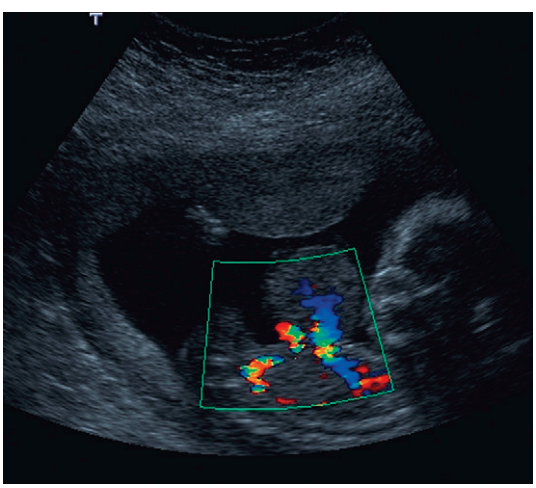

**Fig. 14.15** Omphalocele colour flow Doppler demonstrates abnormal vessels within the anterior abdominal wall defect.

The detailed study of congenital cardiac abnormalities and the role of Doppler techniques are, however, beyond the scope of this chapter.

There is a redistribution of fetal blood flow in response to hypoxia with a selective increase in blood flow to the brain, heart and adrenal glands at the expense of the viscera. This redistribution reflects the morphological findings in IUGR, with the head continuing to grow at the expense of a relatively smaller abdomen. Similarly there is also reduced renal perfusion leading to reduced fetal urine production and hence reduction in amniotic fluid volume in the presence of chronic fetal compromise.

Fetal outcome is thought to relate both to the severity and duration of hypoxia, as well as the gestational age at delivery. It is assumed that hypoxia will tend to increase with increasing gestational age in fetuses with growth retardation and that this will lead to a greater redistribution of blood flow.

## The descending thoracic aorta

The descending thoracic aorta was the subject of significant early research interest since it was thought to afford comparison between the visceral blood supply and cerebral perfusion.[49] Although the waveform has characteristic features and pulsatility and resistance indices are constant throughout gestation[50–52], the haemodynamics of the fetal aorta are complex. Flow within the aorta will reflect flow and impedance not only the visceral vessels and the lower limbs but more especially the umbilical arteries. Thus, while fetal hypoxia may produce alterations in the Doppler waveform of the thoracic aorta, much of the information derived from flow redistribution can also be obtained from examining the umbilical artery waveform. This is generally easier to obtain and, consequently in current routine clinical practice, aortic Doppler studies are very rarely used.

## The fetal cerebral circulation

The common carotid artery can usually be identified on colour Doppler within the neck. It is a relatively straight vessel with a long course and is therefore amenable to pulsed Doppler assessment. The long axis of the vessel is identified and the probe is angled to improve the angle of insonation. The sample volume is placed above the vessel, close to the root of the neck, in order to get a waveform from the common carotid artery and to avoid the external carotid artery.

The middle cerebral artery is the most commonly interrogated of the intracerebral vessels. The skull is scanned as if to perform a biparietal diameter measurement. A colour Doppler examination is then performed in a plane slightly closer to the base of the skull, where the middle cerebral artery will be identified as a vessel coursing towards the probe from the circle of Willis in the Sylvian fissure (Fig. 14.13a). Later in gestation the location of the middle cerebral artery can be identified without colour Doppler simply by demonstrating pulsations within the brain substance. Placement of the sample volume either within these pulsations or within the colour signals will allow recording of the Doppler waveforms.

The common carotid artery pulsatility index remains constant until 32 weeks of gestation and then falls steeply (Fig. 14.7c)[50–52] and this is mirrored by changes seen in the middle cerebral artery (Fig. 14.7d).[53]

The mean pulsatility index of the middle cerebral artery is 2 (SD 0.48) at 20 weeks falling to 1.15 (SD 0.18) at 37 weeks. Fetal haemodynamics suggest a brain sparing effect in IUGR and evidence of cerebral redistribution by a decrease in the pulsatility index in the presence of established growth retardation is commonly considered an indicator for delivery.[54,55] The presence of abnormal Doppler studies can also aid in the postnatal management of growth restricted neonates who are at greater risk of ischaemic complications such as necrotising enterocolitis due to their intrauterine adaptations to a suboptimal environment.[56,57] Clinicians vary as to at what stage in the progress of the growth retardation at any given gestation the fetus should be delivered, given the absence of a clear temporal relationship between an abnormal pulsatility index reduction and incidence of ischaemic complications.[58] Data suggesting decompensation of the cerebral circulation and a consequent increase in the

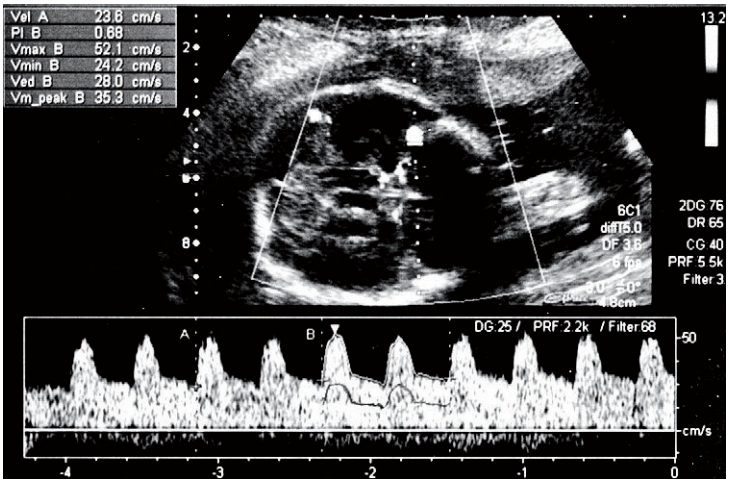


**Fig. 14.16** Middle cerebral artery flow in severe fetal compromise. There is marked reduction of diastolic flow as evidence of cerebral redistribution. The features imply ischaemic complication.

pulsatility index are scanty but this may represent evidence of irreversible ischaemic change (Fig. 14.16). In spite of variation in clinical practice, immediate delivery versus delay does not appear to impact on neonatal or long-term outcomes. It is suggested that the variation in practice simply reflects appropriate clinical response to a wide variety of clinical and laboratory data of which middle cerebral artery Doppler is only one.

## The renal arteries

Oligohydramnios consequent upon poor renal perfusion is cardinal sign of IUGR. Although Doppler evaluation of the renal arteries is technically feasible and Doppler spectra can be recorded (Fig. 14.7f)[59] the fetal kidneys only receive 3% of the fetal cardiac output and the renal artery velocities are low. As a result, demonstration of variation of flow and impedance indices within the renal arteries is an insensitive and unreliable indicator of fetal compromise. It is not clear whether increased sensitivity of ultrasound equipment, particularly to low flow states, will alter this.

Colour Doppler of the renal vessels may also be used to assess congenital renal abnormalities, such as renal agenesis, where the artery is also absent, although care should be taken as hypoplastic arteries may be difficult to demonstrate on ultrasound, and enlarged adrenal glands supplied by large adrenal vessels may be misidentified as kidney (Fig. 14.17).

## The ductus venosus

The ductus venosus is an embryological channel which connects the fetal umbilical vein with the inferior vena cava and hence the right heart. In the fetus it carries most of the blood from the umbilical vein to the right atrium.

The ductus venosus is identified within the liver by following the umbilical vein in a sagittal plane into the fetal liver using colour Doppler. The ductus venosus arises at the junction of the umbilical vein and the right branch of the portal vein angling posteriorly and cephalad towards the inferior vena cava with which it makes an angle

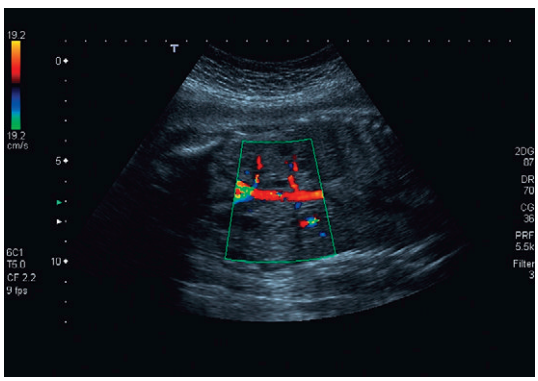


**Fig. 14.17** Coronal colour flow Doppler image of the fetus. There are two renal arteries, one of which arises from the iliac artery.

of 45 to 60°. Colour flow will demonstrate a high velocity pattern with aliasing at low pulse repetition frequency (Fig. 14.18).

Normal Doppler blood flow studies of the ductus venosus show a triphasic forward flowing cycle reflecting ventricular systole, ventricular diastole and atrial systole (Fig. 14.19). Spectral analysis can therefore be used to reflect fetal ventricular function and cardiac afterload (Fig. 14.20). In the presence of end-stage hypoxaemia with hypoxic cardiomyopathy, there is a fall in cardiac function, and hence rise in central venous pressure. This can be identified by reverse flow in the ductus venosus. Presence of reverse flow is associated with decreased fetal maternal perfusion and fetal death.[60,61] In severely growth restricted fetuses where the gestational age is close to viability, use of this technique can help guide the clinician in the exact moment at which delivery is required.

In the presence of a thoracic space occupying lesion, ductus venosus studies can aid in assessing the degree of cardiac restriction. Reduction in flow velocity and reversal of flow may occur.

## Placental abnormalities

The diagnosis of placenta praevia is largely performed by ultrasound imaging. Transabdominal ultrasound has fallen into some disrepute because of reported incidences of low-lying placenta in excess of 40%[62] when scanning is performed before the last trimester; routine screening for placenta praevia in the second trimester is therefore not now widely used. By contrast, when there is antepartum haemorrhage, ultrasound is used to establish the relationship of the placenta to the internal os. This is more commonly now performed using transvaginal ultrasound. The addition of colour Doppler allows the demonstration of the rare but potentially serious vasa praevia. In this situation a vessel, or vessels, can be seen coursing from the margin of the placenta in close proximity to, or covering, the internal os. Similarly, other placental abnormalities can be documented: velamentous insertion of the cord can be identified with colour Doppler and chorioangioma can be differentiated from a placental haematoma by the demonstration of a rich vascular supply.[63]

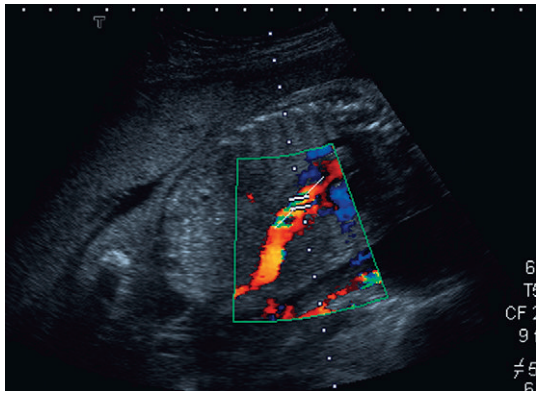

**Fig. 14.18** Oblique scan through the fetal abdomen with colour flow Doppler demonstrating the aliased flow within the ductus venosus. The Doppler sample volume is placed within the area of maximum aliasing.

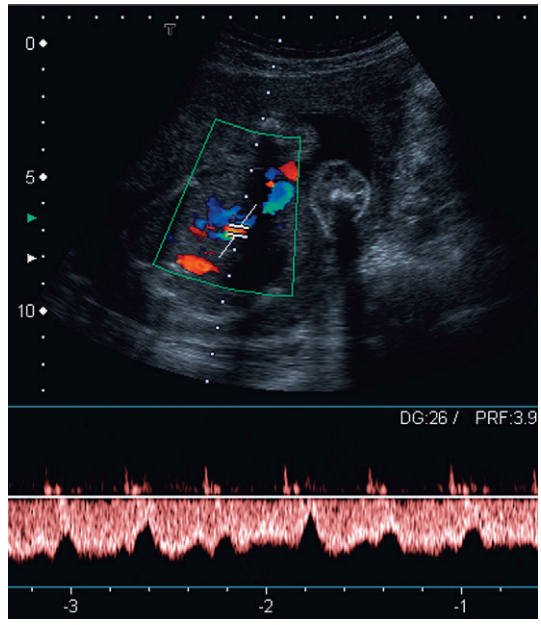


**Fig. 14.19** Normal spectral flow within the ductus venosus.

### *Postpartum*

A small amount of postpartum haemorrhage is a normal feature but where haemorrhage is prolonged, or heavy, the possibility of retained products of conception must be considered.

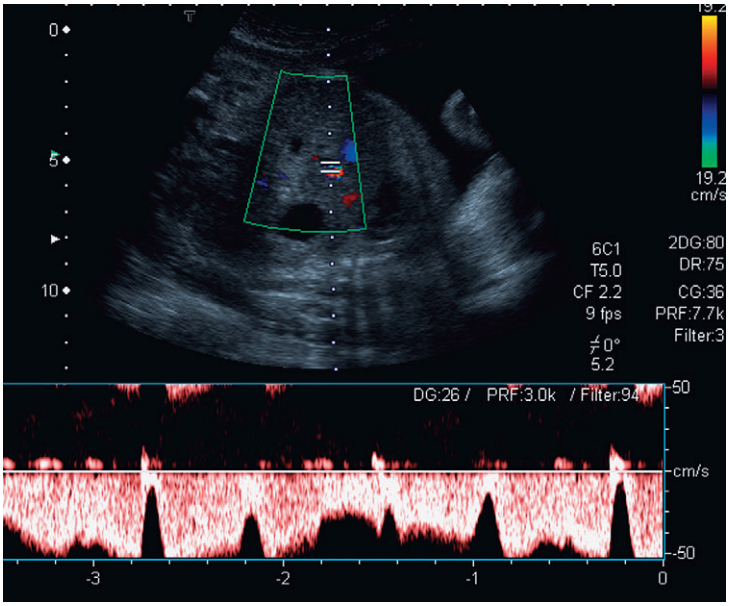


**Fig. 14.20** Intermittent flow reversal within the ductus venosus in a cardiac dysrhythmia.

Transvaginal ultrasound will frequently demonstrate abnormalities within the uterine cavity. As a general rule brightly reflective structures are taken to represent retained placental fragments and/or membrane; while echo-poor contents are thought to represent fresh or clotted blood. However, it is frequently difficult to differentiate between retained products of conception and uncomplicated blood clot.

There is a difference in the blood flow characteristics of the uterine artery when there are retained products of conception. Patients with residual trophoblast exhibit a resistance index in the myometrial vessels of 0.35 ± 0.1 whereas those without residual trophoblast have resistance indices in the myometrial vessels of 0.54 ± 0.15. However, the combination of low-impedance flow and intrauterine material is common after

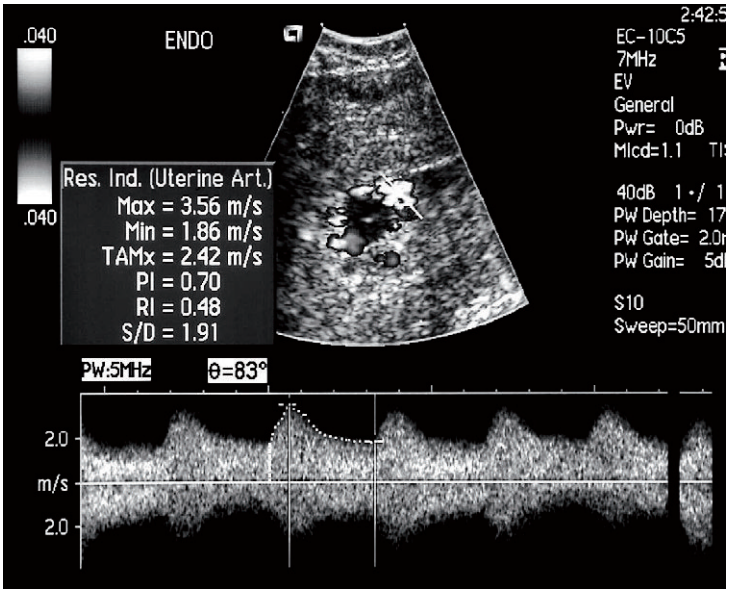


**Fig. 14.21** Spectral Doppler in retained products of conception. The resistance index of 0.48 implies residual trophoblast.

abortion and does not necessarily imply retained products of conception. It may simply reflect physiological involution; the temporal course of return to non-pregnant flow characteristics in the uterine vessels has not been documented[64] (Fig. 14.21).

## TROPHOBLASTIC DISEASE

Transvaginal ultrasound will demonstrate uterine abnormalities in persistent gestational trophoblastic tumour. However, the sensitivity of ultrasound imaging is only 70% but abnormal uterine artery waveforms are seen in 90% of cases with persistent gestational trophoblastic tumour, and raised uterine artery impedance may predict resistance to chemotherapy.[65,66] However, magnetic resonance imaging (MRI) appears to be more sensitive in the detection of trophoblastic tumour, being more accurate at identifying myometrial invasion and therefore establishing a diagnosis of choriocarcinoma.

## MATERNAL HAEMODYNAMICS

Pregnancy is associated with marked changes in maternal haemodynamics. There is an increase in circulating blood volume with a corresponding increase in the cardiac output. This might be expected to have effects on blood flow to a number of the intra-abdominal organs, in addition to the effect that it has on uterine blood flow. Furthermore, it might be hoped that certain conditions, particularly associated with pregnancy and thought to be mediated through an abnormality in maternal physiology, might be reflected in changes in blood flow characteristics detectable by Doppler.

### Doppler ultrasound of the maternal kidney in pregnancy

Doppler blood flow characteristics to the maternal kidney appear to alter little during pregnancy. Although certain authors report a slight reduction in the mean resistance index in renal artery examinations, this is not statistically significant. There is no doubt that volume flow is increased in pregnancy but this appears to be mediated largely by vasodilatation of the large supply vessels, although the absolute changes in flow velocity have not been investigated. There is no change in pulsatility or resistance indices in patients with essential hypertension.[70] There has been no documented change in these indices in pregnancy induced hypertension. However there is significant increase in acceleration time within the intrarenal vessels. This is suggestive of proximal vasospasm as being at least partly responsible for the pathogenesis of pregnancy induced hypertension.[71,72]

There is no change in Doppler indices in patients presenting with progressive physiological dilatation of the collecting system of the kidneys during pregnancy. In the past this has been attributed to a combination of a hormonal effect, together with a degree of mechanical obstruction of the ureter by the enlarging uterus. There is no correlation between the degree of dilatation of the collecting system and any change in the resistance index in uncomplicated cases, but it may be clinically useful in cases of suspected obstruction where Doppler ultrasound may show a significant difference between the affected and unaffected kidney. The obstructed kidney will usually show a resistance index differing by 0.04 or more than that in the unobstructed kidney. In these authors' department, resistance indices are used as a discriminator in deciding which patients with loin pain in association with pregnancy should proceed to an intravenous urogram[73] (see Ch. 8).

### Haemodynamic changes in other vessels

There is naturally a decrease in the resistance index in the aorta and common iliac arteries which reflects the increased flow to the uterus that occurs during pregnancy. However, there are also changes in the flow patterns in other vessels consequent upon changes in volume flow. There is, for example, an increase in volume flow through the portal vein and consequently in the hepatic veins. In the hepatic veins this affects not only the volume of flow but also the Doppler waveform where the

normal pulsatile flow is lost in most patients. This occurs as early as the first trimester in some patients and therefore does not appear to be related to pressure effects from the enlarging uterus. This is of limited diagnostic significance except that some authors have suggested that changes in hepatic venous flow might be useful in the assessment of diffuse liver disease, including pregnancy-related liver disease. However, there is no correlation between liver disease in pregnancy and changes in hepatic venous flow, whatever the severity.[74]

## CONCLUSIONS

The role of Doppler in obstetrics is becoming a mature technology. The advent of colour Doppler has enabled more precise examination of the uteroplacental and fetoplacental circulations, together with more intricate examination of the fetal vasculature. However, this is an expensive modality and its benefits beyond a research tool have yet to be established. Combined analysis of the uteroplacental and fetoplacental (umbilical) circulation may increase diagnostic accuracy.[75] However, fetomaternal haemodynamics are complex, showing variation in their response to many maternal and fetal physiological and pathological states. It is possible, even likely, that other factors will influence fetal maternal blood flow. Currently Doppler methods appear capable only of detecting gross changes in placentation and gross changes of fetal well-being. For example, umbilical artery waveforms may be normal in a morphologically normal but small placenta. Similarly, chronic hypoxia induces placental changes which are presumably responsible for the altered waveform in umbilical and fetal vessels. However, in experimentally induced acute hypoxia there is no alteration in fetomaternal flow as detected by Doppler techniques.[76]

In the same way, the role of uterine artery Doppler in the management of pregnancy is not clear cut. While apparently of value in patients with pre-existing maternal disease, its findings are not sufficiently sensitive or specific, nor does the use of screening Doppler affect perinatal morbidity and outcome.[77] Doppler ultrasound cannot be recommended as a screening procedure for the identification of pregnancy complications in low-risk pregnancies. Doppler examination of the uterine and umbilical arteries between 18 and 26 weeks of gestation in high-risk pregnancies may be predictive of significant pregnancy complications, but at present there is insufficient evidence to suggest that the level of surveillance in the Doppler-negative group can be relaxed. If a relatively safe, cheap and effective treatment for early-onset maternal placental disease becomes established, such as antioxidant therapy, then uteroplacental waveform screening may prove useful in deciding upon early treatment.

Doppler has most potential in the management of high-risk pregnancies such as those with pre-existing maternal disease, previously identified placental disease and those at high risk of fetal IUGR or where IUGR is already established. Umbilical artery studies help identify fetuses at risk of hypoxia and acidaemia; when the results are applied clinically they contribute to reduced perinatal mortality rates. Doppler ultrasound of the fetal circulation may identify chronic hypoxia and there is evidence that documentation of redistribution of flow is important in the identification of fetal compromise (Tables 14.3 and 14.4). Doppler ultrasound has significantly impacted in the care of maternal alloimmunisation pregnancies at risk of severe fetal anaemia. Middle cerebral artery peak velocity measurements have now superceded routine invasive monitoring, which is highly likely to lead to a reduction in fetal loss in this condition.

It is likely that the future lies in comparative investigation of the uteroplacental umbilical and one or more fetal vessels and the development of more sophisticated parameters of flow dynamics.

It is important, however, to stress that fetomaternal haemodynamics are not the only indicator of maternal or placental disease, or of fetal well-being. Doppler ultrasound may contribute to, but not replace, other methods of fetal and maternal surveillance.

## REFERENCES

1. Pijnenborg R, Dixon G, Robertson WB, et al. Trophoblastic invasion of human decidua from 8 to 18 weeks of pregnancy. Placenta 1980; 1:3–19.
2. Bewley S, Campbell S, Cooper D. Uteroplacental Doppler flow velocity waveforms in the second-trimester. A complex circulation. Br J Obstet Gynaecol 1989; 96:1040–1046.
3. Schulman H, Winter D, Farmakides G, et al. Doppler examinations of the umbilical and uterine arteries during pregnancy. Clin Obstet Gynecol 1989; 32:738–745.
4. Bower S, Vyas S, Campbell S, et al. Colour Doppler imaging of the uterine artery in pregnancy: normal ranges of impedance to blood flow, mean velocity and volume flow. Ultrasound Obstet Gynecol 1992; 2:261–265.
5. Schulman H, Fleischer A, Farmakides G, et al. Development of uterine artery compliance in pregnancy as detected by Doppler ultrasound. Am J Obstet Gynecol 1986; 155:1031–1036.
6. Fleischer A, Schulman H, Farmakides G, et al. Uterine artery Doppler velocimetry in pregnant women with hypertension. Am J Obstet Gynecol 1986; 154:806–813.
7. Bower S, Schuchter K, Campbell S. Doppler ultrasound screening as part of routine antenatal screening: prediction of pre-eclampsia and growth retardation. Br J Obstet Gynaecol 1993; 100:989–994.
8. Voigt HJ, Becker V. Doppler flow measurements and histomorphology of the placental bed in uteroplacental insufficiency. J Perinat Med 1992; 20:139–147.
9. Kofinas AD, Espeland M, Swain M, et al. Correcting umbilical artery flow velocity waveforms for fetal heart rate is unnecessary. Am J Obstet Gynecol 1989; 160:704–707.
10. Rightmire DA, Campbell S. Fetal and maternal Doppler blood flow parameters in postterm pregnancies. Obstet Gynecol 1987; 69:891–894.
11. Bewley S, Cooper D, Campbell S. Doppler investigation of uteroplacental blood flow resistance in the second trimester: a screening study for pre-eclampsia and intrauterine growth retardation. Br J Obstet Gynaecol 1991; 98:871–879.
12. Qu LR, Kan A, Masahiro N. Fetal circulation in relation to various maternal body positions. Chung Hua Fu Chan Ko Tsa Chih 1994; 29:589–591.
13. Mulders LG, Jongsma HW, Wijn PF, et al. The uterine artery blood flow velocity waveform: reproducibility and results in normal pregnancy. Early Hum Dev 1988; 17:55–70.
14. Morrow R, Ritchie K. Doppler ultrasound fetal velocimetry and its role in obstetrics. Clin Perinatol 1989; 16:771–778.
15. Hastie SJ, Howie CA, Whittle MJ, et al. Daily variability of umbilical and lateral uterine wall artery blood velocity waveform measurements. Br J Obstet Gynaecol 1988; 95:571–574.
16. Duggan PM, McCowan LM, Stewart AW. Antihypertensive drug effects on placental flow velocity wave forms in pregnant women with severe hypertension. Aust N Z J Obstet Gynaecol 1992; 32:335–338.
17. Hirose S, Yamada A, Kasugai T, et al. The effect of nifedipine and dipyridamole on the Doppler blood flow waveforms of umbilical and uterine arteries in hypertensive pregnant women. Asia Oceania J Obstet Gynaecol 1992; 18:187–193.
18. Castro LC, Allen R, Ogunyemi D, et al. Cigarette smoking during pregnancy: acute effects on uterine flow velocity waveform. Obstet Gynecol 1993; 81:551–555.
19. Morrow RJ, Ritchie JW, Bull SB. Maternal cigarette smoking: the effects on umbilical and uterine blood flow velocity. Am J Obstet Gynecol 1998; 159:1069–1071.
20. North RA, Ferrier C, Long D, et al. Uterine artery flow velocity waveforms in the second trimester for the prediction of pre-eclampsia and fetal growth retardation. Obstet Gynecol 1994; 83:378–386.
21. Ferrier C, North RA, Becker G, et al. Uterine artery waveform as a predictor of pregnancy outcome in women with underlying renal disease. Clin Nephrol 1994; 42:362–368.
22. Johnstone FD, Steel JM, Haddad NG, et al. Doppler umbilical artery flow velocity waveforms in diabetic pregnancy. Br J Obstet Gynaecol 1992; 99:135–140.
23. Ben-Ami M, Battino S, Geslevich Y, et al. A random single Doppler study of the umbilical artery in the evaluation of pregnancies complicated by diabetes. Am J Perinatol 1995; 12:437–438.
24. Kofinas AD, Penry M, Simon NV, et al. Interrelationship and clinical significance of increased resistance in the uterine arteries in patients with hypertension or pre-eclampsia or both. Am J Obstet Gynecol 1992; 166:601–606.
25. Fitzgerald DE, Drumm JE. Non-invasive measurement of human fetal circulation using ultrasound: a new method. Br Med J 1977; 2:1450–1451.
26. Giles WB, Trudinger BJ, Baird PJ. Fetal umbilical artery flow velocity waveforms and placental resistance: pathological correlation. Br J Obstet Gynaecol 1985; 92:31–38.
27. Mires G, Dempster J, Patel NB, Crawford JW. The effect of fetal heart rate on umbilical artery flow velocity waveforms. Br J Obstet Gynaecol 1987; 94:665–669.
28. Gill RW, Trudinger BJ, Garrett WJ, et al. Fetal umbilical venous flow measured in utero by pulsed

Doppler and B-mode ultrasound. Am J Obstet Gynecol 1980; 139:720–725.
29. Kofinas AD, Penry M, Swain M, et al. The effect of placental laterality on uterine artery resistance and development of pre-eclampsia and intrauterine growth retardation. Am J Obstet Gynecol 1989; 161:1536–1539.
30. Erskine RLA, Ritchie JWK. Umbilical artery blood flow characteristics in normal and growth-retarded fetuses. Br J Obstet Gynaecol 1985; 92:605–610.
31. McParland P. Modern approach to the poorly grown fetus. Ir Med J 1992; 85:88–89.
32. Trudinger BJ, Cook CM, Giles WB, et al. Fetal umbilical artery velocity waveforms and subsequent neonatal outcome. Br J Obstet Gynaecol 1991; 98:378–384.
33. Neilson JP. Doppler ultrasound in high-risk pregnancies. In: Enkin MW, Keirse MJNC, Renfrew MJ, et al, eds. Pregnancy and childbirth module. Cochrane Database of Systematic Reviews, No. 03889. London: BMJPublishing; 1993.
34. Poulain P, Palaric JC, Paris-Liado J, et al. Fetal umbilical Doppler in a population of 541 high-risk pregnancies: prediction of perinatal mortality and morbidity. Doppler Study Group. Eur J Obstet Gynecol Reprod Biol 1994; 54:191–196.
35. Devoe LD, Gardner P, Dean C, et al. The significance of increasing umbilical artery systolic-diastolic ratios in the third-trimester pregnancy. Obstet Gynecol 1992; 80:684–687.
36. Zimmermann P, Alback T, Koskinen J, et al. Doppler flow velocimetry of the umbilical artery, uteroplacental arteries and fetal middle cerebral artery in prolonged pregnancy. Ultrasound Obstet Gynecol 1995; 5:189–197.
37. Devine PA, Bracero LA, Lysiliewicz A, et al. Middle cerebral to umbilical artery Doppler ratio in post date pregnancies. Obstet Gynecol 1994; 84:856–860.
38. Faber R, Viehweg B, Burkhardt U. Predictive value of Doppler ultrasound findings in twin pregnancies. Zentralbl Gynäkol 1995; 117:353–357.
39. Giles WB, Trudinger BJ, Cook CM, et al. Umbilical artery flow velocity waveforms and twin pregnancy outcome. Obstet Gynecol 1988; 72:894–897.
40. Nickolaides KH, Fontanarosa M, Gabbe SG, et al. Failure of ultrasonographic parameters to predict the severity of fetal anaemia in rhesus isoimmunization. Am J Obstet Gynecol 1988; 158:920–926.
41. Copel JA, Grannum PA, Green JJ, et al. Pulsed Doppler flow-velocity waveforms in the predicition of fetal hematocrit of the severely isoimmunized pregnancy. Am J Obstet Gynecol 1989; 161:341–344.
42. Hercher K, Snijders R, Campbell S, et al. Fetal venous, arterial, and intracardiac blood flows in red blood cell isoimmunisation. Obstet Gynecol 1995; 85:122–128.
43. Bahodo-Singh R, Oz U, Jones D, et al. Fetal spleen size in anaemia due to Rh-alloimmunization. Obstet Gynecol 1998; 92:828–832.
44. Vyas S, Nicolaides KH, Campbell S. Doppler examination of the middle cerebral artery in anaemic fetuses. Am J Obstet Gynecol 1990; 162:1066–1068.
45. Mari G. Noninvasive diagnosis by Doppler ultrasonography of fetal anemia due to maternal red-cell alloimmunization. N Engl J Med 2000; 342:9–14.
46. Rochelson B, Kaplan C, Guzman E, et al. A quantitative analysis of placental vasculature in the third-trimester fetus with autosomal trisomy. Obstet Gynecol 1990; 75:59–63.
47. Pearce JMF. The application of uteroplacental waveforms to complicated pregnancies. In: Pearce JMF, ed. Doppler ultrasound in perinatal medicine. Oxford: Oxford University Press; 1992:173–174.
48. Jauniaux E, Ramsay B, Campbell S. Ultrasonographic investigation of placental morphologic characteristics and size during the second trimester of pregnancy. Am J Obstet Gynecol 1994; 170:130–137.
49. European Association of Perinatal Medicine. Regulation for the use of Doppler technology in perinatal medicine. In: Consensus of Barcelona. Barcelona: Instituto Barcelona; 1989:22–26.
50. Bilardo CM, Campbell S, Nicolaides KH. Mean blood velocity and flow impedence in the fetal descending thoracic aorta and common carotid artery in normal pregnancy. Early Hum Dev 1988; 18:213–217.
51. Lingman G, Marsal K. Fetal central blood circulation in the third trimester of normal pregnancy – a longitudinal study; aortic and umbilical blood flow. Early Hum Dev 1986; 13:137–150.
52. Griffin D, Bilardo K, Masini L, et al. Doppler blood flow waveforms in the descending thoracic aorta of the human fetus. Br J Obstet Gynaecol 1984; 91:997–1002.
53. Vyas S, Nicolaides KH, Bower S, et al. Middle cerebral artery flow velocity waveforms in fetal hypoxaemia. Br J Obstet Gynaecol 1990; 97:797–803.
54. Rowlands DJ, Vyas SK. Longitudinal study of fetal middle cerebral artery flow velocity waveforms preceding fetal death. [Comment in Br J Obstet Gynaecol 103(8):852.] Br J Obstet Gynaecol 1995; 102:888–890.
55. Laurin J, Lingman G, Marsal K, et al. Fetal blood flow in pregnancies complicated by intrauterine growth retardation. Obstet Gynecol 1987; 69:895–902.
56. Hackett GA, Campbell S, Gamsu H, et al. Doppler studies in the growth-retarded fetus and

prediction of neonatal necrotising enterocolitis, haemorrhage, and neonatal morbidity. Br Med J 1987; 294:13–16.
57. Laurin J, Marsal K, Persson PH, et al. Ultrasound measurements of fetal blood flow in predicting fetal outcome. Br J Obstet Gynaecol 1987; 94:940–948.
58. The GRIT trial study group. Infant wellbeing at 2 years of age in Growth Restriction Intervention Trial (GRIT): mulitcentred randomized controlled trail. Lancet 2004; 364:513–520.
59. Vyas S, Nicolaides KH, Campbell S. Renal artery flow velocity waveforms in normal and hypoxemic fetuses. Am J Obstet Gynecol 1989; 161:168–172.
60. Gudmunsson S, Tulzer G, Huhta JC, et al. Venous Doppler velocimetry in fetuses with absent end-diastolic blood velocity in the umbilical artery. J Matern Fetal Invest 1993; 3:196.
61. Baschat AA, Gembruch U. Triphasic umbilical venous blood flow with prolonged intrauterine survival in intrauterine growth retardation. Ultrasound Obstet Gynecol 1996; 8:201–205.
62. Marsal K, Lindblad A, Lingman G, et al. Blood flow in the descending aorta: intrinsic factors affecting fetal blood flow, i.e. fetal breathing movements and cardiac arrhythmia. Ultrasound Med Biol 1984; 10:339–348.
63. Vyas S, Campbell S, Bower S, et al. Maternal abdominal pressure alters fetal cerebral blood flow. Br J Obstet Gynaecol 1990; 97:740–742.
64. Scherjon SA, Kok JH, Oosting H, et al. Fetal and neonatal cerebral circulation: a pulsed Doppler study. J Perinatol Med 1992; 20:79–82.
65. Ott W. Placenta praevia. Ultrasound Obstet Gynecol 1993; 139:1493–1494.
66. Heinonen S, Ryynanen M, Kirkinen P, et al. Perinatal diagnostic evaluation of velamentous umbilical cord insertion: clinical, Doppler, and ultrasonic findings. Obstet Gynecol 1996; 87:112–117.
67. Dillon EH, Case CQ, Ramos IM, et al. Endovaginal ultrasound and Doppler findings after first-trimester abortion. Radiology 1993; 186:87–91.
68. Dobkin GR, Berkowitz RS, Goldstein DP, et al. Duplex ultrasonography for persistent gestational trophoblastic tumor. J Reprod Med 1991; 36:14–16.
69. Long MG, Boultbee JE, Langley R, et al. Doppler assessment of the uterine circulation and the clinical behaviour of gestational trophoblastic tumours requiring chemotherapy. Br J Cancer 1992; 66:883–887.
70. Zeeman GG, McIntire DD, Twickler DM. Maternal and fetal artery Doppler findings in women with chronic hypertension who subsequently developed superimposed pre-eclampsia. J Matern Fetal Neonat Med 2003; 14(5):318–323.
71. Myake H, Nakai A, Kshino T, et al. Doppler velocimetry of maternal renal circulation in pregnancy induced hypertension. J Clin Ultrasound 2001; 29(8) 449–455.
72. Nakai A, Asakura H, Oya A, et al. Pulsed Doppler US findings of renal interlobar arteries in pregnancy induced hypertension. Radiology 1999; 213(2):423–428.
73. Weston MJ, Dubbins PA. The diagnosis of obstruction: colour Doppler ultrasonography of renal blood flow and ureteric jets. Curr Opin Urol 1994; 4:69–74.
74. Roobottom CA, Hunter JD, Weston MJ, et al. Hepatic venous Doppler waveforms: changes in pregnancy. J Clin Ultrasound 1995; 23:477–482.
75. Campbell S, Hernandez CJ, Cohen-Overbeek T, et al. Assessment of fetoplacental and uteroplacental blood flow using duplex pulsed Doppler ultrasound in complicated pregnancies. J Perinat Med 1984; 12:261–265.
76. Trudinger BJ, Giles WB, Cook CM. Flow velocity waveforms in the maternal uteroplacental and fetal umbilical placental circulations. Am J Obstet Gynecol 1985; 152:155–163.
77. Newnham JP, O'Dea MR, Reid KP, et al. Doppler flow velocity waveform analysis in high-risk pregnancies: a randomised control trial. Br J Obstet Gynaecol 1991; 98:956–963.

# Microbubble ultrasound contrast agents

# 15

Jonathan D. Berry and Paul S. Sidhu

## BACKGROUND

The principle of ultrasound microbubble contrast agents is based on the selective augmentation of echo strength. Unlike other imaging modalities, the majority of which have benefited from contrast enhancing agents for many years, contrast enhancement in ultrasound is a relatively new concept. The phenomenon was first observed when during echocardiography an injection of indocyanine green through a catheter resulted in transient echo enhancement in the region of the catheter tip.[1] This observed enhancement was the result of small air bubbles forming in the region of the catheter tip and strongly reflecting the ultrasound beam back towards the transducer. Following this observation much research has been undertaken in both establishing the physics of ultrasound contrast enhancement as well as developing agents for clinical use.

## CHARACTERISTICS OF MICROBUBBLE ULTRASOUND CONTRAST

Ultrasound contrast agents in current use are typically small (<10 μm in diameter, approximately the size of an erythrocyte) gas filled bubbles (Fig. 15.1). Microbubble contrast agents are physiologically inert, non-toxic and pass through the pulmonary circulation following intravenous injection. The microbubbles contain either air or an inert gas, encapsulated either by a membrane of surfactant only, a soft shell or a firm shell.

The intense echo enhancement observed with microbubbles is a result of their compressibility. A microbubble undergoes volumetric oscillation while being insonated, to a greater degree than a rigid sphere of similar size, and consequently scatters more energy. In addition there is a fortuitous relationship between the size of microbubble that is able to pass through a capillary and that which will resonant at frequencies typically used in medical imaging (3 MHz).[2] As such, at the resonant frequency the returning echoes from a microbubble are maximised in such an effective manner that these microbubbles behave as though they are $10^{14}$ times larger than in reality.[3]

Microbubbles are better able to resist compression than expansion, and consequently as the acoustic power of the ultrasound increases complex non-linear movements of the bubbles occur. The resultant signals emitted from the microbubbles display harmonic characteristics at both fractions and multiples of the insonating frequency. These features can be utilised in the optimisation of contrast to tissue signal ratio. Ultimately as acoustic power is increased physical disruption of the microbubbles begins to occur, a feature that may be used to therapeutic advantage.[4]

## SAFETY OF MICROBUBBLE CONTRAST

Microbubbles are injected intravenously where the volumes of gas involved (typically less than 200 μL) are considered non-hazardous. The safety profile of microbubble contrast agents in general is extremely favourable when compared to other

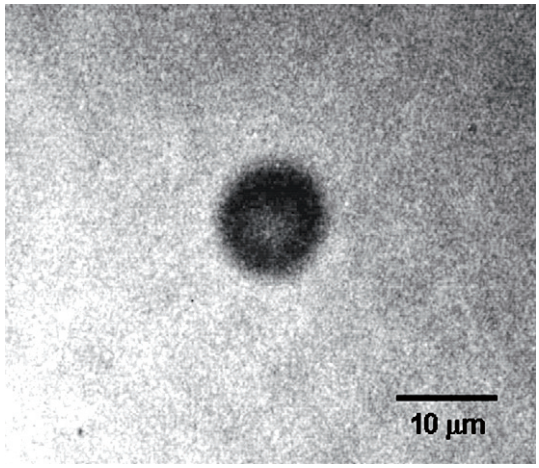


**Fig. 15.1** Electron microscopy of a microbubble (SonoVue®); ultrasound microbubble contrast agents in current use are typically small (<10 µm in diameter) gas filled bubbles. Courtesy of Bracco International BV.

radiographic contrast agents.[5] Limited data suggests that microvascular rupture may occur when gas bubbles are insonated and there is a theoretical risk of injury should structures where vascular damage may be critical, for example the eye or brain, are examined.[6]. Microembolism of particles is a potential hazard. Evidence exists that single microbubbles do not pose a significant embolic risk but if coalescence of particles occurs the evidence is less clear.[7] It is likely that the structure of the microbubbles influences coalescence with, for example, albumin-based shells being unlikely to coalesce.[8] Current ultrasound guidelines recommend that a maximum mechanical index (MI) of 1.9 for diagnostic imaging should not be exceeded; whether this is relevant in the context of microbubble use is unknown.

## COMMERCIALLY AVAILABLE CONTRAST AGENTS

The need to form biologically and physically stable microbubbles in commercial quantities in a simple, cost effective fashion has led to the development of a variety of microbubble technologies. Commercially available contrast agents in Europe approved for transpulmonary transit at the time of writing include Levovist® (Schering AG), Optison® (Amersham Health) and SonoVue® (Bracco International B.V.).[6] Definity® (Bristol-Myers Squibb Medical Imaging) is licensed in North America for cardiac use only.

### Levovist®

In a similar manner as bubbles form on imperfections of the surface of a glass containing a carbonated drink, galactose microcrystals will provide a nidation site upon which air bubbles form in Levovist®, an example of a surfactant encapsulated microbubble.[9] Palmitic acid is the added surfactant that stabilises the bubbles allowing their transit across the pulmonary circulation. Even so, these microbubbles are fragile and disruption of the bubbles occurs at mechanical indexes used for standard B-mode imaging. To overcome this, intermittent imaging and low frame rates must be employed to allow refilling of the vasculature with microbubbles; for example using intermittent imaging of myocardial perfusion triggered by echocardiography to limit bubble bursting.[10] Licensed clinical indications for the use of Levovist® are cardiac, abdominal and transcranial imaging.

### Optison®

Unlike Levovist® which utilises air as the gas agent, both Optison® and SonoVue® use larger gas molecules; perfluoropropane in the case of Optison®. These have the advantage of being long lived relative to air. Excretion of the gas is ultimately via the pulmonary route. Albumin provides the soft shell of the Optison® microbubble and the only licensed clinical indication for use at present is in cardiac imaging.

### SonoVue®

Introduced in 2001, SonoVue® consists of sulfur hexafluoride encased by a phospholipid soft shell.[11] Formation of the microbubbles is achieved by hand mixing of provided carrier fluid and freeze dried powder. Once mixed the bubbles remain stable in the vial for several hours until required for use. The stability of this formulation in vivo allows real time imaging to

occur for several minutes following administration. Licensed clinical indications for use of this agent include cardiac, vascular, liver and breast applications.

### Definity®

Licensed in North America for cardiac use only, Definity® consists of lipid-stabilised octafluoropropane gas. The indication for use is to opacify the left ventricular chamber and to improve the delineation of the left ventricular endocardial border.

A summary of the features of the above agents is provided in Table 15.1.

## ULTRASOUND TECHNOLOGIES USED IN CONTRAST IMAGING

Optimising visualisation of microbubbles has required the development of specific ultrasound imaging modes. Manufacturers attach a variety of propriety names to the techniques employed; however there are several common themes.

### Harmonic imaging

Insonating microbubbles at a given frequency will result in the emission of energy at multiples of the insonating frequency and by tuning reception to only these emitted frequencies, to form an image or Doppler signal, clutter signals from surrounding tissue will be suppressed. An advancement on this technique makes use of the fact that, given the correct conditions of pressure and frequency, microbubbles will scatter the insonating beam at subharmonic frequencies, usually half the insonating frequency.[12] While this technique has the potential of enhancing differentiation between tissues and microbubbles it is currently limited by the need for a narrow band of insonating signals. Such problems are likely to be overcome with further research.[2]

### Phase inversion imaging

Phase or pulse inversion imaging (PII) achieves improved signal to clutter ratio similar to harmonic imaging. Unlike harmonic imaging, PII has the advantage of maintaining spatial resolution in B-mode imaging since it is not compromised by the formers narrow band pulse.[13] PII involves transmission of an initial imaging wave following at a suitable delay by a second wave which is an inverted copy of the original.[14] The resultant echo if these two waves were scattered linearly would be zero. However, as microbubbles are non-linear scatters, the sum of the two signals after encountering a microbubble will not be zero[15] (Fig. 15.2). In addition to the ability to use a wider bandwidth than in harmonic imaging, PII allows relatively low insonating pressures (low MI) therefore reducing the risk of microbubble disruption. This technique allows for continuous real time imaging during the various vascular phases, allowing detection of vascular patterns peculiar to different liver tumours. This technique works best with a robust microbubble agent such as SonoVue®.

**Table 15.1** Characteristics of commercially available ultrasound contrast agents

| Brand name | Producer | Gas | Stabilisation | Applications |
|---|---|---|---|---|
| Levovist® | Schering | Air | Galactose/ Palmitic acid | Cardiac<br>Abdominal<br>Transcranial |
| Optison® | Amersham Health | Perfluoropropane | Sonicated albumin | Cardiac |
| SonoVue® | Bracco | Sulfur hexafluoride | Phospholipids | Cardiac<br>Vascular<br>Hepatic<br>Breast |
| Definity® | Bristol-Myers-Squibb Medical Imaging | Octafluropropane | Phospholipids | Cardiac |

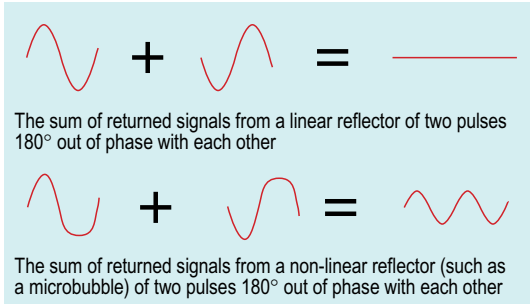


**Fig. 15.2** The concept of phase or pulse inversion imaging involves transmission of an initial imaging wave followed at a suitable delay by a second wave which is an inverted copy of the original. The resultant echo if these two waves were scattered linearly would be zero but as microbubbles are non-linear scatters, the sum of the two signals after encountering a microbubble will not be zero.

## Stimulated acoustic emission

Although the theories and nomenclature regarding this mode of imaging have been the matter of some debate,[16] stimulated acoustic emission (SAE) refers to the strong transient signals associated with microbubble disruption when imaged using two-dimensional (2D) Doppler mode.[16] The principle of this imaging technique relies on the fact that if a microbubble lies in the beam of a train of insonating pulses then disruption of the microbubble by the first pulse in the train will result in an apparent large Doppler shift. This will be registered on screen as extremes in the colour Doppler scale or even what appears to be aliasing. In reality there has been no large movement to account for these extreme changes; it is simply the disappearance of a microbubble. As such, stationary microbubbles are as equally well visualised as ones moving within blood vessels.

SAE has found application in the study of, for example, focal liver lesions using Levovist®.[17,18] By avoiding imaging the organ of interest while the microbubble contrast agent is in the blood pool phase (approximately 2–5 min after injection) early destruction of the microbubbles is prevented. Levovist® uniquely remains in the liver (and splenic tissue) in the late phase. Subsequent imaging demonstrates the normal liver parenchyma to have colour signal whereas malignant tumours will present as defects within this colour pattern (Fig. 15.3). The technique appears sensitive with SAE improving conspicuity of liver metastasis relative to B-mode imaging.[17]

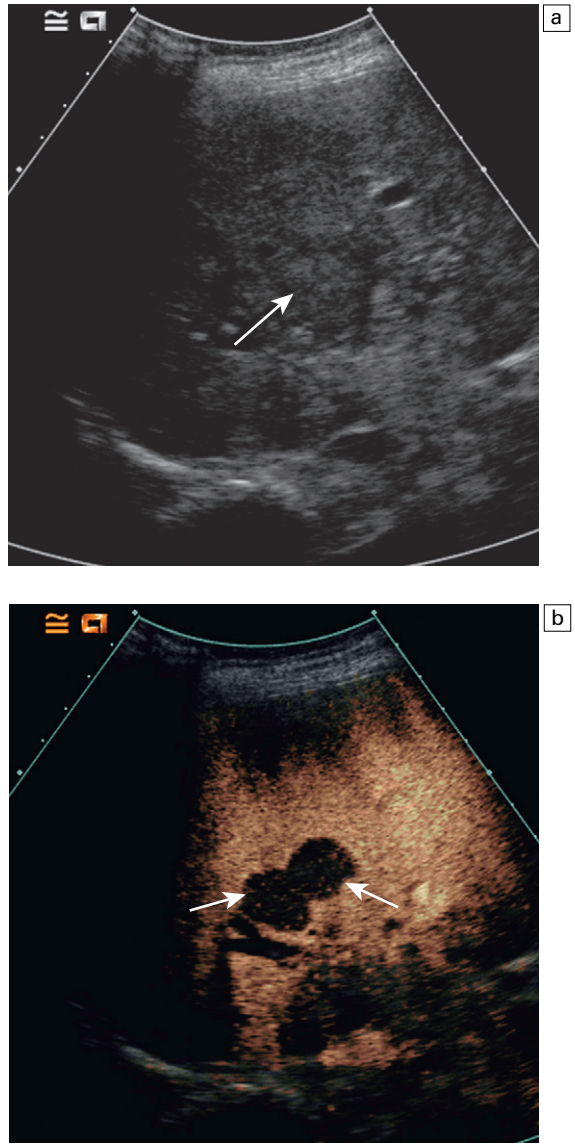


**Fig. 15.3** Agent Detection Imaging (ADI®, Acuson Siemens, Mountain View, CA), a form of late phase destructive imaging; (a) baseline image of the right lobe of the liver with a suggestion of an abnormality (arrow); (b) ADI® in the late phase using Levovist®, demonstrates two lesions with absence of microbubble contrast within the lesions in keeping with metastatic disease (arrows).

## Quantification techniques

Quantification of microbubbles may take several forms including time to arrival, wash-in/wash-out characteristics, time to peak and area under a curve.[3] The situation is complicated by virtue of the fact that there is, unlike for example computed tomography (CT) Hounsfield units, no single variable unit of measurement for ultrasound contrast which can be reliably and reproducibly measured. Furthermore, colour contrast enhancement is subject to multiple artefacts including motion artefact from patient or operator movement which, in long examinations, can be difficult to avoid.

Strategies for attaining 'quantification analyses' include; measurement of the back-scattered signal and Doppler intensity, both of which are related to the microbubble concentration. Using proprietary software regions of interest may be drawn and analysis pre- and postcontrast achieved.

# ARTEFACTS

One of the most commonly seen artefacts when using microbubbles to enhance conventional Doppler studies is that of 'blooming' in which colour pixels appear to extend beyond the bounds of the vessel (Fig. 15.4). The phenomenon may prove problematic when objective computer analysis of contrast enhancement is required. While the problem in part arises from multiple re-reflections between adjacent microbubbles, it is also in part due to limitations of the hardware analysis of the Doppler signal, a problem which may be overcome with technological improvements. A further artefact resulting from limitations in the ultrasound hardware is the apparent reversal of Doppler flow following administration of contrast. This effect represents overloading of the Doppler circuitry and once appreciated is easily recognised.

The administration of contrast may render high velocity signals, which precontrast were not detectable, now detectable.[19] Whilst this may initially appear to be a desirable effect it proves problematic when absolute angle-corrected values are essential to clinical decision making, for example in assessment of internal carotid artery narrowing. Although adding a further layer of

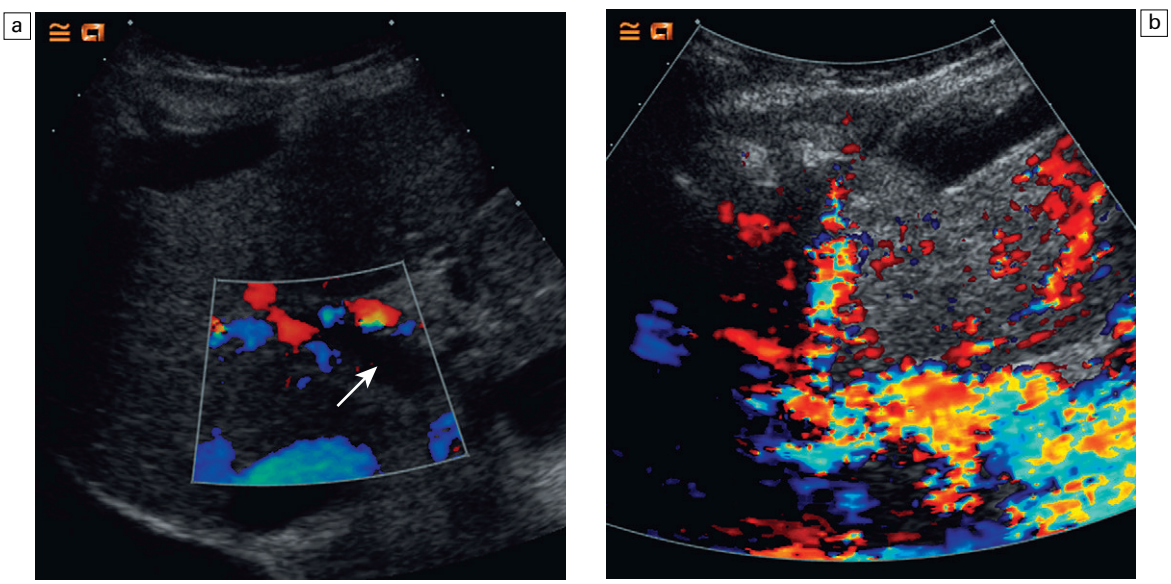


**Fig. 15.4** A commonly seen artefact when using microbubbles to enhance conventional Doppler studies is 'blooming' in which colour pixels appear to extend beyond the bounds of the vessel; (a) baseline colour Doppler image at the level of the porta hepatis demonstrating absence of colour signal in the portal vein (arrow) but colour is present in the overlying hepatic artery; (b) following the administration of SonoVue® 'blooming' from the hepatic artery obscures the portal vein.

complexity to the measurement, the problem may be overcome by use of peak systolic ratios to define limits rather than absolute velocity values.

Sharp spikes of Doppler 'noise' may occasionally be seen (Fig. 15.5). Such effects may arise from collapse of the microbubbles or aggregation of microbubbles.[13]

## CLINICAL APPLICATIONS OF MICROBUBBLE CONTRAST

### Cardiac

Cardiology represents the single greatest area of use of microbubble contrast agents with several established and evolving applications.

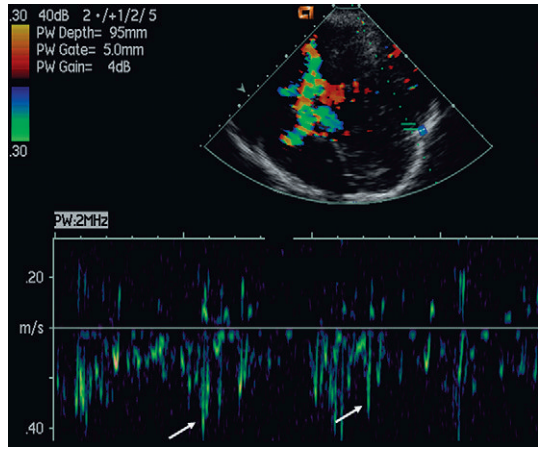


**Fig. 15.5** Sharp spikes of Doppler 'noise' (arrows) are seen in the spectral Doppler trace obtained from a transcranial ultrasound examination following the administration of Levovist®, arising from collapse of the microbubbles or aggregation of microbubbles.

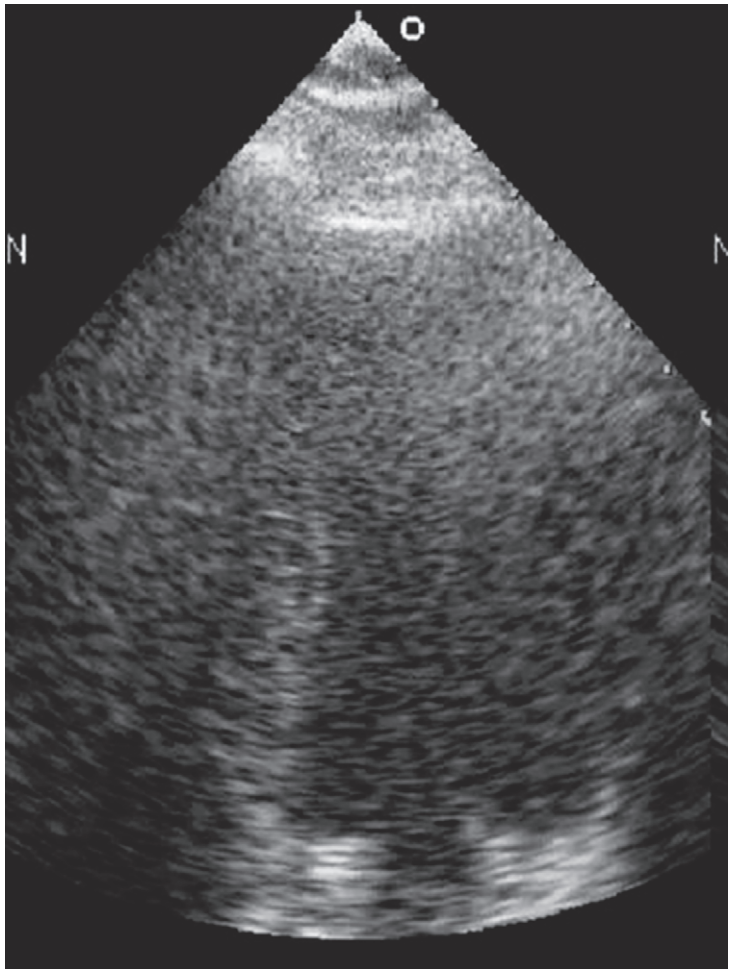


**Fig. 15.6** Apical four chamber view using tissue harmonic imaging (a) in an intensive care unit patient with very poor imaging windows. The patient had been recovering slowly post cardiac surgery and the request was to assess left ventricular function (LV) function. Image quality was so poor that no comment could be confidently made about LV function.

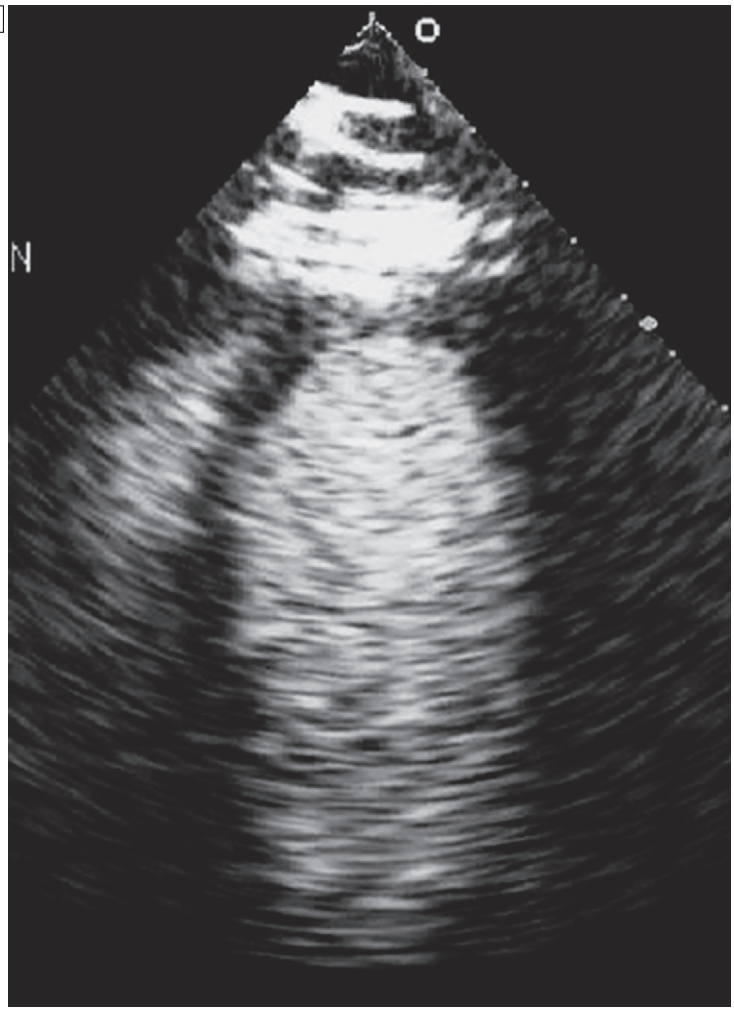


**Fig. 15.6** cont'd Before proceeding to perform a transoesophageal echo a microbubble contrast study was performed using a 0.3 mL injection of Optison® through an existing intravenous line and power modulation low mechanical index contrast imaging (b). Evaluation of the LV endocardial border was significantly enhanced, especially at the apex and the lateral wall, allowing an accurate assessment of LV function without needing to proceed to a transoesophageal echo. The improvement in image quality was even more evident on real-time images than on these still frames. (Copyright MJ Monaghan).

### *Echocardiography*

Microbubble ultrasound contrast allows improved delineation of the endocardial border and detection of wall motion abnormalities.[20,21] This is particularly true in the 10–20% of routine echocardiograms which are technically difficult, for example in lung disease or obesity, where up to 74% of otherwise non-diagnostic studies are 'rescued' by the use of microbubble contrast[22] (Fig. 15.6). Unlike isotope studies, contrast echocardiography is a mobile technique which may be performed at the bedside, avoids the need for ionising radiation and with consequent cost benefits to be gained. Use of microbubble contrast allows additional information regarding regional and global left ventricular function to be acquired during a stress echocardiography examination. Furthermore valvular disease may be more accurately assessed.[3]

### *Myocardial perfusion*

Assessment of myocardial perfusion offers potential for the diagnosis of acute myocardial infarction as well as assessing myocardium which is at risk of infarction and that which has responded to thrombolytic therapy. With use of a more robust microbubble formulation in addition to the development of low MI techniques allows a more comprehensive myocardial assessment. Furthermore, the application of intermittent high power pulses to destroy the microbubbles allows assessment of rate of refilling of the myocardium

microcirculation so providing a measure of microcirculation flow speed.[22]

### *Coronary arteries*

Localisation and quantification of degree of coronary artery stenosis may be performed using intermittent harmonic imaging techniques. Analogous to the assessment of microcirculation described above, coronary artery flow rate may be calculated by intermittent destruction of microbubbles and measurement of time taken to refill.[22]

## Liver

The histological architecture, rich vascular supply and superficial nature, allows the liver to be suited to interrogation with microbubble ultrasound contrast agents. A variety of different contrast agents have been employed to study the liver; consequently, much of our understanding regarding microbubble contrast has been gained from studies of liver pathology.[23,24]

### *Focal liver lesions*

One of the most promising areas of use for microbubble contrast agents is in the study of focal liver lesions. In clinical terms two important aspects of analysis of focal liver lesions are detection and then characterisation into benign and malignant.

In the healthy liver approximately 70% of the blood is supplied by the portal vein with the remaining 30% by the hepatic artery. Venous drainage for the majority of the liver (except the caudate lobe which drains directly into the inferior vena cava) is via the left, right and middle hepatic veins into the inferior vena cava. Analogous to the phases seen with CT and iodinated contrast, microbubble ultrasound contrast displays an early (arterial) phase at around 20 s post intravenous administration followed by a portal venous phase at approximately 90–120 s. Depending on the formulation of the microbubble contrast agent there is then a late phase, greatest with Levovist®, as the agent is cleared from the liver parenchyma. This late phase differs in its pharmacokinetics from the clearance of iodinated radiographic contrast, and is likely to be attributable to uptake of microbubble contrast by normal functioning cells.

Several studies have demonstrated improved detection of liver lesions using microbubble contrast.[25,26] Much of the early data refers to the use of delayed imaging of Levovist® during the late liver specific phase, using the technique of SAE. In these studies malignant focal liver lesions generally appear as defects in an otherwise enhancing liver parenchyma, whereas benign lesions demonstrate microbubble contrast uptake. Data regarding the use of other agents, using continuous non-linear techniques with low MI, is emerging with initial results using SonoVue® proving particularly useful.[27] Imaging of a focal liver lesion during different vascular phases provides clues to the identity of the lesion with good correlation between the findings of microbubble contrast enhanced ultrasound and CT or magnetic resonance (MR) imaging. Generally the current practice is to use non-linear low MI techniques to characterise lesions; the liver lesion is identified with B-mode imaging then, with the probe held stationary over the lesion, continuous imaging is performed for 60–90 s after injection of a bolus of microbubble contrast followed by a saline flush via a peripheral vein.

Using the low MI method the characteristics of different types of focal liver lesions have been established. Haemangiomas, common benign liver lesions, typically display progressive enhancement starting from the periphery of the lesion, as also demonstrated with CT and MR imaging[24] (Fig. 15.7). Focal fatty sparing, focal fatty change and regenerative nodules may have alarming appearances with contrast enhanced CT and MR imaging but reassuringly display isoenhancement compared to surrounding liver parenchyma following microbubble contrast administration. Focal nodular hyperplasia, a benign vascular anomaly, tends to hyperenhance with microbubble contrast with demonstration of a characteristic central hypoenhancing scar. Adenomas, which on occasion may be very large and associated with haemorrhage, generally show hyperenhancement in the arterial and portovenous phases becoming isoenhancing with surrounding parenchyma on

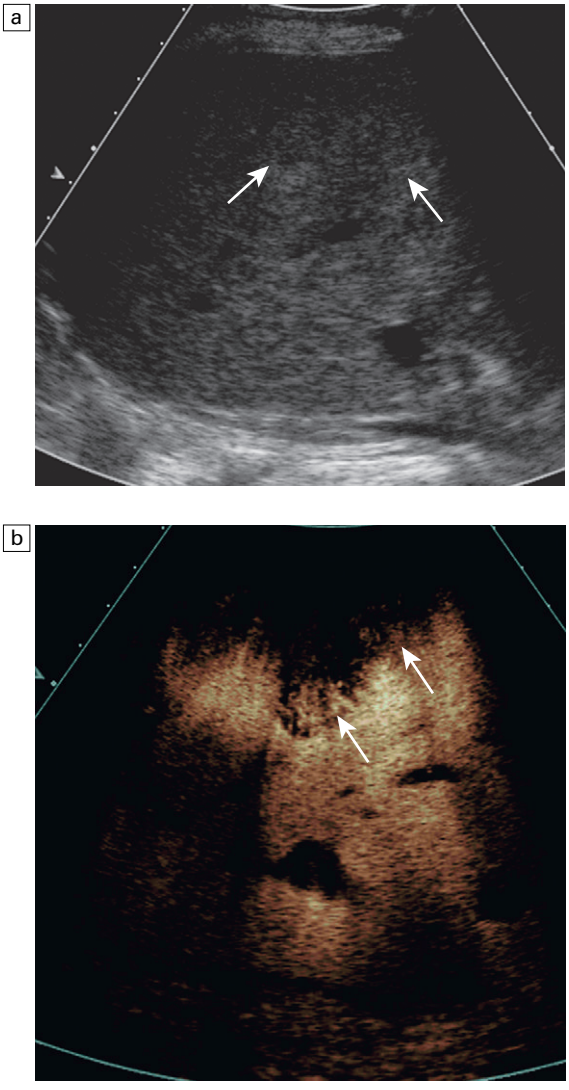


**Fig. 15.7** A haemangioma demonstrates progressive enhancement starting from the periphery of the lesion during the late phase; (a) baseline image of an atypical focal liver lesion (arrows); (b) microbubble enhanced image in the late phase, using SonoVue® and CPS® imaging (Acuson, Siemens) demonstrates 'creeping' enhancement from the periphery (arrows) typical of a haemangioma.

delayed imaging. Simple liver abscesses are often readily diagnosed on B-mode imaging but if there is diagnostic doubt, administration of microbubble contrast displays a hyperenhancing rim and a low reflective central area on arterial phase. Occasionally enhancing septa may be seen within the abscess and the surrounding liver segment may be hyperenhancing (Fig. 15.8).

Unfortunately there is no single feature to differentiate a benign from a malignant lesion on low MI imaging. Hepatocellular carcinomas (HCC) tend to be hyperenhancing in the arterial phase, iso- or hypoenhancing in the portovenous phase

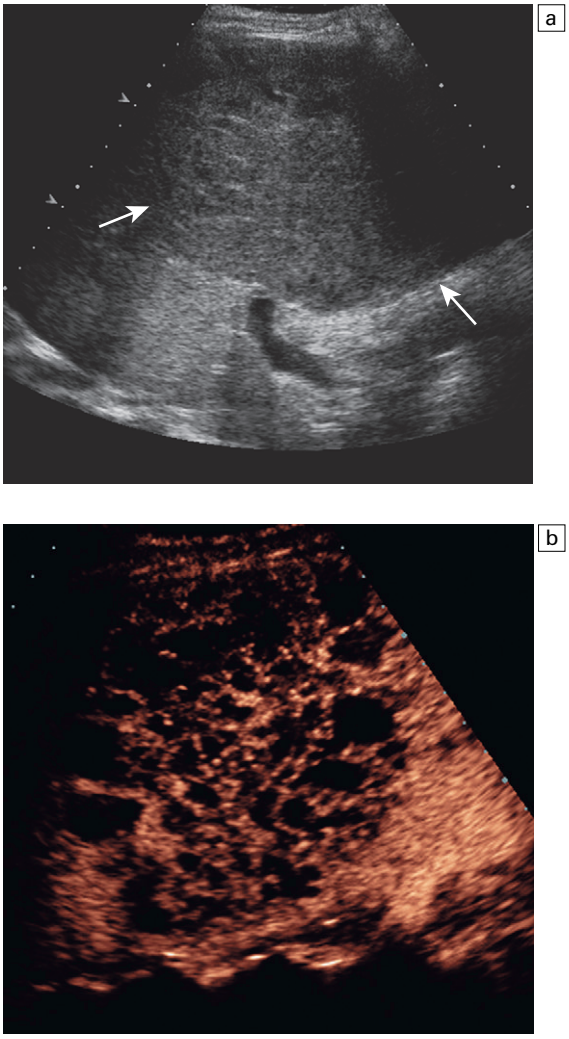


**Fig. 15.8** Complications relating to the liver parenchyma following transplantation that can be effectively interrogated using microbubble contrast include abscesses; (a) on baseline imaging a large heterogeneous mass (arrows) is present in the right lobe of the liver; (b) following administration of SonoVue®, and using CPS®, a multiseptated abscess is demonstrated.

and hypoenhancing on delayed imaging. Occasionally an HCC may show some late phase enhancement (Fig. 15.9). Cholangiocarcinomas generally do not enhance with microbubble contrast although there may be early arterial rim enhancement in some cases. As with other imaging modalities the ultrasound characteristics of liver metastasis depend on the source of the primary. In general metastasis are hypoenhancing however, predictably, hypervascular metastasis are hyperenhancing in the arterial phase of scanning. Although not specific to hepatic malignancies, one development which may in the future provide supplementary evidence of a malignant versus a benign tumour is the study of the disorganised neovascularity which is associated with rapidly growing malignant tumours.[28]

### *Trauma*

Microbubble ultrasound contrast may reveal solid abdominal organ injuries not evident with B-mode imaging.[29] Although at present contrast enhanced CT remains the reference standard in the context of trauma, microbubble enhanced ultrasound has certain inherent advantages including ease of access, the possibility of a bedside examination in the emergency room, lack of ionising radiation absence of nephrotoxicity.

### *Liver transplantation and liver vasculature*

Microbubble contrast agents are a useful diagnostic tool in the practice of liver transplantation ultrasound imaging.[30] Pretransplant patient assessment is essential to select candidates who are most likely to benefit from a liver transplant. Both liver parenchyma and hepatic vasculature need to be assessed; in particular portal vein and superior mesenteric vein (SMV) patency must be documented. Not uncommonly patients will have a cirrhotic highly attenuating liver, large volume ascites or bowel gas rendering visualisation of the vasculature problematic. In such cases demonstration of portal vein and SMV patency is improved by the use of microbubble contrast ('Doppler rescue') (Fig. 15.10). Furthermore in cases of long-term portal vein thrombosis the presence of cavernous transformation may be seen (Fig. 15.11).[31] Diagnostic confidence of hepatic vein and inferior vena cava thrombus

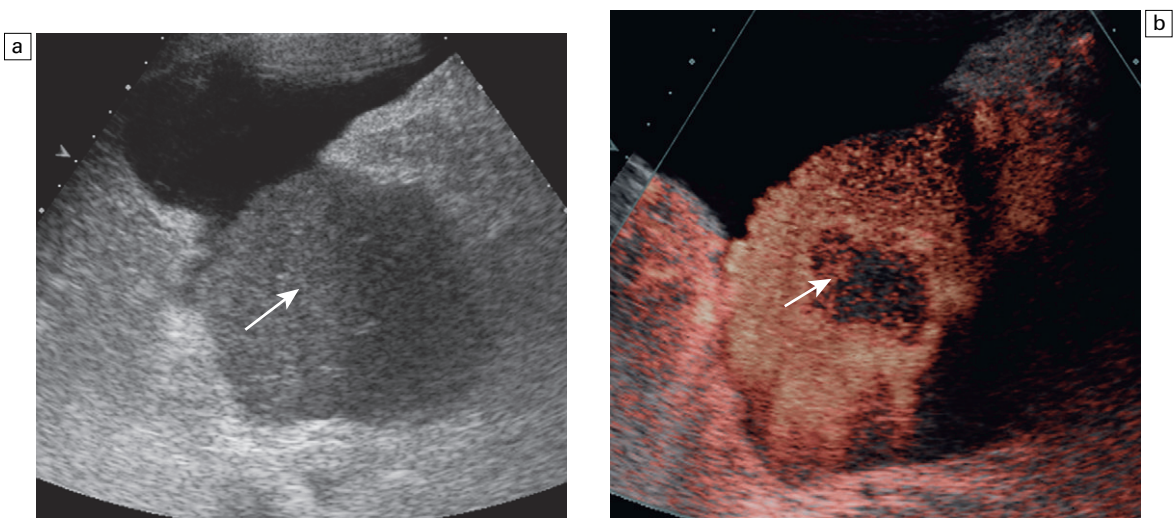


**Fig. 15.9** Benign lesions tend to demonstrate persistence of contrast enhancement in portal venous and late phases whereas malignant lesions tend to show early wash out of contrast in the portal and late phases; a notable exception is hepatocellular carcinoma which can show some late phase enhancement; (a) baseline image of a hepatocellular carcinoma in the right lobe of the liver (arrow); (b) following administration of SonoVue®, there remains some microbubble contrast within the lesion (arrow).

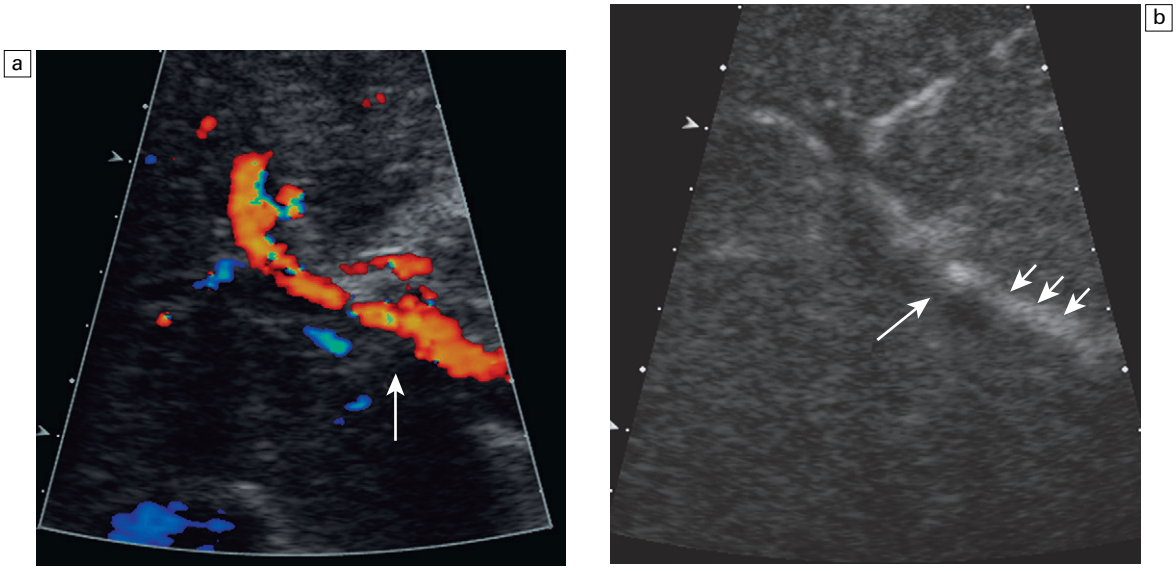


**Fig. 15.10** Demonstration of portal vein patency status is improved by the use of microbubble contrast, 'Doppler rescue'; (a) on baseline imaging there is no colour Doppler signal from the portal vein (arrow) but flow is seen in the hepatic artery; (b) following administration of SonoVue®, and using CCI® (Acuson Siemens, low mechanical imaging) contrast is seen in the hepatic artery (small arrows) but no contrast is present in the portal vein (arrow), confirming occlusion.

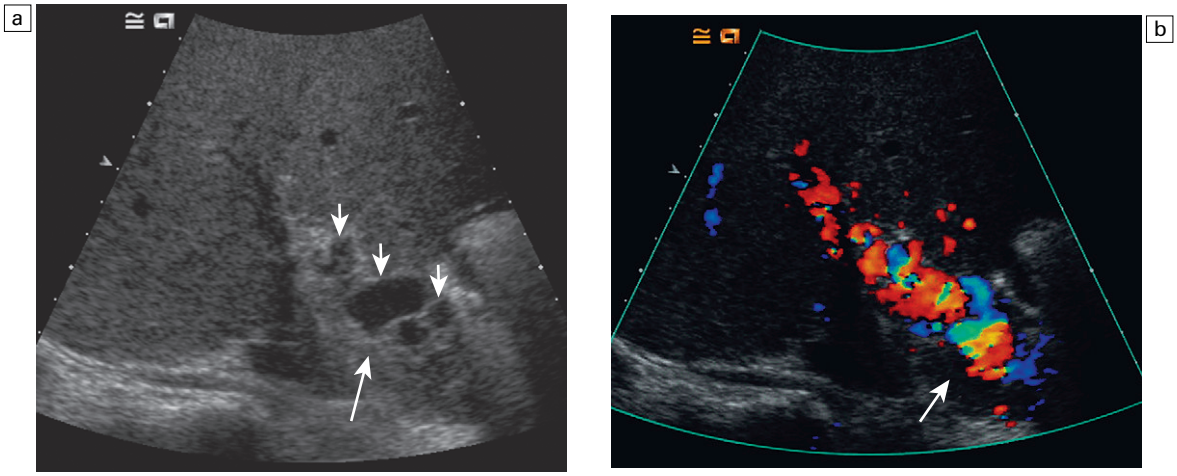


**Fig. 15.11** With long-term portal vein thrombosis the presence of cavernous transformation may be confirmed, 'Doppler rescue'; (a) baseline imaging demonstrates a dilated high reflective portal vein (arrow) and serpiginous low reflective structures (small arrows) in keeping with cavernous transformation; (b) following SonoVue®, the cavernous transformation and the occluded portal vein (arrow) are demonstrated.

occlusion in the Budd–Chiari syndrome can be improved and the spider-web like pattern of intrahepatic veins may be demonstrated following administration of microbubble ultrasound contrast.

Transjugular intrahepatic portosystemic shunt (TIPS) can provide effective palliation in cases of recurrent varicocele haemorrhage or intractable ascites. The principle long-term complication of TIPS, occurring in up to 30% of patients in the

first year, is occlusion.[32] As with other vascular structures in the cirrhotic liver this can be difficult to assess using standard Doppler ultrasound with administration of microbubbles providing evidence of low flow within a TIPS.

In assessing the liver parenchyma pretransplantation, it is important to establish the presence of occult malignancy, in particular HCC. Initial experience suggests microbubble contrast enhanced ultrasound may improve conspicuity of such lesions.

In the post-transplant liver, the principal vascular supply is from the anastomosed hepatic artery, with the portal vein playing a less significant role. When performing ultrasound assessment post-transplant, the single most important structure to visualise and document patency is the hepatic artery; compromise of this vessel may result in bile duct ischaemia, necrosis and bile duct leaks.[33] If a hepatic artery spectral Doppler trace is not demonstrated using standard Doppler the patient often undergoes formal angiography; use of microbubble contrast could negate the need for arteriography in such cases.[34] Pseudoaneurysms of the hepatic artery may arise secondary to localised infection or as a consequence of liver biopsy; rupture may result in fatal haemorrhage. The swirling blood flow within a pseudoaneurysm (the 'yin-yang' sign) may be elegantly demonstrated post microbubble contrast allowing hepatic artery reconstruction or endovascular embolisation to proceed with confidence (Fig. 15.12). Although relatively uncommon post-transplant, both portal vein and hepatic vein thrombosis can be assessed with microbubble contrast. There are a variety of complications relating to the liver parenchyma and surrounding structures that can be effectively interrogated using microbubble contrast including parenchymal infarction (Fig. 15.13), recurrent malignancy, post-transplant lymphoproliferative disorder, localised fluid collections and abscesses.[35]

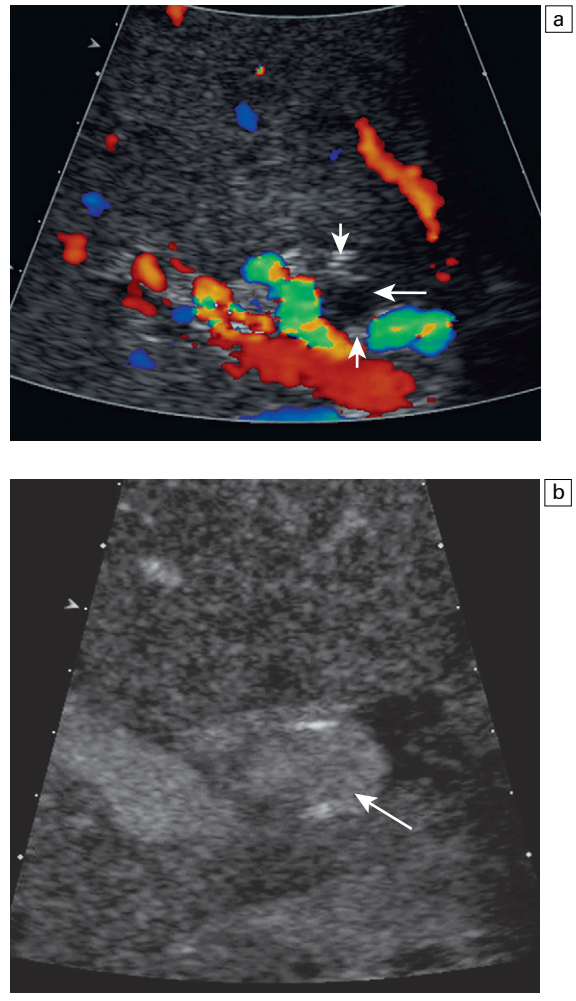


**Fig. 15.12** Following endovascular embolisation of a hepatic artery pseudoaneurysm abdominal haemorrhage continues; (a) baseline colour imaging demonstrates the low reflective pseudoaneurysm (arrow) and embolisation coils (small arrows) without any colour flow signal present; (b) using SonoVue® and CCI®, there is clear demonstration of continuing blood flow (arrow) and the need to perform further endovascular embolisation to stop the haemorrhage.

## Spleen

The spleen is often a technically difficult organ to adequately visualise on B-mode ultrasound, where several conditions within and surrounding the spleen may cause diagnostic confusion; the addition of microbubble contrast will enhance the operators' confidence when assessing such lesions.[36] Splenunculi occur in up to 30% of the population, may be multiple and can be found at locations remote to the spleen with the primary differential for splenunculi, particularly when multiple, that of lymph node enlargement.

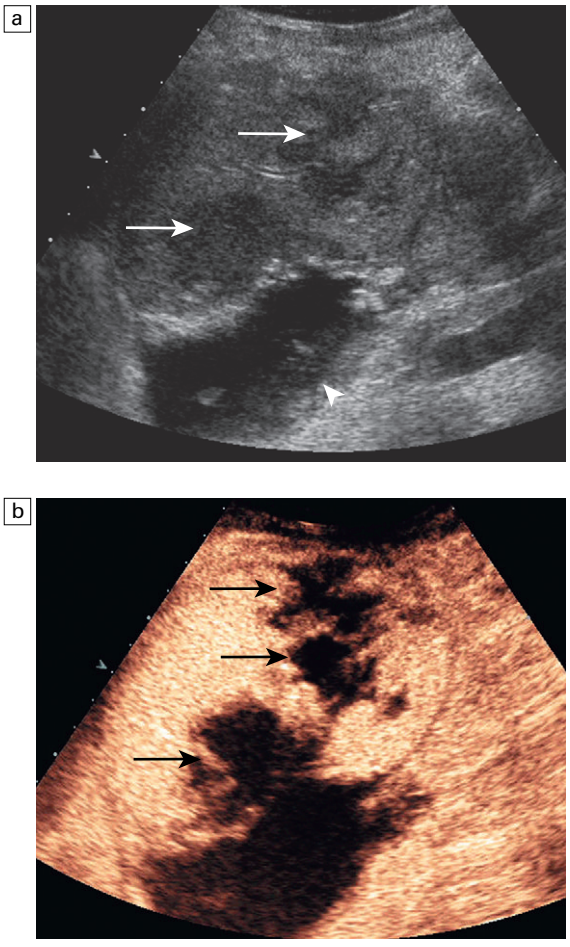


**Fig. 15.13** Complications relating to the liver parenchyma following transplantation that can be effectively interrogated using microbubble contrast include parenchymal infarction; (a) low reflective areas (arrows) are present within the left lobe of the liver and there is a subhepatic collection noted (arrowhead); (b) following the administration of SonoVue® and using CPS®, areas of infarction are demonstrated (arrows) in this patient with a hepatic artery occlusion.

Microbubble contrast enhanced ultrasound accurately demonstrates that the parenchymal enhancement of the splenunculi matches the main spleen with a clear vascular hilum (Fig. 15.14).

### *Focal splenic lesions*

Cavernous haemangiomas are the most common of the benign solid splenic lesions, usually small and solitary but they may occasionally be multiple and greater than 2 cm in diameter. When large, microbubble contrast demonstrates a centripetal enhancement pattern, analogous to haemangiomas found in the liver. Other benign solid lesions are rare but include lymphangioma and hamartoma which both show varying degrees of enhancement post microbubble administration. Whilst primary malignant tumours of the spleen such as lymphoma and angiosarcoma do occur they are both

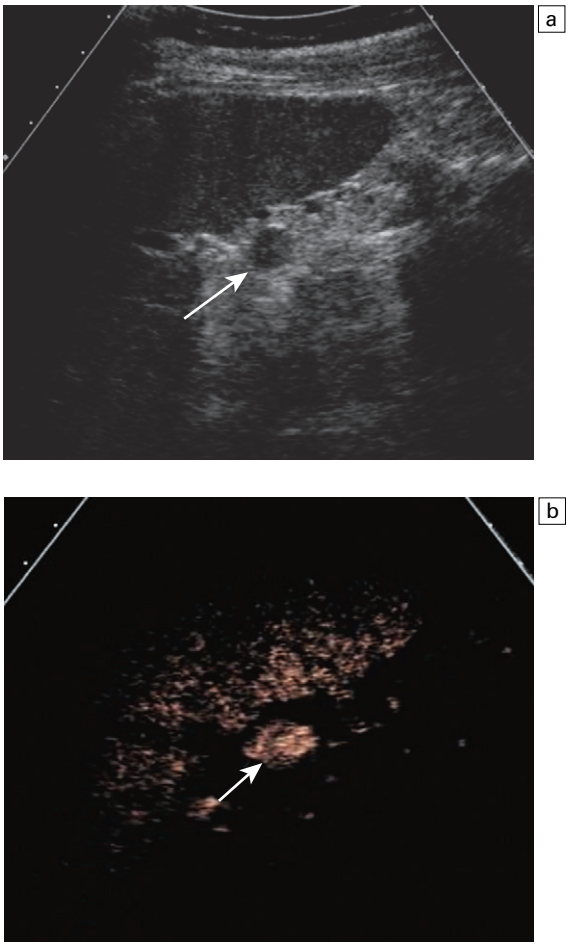


**Fig. 15.14** Microbubble contrast enhanced ultrasound demonstrates the parenchymal enhancement of a splenunculi that matches the spleen; (a) baseline image demonstrates a well circumscribed iso reflective (to spleen) area (arrow) adjacent to the splenic hilum; (b) following the administration of Levovist® using ADI®, there is microbubble contrast uptake in the late phase confirming the presence of splenic tissue (arrow).

rare.[36] More common, although still unusual, are metastatic deposits to the spleen. The majority of these deposits are serosal (cause scalloping of the spleen surface) as opposed to parenchymal and arise from a primary neoplasm in, for example, the ovary.[36] Simple splenic cysts, either congenital or acquired, rarely cause diagnostic uncertainty. Spleen abscesses may have ultrasound appearances ranging from cystic to solid and generally appear avascular on both Doppler ultrasound and microbubble contrast enhanced ultrasound. Splenic infarction typically occurs in patients with infective endocarditis or myeloproliferative disorders, often difficult to visualise on initial B-mode ultrasound but may show lack of vascular perfusion on colour Doppler ultrasound.[37] Conspicuity of infarcts is improved by the use of microbubble ultrasound contrast media (Fig. 15.15).

### *Trauma*

The spleen is prone to injury following blunt abdominal trauma. Prompt diagnosis is central to effective management of this potentially fatal condition. While CT remains the reference standard for diagnosis of splenic injury, microbubble contrast may prove to be a useful adjunct. Following administration of contrast, a non-enhancing linear branching laceration not evident on B-mode imaging may be shown (Fig. 15.16).

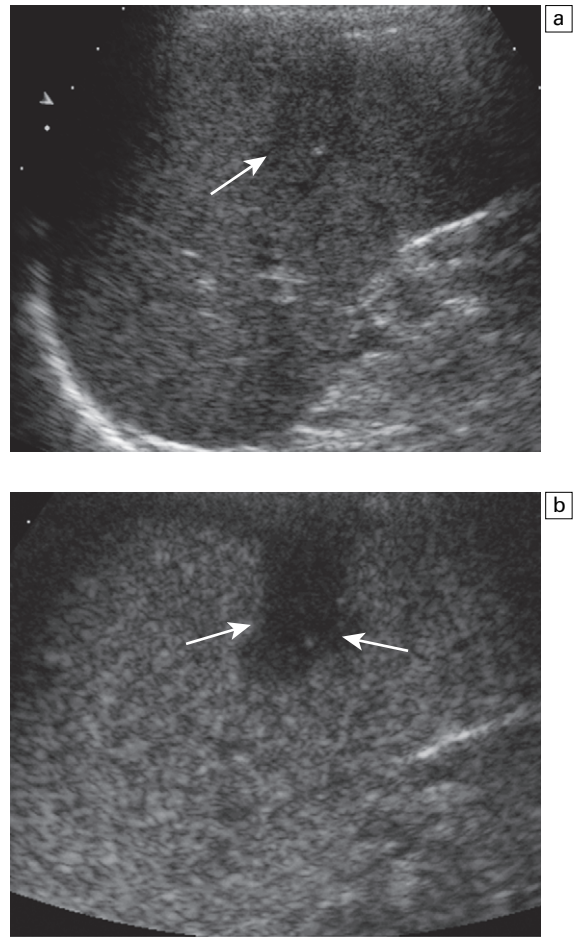


**Fig. 15.15** Splenic infarction may occur in patients with infective endocarditis; (a) on baseline imaging there is a heterogeneous area in the spleen (arrow) without particular characteristics; (b) conspicuity of this area is improved by the use of microbubble contrast (SonoVue® and CCI®) to reveal an area of infarction (arrows).

## Renal

### *Complex renal cysts*

On finding a complex renal cyst most institutions currently undertake contrast enhanced CT to further assess the kidney, looking for a potential malignancy. Microbubble contrast may ultimately prevent the need for so many CT examinations but at present experience is still being accumulated. The vascularity of a soft tissue mass within a renal cyst may be readily demonstrated with microbubble contrast (Fig. 15.17). Microbubble contrast may help delineate 'pseudotumours' from real renal masses as in the case of a prominent column of Bertin. With a true renal mass, microbubble contrast may illustrate the abnormal distorted vasculature and confirm or refute the patency of the renal vein (Fig. 15.18).

### *Renal vasculature*

Whilst Doppler ultrasound of the renal arteries is an accepted screening examination for renal artery stenosis, this technique is technically challenging. Problems arise in visualising the entire renal artery, identifying accessory arteries and obtaining accurate Doppler traces due to patient factors and being unable to access a suitable angle on the artery. Microbubble contrast enhancement may overcome some of these problems with the number of successful examinations increasing

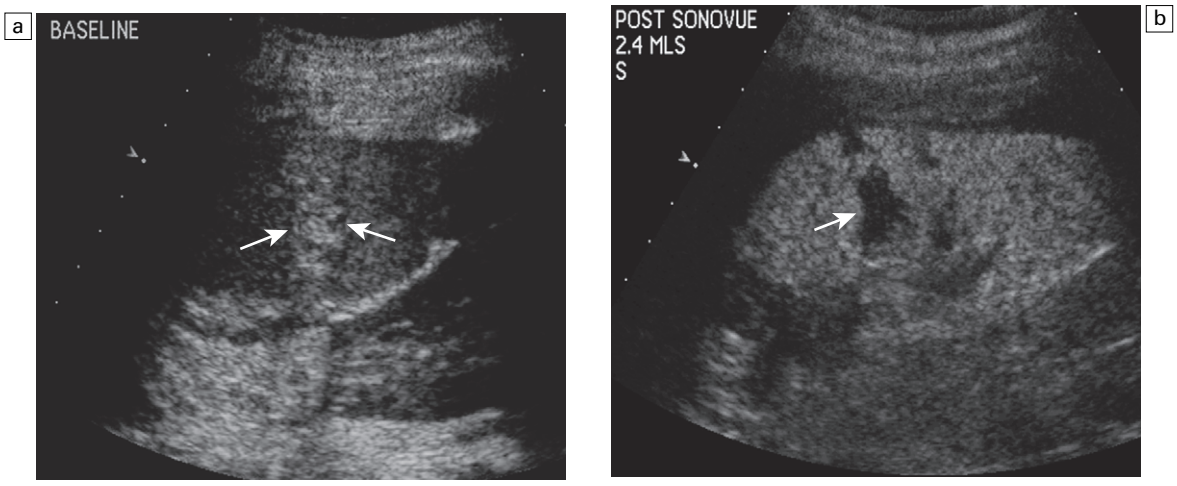


**Fig. 15.16** In blunt abdominal injury microbubble contrast may be a useful adjunct; (a) on the baseline image there is a high reflective heterogeneous pattern observed in the spleen (arrows); (b) following administration of SonoVue®, and imaging with CCI®, a non-enhancing laceration is demonstrated (arrow) as well as other areas of non-perfusion in keeping with significant splenic trauma.

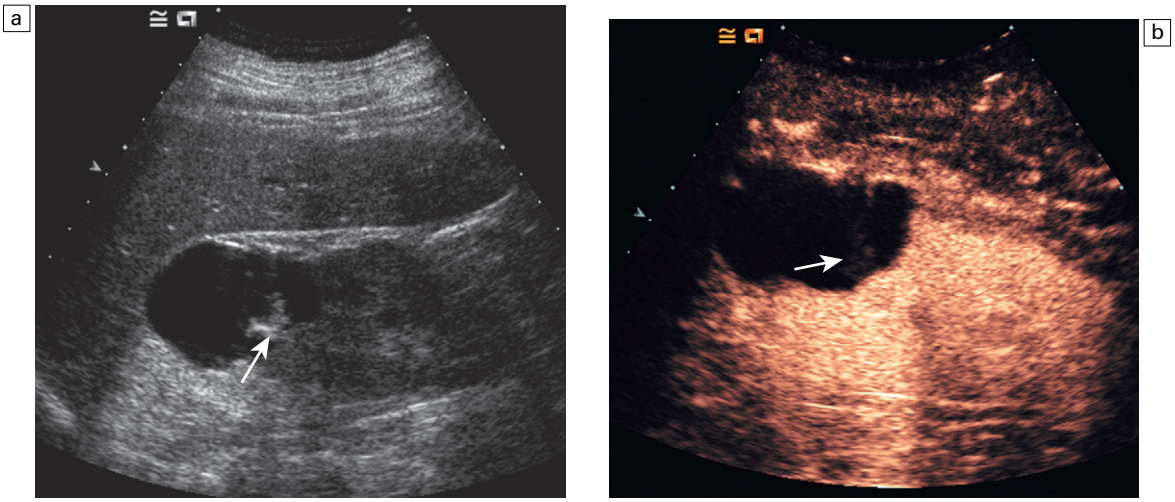


**Fig. 15.17** With a complex renal cyst the vascularity of a soft tissue mass within the cyst may be readily demonstrated with microbubble contrast; (a) on baseline imaging a soft tissue component (arrow) makes this renal cyst suspicious for a malignant lesion; (b) following the administration of SonoVue® and using CPS®, the soft tissue component does not enhance (arrow) demonstrating that there is no vascularity to this area, and it is likely benign.

by as much as 20%.[38] Microbubble ultrasound contrast is employed in the visualisation of the vasculature post renal transplantation. In such cases viability of the transplant is dependent on the patency of the renal artery and vein and microbubble contrast can aid in the diagnosis of renal artery stenosis or renal vein thrombosis.

Aside from vascular applications in the renal tract, microbubble contrast is used to investigate ureteric reflux via direct installation of micro-

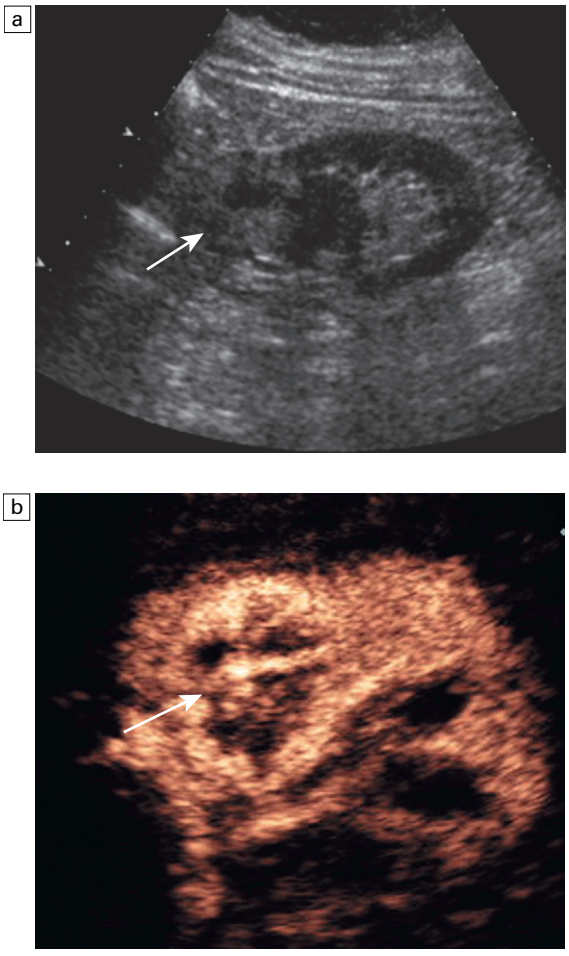


**Fig. 15.18** In a true renal mass, microbubble contrast will demonstrate abnormal distorted vasculature; (a) on the baseline image a complex mass is present at the upper aspect of the left kidney (arrow); (b) following the administration of SonoVue®, and using CPS®, abnormal vessels are demonstrated within the tumour (arrow).

bubble contrast into the bladder and observing reflux on ultrasound. Although this is appealing in that ionising radiation could be avoided in young patients, practical difficulties remain in the implementation of the method.[39]

## Hystero-contrast salpingography

In the investigation of subfertility, Fallopian tube patency has traditionally been established by hysterosalpingography (HSG), a technique requiring both iodinated contrast and irradiation of the pelvic organs. The use of *hystero-contrast salpingography* (HyCoSy) avoids these risks. Instillation of microbubble contrast in to the uterine cavity is performed and using transvaginal ultrasound, the passage of contrast through the Fallopian tubes and spillage into the pelvis may be followed in real time.[40] While this serves as a good screening test for tubal patency, it cannot at present provide detailed anatomical delineation of tubal pathology. As such in cases where tubal occlusion is demonstrated the patients may progress to a formal HSG prior to therapeutic intervention. Both HSG and HyCoSy can result in significant patient discomfort, with some studies suggesting pain is more common with HyCoSy.[41]

## Neurological

### *Transcranial ultrasound*

Accurate visualisation of the intracerebral vasculature allows diagnosis and monitoring of arterial spasm after stoke or subarachnoid haemorrhage and vessel occlusion in sickle cell disease. Assessment of these vessels using standard Doppler ultrasound is limited by the severe attenuation of the signal due to the skull vault. Use of microbubble contrast agents can overcome this difficulty and allow accurate visualisation of the vessels (Fig. 15.19).[42] Indeed in one study the use of microbubble contrast technically improved the images in 77% of patients.[43]

### *Carotid artery*

Microbubble contrast use in the assessment of carotid arteries is focused on two areas. First is to accurately visualise flow within the carotid artery, a task that is frequently made complex by overlying calcified plaque and vessel tortuosity. In one study, on baseline colour Doppler imaging 21% of vessel stenosis was not identified in comparison to only 6% post microbubble contrast.[44] Second, is to differentiate between vessel occlusion and high grade stenosis, a distinction which can be difficult to make with standard colour Doppler. Microbubble contrast improves this, decreasing the false-negative rate from 30% to 17%.[45]

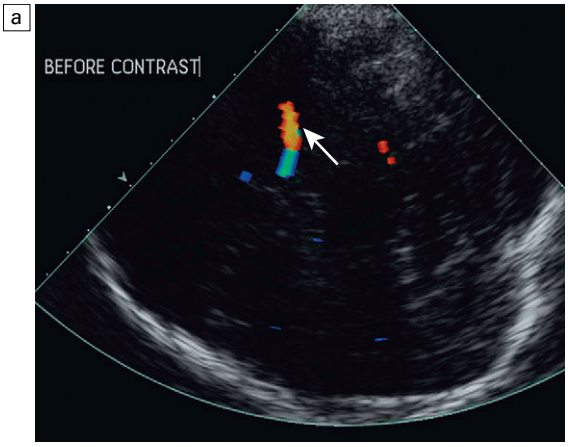


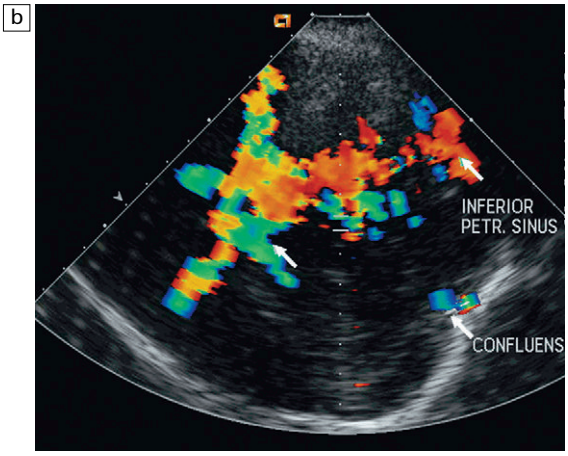


**Fig. 15.19** The application of microbubble contrast in transcranial ultrasound is useful; (a) on the baseline image a single vessel is visualised on colour Doppler ultrasound (arrow); (b) following the administration of Levovist® and using conventional colour Doppler ultrasound, both the circle of Willis and the draining veins of the brain are demonstrated (arrows).

## Musculoskeletal

Currently principally a research tool, microbubble contrast is finding application in the study of articular inflammatory disease. Several studies have shown synovial enhancement in patients with synovial inflammation confirmed with MR imaging (Fig. 15.20).[46,47] Such findings may offer opportunity not only in terms of diagnosis but also monitoring disease progression and response to therapy.

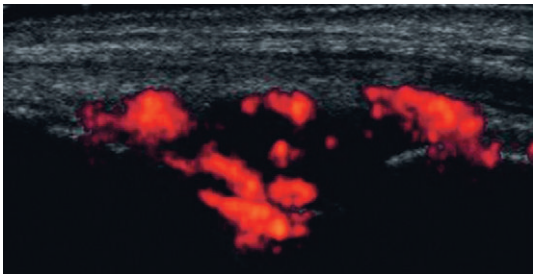

**Fig. 15.20** Inflammatory change in the proximal inter-phalangeal joint of a patient with rheumatoid disease and synovitis is demonstrated following the administration of SonoVue® as a microbubble contrast agent.

## Treatment

The currently available microbubbles consist of gas contained within a shell. Potential exists to replace this gas with a 'cargo' and effectively use the microbubble as a vehicle to transport a therapeutic agent to a specified site. Ultimately this may prove to be an application of microbubbles more important than any of those discussed above. Perhaps the most interesting use would be in the area of gene therapy where the initial hopes of effective treatments have often been limited by lack of suitable delivery mechanism. Sonoporation, the mechanism by which cell membranes are rendered porous to large molecules by ultrasound, is enhanced in the presence of microbubbles. The ability of this process to deliver gene therapy has been shown.[48] Aside from gene therapy the possibility for delivery of other therapeutic agents also exists. These include chemotherapeutic agents whose site of delivery could be dictated by selective microbubble disruption at the tumour site. Alternatively, drug delivery could be directed by use of ligands within the microbubble membrane which bind to specific cell receptors at target tissue.

## REFERENCES

1. Gramiak R, Shah PM. Echocardiography of the aortic root. Invest Radiol 1968; 3:356–366.
2. Stride E, Saffari N. Microbubble ultrasound contrast agents: a review. Proc Inst Mech Eng [H] 2003; 217:429–447.
3. Harvey CJ, Blomley MJK, Eckersley RJ, et al. Developments in ultrasound contrast media. Eur Radiol 2001; 11:675–689.
4. Porter TR, Xie F, Li S, et al. Increased ultrasound contrast and decreased microbubble destruction rates with triggered ultrasound imaging. J Am Soc Echocardiogr 1996; 9:599–605.
5. Nanda NC, Carstensen C. Echo-enhancing agents: safety. In: Nanda NC, Goldberg BB, eds. Advances in echo imaging using contrast enhancers. Dordrecht: Kluwer; 1997:115–131.
6. Albrecht T, Blomley MJK, Bolondi L, et al. Guidelines for the use of contrast agents in ultrasound. Ultraschall Med 2004; 25:249–256.
7. Nyborg WL. Biological effects of ultrasound: development of safety guidelines. Part II; general review. Ultrasound Med Biol 2001; 27:301–333.
8. Gromley G, Wu J. Observation of acoustic streaming near Albunex spheres. J Acoust Soc Am 1998; 104:3115–3118.
9. Schlief R. Developments in echo-enhancing agents. Clin Radiol 1996; 51:5–7.
10. Wei K, Kaul S. Recent advances in myocardial contrast echocardiography. Curr Opin Cardiol 1997; 12:539–546.
11. Bokor D. Diagnostic efficacy of SonoVue. Am J Cardiol 2001; 86:19G–24G.
12. Neppiras EA. Acoustic cavitation. Phys Rep 1980; 61:159–251.
13. Cosgrove DO. Ultrasound contrast agents. In: Meire H, Cosgrove DO, Dewbury K, et al, eds. Clinical Ultrasound: a comprehensive text. London: Churchill Livingstone; 2000:67–79.
14. Simpson DH, Chin CT, Burns PN. Pulse inversion Doppler: a new method for detecting nonlinear echoes from microbubble contrast agents. IEEE Trans Biomed Eng 1999; 46:372–382.
15. Albrecht T, Hoffmann CW, Schettler S, et al. B-mode enhancement at phase-inversion US with air-based microbubble contrast agent: initial experience in humans. Radiology 2000; 216:273–278.
16. Tiemann K, Becher H, Bimmel D, et al. Simulated acoustic emission nonbackscatter contrast effect of microbubbles seen with harmonic power Doppler imaging. Echocardiography 2000; 14:65–70.
17. Blomley MJK, Albrecht T, Cosgrove DO, et al. Improved imaging of liver metastases with stimulated acoustic emission in the late phase of enhancement with the US contrast agent SH U 508A: early experience. Radiology 1999; 210:409–416.
18. Forsberg F, Liu JB, Burns PN, et al. Artifact in ultrasonic contrast agents studies. J Ultrasound Med 1994; 13:357–365.
19. Petrick J, Zomack M, Schlief R. An investigation of the relationship between ultrasound echo enhancement and Doppler frequency shift using a pulsatile arterial flow phantom. Invest Radiol 1997; 32:225–235.
20. Nihoyannopoulos P. Contrast echocardiography. Clin Radiol 1996; 51:28–30.
21. Kaul S. New developments in ultrasound systems for contrast. Clin Cardiol 1997; 20:127–130.
22. Blomley MJK, Cooke JC, Unger EC, et al. Microbubble contrast agents; a new era in ultrasound. Br Med J 2001; 322:1222–1225.
23. Leen E, McArdle CS. Ultrasound contrast agents in liver imaging. Clin Radiol 1996; 51:35–39.
24. Leen E. Ultrasound contrast harmonic imaging of abdominal organs. Semin Ultrasound CT MRI 2001; 22:11–24.
25. Bryant TH, Blomley MJK, Albrecht T, et al. Liver phase uptake of a liver specific microbubble improves characterization of liver lesions: a prospective multi-center study. Radiology 2004; 232:392–399.
26. Blomley MJK, Sidhu PS, Cosgrove DO, et al. Do different types of liver lesions differ in their uptake of the microbubble contrast agent SH U 508A in the late liver phase? Early experience. Radiology 2001; 220:661–667.
27. Albrecht T, Oldenburg A, Hohmann J, et al. Imaging of liver metastases with contrast-specific low-MI real-time ultrasound and SonoVue. Eur Radiol 2003; 13:N79–N86.
28. Cosgrove DO. Microbubble enhancement of tumour neovascularity. Eur Radiol 1999; 9:S413–S414.
29. Kraemer N, Cosgrove DO, Blomley MJK. Microbubble ultrasound demonstrates liver trauma. J Trauma 2004; 56:913–914.
30. Berry JD, Sidhu PS. Microbubble contrast-enhanced ultrasound in liver transplantation. Eur Radiol 2004; 14:P96–P103.
31. Marshall MM, Beese RC, Muiesan P, et al. Assessment of portal venous patency in the liver transplant candidate: a prospective study comparing ultrasound, microbubble-enhanced colour Doppler ultrasound with arteriography and surgery. Clin Radiol 2002; 57:377–383.
32. Shaw AS, Ryan SM, Beese RC, et al. Liver transplantation. Imaging 2002; 14:314–328.
33. Zajko AB, Campbell WL, Logsdon G. Cholangiographic findings in hepatic artery occlusion after liver transplantation. AJR Am J Roentgenol 1987; 149:485–489.

34. Sidhu PS, Shaw AS, Ellis SM, et al. Microbubble ultrasound contrast in the assessment of hepatic artery patency following liver transplantation: role in reducing frequency of hepatic artery arteriography. Eur Radiol 2004; 14:21–30.
35. Shaw AS, Ryan SM, Beese RC, et al. Ultrasound of non-vascular complications in the post-transplant patient. Clin Radiol 2003; 58:672–680.
36. Peddu P, Shah M, Sidhu PS. Splenic abnormalities: a comparative review of ultrasound, microbubble enhanced ultrasound and computed tomography. Clin Radiol 2004; 59:777–792.
37. Goerg C, Schwerk WB. Color Doppler imaging of focal splenic masses. Eur J Radiol 1994; 18:214–219.
38. Claudon M, Plouin PF, Baxter GM, et al. Renal arteries in patients at risk of renal arterial stenosis: multicentre evaluation of the Echo-enhancer SH U 508A at color and spectral Doppler US. Radiology 2000; 214:737–746.
39. Mentzel HJ, Vogt S, Patzer L, et al. Contrast-enhanced sonography of vesicoureterorenal reflux in children: preliminary results. AJR Am J Roentgenol 1999; 173:737–740.
40. Ayida G, Harris P, Kennedy S, et al. Hysterosalpingo-contrast sonography (HyCoSy) using Echovist-200 in the outpatient investigation of infertility patients. Br J Radiol 1996; 69:910–913.
41. Stacey C, Brown C, Manhire A, et al. HyCoSy – as good as claimed? Br J Radiol 2000; 73:133–136.
42. Bauer A, Becker G, Krone A, et al. Transcranial duplex sonography using ultrasound contrast enhancers. Clin Radiol 1996; 51:19–23.
43. Otis SM, Rush M, Boyajian R. Contrast-enhanced transcranial imaging. Results of an American phase-two study. Stroke 1995; 26:203–209.
44. Sitzer M, Furst G, Siebler M, et al. Usefulness of an intravenous contrast medium in the characterization of high-grade internal carotid stenosis with color Doppler-assisted duplex imaging. Stroke 1994; 25:385–389.
45. Furst G, Saleh A, Wenserski F, et al. Reliability and validity of noninvasive imaging of internal carotid artery pseudo-occlusion. Stroke 1999; 30:1444–1449.
46. Carotti M, Salaffi F, Manganelli P, et al. Power Doppler sonography in the assessment of synovial tissue of the knee joint in rheumatoid arthritis: a preliminary experience. Ann Rheum Dis 2002; 61:877–882.
47. Margarelli N, Guglielmi G, Matteo L, et al. Diagnostic utility of an echo-contrast agent in patients with synovitis using power Doppler ultrasound: a preliminary study with comparison to contrast-enhanced MRI. Eur Radiol 2001; 11:1039–1046.
48. Price RJ, Skyba DM, Kaul S, et al. Delivery of colloidal particles and red blood cells to tissue through microvessel ruptures created by targeted microbubble destruction with ultrasound. Circulation 1998; 98:1264–1267.

# Appendix: System controls and their uses

In addition to the basic choice of transducer type and frequency for the examination in hand, there are many other factors on a Doppler ultrasound system which need to be adjusted. Despite the efforts of the manufacturers to automate and simplify things, it is still necessary to adjust continually many of the scan and Doppler parameters during the course of an examination. Is the vessel superficial or deep? Is flow fast or slow, high volume or low volume? Most systems now come with a variety of preset programs for different situations: peripheral arteries, veins, cerebrovascular, etc. Many also have the facility to allow users to save their own program preferences. Whilst these presets allow the basic appropriate settings to be entered, fine adjustments will still be required during the course of the examination to make the most of the available information. Familiarity with the ultrasound system and experience enable skilled operators to set up their system appropriately for the examination being performed. Different manufacturers sometimes use different names for the same controls or functions; it is not possible to give an exhaustive list of all the possible options but the following notes describe the basic controls, or parameters on most systems that can be adjusted during the course of an examination to improve and maximise the information that is obtained from the examination.

## GENERAL PRINCIPLES

### Transducer frequency

The highest frequency which will achieve the highest resolution consistent with adequate penetration for imaging is normally chosen. The Doppler frequency used by any transducer is often 1–2 MHz below the imaging frequency, although modern equipment has a wide range of receive frequencies such as 5–14 MHz. In addition to the basic imaging requirements, it should be remembered that the deeper a vessel lies, the longer it takes a sound pulse to travel there and back, so that the Nyquist limit becomes very relevant (Ch. 1) and limits the Doppler frequencies that can be used and therefore velocities that can be recorded accurately.

### B-mode image

For colour Doppler examinations this should be set up with relatively low overall gain, so that the image is a little on the dark side as the software tends to allocate colour to darker areas, rather than to areas which contain echoes. See ‘colour write priority’ below.

### Transmit power

The transmit power of the system should be set at the lowest level consistent with an adequate examination, especially during obstetric and gynaecological examinations. It is better to start at a medium level and increase the power only after other measures to improve system sensitivity have been tried, such as adjusting colour gate size, removing filters, adjusting the scale/pulse repetition rate. For low mechanical index (MI) contrast studies (see Ch. 15) the transmit power should be set as low as possible and the MI reading ideally should be less than 0.4; modern systems may have contrast agent-specific programs already installed, or the relevant

settings can be obtained from the supplier of the contrast agent.

### Update/duplex/triplex

In duplex ultrasound there is the ability to acquire and display both imaging and Doppler information either simultaneously, or alternately. Simultaneous display results in degradation of both the image and the spectral display as the computer has to process data from both sources. The update facility allows the operator to set the system to handle either imaging data, or Doppler data. This results in a higher quality of display for the selected mode and it is usually used for acquisition of the best-quality spectral display for analysis. Duplex scanning is of some value in the initial stages of an examination in order to position the sample volume in the area of interest. Triplex mode refers to the simultaneous acquisition, processing and display of colour Doppler, spectral display and imaging information. As with duplex scanning, this requires significant division of processing power and consequent compromise in the quality of the display. Newer systems with more powerful computers are less prone to these problems but there is still a division of processing power and experienced operators will still tend to switch between imaging and spectral Doppler for optimal results.

### Automatic image optimisation

Many systems now have automatic image optimisation controls which adjust factors such as time gain compensation, receiver gain and colour Doppler gain to improve the image. In some cases this facility can also be applied to the spectral display. These can be useful in getting a reasonable display but should not be relied upon entirely and the operator needs to make the final adjustments for the best images.

## COLOUR DOPPLER CONTROLS

### Colour map

Choose one that has good contrast for the identification of aliasing. Maps which grade to white at each end, or to very pale colours, do not give as much information about aliasing as those which have significantly different colours, such as pale green and pale orange. Variance maps were said to register the amount of spectral broadening in the colour map, although this is not easy to appreciate and may, in fact, not be true as this 'variance' seems to reflect the velocity, rather than spectral broadening. Variance maps are most frequently used in cardiological examinations. In addition, colour tags can be put into the scale so that velocities above or below the chosen range can be identified.

### Colour gain

The colour gain is set to the optimal level. This can be identified by turning up the gain until noise/colour speckle is seen in the colour box and then backing off slightly on the overall colour gain. It should also be adjusted to remove any spill of the colour map over the boundaries of the vessel seen on the B-mode images; this is sometimes called colour bleeding.

### Colour scale

The colour scale should be set to levels appropriate for the range of velocities under investigation. It should be remembered that colour Doppler only gives information on the mean Doppler shift in a pixel; the mean velocity in a pixel is only calculated when an angle correction for that pixel is performed. The scale is closely related to the pulse repetition frequency, or sampling rate; this has to be above the Nyquist limit for the frequency shift being measured. If it is set too low then aliasing will occur; this can be removed by increasing the colour scale range, also known as the pulse repetition frequency. If it is set too high then there will be poor colour sensitivity for slower velocities, resulting in inadequate colour fill-in across the vessel.

### Colour inversion

This changes the colour map display for mapping the direction of blood flow in relation to the transducer, e.g. red for flow towards the transducer and blue for away from the transducer, or vice versa.

### Colour gate
This relates to the size of the colour pixels, a smaller size gives better spatial resolution, whereas a larger size provides better sensitivity at the expense of spatial and sometimes temporal resolution.

### Colour baseline
The colour baseline can be adjusted to provide a wider range of shifts on one side or the other, depending on the characteristics of the blood flow in the vessel being examined and particularly if the flow is in only one direction.

### Colour filters
These help remove low-frequency noise and clutter from the image. It is best to set filters at the lowest level compatible with an acceptable image as they also remove low-frequency shift information from the image.

### Colour write priority
A pixel in the image can display either B-mode imaging information, or colour Doppler information. The colour write priority facility allows the relative priorities for these two types of information to be defined. High colour priority results in colour information being displayed in areas which might contain low-intensity imaging information, for instance at the margins of vessels. Alternatively, high imaging priority results in grey-scale information displacing colour information, such as might occur with reverberation artefacts appearing within the vessel lumen amongst the colour Doppler information.

### Colour box
This defines the volume of tissue from which colour Doppler information will be gathered. It is better to keep the box as small and as superficial as practical, because larger areas take more processing power and time; deeper boxes need slower pulse repetition frequencies. Most systems now allow the direction of the box to be steered but this also reduces sensitivity for Doppler information.

### Colour persistence
This reflects the amount of frame-averaging which occurs. A low level of persistence results in an image which has a fast temporal response but may have a poor signal to noise ratio. A high level of persistence improves the signal to noise ratio by summating data from several frames, but this results in an impaired temporal response, so that pulsatile flow information is dampened.

## POWER DOPPLER CONTROLS

Although the power mode is intrinsically simpler than velocity mode, there are still several controls and options which influence the power image.

### Power maps
Most systems offer a variety of colour maps from which the operator can select according to personal preference, usually a yellow- or magenta-based scale is used for display of power Doppler information. The threshold or sensitivity can be varied; this results in changes in the transparency of the power box. When the power map background is opaque the sensitivity is maximal. Various degrees of increasing translucency are available so that sensitivity can be traded for imaging and anatomical information.

### Power gain
This is similar to colour gain and amplifies the received Doppler signal. Excessive gain will result in unnecessary noise and artefact in the image.

### Scale
The energy scale affects the sensitivity of the system for signal intensities of varying strengths: lower scales are more sensitive to lower-intensity signals; on some systems the scales are linked to the filters.

### Dynamic range
As in spectral Doppler, this affects the range of signal intensities over which the available colour scale is spread and the appearance of the Doppler information on the screen: increasing the dynamic

range will tend to increase the amount of colour on the screen.

### Power box steering angle

Although the power display is much less dependent on angle than the velocity display, there may still be loss of the power signal at 90° because these low Doppler frequencies fall below the motion discrimination filter cut-off level. In most situations, steering the power Doppler box does not have much effect on the display; however, the loss of signal at 90° may be overcome by having a degree of angulation of the transducer.

### Filters

Motion discrimination filters are used to filter out excessive signal noise from structures, other than blood, which are moving in the Doppler box. Low filter settings provide more sensitivity but are more prone to flash artefacts, whereas higher filter settings reduce flash artefacts but will also filter out some blood flow information.

## SPECTRAL CONTROLS

### Spectral gain

This affects the receiver gain for the spectral display. As in B-mode imaging, the level should be adjusted in order to give a balanced distribution of grey shades across the displayed spectra. Excessive gain will produce erroneous estimates of Doppler shift/velocity.

### Spectral dynamic range

This can be varied to optimise the display of particular frequency shifts. A narrow dynamic range results in the loss of low-intensity shifts above and below the main shift frequencies. Conversely a wide dynamic range, particularly if associated with a high level of spectral receiver gain, can result in artefactual broadening of the spectra displayed. Further manipulation of the spectral display can be performed by altering the postprocessing algorithms in order to emphasise, or suppress, particular frequency shifts. In normal practice a simple linear allocation is most convenient.

### Spectral scale

Altering the scale affects the pulse repetition frequency and thus the range of shifts which can be registered without aliasing. In practice the scale is adjusted so that the Doppler waveform is displayed without wrap-around, which indicates aliasing. The scale may be displayed with either a KHz scale for frequency shift, or m $s^{-1}$ for velocity. The use of m $s^{-1}$ allows some comparison of different examinations, performed with different transducer frequencies and with different angles of insonation.

### Spectral inversion

This allows the operator to change the orientation of the display. Many operators prefer to display arterial and venous waveforms above the baseline, even if flow is away from the transducer. However, care is therefore required when assessing the vertebral arteries for reverse flow, or the leg veins for reflux, as errors may occur if spectral inversion is not recognised. Some centres do not allow spectral inversion because of the potential for misinterpretation, particularly in relation to examinations for venous insufficiency.

### Spectral sweep speed

A medium speed is adequate for most arterial work, with a slower speed for venous flow. A fast sweep speed is useful for acceleration time measurement and waveform analysis, particularly if there is tachycardia.

### Angle correction

The measurement of the angle of insonation relative to the direction of flow is required in spectral Doppler in order to convert frequency shift information into velocity information and also in colour Doppler to convert mean pixel shifts into mean velocities. The main direction of flow may not necessarily be parallel to the vessel wall and colour Doppler is useful in precise positioning of the angle-correction cursor along the line of the jet. The angle of insonation should be less than 60° or the errors in velocity calculation become significant.

## Gate size

This defines the range of depths from which Doppler data are collected. The gate should be positioned across the lumen of the vessel but clear of the walls in order to reduce wall thump. The position of the gate which corresponds to the maximum Doppler shift is located with the use of the colour map and the operator's ears, which are the most sensitive and efficient spectral analyser available; with experience, the ears will register when the peak frequency shift is obtained. If an assessment of volume flow is being made, the gate should be wide enough to encompass the entire vessel width so that all the flow contributes to the signal and the time-averaged mean velocity will be most representative. Smaller gates give a cleaner signal, especially with laminar flow, but at the expense of a reduction in sensitivity.

## Filters

Removal of low-frequency noise and clutter arising from the vessel wall and surrounding tissues contributes to a cleaner signal, but filters should be set as low as is practical, otherwise low-frequency shifts from slow blood flow will be filtered out, which could result in the mistaken impression of absent diastolic flow in arteries, or occlusion in veins. In practice it is best to keep the filters set at the lowest setting and only increase filtration as required during an examination.

Modern systems allow the operator to preset many of these parameters and create different profiles for different types of examination such as veins, carotids, renal, etc. However, it should be remembered that ultrasound is a dynamic examination and the best results will be obtained if the system controls are adjusted to optimum settings for the task in hand, rather than relying on the preset profiles alone.